

This electronic thesis or dissertation has been downloaded from the King's Research Portal at <https://kclpure.kcl.ac.uk/portal/>



Investigating the contribution of microglia to the pathophysiology of schizophrenia and autism spectrum conditions using human induced pluripotent stem cells with copy number variants at the 22q11.2 locus

Hanger, Bjørn

Awarding institution:
King's College London

The copyright of this thesis rests with the author and no quotation from it or information derived from it may be published without proper acknowledgement.

END USER LICENCE AGREEMENT



Unless another licence is stated on the immediately following page this work is licensed

under a Creative Commons Attribution-NonCommercial-NoDerivatives 4.0 International

licence. <https://creativecommons.org/licenses/by-nc-nd/4.0/>

You are free to copy, distribute and transmit the work

Under the following conditions:

- Attribution: You must attribute the work in the manner specified by the author (but not in any way that suggests that they endorse you or your use of the work).
- Non Commercial: You may not use this work for commercial purposes.
- No Derivative Works - You may not alter, transform, or build upon this work.

Any of these conditions can be waived if you receive permission from the author. Your fair dealings and other rights are in no way affected by the above.

Take down policy

If you believe that this document breaches copyright please contact librarypure@kcl.ac.uk providing details, and we will remove access to the work immediately and investigate your claim.

**Investigating the contribution of
microglia to the pathophysiology of
schizophrenia and autism spectrum
conditions using human induced
pluripotent stem cells with copy number
variants at the 22q11.2 locus**

Bjørn Hanger

Thesis submitted for the degree of Doctor of Philosophy

Department of Basic and Clinical Neuroscience

Institute of Psychiatry, Psychology and Neuroscience

King's College London

April 2023

To my parents

Abstract

There are converging lines of the evidence that microglia, innate myeloid cells of the central nervous system, might be implicated in psychiatric disorders with a putative neurodevelopmental origin such as schizophrenia and autism spectrum conditions (ASCs). The complex genetic and environmental aetiology of these disorders and heterogeneous clinical presentations have restricted translational potential of disease modelling with animals. Human *postmortem* studies exist but represent microglia phenotypes at end of life rather than during development, and studies using induced microglia models from blood monocytes is limited by not recapitulating authentic microglia ontogeny while also representing post-diagnosis phenotypes. Alternative human *in vitro* models are needed, with human fetal primary tissue being limited and not ethically suitable. Therefore, this thesis reviewed evidence for microglia involvement in schizophrenia and ASC and proposes that human induced pluripotent stem cells (hiPSCs) could be a useful model due the potential of generating microglia-like cells (MGLs) with authentic microglia ontogeny. To study the potential contribution of microglia in the development of schizophrenia and ASC, I characterised hiPSC-derived MGLs from donors with a highly penetrant risk factor risk factor for both conditions, 22q11.2 deletion syndrome (22q11.2DS), which is caused by one or more hemizygous microdeletions in the 22q11.2 chromosome region.

Genotyping of hiPSCs from donors with 22q11.2DS was performed, identifying several deleted genes expressed in microglia. Polygenic risk was calculated, highlighting potential sources of variance among 22q11.2DS donors. Following confirmation that hiPSCs from donors with 22q11.2DS can successfully differentiate to MGLs, this thesis showed that 22q11.2DS affects MGL form and function. Compared to hiPSC-derived MGLs from neurotypical donors, 22q11.DS MGLs have reduced arborisation, higher TMEM119:IBA1 colocalisation, increased phagocytosis, a transcriptomic profile suggesting differences in cytokine signalling, and reduced IL-6 and IFN γ cytokine secretion.

Differences between 22q11.2DS MGLs and control MGLs also appears to be context-dependent. Transcriptomic analysis following lipopolysaccharide (LPS) challenge identified differences in pathways associations and differentially expressed genes, with interaction analysis suggesting a stronger effect of LPS on the expression of *CXCL10* and *CHN1* in 22q11.2DS MGLs. Additionally, LPS challenge induced higher phagocytic activity, inferred lysosome levels using lysotracker, and secretion of IL-10 and TNF α alongside reduction in TMEM119:IBA1 colocalisation in control MGLs compared to 22q11.2DS MGLs. On the other hand, LPS challenge did not impact 22q11.2DS MGLs morphological state even though it reduced polarity in control LPS MGLs but induced enhanced IL-6 secretion compared to control MGLs.

This thesis not only provides the first characterisation of microglia with 22q11.2DS, but also is the first hiPSC study investigating microglia contribution to schizophrenia and ASC pathophysiology. The context-dependent impact of 22q11.2DS on MGLs highlights key mechanisms which could contribute to the development of schizophrenia and ASC. Findings both overlapped and contrasted with previous evidence from *in vitro* and *in vivo* human and animal models, including data on human induced microglia from blood monocytes. This suggests that models with authentic microglial ontogeny may be important in studying the contribution of microglia to the development of 22q11.2DS-associated schizophrenia and ASC. Increased replication with stratification of donors by diagnosis and polygenic risk, comparison to idiopathic donors, and use of isogenic lines is recommended. Subsequently, characterisation should be extended to more complex model system like co-cultures and organoids to assess microglial interaction with other cell types including neurons, and in the future also to chimeric animals to examine impact on behavioural phenotypes.

COVID-19 Impact Statement

How COVID-19 impacted this PhD study

Severe disruption to the progress of this PhD study was caused by the COVID-19 pandemic. During the period of the first national lockdown in response to C19 (March 23rd 2020 – 31st July 2020) the wet labs were completely closed and all access was restricted. All cell lines currently in culture at that moment, which included all the 22q11.2DS and control donor line factories for microglia-like cells, had to be disposed of, since they could not be maintained. Due to the lengthy cell cultures ongoing upon initial facility closures, from requiring expansion of human induced pluripotent stem cell cultures to appropriate passage number to differentiation to microglia-like cells, this meant that cell culture started from January 2020 was lost. Expansion and differentiation were restarted upon return to the lab in August 2020, however there were capacity limits which were gradually lifted until June 2021, amounting to 14 months of disrupted wet lab access in addition to the initial loss of 2.5 months' worth of cell culture, making it impossible to recover lost time during this period.

Impact on planned thesis work

This impacted the scope of this project, removing all plans of co-culture experiments and changing the focus to characterisation of 22q11.2DS cell lines in monoculture. It also prevented the completion of all experiments planned, with there also being no time for optimisation of experiments and additional replications. Planned experiments and analyses not completed that would have strengthened the thesis narrative and could have been performed with more time available included:

- Additional hiPSC quality control: It was elected to rely on previous quality control performed on cell lines utilised and only characterise positive pluripotency surface marker expression of those previously not published (Chapter 3).
- Additional validation of findings: This includes not expanding pilot datasets to 22q11.2DS donor lines (Chapter 3), testing of different treatment lengths (Chapter 3, but might in turn have impacted Chapter 4 and Chapter 5), live cell motility assay (Chapter 3) and quantitative PCRs following RNA sequencing (Chapter 4).
- Effect of 22q11.2DS on MGL rate of ATP production, assessing impact on glycolysis and oxidative phosphorylation using a Seahorse XF ATP Real-Time rate assay (Chapter 5).
- More extensive analyses of acquired data which also would require additional training: 3D morphology analyses (Chapter 3) and quantification of relationship between morphology and phagocytic uptake (Chapter 5) using confocal images. Additional analysis of RNA sequencing data including power analysis, and classification of differentially expressed genes outside versus inside of the 22q11.2 region (Chapter 4).

Mitigation

In addition to changing the scope of this project, other efforts were made to mitigate the impact of COVID-19. A 3-month extension was obtained which could be used in the wet lab setting. Careful planning allowed for key sample collection during the period of disrupted access. During lockdown, time was spent independently to learn R and Ubuntu Linux software to perform data processing for a future RNA sequencing experiment, a skillset which also later allow calculation of polygenic risk scores. Lastly, various analysis was carried on into write-up status period but was stopped when there were no time remaining.

This Impact of COVID-19 Impact Statement is referred to in relevant thesis sections for transparency and clarity.

Statement of work completed

All writing and data presented within this thesis was the result of work completed by me unless otherwise stated.

Chapter 3: The location and size of the deleted and duplicated regions at the 22q11.2 locus were mapped for all 22q11.2 deletion carrier lines by Miss Kaarin Sabad in partial fulfilment for the degree of MSc in Neuroscience under supervision of myself and Dr Anthony C. Vernon. This work resulted in gene lists shown in **Figure 3.1**, **Figure 3.2**, **Figure 3.3**, **Table 3.2** and **Table 3.3**. Work by Miss Kaarin Sabad was later validated by me as well as further classified as described in Methods section of **Chapter 3**, which led to other data and figures associated with this dataset. Training was given to both me and Miss Kaarin Sabad by Dr. Dwaipayan Adhya in use of and understanding of associated software to support analysis of Psycharray data files. Psycharray data files, which included cell lines CTR_M3_36S, 127_CTM_03, 007_CTF_10, 287_SZM_01, 191_SZM_09, and 509_CXF_13, had previously been obtained by the Srivastava laboratory. Clinical status of 22q11.2 deletion line donors was obtained from Dr. Maria Rogdaki and collaborators, with recruitment and reprogramming in addition also being supported by Mr Matthew Reid and Mr Roland Nagy.

Chapter 5: The cytokine secretion experiment that resulted in **Figure 5.5** and **Figure 5.6** was performed together with Dr. Alessandra Borsini. I prepared all the samples and Dr. Borsini ran the MSD instrument with me present. Analysis of the output data was performed by me independently following training by Dr. Borsini. I would also like to acknowledge Dr. Shiden Solomon for support in designing the phagocytosis assay and training for the IMARIS 3D reconstruction analysis.

Acknowledgements

First, I would like to thank my first supervisor, Dr Anthony C. Vernon. I'm thankful for you taking the time to entertain my crazy ideas for projects and the broader implications for findings even when they did not make sense. The fact that you also encouraged these discussions made me a better scientist. I would also like to thank for second supervisor Dr Deepak P. Srivastava for not only making all the cell lines used in study available for me to use, but for your never-ending enthusiasm. Although one day you will hopefully admit that, of course, microglia are cooler than neurons. Without both of you this would not be possible. I don't think I could have asked for better supervisors and this was evident once COVID-19 arrived in the UK. You encouraged safety above all, prepared us what might happen in advance, and made sure that fellow lab members and I were well taken care of.

I would like to thank members both past and present of the Vernon and Srivastava labs that have been there alongside me throughout or temporarily during this journey for their support and contribution to a fantastic working environment: Dr. Deep Adhya, Dr. Ester Coutinho, Amalie Couch, Rugile Matuleviciute, Dr. Lucia Dutan Polit, Laura Sichlinger, Dr. Nick Gatford, Dr. Deborah Reyes, Dr. Pooja Raval Chudasama, Iain Watson, Roland Nagy, Kelly O'Toole, Fiona Coutes. Dr. Marie-Caroline Cotel, and Dr. Elise Halff. Special thanks to Dr. Maria Rogdaki for making work on 22.11.2DS possible. My thanks also extend to students whom I have co-supervised during my PhD candidacy: Thank you to Tharshini Ragupathy, Kaarin Sabad, Cecily Jacobs, Alessia Fisher, and Elif Somer.

Furthermore, I would like to thank the people that I have met during my time at the Maurice Wohl Institute for contributing to a fantastic working environment through a conversation

here, a piece of advice there. Of the Wohl cellular imaging centre: Dr. George Chennell and Chen Liang. Of the Wohl second floor: Dr. Edina Silajdzic, Dr. Hyunah Lee, Dr. Thomas Berger, and Jordan Guthrie. A special mention to (now Dr.) Shiden Solomon, which I for the second time acknowledge in a thesis for his ongoing support for not only me but also others in the Wohl. Speaking of this other thesis, I want to thank my MSc supervisor Dr. Agnes Nishimura. Without your guidance and teaching during my MSc I would not be doing a PhD.

I would like to express gratitude to Celeste Kolanko and my colleagues, both past and current, at Liberum IME, for not only giving me the opportunity to work alongside you while I've been writing this thesis during my final year, but for being wonderful human beings.

To the people that have contributed to keeping me sane throughout this experience, I really appreciate you and am thankful to have you in my life. My friends, who been supportive no matter where they are in the world: Mathew Chan, Stefan Lay, Anamul Hoque, Palwasha Najeeb, Samuel Clarke, Emma Grønning, Magnus Andresen, and the closest thing I have to a sibling, Martin Langen. And of course, a special thank you to my supportive partner Laura Luengo González, who has been a patient, optimistic rock throughout this journey.

Lastly, I want to thank my parents, Bjørn and Karin Hanger. Words cannot express how grateful and how lucky I am to have the best parents in the world. You have supported me no matter how crazy my adventures have been, from living in different countries including the USA, Australia, and the UK, to throughout my studies starting with Exercise Science and now having written a PhD thesis in the Neuroscience field. I don't think anyone would have guessed this is where I would end up, but it is all thanks your never-ending support and love. Kjempeglad i dere.

Table of Contents

Abstract.....	1
COVID-19 Impact Statement	3
Statement of work completed	5
Acknowledgements	6
Table of Contents	8
List of Figures.....	13
List of Tables	16
Abbreviations	20
Chapter 1: General introduction.....	27
<i>1.1 Microglia.....</i>	<i>27</i>
1.1.1 A short note on the study of microglia	27
1.1.2 Microglia ontogeny	28
1.1.3 Roles of microglia	34
1.1.4 “Activation” of microglia.....	36
1.1.5 Heterogeneity of microglia	38
<i>1.2 Role of microglia in the pathophysiology of psychiatric disorders with a putative neurodevelopmental origin</i>	<i>44</i>
1.2.1 Autism spectrum conditions	44
1.2.2 Schizophrenia	45
1.2.3 Aetiology of schizophrenia and ASC	46
1.2.4 Immune system-associated phenotypes in ASC and schizophrenia	48
<i>1.3 Using human induced pluripotent stem cells to model ASC and schizophrenia in vitro </i>	<i>51</i>
1.3.1 Potential of human induced pluripotent stem cells	52
1.3.2 Protocols for the generation of hiPSC-derived microglia	60
<i>1.4 Thesis aims and outline</i>	<i>70</i>
Chapter 2: General Materials and Methods	74
2.1 Use of human materials and cell line information	74

2.3 Differentiation of hiPSCs to pre-Macpre factories	79
2.4 Differentiation of microglia-like cells and macrophages from macrophage precursors	81
2.5 Microglia-like cell and macrophage immune challenge	82
2.6 RNA extraction, cDNA synthesis and RT-qPCR	83
2.7 Experiment design	86
2.8 Statistical analysis and data visualisation	87
Chapter 3: Characterisation of 22q11.2 copy number variants and generation of hiPSC microglia-like cells	88
3.1 Introduction	88
3.1.1 Using hiPSC-derived microglia-like cells to assess microglia contribution to pathophysiology of psychiatric disorders with putative neurodevelopmental origin	88
3.1.2 22q11.2 deletions – a highly penetrant risk factor for schizophrenia and ASC	90
3.1.3 Why is microglia a relevant cell type to model the effect of 22q11.2 deletions?	92
3.1.4 Aims and hypotheses	95
3.2 Methods	97
3.2.1 Analysis of Infinium Psycharray dataset	99
3.2.3 Surface marker immunocytochemistry	102
3.2.4 hiPSC signature marker image acquisition	106
3.2.5 Microglia morphology and surface marker analysis	107
3.3 Results	110
3.3.1. Characterisation of 22q11.2 deletions in patient lines	110
3.3.2. Polygenic risk profiles vary among 22q11.2DS and control cell lines	116
3.3.3. Quality control of hiPSCs	118
3.3.4. Validation of MGL differentiation protocol using control lines	128
3.3.5. Key suspected gene within 22q11.2DS deletion are qualitatively lower expressed than in control MGLs	136
3.3.6. Comparison of morphology and key signature protein expression as a function of genotype and under the context of LPS stimulation	137
3.3.7. 22q11.2DS MGL surface marker TMEM119:IBA1 colocalisation is altered	149
3.4 Discussion	152

3.4.1. Data summary	152
3.4.2. 22q11.2DS cell line gene variants and polygenic risk towards 22q11.2DS - associated conditions are highly heterogeneous	154
3.4.3. hiPSC-derived MGLs exhibit signature markers and functions	160
3.4.4. Characterisation of 22q11.2DS effect on hiPSC-derived MGL morphology	161
3.4.5. Altered colocalisation of TMEM119 and IBA1 in both vehicle and LPS-treated 22q11.2DS MGLs compared to control MGLs	164
3.4.6. Limitations and considerations for future work	165
3.5 Conclusions	167
Chapter 4: Transcriptomic profiling of 22q11.2DS MGLs and their response to LPS	169
4.1 Introduction	169
4.1.1. Utility of bulk RNA sequencing	169
4.1.2. Relevance for transcriptomic profiling of hiPSC-derived 22q11.2DS MGLs	170
4.1.3. Importance of exploring the effect of LPS challenge on the hiPSC-derived 22q11.2DS MGL transcriptome	172
4.1.4. Aims and hypotheses	174
4.2 Methods	175
4.2.1 RNA library preparation and NovaSeq Sequencing	175
4.2.2. RNAseq sample processing	177
4.2.3. Differential gene expression	178
4.2.4. Gene enrichment analysis	179
4.2.5. Gene ontology analysis	179
4.3 Results	180
4.3.1. Control and 22q11.2DS MGLs express key microglia genes and qualitative confirmation of common deleted genes in 22q11.2DS MGLs cell lines	180
4.3.2. PCA analysis of RNA sequencing data demonstrates presence of variance based on sex and treatment condition, but not control and 22q11.2DS genotypes	183
4.3.3. Differentially expressed genes across different analysis thresholds in Signature A	185
4.3.4. Microglia gene set enrichment of differentially expressed in Signature A ...	194
4.3.5. Gene ontology analysis of differentially expressed genes in Signature A	196
4.3.6. Signature B	212
4.3.7. Signature C	219

4.3.8. Common differentially expressed genes between control and 22q11.2DS in response to LPS	226
4.3.9. Microglia gene set enrichment of uniquely differentially expressed genes in LPS treated control and 22q11.2DS MGLs	227
4.3.10. Gene ontology of uniquely differentially expressed genes in Signature B and C	229
4.3.11. Signature D	235
4.4 Discussion	238
4.4.1. Differentially regulated genes in Signature A are associated with 22q11.2DS-associated conditions and aberrancies in immune response	243
4.4.2. Signature B and Signature C showcases broad immune responses, but secondary analysis identifies differences in pathways utilised	249
4.4.3. Signature D analysis reveals potential key drivers in differential response to LPS	252
4.4.4. Limitations and future direction	254
4.5 Conclusions	255
Chapter 5: Functional characterisation of control versus 22q11.2DS hiPSC-derived microglia-like cells	256
5.1 Introduction	256
5.1.1. Functional characterisation of 22q11.2DS MGLs based on morphological and transcriptomic profiling	256
5.1.2. Microglia-associated phagocytosis in psychiatric disorders	257
5.1.3. The role of lysosomes in microglial functions	258
5.1.4. Relevance of studying cytokine secretion by control and 22q11.2DS microglia	259
5.1.5. Aims and hypotheses	261
5.2 Methods	263
5.2.1 Cargo uptake and lysotracker red™ assay	263
5.2.2 Cytokine secretion assay	266
5.3 Results	268
5.3.1 Effect of 22q11.2DS on particle uptake is dependent on cargo size	268
5.3.2 Abnormal lysosome:cell body ratio in 22q11.2DS MGLs compared to controls	276
5.3.3 Altered cytokine release in 22q11.2DS MGL culture media compared to controls	278
5.4 Discussion	286

5.4.1 Genotype effects of 22q11.2DS on MGL phagocytosis is cargo and context-dependent	286
5.4.2 22q11.2DS MGL acidity is not increased the level of control MGLs in response to LPS	290
5.4.3 22q11.2DS MGLs have context-dependent abnormalities in cytokine secretion	292
5.4.4 Limitations and future directions	296
5.5 Conclusions	300
Chapter 6: General Discussion	301
6.1 Overview and discussion of key findings.....	301
6.1.1 Genetic heterogeneity of cell lines	305
6.1.2 Genotype-driven differences between control and 22q11.2DS MGLs	306
6.1.3 Distinct phenotype in 22q11.2DS MGLs following LPS challenge	307
6.2 Implications	310
6.2.1 Studying microglia and their immune response <i>in vitro</i> using hiPSCs	311
6.2.2 Understating the contribution of microglia to 22q11.2DS-associated conditions	312
6.3 Limitations and future work	316
6.3.1 The hiPSC model and hiPSC-derived MGLs	316
6.3.2 Studying CNVs and 22q11.2DS	318
6.3.3 General future considerations for examining whether microglia play a role in schizophrenia and ASC by using 22q11.2DS MGLs	321
6.4 Concluding remarks	324
Bibliography	325

List of Figures

Chapter 1

Figure 1. 1: Overview of key microglia events during brain development and other notable events	33
---	----

Chapter 2

Figure 2. 1: Overview of MGL differentiation protocol	80
---	----

Chapter 3

Figure 3. 1: Diagram illustrating genomic locations of 22q11.2 locus CNVs in 22q11.2DS hiPSC lines.....	112
Figure 3. 2: Heterogeneity of [22q11.2DS-associated neurodevelopmental psychiatric disorder PRS across control and 22q11.2 deletion lines	117
Figure 3. 3: Heterogeneity of neurodegenerative disease-associated PRS towards neurodegenerative diseases across control and 22q11.2 deletion lines	118
Figure 3. 4: Karyograms of cell lines included in Infinium Psycharray	120
Figure 3. 5: Validation of hiPSC lines	126
Figure 3. 6: Signature marker assessment of differentiated MGLs compared to macrophages	131
Figure 3. 7: Percentage of cells per well positive for PU.1 and either P2RY12 or TMEM119	133
Figure 3. 8: MGL functional response to 4-hour treatment of IL-1 β	134
Figure 3. 9: Macrophage functional response to 4-hour treatment of IL-1 β	135

Figure 3. 10: Qualitative confirmation of deleted genes in 22q11.2DS cell lines	137
Figure 3. 11: Illustration of microglia signature protein expression and morphology in control MGLs treated with either H ₂ O vehicle or LPS for 3 hours	140
Figure 3. 12: Illustration of microglia signature protein expression and morphology in 22q11.2DS MGLs treated with either H ₂ O vehicle or LPS for 3 hours	140
Figure 3. 13: MGL whole cell morphology and signature markers in 22q11.2DS cell lines compared to control MGLs	141
Figure 3. 14: MGL polarity in differentiated vehicle-treated and LPS-treated 22q11.2DS lines compared to vehicle-treated and LPS-treated control lines. cal analysis	142
Figure 3. 15: Assessment of nuclei morphology in vehicle-treated control and 22q11.2DS MGLs	143
Figure 3. 16: MGL whole cell morphology and signature markers in 22q11.2DS cell lines compared to control MGLs in response to LPS	144
Figure 3. 17: MGL signature protein markers in 22q11.2DS cell lines compared to control MGLs	146
Figure 3. 18: MGL signature protein markers in 22q11.2DS cell lines compared to control MGLs in response to LPS	148
Figure 3. 19: Colocalisation of IBA1 and TMEM119 in control MGL compared to 22q11.2DS MGLs	150
Figure 3. 20: Colocalisation of IBA1 and TMEM119 in control MGL compared to 22q11.2DS MGLs in response to LPS.....	151

Chapter 4

Figure 4. 1: Validation of MGL gene expression based on consensus human microglia/monocyte markers as assessed in Haenseler et al. (2017)	181
Figure 4. 2: Heatmap showing expression of selected deleted gene common among all 22q11.2DS cell lines	183
Figure 4. 3: PCA analysis of H ₂ O vehicle- and LPS-treated control and 22q11.2DS MGLs	185
Figure 4. 4: Volcano plot of up and down-regulated genes in Signature A-StringentT	189
Figure 4. 5: Volcano plot of up and down-regulated in Signature A-ModerateT.....	190
Figure 4. 6: Volcano plot of up and down-regulated genes in Signature A-LenientT.....	192
Figure 4. 7: Gene ontology analysis of down-regulated differentially expressed genes in Signature A-StringentT	200
Figure 4. 8: Gene ontology analysis of up-regulated differentially expressed genes in Signature A-StringentT	202
Figure 4. 9: Gene ontology analysis of down-regulated differentially expressed genes in Signature A-ModerateT	204
Figure 4. 10: Gene ontology analysis of up-regulated differentially expressed genes in Signature A-ModerateT	206
Figure 4. 11: Gene ontology analysis of down-regulated differentially expressed genes in Signature A-LenientT	208
Figure 4. 12: Gene ontology analysis of up-regulated differentially expressed genes in Signature A-LenientT	210
Figure 4. 13: Volcano plot of up and down-regulated genes in Signature B	213
Figure 4. 14: Gene ontology analysis of Signature B	217
Figure 4. 15: Volcano plot of up and down-regulated genes in Signature C	220

Figure 4. 16: Gene ontology analysis of Signature C	224
Figure 4. 17: Venn diagram showing the total number of overlapping and uniquely differentially expressed genes in Signature B and Signature C	226
Figure 4. 18: Gene ontology analysis of DEGs up-regulated in Signature B but not Signature C	231
Figure 4. 19: Gene ontology analysis of DEGs up-regulated in Signature C but not Signature B	233
Figure 4. 20: Volcano plot of up- and down-regulated genes in Signature D	236
Figure 4. 21: Normalised gene counts of gene hits in Signature D	237
Figure 4. 22: Overview of Signature A MGENrichment gene set enrichment analyses	239
Figure 4. 23: Overview of Signature B and Signature C MGENrichment gene set enrichment analyses	240
Figure 4. 24: Overview of Signature A gene ontology analyses	241
Figure 4. 25: Overview of Signature B and Signature C gene ontology analyses	242

Chapter 5

Figure 5. 1: Effect of 22q11.2DS on uptake of Alexa Fluor™ 594-zymosan in vehicle- and LPS-treated conditions	271
Figure 5. 2: Effect of 22q11.2DS on uptake of mouse brain purified ^{td} Tomato-tagged synaptosomes in vehicle- and LPS-treated conditions	273
Figure 5. 3: Effect of 22q11.2DS on uptake of 4 kDa FITC-dextran (green) in vehicle- and LPS-treated conditions	275
Figure 5. 4: Effect of 22q11.2DS on MGL acidic endolysosomal vesicle levels	277
Figure 5. 5: Effect of 22q11.2DS on cytokine release	280
Figure 5. 6: Effect of 22q11.2DS on cytokine release when treated with LPS	283

List of Tables

Chapter 1

Table 1. 1: Overview of species differences between human and mouse microglia of potential relevance to studying microglia contribution to pathophysiology of psychiatric disorders with a putative neurodevelopmental origin	43
Table 1. 2: ASC Category 1 Risk Genes and expression profile in microglia	55
Table 1. 3: An overview of hiPSC-derived microglia systems for psychiatric disorder modelling and their benefits, drawbacks, and potential uses	58
Table 1. 4: Overview of published protocols that generate hiPSC-derived microglia	69

Chapter 2

Table 2. 1: Overview of hiPSC donor details and clinical status	76
Table 2. 2: Overview of primers utilised	85

Chapter 3

Table 3. 1: Overview of which cell lines were used across different results sections within this chapter	98
Table 3. 2: GWAS data set training samples in polygenic risk scoring analysis	102
Table 3. 3: Overview of primary and secondary antibodies used for immunocytochemistry	106
Table 3. 4: Description of measurements performed in FIJI v2.3.1	108
Table 3. 5: Deleted genes within the 22q11.2 region of 22q11.2DS hiPSC lines	113
Table 3. 6: Duplicated genes within the 22q11.2 region of 22q11.2DS hiPSC lines	114

Table 3. 7: Summary of affected genes within 22q11.2 region donor clinical status	115
Table 3. 8: Overlap of deleted protein-coding genes in 22q11.2DS hiPSC lines with known positive expression in microglia or macrophages	115

Chapter 4

Table 4. 1: Overview of sequencing sample details	176
Table 4. 2: Down-regulated differentially expressed genes in Signature A-StringentT	189
Table 4. 3: Up-regulated differentially expressed genes in Signature A-StringentT	190
Table 4. 4: Down-regulated differentially expressed genes in Signature A-ModerateT	191
Table 4. 5: Up-regulated differentially expressed genes in Signature A-ModerateT	191
Table 4. 6: Down-regulated differentially expressed genes in Signature A-LenientT	193
Table 4. 7: Up-regulated differentially expressed genes in Signature A-LenientT	193
Table 4. 8: Gene set enrichment analysis of Signature A-StringentT	194
Table 4. 9: Gene set enrichment analysis of Signature A-ModerateT	195
Table 4. 10: Gene set enrichment analysis of Signature A-LenientT	196
Table 4. 11: Differentially expressed genes in Signature B	214
Table 4. 12: Gene set enrichment analysis of Signature B	215
Table 4. 13: Differentially expressed genes in Signature C	221
Table 4. 14: Gene set enrichment analysis of Signature C	222
Table 4. 15: Overlap of differentially expressed genes in Signature B and Signature C	227
Table 4. 16: Uniquely differentially expressed genes in Signature B vs Signature C	227
Table 4. 17: Uniquely differentially expressed genes in Signature C vs Signature B	228
Table 4. 18: Gene set enrichment analysis of unique DEGs in Signature C vs Signature B	229

Chapter 6

Table 6. 1: Overview of key thesis findings	304
---	-----

Abbreviations

<i>Abbreviation</i>	<i>Description</i>
<i>22q11.2DS</i>	22q11.2 deletion syndrome/ DiGeorge Syndrome
<i>2D</i>	Two-dimensional
<i>3D</i>	Three-dimensional
μM	Micromolar
μm	Micrometer
<i>ADHD</i>	Attention deficit hyperactivity disorder
<i>AIF1</i>	Allograft Inflammatory Factor 1 (also known as IBA1)
<i>ASC</i>	Autism spectrum condition
<i>ASD</i>	Autism spectrum disorder
<i>ATAC</i>	Assay for transposase-accessible chromatin
<i>Atg7</i>	Autophagy Related 7
<i>ATP</i>	Adenosine triphosphate
<i>BD</i>	Bipolar disorder
<i>BDNF</i>	Brain-derived neurotrophic factor
<i>BH</i>	Benjamini-Hochberg
<i>BH4</i>	Tetrahydrobiopterin
<i>BMP4</i>	Bone morphogenetic protein 4
<i>BV2</i>	Immortalised microglial cell derived from C57/BL6 murine
<i>C</i>	Celsius
<i>c-Myc</i>	MYC proto-oncogene, BHLH transcription factor
<i>C1q</i>	Complement component 1q
<i>C1QA</i>	Complement C1q A chain
<i>C3</i>	Complement C3
<i>C4</i>	Complement C4
<i>C4A</i>	Complement C4A
Ca^{2+}	Calcium ion
<i>CatS</i>	Cathepsin S
<i>CAARMS</i>	Comprehensive Assessment of At Risk Mental States

<i>CASPR2-IgG</i>	Anti-contactin-associated protein-like 2-immunoglobulin G
<i>CCL13</i>	Chemokine (C-C motif) ligand 13
<i>CD11b</i>	Integrin Subunit Alpha M (also known as ITGAM)
<i>CD40</i>	CD40 Molecule, TNF Receptor Superfamily Member 5
<i>CD58</i>	CD58 Antigen, Lymphocyte Function-Associated Antigen 3
<i>CD68</i>	CD68 Molecule, Scavenger Receptor Class D, Member 1
<i>CD163</i>	CD163 Molecule, Scavenger Receptor Cysteine-Rich T1 Protein M130
<i>cDNA</i>	Complementary/copy deoxyribonucleic acid
<i>CHAMP1</i>	Chromosome Alignment Maintaining Phosphoprotein 1
<i>ChIP</i>	Chromatin immunoprecipitation
<i>CHN1</i>	Chimerin 1
<i>CHRFAM7A</i>	CHRNA7 (Cholinergic Receptor, Nicotinic, Alpha Polypeptide 7, Exons 5-10) And FAM7A (family With Sequence Similarity 7A, Exons A-E) Fusion
<i>CNS</i>	Central nervous system
<i>CNV</i>	Copy number variant
<i>CO₂</i>	Carbon dioxide
<i>COMT</i>	Catechol-O-Methyltransferase
<i>CMPK2</i>	Cytidine/Uridine Monophosphate Kinase 2
<i>CRISPR/Cas9</i>	Clustered regularly interspaced short palindromic repeats/ CRISPR-associated protein 9
<i>CSF-1</i>	Colony Stimulating Factor 1
<i>Ct</i>	Cycle threshold
<i>CX3CL1</i>	C-X3-C Motif Chemokine Ligand 1
<i>CXCL10</i>	C-X-C Motif Chemokine Ligand 10
<i>CX3CR1</i>	C-X3-C Motif Chemokine Receptor 1
<i>D</i>	Day
<i>DAMP</i>	Disease-associated molecular pattern
<i>DAPI</i>	4',6-diamidino-2-phenylindole
<i>DEG</i>	Differentially expressed gene
<i>DGCR8</i>	DGCR8 Microprocessor Complex Subunit, DiGeorge Syndrome Critical Region Gene 8
<i>DLG4</i>	Discs Large MAGUK Scaffold Protein 4 (also known as PSD95)
<i>DMEM/F12</i>	Dulbecco's Modified Eagle Medium/Ham's F-12

<i>DMSO</i>	Dimethylsulfoxide
<i>DNA</i>	Deoxyribonucleic acid
<i>E (i.e. E15.5)</i>	Embryonic day (embryonic day 15.5)
<i>EB</i>	Embryoid body
<i>eIF4E</i>	Eukaryotic translation initiation factor 4E
<i>ELISA</i>	Enzyme-linked immunosorbent assay
<i>EMBL-EBI</i>	European Molecular Biology Laboratory- European Bioinformatics Institute
<i>ER</i>	Endoplasmic reticulum
<i>ERAP2</i>	Endoplasmic reticulum aminopeptidase 2
<i>ERK</i>	Extracellular signal-regulated kinase
<i>F4/80</i>	EGF-like module-containing mucin-like hormone receptor-like 1
<i>FDR</i>	False discovery rate
<i>FITC</i>	Fluorescein isothiocyanate
<i>FMR1</i>	Fragile X Messenger Ribonucleoprotein 1
<i>FPKM</i>	Fragments Per Kilobase of transcript per Million mapped reads
<i>GAS6</i>	Growth Arrest Specific 6
<i>GAPDH</i>	Glyceraldehyde-3-phosphate dehydrogenase
<i>GCH-1</i>	Guanosine 5'-Triphosphate Cyclohydrolase I
<i>GM-CSF</i>	Granulocyte-macrophage colony-stimulating factor
<i>GNLY</i>	Granulysin
<i>GO</i>	Gene ontology
<i>GPR34</i>	G Protein-Coupled Receptor 34
<i>GW (i.e. GW4)</i>	Gestational week (gestational week 4)
<i>GWAS</i>	Genome-wide association study
<i>H₂O</i>	Dihydrogen monoxide
<i>HAMs</i>	Human AD microglia patterns
<i>HLA-A</i>	Human Leukocyte Antigen A, Major Histocompatibility Complex, Class I, A
<i>HLA-DR</i>	Histocompatibility Antigen HLA-DR Alpha, Major Histocompatibility Complex, Class II, DR Alpha
<i>hiPSC</i>	Human induced pluripotent stem cells
<i>IFN-α</i>	Interferon Alpha

<i>IFNγ</i>	Interferon Gamma
<i>IGF</i>	Insulin Like Growth Factor 1
<i>kDa</i>	Kilodalton
<i>Klf4</i>	Krueppel-Like Factor 4
<i>IBA1</i>	Ionized calcium binding adaptor molecule 1
<i>IL-1α/ IL1A</i>	Interleukin 1 alpha
<i>IL-1β</i>	Interleukin 1 beta
<i>IL-2</i>	Interleukin 2
<i>IL-3</i>	Interleukin 3
<i>IL-4</i>	Interleukin 4
<i>IL-6</i>	Interleukin 6
<i>IL-8</i>	Interleukin 8
<i>IL-10</i>	Interleukin 10
<i>IL-12p70</i>	Interleukin 12
<i>IL-13</i>	Interleukin 13
<i>IL-34</i>	Interleukin 34
<i>ID</i>	Identifier
<i>IGV</i>	Integrative Genomics Viewer
<i>iNOS</i>	Inducible nitric oxide synthase
<i>IP-10</i>	Interferon γ -induced protein 10 kDa
<i>ITGAM</i>	Integrin Subunit Alpha M
<i>IRF8</i>	Interferon Regulatory Factor 8
<i>JNK</i>	c-Jun N-terminal kinase
<i>LAMP2</i>	Lysosomal Associated Membrane Protein 2
<i>LCR</i>	Low copy repeat
<i>LCR-A</i>	Low copy repeat A
<i>LCR-B</i>	Low copy repeat B
<i>LCR-C</i>	Low copy repeat C
<i>LCR-D</i>	Low copy repeat D
<i>LD</i>	Learning disorder
<i>LIN28</i>	Lin-28 Homolog A, Zinc Finger CCHC Domain-Containing Protein 1
<i>LPS</i>	Lipopolysaccharide

<i>LRRK2</i>	Leucine Rich Repeat Kinase 2
<i>M-CSF</i>	Macrophage colony-stimulating factor
<i>M1</i>	Outdated term for “toxic” microglia
<i>M2</i>	Outdated term for “protective” microglia
<i>MAF</i>	Minor allele frequency
<i>Mb</i>	Megabase
<i>MeCP2</i>	Methyl-CpG Binding Protein 2
<i>MERTK</i>	Tyrosine-Protein Kinase Mer
<i>MGL</i>	Microglia-like cell
<i>MHCI</i>	Major histocompatibility complex class 1
<i>MiMS</i>	Microglia inflamed in MS
<i>MIA</i>	Maternal immune activation
<i>mL</i>	Milliliter
<i>MPZL1</i>	Myelin Protein Zero Like 1
<i>mRNA</i>	Messenger RNA
<i>MRPL40</i>	Mitochondrial Ribosomal Protein L40
<i>MSD</i>	Meso scale discovery
<i>mtDNA</i>	Mitochondrial DNA
<i>MYB</i>	Transcriptional Activator Myb
<i>NAMP</i>	neurodegeneration associated damage pattern
<i>NANOG</i>	Homeobox Transcription Factor Nanog
<i>NCBI</i>	National Center for Biotechnology Information
<i>NF-κB</i>	Nuclear factor kappa-light-chain-enhancer of activated B cells
<i>NGF</i>	Nerve Growth Factor
<i>NHS</i>	National health service
<i>NLRP2</i>	Nucleotide-Binding Oligomerization Domain, Leucine Rich Repeat And Pyrin Domain Containing 2
<i>NLRP3</i>	Nucleotide-Binding Oligomerization Domain, Leucine Rich Repeat And Pyrin Domain Containing 3
<i>nm</i>	nanometer
<i>NRXN1</i>	Neurexin 1
<i>Oct3</i>	Octamer-Binding Transcription Factor 3

<i>Oct4</i>	Octamer-Binding Protein 4
<i>p</i>	Passage
<i>p38</i>	Cytokine Suppressive Anti-Inflammatory Drug Binding Protein
<i>P2RY12</i>	Purinergic Receptor P2Y, G-Protein Coupled, 12
<i>PAMP</i>	Pathogen-associated molecular pattern
<i>PBS</i>	Phosphate-buffered saline
<i>PC1</i>	Principal component 1
<i>PC2</i>	Principal component 2
<i>PCA</i>	Principal component analysis
<i>PCR</i>	Polymerase chain reaction
<i>PDD-NOS</i>	Pervasive developmental disorder-not otherwise specified
<i>PET</i>	Positron emission tomography
<i>PiNDs (study)</i>	Patient iPSCs for Neurodevelopmental Disorders (study)
<i>PKCα</i>	Protein kinase C alpha
<i>pMacpre</i>	Macrophage precursors
<i>POC1</i>	Proteome Of Centriole Protein
<i>Poly(I:C)</i>	Polyinosinic:polycytidylic acid
<i>PROS1</i>	Protein S
<i>PRS</i>	Polygenic risk score
<i>PSD95</i>	Post-Synaptic Density Protein 95
<i>P^T</i>	P-value threshold
<i>PU.1</i>	31 KDa-Transforming Protein
<i>qPCR</i>	Quantitative polymerase chain reaction
<i>R&D</i>	Research & development
<i>RelA</i>	Nuclear Factor NF-Kappa-B P65 Subunit
<i>RFP</i>	Red fluorescent protein
<i>RIP</i>	Receptor-interacting protein
<i>RNA</i>	Ribonucleic acid
<i>RNAseq</i>	RNA sequencing
<i>ROCK</i>	Rho-associated, coiled-coil containing protein kinase
<i>ROI</i>	Region of interest
<i>ROS</i>	Reactive oxygen species

<i>RPL13</i>	Ribosomal Protein L13
<i>RT-qPCR</i>	Real time quantitative polymerase chain reaction
<i>RUNX1</i>	Runt-Related Transcription Factor 1
<i>S100A12</i>	S100 Calcium Binding Protein A12
<i>S100B</i>	S100 Calcium Binding Protein B
<i>SCF</i>	Stem cell factor
<i>SCZ</i>	Schizophrenia
<i>SCRNA-seq</i>	Single-cell RNA sequencing
<i>SETD1A</i>	SET Domain Containing 1A, Histone Lysine Methyltransferase
<i>SH-SY5Y</i>	Subline clone of the SK-N-SH neuroblastoma line
<i>SSH</i>	Secure shell
<i>SLaM</i>	South London and Maudsley
<i>SNL</i>	Sambucus nigra lectin
<i>SNP</i>	Single nucleotide polymorphism
<i>SORL1</i>	Sortilin Related Receptor 1
<i>Sox2</i>	SRY-Box Transcription Factor 2
<i>SSEA4</i>	Stage-specific embryonic antigen 4
<i>TANGO2</i>	Transport And Golgi Organization 2
<i>TLR</i>	Toll-like receptor
<i>TLR3</i>	Toll-like receptor 3
<i>TLR4</i>	Toll-like receptor 4
<i>TMEM119</i>	Transmembrane Protein 119
<i>TMEM59</i>	Transmembrane Protein 59
<i>TNF-α</i>	Tumor necrosis factor alpha
<i>TRA-1-81</i>	Podocalyxin
<i>TREM2</i>	Triggering Receptor Expressed On Myeloid Cells 2
<i>TSPO</i>	18 kDa translocator protein
<i>UK</i>	United Kingdom
<i>VEGF</i>	Vascular endothelial growth factor
<i>VEH</i>	Vehicle
<i>WebGestalt</i>	WEB-based GEne SeT AnaLysis Toolkit
<i>WGCNA</i>	Weighted correlation network analysis

Chapter 1:

General introduction

1.1 Microglia

1.1.1 A short note on the study of microglia

Microglia are the primary immunocompetent cells of the central nervous system (CNS). Historically, after their initial description by del Río-Hortega in the early 20th century (del Río-Hortega, 1919), the role of microglia has conventionally been investigated in human and rodent models *en bloc* through low-resolution *in vivo* positron emission tomography (PET) and *postmortem* brain tissue (Mondelli et al., 2017; Hanger et al., 2020). *In vitro* studies have primarily relied on the use of immortalised cell lines derived from mouse and human sources such as BV2 and SV40 cell lines, respectively (Gosselin et al., 2017; Timmerman et al., 2018; Tewari et al., 2021). However, it has now been shown that immortalised cell lines have reduced or no expression of genes that are associated with the core human microglial transcriptomic signature such as *P2RY12*, *CIQA*, and *GAS6*, while phagocyte functions, which are displayed by microglia, such as engulfment of live particles are reduced in immortalised cell lines when compared to microglia isolated from human hippocampal *postmortem* (Butovsky et al., 2014; Sellgren et al., 2017). Primary human microglia from post-surgical samples, being a less accessible alternative, were also only recently described as possible to culture in a serum-free environment (Gosselin et al., 2017; Timmerman et al., 2018; Tewari et al., 2021). Most of our understanding of microglia biology hence comes thanks to rodent data as access to human primary tissue is limited, particularly to fetal tissue which is relevant if studying neurodevelopmental conditions. While it is unclear how some data generalises to humans, for example due to differences in transcriptomic profile such as

no full conservation of microglial sensome genes across mice and human, and potential differences in response to immune challenge such as lipopolysaccharide (LPS) (Nakamura et al., 1999; Owen et al., 2017; Abels et al., 2021), our understanding of microglia, which here now will be reviewed in this section of Chapter 1, has greatly increased since their discovery (Paolicelli et al., 2022). This will then lead into the potential use of human induced pluripotent stem cells (hiPSC) for the study of these cells, psychiatric conditions, and the aims of this thesis, which are to study microglia from individuals with copy number variants (CNVs) within the 22q11.2 region.

1.1.2 Microglia ontogeny

Two theories have dominated the literature on the topic of the origin of microglia, with the arguments being on whether microglia precursors originate in the mesoderm or neuroectoderm. The neuroectoderm theory suggests that microglia within the same lineage as astrocytes and oligodendrocytes (Fujita and Kitamura, 1975; Hao et al., 1991; de Groot et al., 1992; Rezaie and Male, 1999). On the other hand, a hematopoietic yolk sac origin is the basis of the mesoderm theory placing microglia alongside the monocyte-derived macrophage lineage (Huang et al., 2018; Schulz et al., 2012; Swinnen et al., 2013; Kierdorf et al., 2013; Menassa and Gomez-Nicola, 2018), which is also why they are often referred to as CNS tissue-resident macrophages. While studies on human *postmortem* tissue from various developmental stages have provided evidence for microglial morphological and antigenic features, human tissue from embryonic and fetal stages have been limited by use of markers which distinguish microglia and macrophages, with studies on how microglia populate, develop and expand throughout the brain being primarily limited to rodent models (Menassa and Gomez-Nicola, 2018).

The neuroectoderm theory proposes that while during ontogeny, monocyte-derived MOMA-1-, Mac-1-alpha-, and F4/80- positive macrophages infiltrate the CNS parenchyma, they gradually disappear after postnatal day 7 (P7) and cannot stay unless there is persistence of pathological alteration (Fujita & Kitamura, 1975; de Groot et al., 1992). Mac-1-alpha- and F4/80-positive cells are however later observed within the mouse brain parenchyma from P17 in the form of “ramified” microglia, unlike the infiltrating macrophages which take on a more “amoeboid” morphology before their disappearance (de Groot et al., 1992). This is also supported by experiments suggesting that astrocytes, neuropallial, and neuro-epithelial cells can differentiate into cells with microglia characteristics *in vitro* (Hao et al., 1991; Fedoroff et al., 1997).

The idea of a mesodermal origin was first introduced by del Río-Hortega (1932, 1939), but was initially largely overlooked due to the majority of evidence supporting the neuroectodermal theory at the time (Rezaie and Male, 1999; Ginhoux et al., 2013). The mesoderm theory was later supported when it was found that microglia during development display morphological features of macrophages and reacts positively to antisera that recognises monocytes and monocyte-derived macrophages, but the lack of homology between mature microglia and monocytes in specific antigen expression still complicated the theory (Oehmichen et al., 1979, 1979; Wood et al., 1979; Murabe and Sano, 1982; Hume et al., 1983; Murabe and Sano, 1983). However, homologies such as expression of *CD11b* were later established alongside the revelation that disrupted expression of *PU.1*, an essential transcription factor for myeloid cells, results in obliteration of microglia in mice but in humans have only been shown to decrease microglia viability in adult brain tissue (Akiyama and McGeer, 1990; Perry et al., 1985; McKercher et al., 1996; Beers et al., 2006; Kierdorf et al., 2013; Smith et al., 2013; Cakir et al., 2022). Now studies such as by Ginhoux et al. (2010)

using *in vivo* lineage tracing have also revealed that microglia in, at least in mice, originate from primitive macrophages in the yolk sac, which is now generally inferred to be the case also in humans although as noted such studies are not currently possible in human tissue (Janossy et al., 1986; Kierdorf et al., 2013; Menassa and Gomez-Nicola, 2018; Cuadros et al., 2022; Dermitzakis et al., 2023)

At least in rodents, erythromyeloid cells, which give rise to yolk sac-derived macrophages and later go on to become microglia, infiltrate the developing brain parenchyma through blood vessels during E8.5-9.5 (Ginhoux et al., 2010, 2013; Li and Barres, 2018). A gradual increase of microglia proliferation and migration occurs at phases until E15.5, where the rate of increase of microglia proliferation in what becomes the cortex begins to slow (Swinnen et al., 2013). Separating the development of yolk-sac derived macrophages from non-yolk sac macrophages and monocytes is their key characteristic of Myb-independence, which is required for the development of monocytes and non-yolk sac macrophages (Schulz et al., 2012; Buchrieser et al., 2017; Haenseler et al., 2017; van Wilgenburg et al., 2013). Fate determination, survival and proliferation of early macrophages and subsequent microglia have been shown to be regulated by transcription factors RUNX1, PU.1, and IRF8 while also being dependent on capacity to express the CSF-1 receptor (Ginhoux et al., 2010; Kierdorf et al., 2013; Kierdorf & Prinz, 2013). Critically, one could argue that since these supporting studies have been performed in rodents, it would not translate to human models. There is some evidence supporting that the mesoderm theory fits, for example that human haematopoiesis begins in the yolk sac around day 19 of estimated gestational age, and these hematopoietic stem cells are fated to erythromyeloid development akin to what is observed in rodents (Tavian & Peault, 2005; Ginhoux et al., 2013). While likely not microglia, what are likely primitive macrophages or highly immature microglia-like cells have also been

observed as early 3 weeks of human estimated gestational age before the development and subsequent colonisation of CNS-like structures (Hutchins et al., 1990).

The appearance of macrophage precursors importantly predates neurogenesis (Menassa et al., 2018), putting these precursors in a position to support normal neuronal development (Paolicelli et al., 2011). While neurogenesis and neural migration is not initiated until human gestational week (GW) 9, amoeboid-like morphology of microglia in the intermediate, telencephalic ventricular, and marginal zones at GW4, and ramified microglia are observed at GW6 (Migliaccio et al., 1986; Rakic, 1988; Monier et al., 2006, 2007; Bystron et al., 2008; Menassa and Gomez-Nicola, 2018). Functional ability to detect and react to local environmental changes, characterised by high expression of a set of genes termed the microglial “sensome”, is suggested to be gained at E16.5 in mice, which is around GW8 in humans (Hickman et al., 2013; Thion et al., 2018). This is almost at the time in which microglia with amoeboid morphology appear in the spinal cord around GW9 (Rezaie and Male, 1999). Following this developmental stage, rate of microglial proliferation and distribution increases, notably appearing at the cortical plate-subplate junction at GW10-12 where synapses are first observed, followed by appearance in the mesencephalon at week 19 (Verney et al., 2010; Cho et al., 2013). Peak density and ramified morphology of microglia alongside further distributions in the intermediate zone occurs up to GW22 beside the appearance of astrocyte precursors and oligodendrocytes during GW20-22 (Choi and Lapham, 1978; Rezaie and Male, 1999; Rezaie et al., 2004; Jakovcevski et al., 2009; Verney et al., 2010; Cho et al., 2013). Widely differentiated microglia populations throughout the brain is observed by around GW35 (Esiri et al., 1991; Verney et al., 2010). An overview of this information is provided in **Figure 1.1**, which also summarises recent key findings by Menassa and colleagues (2022) on prenatal human *postmortem* tissue published following the

initiation of thesis write-up. **Figure 1.1** additionally illustrates the periods in which synaptogenesis and synaptic pruning occurs (Huttenlocher, 1979; Petanjek et al., 2009), processes in which microglia play key roles in, suggesting that microglia can play an intricate role in brain development (Paolicelli et al., 2011; Miyamoto et al., 2016; Menassa and Gomez-Nicola, 2018; Andoh and Koyama, 2021; Gallo et al., 2022). The establishment of both presence and supposed functionality of microglia at this stage also allows for them to be hypothetically implicated in various conditions associated with abnormal development of neural circuitry (Zhan et al., 2014; Paolicelli and Ferretti, 2017; Konishi et al., 2019; Hanger et al., 2020; Cabirol et al., 2022)

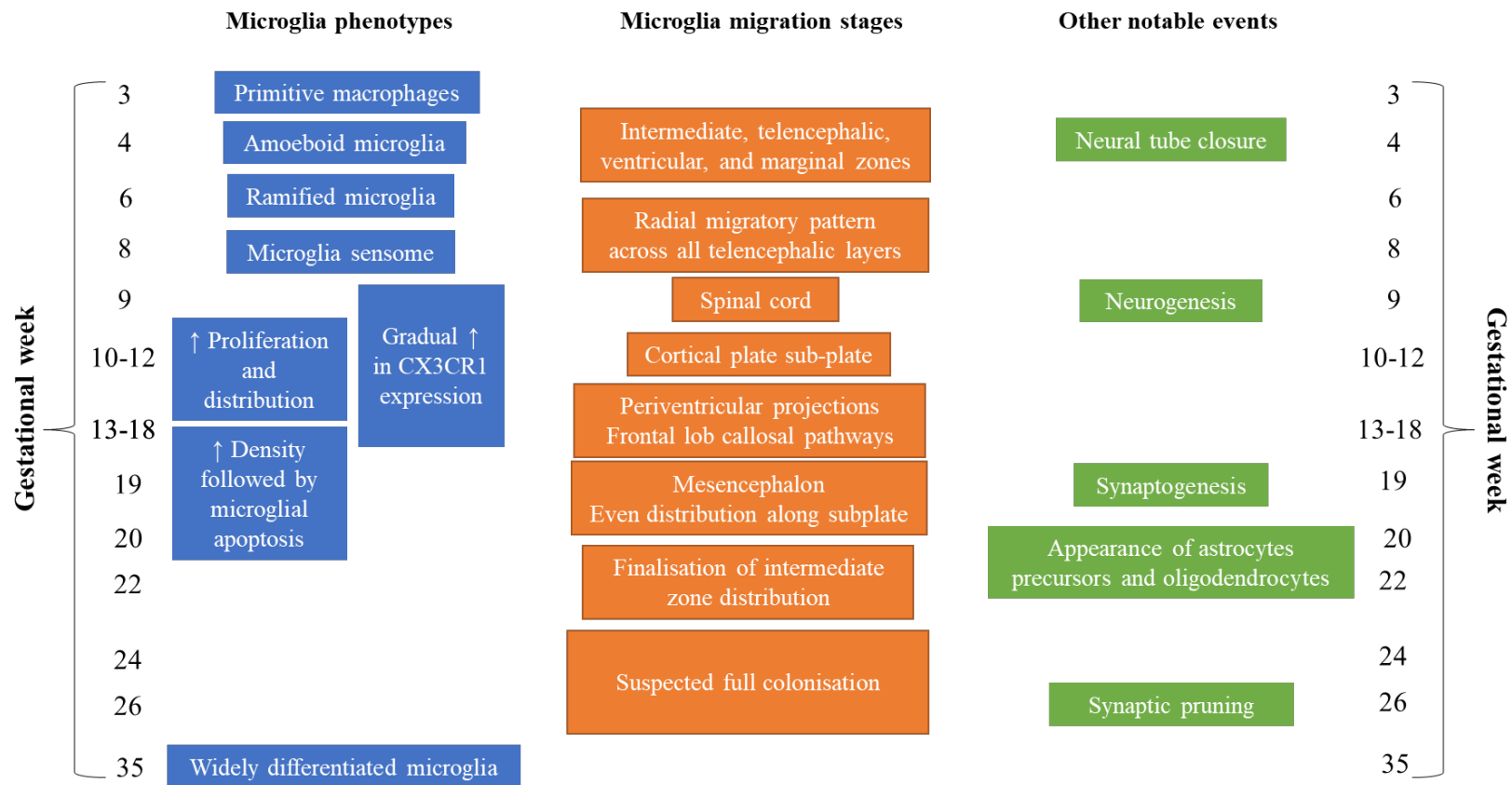


Figure 1. 1: Overview of key microglia events during brain development and other notable events. Information based on data from Menassa et al. (2022) was added following its publication during the write-up period of this thesis. This information included: Radial migratory pattern across all telencephalic layers, periventricular projections, frontal lob callosal pathways, even distribution along subplate, Gradual ↑ in CX3CR1 expression, and ↑ Density followed by microglial apoptosis. Menassa et al. (2022) notably found that homeostatic marker P2RY12 and AIF1, which encodes the microglia IBA1 protein, was expressed at stable levels up to gestational week 11-15. During development, expression of the homeostatic marker TMEM119 also appears to be sporadic, with a significantly lower density of cells being TMEM119+ compared to IBA1+ during gestational weeks 7 and 14 but density changes in TMEM119+ cells do correlate with changes in IBA1+ cells. Additionally, differences observed in microglia transcriptomic states in Menassa et al. (2022) suggest that maturation timings may be different across brain regions

1.1.3 Roles of microglia

In the healthy brain, the phenotype of microglia undergoes dynamic changes throughout the human lifespan due to a demand to perform different functions at different times. During development, microglia play key roles in brain homeostasis. In early brain developmental stages, microglia remove unwanted cells such as excess neural stem cell and progenitor cells, as well as debris such as apoptotic cells, primarily by phagocytic engulfment (Bessis et al., 2007; Sierra et al., 2010; Cunningham et al., 2013; Cserép et al., 2022). Removal of these excess cells to help shape neuronal circuitry could for example be done through DAP12/CD11b-dependent reactive oxygen species (ROS) production by microglia which promotes the engulfment of hippocampal neurons and cerebellar Purkinje neurons during development in mice, although not all neurons might express apoptotic signals which initially induce this signalling across all brain regions (Marín-Teva et al., 2004; Wakselman et al., 2008). Microglia also provide immune surveillance by detecting threats such as infections, inflammation, or injury, regulating the local immune response through release of pro-inflammatory cytokines such as IL-1 β , TNF- α , and IL-6, and anti-inflammatory cytokines such as IL-10 and IL-4 (Lively and Schlichter, 2018; Da Pozzo et al., 2019; Shemer et al., 2020). The release of these cytokines can produce effects on various cell types including neurons and astrocytes as well as other immune cells that may or may not originate in the CNS and may increase in abundance following infiltration during injury such as macrophages, T cells, and B cells (Szepesi et al., 2018; Tanabe and Yamashita, 2018; Zrzavy et al., 2018; Liu et al., 2020; Lyu et al., 2021; Xu et al., 2021; Jain and Yong, 2022). Additionally, microglia support other cell types in the local environment such as promoting oligodendrocyte formation and myelination, while also being involved in vascular formation in the CNS, cerebral blood flow regulation, and regulation of blood brain barrier permeability (da Fonseca et al., 2014; Butovsky and Weiner, 2018; Kisler et al., 2021; Császár et al., 2022;

Hattori, 2023; McNamara et al., 2023). Lastly, other key functions of microglia during brain development is synapse formation and elimination, in which removal of non-functional synapses and refinement of others support normal development and maintenance of neural circuitry (Cunningham et al., 2013; Miyamoto et al., 2016; Lehrman et al., 2018; Weinhard et al., 2018; Basilico et al., 2022). Reduced expression of genes such as in *CX3CR1*, whose activity is normally promoted by secretion of the CX3CL1 chemokine by neurons, has been observed in brain and blood of individuals with schizophrenia and based on data from mouse models, can impair this synapse elimination, which is often referred to as “synaptic pruning”(Zhan et al., 2014; Bergon et al., 2015). Growth of neuronal networks is also supported by modulation of axon growth cone guidance and synaptogenesis as well as through other bidirectional communication with neurons such as by secretion of growth factors such as BDNF, NGF and IGF (Kettenmann et al., 2011; Squarzoni et al., 2014; Wu et al., 2015; De Biase et al., 2017; Illes et al., 2021). Conversely and critically for the study of microglia, this bidirectional communication with neurons may provide cues directing microglia homeostatic state (Biber et al., 2007; Szepesi et al., 2018). As demonstrated in a human induced pluripotent stem cell (hiPSC) system, microglia-like cells co-cultured with cortical neurons changes their morphological and transcriptomic state compared to monocultured microglia-like cells (Haenseler et al., 2017).

As inferred primarily by rodent data, microglia largely retain their key functions with age, not becoming dormant in the adult brain. Microglia immune surveillance and response is retained, as well as interaction with cells in their local environment (Davalos et al., 2005; Nimmerjahn et al., 2005; Kettenmann et al., 2013). The microglia population also remains steady through efficient turnover through spatial and temporal coupling of apoptosis and proliferation (Askew et al., 2017). There are however key differences that are of note when

considering the more aged brain, including a decrease in microglial process motility as well increased cell soma motility has been observed in the ageing brain (Hefendehl et al., 2014). Matching this, studies have also suggested that microglia in the aged brain have a more amoeboid morphology explaining that cell soma mobility is the primary form of immune surveillance as processes are less branched (Davies et al., 2017). In ageing, further differences might also include elevated expression of markers associated with an immune challenged environment alongside lower levels of neuroprotective factors, which have led to suggestions that microglia in the aged brain are vulnerable to secondary insults such as infections and stress (Niraula et al., 2017). This highlights the importance of studying microglia at specific developmental stages during disease modelling.

1.1.4 “Activation” of microglia

Historically, terms “resting” and “activated” microglia appeared in the literature in the 1960s and started becoming more popular in the 1980s, with the terms describing physiological and pathological conditions, respectively (Streit et al., 1988; Paolicelli et al., 2022). “Resting” microglia, described in the absence of injury or pro-inflammatory stimuli, have long an accepted term characterised with rodents both *in vivo* and *in vitro* as the most dynamic cells of the healthy brain continuously remodel their shape through extension and retraction of processes to support motility and survey of the environment (Davalos et al., 2005; Nimmerjahn et al., 2005; Tremblay et al., 2012). “Activated” microglia on the other hand is classified as a shift from this more homeostatic state toward activation of a defense response triggering downstream stress signals (Deczkowska et al., 2018; Pape et al., 2019). These signals are collectively known as “disease-associated molecular patterns”(DAMPs) and “pathogen-associated molecular patterns” (PAMPs) and are recognised via pattern recognition receptors (Deczkowska et al., 2018). Such receptors expressed in microglia

include Toll-like receptors (TLRs), with for example TLR4 and TLR3 sensing components of bacterial and viral pathogens, respectively. TLR4 agonists such as LPS can and have hence been used model microglia “activation” *in vitro*, *in vivo* with rodents, as well as in healthy humans, but it is critical to understand that these studies utilise different end-points, with human *in vivo* work utilising TSPO PET, a marker which is not specific to microglia (Hoogland et al., 2015; Sandiego et al., 2015; Zhang et al., 2015; Haenseler et al., 2017). Together, these studies have inferred that microglia challenged by factors such as LPS undergo shifts in form, promoting morphological state change to be more circular, as well as in functions, including metabolic shifts towards an anaerobic profile accompanied with elevated ROS production, as well as increases in synthesis and release of cytokines and chemokine, clustering, migration, and phagocytic activity.

Expanding on classifications of microglia activation, *in vitro* studies using stimuli such as LPS have categorised the activation of microglia into “toxic” (M1) or “protective” (M2) states (Ransohoff, 2016; Paolicelli et al., 2022). Problematically however, *in vivo* studies show that microglia in rodents can express genes associated with M1 and M2 states simultaneously, leading to such classifications being challenged (Salter and Stevens, 2017; Paolicelli et al., 2022). Transcriptional profiles associated with these states are also unlikely to correspond to conditions where microglia potentially are hypersensitive to stimulation, bringing in the term “primed” microglia, which have been described in early development following environmental insults such as infection affecting the CNS during childhood or severe systemic exposure, and in ageing and age-related disorders, specifically being defined as a microglia which are more sensitive to potentially minor stimuli and respond through a heightened or in an exaggerated manner to environmental interruption compared to microglia that are “activated”(Chiu et al., 2013; Holtman et al., 2015; Niraula et al., 2017; Li et al.,

2018). These terms also do not encompass unique transcriptomic patterns observed in a variety of conditions, including the more generalised “neurodegeneration associated damage patterns’ (NAMPs) and disease-specific profiles such as “human AD microglia patterns” (HAMs) and “microglia inflamed in MS” (MiMS) (Srinivasan et al., 2020; Absinta et al., 2021; Wendimu and Hooks, 2022). The term “neuroinflammation” has also been widely used in the literature as synonym for microglia activation, however its definition varies drastically among authors including for example limiting it to conditions where there is infiltration of other immune cells to the CNS or simply calling the term too unclear and imprecise, condemning its use (Paolicelli et al., 2022). Considering the complex nature of describing microglia state an in agreement with the published consensus by Paolicelli et al. (2022) published following the initiation of thesis write-up, description of data in this thesis has been adapted to avoid categorisation of data into groups and avoiding terms such as “activation” and “neuroinflammation” which might promote misinterpretation of findings. Rather, specificity and detail are emphasised to provide a clear description of data when assessing differences in microglia genotypes and context-dependent states including when detailing overlap with previously published data.

1.1.5 Heterogeneity of microglia

Microglia heterogeneity is not limited to differences during development, ageing and their change in behaviour in response to injury, disease, or infection (Thion et al., 2018; Böttcher et al., 2019). Heterogeneous microglia populations exist within both development and adulthood whose form and function likely are dependent on genetics and local cues (Zhong et al., 2018; Hammond et al., 2019; Masuda et al., 2019; Sankowski et al., 2019; Kracht et al., 2020). Diversity of microglia populations are observed as early as mouse E18.5, a period which corresponds to female/male differentiation with the initiation of sex hormone

production (Nelson et al., 2017; Nelson & Lenz, 2017; Thion et al., 2018). Microglia acquire sexually dimorphic signatures at the transcriptomic level with differentially expressed genes (DEGs) being found primarily on the X and Y chromosomes (Thion et al., 2018). This might have implications for microglia functions as it has been suggested that female microglia might have an enhanced immune response compared to male microglia based on their transcriptomic signature in aged human *postmortem* entorhinal and somatosensory neocortical grey matter, while differences in microglia morphology, number and gene expression have been observed in the postnatal rat brain (Schwarz et al., 2012; Lenz et al., 2013; Coales et al., 2022). In the postnatal rat brain, female microglia, for example, has been observed to have higher expression of genes associated with immune response such as *IL-10* across postnatal day 0, 4 and 60, while morphological states are different to male microglia depending on postnatal development stage and brain region (Schwarz et al., 2012). Additionally, female mice has been observed to have a higher amount of phagocytic microglia in the neonatal hippocampus as well as increase proliferation compared to microglia from male mice in response to estradiol (Nelson et al., 2017). Phenotype differences also extend to response to LPS in rats *ex vivo*, with male microglia expression of IL-1 β being significantly higher in males compared to females following LPS treatment even though female microglia have higher expression of TLR4 (Loram et al., 2012). Adult female mouse microglia have been suggested to have a neuroprotective effect in an experiment where they were transferred into adult male mouse brains (Villa et al., 2018). While there remains questions regarding the corresponding intrinsic functional differences of microglia for example in terms of phagocytosis and cytokine secretion and how much these functional data is dependent on cues received by non-microglial cells during brain development, one could speculate that further work taking these data into account could help explain sex differences observed in terms of prevalence in disorders microglia are increasingly thought to

be implicated in such as schizophrenia and ASC (Werling and Geschwind, 2013; Mondelli et al., 2017; Hanger et al., 2020). Therefore, studies investigating such disorders should always ideally utilise matched sex controls when possible. However, it is important to note that all sex-dependent microglia phenotypes might not translate to humans, as Menassa and colleagues (2022), did not note sex-dependent differences in microglia development, for example in microglia densities as observed in Schwarz et al. (2012). It will also be important for the field to delineate whether these differences are observed across relevant brain regions, in which the diversity of microglia phenotypes also is extensively heterogeneous.

Across brain regions, microglia are likely more diverse in the developing brain compared to the adult brain, at least in rodents, but there is substantial evidence that this is retained, with some even supporting enhanced transcriptional heterogeneity during ageing (Hammond et al., 2019). In the adult mouse, heterogeneity has been observed throughout fore-, mid- and hindbrain regions in isolated microglia using microarray gene expression mapping (Grabert et al., 2016). A unique phenotype has also been observed in the basal ganglia at both transcriptomic and protein characterisation including diversity of lysosomal content levels across regional mouse microglia (De Biase et al., 2017). In mice, differences in morphology, region-specific densities, and in the expression of immunoregulatory proteins such as CD40 which is significantly different between the cerebellum and cerebral cortex (Lawson et al., 1990; de Haas et al., 2008). Multiplexed single-cell mass cytometry analyses, providing a deep profile of microglia phenotype at the protein level, investigating adult and aged microglia in subventricular zone, thalamus, cerebellum, temporal lobe, and frontal lobe *postmortem* tissue have also suggested that regional differences are present in humans, with distinct populations being found even though phenotypic variability have been observed between donors (Böttcher et al., 2019). For example, the subventricular zone microglia

phenotype is similar to what is found in the thalamus, and the profile in the cerebellum is distinct from other brain regions, at least of those examined in Böttcher et al., (2019). The difference observed in the cerebellum aligns with mouse data suggesting a notable replicated difference between forebrain and cerebellar microglia phenotypes (Grabert et al., 2016). It is evident that local cues play a role in defining the cerebellar and forebrain microglial phenotypes as when CSF-1, which is normally required to maintain microglia populations by stimulating the CSF-1 receptor in microglia, is knocked out in nestin-positive cells, which secrete CSF-1 such as neurons and astrocytes, it depletes microglia in the cerebellum, but not the forebrain based on mouse data (Kana et al., 2019). This is potentially due to differences in expression levels of alternate CSF-1 receptor ligand, for example IL-34 (Lin et al., 2008; Stanley and Chitu, 2014; Kana et al., 2019). Distinct microglia-related behaviour have also been reported in disease, with for example increased microglia density having been observed in hippocampal dentate gyrus subregions in human *postmortem* Alzheimer's disease samples compared to cognitively intact controls samples, age-associated hippocampal sclerosis samples, and dementia with lewy body samples (Bachstetter et al., 2015). This means that microglia behave differently potentially through either elevated proliferation or directed migration in this specific disease context. Other differences may also exist within the temporal lobe white and grey matter when comparing apparently healthy *postmortem* tissue from individuals with that from glioblastoma or epilepsy (Sankowski et al., 2019). For example, density of HLA-DR-positive cells and protein expression levels including for homeostatic microglia marker TMEM119 might be higher in white matter (Sankowski et al., 2019). In further analysis from the same study, these already noted markers alongside others also appear to be more elevated in disease based on comparison of apparently healthy white matter versus diseased white matter, at least in glioma (Sankowski et al., 2019). Distinct microglia transcriptional states has also been observed in human *postmortem* tissue between

cortical grey matter and corpus callosum white matter, including for transcriptional differences in samples from individuals with multiple sclerosis (van der Poel et al., 2019). Increasing this complexity, transcriptional profiling studies suggest that regional heterogeneity can be time- and region dependent, and even extend to grey-white matter specific profiles (Masuda et al., 2019; Sankowski et al., 2019; van der Poel et al., 2019). As reviewed in Hanger et al. (2020), while the functional significance of regional heterogeneity is unclear, it corresponds with evolutionary innate immune cell demand to flexibly be able to respond to tissue injuries or pathogens. Local cues likely play an important role in this heterogeneity at both protein and transcriptome levels (Paolicelli et al., 2022).

Even though microglia are suspected to be highly heterogeneous during development, existing human data is limited to *postmortem* studies, and this has high relevance for studying neurodevelopmental disorders (Hanger et al., 2020). Animal models have attempted to characterise these early periods, however species-related heterogeneity remains a challenge. Models using gene editing and environmental stimuli retain limitations as well, as behavioural measurements cannot always directly correlate to what is observed in humans. While a shared microglial sensome has been proposed consisting of 57 transcripts, partially supporting the use of animal models, other parts of the sensome remain unique for across species (Abels et al., 2021). Originally published in Hanger et al. (2020), **Table 1.1** highlights established species-associated differences which may have implications the study of psychiatric disorders with a putative neurodevelopmental origin.

<i>Phenotype</i>	<i>Species differences with potential relevance to studying microglia involvement in human psychiatric disorders with a putative neurodevelopmental onset</i>	<i>References</i>
Microglia turnover and maintenance	<ul style="list-style-type: none"> • Rates of turnover for rodent microglia vary from 0.05% to 0.7% depending on the method used • Human microglia may be longer lived with slower turnover relative to the lifespan of the host species although chimeric model data suggest fast turnover and proliferation of human microglia in the neonatal rodent brain 	Lawson et al. (1992) Askew et al. (2017) Réu et al. (2017)
Microglia gene expression signature (homeostatic state)	<ul style="list-style-type: none"> • While 57 genes potentially are conserved between human and mouse microglia sensome, as low as 53% (477 of 900) of genes highly specific to mouse microglia may be expressed at a comparable level human microglia • Rodent microglia show regional and time dependent heterogeneity, which is maximal during development, but so far only a partial overlap has been reported with human microglia • With age, less overlap is seen between mouse and human microglia, highlighting the importance for studies at the developmental stage • Some innate immune system genes, such as <i>CD58</i>, <i>ERAP2</i>, <i>GNLY</i>, <i>MPZL1</i>, <i>S100A12</i>, <i>SORL1</i>, and <i>POC1</i> are only expressed in human microglia. 	Grabert et al. (2016) Galatro et al. (2017) Gosselin et al. (2017) Dubbelaar et al. (2018) Hammond et al. (2019) Masuda et al. (2019) Abels et al. (2021)
Microglia response to stimulation (IFN- γ /LPS) <i>in vitro</i>	<ul style="list-style-type: none"> • Rodent microglia become more rounded/amoeboid, retract processes, and increase TSPO and iNOS/Arginase1 expression • Human microglia in extend processes and become bipolar, decrease TSPO expression without change in iNOS/Arginase1 	Nakamura et al. (1999) Owen et al. (2017)

Table 1. 1: Overview of species differences between human and mouse microglia of potential relevance to studying microglia contribution to pathophysiology of psychiatric disorders with a putative neurodevelopmental origin. Updated from published version in Hanger et al. (2020).

1.2 Role of microglia in the pathophysiology of psychiatric disorders with a putative neurodevelopmental origin

1.2.1 Autism spectrum conditions

ASCs are a clinically heterogeneous group of neurodevelopmental disorders encompassing diagnoses such as autism, Asperger's Syndrome, and pervasive developmental disorder-not otherwise specified (PDD-NOS) (Sharma et al., 2018). Behavioural symptoms described in the core DSM-5 criteria for ASC diagnosis includes social communication deficits, stereotype, and often intellectual disability, but heterogeneous presentations (APA, 2013; Lord et al., 2020). The global estimate of ASC prevalence is 0.6% following a meta-analysis, but in countries such as the U.S., estimated prevalence has been suggested to be as high as 1 in 36 children, perhaps owing to differences support for diagnoses worldwide (Zablotsky et al., 2017; Salari et al., 2022). The global burden of ASCs continues to increase, and with increased knowledge of the disorders, a sex difference with 4 times higher prevalence in males has also shrunk with more females becoming diagnosed (Werling and Geschwind, 2013; Li et al., 2022). Except some use of antipsychotics to treat irritability and/or aggression and repetitive behaviours, the primary interventions for ASC are psychosocial therapies (D'Alò et al., 2021; Gosling et al., 2022). Complicating diagnoses in the first place is also the lack of validated biomarkers, a field which is currently in the early stages (Jensen et al., 2022). Biomarker methods investigating autoantibody and cytokine dysregulation are notable based on aberrant immune system phenotypes in the disorders. However, biomarker-driven diagnoses will be complicated by the high prevalence of comorbidities observed in ASC, with nearly 75% of individuals suffering from one or more additional psychiatric illnesses

(Sharma et al., 2018), which may include schizophrenia as approximately 34.8% of individuals with ASC experience psychosis (Ribolsi et al., 2022)..

1.2.2 Schizophrenia

Schizophrenia is a chronic, complex, often debilitating, and relapsing mental disorder with symptoms that manifest as a combination of positive, negative, positive, and/or cognitive features (Kahn et al., 2015; Correll et al., 2022). Negative symptoms reflect reduction or absence of normal functions associated with interest and motivation, or expression, including behaviours such as asociality, avolition, anhedonia, and alogia. Positive symptoms refer to a distortion of or surplus unwanted normal functions such as hallucinations, delusions, and disorganised behaviour. When cognitive deficits occur, they are sometimes detectable even before the emergence of positive symptoms, with these including reduced working memory, executive functioning, processing speed, superimposed severe deficits in declarative verbal memory, although there is no clear neuropsychological signature of these in schizophrenia (Bowie and Harvey, 2006). Global estimates of schizophrenia are 0.28% without sex difference following a systematic review, however sex differences have been found in symptomology and onset, with earlier age of onset in males along with more negative symptoms, while female experience may experience more affective symptoms but often experiencing a reduced disease burden compared to males (Charlson et al., 2018; Gogos et al., 2019; Giordano et al., 2021). Lifelong treatment with antipsychotics is often required to adequately control positive symptoms such as psychosis, however, severe metabolic and neurological side effects can accompany their use, with also a portion of individuals with schizophrenia having treatment resistance to antipsychotics, increasing the treatment difficulty (Patel et al., 2014; Haddad and Correll, 2018; Stepnicki et al., 2018; Potkin et al., 2020). Neuroimaging strategies are perhaps the most promising biomarker candidate method

in development for schizophrenia investigating options such as immune dysregulation and dysconnectivity, however, like ASC, no there is currently clear option that is currently viable for individuals with suspected diagnosis (García-Gutiérrez et al., 2020; Kraguljac et al., 2021). Comorbidities of schizophrenia without or alongside ASC may often include other psychiatric disorders such as anxiety disorders, obsessive-compulsive disorders, depression, panic disorder, or posttraumatic stress disorders (Buckley et al., 2009), as well as metabolic disorders including dyslipidemia, hypertension, type 2 diabetes, and obesity (Jacob & Chowdhury, 2008).

1.2.3 Aetiology of schizophrenia and ASC

The exact causes of both schizophrenia and ASC remain elusive, but it is clear both disorders are highly heritable, although their genetic risk architecture reflects their clinical presentation. In ASC, less than 1% of cases have been linked to single gene mutation, some being more high confidence than others, while a notable fraction has been linked to polygenic risk (Grove et al., 2019). Likewise, single nucleotide polymorphisms (SNPs) in at least 145 independent loci contribute to polygenic risk in schizophrenia, with perhaps the strongest single gene associations being *SETD1A* and *C4A* which are expressed in microglia with animal models having demonstrated alterations in connectivity-related phenotypes associated with the disorder (Singh et al., 2016; Mukai et al., 2019; Weinberger, 2019; Yilmaz et al., 2021). Among high confidence genetic risk factors for schizophrenia as well as ASC beyond single gene mutations such as *NRXN1*, some highly penetrant CNVs in some are also associated with increased risk for both disorders (gene.sfari.org) (Bassett and Chow, 2008; Kirov et al., 2009; Uchino and Waga, 2013; Onay et al., 2016; Flaherty et al., 2019). In fact, the strongest known single genetic risk factor for schizophrenia is deletions in the 22q11.2 genomic region, often just referred to as 22q11.2 deletion syndrome (DiGeorge Syndrome, 22q11.2DS),

which bears 20- to 25-fold increased risk for schizophrenia, with an estimated 1% of individuals with schizophrenia being carriers, but there is also a high prevalence of 22q11.2DS in people with ASC, with this number being between 0.3% and 1% (Shprintzen et al., 1992; Murphy et al., 1999; Vorstman et al., 2006; Bassett and Chow, 2008; Bassett et al., 2010; Karayiorgou et al., 2010; Levinson et al., 2011; McDonald-McGinn et al., 2015; Fiksinski et al., 2017; Ousley et al., 2017; Karbarz, 2020; McDonald-McGinn et al., 2020). It is however also notable that other psychiatric disorders such as bipolar disorders and attention deficit hyperactivity disorder (ADHD) has been associated with 22q11.2DS (Niarchou et al., 2018), hence human studies should consider individual diagnoses when investigating this genetic risk factor.

In addition to genetic factors, the environment also modulates risk for both ASC and schizophrenia (Modabbernia et al., 2017; Bölte et al., 2019; Stilo and Murray, 2019). Environmental precedes the disorders and can mediate the causal chain between genetic susceptibility and appearance of symptoms. The environment factors can be biological, including physical, chemical, viral, and bacterial influences, and psychosocial which denotes environments primarily acting on mental functions and secondarily on physiology (Bölte et al., 2019). In the context of biological environment, epidemiological, clinical, and preclinical evidence suggests that prenatal period is of particular interest for further study, suggesting that infection across all trimesters infers elevated risk for both schizophrenia and ASC (Atladóttir et al., 2010; Brown and Derkits, 2010; Lee et al., 2015). However, the relevance of the maternal infection to psychiatric disorder risk is not necessarily associated to the infection itself, with it rather having been suggested to be related to the consequently invoked immune response which is a hypothesis supported by elevated C-reactive protein, a non-specific biomarker of inflammation, and cytokine levels in pregnant women with diagnosed

offspring (Brown et al., 2014; Canetta et al., 2014; Brown and Meyer, 2018). Support for this theory of maternal immune activation (MIA) is found in animal models, including in rodents and rhesus macaques (Kaidanovich-Beilin et al., 2011; Malkova et al., 2012; Bauman et al., 2014), where maternal administration of for example poly(I:C) results in abnormal repetitive behaviours, reduced social Interaction and reduced vocalisation. Notably, one could argue that the model is more reliable for ASCs, as MIA does not induce hallucination, at least in a way that is measurable. Potentially explaining these developmental aberrancies is that MIA induces sustained changes in fetal mouse microglia motility, including increased IL-6 expression, as well as motility when induced at earlier time points (Smith et al., 2007; Ozaki et al., 2020). Based on these data, there hence appears to be evidence that microglia phenotypes are affected, and hence could be contributors to pathophysiology of these conditions. Of note, genetic risk factors have been hypothesised to confer elevated susceptibility to the development of these conditions by interacting with environmental exposure, including MIA (Brown and Meyer, 2018)

1.2.4 Immune system-associated phenotypes in ASC and schizophrenia

Most human research of microglia in the context of psychiatric disorders utilises *in vivo* neuroimaging methodology such as radioligand targeting of TSPO, which only non-specifically assesses microglia and it is possible that it only assesses density of TSPO-cells, failing to characterise microglial states in humans (Eme-Scolan and Dando, 2020; Hanger et al., 2020; Beaino et al., 2021). Alternatively, *postmortem* tissue from brain banks are used (Hanger et al., 2020). Abnormalities in the immune process in ASC have been shown *in vivo* with [¹⁸F]FEPPA and [¹¹C]PBR28 (radiotracer ligands that binds to TSPO) PET studies suggesting lower regional levels of TSPO (Zürcher et al., 2021; Simpson et al., 2022), however, high expression has also been suggested, for example using [¹¹C](R)-PK11195,

another ligand binding to TSPO, PET (Suzuki et al., 2013). Similarly, lower total distribution volume has been suggested in schizophrenia based on a meta-analysis of studies using second-generation TSPO ligands (Plavén-Sigraý et al., 2018), however, many studies have also shown either increased TSPO or no difference (De Picker and Morrens, 2020). There are several concerns regarding the method of measuring putative microgliosis, as the protein is also expressed by astrocytes and endothelial cells (Notter et al., 2018). Hence, this evidence is by no means unequivocal towards the involvement of microglia activation *in vivo*, and microglial functional state cannot be measured using PET (Mondelli et al., 2017).

Postmortem data is hence perhaps more useful. Studies on brain tissue from ASC cases has for example suggested increased microglia density, which is often associated with an immune response state (Vargas et al., 2005; Morgan et al., 2010; Edmonson et al., 2014).

Additionally, in schizophrenia, elevated serum levels and expression of IL-1 β and TNF- α have been observed, which both being linked to immune response and associations also being made to disease progression and symptom severity (Mohammadi et al., 2018; Zhu et al., 2018). Other findings include altered expression of immune response mediators such as decreased IL-1 α and IP-10, and increased IFN- α in human *postmortem* superior temporal gyrus tissue (Izumi et al., 2021), and region-dependent microglia density differences but reduced arborisation and increased soma size across human *postmortem* cingulate, frontal, and temporal cortical gray matter and subcortical white matter sections (Gober et al., 2021).

Postmortem data, however informative, is subject to limitations such as age-related changes and, in schizophrenia and some cases ASC, prolonged exposure to psychotropic medications (Hanger et al., 2020). Chronic antipsychotic exposure has for example been reported to affect microglia density and morphology in rodents (Cotel et al., 2015; Bloomfield et al., 2018), highlighting the importance of animal models in this field as these studies could not have been performed with using standard human psychiatric disorder modelling, but also

showcases how the lack of an established human *in vitro* system for psychiatric disorders limits the field as it is unclear how this would translate to humans.

Regardless of problems with current human models, animal models have described abnormal brain co abnormal brain connectivity and asocial behaviour arising from a primary deficit in microglia-neuron signalling (Zhan et al., 2014; Kim et al., 2017). Media secreted by mouse microglia deficient in MeCP2, a risk factor for both ASC and schizophrenia, impairs normal dendrite development when added to neuron primary mouse cultures, potentially through increased glutamate release (Maezawa and Jin, 2010; Chen et al., 2020). Additionally, during postnatal development, knockout of the schizophrenia risk factor C4 in mice results in abnormal synapse loss (Sekar et al., 2016). Environmental modelling has also revealed additional data suggesting increased microglia activation and concurrent synapse loss. For example, prenatal exposure of mice to CASPR2-IgG collected from clinical cases causes microglia immune response-like phenotypes and disrupts social behaviour of offspring (Coutinho et al., 2017). In MIA mice studies on microglia, transcriptomic data have shown higher expression of genes associated with immune response, and reduced expression of schizophrenia-associated cell adhesion genes, with functional data suggesting reduced phagocytic activity in hippocampal tissue slices compared to placebo-treated controls (Mattei et al., 2017; Handunnetthi et al., 2021). Collectively, these data suggest that during critical periods of brain development, gain or loss of microglia function could lead to abnormal synaptic pruning, failure to eliminate excess neurons, aberrant trophic factor secretion and higher cytokine levels, with later emergence of psychopathology.

As previously established in **Table 1.1**, there are several issues with using animal models to model psychiatric disorders. So far, the closest possible human model systems that have

attempted to investigate the contribution of microglia to these conditions are induced microglia, which are blood monocytes treated with factors making them more microglia-like in phenotype that can be harvested from diagnosed individuals and hence model both genetic and non-genetic factors of the conditions (Sellgren et al., 2017). So far, the protocol has been able to support animal data suggesting that abnormalities in the C4 complement cascade, specifically *C4A* is associated with increased phagocytic activity in induced microglia from individuals with idiopathic schizophrenia when compared to neurotypical controls (Sekar et al., 2016; Sellgren et al., 2019). Additionally, it has been found that induced microglia from a different idiopathic schizophrenia cohort has an enhanced response to LPS compared to neurotypical controls (Ormel et al., 2020). However, this model is also not perfect, as these microglia are potentially more akin to infiltrating macrophages due to not having developed through authentic yolk sac ontogeny.

1.3 Using human induced pluripotent stem cells to model ASC and schizophrenia in vitro

While knowledge surrounding the roles of microglia in health and disease is vast, there is a clear need for a flexible and reliable human *in vitro* model which can be used to study early developmental stages of psychiatric disorders. To address this challenge, the hiPSC model is proposed as a potential system. The model system has reliably generated interesting data in the study of hiPSC-derived neuronal cell types, however, no studies have been published characterising hiPSC-derived microglia in psychiatric disorders, even though modelling have extended to co-cultures with neurons to model other conditions, as the primary focus has

been neurodegeneration (Haenseler et al., 2017; Vahsen et al., 2022). It would be desirable to use this system to confirm human *in vivo*, *postmortem* and animal model findings in human microglia at a developmental stage that are generated with an authentic, yolk-sac ontogeny, as previously alluded to in the preceding section.

1.3.1 Potential of human induced pluripotent stem cells

HiPSCs represent a patient-specific approach, in which somatic cells may be reprogrammed to a pluripotent state capable of differentiating into both neural and myeloid lineages, whilst retaining the genetic make-up of the donor, which may offer one solution to this challenge (Takahashi and Yamanaka, 2006; Takahashi et al., 2007). Reversion to pluripotency is performed through delivery of transcription factors, typically the ones now known as the Yamanaka factors Oct3/4, Sox2, Klf4, c-Myc following characterisation by Takahashi and Yamanaka (2006; Takahashi et al., 2007). Alternatively, reprogramming can also be performed with the Thomson plasmid factors (*OCT4*, *SOX2*, *NANOG*, and *LIN28*) (Yu et al., 2007). Reprogramming is typically done via viral, mostly adenoviral, retroviral, and lentiviral, vectors (Hu, 2014). It is now possible to reliably generate and culture multiple hiPSC lines, at scale, from many donors (Cuomo et al., 2020) if funding allows, which may in turn be guided towards several neuronal or non-neuronal fates. Consequently, cell-specific phenotypes with direct relevance to patients can be explored. Consistent with this view, the study of neurons, glia and even organoids differentiated from hiPSC collected from syndromic ASC and schizophrenia cases have provided important new leads into the pathophysiology of the disorders (Ben-Reuven and Reiner, 2016; Kathuria et al., 2019, 2020; Ross et al., 2020; Adhya et al., 2021; Mansur et al., 2021; Bhat et al., 2022; Page et al., 2022; Reid et al., 2022). Most studies have however focused on neurons despite evidence suggesting a key role of innate immune cells, particularly microglia, in ASC and

schizophrenia pathophysiology (Gonzalez et al., 2017; Salter and Stevens, 2017; Smolders et al., 2018). Additionally, in ASC, a substantial amount of the associated high-risk genes identified are indeed expressed in microglia (**Table 1.2**). In a timely step forward, it is now possible to generate microglia from hiPSCs which faithfully replicate human microglia ontogeny during differentiation (Buchrieser et al., 2017; Haenseler et al., 2017).

ASD Category 1 risk genes and their expression profile in microglia

ADNP	ADSL	AFF2	AHDC1	ALDH5A1	ANK2	ANK3
ANKRD11	ARHGEF9	ARID1B	ARX	ASH1L	ASXL3	AP2S1
ATRX	AUTS2	BAZ2B	BCKDK	BCL11A	BRAF	BRSK2
CACNA1C	CACNA1E	CACNA2D3	CASK	CDKL5	CELF4	CHAMP1 (CAMP)
CHD2	CHD3	CHD7	CHD8	CIC*	CNOT3	CREBBP
CTCF	CTNNB1*	CUL3	CORO1A	DDX3X	DEAF1*	DHCR7
DIP2A	DLG4 (PSD95)*	DMPK	DNMT3A	DPYSL2	DSCAM	DYNC1H1
DYRK1A	EBF3	EHMT1	EIF3G	ELAVL3	EP300	FMR1
FOXG1	FOXP1	FOXP2	GABRB3	GABRB2	GFAP	GIGYF1
GIGYF2	GRIA2	GNAI1	GRIN2B	HDLBP	HECTD4	HIVEP2
HNRNPH2	HNRNPU	HRAS (HRAS1)	IQSEC2	IRF2BPL	KANSL1 (NSL1)	KATNAL2
KCNB1	KCNQ3	KDM3B	KDM5B	KDM6B	KIAA0232	KMT2A (MLL1)
KMT2C (MLL3)	KMT2E (MLL5)	KMT5B (MLL2)	LZTR1	MAGEL2	MBD5	MBOAT7
MECP2	LDB1*	LRRC4C	MED13	MED13L	MEIS2	MYT1L
MAP1A (MTAP1a)*	MKX	NAA15	NACC1	NBEA	NCKAP1	NF1
NEXMIF	NFIX*	NIPBL	NLGN2	NLGN3	NR3C2	NR4A2
NCOA1	NRXN1*	NRXN2*	NRXN3	NSD1	PACS1	PAX5
PCDH19	PHF2	PHF21A	PHF3	PHIP	POGZ*	POMGNT1*
PPP2R5D	PRR12	PHF12	PPP1R9B	PPP5C	PTCHD1	NUP155
PTEN	PTK7	PTPN11	RAI1*	RELN	RERE	RFX3
RIMS1	RORB	SCN1A	SCN2A (SCN2A1)	SATB1	SCN8A	SETBP1
SETD2	SETD5	SHANK2	SHANK3	SIN3A*	SLC6A1	SKI
SLC9A6	SMARCC2*	SON	SOX5	SPAST	SRCAP (EAF1)	STXBP1*
SYNGAP1 (RASA1)	TANC2	SRPRA	TAOK1	TBL1XR1	TBR1	TCF20*
TCF4*	TCF7L2	TLK2	TM4SF20	TEK	TM9SF4	TRAF7*
TRIM23	TRIO	TRIP12	TSC1	TSC2*	TSHZ3	UBE3A
UPF3B	VEZF1	VPS13B	UBR1	WAC*	WDFY3	ZBTB20
ZMYND8	ZNF292 (ZFP292)	ZNF462 (ZFP462)				

Not detected	Below cut-off (<0.5 FPKM)	Low (0.5-10 FPKM)	Moderate (11-1000 FPKM)	High (1000< FPKM)
--------------	------------------------------	----------------------	----------------------------	----------------------

Table 1. 2: ASC Category 1 Risk Genes and expression profile in microglia. Genes were scored and classified as Category 1 by the SFARI Gene database (gene.sfari.org). Expression level classifications were categorised as per the Expression Atlas database (Papatheodorou et al., 2020). Genes detected but classified as below cut-off are potentially not active in microglia and could be present because of phagocytosis or variation in tissue isolation procedures. Cut-offs are set based on overall read depths. In boxes with parentheses, homolog, and commonly utilised aliases such as *DLG4* (*PSD95*) and *CHAMP1* (*CAMP*) are noted. Genes annotated with an asterisk (*) have variable isoforms either fluctuating with a FPKM score more than 10 or if one or more isoforms had below cut-off values. Isoform values were checked using the Brain RNA-Seq database of the Barres lab (Zhang et al., 2014). Expression levels compared to other conditions were not compared. Abbreviations: ASC, autism spectrum condition; FPKM, Fragments Per Kilobase of transcript per Million mapped reads



HiPSC-derived microglia could be used to study both genetic and environmental factors. To model for example MIA *in vitro*, either single or combinations of specific cytokines can be applied to either mono- and co-culture neuron-microglia systems, assessing potential increases in IL-6, which has direct correlation to altered frontal cortex transcription profile in mouse offspring (Smith et al., 2007). As such, several MIA-related microglia phenotypes would be interesting to investigate using hiPSCs when modelling ASC and schizophrenia based on findings in rodent models. Microglia that are subject to MIA develop differently in a poly I:C mouse model, shifting to a more adult-like transcriptomic phenotype both before and a few weeks after birth (Matcovitch-Natan et al., 2016). RNA sequencing studies could investigate whether a similar phenotype is observed in humans. The same studies could also assess whether MIA affects downstream targets of *FMRI* (Fragile X syndrome, an ASC) and *CHD8* as seen in fetal rat brain (Lombardo et al., 2018), both being genes that are associated with ASC and notably also expressed in microglia. Hence MIA might cause the development of ASC and schizophrenia-like behaviour without genetic deficits being required.

Functionally, microglia affected by MIA could be less phagocytic likely caused by the downregulation of genes associated with phagocytosis including *CX3CR1*, which is also

linked to microglia-neuron communication (Mattei et al., 2017). In vitro model systems also naturally provide an easy method to assess uptake of a variety of cargos (Maguire et al., 2022). Elevated levels of cytokines such as TNF α positively associated with MIA in mice (Paraschivescu et al., 2020) could also be easily measured in this model. Furthermore, reduced cortical neuron dendrite node number and dendrite length has also been shown to potentially be caused by prenatal exposure to cytokines such as IL-6 and TNF α elevated in MIA in rat (Gilmore et al., 2004). This would also be interesting to investigate in hiPSC co-cultures. Taken together, MIA models provide a unique way to investigate psychiatric disorders with cell lines not even being required to be donated by a diagnosed individual, but the potential effect in genetic models must also be investigated.

As underscored by the work of Sellgren and colleagues on *C4A*, the potential of novel human *in vitro* microglia model system in determining the effect of genetic risk factors for psychiatric disorders on microglia phenotypes is clear. HiPSC studies specifically have also established that hiPSC-derived microglia can elicit an activation response following LPS and IFN γ , which can be influenced by genetic variants such as a *TREM2* missense mutation (Haenseler et al., 2017; Garcia-Reitboeck et al., 2018). Based on the potential of hiPSC-derived microglia studies, an overview of potential applications for this model in the context of psychiatric disorders are shown in **Table 1.3**. It should however be noted that monoculture systems will be the preferred starting point for most laboratories, as there is a need to ensure validity of the differentiation protocol used.

Utilising hiPSC-derived microglia to study schizophrenia and ASD by model system

Model system	Advantages (+) and disadvantages (-)	Used to investigate	Useful experiments
<p>Monoculture</p>  <p>Microglia</p>	<p>+</p> <p>Can be used to highlight microglia-specific defects</p> <p>No isolation steps required</p> <p>-</p> <p>Cannot directly study interaction with non-microglial cells</p>	<p>Intrinsic microglia form and function in an easily manipulated environment such as through immune challenge. Morphology changes, cytokine secretion, phagocytic capacity</p>	<p>Phagocytosis of isolated synaptic material</p> <p>ROS production</p> <p>Cytokine profiling</p> <p>RT-qPCR or more extensive RNA sequencing</p> <p>Chromatin state analysis</p> <p>Immunocytochemistry</p> <p>Proteomics of cells and conditioned media</p>
<p>Multi-cell culture</p>  <p>Neuron and microglia</p>	<p>+</p> <p>Addition of other relevant cells such as neurons and astrocytes can be used to form more complex environments in co- and tri-cultures</p> <p>-</p> <p>Increasing complexity of assays</p>	<p>Changes related to neuronal environment, including morphology</p> <p>Maternal immune activation</p> <p>Engulfment of synaptic material</p> <p>Synapse refinement</p> <p>Sex differences</p>	<p>Live cell imaging, phagocytosis assays and <i>in situ</i> RNA sequencing to characterise motility and synaptic refinement</p> <p>RNA sequencing following isolation or single cell sequencing</p> <p>Chromatin state analysis following isolation or single-cell chromatin state analysis</p> <p>Cytokine profiling</p> <p>Immunocytochemistry</p> <p>Proteomics of cells and conditioned media</p> <p>Uptake of synaptic material i.e. by PSD95 internalisation</p>

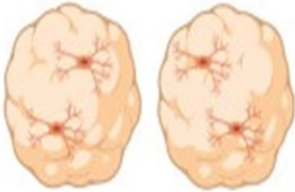

<p>Organoids</p>  <p>Cerebral organoids with microglia</p>	<p>+</p> <p>Cell-cell interaction more resemble <i>in vivo</i> systems</p> <p>Can include BBB</p> <p>Studying early developmental stages less time-consuming compared to ageing-related studies</p> <p>-</p> <p>Difficult to image even with high resolution microscopy</p>	<p>CNS-like environment-related changes</p> <p>Maternal immune activation</p> <p>Peripheral immune activation</p> <p>BBB characterisation</p> <p>Sex differences</p>	<p>Single-cell sequencing</p> <p>Single-cell chromatin state analysis</p> <p>Immunohistochemistry</p> <p>Proteomics of cells and conditioned media</p> <p>Cytokine profiling</p>
<p>Chimeric animals</p>  <p>Chimeric rodent</p>	<p>+</p> <p><i>In vivo</i> system</p> <p>Human microglia distinguishable from mouse microglia</p> <p>Possible to study behavioural correlations</p> <p>-</p> <p>Requires extensive planning and long-term investment in two previously separate models</p> <p>Requires immune-deficient recipient</p>	<p>Environment-related morphology changes</p> <p>Maternal immune activation</p> <p>Peripheral immune activation BBB characterisation</p> <p>Sex differences</p>	<p>Single-cell sequencing</p> <p>Single-cell chromatin state analysis</p> <p>Immunohistochemistry</p> <p>Proteomics of cells and conditioned media</p> <p>Assess ASD-related behavioural symptoms linking to microglia phenotype,</p> <p>Ex vivo assessment of biomarkers</p> <p>Peripheral immune activation</p>

Table 1. 3: An overview of hiPSC-derived microglia systems for psychiatric disorder modelling and their benefits, drawbacks, and potential uses. Investigating highlighted phenotypes with suggested experiments provide a starting point for future characterisation of schizophrenia and ASC pathology modelling using hiPSC-derived microglia. Immune challenge can be simulated using agents such as *IL-1 β* and *IL-6* or *LPS* through addition to media, with systemic *LPS* injection being an option for *in vivo* chimera models. Illustrations created

in BioRender.com. Abbreviations: ASC, autism spectrum condition; BBB, blood brain barrier; CNS, Central nervous system; hiPSC, human induced pluripotent stem cells; LPS, lipopolysaccharide

It is worth noting that the complexity of ASC and schizophrenia genetics means that the presence of genetic risk factors alone might not yield substantial phenotypic differences. Hence an investment in studying differential responses to immune challenge is important as it is possible that genetic and environmental risk factors interact in their contribution to pathophysiology. This is because, for example, prenatal immune stress can impact long-term transcriptional profile and chromatin state of microglia based on rodent MIA models following MIA (Hayes et al., 2022; Johnson et al., 2022). While a genetic risk variant alone being present might not be causal to symptoms, one may establish a polygenic risk score (PRS) of donated cell lines to assess polygenic risk which is usually not represented in single gene mutation studies. This can be performed at the hiPSC maintenance stage before differentiation. Accumulation of a variety of genetic variants can trigger the disorder rather than a singular high-risk gene (Manolio et al., 2009). For example, in the case of the previously discussed 22q11.2DS, each variant within this risk region is scored based on associated risk, but the risk can increase based on the presence of other variants outside this region (Manolio et al., 2009). Individuals scoring higher in clinical measures associated with ASC and schizophrenia could also be prioritised for donor selection to ensure a phenotype is observed *in vitro*, although it would be preferable to also include asymptomatic donors that score highly when studying specific genetic risk factors to investigate whether there are any protective mechanisms, which potentially could be explained by lower PRS (Reid et al., 2022). For selection of control donors, a low PRS with no history of psychiatric illness would be ideal, and in higher scale studies, cellular phenotype correlations might be made with PRS (Coleman, 2022). To further accommodate issues of genetic heterogeneity as isogenic lines

does in genetic cases, the healthy control would also ideally be a close genetic match. An ideal example would be a healthy family member such as a parent or twin if possible.

1.3.2 Protocols for the generation of hiPSC-derived microglia

As reviewed by Hanger et al. (2020), there are several differentiation protocols to obtain hiPSC-derived microglia *in vitro* that could be used to study psychiatric disorders. At the time of review, the protocols by Almeida et al. (2012), Muffat et al. (2016), Abud et al. (2017), Takata et al. (2017), Pandya et al. (2017), Haenseler et al. (2017), and McQuade et al. (2018) were assessed as to show advantages and limitations of current methods. The review also discussed the protocol established by Ormel et al. (2018), which was the first to show innate development of microglia within cerebral organoids. Since this review, new protocols as well as improvement to these protocols have been published. As a result, an extended version of the table in Hanger et al. 2020 is shown in **Table 1.4**, providing a brief overview of the protocol as well as notable findings and potential disadvantages, including organoid protocols which have demonstrated innate development of microglia, but not those that are incorporated through co-culture methods (Fagerlund et al., 2022; Sabate-Soler et al., 2022).

Article	Overview of protocol	Notable findings	Notable disadvantages
2D systems			
Almeida et al. (2012)	Not described in publication	First to produce hiPSC-microglia	Transcriptomic profile not unlike immortalised microglia cell lines (BV2) Generated through neuronal rather than myeloid pathway.
Muffat et al. (2016)	Embryoid bodies were generated and resuspended in neuroglial differentiation media containing (supplement) with the addition of CSF-1/M-CSF and IL-34	First published study with similar characteristics of fetal primary human and mouse microglia.	Appears to generate a mixed population of cells and is limited to monoculture experiments.
Abud et al. (2017)	Microglia differentiation media utilises neuronal base media DMEM/F-12 + +N2+B27 with small molecules M-CSF, IL-34, and TGF β -1. An additional maturation media is utilised consisting of CD200 and CX3CL1, which is notably secreted by neurons for the final three days.	Successful transplantation of already ramified microglia within Alzheimer's disease model mice. Subsequent in vivo evidence shows ability to interact with neurotoxic amyloid β	Requires an isolation step to begin differentiation part of haematopoiesis step, making it highly complex compared to pure single molecule methods. Not authentic yolk sac ontogeny.
McQuade et al. (2018)	Proprietary composition of initial hematopoietic differentiation media (STEMdiff hematopoietic kit) for an 11-day period followed by differentiation with IL-34, TGF- β 1 and M-CSF/CSF-1. Includes the additional maturation step with CX3CL1 (fractalkine) and CD200 to induce ramification.	Successfully ramify following transplantation in mouse brain. Suggests <i>IDE1</i> as a small molecule able to replace TGF- β in protocols utilising this for differentiation.	Describes itself as resembling developmental microglia but does not separate cited fetal vs adult datasets. Not authentic yolk sac ontogeny

Takata et al. (2017)	Generation of hematopoietic lineage macrophages terminally differentiated with SCF, IL-3 and CSF-1/M-CSF. Cells then co-cultured with mouse iPSC-derived neurons to further drive towards microglia phenotype	Described the requirement for tissue-dependent cues to make cells more microglia-like. Demonstrated potential of modelling infiltrating macrophages during adulthood.	Primary characterisation with mouse iPSCs. Not authentic yolk sac ontogeny
Pandya et al. (2017)	HiPSCs were differentiated on OP9 feeder layers with OP9 differentiation medium (ODM) to myeloid progenitors. CD34 ⁺ /CD43 ⁺ cells were sorted with MACS into myeloid progenitor media with GM-CSF and subsequently passaged and plated in astrocyte differentiation medium (ADM-IMDM base medium + GM-CSF, M-CSF, and IL-3) then CD11 ⁺ cells were further isolated. Additionally, some experiments used CD39 ⁺ microglia sorted from a specific co-culture system with astrocytes.	Utilises hematopoietic stem cells paired with astrocytes to obtain hiPSC-derived microglia. Mouse iPSC-derived cells consistent with primary neonatal microglia profile.	Gene expression data primarily from mouse iPSC-derived microglia. The human microglia model requires an isolation step. Majority of characterisation done in mouse model and the system does not utilise neuronal cells. Not authentic yolk sac ontogeny

Douvaras et al. (2017)	Initial induction with supplemented BMP4 in mTeSR custom media before later adding SCF and VEGF in StemPro-34FM media with GlutaMAX. Subsequently, supplementation is changed to SCF, IL-3, Flt3l, thrombopoietin and M-CSF. For maturation. M-CSF, Flt3l and GM-CSF were used. To establish a pure culture, CD14 or CD14 and CX3CR1 positive progenitors were isolated. Isolated cells are terminally plated in RPMI-1640 Microglia base media with GlutaMAX-I, and GM-CSF	<p>Similar to Muffat et al., 2016, established potential similarities to human primary microglia</p> <p>Highlighted importance of differentiation timing, as variable expression of TMEM119, which could be developmentally regulated, had been observed across protocols at this time</p>	<p>Unclear how base media supports replication of CNS-like conditions due to use of custom formulations</p> <p>45-60 days to generate single batch of mature hiPSC-derived microglia. Unclear how phenotypes would be different at earlier stage of differentiation as maturation starts at day 14</p> <p>Requires potentially complicated isolation step</p> <p>Not authentic yolk sac ontogeny</p>
Haenseler et al., 2017	Utilises IL-3 and M-CSF to drive myelopoiesis yielding a pure macrophage precursor population. Microglia differentiation and ramification of these cells is successfully induced using a neuronal base media (DMEM/F-12+N2 as a base media) + small molecules IL-34 and GM-CSF compared to X-VIVO which is used in the cultivation of monocytes and macrophages. The protocol utilises X-VIVO and M-CSF for the maturation to macrophages as comparison.	<p>Once set up, fully matured microglia can be generated at 2-week intervals for a 5-month period.</p> <p>Functional validation completed in a co-culture system.</p> <p>Demonstrated a MYB-independent yolk sac origin using a MYB knockout hiPSC line in previous work (Buchrieser, James and Moore, 2017),</p> <p>Protocol later been shown to be able to integrate into organoids in Sabate-Soler et al., (2022)</p>	<p>Requires a very sensitive 6–7-week period before microglia precursors can be collected.</p> <p>No assays showing functional integration into an animal model.</p>
Washer et al. (2022)	A modified improved version of the Haenseler et al. (2017) protocol. Rather than using DMEM/F-12+N2 as a base media, N2 is removed potentially due to suspected	Trialled 15 media combinations, initially removing options due to poor morphological (three) and qPCR gene expression (four) outcomes. Effective	<p>Only characterised in monoculture</p> <p>Functional assay outcomes like previously published protocol (Haenseler et al. 2017)</p>

	<p>immunosuppressive properties. In addition to IL-34 and GM-CSF being used as maturation factories in the original protocol, this protocol demonstrated potential improvements with the addition of TGF-β1 and M-CSF.</p>	<p>reagents were IL-34, TGF-β1, M-CSF, and GM-CSF, with further exclusions being due to poor microglial identify following single-cell RNA sequencing and morphology analyses.</p> <p>Overall, compared to Haenseler et al. (2017), the new protocol was demonstrated to have improved survival, with more extensive validation of microglia transcriptome status.</p>	<p>No assays showing functional integration into an animal model.</p>
<p>Banerjee et al. (2020)</p>	<p>As per Haenseler et al. (2017), but after 7 days, microglia media was supplemented with an increasing gradient (10, 20, 30, 40, 50%) of neural precursor cell-conditioned media every other day until fully differentiated, with differentiation lasting for at least 15 days rather than 14 as in Haenseler et al. (2017).</p>	<p>Significantly higher percentage of TMEM119-positive cells compared to Haenseler et al. (2017).</p> <p>Similar transcriptomic profile to Haenseler et al. (2017).</p> <p>Higher expression of the following genes compared to Haenseler et al. (2017): <i>MERTK</i>, <i>GPR34</i>, <i>CSF1R</i>, <i>CX3CR1</i>, <i>TREM2</i>, <i>TMEM119</i>, <i>SALL1</i>, and <i>SIGLEC11</i>. Significantly lower expression of <i>ITGAM</i>.</p>	<p>Yolk-sac ontogeny inferred based on using similar initial differentiation as Haenseler et al. (2017).</p> <p>Not as extensive functional analysis as Haenseler et al. (2017), but notably did demonstrate integration into rodent slices and central nervous system-patterned spheroids.</p> <p>Unclear what differences in gene expression impacts on a functional level.</p> <p>Requires ongoing hiPSC-derived neural progenitor cell cultures alongside the differentiating hiPSC-derived microglia cultures</p>

Chen et al. (2021)	<p>Adopted the established possibility of using forced expression of NGN2 to rapidly convert hiPSCs to neurons for microglia. Authors created established cell lines that were infection with FUW-rtTA and pTetO-CEBPA-T2A-SPI1-T2A-Puro causing overexpression of SPI1 and CEBPA. For differentiation, DMEM/F12+N2 and non-essential amino acids are used as a base media. Dox which promote TetO downstream gene expression is added throughout the differentiation. Initially, BMP4, bFGF, and activin-A is used, which are replaced with VEGF, SCF, and FGF2 alongside puromycin after 1 day. On the next day, media is replaced with the same base media but containing IL-34, M-CSF, and TGF-β1. Concentrations are then changed after three days with the addition of GM-CSF.</p>	<p>Typical microglia markers IBA1, TMEM119, P2RY12, PU.1, TREM2, and CD11b is observed at day 9 of differentiation</p> <p>Functional experiments could start within day 10</p> <p>No need for EB formation</p> <p>Successful coculture with NGN2 induced neurons</p>	<p>Unclear how yolk sac ontogeny is accurately replicated and how a potential lack of this would affect studies of neurodevelopment</p> <p>No assays showing functional integration into an animal model.</p>
--------------------	---	--	---

<p>Lopez-Lengowski et al. (2021)</p>	<p>Adapted protocol from Douvaras et al. (2017). Initial induction in stem cell media supplemented with BMP-4 followed by change to hematopoietic medium supplemented with SCF, FGF, and VEGF. This media is replaced with Y-27632 containing media to support survival. Floating cells are then collected and plated in hematopoietic medium supplemented with M-CSF, TPO, Flt3-L, and SCF. Floating cells are then collected again at a later stage and plated in hematopoietic media supplemented with GM-CSF, M-CSF and Flt3-L. Cell can be maintained for 25+ days at this stage if need. Floating cells can then be recollected and plated for terminal differentiation in RPMI supplemented with L-alanyl-L-glutamine dipeptide in 0.85% NaCl, GM-CSF, IL-34 and Y-27632 on LDEV-free reduced growth factor basement membrane matrix-coated plates treated with poly-L-ornithine and laminin in DPBS following by a 14-day maturation period</p>	<p>First publication to provide a fully accessible step-by-step protocol</p> <p>Step-by-step protocol additionally provides method for co-culture</p>	<p>Unclear how changes to Douvaras et al. (2017) protocol affects microglia phenotype. Only microglia phenotyping performed in monoculture is positive expression of TMEM119, P2RY12, CD11c, and IBA1 proteins alongside gene expression of CX3CR1, ITGAM, AIF1/IBA1, ITGAX, P2RY12, and TMEM119.</p> <p>Cells appears potentially functional in co-culture, but unclear what the phenotypes are in monoculture</p> <p>Unclear how different haematopoietic stem cell media will affect differentiation</p> <p>Likely similar long timeline as Douvaras et al. (2017)</p> <p>Unclear how base media supports replication of CNS-like conditions due to use of custom formulations</p> <p>Not authentic yolk sac ontogeny</p>
--------------------------------------	---	---	--

Speicher et al. (2022)	Similar to Chen et al., 2021, this is a forced expression protocol which generated cell lines overexpressing PU.1 (encoded by SPI1) and C/EBPβ (encoded by CEBPB). At the start of differentiation, DMEM/F12 base media is used supplemented with B27, N2, GlutaMAX and P/S). The following factors are used at different stages of differentiation: At day 0: BMP4, Activin A, VEGF-A, LY, CHIR, and Dox. At day 2 and 4: FGF, SCF, IL-3, M-CSF, IL-6, and doxycycline. Days 6 and 8: CSF1 and Dox. Detached floating cells are collected at day 10 and replated in PLL-coated wells washed with PBS. Maturation is then replicated similarly to Muffat et al., 2016, supplementing with IL-34, CSF1, and TGF-β, while changing media every 3-4 days until analysis between day 16-20	Successful coculture with Tau-mutant hiPSC-derived neurons Compared transcriptome with multiple established protocols and known non-hiPSC microglia datasets using both bulk and single-cell RNA sequencing technology HiPSC-derived microglia exhibited <i>in vivo</i> -like phenotypes when incorporated into 3D organoids through addition to media	Monoculture gene expression profile is similar to <i>ex vivo</i> human activated microglia Uses P/S and B27 in base media which has commonly been avoided due to potentially affecting differentiation and phenotypes Not authentic yolk sac ontogeny No assays showing functional integration into an animal model.
------------------------	--	--	---

Trudler et al. (2021)	Differentiation from hiPSCs is initiated with formation of floating EBs in low attachment plates. Erythro-myeloid lineage is promoted using a combination of VEGF, bFGF, IL6, IL3, and SCF before later exchanging bFGF with TPO. Expansion of and maturation from primitive macrophages from to microglia is performed using IL-34 and GM-CSF in a base media consisting of Iscove's Modified Dulbecco's Medium (IMDM), N2, BSA, AlbuMAX®, L-ascorbic acid 2-phosphate, and MTG	<p>Subset of EB cells display co-expression of yolk sac markers C235a , CD144, and CD41</p> <p>Transcriptome signature consistent with human microglia transcriptomes</p> <p>Successfully cultured hiPSC-derived microglia with hiPSC-derived neurons with A54T αSyn showing potential for disease modelling in multi-cell cultures</p> <p>Rapid 21-day differentiation from hiPSCs</p>	<p>Need for multiple differentiations to achieve suitable number of replicates might cause increased variability because of need for EBs throughout each differentiation and will make timelines longer. These are notably not very significant disadvantages in what seems to be a very effective protocol.</p> <p>No assays showing functional integration into an animal model.</p>
-----------------------	--	---	--

Microglia in organoids

Ormel et al. (2018)	This protocol was adapted from Lancaster and Knoblich, (2014), with the only change made in media composition being increasing the concentration of Heparin (0.1 ug/mL to 1 ug/mL).	Characterises innate development of microglia in hiPSC-derived brain organoids, which exhibit some phagocytic function as synaptic material is present within the cells.	<p>Replication of these findings is currently lacking in the literature regarding the spontaneous differentiation of microglia in the organoid</p> <p>Likely to contain unhealthy cells at later stages of development which may lead to premature activation of microglia</p>
---------------------	---	--	--

Cakir et al., (2022)	Employs a guided protocol of cortical organoids through PU.1 induction during human cortical organoid formation, reducing variability that can be caused by unguided protocols such as Ormel et al. (2018) which relies more on controlling the amount of neuroectoderm stimulation	Found that overexpression of PU.1 can induce generation of hiPSC microglia in cortical organoids	Authors noted a that distribution of microglia can still vary between each microglia-containing human cortical organoid Likely to contain unhealthy cells at later stages of development which may lead to premature activation of microglia
Gabriel et al. (2021)	Uses neurospheres to generate optic vesicle-containing organoids, deviating from the normal EB-approach to generating cortical organoids	First to characterise innate development of microglia in non-cortical CNS organoids by identified AIF1/IBA1 positive cells which are uniquely expressed in microglia within the brain	Neurosphere aggregation to generate organoids have previously been described as limited due to lack of clear organisation (Lancaster et al., 2014). It is also unclear how microglia ontogeny is recapitulated in this protocol

Table 1. 4: Overview of published protocols that generate hiPSC-derived microglia. While all these protocols can be concluded to produce microglia-like phenotypes, co-culture models that provide cues associated with a CNS environment are the most promising. It should be noted that disadvantages of some protocols are simply present due to extensive characterisation performed, and the extent to which these are present in other protocols is simply unknown. The precise protocol used however is likely to be dependent on the experimental question under investigation. Abbreviations: CNS, central nervous system; EB, embryoid body; hiPSC, human induced pluripotent stem cell.

The majority of published protocols utilise growth factors to guide hiPSCs towards a mesodermal fate to create primitive haematopoietic progenitors which are then matured using more specific growth factor cocktails. Naturally, there is debate regarding authenticity of microglial ontogeny, however, some protocols have characterised the presence of yolk sac-specific proteins or gone further using MYB knockout hiPSCs (Buchrieser et al., 2017; Trudler et al., 2021) which provides substantial support for their use. Although it is important that this is not too much a limiting factor for utilising a protocol, as it could be argued that for some studies using hiPSC-derived microglia with authentic ontogeny should be avoided. This

because a scientific question might rather be focused on the study of infiltrating macrophages upon injury.

At the start of this project, it was elected to utilise the protocol established by Haenseler et al. (2017), which then was then only protocol with well characterised developmental stages, suggesting that indeed the protocol recapitulated an authentic ontogeny. Ideally, this project would now utilise the improved version of Haenseler et al. (2017), Washer et al. (2022), especially as it excludes the potentially immunosuppressive N2 media, which previously was believed to be a necessity in inducing a CNS-like environment, but the article was published following completion of laboratory work. Other protocols now offer faster differentiation timelines, which would in some scenarios be more useful. For example, the laboratory work of this project took place during COVID-19-associated national lockdowns, and hence the longer differentiation stages of Haenseler et al (2017) proved problematic even though the protocol was robust and final yields were very lucrative. Hence it could be argued that protocols using inducible microglia (Chen et al., 2021; Speicher et al., 2022) or the one published by Trudler et al. (2021) are good alternatives for laboratories where consistent long-term presence in the laboratory is not possible.

1.4 Thesis aims and outline

There is strong evidence for the involvement of innate immune system pathways in the pathology of schizophrenia and ASC. The vast majority of *in vitro* microglia characterisation have come from animal models due to the lack of access to human primary tissue. Even with access it also remains unclear how microglia harvested from peri-lesional areas during surgical resections and subsequent analyses, or further isolation might reflect “normal” homeostatic microglia. The hiPSC system offers a human, patient specific approach to study

a diverse population of microglia in both 2D and 3D environments. The value of this model is currently clear, primarily due to limited access to fetal brain tissue (Hanger et al., 2020).

HiPSC-derived microglia has however yet to be applied to investigate the contribution of microglia to the pathophysiology of schizophrenia and ASC. It is not yet known how data from animal studies will translate to the cells with human genetic background. This includes baseline properties of microglia in studies on specific genetic variants as well as their response to immune challenge.

This thesis asks the question “Can a hiPSC with a highly penetrant risk factor be used to understand how microglia contribute to schizophrenia and ASC pathogenesis” by aiming to characterise how the highly penetrant deletions in the 22q11.2 region affects intrinsic properties of microglia by studying them in monoculture. The 22q11.2 deletion risk factor, which is further discussed in the first results chapter of this thesis (**Chapter 3**), was chosen due to being the strongest known genetic risk factor for schizophrenia while also conferring high risk towards ASC as noted as part of this chapter. As such, the objective of the thesis is to assess abnormalities in hiPSC-derived microglia-like cells that will be referred to as MGLs from individuals with a genetic background of 22q11.2DS with a diagnosis of schizophrenia and/or ASC.

This project has a general hypothesis that **22q11.2 deletion carriers will highlight microglial phenotypes that may contribute to the pathophysiology of 22q11.2DS-associated conditions, with an emphasis on psychiatric disorders schizophrenia and ASC with a putative neurodevelopmental origin.** This extends to more specific hypotheses that **22q11.2DS will affect the form and function of hiPSC-derived microglia**, and that **22q11.2DS-associated abnormalities will be present with and without LPS challenge.**

As for the project's null hypotheses, the general null hypothesis is that there will be no significant differences in microglial phenotypes between individuals with the 22q11.2 deletion and non-carriers, showing no contribution to the pathophysiology of 22q11.2DS-associated psychiatric disorders such as schizophrenia and ASC. For specific null hypotheses, The presence of the 22q11.2 deletion will not affect the form and function of hiPSC-derived microglia, with any observed differences being attributed to random variations rather than the 22q11.2 deletion status. Additionally, abnormalities associated with 22q11.2DS will not be present in hiPSC-derived microglia, regardless of whether they are subjected to LPS challenge or not, meaning any differences observed in microglial response to LPS would be independent of the 22q11.2 deletion carrier status and considered as random fluctuations.

Sex-matched control lines from donors with no known history of psychiatric disorders will be utilised. Both bioinformatics and lab-based approaches will be used to characterise these cell lines and interrogate the effect of 22q11.2DS. Bioinformatic approaches include cell line PRS calculation based on genotyping data sets and determining differential gene expression, gene ontology, and gene set enrichment through RNA sequencing. Laboratory-based methods will encompass immunocytochemistry, high-content screening, super-resolution microscopy, immune challenge assays, uptake assays, gene expression analysis, and cytokine secretion by media concentration quantification.

Chapters of this thesis will investigate the defined hypotheses as follows, with more specific hypotheses being provided within results chapters:

Chapter 2: Will describe the general materials and methods utilised this project.

Chapter 3: Will aim to set the scene for investigating microglia form and function in the context of 22q11.2DS through genotyping of hiPSCs used in this study and characterisation of the successful differentiation of hiPSCs to hiPSC-derived MGLs in monoculture.

Chapter 4: Will aim to determine the impact of CNVs that confer increased risk for the development of schizophrenia and ASC, specifically 22q11.2DS-associated CNVs, on the transcriptomic profile of MGLs in monoculture using RNA sequencing.

Chapter 5 will aim to utilise results described in Chapters 3 and 4 to identify functional assays which are relevant to study in monoculture in the context of 22q11.2DS MGLs.

Chapter 6 will aim to summarise and findings across chapters 3-5 and discuss the potential implications of the results.

Experiments performed as part of this project will be the first to investigate the potential of using hiPSCs to assess the contribution of microglia to the pathophysiology of 22q11.2DS-associated schizophrenia and ASC.

Chapter 2:

General Materials and Methods

2.1 Use of human materials and cell line information

Relevant for Chapter 3, 4 and 5

Participants were recruited and methods carried out in accordance with the ‘Patient iPSCs for Neurodevelopmental Disorders (PiNDs) study’ (REC No 13/LO/1218). Informed consent was obtained from all subjects for participation in the PiNDs study. Ethical approval for the PiNDs study was provided by the NHS Research Ethics Committee at the South London and Maudsley (SLaM) NHS R&D Office.

HiPSCs were originally derived from hair follicle keratinocytes collected and reprogrammed from n=3 individuals with a confirmed deletion CNV within the 22q11.2 region (locations later characterised in **Figure 3.1, Chapter 3**), termed 22q11.2DS lines. An n=5 individuals without this CNV and no history of psychiatric illness had also been collected and reprogrammed. 22q11.2DS donor lines were chosen based on the confirmed presence of a 22q11.2 deletion CNV and/or existing data on psychiatric evaluations part of a study now published by Rogdaki et al. (2021) using the Comprehensive Assessment of At Risk Mental States (CAARMS) questionnaire and Ki^{cer} scores. CAARMS measures sub-clinical psychotic-like symptoms to predict whether an individual meets criterion for being at clinical high risk of psychosis. Ki^{cer} scores indicated dopamine influx rate constant which was assessed by Rogdaki et al. (2021) in the whole striatum, which was chosen based on the hypothesis that dopaminergic alterations are a potential biomarker of schizophrenia and that it is more pronounced in the striatum (McCutcheon et al., 2018). Ki^{cer} parametric images were

constructed from movement-corrected brain PET images using the wavelet-based Patlak-Gjedde approach (Patlak et al., 1983). The Ki^{cer} parametric image for each donor had been normalised into Montreal Neurological Institute standard space, using the [18F]-DOPA template and donor PET summation image and statistical mapping was performed using SPM8 software and a striatal mask with criteria established in Martinez et al. (2003). For CAARMS categorisation, scores of 0 to 2 indicated asymptomatic or questionably present at most, while a score of >2 indicated symptomatic. Findings suggested that Rogdaki et al. (2021) suggested that there is a correlation between CAARMS symptom severity and Ki^{cer} scores. The control group used by Rogdaki et al. (2021) is not related to the control group of this study but were rather chosen from available stock options based a history of thorough characterisation by the Srivastava and Vernon laboratories. Out the 22q11.2DS donor lines used in this study, all but one, being 509_CXF_13, underwent this evaluation. The donors of the control cell lines used in this thesis did not undergo these assessments. Importantly, at the end stages of laboratory work, details emerged that 069_CTF_01 has a SNP in the *CHRFAM7A* gene which has been associated with altered inflammatory microglia phenotype (Ihnatovych et al., 2020). The SNP also incurs elevated schizophrenia and Alzheimer's disease (Sinkus et al., 2015). While there was no time to confirm the presence of this SNP during this project, this could impact potential variance related to this cell line.

One clone of each cell line was chosen for use throughout this thesis. As per submission guidance in Stem Cell Reports (<https://www.cell.com/stem-cell-reports/authors>), which suggests several clones be used per donor, this is not ideal. However, genotyping data was only available for one clone per 22q11.2DS donor. Expansion and quality control of additional clones was also deemed not feasible based on time and available resources. Studying rare genetic variants such as deletions in the 22q11.2 region allows for donor

numbers to be smaller, but rather than focus on increasing clone number, it was elected to increase the number of 22q11.2DS cell lines used in experiments to accommodate for phenotype heterogeneity which could be a result of differing donor clinical presentation. Lastly, at the end of the laboratory period of this project, most submitted manuscripts use a single clone per cell line without isogenic lines being used and are still published. This is importantly dependent on the novelty of the data, but the work in thesis is completely novel.

An overview of last recorded details on the hiPSC donor lines used in this project is provided in **Table 2.1**.

Donor detail overview					
Cell line	Known 22q11.2 deletion	Sex	Age	Clinical status	Psychiatric disorder family history
CTR_M3_36S	No	Male	18-30	Neurotypical	Unknown
007_CTF_10	No	Female	18-30	Neurotypical	Unknown
069_CTF_01	No	Female	47	Neurotypical	Unknown
127_CTM_03	No	Male	53	Neurotypical	Unknown
014_CTM_02	No	Male	18-30	Neurotypical	Unknown
287_SZM_01	Yes	Male	30	ASC, SCZ, mild LD	No
191_SZF_09	Yes	Female	19	Neurotypical	No
509_CXF_13	Yes	Female	17	Atypical ASC	Unknown

Table 2. 1: Overview of hiPSC donor details and clinical status. All cell lines were reprogrammed using Cytotune (Invitrogen) Neurotypical indicates no current clinical diagnosis of psychiatric illness. By known 22q11.2 deletion it is indicated that this was tested and confirmed prior to obtaining the donor lines, but the data was not available for this project and hence characterisation of genotyping data is later performed as part of this project. 069_CTF_01 and 509_CXF_13 have not been previously characterised. Characterisation of male control lines have been published by the Srivastava and Vernon labs (Cocks et al., 2014; Couch et al., 2023; Shum et al., 2020; Adhya et al., 2021; Warre-Cornish et al., 2020). 007_CTF_10 have been characterised

by the Srivastava lab (Adhya et al., 2021). 191_SZF_09 and 287_SZM_01 characterisation have been published by Vernon and Srivastava lab (Reid et al., 2022). Abbreviations: ASC, autism spectrum condition; CNV; copy number variant; LD, learning disorder; SCZ, Schizophrenia.

2.2 HiPSC expansion and maintenance

Relevant for Chapter 4, 5 and 6

A cell line bank had previously been established by the Srivastava laboratory for all cell lines. Cell line aliquots were stored in liquid nitrogen containers. Prior to thawing, a 6 well plate coated with Geltrex (A1413201, ThermoFisher) for 1 hour at 37 °/5% CO₂ as per manufacturer's instructions. HiPSC vials were then thawed in a 37° water bath. Then, content was reverse pipetted to a 15 mL falcon tube and centrifuged to remove DMSO/StemFlex (ThermoFisher, 85190/ThermoFisher, A3349401) which the hiPSC previously had been stored in. Subsequently, Geltrex-coating was reverse pipetted and discarded. Cells were then plated in 1-2 wells, 2 if a large pellet is observed, after being suspended in warm StemFlex supplemented with μ M Y27632 (LKT Labs, 129830-38-2), a dihydrochloride Rho-associated, coiled-coil containing protein kinase (ROCK) inhibitor, to support survival during thawing. The plate with cells was then stored in a hypoxic incubator at 37 °/5% CO₂ for all continued work at this stage. Media was then changed to 100% warm StemFlex the day after thawing. HiPSCs survival and proliferation rate was monitored every 1-3 days depending on stage of expansion, with 1 day monitoring equalling days after thawing or passaging, and 3 day monitoring for healthy cultures still requirement a large amount of proliferation. HiPSCs were fed with a 100% media change of StemFlex every 2 days. Upon reaching 70-80% confluency, cells were passaged with Versene (ThermoScientific, 15040-33). Warm StemFlex culture media was removed prior to the addition of 1 mL Versene. The plate, or

plates if multiple were done simultaneously, were moved back to the incubator for 5-10 minutes. Cells were then taken back to a sterile hood and gently lifted from wells using a cell lifter (Fisher Scientific, 11577692). Warm StemFlex was then added the wells so support further suspension during forward pipetting. Cells were then moved to through reverse pipetting to a 15 mL falcon tube, which was centrifuged to create a pellet of cells. Media was then aspirated to remove any Versene present before resuspension in StemFlex. HiPSCs were then re-plated in a new Geltex coated 6 well plate. Media was then changed the subsequent day before repeating maintenance and expansion procedures until 70-80% confluency. One well with 70-80% confluence was passaged to up to 6 wells pending expansion needs. A large amount of time was spent establishing hiPSC banks for the Vernon laboratory for each cell line used in this study. When banking, cells were removed from wells and centrifuged as per the passaging method. Instead of resuspending in just StemFlex, it was supplemented with 10% DMSO. HiPSCs were then pipetted to a labelled eppendorf that was put in a frozen Nalgene ® Mr. Frosty freezing container (Sigma-Aldrich, C1562) and put in a -80° C freezer overnight before transportation to liquid nitrogen tanks. Cell line banks consisted of vials with cells at low passage numbers (p 10-15) to avoid genetic drift as well as being ready rapid differentiation. HiPSC lines were maintained and expanded using StemFlex on plates coated with Geltrex. When not changing media in a sterile hood, which was performed approximately every 48 hours, hiPSCs were stored in a hypoxic incubator to supports stemness (Caballano-Infantes et al., 2021; Matthiesen, Jahnke, and Knittler, 2021). A minimum of 2 passages was performed before initiation of differentiation to ensure that cells were healthy. Quality control of hiPSC lines is later described in **Section 3.3.3, Chapter 3**, including references to previous quality control performed by the Srivastava and Vernon labs.

2.3 Differentiation of hiPSCs to pMacpre factories

Relevant for Chapter 3, 4 and 5

To generate MGLs the protocol reported in Haenseler et al. (2017) was used. Protocol steps are illustrated in **Figure 2.1**. One alteration was made to this protocol, this being to exclude the use of penicillin-streptomycin across our differentiation. Antibiotics are commonly used to avoid microbial contamination in culture, these compounds can affect cell biochemistry and hence impact cell biochemistry (Llobet et al., 2015; Ryu et al., 2017). While not peer-reviewed, pilot data from Zhao and colleagues (2020) have also indicated that penicillin-streptomycin can influence macrophages morphology and ability to respond to extracellular matrix change. Hence it was decided to rely purely on aseptic techniques in the tissue culture room and hood.

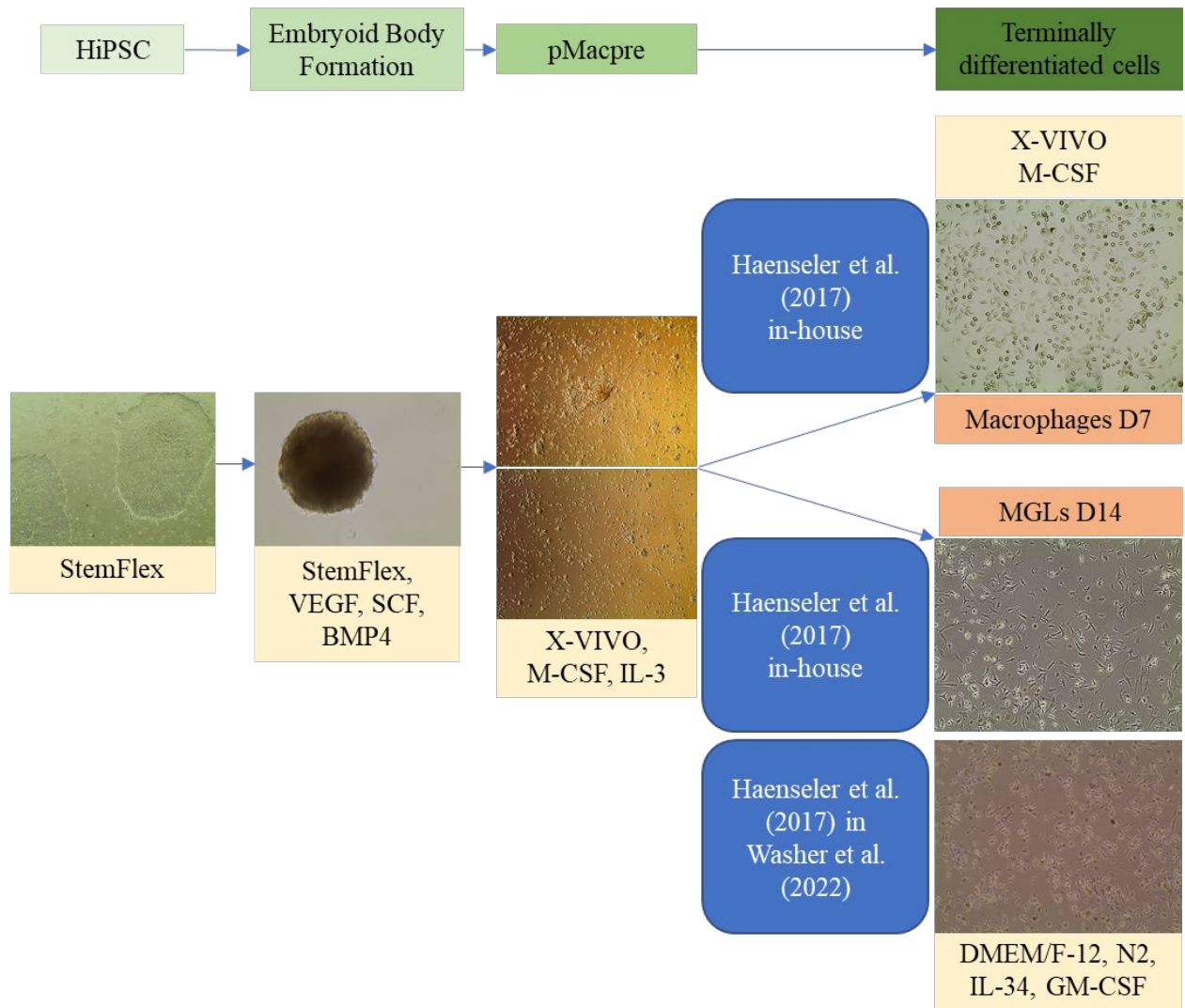


Figure 2. 1: Overview of MGL differentiation protocol. As described in more detail in the main text; at the embryoid body stage (picture from day 3), media was changed every day. At the pMacpre stage (pictures from week 4), media was added every week for 4-6 weeks. Media was replaced following collection and plating of pMacpres. For terminal differentiation, media was changed every 3 days (pictures from day 7 macrophages and day 14 MGLs). Abbreviations: D, day; hiPSC, human induced pluripotent stem cell; MGL, microglia-like cell; pMacpre, macrophage precursors.

On day 0, embryoid bodies was formed by passaging hiPSC at a passage number between 15-20 onto Nunclon Delta Surface low adherence round bottom 96-well plates in a medium consisting of StemFlex supplemented with BMP4 (50 ng/mL, ThermoFisher, PHC9534), VEGF (50 ng/mL, 100-20) and SCF (20 ng/mL, 130-094-303). Daily 75 % medium changes

were repeated for 3 days. On day 4, embryoid bodies were gently pipetted up and strained through a 40 μ M cell strainer inverted over a 50 mL centrifuge tube with a 1000 μ L, which is large enough not to damage EBs. The remaining EBs were dislodged using forward pipetting with PBS and again picked up using reverse pipetting and strained as before. The cell strainer was rapidly moved over a new 50 mL centrifuge tube and EBs were washed off the strainer into the centrifuge tube in factory medium consisting of X-VIVO15 (1x, Lonza, BE02-060Q) medium supplemented with GlutaMax (1:100, ThermoFisher, 10565018), β -mercaptoethanol (1:1000, SigmaAldrich, CAS 60-24-2), M-CSF (100 ng/mL, ThermoFisher, PHC9501), and IL-3 (25 ng/mL, ThermoFisher, PHC0035). EBs were then transported via pipetting with a 1000 μ L to a T175 Nunc EasyFlask and differentiated in the factory medium, which was added weekly for a minimum of 4-6 weeks. Once differentiated, for example at week 5, macrophage precursors were harvested (term used for collection from and plating of pMacpre weekly for experiments. The first harvest was discarded to minimise transfer of potential dead cells to terminal differentiation conditions. Harvests were performed until week 14 during which factories were taken down, as qualitative observation suggested that minor phenotype changes in such as reduced yield began arising. This was based on in-house experience of yields reducing, and conversations with other laboratories using the protocol.

2.4 Differentiation of microglia-like cells and macrophages from macrophage precursors

Relevant for Chapter 3, 4 and 5

To differentiate pMacpres to MGLs, macrophage precursors collected from factories were strained through a 40 μ M cell strainer in a 50 mL centrifuge tube. Clumps in the strainer were discarded and precursors in the tube were centrifuged down at 400 g for 5 minutes. Pellets

were resuspended in MGL differentiation medium consisting of DMEM/F12 (SigmaAldrich, D6421) supplemented with N2 (1x, Gibco, 17502048), GlutaMax (1mM, ThermoFisher, 35050061), IL-34 (100 ng/mL, ThermoFisher, 34-8684-61), GM-CSF (10 ng/mL SigmaAldrich, G-5035-5UG), and β -mercaptoethanol (50 μ M). Cells were then plated according to specific experiment designs (see individual results chapters for details) and differentiated for 14 days with 50 % medium changes being performed twice every three days. Number of cells were counted using a TC10 automated cell counter (Bio-Rad). Initial quality control of MGL differentiation is described in **Chapter 3**. Additional characterisation of MGL form and function is described further in **Chapter 3**, as well as later in **Chapter 4** and **Chapter 5**.

For differentiation to macrophages, macrophage medium was used instead of MGL medium. Macrophage medium contained XVIVO15 (1x) supplemented with 1:100 GlutaMax and M-CSF at 100 ng/mL. Differentiation length of macrophages was 7 days instead of 14. Media changes was performed as with MGLs until differentiated.

2.5 Microglia-like cell and macrophage immune challenge

Relevant for Chapter 3, 4 and 5

Experiments using Escherichia coli-derived LPS (Sigma-Aldrich, L2630. Serotype: O111:B4) on MGLs (day 14 of differentiation) were treated with either 100 ng/mL LPS diluted in sterile H₂O or vehicle (sterile H₂O) for 3 or 24 hours before sample collection unless otherwise specified. The concentration was chosen based on similar work on hiPSC-derived microglia (Garcia-Reitboeck et al., 2018). For experiments using IL-1 β (PeproTech, 200-01B), differentiated cells were treated with either 1 ng/mL IL-1 β diluted in sterile H₂O or

vehicle (sterile H₂O) for 4 hours before sample collection. Concentration and timing of this experiment was determined using pilot data that was performed earlier within the Vernon laboratory by Maneet Verdi under supervision by Dr Lucia Dutan Polit of the Srivastava laboratory. For both treatments, a high number of smaller aliquots were made up following dilution in sterile H₂O and stored in -20° Celsius. This was done to avoid repeated thawing and freezing of the reagents. Treatments were administered to cell cultures via being added as supplement to culture media as part of a full media change.

2.6 RNA extraction, cDNA synthesis and RT-qPCR

Relevant for Chapter 3 and 4

Differentiated cells, day 14 for MGLs and day 7 for macrophages, were first collected after aspiration of media in TRI Reagent™ Solution (Invitrogen; AM9738) and stored at -80°C until RNA extraction. RNA was isolated from each sample by centrifugation at 12000 g for 5 minutes with 200 µl of 100 % Chloroform. The top aqueous layer was placed in a new 1.5ml tube with a 1:1 100 % isopropanol to sample amount ratio. Samples were mixed x15 and incubated 15 minutes at room temperature. After incubation, the RNA was precipitated by centrifugation at 12000 g for 15 minutes. The supernatant was removed, and the pellet was suspended in 1 ml of 75 % ethanol followed by centrifugation 12000 g, for 5 minutes. The ethanol was removed, and the pellet was air dried for 15 minutes at room temperature. Further precipitation of RNA by 0.3 M Sodium-acetate and 100 % ethanol overnight was performed to further clean samples before resuspension in RNaseq-free water. Nucleic acid content and quality was measured using NanoDrop™ One. Reverse transcription of RNA to complementary DNA was then conducted using commercial reagents according to the manufacturer's instruction (SuperScript™ III Reverse Transcriptase Invitrogen 18080093 and 40 U RNaseOUT Invitrogen 10777019). Quantitative PCRs (qPCRs) were performed using

Forget-Me-Not™ EvaGreen® qPCR Master Mix (Biotium; 31041-1) with the QuantStudio 7 Flex Real-Time PCR System (ThermoFisher). Cycling parameters were as follows: Initial denaturation at 95°C for one cycle of 10 minutes, denaturation, annealing, and extension were then performed at 95°C, 60°C and 72°C for 15, 30, and 30 seconds respectively for forty cycles. Normalisation of data was done by normalising cycle threshold (Ct) data to an average of GAPDH and RPL13 housekeeper expression Ct values. Housekeeper genes are often used as internal controls during gene expression experiments due to being cellular maintenance genes which regulate basic cellular functions and typically have stable expression in RT-qPCR reactions (Suzuki, Higgins, and Crawford, 2000; Nygard et al., 2007). Yet, it is ideal to characterise prior to each experiment as their expression can vary depending on the condition such as under LPS challenge (Tanaka et al., 2017). As objective assessment of housekeepers across conditions were not performed, cT values are provided for each condition to show consistency across conditions. Primers used for qPCR can be found in **Table 2.2**. All primers were diluted from 100 µM stock to 2 µM working solutions in RNase- and DNase-free H₂O immediately prior to use in any experiments.

Primers used for RT-qPCR		
Gene	Forward primer sequence: (5' to 3')	Reverse primer sequence: (5' to 3')
<i>CIQA</i>	GTGACACATGCTCTAAGAAG	GACTCTTAAGCACTGGATTG
<i>GAS6</i>	CGAAGAACTCAAGAAGCAG	AGACCTTGATCTCCATTAGG
<i>GPR34</i>	GAAGACAATGAGAAGTCATACC	TGTTGCTGAGAAGTTTTGTG
<i>PROS1</i>	AAAGATGTGGATGAATGCTC	TCACATTCAAATCTCCTGG
<i>MERTK</i>	AGGACTTCCTCACTTTACTAAG	TGAACCCAGAAAATGTTGAC
<i>P2RY12</i>	AAGAGCACTCAAGACTTTAC	GGGTTTGAATGTATCCAGTAAG
<i>TMEM119</i>	AGTCCTGTACGCCAAGGAAC	GCAGCAACAGAAGGATGAGG
<i>TREM2</i>	TCTGAGAGCTTCGAGGATGC	GGGGATTTCCTTCAAGA
<i>CD163</i>	CGGAAATGAACTTCTCTTTGG	CACTTCAACACGTCCAGAACA
<i>IL-6</i>	TGGAGATGTCTGAGGCTCATT	GCGCTTGTGGAGAAGGAGT
<i>IL-10</i>	ACCTGCCTAACATGCTTCGAG	CCAGCTGATCCTTCATTTGAAAG
<i>TSPO</i>	CTACTCAGCCATGGGGTACG	CAGCTGCCCAGTGTAGAGG
<i>GAPDH</i>	GCTGAGAACGGGAAGCTTGT	ACGTACTCAGCGCCAGCAT
<i>RPL13</i>	CCCGTCCGGAACGTCTATAA	CTAGCGAAGGCTTTGAAATTCTTC

Table 2. 2: Overview of primers utilised. The following primer designs were replicated from the Haenseler et al. (2017) publication describing these MGLs: *PROS1*, *GAS6*, *CIQA*, *GPR34*, *MERTK*, *TMEM119*, *TREM2*, *P2RY12*. Other primers were designed using Genome Browser™ UCSC software (Genome Reference Consortium Human GRCh38.p14, <https://genome.ucsc.edu>, patch release 14) the Primer3Plus™ online tool version 3.0.0 (<https://www.primer3plus.com/index.html>). *CD163*, *TSPO* and *GAPDH* were previously designed by Maneet Verdi under supervision by Dr Lucia Dutan Polit before the initiation of this project. *IL-6*, *IL-10* and *RPL13* primers were designed by me and Kelly O'Toole with support from Dr Lucia Dutan Polit during the initiation of this project. Primers designed in-house aimed for an amplicon size of 80-150. Melting temperatures were not checked for in-house designed primers. Abbreviation: RT-qPCR, real time quantitative polymerase chain reaction.

2.7 Experiment design

Relevant for Chapter 3, 4 and 5

Design of experiments varied depending on the goal of experiments and is detailed further in individual chapters. One biological replicate was defined as one fully differentiated harvest, with separate wells plated within a harvest being defined as technical replicates. To account for variability, three biological replicates were used for each cell line in experiments evaluated for statistical significance. The only exceptions of are PRS in **Chapter 3**, and RNA sequencing in **Chapter 4**. One well of highly confluent (70-80% of well) hiPSCs were collected for the PRS experiment. One fully biological replicate per line was used for the RNA sequencing experiment. Ideally, multiple differentiated harvests would be used and PRS results were viewed as qualitative as a result. The reliability of RNA sequencing analysis however justifies this approach to conserve resources without need for additional validation (Griffith et al., 2010; Shi and He, 2014; Wu et al., 2014). Of note, we previously identified that greatest source of variability is likely to be individual differences between symptomatic donors rather than replicates (Bhat et al., 2022), highlighting the importance of prioritising including as many 22q11.2DS cell lines as possible rather than adding replicates. This approach with transcriptomic analyses was also used in the original publication of the protocol used in Haenseler et al. (2017). Number of harvests from a factory for each experiment were tracked and matched across cell lines, when possible, to minimise variability, as has been done in other publications using the protocol (Hall-Roberts et al., 2020). It was elected to take this approach of harvest matching to avoid potential issues as have been seen by using high and low passage numbers of hiPSCs for differentiation. It would also support future work trying to replicate the data if potential phenotype differences exist as it potentially does beyond the harvest at week 14.

2.8 Statistical analysis and data visualisation

Relevant for Chapter 3, 4 and 6

Statistical analyses were primarily performed in GraphPad Prism 9.3 for Windows 11 (GraphPad Software, La Jolla California USA, <https://www.graphpad.com/scientific-software/prism>) except for RNAseq analyses. RNAseq analyses (**Chapter 4**) were carried out using the research computing facility at King's College London, Rosalind, and R version 4.0.2 (R Core Team, 2020). were considered significant if p was lower than 0.05 ($p < 0.05$) other than in RNAseq analyses in which multiple thresholds were tested as described in **Section 4.2, Chapter 4**. When using more than one biological replicate per cell line, the mean of all biological replicates was calculated and used during statistical analysis. After checking data for normal distribution, unpaired two-tailed parametric t -test was the primary test used unless otherwise specified. Significant p values were indicated at follows: * = $p < 0.05$, ** = $p < 0.01$, *** = $p < 0.001$, **** = $p < 0.0001$. Error bars represent standard deviations of the mean unless stated otherwise.

All data visualisations except for data in **Chapter 4** were generated in GraphPad Prism 9.3 for Windows 11 (GraphPad Software, La Jolla California USA, <https://www.graphpad.com/scientific-software/prism/>). All data analysed in **Chapter 3** and **Chapter 5** are shown with the mean of each cell line and with biological replicates illustrating variability within each cell line unless otherwise specified. Figures in **Chapter 4** were visualised in R version 4.0.2 (R Core Team, 2020) or extracted from WebGestalt (WEB-based GENE SeT AnaLysis Toolkit) following data input (Liao et al., 2019).

Chapter 3:

Characterisation of 22q11.2 copy number variants and generation of hiPSC microglia-like cells

3.1 Introduction

3.1.1 Using hiPSC-derived microglia-like cells to assess microglia contribution to pathophysiology of psychiatric disorders with putative neurodevelopmental origin

There is increasing evidence that implicates microglia in the pathophysiology of psychiatric disorders with a neurodevelopmental origin such as schizophrenia and ASC (Hanger et al., 2020). This argument is based on the critical role of microglia in synapse formation and elimination during brain development and their potential relationship with immune system dysregulation observed across genome, *postmortem*, and *in vivo* studies on psychiatric disorders (Paolicelli et al., 2011; Lim et al., 2013; Corvin and Morris, 2014; Gupta et al., 2014; Miyamoto et al., 2016; Lee et al., 2017; Mondelli et al., 2017; Sellgren et al., 2019; Marques et al., 2019; Smigielski et al., 2020; De Picker et al., 2021; Williams et al., 2022). As reviewed in **Section 1.2.4, Chapter 1**, findings that have supported potential microglia involvement in psychiatric disorders have been driven by human *in vivo* work. *Postmortem* studies primarily driving association with specific cell types in humans due to non-specificity of the classic neuroimaging marker TSPO in PET imaging which also binds to other cells such astrocytes (Lavis et al., 2012). *In vitro* and *in vivo* animal models have supported the microglia-focused hypothesis, characterising both genetic and environmental factors of schizophrenia and ASC (**Section 1.2.4, Chapter 1**). As reviewed in **Section 1.1.5, Chapter**

1, species-related microglia heterogeneity is evident, so translational possibility of the data cannot be guaranteed. As human- focused studies have been limited to *in vivo* neuroimaging and *in vitro* postmortem tissue, neurodevelopmental stages are also understudied (Hanger et al., 2020). This is because legislations restrict *in vitro* human embryo research to a maximum period of 14 days from fertilisation or equivalent stage of development. With gastrulation not occurring until between weeks 2-3 of human development, the stage at which three-layered organism features are defined, direct study of further developed cells *in vitro* associated with mesoderm-, ectoderm- and endoderm-specific lineages cannot be performed (Ghimire et al., 2021). Hence, we must look to other methods to study human microglia *in vitro* at the neurodevelopmental stages. The characterisation of hiPSCs published in 2007 put researchers a step closer (Takahashi and Yamanaka, 2006; Takahashi et al., 2007), allowing the beginning of differentiation studies on CNS cells by using knowledge on developmental cues obtained from animal models. Several protocols have now emerged that reliably derives microglia-like cells from hiPSCs, and an overview of these was provided in **Section 1.3.2, Chapter 1**.

The protocol published by Haenseler and colleagues (2017) was the first to characterise hiPSC-derived microglia with *MYB*-independent, *RUNX1*- and *PU.1*-dependent lineage (Karlsson et al., 2008; van Wilgenburg et al., 2013; Vanhee et al., 2015; Buchrieser et al., 2017). *MYB*-independent development is a highly relevant trait for a microglia-like model system to have it has been described to be characteristic of microglia and macrophages (Schulz et al., 2012). Similarly, *PU.1* and *RUNX1* have been described to play a role in microglia fate determination, proliferation, and regulation of inflammatory state (Ginhoux et al., 2010; Zusso et al., 2012; Kierdorf and Prinz, 2013; Kierdorf et al., 2013; Deng et al., 2020; Pimenova et al., 2020). Using embryoid bodies to mimic yolk sac formation,

macrophage precursors can reliably be harvested weekly following 5 weeks of differentiation and further pushed towards a microglia-like phenotype. The timing of this characterisation presented an ideal system for this project to study hiPSC-derived microglia with rigorous experimental design when compared to other protocols available at project initiation (**Section 1.3.2, Chapter 1**). It also presents an ideal model for diseases with suspected neurodevelopmental origin as the differentiated phenotype, when co-cultured with neurons, was suggested to align most closely to fetal-stage microglia at the transcriptomic level (Haenseler et al., 2017). The impact of the neuronal presence during differentiation should importantly be considered, but critically, the expression levels of key homeostatic genes in fetal microglia samples such as *TMEM119* and *CIQA* did most resemble monocultured MGLs (Haenseler et al., 2017). Fetal microglia samples also closely clustered with monocultured MGLs in principal component analysis (PCA) (Haenseler et al., 2017).

3.1.2 22q11.2 deletions – a highly penetrant risk factor for schizophrenia and ASC

Both ASC and schizophrenia whose pathogenesis is thought to occur during neurodevelopment are highly heritable, having complex polygenic architecture (Smeland et al., 2019, 2020; Antaki et al., 2022; Schendel et al., 2022). To support study of these psychiatric disorders, highly penetrant variants associated with increased risk of both disorders exist. One such risk factor is one or more sizeable deletions at 22q11.2DS. CNVs found in 22q11.2DS are the most impactful genetic risk factors for schizophrenia identified (Marshall et al., 2017), inferring 20- to 25-fold increase in risk for schizophrenia (Shprintzen et al., 1992; Murphy et al., 1999; Vorstman et al., 2006; Bassett and Chow, 2008; Karayiorgou et al., 2010; Schneider et al., 2014). Up to 1 % of individuals with schizophrenia in the general population are estimated to be carriers (Bassett and Chow, 2008; McDonald-McGinn et al., 2015). Rate of 22q11.2DS CNV associated risk for ASC is highly varied

across studies, suggesting 14-50 % of carriers develop an ASC, with estimations proposed to be dependent on diagnostic criteria which can be variable (Angkustsiri et al., 2014; Ousley et al., 2017b; Schneider et al., 2014; Wenger et al., 2016). Individuals with 22q11.2DS and ASC are not at elevated risk of developing schizophrenia (Vorstman et al., 2013). In fact, it is possible other parts of the genetic background in 22q11.2 deletion carriers, such as presence of other risk variants or higher accumulated polygenic risk towards one disorder might act as risk modifiers driving development of one disorder over the other (Bassett et al., 2017; Bergen et al., 2019; Davies et al., 2020; Nehme et al., 2022; Lin et al., 2023) . The high risk associated risk with schizophrenia and ASC however makes 22q11.2DS appealing to study.

To get a diagnosis of 22q11.2DS the individual must have one or a variation of deletions within the critical region. The region includes low copy repeats (LCRs) throughout the region which may result in breakpoints for deletions which help categorise the 22q11.2DS-associated deletion. The most common deletion spans LCR-A to LCR-D at genomic location chr22:18,912,231-21,465,672 , which is found in 85% of individuals with 22q11.2DS (McDonald-McGinn et al., 2020). However, 15% of individuals with 22q11.2DS have smaller nested deletions, which span LCR-A to LCR-B, LCR-A to LCR-C, LCR-B to LCR-C, or LCR-C to LCR-D (later illustrated in **Figure 3.1**). The fact that a diagnosis of 22q11.2DS can refer to either classic or nested deletions variations is relevant as it has been proposed that different regions within the classic 22q11.2 deletion contribute differently to disease risk (Clements et al., 2017; McDonald-McGinn et al., 2020). The presence of a deletion in the nested LCR-A to LCR-B region has been suggested to infer elevated risk for ASC compared to those without this region being affected (Clements et al., 2017). It is hence important to accurately confirm deletion information of donors when working on 22q11.2DS.

3.1.3 Why is microglia a relevant cell type to model the effect of 22q11.2 deletions?

22q11.2DS has previously only been studied *in vitro* using animal, human *postmortem*, and hiPSC-derived neuronal and blood-brain barrier models (Kiehl et al., 2009; Napoli et al., 2015; Wang et al., 2017; Gokhale et al., 2019; Li et al., 2019; Crockett et al., 2021; Rogdaki et al., 2021; Nehme et al., 2022). Several hiPSC models have found significant effects of deletions in neuronal and blood-brain barrier systems (Zhao et al., 2015; Toyoshima et al., 2016; Li et al., 2019; Khan et al., 2020; Arioka et al., 2021; Crockett et al., 2021; Li et al., 2021; Reid et al., 2022; Nehme et al., 2022; Li et al., 2023). While no models have used microglia, several published findings have notable relevance to microglia. First, deficiencies in energy metabolism mechanisms glycolysis and oxidative phosphorylation, which have been observed in neurons, are also utilised by microglia and is important to modulate their response to immune challenge (Li et al., 2019; Lauro and Limatola, 2020). Secondly, changes in dopamine metabolism in neuronal cells and potential release could affect dopamine-associated cross-talk with microglia, modulating immune response (Vidal and Pacheco, 2020; Pike et al., 2022; Reid et al., 2022). Thirdly, dysregulation akin to an immune challenged environment was observed in a blood brain barrier and was linked to astrocytes, but the role of microglia in this context was not studied (Crockett et al., 2021). This is despite the potential contribution of microglia to psychiatric disorder pathophysiology including for both schizophrenia and ASC (Pardo et al., 2005; Rodriguez and Kern, 2011; Edmonson et al., 2016; van Rees et al., 2018). Other data from a 22q11.2DS transcriptomic profiling study on blood samples by Lin et al. (2021) have also of relevance indicated that down-regulated genes within deleted regions in 22q11.2DS in carriers are associated with immune and inflammatory processes, including in macrophages which share a similar ontogeny to microglia. Lin et al (2021), in a transcriptomic profiling study using whole blood samples from 22q11.2DS carriers, also identified significantly higher proportions in what was termed

M1 activated macrophages, although which exact markers this was based on is unclear.

While this aligns with changes in inflammatory markers that has been observed in blood samples from individuals with 22q11.2DS (Aresvik et al., 2016; Mekori-Domachevsky et al., 2017; Grinde et al., 2020), it is unclear how it translates to microglia. Genomics approaches have also identified a link between 22q11.2 deletions and synaptic pathways, which speculatively could affect normal microglia interaction with synapses (Wu et al., 2015; Forsyth et al., 2020). Modelling using mice have further supported synaptic abnormalities, specifically in synaptic plasticity (Devaraju et al., 2017).

Based on *postmortem* data one could speculate that microglia in a pro-inflammatory state may be a causative phenotype with the cells being in a pro-inflammatory state from the time they reach a functional state (Gober et al., 2021), but it is unclear whether they have been in this state through the individuals lifespan. Hence a developmental model is necessary. They might also however, rather than being causative to the disorder, already be responding to a diseased brain, but this is unknown (Hanger et al., 2020). It is also possible that when at risk microglia are exposed to environmental immune challenges as seen in MIA models (Fernández de Cossío et al., 2017), possibly resulting in epigenetic modification causing the microglia to have more difficulty in returning to a normal regulatory, or resting, states (Dunaevsky and Bergdolt, 2019). The evidence for microglia involvement in MIA is however mixed, and more data alongside consistent methodological approaches is needed (Smolders et al., 2018). While the evidence surrounding the immune challenged-like state microglia is not unequivocal (Mondelli et al., 2017) it is clear they play a role in these psychiatric disorders regardless of the current homeostatic state (Snijders et al., 2021). To focus in on the contribution of microglia to the potentially microglial state observed in these disorders, an intrinsic monoculture experimental approach might be preferred allowing characterisation of

microglia phenotypes without cues for other glia or neuronal cells. This would simplify characterisation of potentially altered functions identified in the context of 22q11.2 deletion risk.

Some relevant key features of microglia state when investigating the intrinsic effect of 22q11.2 deletions on microglia in ASC and schizophrenia models include a more amoeboid morphological state, meaning reduced or loss of ramification seen respectively in animal and *postmortem* models for each disorder (Gober et al., 2021; Sanagi et al., 2019). Relevant features also include altered localisation of key homeostatic marker IBA1 seen in an ASC animal model, as well as loss of TMEM119 expression in IBA1-positive cells in human *postmortem* tissue from individuals with schizophrenia (Sanagi et al., 2019; Snijders et al., 2021). Deficiency of *IBA1* in a knockout model has also been associated with reduced synaptic connectivity and microglia ramifications in mouse brains (Lituma et al., 2021). The transcription factor *PU.1*, which as described in **Section 1.1.2, Chapter 1** is critical in normal microglia development, is also a regulator of microglia immune response including phagocytic activity, so it is a relevant marker in the study of schizophrenia and ASC due to links with abnormal synaptic pruning (Sellgren et al., 2019; Zhou et al., 2019; Pimenova et al., 2020, 2021).

3.1.4 Aims and hypotheses

The overall aim of this chapter is to set the scene for investigating microglia form and function in the context of 22q11.2DS.

In line with this, it is hypothesised that 22q11.2DS cell lines will have one or more deletions in the corresponding region, and that diagnosis will match polygenic risk towards clinical status demonstrated by having higher PRS relative to control lines. It is further hypothesised that 22q11.2DS MGLs, in line with literature on potential microglial morphological state in schizophrenia and ASC, will take on more circular or amoeboid-like morphology.

Additionally, expression of key signature protein markers proteins in MGLs, specifically IBA1 and PU.1, is hypothesised to be elevated without immune challenge.

Null hypotheses aligning with these hypotheses are: There will be no deletions detected in the corresponding region of 22q11.2DS cell lines, and the presence of the 22q11.2 deletion will not imply higher polygenic risk relative to control lines. There will be no significant difference in the morphological state of MGLs derived from 22q11.2DS donors compared to controls. Specifically, there will be no difference in the circular or amoeboid-like morphology of microglia between individuals with 22q11.2DS and those without the deletion. Lastly, expression levels of key signature marker proteins IBA1 and PU.1 in MGLs will not be elevated in 22q11.2DS cell lines compared to control lines, in the absence of immune challenge.

To investigate these hypotheses, the aims of this chapter are to:

1. Confirm genotypes in cell lines with suspected 22q11.2 deletion.
2. Confirm successful MGL differentiation irrespective of genotype
3. Assess whether 22q11.2DS MGLs have altered morphology and protein marker expression compared to control MGLs

3.2 *Methods*

Table 3.1 illustrates which cell line as well as the number of biological replicates that were utilised for each section in the sub-section. Cell line information is found in **Section 2.1, Chapter 2**. MGLs and macrophages were differentiated as described in **Section 2.3, Chapter 2** and **Section 2.4, Chapter 2**. Treatments with either vehicle or LPS for 3 hours, or vehicle or IL-1 β for 4 hours, respectively, was performed as described in **Section 2.5, Chapter 2**. RNA extraction and qPCR protocols are outlined in **Section 2.6, Chapter 2**. Experiment design and statistical analysis was performed as per **Section 2.7** and **Section 2.8, Chapter 2**, respectively.

Section	Cell line							
	CTR_M3_36S	007_CTF_10	069_CTF_01	127_CTM_03	014_CTM_02	287_SZM_01	191_SZF_09	509_CXF_13
3.3.1	n=1	n=1		n=1		n=1	n=1	n=1
3.3.2	n=1	n=1		n=1		n=1	n=1	n=1
3.3.3	n=1	n=1	n=1	n=1		n=1	n=1	n=1
3.3.4	n=3	n=3		n=3				
3.3.5	n=1	n=1			n=1	n=1	n=1	n=1
3.3.6	n=3	n=3	n=3	n=3	n=3	n=3	n=3	n=3
3.3.7	n=3	n=3	n=3	n=3	n=3	n=3	n=3	n=3

Table 3. 1: Overview of which cell lines were used across different results sections within this chapter. *n=number of biological replicates for each cell line in each experiment. One clone per cell line was utilised.*

3.2.1 Analysis of Infinium Psycharray dataset

To confirm 22q11.2 cell line genotypes, a SNP array (Infinium Psycharray) was used. These Infinium Psycharray datasets were previously acquired by the Srivastava laboratory. Output files following genotyping using an Infinium PsychArray 24 Kit (Illumina) was inputted into The Integrative Genomics Viewer (IGV) (Robinson et al., 2011; Thorvaldsdóttir et al., 2013). CNV locations for 22q11.2DS cell lines were visualised and classified as deletions or duplications using automated colour coding by IGV. Gene IDs within these regions were individually checked for known expression in human microglia and macrophage tissue using EMBL-EBI Expression Atlas (Papatheodorou et al., 2020) platform.

To generate karyograms, Infinium Psycharray datasets were loaded into the no longer supported Illumina GenomeStudio 2011.1 software. All SNPs were clustered using the “Cluster all SNPs” analysis tool. This allowed export of a cluster file (.egt) compatible with Illumina KaryoStudio v1.4, which was required as this software does not support cluster files provided by Illumina alongside Infinium Psycharrays, which are generated using GenTrain v3.0. Generation of a custom cluster file with Illumina GenomeStudio 2011.1 allowed generation of cluster file relevant for the Infinium Psycharray data in GenTrain v2.0, which is supported by Illumina KaryoStudio v1.4. This method of generating a custom cluster file to make the software compatible was suggested by Illumina technical support team. In Illumina KaryoStudio v1.4, karyograms were exported with detected chromosomal regions displayed in a track for each cell line. This was done by selecting “show karyotype” for each sample and using the export as a .bmp file function.

3.2.2 Calculation of polygenic risk scores

To estimate whether 22q11.2DS or control lines have elevated genetic risk for developing schizophrenia and ASC, exploratory PRS was calculated. PRS was also calculated for bipolar disorder type 2, Parkinson's disease, and Alzheimer's disease. This was performed due to Parkinson's disease and bipolar affective disorders having previously been associated with 22q11.2DS, but it is important to note that the link with bipolar affective disorders was more prevalent in early studies and 22q11.2 deletions are no longer considered to elevate risk for this disorder in particular (Gothelf et al., 1999; Schneider et al., 2014; Boot et al., 2018). Alzheimer's disease also sharing several genetic risk variants with schizophrenia and was hence included for exploratory purposes (Chen et al., 2022)

Output files from two Infinium PsychArray 24 Kits, Illumina) consisting of eighteen different cell lines including clonal replicates were imported to Illumina GenomeStudio (v2.0.5). Out of these cell lines, the following final scores of the following lines were extracted: CTR_M3_36S, 007_CTF_10, 127_CTM_03, 287_SZM_01, 191_SZF_09, and 509_CXF_13. Scores for the other cell lines used in this project, being 069_CTF_01 and 014_CTM_02, were not extracted as these lines were not included in this dataset and no SNP array experiment was performed on these lines. The dataset otherwise consisted of neurotypical control lines, idiopathic schizophrenia lines (scores published in Bhat et al., 2022), idiopathic ASC, and cell lines with high risk gene variants associated with ASC. Inclusion of additional lines in processing to generate PRS does not impact final scoring as PRS is generated independently per sample later by PRSice. However, with an n=18, quality control processing becomes less stringent although adjustments such as linkage disequilibrium correlation calculations is made (Choi et al., 2020). As such, statistical comparison of PRS estimated in this study cannot be made to other results linking PRS with phenotype due to insufficient power (Coleman, 2022).

PRS was calculated limiting to autosomal variants in common between each set of GWAS summary statistics (**Table 3.2**), Infinium Psycharray data, and the 404 non-Finnish European participants in 1000 Genomes study (The 1000 Genomes Project Consortium et al., 2015). The non-Finnish European participant dataset was chosen based on donor ancestry but was not estimated as part of the analysis. Low-quality SNPs were filtered out with software recommended settings using a 0.15 GenCall cutoff score in Illumina GenomeStudio (v2.0.5). Data was then exported to PLINK (v1.5.1, Purcell et al. 2007, Purcell, 2017) format using the GenomeStudio associated plugin (PLINK Input Report Plugin v2.1.4). Quality control was performed on these files. Variants with < 99% call rate, minor allele frequency (MAF) of < 1 %, missing genotype rate of < 1 %, and that were outside of the Hardy-Weinberg equilibrium ($p < 10^{-5}$) were excluded (Coleman, 2022). Due to low sample size, $n=18$ with ≤ 100 recommended, linkage disequilibrium ($r^2 > 0.1$) was estimated from the 404 non-Finnish European participants in the 1000 Genomes study, and variant with a lower p-value within 250 kilobases were removed (The 1000 Genomes Project Consortium, 2015; Choi et al., 2020; Coleman, 2022). Imputation performed using the Sanger imputation Service to the Haplotype Reference Consortium panel using the EAGLE2+PBWT panel (Durbin, 2014; Loh et al., 2016; The Haplotype Reference Consortium et al., 2016). In PLINK, the same quality control was repeated after merging files. Generation of PRS was performed by calculating multiple scores made up of variants with a p-value in the base GWAS smaller than the given threshold (Coleman, 2022). Using the PRSice2 software (Choi and O'Reilly, 2019) run with default options for each base GWAS (**Table 3.2**), the `--all-score` output was used to designate individual PRS for each cell line at these p-value thresholds (P^T 0.001, 0.05, 0.1, 0.2, 0.3, 0.4, 0.5 and 1.0). GWAS datasets were used as training samples in PRSice2 targeting the imputed Infinium Psycharray files are shown in **Table 3.2**. The p-value threshold that explained the

greatest the proportion of variance, being P^T 0.001 for all datasets, was used to designate cell line PRS (Coleman, 2022). A pseudo measure is performed by PRSice2 to approximate proportion of variance on the liability scale, which is comparable to proportion of variance estimated by linear regression (Coleman, 2022; Lee et al., 2012).

Disorder	Dataset (training sample)	Reference
Schizophrenia	scz2022	Trubetskoy et al., 2022
Autism spectrum condition	asd2019	Grove et al., 2019
Bipolar disorder type 2	Bip2021 (for bipolar type 2)	Mullins et al., 2021
Alzheimer's Disease	alz2019	Jansen et al., 2019
Parkinson's Disease	META5 excluding 23andMe	Nalls et al., 2019

Table 3. 2: GWAS data set training samples in polygenic risk scoring analysis.

3.2.3 Immunocytochemistry

For experiments investigating surface protein markers hiPSCs were stained within Falcon 96 Well Black with Clear Flat Bottom TC-Treated Microplate with Lid Sterile (353219, Scientific Laboratory Supplies) at a density of 2.5×10^4 and expanded for two days with a medium change at day 1 to remove any dead cells. HiPSCs were fixed for twenty minutes in 4 % paraformaldehyde (w/v; made in 4 % sucrose in PBS) at room temperature. Wells were

gently washed twice in PBS. Permeabilisation and blocking was then performed by adding 2 % normalised goat serum (5425S, Cell Signaling Technology) and 0.1 % Triton X-100 (9036-19-5, Merck) in PBS for 2 hours at room temperature.

MGLs (day 14) and macrophages (day 7) were plated on Nunclon Delta Surface 12-well plates with each well containing a single sterile coverslip at a density 7.5×10^4 per well. When differentiated, coverslips were fixed for twenty minutes in 4 % paraformaldehyde (w/v; made in 4 % sucrose in PBS) in the wells at room temperature. Coverslips were gently washed twice in PBS and then permeabilised and blocked in the same wells using 2 % normalised goat serum and 0.1 % Triton X-100 in PBS at room temperature for 2 hours.

Primary and secondary antibodies were diluted with 2 % normalised goat serum in PBS to concentrations listed in **Table 3.3**. For antibody incubation, experiments with coverslips were moved to a humidified chamber without light access. Chambers were humidified by placing strips of paper towel soaked in H₂O along the sides of the chambers. Chambers were sealed with parafilm during incubations. Primary antibodies were then added on top of coverslips on the side with cells and incubated overnight at 4°C, followed by three gentle washes with PBS. Coverslips were moved back to sterile 12-well plates, one coverslip per well, containing PBS. Secondary antibody incubation was then performed for 1 hour at room temperature after moving the coverslips back to the incubation chamber. The same washing method was then repeated. Coverslips were then mounted onto glass slides with VECTASHIELD® HardSet™ Antifade Mounting Medium with DAPI (H-1500-10) and left in a dark chamber overnight to ensure coverslip attachment before image acquisition. At the time of mounting, glass slides were also coded to avoid bias during image acquisition and analysis. Experiments without

coverslips were not blinded, and antibody incubations were performed as with coverslips, but cells were not removed from wells and plates were wrapped in aluminium foil to block light. Light was blocked to prevent fading of signal as secondary antibodies used were light sensitive fluorescence antibodies.

Antibody	Host	Application, dilution	Manufacturer, catalogue number	Reactivity tested in human tissue
TMEM119	Rabbit	Primary, 1:100	Abcam, ab185333	Yes
PU.1	Mouse	Primary, 1:100	Santa Cruz, sc-390405	Yes
IBA1	Goat	Primary, 1:300	Abcam. ab5076	Yes
DAPI	N/A	1:5000	Sigma Aldrich, D9642	Yes
OCT-4	Rabbit	Primary, 1:500	Invitrogen, 701756	Yes
SSEA4	Mouse	Primary, 1:500	Invitrogen, MA1021	Yes
TRA-1-81	Mouse	Primary, 1:500	Invitrogen, MA1024	Yes
Nanog	Rabbit	Primary, 1:500	Abcam, ab80892	Yes
Anti-Rabbit AlexaFluor 488	Goat	Secondary, 1:750	ThermoFisher, A11034	Yes, cross absorption against human IgG
Anti-Mouse AlexaFluor 568	Goat	Secondary, 1:750	ThermoFisher, A11031	Yes, cross absorption against human IgG and serum
Anti-Goat AlexaFluor 647	Donkey	Secondary, 1:500	ThermoFisher, A32849	Yes, cross absorption against human IgG
Anti-Rabbit AlexaFluor 488	Goat	Secondary, 1:500	Abcam, A11034	Yes, cross absorption against human IgG
Anti-Mouse AlexaFluor 568	Goat	Secondary, 1:500	Abcam, A11004	Yes, cross absorption against human IgG and serum

Table 3. 3: Overview of primary and secondary antibodies used for immunocytochemistry. *Reactivity to human was checked by reading descriptions on manufacturer product websites and published applications. Effectiveness of pluripotency markers OCT-4, SSEA4, TRA-1-81 and Nanog have additionally previously been confirmed by the Srivastava laboratory (Warre-Cornish et al., 2020).*

3.2.4 hiPSC signature marker image acquisition

Qualitative images of hiPSC signature markers OCT-4, SSEA4, TRA-1-81 and Nanog were taken following immunocytochemistry methods described in **Section 3.2.3, Chapter 3** through a series of z-stack confocal microscopy images obtained using the 20x water immersion objective, which has high numerical aperture, in the Opera PhenixTM High Content Screening confocal microscope (PerkinElmer Inc.). The Falcon 96 Well Black with Clear Flat Bottom TC-Treated Microplate with Lid Sterile (353219, Scientific Laboratory Supplies) used to incubate antibodies was secured at the designated slot of the microscope. Once securely in place, the plate was sent into the microscope using the load button of the microscope. Focus was then adjusted using device software to identify nuclei visibility based on DAPI staining using the 405 nm laser. To acquire the images, 488 and 568 channels were scanned to evaluate the top and bottom part of cells within the field. Specifically. Five images were taken per well, one in each of the following spots: centre, upper middle left, upper middle right, lower middle left, and lower middle right. Focal adjustments in z were set up in one well and briefly confirmed in other wells before allowing the confocal microscope to image all selected wells in one run. Number of stacks were the same for each well. Position of each image for each well was also selected to be the same. Laser intensity and gain were set to the same levels for each well.

3.2.5 Microglia morphology and protein marker analysis

Images of TMEM119, PU.1 and IBA1 were acquired using a Nikon A1R inverted confocal microscope (Nikon) with the 60 x oil immersion lens, which has a numerical aperture of 1.49, following immunocytochemistry methods described in **Section 3.2.3, Chapter 3**. Image acquisition was set up to acquire multiple channels of singular planes at 18 Z stacks, which was sufficient to cover all expected fluorescence signals, with step size 0.9 μm at a resolution of 1024×1024 yx. Lasers used were 405.7 nm (DAPI; blue), 487.7 nm (green), 561.9 nm (red) and 638.9 nm (far-red). Optical section was set by pinhole size which was 28.0970625798212 (a.u.). Laser power setting was adapted in Nikon A1R optimisation of image acquisition for each channel and kept the same for each condition for all cell lines.

Data was extracted from each image field using a per cell method where individual cells were drawn around using the freehand selection tool in FIJI v2.3.1 (<https://imagej.net/software/fiji/>, Schindelin et al., 2012) to ensure appropriate selection of regions of interest (ROIs). All threshold settings were optimised to work for all fields of view in maximum projection then applied universally across all images for ROI selection for subsequent intensity analyses. Cell selection was done by randomly identifying DAPI positive cells and then with freehand selection and subsequently outlining the TMEM119 stain of the DAPI positive cell. These TMEM119 ROIs were saved and used for intensity analysis of TMEM119 and IBA1. The ROI for PU.1 was generated using freehand selection of the DAPI nuclei stain in order to measure PU.1 only within the nuclei. Thresholds for each channel was generated separately. The same settings for each threshold was used across all samples. Images obtained during image acquisition of TMEM119 surface protein expression were used for whole cell morphological analysis. Selected output measurements in FIJI v2.3.1 were mean intensity, integrated density

intensity, percentage positive area, area, circularity, roundness, solidity, perimeter, and aspect ratio. A description of these measures is provided in **Table 3.4**

Assessment	Description
Area	Area of cell in calibrated units
Circularity	Formula: $4\pi(\text{area}/\text{perimeter}^2)$. While a value of 1.0 indicates a perfect circle, values closer to 0.0 indicates an increasingly elongated shape
Roundness	Formula: $4*\text{area}/(\pi*\text{major_axis}^2)$. Like circularity, but incorporates the major axis of the cell rather than perimeter to calculate how perfectly round cells are
Solidity	Ratio of the ROI contour area (area) to its convex hull area. Formula: $\text{Area}/\text{convex area}$. Measures the overall concavity of the particles within the ROI
Aspect ratio	Ratio of the length of major and minor axis. Formula: $\text{Major_axis (width)}/\text{minor_axis (height)}$.
Perimeter	Measures the length around the outside of the ROI selection
Mean intensity	Mean grey value of pixels within ROI
Integrated density intensity	Formula: $\text{Mean intensity}*\text{area}$
Percentage positive area	Percentage of cell ROI positive for the fluorescent marker analysed

Table 3. 4: Description of measurements performed in FIJI v2.3.1. ROIs were drawn using freehand selection. “Set scale” was used to spatially calibrate output measurements. Abbreviation: ROI, region of interest.

Colocalisation output was generated using FIJI v2.3.1's built-in colocalisation plugin which allowed specific channels to be independently separated and have the threshold applied before being re-merged and subsequently allowing output data to be collected. Thresholds were established visually and remained the same across all signature marker analysis for each protein, including in vehicle and LPS conditions.

To assess polarity of the cells, the number of projections coming off the cells were counted using a per cell method as in with morphology and protein marker analyses. This being up to 5 cells being randomly selected, with projections being counted based on TMEM119 staining. The cells were categorised as follows based on the number of primary projections coming out of the cell soma: amoeboid (no projections), unipolar (one projection), bipolar (two projections), or multipolar (three or more projections). Secondary projections were not assessed.

For both signature marker and morphology analyses, data was collected from up to 5 cells per field of view, with 3 fields of view being imaged per coverslip and defined as n=1 technical replicate. n=1 biological replicate consisted of the average of n=3 technical replicates being n=3 MGLs on coverslips from the same harvest but independently cultured in separate wells. Data from a total n=3 biological replicates were extracted per condition (vehicle/LPS) of each cell line, totalling 27 fields of view analysed per condition. For analyses, the values of the n=3 technical replicates were averaged to make up 1 numerical value per n=1 biological replicate. n=3 biological replicates per cell line was used for statistical comparisons. Statistical analyses were carried out as per **Section 2.8, Chapter 2**.

3.3 Results

As per the introduction of this chapter, **Section 3.1.4, Chapter 3**, the scope of this chapter is to 1) confirm genotypes in cell lines with suspected 22q11.2 deletion, 2) confirm successful MGL differentiation irrespective of genotype, and 3) assess whether 22q11.2DS MGLs have altered morphology and protein marker expression compared to control MGLs.

3.3.1. Characterisation of 22q11.2 deletions in patient lines

To confirm the genotype of 22q11.2 deletion lines, CNV locations and sizes were first mined (**Section 3.1, Chapter 3**) using an Illumina Psycharray dataset to assess variance in the 22q11.2 region of these cell lines. Genomic locations were identified and illustrated in **Figure 3.1**. Classically, approximately 85% of individuals with the diagnosis of 22q11.2DS have a heterozygous 2.54-Mb deletion, historically described as a 3-Mb deletion, based on chromosomal microarray designs at the approximate location chr22:18,912,231-21,465,672 (LCR-A to LCR-D) within the NCBI Build GRCh37/hg19 reference genome (Guo et al., 2016; McDonald-McGinn et al., 2020). The remainder of individuals with 22q11.2DS can have variants with different endpoints or smaller atypical “nested” deletions in the previously described LCR regions which are also illustrated in **Figure 3.1** (McDonald-McGinn et al., 2015, 2020).

Mining (**Section 3.1, Chapter 3**) discovered a variety of deletions but also multiple duplications and one double deletion. The locations of these CNV locations are visualised in **Figure 3.1**. Descriptively, cell line 287_SZM_01 has a deletion at chr22:18,892,575-21,460,220, beginning slightly before the classic deletion as well as ending before it by a small margin (**Figure 3.1**). 509_CXF_13 has a shorter deletion at chr22:18,892,575-20,302,922,

covering the LCR-A to LCR-B nested deletion region. The line also notably has two larger duplications earlier in the 22q11.2 region at chr22:16,052,962-17,586,805 and chr22:17,605,899-18,801,657 (**Figure 3.1**). Cell line 191_SZF_09 was noted to have four separate deletions, including at chr22:19,125,772-19,868,218 and chr22:19,968,932-20,057,143 which together cover a large part of the LCR-A to LCR-B nested deletion region (**Figure 3.1**). The other two deletions cover a large part of the LCR-B to LCR-D nested region, specifically at chr22:20,103,736-21,349,277 and chr22:21,369,606-21,991,357, with the latter deletion notably extending beyond LCR-D (**Figure 3.1**). Together, these deletions cover a large part of the classic, most common LCR-A to LCR-D deletion (**Figure 3.1**). However, segments within this region in 191_SZF_09 contains three duplications at chr22:19,951,803-19,967,543, chr22:20,071,737-20,103,645, and chr22:21,350,082-21,367,590 (**Figure 3.1**). There is also a double deletion at chr22:19,870,918-19,921,103 (**Figure 3.1**).

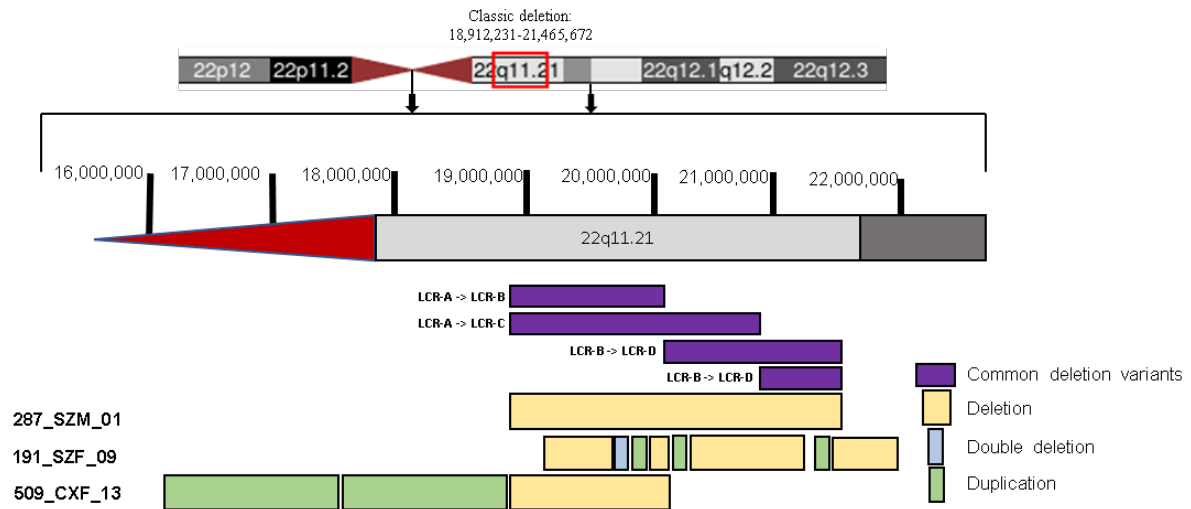


Figure 3. 1: Diagram illustrating genomic locations of 22q11.2 locus CNVs in 22q11.2DS hiPSC lines.

Genome-wide SNP genotype was used to estimate locations. The classic, most common 22q11.2DS-associated deletion encompasses LCR-A to LCR-D. The most common deletions in the region linked to 22q11.2DS outside of the LCR-A to LCR-D deletion are shown as common deletion variants. A version of this figure was published in (Reid et al., 2022) which did not include 509_CXF_13.

In order to determine what exact genes were affected within each CNV, the Infinium Psycharray data set was further mined (Section 3.1, Chapter 3). For each 22q11.2DS cell line, deleted genes are highlighted in **Table 3.4**. Duplicated genes are highlighted in **Table 3.5**

287_SZM_01

FAM230F	DVL1P1	RPL7AP70	LINC00896	CCDC748P1	P2RX6	LOC105377190
DGCR6	KRT18P62	RTL10	LOC105372864	SMPD4P1	SLC7A4	SUSD2P1
PRODH	LOC105372859	TXNRD2	RTN4R	IGLL4P	MIR649	RIMBP3B
DGCR5	HIRA	RPL8P5	LOC105372864	LOC100421121	P2RX6P	RN7SKP63
DGCR9	RN7SL168P	COMT	MIR1286	SLC9A3P2	LRRC74B	HIC2
DGCR10	MRPL40	MIR4761	LOC440792	ABHD17AP4	TUBA3GP	LOC105377191
CA15P1	C22orf39	ARVCF	DGCR6L	POM121L4P	LOC112268300	
DGCR2	LOC105372860	TANGO2	FAM230G	BCRP5	BCRP2	
DGCR11	UFD1	MIR185	USP41	LOC107985584	POM121L7P	
LOC100129263	CDC45	DGCR8	ZNF74 -	TMEM191A	LOC112269299	
TSSK1A	CLDN5	MIR3618	RNU6-225P	PI4KA	E2F6P2	
ESS2	LINC00895	MIR1306	SCARF2	SERPIND1	FAM230B	
TSSK2	LOC100129254	TRMT2A	LOC107985588	SNAP29	LOC105372935	
LOC112268297	LOC100420103	MIR6818	KLHL22	CRKL	GGT2	
GSC2	SEPTIN5	RANBP1	LOC100420177	LINC01637	E2F6P3	
LINC01311	SEPT5-GP1BB	SNORA77B	RNY1P9	AIFM3	POM121L8P	
SLC25A1	GP1BB	ZDHHC8	RN7SL812P	LZTR1	BCRP6	
CLTCL1	LOC105372861	CCDC188	KRT18P5	THAP7	FAM230H	
LOC112268289	TBX1	LOC284865	LOC101928824	THAP7-AS1	PPP1R26P5	
RPL34P35	GNB1L	LOC105372862	MED15	TUBA3FP	CA15P3	

46 Coding genes
7 MicroRNAs
5 lncRNAs

191_SZF_09

TSSK1A	CDC45	RANBP1	KLHL22	CRKL	GGT2	MIR130B
ESS2	CLDN5	SNORA77B	LOC100420177	LINC01637	E2F6P3	LOC107985532
TSSK2	LINC00895	ZDHHC8	RNY1P9	AIFM3	POM121L8P	PPIL2
LOC112268297	LOC100129254	CCDC188	RN7SL812P	LZTR1	BCRP6	YPEL1
GSC2	LOC100420103	LOC284865	KRT18P5	THAP7	FAM230H	RN7SL280P
LINC01311	SEPTIN5	LOC105372862	LOC101928824	THAP7-AS1	PPP1R26P5	MAPK1
SLC25A1	SEPT5-GP1BB	LINC00896	MED15	TUBA3FP	SUSP2P1	RNA5SP493
CLTCL1	GP1BB	LOC105372864	CCDC748P1	P2RX6	RIMBP3B	PPM1F
LOC112268289	LOC105372861	RTN4R	SMPD4P1	SLC7A4	RN7SKP63	LOC100286925
RPL34P35	TBX1	LOC105372864	IGLL4P	MIR649	HIC2	TOP3B
DVL1P1	GNB1L	MIR1286	LOC100421121	P2RX6P	LOC105377191	PRAMENP
KRT18P62	RTL10	LOC440792	SLC9A3P2	LRRC74B	TMEM191C	TXNRD2
LOC105372859	COMT	LOC440792	ABHD17AP4	TUBA3GP	PI4KAP2	RPL8P5
HIRA	MIR4761	DGCR6L	POM121L4P	LOC112268300	RN7SKP221	TANGO2
RN7SL168P	ARVCF	FAM230G	BCRP5	BCRP2	RIMBP3C	
RPL7AP70	DGCR8	USP41	LOC107985584	POM121L7P	UBE2L3	
MRPL40	MIR3618	ZNF74 -	TMEM191A	LOC112269299	YDJC	
C22orf39	MIR1306	RNU6-225P	PI4KA	E2F6P2	CCDC116	
LOC105372860	TRMT2A	SCARF2	SERPIND1	FAM230B	SDF2L1	
UFD1	MIR6818	LOC107985588	SNAP29	LOC105372935	MIR301B	

43 Coding genes
12 Coding genes
outside LCR-A to LCR-D
7 MicroRNAs
3 lncRNAs
2 Homozygous
deletions

509_CXF_13

LOC100292922	CCT8L2	SLC25A1	LOC100419811	GNB1L	MIR4761	LOC284865
FAM230F	LOC105372853	CLTCL1	LOC105372860	RPL7AP70	ARVCF	LOC105372862
ZNF72P	LOC100129262	LOC105372942	UFD1	RTL10	TANGO2	LINC00896
BCL2L12	TSSK1A	LOC112268289	LOC105372871	TXNRD2	MIR185	LOC105372864
DGCR6	LOC112268292	RPL34P35	CDC45	TERF2IPP1	DGCR8	RTN4R
PRODH	ESS2	DVL1P1	CLDN5	LOC105372850	MIR3618	MIR1286
DGCR5	TSSK2	LOC107987325	RPL31P62	LOC101929372	MIR1306	LOC440792
DGCR9	LOC112268297	KRT18P62	LINC00895	RPL8P5	TRMT2A	FABP5P11
DGCR10	LOC105372858	LOC105372859	LOC100129254	GP1BB	MIR6818	
CA15P1	GSC2	HIRA	LOC100420103	LOC107985573	RANBP1	
LOC100422375	LOC101060852	RN7SL168P	LOC105377182	LOC105372861	SNORA77B	
DGCR2	LINC01311	MRPL40	SEPTIN5	TBX1	ZDHHC8	
DGCR11	LOC105379518	C22orf39	SEPT5-GP1BB	COMT	CCDC188	

31 coding genes
1 coding gene
outside Coding
genes outside
LCR-A to LCR-D
5 MicroRNAs
8 lncRNAs
1 SnoRNA

Table 3. 5: Deleted genes within the 22q11.2 region of 22q11.2DS hiPSC lines. Deleted genes within the 22q11.2 region are shown in roman format, while deleted genes are shown italicised. Protein coding genes are shown in black font, while non coding genes other than microRNAs (red) lncRNAs (blue), snoRNAs (green), and hemizygous deletions (gold) for example pseudogenes, are transparent. Abbreviations: LCR-A. Low copy repeat

A; LCR-D. Low copy repeat D; lncRNA, long non-coding RNA; RNA, ribonucleic acid; SnoRNA, Small nucleolar RNA.

191_SZF_09

CA15P3	LOC105377190
MIR4761	MIR3618
MIR1306	

2 Coding genes
3 MicroRNAs

509_CXF_13

ABCD1P4	ANKRD62P1	IGKV1OR22-1	FAM32BP	MICAL3	PPP1R26P3	FAM230E
PABPC1P9	VWFP1	GAB4	CECR3	MIR648	FAM230A	GGT3P
SLC9B1P4	LINC01665	VN1R9P	RN7SL843P	RHEBP3	GGTLC3	
ACTR3BP6	XKR3	CECR7	CECR2	LINC01634	TMEM191B	
CHEK2P4	HSFY1P1	IL17RA	CLCP1	PEX26	PI4KAP1	
KCNMB3P1	GPM6BP3	TMEM121B	DNAJA1P6	ARL2BPP10	RN7SKP131	
TPTEP1	ZNF402P	LINC01664	SLC25A18	TUBA8	RIMBP3	
SLC25A15P5	MTND1P17	HDHD5	ATP6V1E1	USP18	SUSD2P2	
PARP4P3	IGKV2OR22-4	HDHD5-AS1	BID	FAM230D	CA15P2	
PABPC1P9	IGKV2OR22-3	ADA2	MIR3198-1	GGTLC5P	PPP1R26P2	
ANKRD62P1- PARP4P3	IGKV3OR22-2	RPL32P5	LINC00528	FAM230J	PPP1R26P4	

18 Coding genes
13 Coding genes
outside LCR-A to
LCR-D
2 MicroRNAs
12 lncRNAs

Table 3. 6: Duplicated genes within the 22q11.2 region of 22q11.2DS hiPSC lines. Deleted genes within the 22q11.2 region are shown in roman format, while deleted genes are shown italicised. Protein coding genes are shown in black font, while non coding genes other than microRNAs (red) and lncRNAs (blue), for example pseudogenes, are transparent. Abbreviations: LCR-A. Low copy repeat A; LCR-D. Low copy repeat D; lncRNA, long non-coding RNA; RNA, ribonucleic acid.

To further estimate the potential impact of these deletions and duplications, the number of total genes affected within the 22q11.2 region by each type of variant was calculated and is shown in **Table 3.6**, which also provides a summary donor clinical status and total number of CNVs. Genes were then inputted methodically one at a time into the EMBL-EBI Expression Atlas (Papatheodorou et al., 2020) to provide additional evidence that microglia are a relevant cell type to study (**Table 3.7**).

	287_SZF_01	191_SZF_09	509_CXF_13
Altered genes	126	139	154
Deletions	126	134	86
Duplications	0	5	68
Total CNVs	1	8	3
Diagnosis	ASC + SCZ + mild LD	Congenital heart deficits	Atypical ASC

Table 3. 7: Summary of affected genes within 22q11.2 region donor clinical status. Table shows the total amount of affected genes within the 22q11.2 region along with the number of deleted and duplicated genes which contributes to this total. Total CNVs in each within the 22q11.2 region illustrates how segmented these variants are. Additionally, Donor clinical status is shown to further highlight variability of these lines.

Abbreviations: ASC, autism spectrum condition; CNV; copy number variant; LD, learning disorder; SCZ, Schizophrenia.

<u>All 22q lines</u>						
MRPL40	TANGO2	COMT	HIRA	SLC25A1	RTL10	TBX1
TRMT2A	ESS2	ARVCF	RTN4R	ZDHHC8	GSC2	GP1BB
CLDN5	GNB1L	CDC45	RIMBP3	CLTCL1	SEPT5-GP1BB	TXNRD2
TSSK1A	TSSK2	DVL1P1	MIR185	MIR1286	RTL10	DGCR8
MIR4761						
<u>287+191</u>						
CRKL	SNAP29	PI4K	MED15	HIC2	SERPIND1	LZTR1
KLHL22	THAP7-AS1	ZNF74	DGCR6L	SCARF2	AIFM3	THAP7
SLC7A4	TMEM191A	RIMBP3B	POM121L4P	POM121L8P	P2RX6	P2RX6P
MIR3618						
<u>191 + 509</u>						
N/A						
<u>287 + 509</u>						
DGCR2	DGCR11	DGCR10	PRODH	DGCR6	DGCR5	DGCR9

Table 3. 8: Overlap of deleted protein-coding genes in 22q11.2DS hiPSC lines with known positive expression in microglia or macrophages. To identify common genes which could potentially affect 22q11.2DS MGL phenotype, overlap between all as well as individual lines are shown. Overlapping gene lists between two individual lines do not include the genes which are deleted in all lines. Positive expression was determined based on hits in the EMBL-EBI Expression Atlas (Papatheodorou et al., 2020). In the table, 287 denotes 287_SZM, 191 denotes 191_SZF_09, and 509 denotes 509_CXF_13.

3.3.2. Polygenic risk profiles vary among 22q11.2DS and control cell lines

Due to the heterogeneity of deletions and duplications within 22q11.2DS cell lines and that 22q11.2DS is associated with a variety of disorders (McDonald-McGuin et al., 2020), PRS for these lines were generated from the same dataset alongside available control lines (**Figure 3.2**). This was done to observe whether 22q11.2DS lines widely separate from control lines as have been previously demonstrated to occur in Bhat et al., (2022) which used idiopathic schizophrenia lines and Reid et al., (2022) which used the 22q11.2DS donor lines 287_SZM_01 and 191_SZF_09 also being characterised as part of this project. PRS for schizophrenia, ASC, bipolar disorder II, Parkinson's disease, and Alzheimer's disease were generated. Justification for the inclusion of bipolar disorder II, Parkinson's disease and Alzheimer's disease was provided in alongside base GWAS datasets in **Section 3.2.2, Chapter 3**. It was found that based on this output, relative to all other cell lines including 22q11.2 deletion and control lines, 509_CXF_13 had higher polygenic risk for schizophrenia compared to other cell lines, whereas 191_SZF_09 notably had lower polygenic risk (**Figure 3.2**). 191_SZF_09 also had the lowest polygenic risk for bipolar disorder II compared to other 22q11.2 deletion as well as control lines risk (**Figure 3.2**). 287_SZF_01 had higher polygenic risk for bipolar disorder II, Parkinson's disease, and Alzheimer's disease compared to the other 22q11.2 deletion lines as well all control lines risk (**Figure 3.2, Figure 3.3**). 509_CXF_13 had the lowest polygenic risk for Parkinson's disease of all cell lines compared, including 22q11.2DS and control lines (**Figure 3.2, Figure 3.3**).

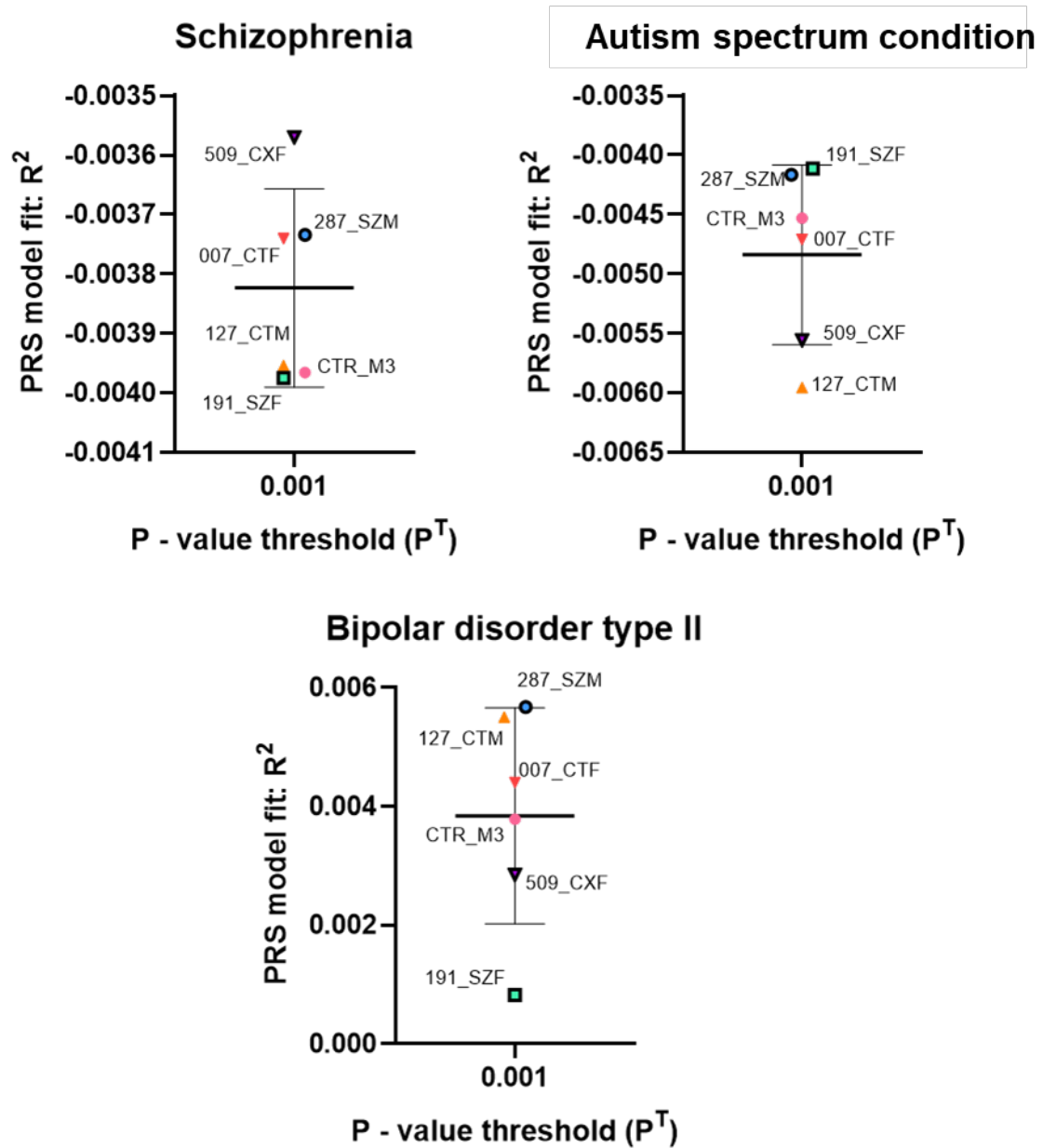


Figure 3. 2: Heterogeneity of [22q11.2DS-associated neurodevelopmental psychiatric disorder PRS across control and 22q11.2 deletion lines. The p-value threshold of $P < 0.001$ was used to designate individual cell line PRS as it explained the largest proportion of variance. Graphs show the standard deviation of available data of cell lines used in this study to qualitatively identify polygenic risk relative to the rest of the cell lines that were scored. A higher PRS model fit (R^2) indicates higher polygenic risk and vice versa. Abbreviations: PRS, polygenic risk score, P^T , p-value threshold. In figures, \blacktriangledown = 007_CTF_10, \blacktriangle = 127_CTM_03, \bullet = CTR_M3_36S, ∇ = 509_CXF_13, \circ = 191_SZF_09, and \square = 287_SZM_01.

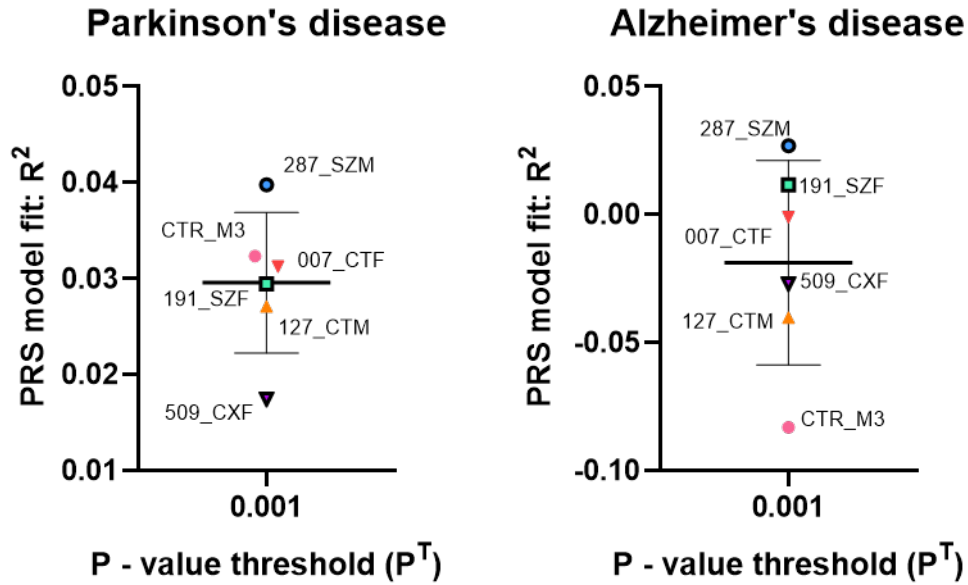


Figure 3. 3: Heterogeneity of neurodegenerative disease-associated PRS towards neurodegenerative diseases across control and 22q11.2 deletion lines. The p -value threshold of $P < 0.001$ was used to designate individual cell line PRS as it explained the largest proportion of variance. Graphs show the standard deviation of available data of cell lines used in this study to qualitatively identify polygenic risk relative to the rest of the cell lines that were scored. A higher PRS model fit (R^2) indicates higher polygenic risk and vice versa. Abbreviations: PRS, polygenic risk score, P^T , p -value threshold. In figures, \blacktriangledown = 007_CTF_10, \blacktriangle = 127_CTM_03, \bullet = CTR_M3_36S, ∇ = 509_CXF_13, \circ = 191_SZF_09, and \square = 287_SZM_01.

3.3.3. Quality control of hiPSCs

Conventional karyotyping is a standard for quality control of hiPSCs (Lund et al. 2012). However, due to a server blackout at King's College London, all original karyotyping data was lost. To accommodate for this ensuring quality of the majority of hiPSC lines used in this study, karyograms were generated from Infinium Psycharray data to qualitatively represent abnormalities present across the genome (**Figure 3.4**). Importantly 069_CTF_01 and 014_CTM_02 was not part of this dataset and karyotyping data has not previously been published for them. The Vernon and Srivastava labs are currently in the process of karyotyping all these cell lines to ensure adequate hiPSC quality control for publication as the

Illumina Infinium Psycharray 24-Kit is designed to study psychiatric predisposition and risk, not to quality control hiPSCs so there might still be missing genetic information.

Karyograms generated here importantly supported that there is at least one deletion across 22q11.2DS cell lines while also supporting that there are no deletions at 22q11.2 specifically in the control lines that were assessed. The karyograms did however critically identify that there might be several CNVs across control cell lines, and that there might be CNVs outside 22q11.2 in 22q11.2DS cell lines. This highlights the importance of having performed the previously described characterisation of cell line polygenic risk. Comparisons cannot be made to original karyotyping data as this was lost in the aforementioned server blackout.

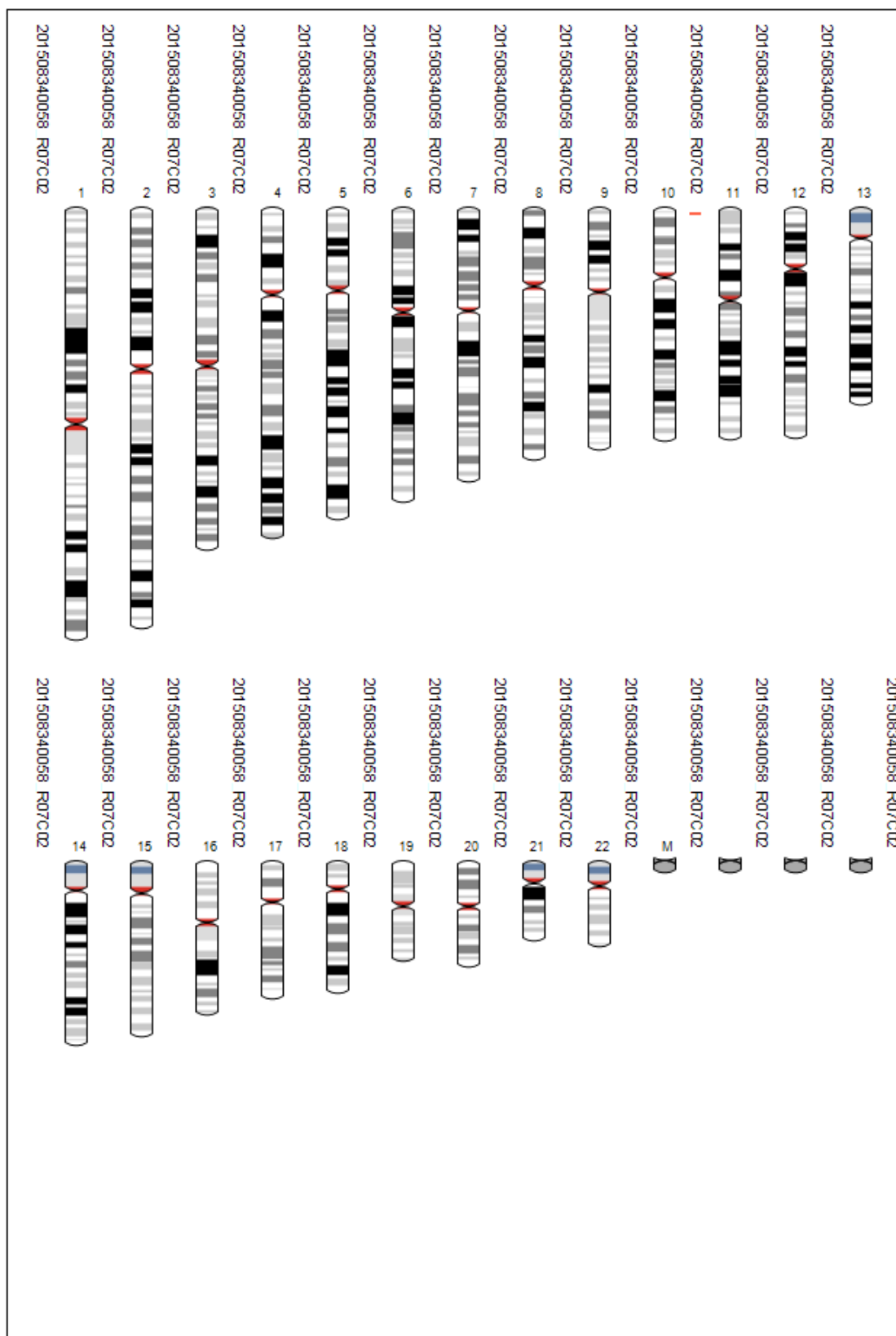


Figure 3. 4: Karyograms of cell lines included in Infinium Psycharray. This karyogram shows CTR_M3_36S. The detected chromosomal regions are displayed in a track for each cell line. Events within regions are colour coded: Green = gain (duplication), red = loss (deletion), and purple = copy-neutral event.

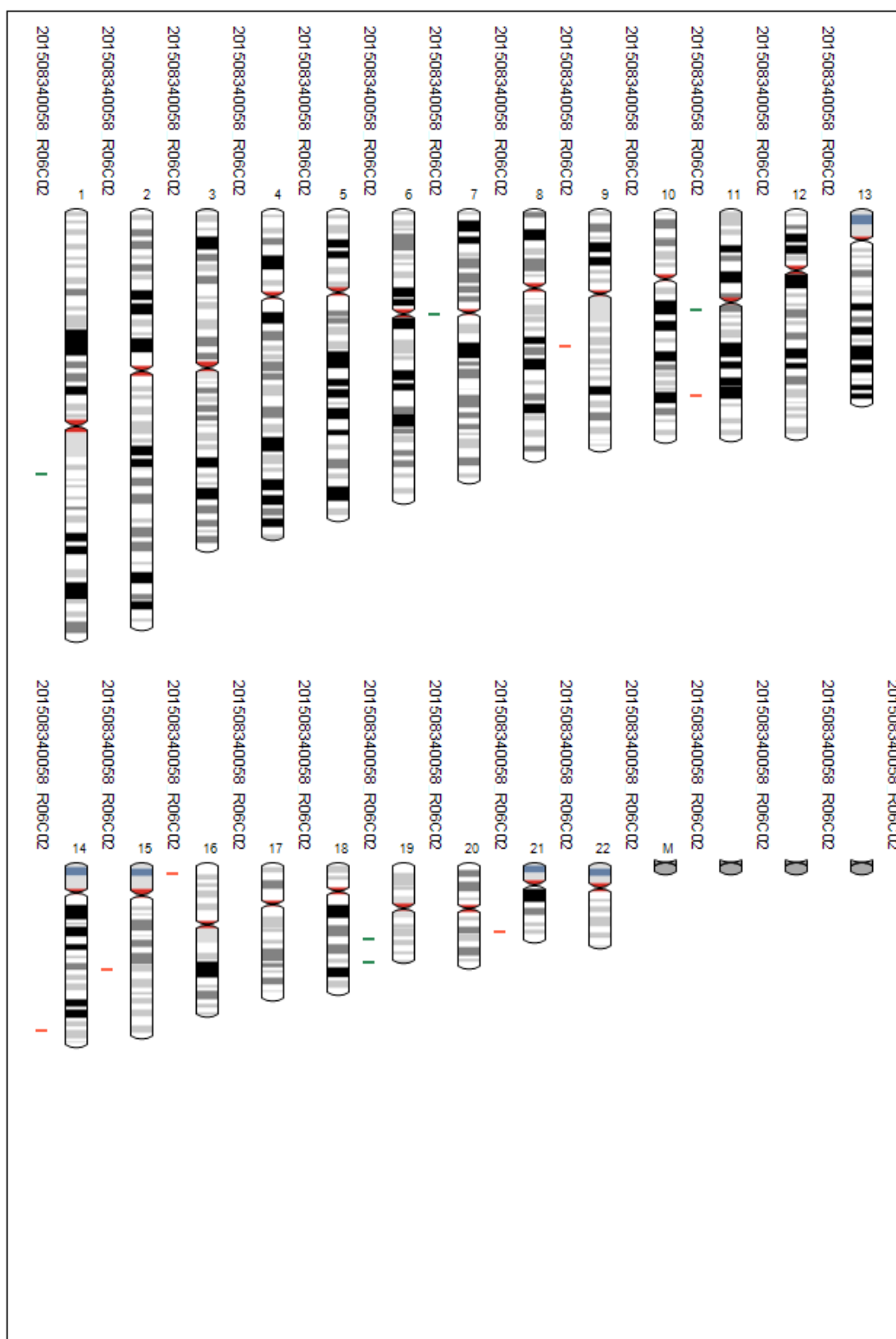


Figure 3. 4 continued. Karyograms of cell lines included in Infinium Psycharray. This karyogram shows 127_CTM_03. The detected chromosomal regions are displayed in a track for each cell line. Events within regions are colour coded: Green = gain (duplication), red = loss (deletion), and purple = copy-neutral event.

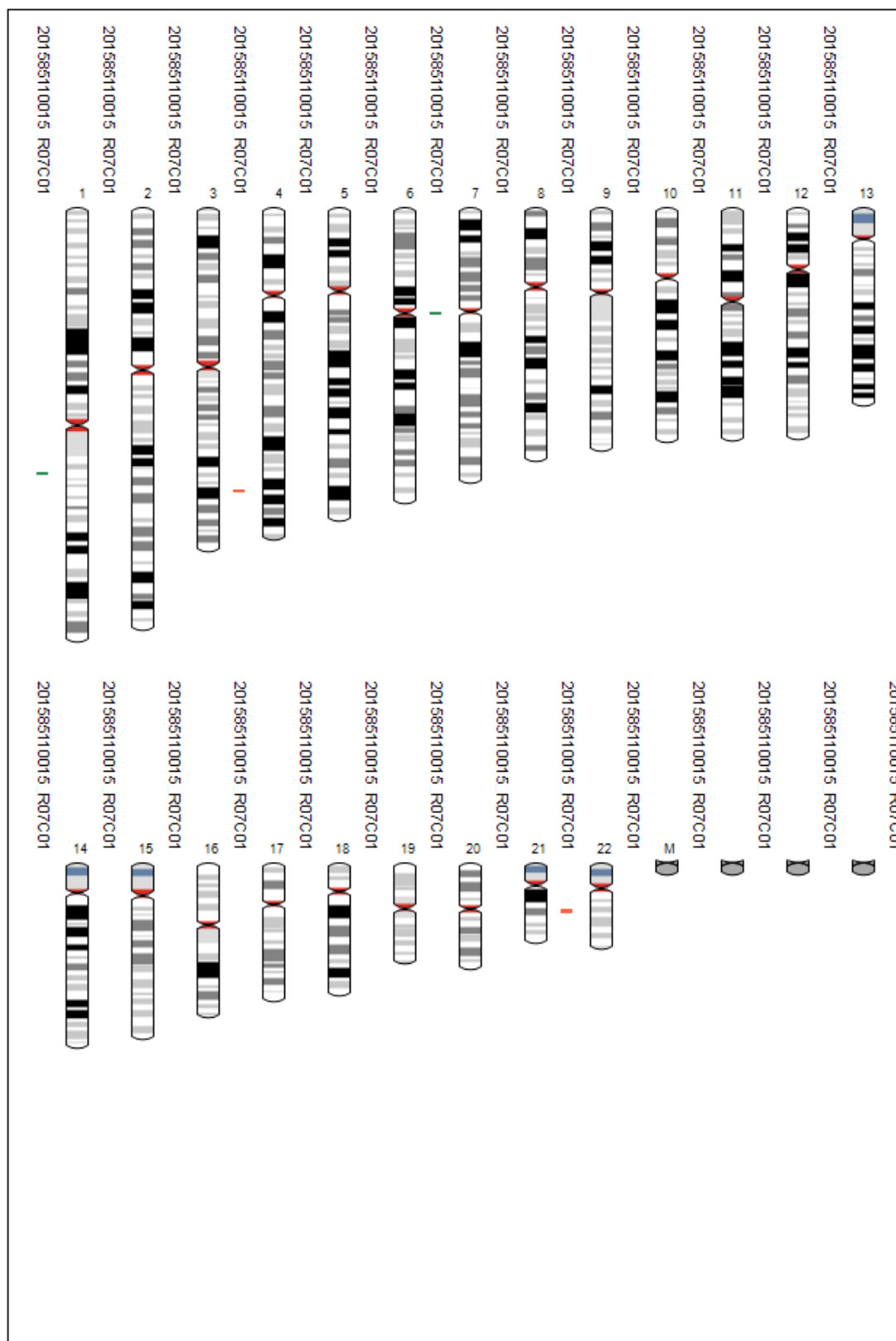


Figure 3. 4 continued. Karyograms of cell lines included in Infinium Psycharray. This karyogram shows 007_CTF_10. The detected chromosomal regions are displayed in a track for each cell line. Events within regions are colour coded: Green = gain (duplication), red = loss (deletion), and purple = copy-neutral event.

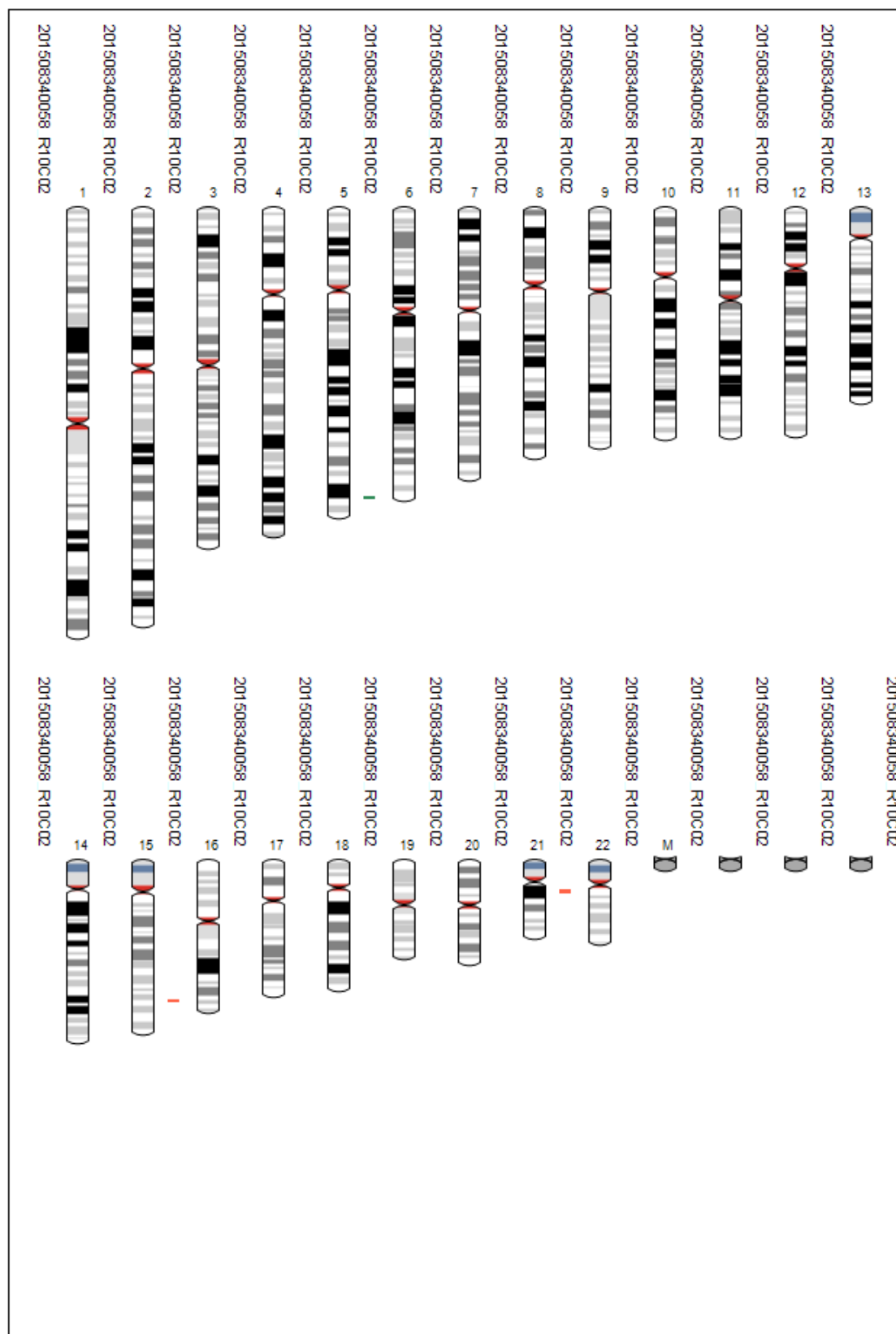


Figure 3. 4 continued. Karyograms of cell lines included in Infinium Psycharray. This karyogram shows 287_SZM_01. The detected chromosomal regions are displayed in a track for each cell line. Events within regions are colour coded: Green = gain (duplication), red = loss (deletion), and purple = copy-neutral event.

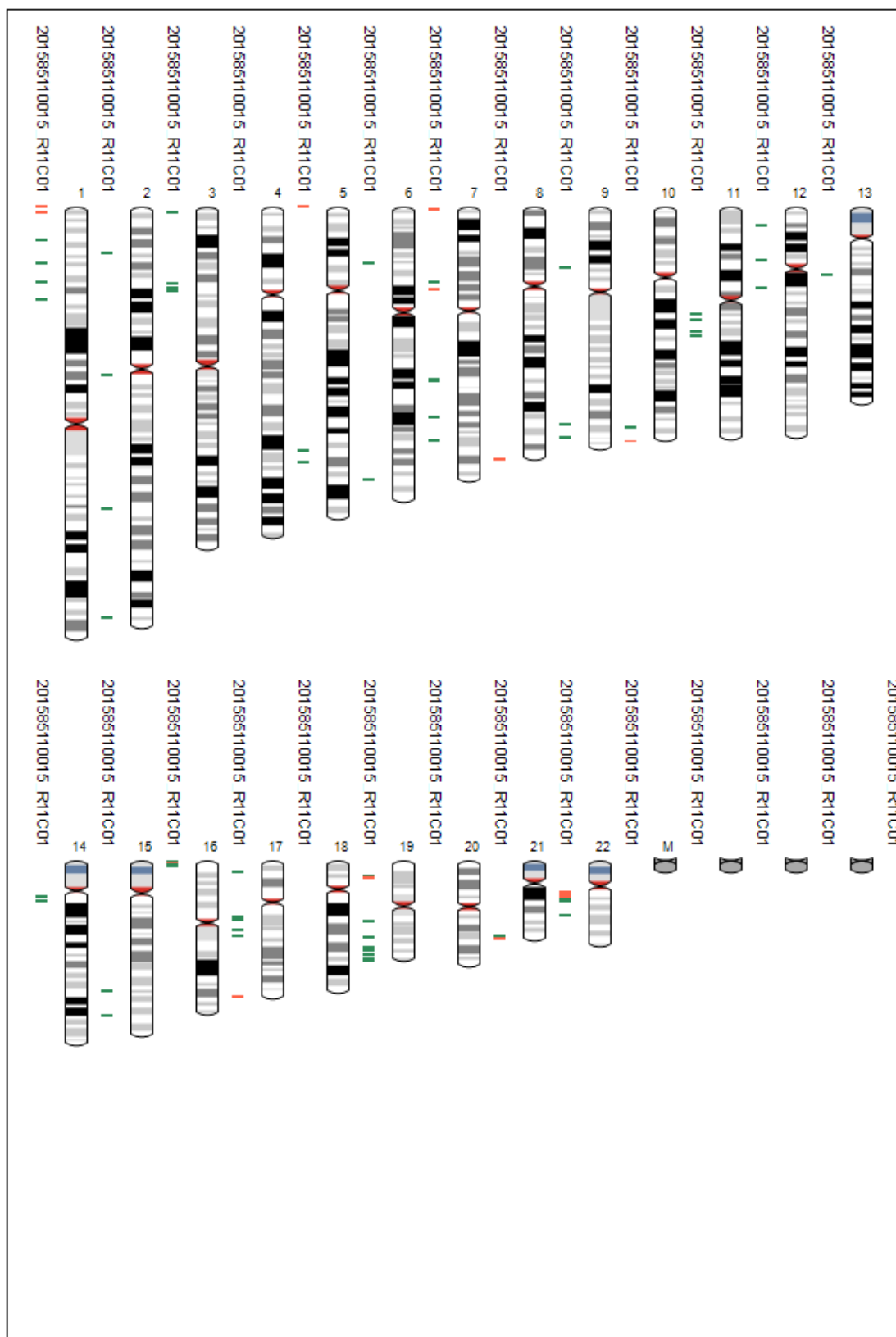


Figure 3. 4 continued. Karyograms of cell lines included in Infinium Psycharray. This karyogram shows 191_SZF_09. The detected chromosomal regions are displayed in a track for each cell line. Events within regions are colour coded: Green = gain (duplication), red = loss (deletion), and purple = copy-neutral event.

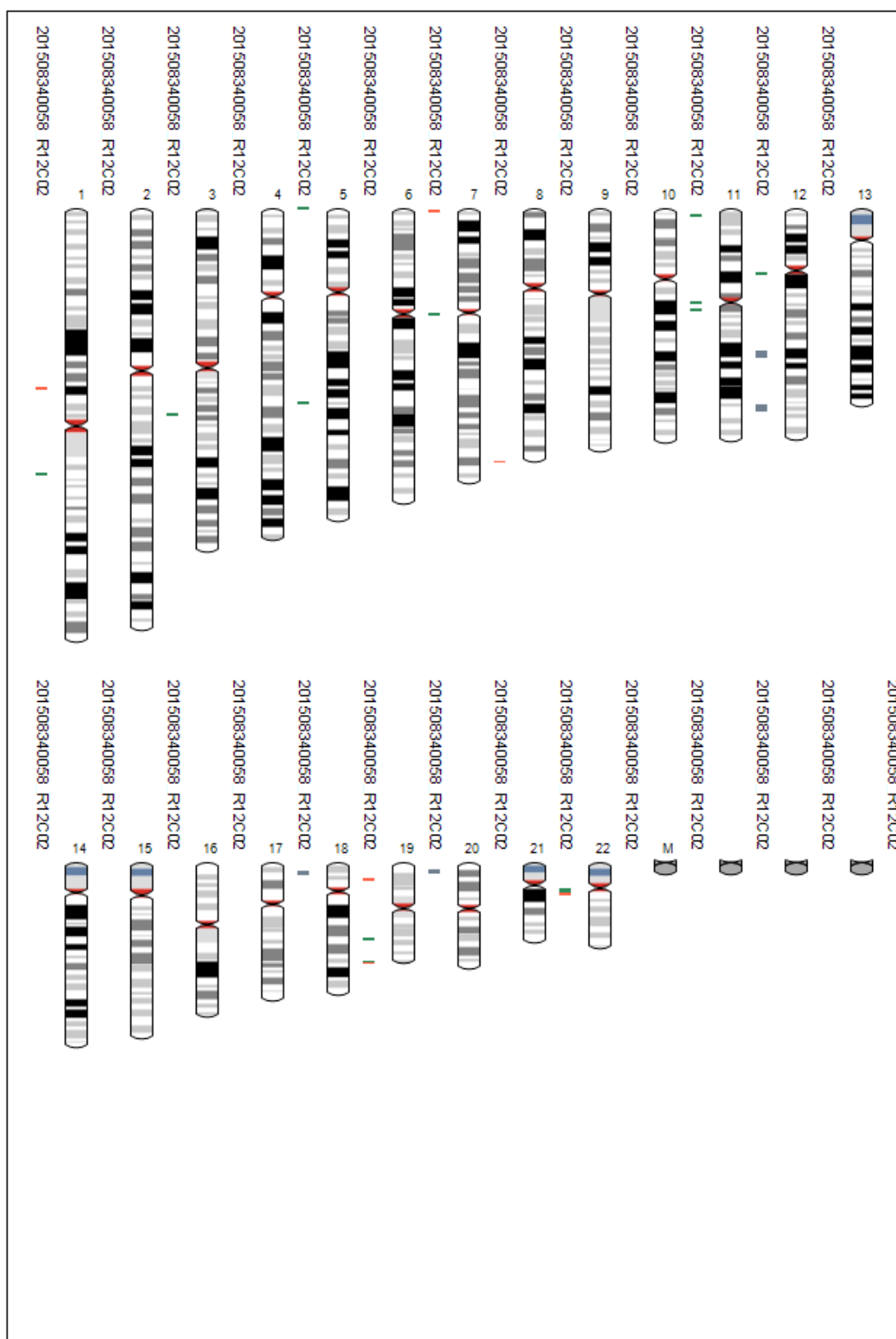


Figure 3. 4 continued. Karyograms of cell lines included in Infinium Psycharray. This karyogram shows 509_CXF_13. The detected chromosomal regions are displayed in a track for each cell line. Events within regions are colour coded: Green = gain (duplication), red = loss (deletion), and purple = copy-neutral event.

Positive surface protein expression of at least two pluripotency markers should be the expected for all hiPSC lines (Sullivan et al., 2018). To ensure pluripotency of cell lines in the hands of experimenter, hiPSC lines 069_CTF_01 and 509_CXF_13 which had previously not undergone testing for pluripotency marker expression, were tested for positive expression of NANOG, SSEA-4, OCT-4 and TRA-1-81 using immunocytochemistry to confirm pluripotency (**Figure 3.5**). These lines were tested alongside CTR_M3_36S, a well-characterised cell line in the Srivastava and Vernon labs, to qualitatively compare similarity in expression. Marker expression levels appeared similar by eye.

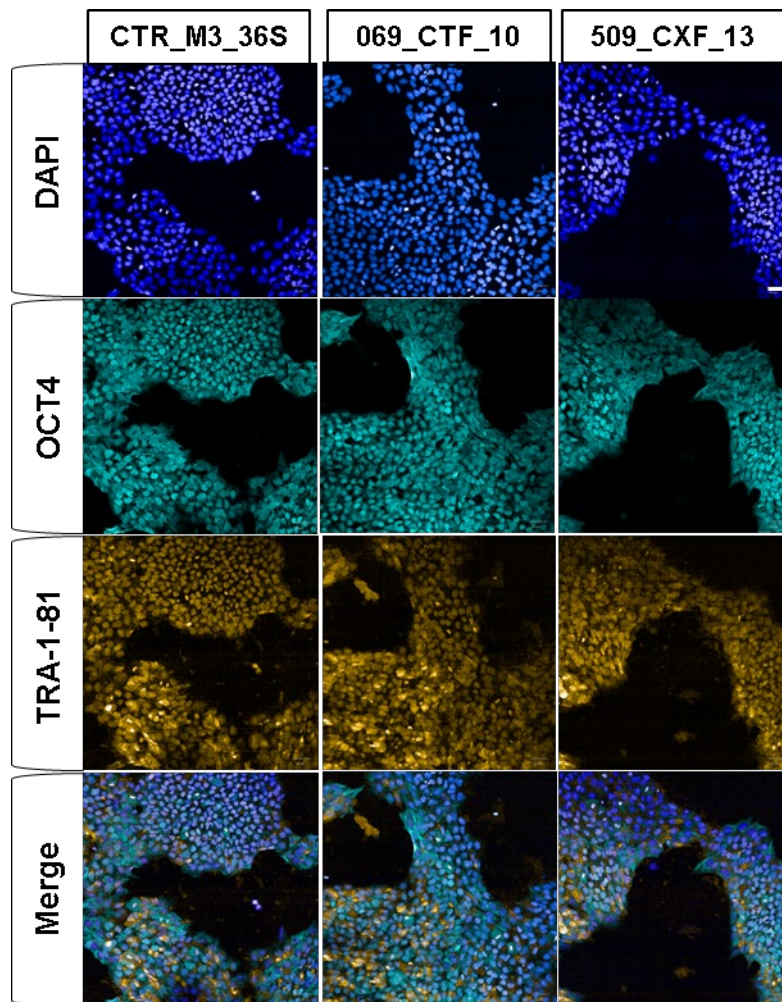


Figure 3. 5: Validation of hiPSC lines. Qualitative immunostaining illustration of pluripotency markers OCT-4 and TRA-1-81 in iPSCs. Scale bar = 50 μ m.

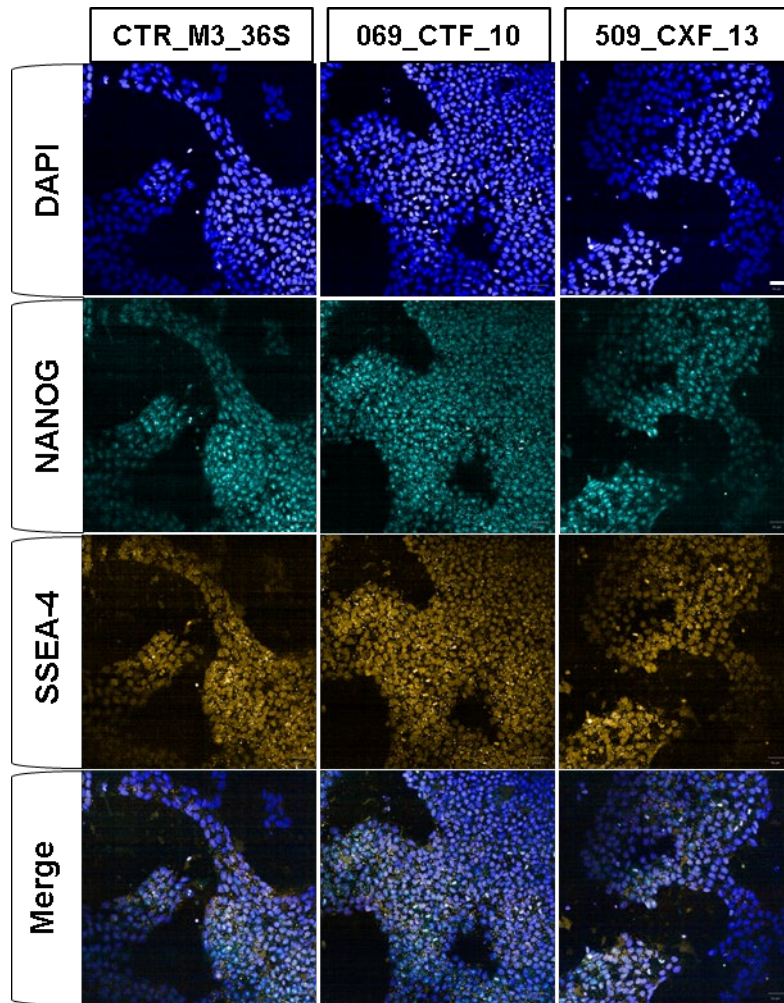


Figure 3. 5: Validation of hiPSC lines continued. *Qualitative immunostaining illustration of pluripotency markers NANOG and SSEA-4. Scale bar = 50 μ m.*

Control lines excluding 069_CTF_01 and 22q11.2DS lines excluding 509_CXF_13 have been previously characterised. Characterisation of male control lines have been published by the Srivastava and Vernon labs (Cocks et al., 2014; Couch et al., 2023; Shum et al., 2020; Adhya et al., 2021; Warre-Cornish et al., 2020). Characterisation of the female control line 007_CTF_10 have been published by the Srivastava lab (Adhya et al., 2021).

Characterisation of 191_SZF_09 and 287_SZM_01 have been published by Vernon and Srivastava lab (Reid et al., 2022). In these publications, previous quality control in these included at least expression of pluripotency surface marker proteins, with all lines except for

014_CTM_02 also having been tested for tri-lineage differentiation potential by EB formation.

3.3.4. Validation of MGL differentiation protocol using control lines

To confirm the Haenseler et al. (2017) protocol could be used to successfully generate MGLs from hiPSCs a selection of control lines, CTR_M3_36S, 007_CTF_10, and 014_CTM_02 were tested in pilot experiments. 22q11.2DS and other control lines used in this study did not undergo this testing to conserve resources and focus on functional data generation in later chapters due to time restrictions described in the **COVID-19 Impact Statement**. The differentiation protocol is described in **Section 2.3** and **Section 2.4, Chapter 2**. qPCR was performed to confirm expression of key signature genes in these lines. The percentage of cells positive for key proteins markers within the cultures were also identified using immunocytochemistry but only for CTR_M3_36S and 007_CTF_10 due to lack of time (**COVID-19 Impact Statement**). Response to IL-1 β by qPCR was additionally tested in all three control lines as described in **Section 2.5, Chapter 2**, but not for other lines also due to lack of time (**COVID-19 Impact Statement**). Normalisation of qPCR data was done as per **Section 2.6, Chapter 2**.

Expected gene expression of signature markers based on the original publication of the protocol was confirmed in all cell lines as shown in **Figure 3.6**, specifically *CIQA*, *GAS6*, *GPR34*, *PROS1*, *MERTK*, *P2RY12*, *TMEM119*, and *TREM2* (Haenseler et al., 2017) for hiPSC differentiated to either macrophages or MGLs. *P2RY12* expression was significantly higher ($p < 0.05$) in MGLs compared to macrophages, which was not the case in Haenseler et al. (2017). Additionally, expression was confirmed of other genes expected to be expressed in these cells including *CD163*, *HLA-A*, and *CX3CR1* (**Figure 3.6**) (Fabrick et al., 2005; Schaefer et al.,

2008; Pey et al., 2014; Haenseler et al., 2017; Murai et al., 2020). Expression change from hiPSC stage was not measured for this project, but validation of significant expression increase in *P2RY12*, *TMEM119*, *MERTK*, *CX3CR1* alongside significant expression decrease in the pluripotency marker *NANOG* was published in Couch et al. (2023) for cell lines CTR_M3_36S, 014_CTM_02, and 127_CTM_03.

The percentage of cells within wells positive for key developmental marker PU.1 alongside signature markers *TMEM119* or *IBA1* was assessed, qualitatively showing that almost all cells are positive for a combination of these markers (**Figure 3.7**).

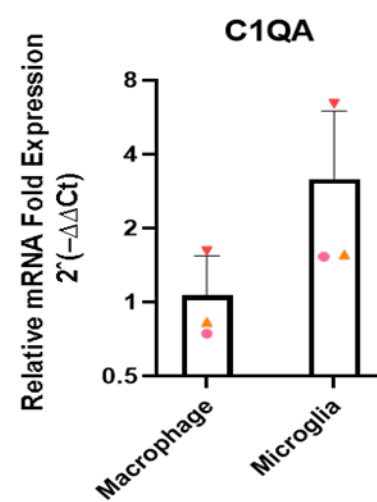
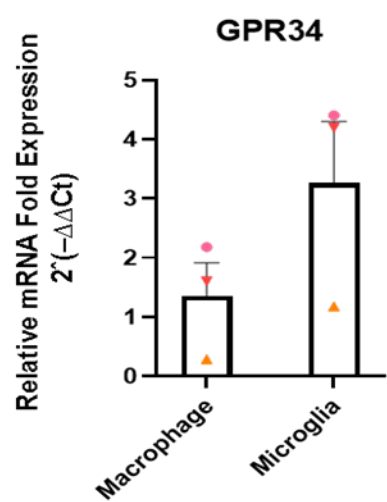
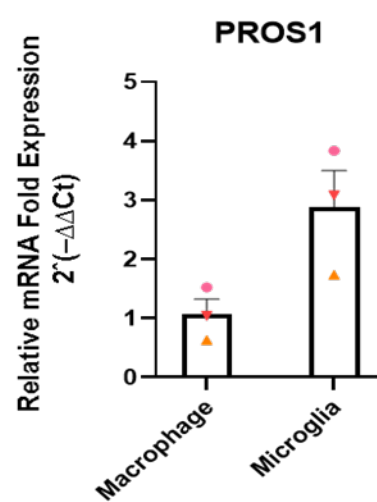
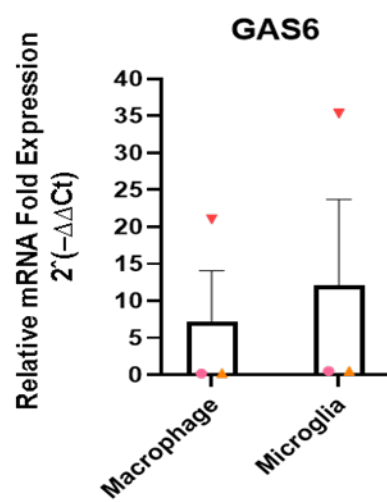
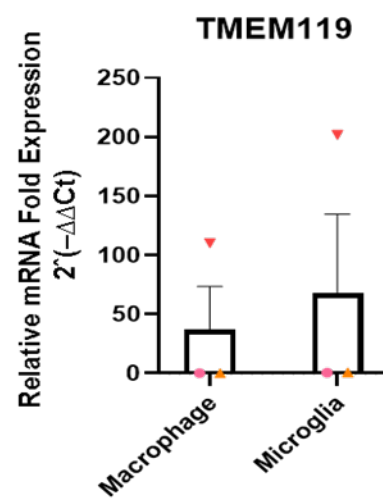
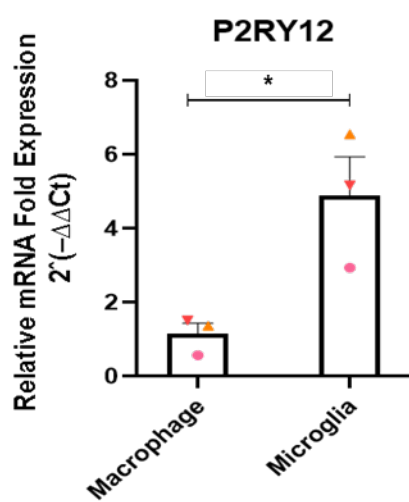


Figure 3. 6: Signature marker assessment of differentiated MGLs compared to macrophages. Gene expression comparison of hiPSC-derived macrophages and MGLs using qPCR. Expression changes are relative to average normalised macrophage Ct. In figures, ▼ = 007_CTF_10, ▲ = 014_CTM_02, ● = CTR_M3_36S. Comparison groups consisted of N=3 day 14 untreated differentiated control MGLs vs N=3 day 7 untreated differentiated control macrophages, with n=3 biological replicates being performed for each cell line. For statistical comparisons, means of macrophages were compared to means of MGLs in one statistical test, not separately for each cell line. For each cell line, the mean of all biological replicates was calculated and used during statistical analysis. Data was checked for normal distribution. Unpaired two-tailed parametric t-test was used for statistical comparisons. Significant p values are indicated at follows: * = $p < 0.05$. Error bars represent the standard deviation of each group. Average housekeeper cT values in this experiment were as follows: Macrophage GAPDH = 17.287 (▼), 17.790 (▲), 17.754 (●), Macrophage RPL13 = 18.170 (▼), 17.552 (▲), 17.676 (●), Microglia GAPDH = 17.247 (▼), 17.814 (▲), 17.319 (●), Microglia RPL13 = 17.816 (▼), 17.961 (▲), 17.917 (●).

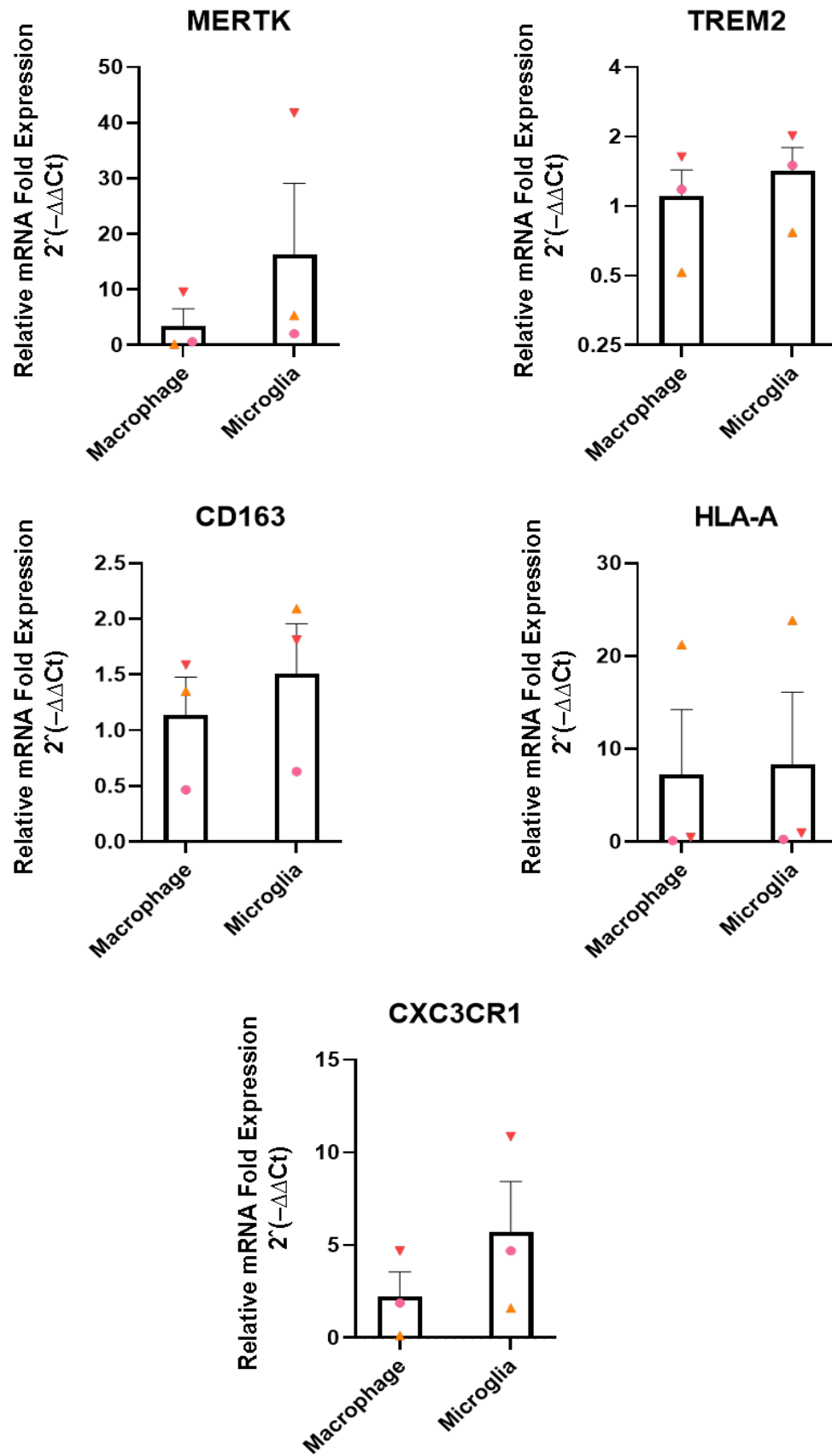


Figure 3. 6. Continued: Signature marker assessment of differentiated MGLs compared to macrophages. Gene expression comparison of hiPSC-derived macrophages and MGLs using qPCR. Expression changes are relative to average normalised macrophage Ct. In figures, ▼ = 007_CTF_10, ▲ = 014_CTM_02, ● = CTR_M3_36S. Comparison groups consisted of N=3 day 14 untreated differentiated control MGLs vs N=3 day 7 untreated differentiated control macrophages, with n=3 biological replicates being performed for each cell line. For statistical comparisons, means of macrophages were compared to means of MGLs in one statistical test, not separately for each cell line. For each cell line, the mean of all biological replicates was calculated and used during statistical analysis. Data was checked for normal distribution. Unpaired two-tailed parametric t-test was used for statistical comparisons. Significant p values are indicated at follows: * = $p < 0.05$. Error bars represent the standard deviation of each group. Average housekeeper cT values in this experiment were as follows: Macrophage GAPDH = 17.287 (▼), 17.790 (▲), 17.754 (●), Macrophage RPL13 = 18.170 (▼), 17.552 (▲), 17.676 (●), Microglia GAPDH = 17.247 (▼), 17.814 (▲), 17.319 (●), Microglia RPL13 = 17.816 (▼), 17.961 (▲), 17.917 (●).

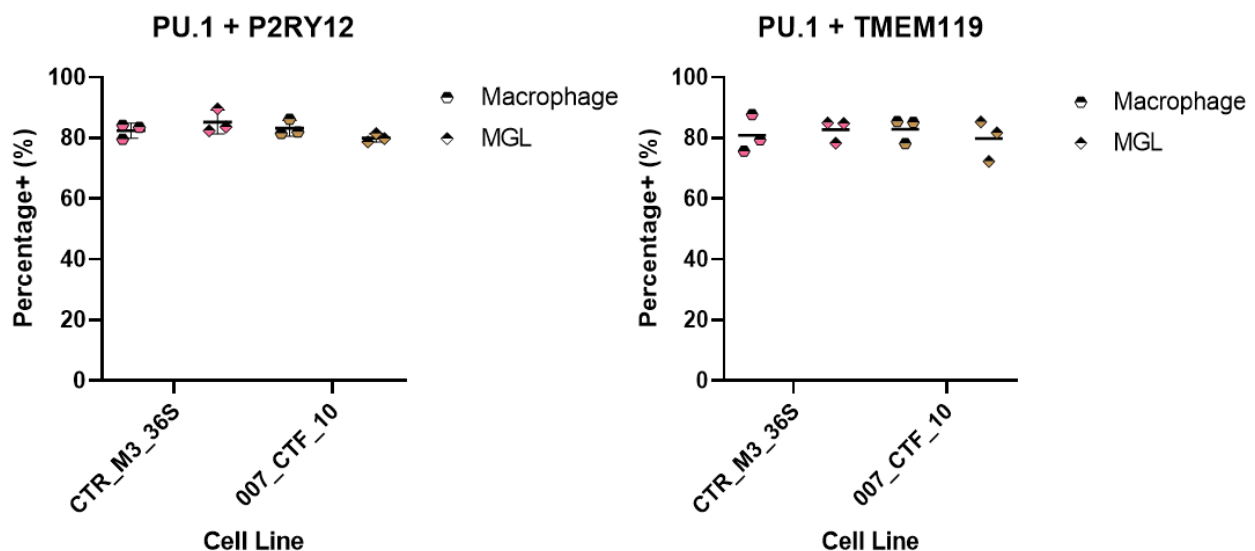


Figure 3. 7: Percentage of cells per well positive for PU.1 and either P2RY12 or TMEM119. The percentage positive population of MGLs and macrophages were calculated compared to the total number of DAPI positive cells. Each biological replicate indicates the average of n=3 technical replicates being three independently cultured wells in one plate. No statistical tests were performed. Error bars represent the standard deviation of each group.

When testing IL-1 β response, a significant ($p < 0.05$) response to 4 hour treatment was shown at the transcriptome level, but only in MGLs, for *IL-6* and *IL-10*, but not in *TSPO* (Figure 3.8 and Figure 3.9).

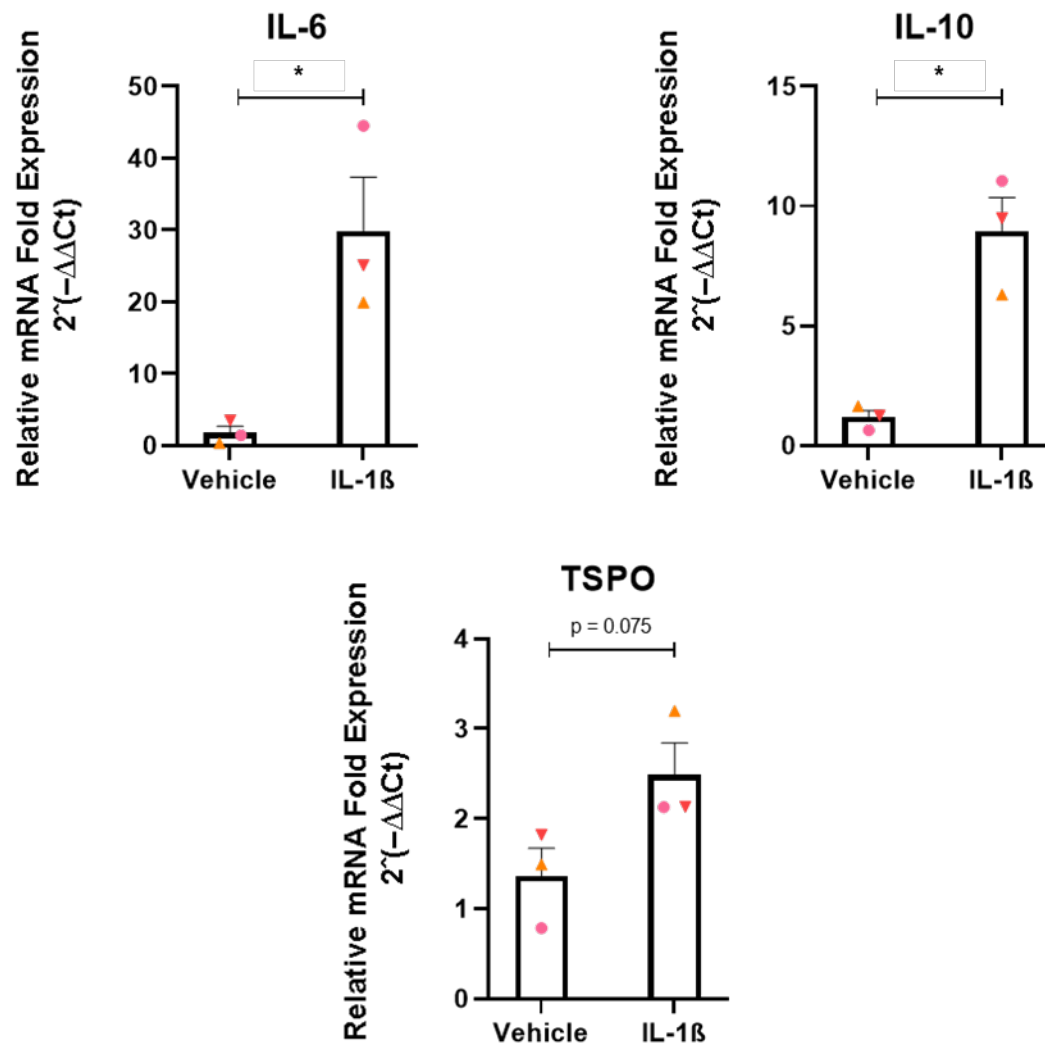


Figure 3. 8: MGL functional response to 4-hour treatment of IL-1 β . MGLs were tested for positive expression of genes associated with MGL immune challenged state. Expression changes are relative to average normalised vehicle Ct. In figures, \blacktriangledown = 007_CTF_10, \blacktriangle = 014_CTM_02, \bullet = CTR_M3_36S. Comparison groups consisted of N=3 day 14 differentiated control MGLs treated with H₂O for 4 hours vs N=3 day 14 differentiated control MGLs treated with IL-1 β for 4 hours, with n=3 biological replicates being performed for each cell line. For statistical comparisons, means of vehicle-treated MGLs were compared to means of IL-1 β -

treated MGLs in one statistical test, not separately for each cell line. For each cell line, the mean of all biological replicates was calculated and used during statistical analysis. Data was checked for normal distribution. Unpaired two-tailed parametric t-test was used for statistical comparisons. Significant p values are indicated at follows: * = $p < 0.05$. Error bars represent the standard deviation of each group. Average housekeeper cT values in this experiment were as follows: Vehicle GAPDH = 17.247 (▼), 17.814 (▲), 17.319 (●), Vehicle RPL13 = 17.816 (▼), 17.961 (▲), 17.917 (●), IL-1 β GAPDH = 17.277 (▼), 17.515 (▲), 17.708, IL-1 β RPL13 = 17.596 (▼), 17.482 (▲), 17.041 (●).

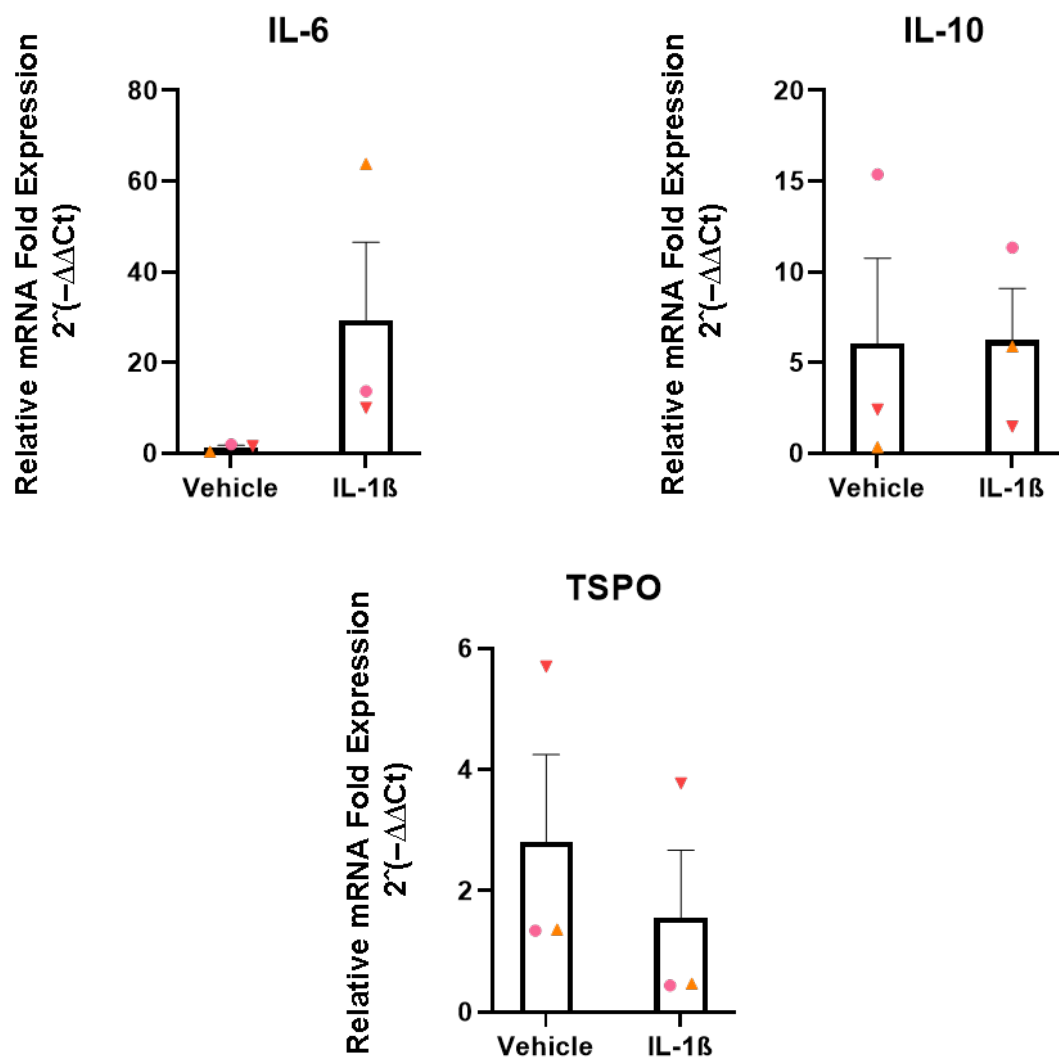


Figure 3. 9: Macrophage functional response to 4-hour treatment of IL-1 β . Macrophages were tested for positive expression of genes associated with MGL immune challenged states. Expression changes are relative to average normalised vehicle Ct. In figures, ▼ = 007_CTF_10, ▲ = 014_CTM_02, ● = CTR_M3_36S.

Comparison groups consisted of N=3 day 7 differentiated control macrophages treated with H₂O for 4 hours vs N=3 day 7 differentiated control macrophages treated with IL-1 β for 4 hours, with n=3 biological replicates being performed for each cell line. For statistical comparisons, means of vehicle-treated MGLs were compared to means of IL-1 β -treated MGLs in one statistical test, not separately for each cell line. For each cell line, the mean of all biological replicates was calculated and used during statistical analysis. Data was checked for normal distribution. Unpaired two-tailed parametric t-test was used for statistical comparisons. Error bars represent the standard deviation of each group. Average housekeeper cT values in this experiment were as follows: Vehicle GAPDH = 17.287 (▼), 17.790 (▲), 17.754 (●), Vehicle RPL13 = 18.170 (▼), 17.552 (▲), 17.676 (●), IL-1 β GAPDH = 17.057 (▼), 17.624 (▲), 17.533, IL-1 β RPL13 = 17.951 (▼), 17.620 (▲), 17.318 (●).

3.3.5. Key suspected gene within 22q11.2DS deletion are qualitatively lower expressed than in control MGLs

Colleagues in the Srivastava lab has previously shown that *COMT*, one of the commonly deleted genes across 22q11.2DS hiPSC lines in this study, is reduced in two of the three 22q11.2DS lines, 287_SZM_01 and 191_SZF_09 in hiPSC-derived midbrain dopaminergic neurons (Reid et al., 2022). In **Figure 3.10**, it is shown that a reduction of at least 50% gene expression is also true, including for the final line 509_CXF_13, in MGLs. While more genes noted to be in the deleted regions of 22q11.2 deletions lines would ideally be tested by qPCR, they were not tested due to lack of time (**COVID-19 Impact Statement**). The transcriptomic profile of 22q11.2 deletion lines is characterised in **Chapter 4**.

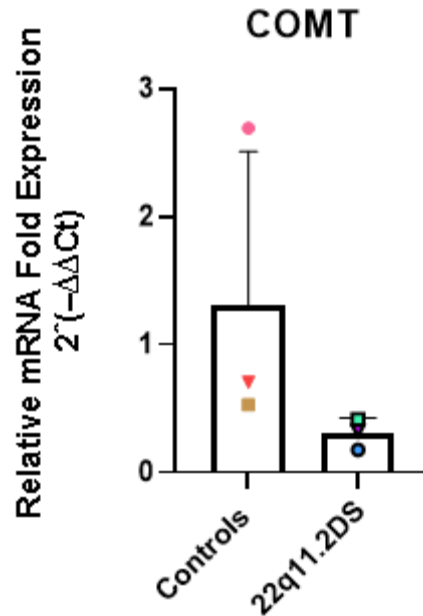


Figure 3. 10: Qualitative confirmation of deleted genes in 22q11.2DS cell lines. Relative gene expression of deleted genes in 22q11.2DS cell lines relative to average normalised Ct in control lines. In figure, ▼ = 007_CTF_10, ▲ = 014_CTM_02, ● = CTR_M3_36S, ▽ = 509_CXF_13, ○ = 191_SZF_09, and □ = 287_SZM_01. No statistical comparison was performed.

3.3.6. Comparison of morphology and key signature protein expression as a function of genotype and under the context of LPS stimulation

To assess whether genotype differences affects the differentiation of MGLs using the Haenseler et al. (2017) protocol, morphology and key protein markers were compared using immunocytochemistry. Additionally, this comparison was also extended to determine whether 22q11.2DS MGLs respond differentially to LPS. A change from IL-1 β to LPS as immune challenge agent was made due to lack of time (**COVID-19 Impact Statement**). While initial interest was in using IL-1 β to characterise its effect on MGLs, using a more well-characterised immune system challenge agent in LPS was deemed necessary to best support results (Haenseler et al., 2017; Lively and Schlichter, 2018; He et al., 2021; Ishijima and Nakajima, 2021). Different treatment times were not tested due to lack of related time

and laboratory access constraints (**COVID-19 Impact Statement**). A 3-hour treatment was selected due to relevance in studying key microglial functions as later investigated in **Chapter 5**. Microglia phagocytosis have been described to plateau after 3 hours in primary mouse microglia, with LPS-treated microglia phagocytosis being enhanced compared to non-treated microglia (He et al., 2021). Hence it was deemed that microglia should be able to demonstrate a response by the end of this treatment period for LPS experiments even though testing different treatment lengths would have been beneficial to help accommodate for potential species-related heterogeneity (**Section 1.1.5, Chapter 1**).

Visualisations of positive expression of key proteins and morphology can be seen in **Figure 3.11** and **Figure 3.12**. When effect of genotype on MGL morphology, it was found that on average 22q11.2DS MGLs take on different morphological phenotype compared to controls. When comparing vehicle-treated conditions, a significant difference ($p < 0.05$) was observed in circularity, with 22q11.2DS MGLs being more circular compared to control MGLs (**Figure 3.13**). 22q11.2DS MGLs average cell polarity was also different, having a significantly higher ($p < 0.05$) percentage of cells being in an amoeboid state, and a significantly lower ($p < 0.05$) percentage of cells in a bipolar state compared to control MGLs (**Figure 3.14**). No significant change was observed in nuclei area within vehicle-treated conditions (**Figure 3.15**). In response to LPS, a significant increase ($p < 0.05$) in percentage of amoeboid cells were observed in control MGL cultures, but no significant response was observed in 22q11.2DS MGL cultures (**Figure 3.14** and **Figure 3.16**). No morphological change differences were observed in response to LPS between control and 22q11.2DS MGLs (**Figure 3.13** and **Figure 3.15**). Together, this might indicate that 22q11.2DS MGL morphology does not shift morphological state in response to LPS as MGLs in 22q11.2DS

In protein marker analysis, which included TMEM119, PU.1, and IBA1 (**Figure 3.17**), no significant differences were found when comparing control and 22q11.2DS MGL vehicle-treated conditions. There was of note a trend towards a difference in PU.1 mean fluorescence intensity in 22q11.2DS MGLs compared to control MGLs ($p = 0.0537$), potentially due to data points of the 22q11.2DS line 191_SZF_09 more closely aligning with control MGLs. No change in protein expression was observed in either control or 22q11.2DS MGLs in response to LPS and no difference in protein expression change in response LPS was observed between genotypes (**Figure 3.18**).

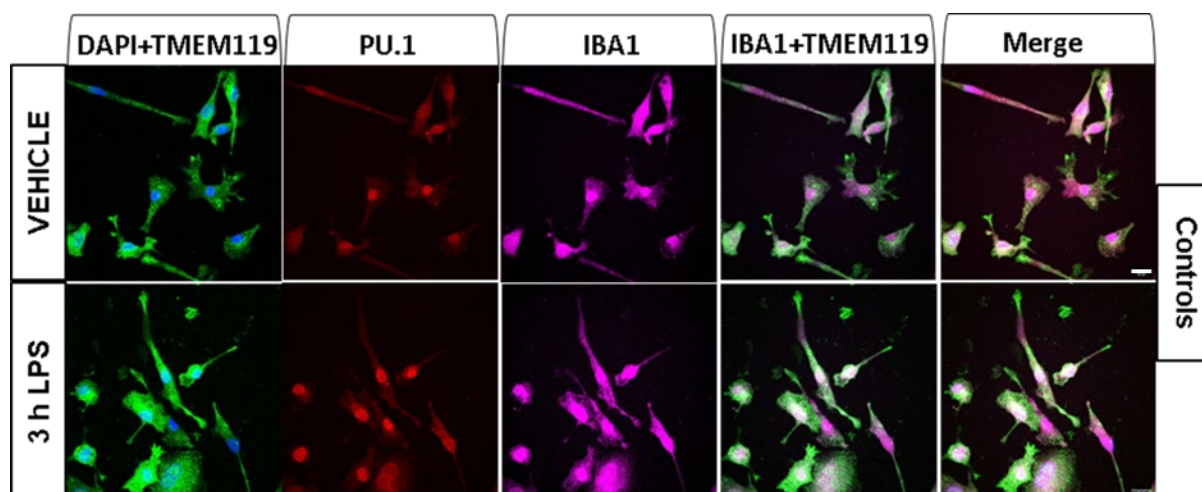


Figure 3. 11: Illustration of microglia signature protein expression and morphology in control MGLs treated with either H₂O vehicle or LPS for 3 hours. Immunofluorescence assay shows positive expression of microglia signature protein markers TMEM119 (green), PU.1 (red) and IBA1 (pink). Visual illustration of IBA1 and TMEM119 colocalisation is also shown. Merge image displays all channels merged including DAPI, TMEM119, PU.1, and IBA1. DAPI was used to stain nuclei (blue). Scale bar = 20 μ m. Abbreviations: LPS, lipopolysaccharide; MGL, microglia-like cell.

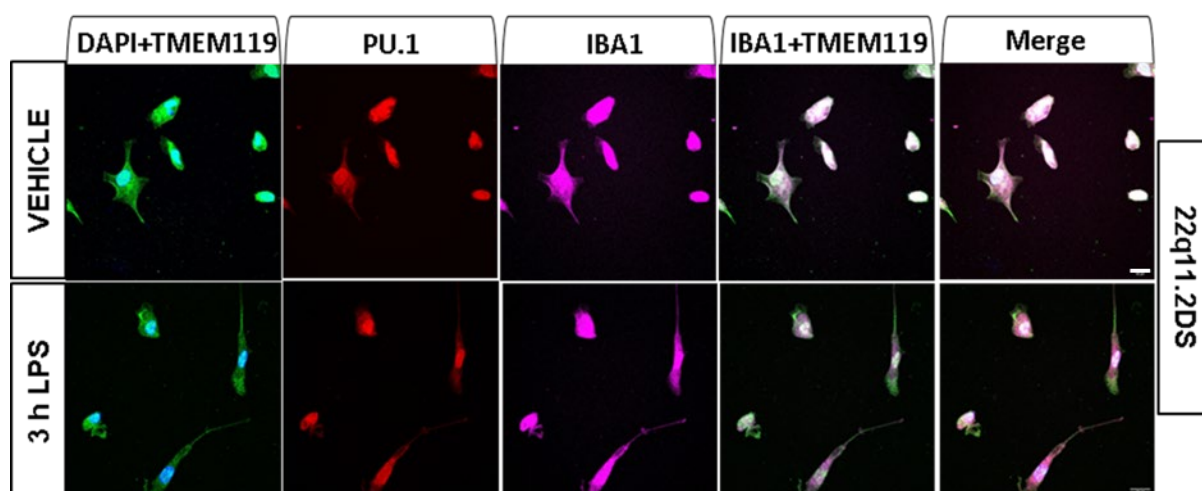


Figure 3. 12: Illustration of microglia signature protein expression and morphology in 22q11.2DS MGLs treated with either H₂O vehicle or LPS for 3 hours. Immunofluorescence assay shows positive expression of microglia signature protein markers TMEM119 (green), PU.1 (red) and IBA1 (pink). Merge image displays all channels merged including DAPI, TMEM119, PU.1, and IBA1. Visual illustration of IBA1 and TMEM119 colocalisation is also shown. DAPI was used to stain nuclei (blue). Scale bar = 20 μ m. Abbreviations: LPS, lipopolysaccharide; MGL, microglia-like cell.

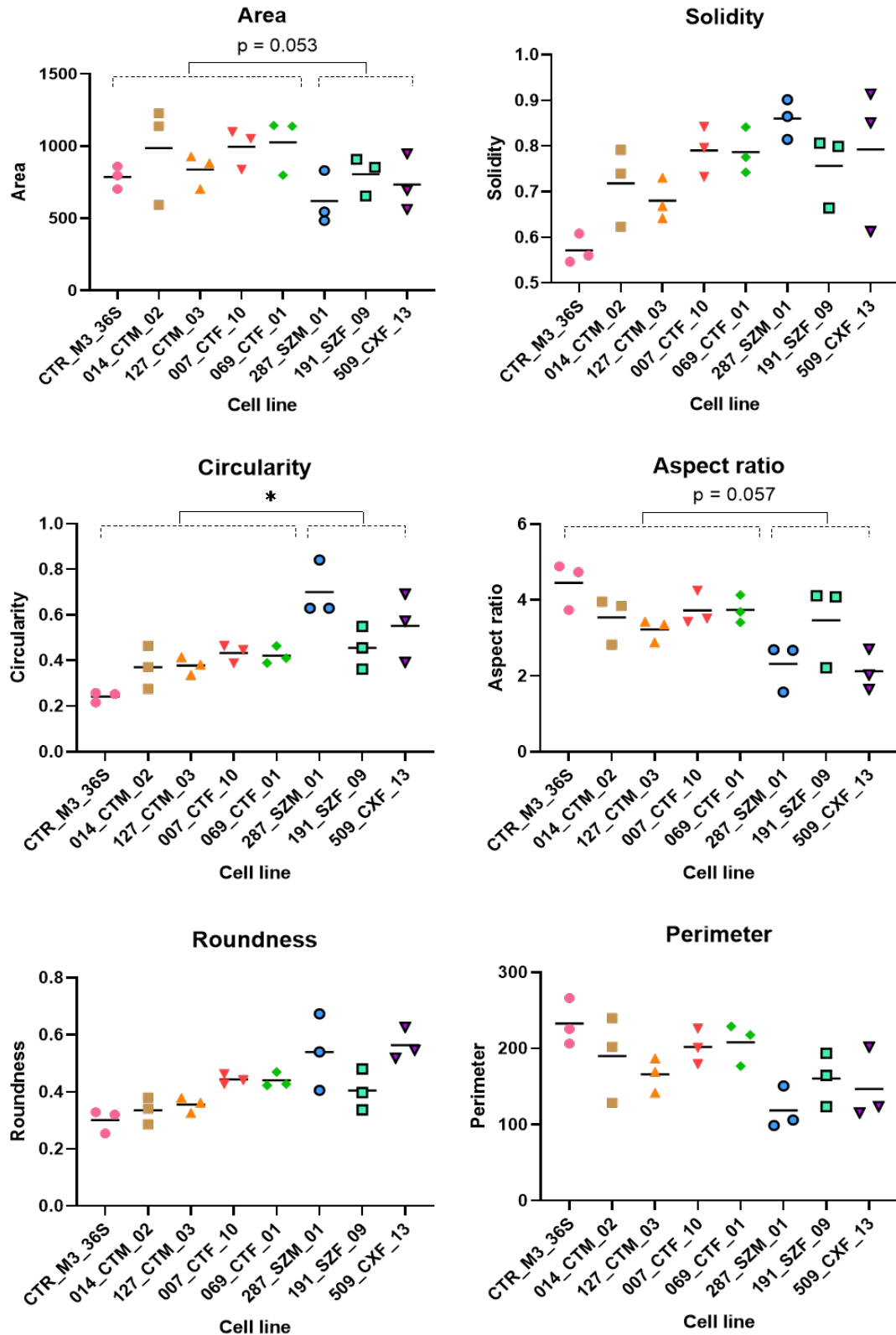


Figure 3. 13: MGL whole cell morphology and signature markers in 22q11.2DS cell lines compared to control MGLs. Morphological analysis of differences between control and 22q11.2DS MGLs treated with H_2O vehicle for 3 hours. Comparison groups consisted of N=3 day 14 differentiated 22q11.2DS MGLs vs N=5 day

14 differentiated control MGLs, with $n=3$ biological replicates being performed for each cell line. For statistical comparisons, means of control MGLs were compared to means of 22q11.2DS MGLs in one statistical test, not separately for each cell line. For each cell line, the mean of all biological replicates was calculated and used during statistical analysis. Data was checked for normal distribution. Unpaired two-tailed parametric t -test was used for statistical comparisons. Significant p values are indicated at follows: * = $p < 0.05$. Bars represent the mean of $n=3$ biological replicates for each cell line. Abbreviation: MGL, microglia-like cell.

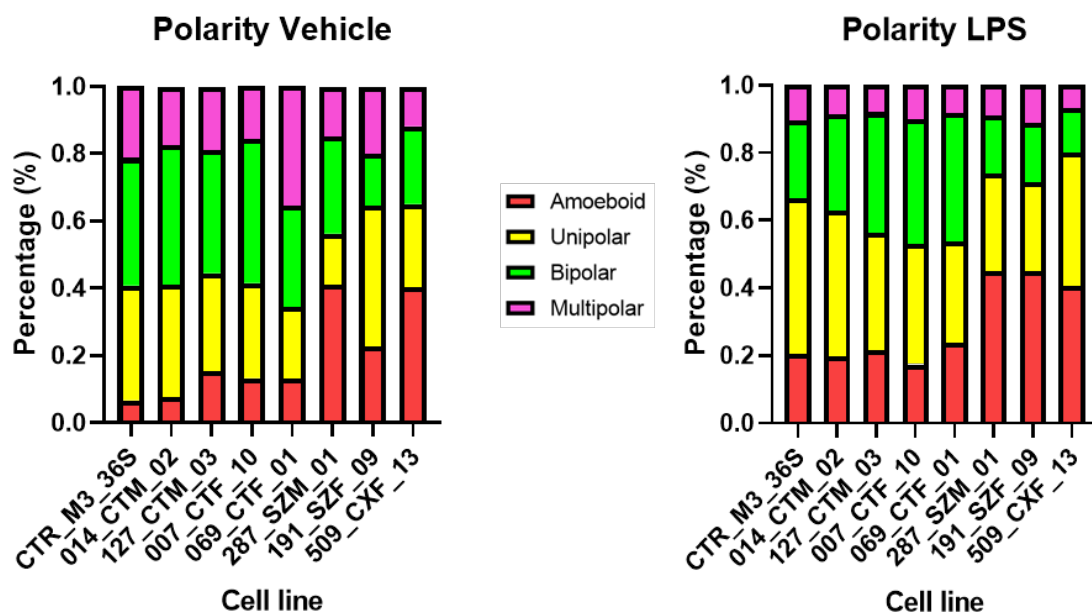


Figure 3. 14: MGL polarity in differentiated vehicle-treated and LPS-treated 22q11.2DS lines compared to vehicle-treated and LPS-treated control lines. Polarity analysis of differences between control and 22q11.2DS MGLs treated with LPS or H₂O vehicle for 3 hours. The figures illustrate the ratio between different polarity categories for each cell line. Average percentage of total cells within each polarity category for vehicle-treated control MGLs (left figure) were 21% amoeboid, 38% unipolar, 32% bipolar, and 9% multipolar. For vehicle-treated 22q11.2DS MGLs (left figure), this was 43% amoeboid, 32% unipolar, 16% bipolar, and 9% multipolar. Average percentage of total cells within each polarity category for LPS-treated control MGLs were 11% amoeboid, 29% unipolar, 38% bipolar, and 22% multipolar. For LPS-treated 22q11.2DS MGLs, this was 35% amoeboid, 27% unipolar, 23% bipolar, and 16% multipolar. Comparison groups consisted of $N=3$ day 14 differentiated 22q11.2DS MGLs vs $N=5$ day 14 differentiated control MGLs, with $n=3$ biological replicates being performed for each cell line. For statistical comparisons, means of control MGLs were compared to means of 22q11.2DS MGLs in one statistical test, not separately for each cell line. For each cell line, the mean

of all biological replicates was calculated and used during statistical analysis. Data was checked for normal distribution. By using a 2 x 2 ANOVA model for analysis with Bonferroni multiple correction, it was found that vehicle-treated 22q11.2DS MGL cultures had a significantly higher ($p < 0.05$) percentage of amoeboid cells and a significantly lower ($p < 0.05$) percentage of bipolar cells compared to control lines. In the context of LPS response, there was also an effect of genotype. The percentage of cells within control cultures became significantly more amoeboid ($p < 0.05$), but 22q11.2DS cultures did not significantly shift polarity after 3 hours with LPS. Abbreviations: LPS, lipopolysaccharide; MGL, microglia-like cell.

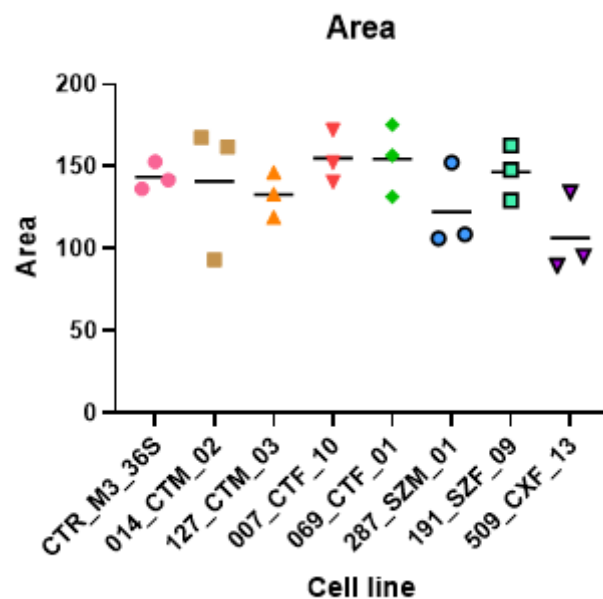


Figure 3. 15: Assessment of nuclei morphology in vehicle-treated control and 22q11.2DS MGLs. Analysis of differences between control and 22q11.2DS MGLs treated with H₂O vehicle for 3 hours. Comparison groups consisted of N=3 day 14 differentiated 22q11.2DS MGLs vs N=5 day 14 differentiated control MGLs, with n=3 biological replicates being performed for each cell line. For statistical comparisons, means of control MGLs were compared to means of 22q11.2DS MGLs in one statistical test, not separately for each cell line. For each cell line, the mean of all biological replicates was calculated and used during statistical analysis. Data was checked for normal distribution. Unpaired two-tailed parametric t-test was used for statistical comparisons. Bars represent the mean of n=3 biological replicates for each cell line. Abbreviation: MGL, microglia-like cell.

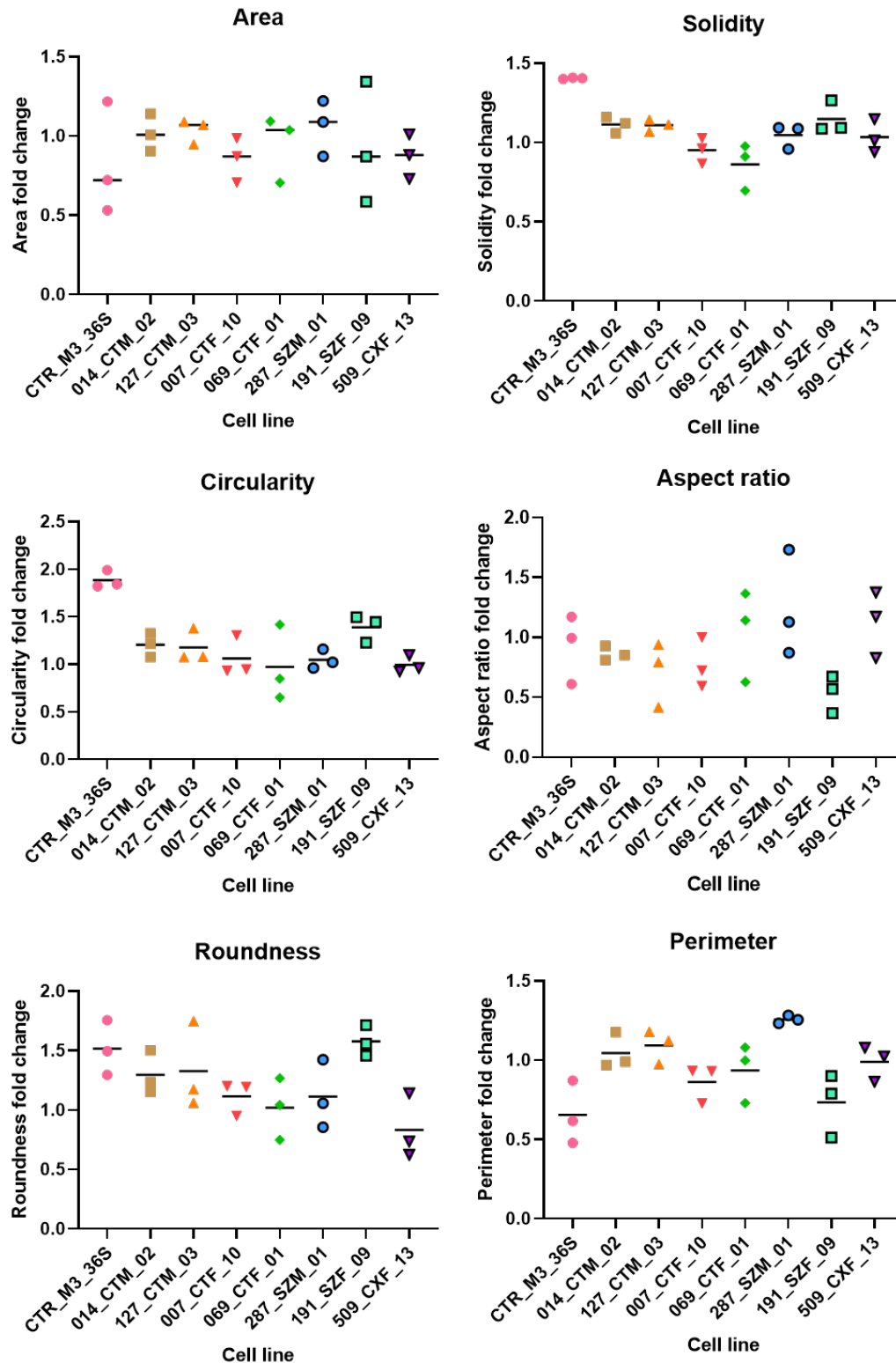


Figure 3. 16: MGL whole cell morphology and signature markers in 22q11.2DS cell lines compared to control MGLs in response to LPS. Morphological analysis of differences between control and 22q11.2DS MGLs treated with either H₂O vehicle or LPS for 3 hours. Effect of LPS treatment is shown as a fold change of the 3-hour LPS condition compared to the H₂O vehicle condition. Comparison groups consisted of N=3 day 14 differentiated 22q11.2DS MGLs vs N=5 day 14 differentiated control MGLs, with n=3 biological replicates

being performed for each cell line. For statistical comparisons, means of control MGLs were compared to means of 22q11.2DS MGLs in one statistical test, not separately for each cell line. For each cell line, the mean of all biological replicates was calculated and used during statistical analysis. Data was checked for normal distribution. Unpaired two-tailed parametric t-test was used for statistical comparisons. Bars represent the mean of n=3 biological replicates for each cell line. Abbreviations: LPS, lipopolysaccharide; MGL, microglia-like cell.

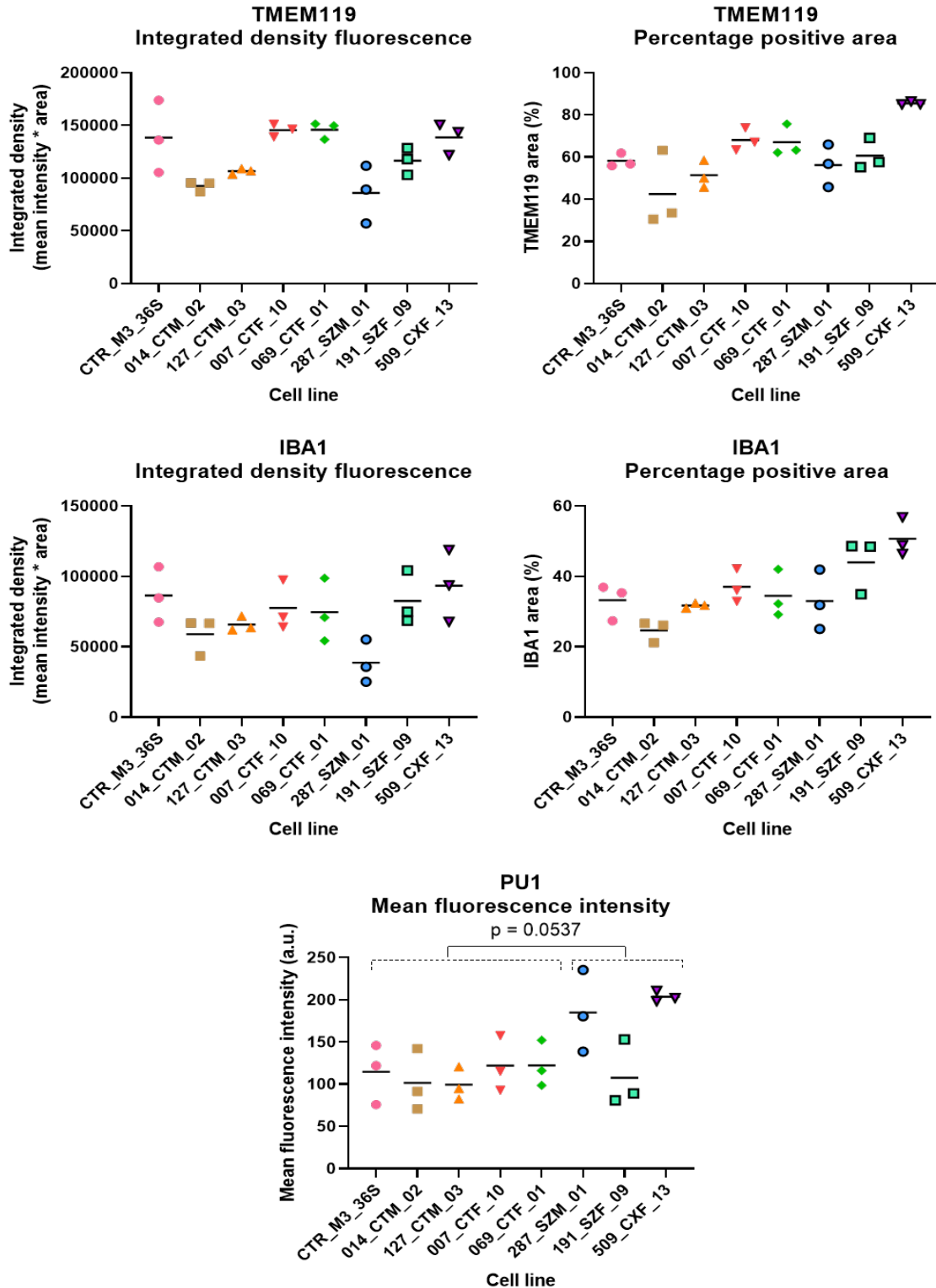


Figure 3. 17: MGL signature protein markers in 22q11.2DS cell lines compared to control MGLs. Protein marker analysis of microglia markers TMEM119, IBA1, and PU.1 including IBA/TMEM119 colocalisation in control and 22q11.2DS microglia treated with H₂O vehicle for 3 hours. Comparison groups consisted of N=3 day 14 differentiated 22q11.2DS MGLs vs N=5 day 14 differentiated control MGLs, with n=3 biological

replicates being performed for each cell line. For statistical comparisons, means of control MGLs were compared to means of 22q11.2DS MGLs in one statistical test, not separately for each cell line. For each cell line, the mean of all biological replicates was calculated and used during statistical analysis. Data was checked for normal distribution. Unpaired two-tailed parametric t-test was used for statistical comparisons. Bars represent the mean of n=3 biological replicates for each cell line. Abbreviations: MGL, microglia-like cell.

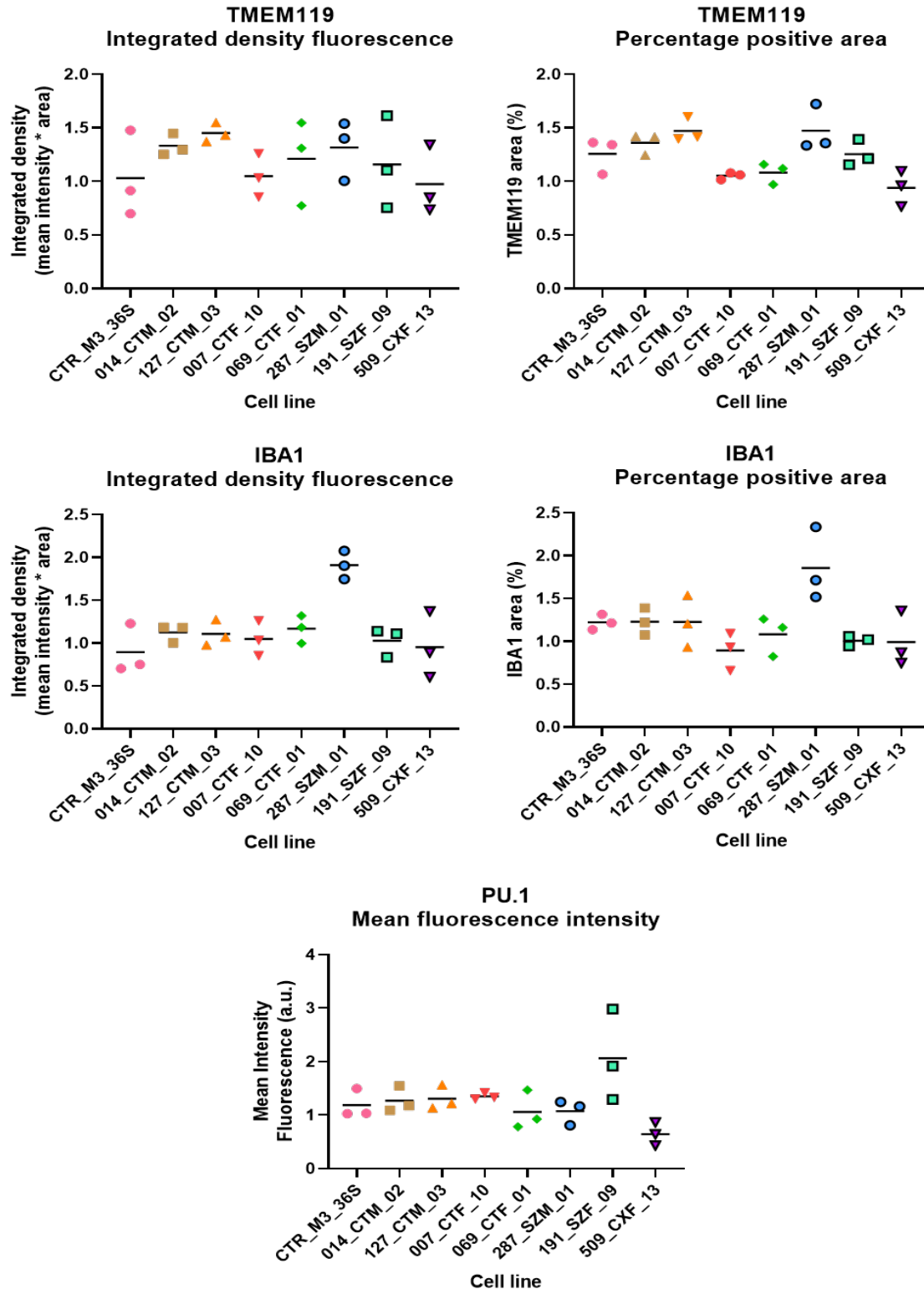


Figure 3. 18: MGL signature protein markers in 22q11.2DS cell lines compared to control MGLs in response to LPS. Protein marker analysis of microglia markers TMEM119, IBA1, and PU.1 including IBA/TMEM119 colocalisation in control and 22q11.2DS MGLs treated with either vehicle or LPS for 3 hours. Effect of LPS treatment is shown as a fold change of the 3 hour LPS condition compared to the H2O vehicle condition. Comparison groups consisted of N=3 day 14 differentiated 22q11.2DS MGLs vs N=5 day 14 differentiated

control MGLs, with n=3 biological replicates being performed for each cell line. For statistical comparisons, means of control MGLs were compared to means of 22q11.2DS MGLs in one statistical test, not separately for each cell line. For each cell line, the mean of all biological replicates was calculated and used during statistical analysis. Data was checked for normal distribution. Unpaired two-tailed parametric t-test was used for statistical comparisons. Bars represent the mean of n=3 biological replicates for each cell line. Abbreviations: LPS, lipopolysaccharide; MGL, microglia-like cell.

3.3.7. 22q11.2DS MGL TMEM119:IBA1 colocalisation is altered

For further analyses of proteins TMEM119 and IBA1 expression it must be noted that the majority of MGLs differentiated in this protocol are suspected be positive for both TMEM119 and IBA1 in control lines based initial pilot experiments (**Figure 3.7, Section 3.3.4, Chapter 3**). Also, while not quantified can be qualitatively observed in images from protein marker analysis as seen in **Figure 3.11** and **Figure 3.12, Section 3.3.6, Chapter 3** for all cell lines. Together this validates the protocol and could imply that the MGLs in these cultures are homogenous as least in the context of positive TMEM119 and IBA1 protein marker expression. Hence to best compare protein expression data collected in this project to Snijders et al. (2021), which found significant reduction of TMEM119 positive microglia also positive for IBA1, colocalisation analyses was deemed appropriate as it would take into account the ratio of both markers within each cell.

A significant ($p < 0.05$) difference was found in colocalisation of TMEM119 and IBA1 in vehicle-treated MGLs, with colocalization being higher in control MGLs compared to 22q11.2DS MGLs (**Figure 3.19**). In response to LPS, a significant difference was found between TMEM119 and IBA1 colocalisation fold change, with colocaliation decreasing more in control MGLs compared to 22q11.2DS MGLs (**Figure 3.20**).

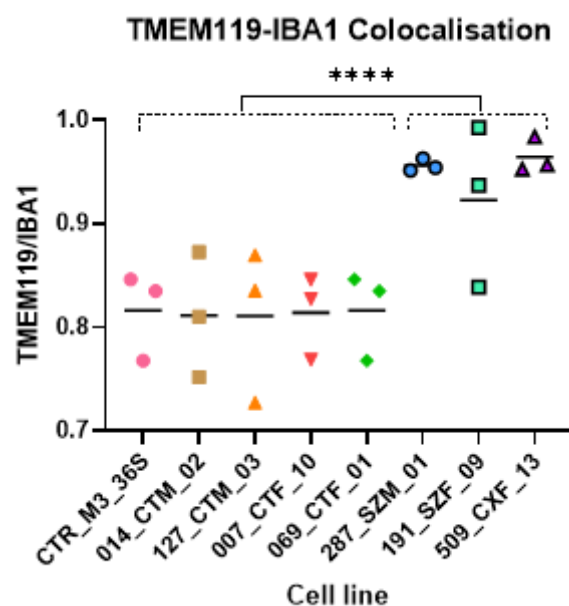


Figure 3. 19: Colocalisation of IBA1 and TMEM119 in control MGL compared to 22q11.2DS MGLs.

Analyses is performed on MGLs treated with H₂O vehicle for 3 hours. Comparison groups consisted of N=3 day 14 differentiated 22q11.2DS MGLs vs N=5 day 14 differentiated control MGLs, with n=3 biological replicates being performed for each cell line. For statistical comparisons, means of control MGLs were compared to means of 22q11.2DS MGLs in one statistical test, not separately for each cell line. For each cell line, the mean of all biological replicates was calculated and used during statistical analysis. Data was checked for normal distribution. Unpaired two-tailed parametric t-test was used for statistical comparisons. Significant p values are indicated at follows: **** = $p < 0.0001$. Bars represent the mean of n=3 biological replicates for each cell line.

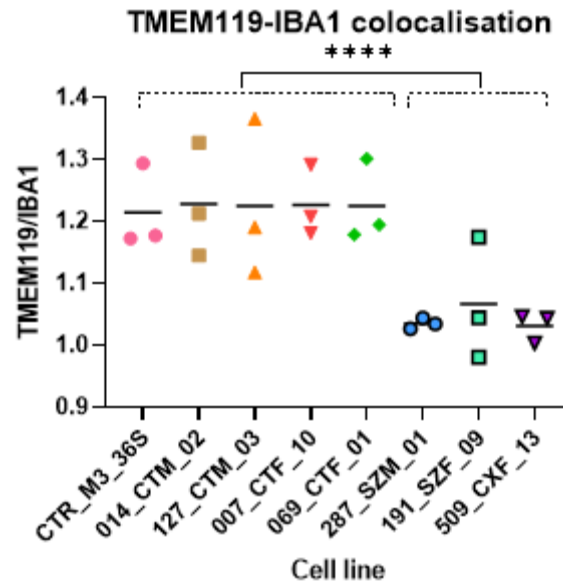


Figure 3. 20: Colocalisation of IBA1 and TMEM119 in control MGL compared to 22q11.2DS MGLs in response to LPS. MGLs were treated with either vehicle or LPS for 3 hours. Effect of LPS treatment is shown as a fold change of the 3-hour LPS condition compared to the H20 vehicle condition. Comparison groups consisted of N=3 day 14 differentiated 22q11.2DS MGLs vs N=5 day 14 differentiated control MGLs, with n=3 biological replicates being performed for each cell line. For statistical comparisons, means of control MGLs were compared to means of 22q11.2DS MGLs in one statistical test, not separately for each cell line. For each cell line, the mean of all biological replicates was calculated and used during statistical analysis. Data was checked for normal distribution. Unpaired two-tailed parametric t-test was used for statistical comparisons. Significant p values are indicated at follows: = $p < 0.0001$. Bars represent the mean of n=3 biological replicates for each cell line.

3.4 Discussion

This chapter provided confirmed 22q11.2DS cell line genotypes and established heterogeneity in genes affected by CNVs as well as PRS across 22q11.2DS cell lines. Initial evidence that differentiated MGLs using the Haenseler et al., (2017) obtain microglia-like phenotypes was provided. This study confirmed that a phenotype associated with typically microglia immune response could be observed in MGLs when stimulated with 1 ng/mL IL-1 β for 4 hours by or 100 ng/mL LPS for 3 hours. The data in this chapter demonstrates novelty by showing the first characterisation of 22q11.2DS MGLs. Morphology was found to be similar to what is observed in immune challenged microglia states without LPS stimuli, while colocalisation of TMEM119:IBA1 in MGLs both with and without LPS is affected by 22q11.2DS genotype.

3.4.1. Data summary

In terms of genotyping, only one cell line has the most common 22q11.2DS associated classic deletion, with others having distinct nested deletions within the critical region. The identification of duplications in two of the cell lines will have to be kept in mind due to potential alterations to genetic risk (Rees et al., 2014; Fiksinski et al., 2017), with 191_SZF_09 notably having three within the classic deletion region. Following the revelation of heterogenous deletions and identification of duplications, this diversity also applied to the estimated PRS of these cell lines. PRS calculations qualitatively showed that, relative to all other cell lines tested including control lines, the 509_CXF donor line has the highest polygenic risk for schizophrenia, 287_SZM has the highest PRS for neurodegenerative diseases Alzheimer's disease and Parkinson's disease, but also bipolar disorder type 2. 191_SZF on the other hand notably has the lowest PRS for schizophrenia of all these cell lines, while 509_CXF had the lowest risk for Parkinson's disease. Together, these data highlight that future 22q11.2DS data

outputs in this project cannot strictly be directly associated with a specific psychiatric disorder and any phenotypes identified should only be classified as potentially contributing phenotype to the pathophysiology of 22q11.2DS-associated conditions. Although potential relevance of Alzheimer's disease risk in 287_SZM might hurt validity of trying to categorise findings as a common phenotypes of 22q11.2DS-associated conditions, other conditions that PRS were calculated for have been previously associated with 22q11.2DS (Gothelf et al., 1999; Ousley et al., 2017; Boot et al., 2018; Mullins et al., 2021).

While no control lines indicate that they have the highest PRS for any assessed condition, it should re-highlighted that 069_CTF_01, which did not have PRS estimated, is suspected to carry a SNP in CHRFAM7A, as described in **Section 2.1, Chapter 2**, which could infer elevated risk for schizophrenia and Alzheimer's disease while being associated with an immune challenged microglia state (Sinkus et al., 2015; Ihnatovych et al., 2020). Hence while control lines appear to be suitable control lines, any differences in phenotype by 069_CTF_01 should be highlighted alongside 014_CTM_02, which did not have PRS estimated.

In experiments assessing the effect of 22q11.2DS on MGLs, an abnormal morphological state was observed which included increased circularity and percentage of amoeboid cells, and decreased percentage of bipolar MGLs in cultures. A change in morphological state was also observed in control MGLs following LPS treatment, making a significantly higher percentage of cells more amoeboid, while no change was observed in 22q11.2DS MGLs. 22q11.2DS also affects spatial proteomic state of MGLs, leading to lower colocalization of TMEM119:IBA1 MGLs without LPS treatment, and less reduction of TMEM119:IBA1 colocalisation following LPS. Together, these findings aligns with previously observed

morphological state observed in ASC and schizophrenia, and spatial proteomics state schizophrenia (Sanagi et al., 2019; Gober et al., 2021; Snijders et al., 2021), supporting this

3.4.2. 22q11.2DS cell line gene variants and polygenic risk towards 22q11.2DS - associated conditions are highly heterogeneous

As stated, the identification of distinct 22q11.2DS genotypes across 22q11.2DS cell lines may have implications for phenotypes in future work. Genotyping confirmed the presence of deletions in all 22q11.2DS cell lines which have been implicated as drivers of 22q11.2DS risk. This included *COMT*, whose expression was qualitatively confirmed to be decreased by at least 50% in MGLs, supporting validity of genotyping analysis. Work published by the Srivastava lab has also confirmed that *COMT* is reduced in hiPSC-derived midbrain dopaminergic neurons in a pilot study on 287_SZM and 191_SZF (Reid et al., 2022), validating the genotyping.

22q11.2DS line donors also do not have the same clinical presentation, which potentially could be explained by their genomic profiles. 509_CXF and 287_SZM have a clinical profile which includes ASC. Cell lines 509_CXF has nested deletion overlapping the LCR-A to LCR-B region, which is associated with increased risk of ASC (Clements et al., 2017). The classic LCR-A to LCR-D deletion in 287_SZM, whose done donor also has schizophrenia, also covers this area. Heterogeneity of clinical presentations has some implications for the study of MGLs. Without multiple donors with and without each clinical presentations it cannot be concluded that findings relate to diagnosis-associated symptoms (Li et al., 2019; Khan et al., 2020; Nehme et al., 2022). The importance of this was exemplified in Reid et al. (2022), which showed that a greater number of differentially regulated genes associated with dopamine metabolism and signalling in hiPSC-derived midbrain dopaminergic neurons in the

schizophrenia-positive 287_SZM line compared to the asymptomatic 191_SZF line, both of which are lines used in this study as well.

Cell line 191_SZF, whose donor has no clinical history, has several segmented CNVs in the 22q11.2 region. Deletions in 191_SZF also only partially cover the most common risk regions and is accompanied by a number of duplications. The presence of duplications within the 22q11.2 region is highly relevant, as they have previously been linked with increased risk of ASC as well as having been suggested to be a putative protective mechanism against schizophrenia, with no reported cases of schizophrenia being observed in individuals with 22q11.2 duplication syndrome (Rees et al., 2014; Fiksinski et al., 2017). In the large CNV study by Rees and colleagues which generated the protective mechanism hypothesis (Rees et al., 2014), the authors made this link to 1.5 Mb - 3 Mb duplications when describing this phenomenon, which are larger than what is present in 191_SZF. However, it is unclear to what extent each gene within duplications contributes to this protection and speculatively might explain the lack of schizophrenia diagnosis in the 191_SZF donor which is supported by aforementioned evidence published in Reid et al. (2022). A protective mechanism could hence be present in 191_SZF even though the donor of the 191_SZF cell has higher Ki^{cer} scores compared to control subjects tested in Rogdaki et al. (2021) (**Section 2.1, Chapter 2**; Reid et al., 2022). Genotype information is also hence critical alongside clinical history during interpretation of data.

In 22q11.2DS, several genes within the classic 22q11.2 deletion have been suggested to be driving forces behind several phenotypes in schizophrenia and ASC, including *COMT*. For example, virus-mediated reintroduction of *COMT* in mice with a 22q11.2DS rescues schizophrenia-like behavioural phenotypes (Kimoto et al., 2012). Other genes which are

suspected to be deleted in 22q11.2DS cell lines of this project includes *MRPL40* and *DGCR8*, but without additional validation to confirm this their expression levels are not clear. A study on 22q11.2DS mice identified *MRPL40* haploinsufficiency as a contributor to disruption of short-term synaptic plasticity via impaired calcium extrusion from the mitochondrial matrix (Devaraju et al., 2017). Reduced mitochondria ATP production and mitochondria protein levels has also been observed in 22q11.2DS hiPSC-derived neurons and in *MRPL40* heterozygous hiPSC-derived neurons (Li et al., 2019). Abnormalities in mitochondrial function would also have implications for MGL metabolomic state shifting for example when stimulated with LPS (Montilla et al., 2021). In isolated neurospheres from *DGCR8* knock-out mice and hiPSC-derived neurospheres from donors with 22q11.2DS, neurospheres for example appear smaller in size (Ouchi et al., 2013; Toyoshima et al., 2016). HiPSC-derived neurons with 22q11.2DS have also been suggested to display abnormal morphology when differentiated, but were not quantified (Toyoshima et al., 2016). Abnormal morphological states would match what is observed in 22q11.2DS MGLs, speculatively suggesting that 22q11.2DS impacts normal development of multiple cell types, but it is unclear if there is any genes that are drivers of this phenotype. However, these studies serve to show that single genes can be drivers of cellular phenotypes, and hence the heterogeneity of CNV numbers and sizes observed in 22q11.2DS hiPSCs may affect the phenotypes observed in 22q11.2DS MGLs. Again aforementioned work published in Reid et al. (2022) adds credence to this theory due to differences observed between 287_SZM, which has one CNV being the most common 22q11.2 deletion, and 191_SZF, which has multiple duplications that might interfere with MGL phenotypes. This potentially also extends to 509_CXF which has two larger duplications, although they are notably outside the LCR-A to LCR-D region which as noted in **Section 3.1.2, Chapter 3** is the deleted region with highest prevalence in individuals with 22q11.2DS.

Due to the access to the Infinium Psycharray dataset provided by the Srivastava lab, it was also possible to perform PRS of the 22q11.2DS lines as well as some control lines.

Cumulative risk estimated from genetic variants was generated for schizophrenia, ASC, bipolar disorder type 2, and Parkinson's disease which are all 22q11.2DS-associated psychiatric disorders, but also for Alzheimer's disease. Several studies have identified that higher PRS increases risk of schizophrenia in individuals with 22q11.2DS (Bassett et al., 2017; Bergen et al., 2019; Davies et al., 2020; Lin et al., 2023). The functional importance of estimating polygenic risk has also been established by Cleynen et al. (2021), which in their 22q11.2DS cohort found that individuals with high polygenic risk of schizophrenia had a higher rate of psychotic illness regardless of the presence of 22q11.2DS. Similarly, high schizophrenia PRS in individuals with 22q11.2DS additionally appears to strengthen behavioural symptoms as well as being associated with full scale cognitive decline as well as longitudinal volumetric reduction of left and right hippocampi (Alver et al., 2022). No data supporting on additional risk caused by high PRS in 22q11.2 deletion carriers have been published in the context of the other disorders. However, the effect of cell type must also be considered. Alzheimer's disease risk genes, but not schizophrenia and Parkinson's disease risk genes, have for example been characterised to be enriched in microglia (Skene et al., 2018). It should be noted that GWAS datasets utilised in this study are older than the ones used to generate PRS in this study. Enrichment results might hence be different if the more recently published datasets, which identified higher amounts of risk variants, are analysed (datasets used can be found in **Section 3.2.2, Chapter 3**). Additionally, it would be interesting if the analysis performed in Skene et al. (2018) could be performed on ASC and bipolar disorder type 2 GWAS summary statistics datasets.

In 22q11.2DS lines, 287_SZM was found to have high risk relative to other lines for Parkinson's disease and Alzheimer's disease, while 509_CXF had a high risk relative to other cell lines for schizophrenia. 509_CXF also presented low polygenic risk for Parkinson's disease compared to other lines. While the risk was not classified as low, 191_SZF has the lowest polygenic risk of all lines for schizophrenia. 191_SZF also as low polygenic risk of bipolar disorder type 2 compared to other cell lines. It is hence possible that disease-associated phenotypes might be less evident in this cell line, or rather that enough protective variants serve to reduce its overall PRS calculated with PRSice2, at least for schizophrenia (Rees et al., 2014). Together, this establishes PRS as potential source of variance among donors, which perhaps more so could affect 287_SZM due to established presence of Alzheimer's disease risk genes in microglia (Skene et al., 2018). Comparing the evidence previously described by Cleyne et al. (2021) to these findings, one would estimate that 509_CXF has a greater likelihood of developing psychosis symptoms compared to 287_SZM. However, 287_SZM is the only line with a clinical presentation of schizophrenia, implying that the differences in types of deletions might play a role.

When considering control lines with estimated PRS, no control lines had the highest PRS in any assessed condition when compared to other cell lines. However, the only control lines with the lowest PRS among tested lines were 127_CTM, which had the lowest estimated PRS for ASC and CTR_M3, which had the lowest estimated PRS for Alzheimer's disease relative to other lines. This suggests that some degree of polygenic risk exists in non-22q11.2DS cell lines, which could be relevant for potential findings and suggested that deeper sequencing studies are important. PRS estimation notably did not include control cell lines 069_CTF and 014_CTM as noted in methods **Section 3.2.2, Chapter 3**. This is relevant to re-emphasise here as it was revealed during the course of this study that 069_CTF has a suspected SNP

which confers elevated risk for schizophrenia with Alzheimer's disease as noted in **Section 2.1, Chapter 2**. This is specifically a missense mutation in the *CHRFAM7A* gene which has been associated with altered transcriptomic microglia state in an hiPSC-derived MGL model including NF- κ B activation and NF- κ B target transcription (Sinkus et al., 2015; Ihnatovych et al., 2020). It hence important to display data from individual donors even though means of control and 22q11.2DS MGLs are compared. This also serves as an example of why all utilised cell lines should undergo some degree of genotyping before proceeding with experiments.

When looking beyond the presence of 22q11.2 deletion on the effect of PRS on microglia form and function, there is relevant data for schizophrenia. PRS for schizophrenia based on microglial-expressed genetic risk variants have been associated with lower performance of several cognitive function in a manner comparable to PRS for schizophrenia based on neuronal risk variants (Corley et al., 2021). The association of lower performance in cognitive testing with microglial schizophrenia PRS was also found to be mediated via total grey matter volume in the UK Biobank (Corley et al., 2021). Of interest due to 22q11.2-associated risk, microglial PRS based on open chromatin regions has the strongest association with Parkinson's disease out of other compared cell types including neurons, astrocytes, oligodendrocytes and other immune cells (Andersen et al., 2021). This not only supports that microglia are also relevant to in the study of Parkinson's disease but is relevant for this study due to 287_SZM having the highest PRS for Parkinson's disease and 509_CXF having the lowest PRS of cell lines tested.

This underlines that phenotypes observed in 22q11.2DS MGLs might be varied dependent on CNV size and location, presence of duplications, clinical history, as well as PRS, highlighting the complexity of studying 22q11.2DS.

3.4.3. hiPSC-derived MGLs exhibit signature markers and functions

In order to check that the Haenseler et al. (2017) protocol could be independently replicated. Morphology was quickly distinguished qualitatively. It was also confirmed by qPCR that *P2RY12* expression is significantly higher in MGLs compared to macrophages, although this was notably not observed in Haenseler et al. (2017). It is however a relevant finding supporting that MGLs might, for example, have higher capability in motility and migration compared to macrophages which would be important for capturing cargo in eventual uptake experiments (Gómez Morillas et al., 2021). Live cell motility however is not assessed in this project to due constraints to time and resources (**COVID-19 Impact Statement**).

Furthermore, expression of other key signature genes *CIQA*, *GAS6*, *GPR34*, *PROS1*, *MERTK*, *TMEM119*, and *TREM2* assessed in the original publication was confirmed (Haenseler et al., 2017) while also adding *CD163*, *HLA-A*, and *CX3CR1*. A significant ($p < 0.05$) response to 4-hour IL-1 β treatment was shown at the transcriptome level, but only in MGLs, for *IL-6*, *IL-10* and *TSPO*. Together this pilot data implies that MGLs could be generated at a superficial level. Successful differentiation of male control hiPSC lines used in this study to MGLs has notably been further characterised in Couch et al. (2023)

Positive expression of all these genes were also confirmed for other cell lines in the RNAseq experiment later performed in **Chapter 4** alongside a transcriptomic response to LPS challenge. This transcriptomic profiling included all lines except for 127_CTM_03, but

characterisation of MGLs alongside RNAseq of MGLs from this cell line has importantly been published in Couch et al. (2023).

3.4.4. Characterisation of 22q11.2DS effect on hiPSC-derived MGL morphology

The altered morphology observed in MGLs is partially in line with previous evidence from non-iPSC models investigating schizophrenia and ASC in microglia. A significant increase in circularity and less ramified cells were seen in 22q11.2DS MGLs suggest that 22q11.2DS MGL morphological state have reduced arborisation compared to control MGLs.

Additionally, ratios of amoeboid, unipolar, bipolar and multipolar cells did not shift in 22q11.2DS MGLs following LPS stimuli. However, a higher percentage of cells in control MGL cultures became more amoeboid following the stimuli, perhaps suggesting that 22q11.2DS MGLs did not significantly shift morphological state in a similar way as a higher number of cells were already in this state. Control data is in line with live cell characterisation performed by Haenseler et al. (2017), with MGLs morphology becoming more amoeboid during LPS stimulation.

Altered microglial morphological state in schizophrenia have been shown in multiple studies on *postmortem* brains (Uranova et al., 2018; De Picker et al., 2021; Guber et al., 2021). In line with this study, reduced arborization has been observed in microglia in schizophrenia compared to neurotypical controls in *postmortem* tissue across frontal, temporal, and cingulate grey matter, as well as in subcortical white matter regions (Guber et al., 2021). There is however contrasting evidence. For example, De Picker and colleagues (2021) found microglia in the dorsal prefrontal cortex of individuals with schizophrenia to be less spherical. Cause of death and medication history are key factors limiting *postmortem* studies. It is important to note that De Picker and colleagues used 3D rendering to assess microglia

sphericity in their model, while most studies including this one has characterised microglia shape in 2D. It was elected to follow the more commonly utilised analysis approach to more accurately compare the data in this project to a higher amount of previously published data. But importantly, 3D sphericity and 2D circularity could hence, crucially, be different enough assessments to require a need for additional analysis in future work. A notable *postmortem* study by Uranova et al. (2018) importantly observed area of microglia could be related the onset of disease in schizophrenia, with *postmortem* tissue from those with early onset having microglia with larger area, with there being no difference in microglial area between controls and individuals with onset after the age of 21.

In ASC, reduced ramification of microglia has previously characterised using human *postmortem* tissue in the dorsolateral prefrontal cortex and grey matter but not in white matter of the temporal cortex when compared to samples from neurotypical individuals (Morgan et al., 2010; Lee et al., 2017; Fetit et al., 2021). This conflicts with evidence in animal models of ASC, highlighting the importance of a human model system. For example, conflicting evidence includes data from the medial prefrontal cortex of 2-week old mice with overexpression of *eIF4E*, which showed increased area of microglia, at least in male mice microglia measured by area (Xu et al., 2020). Analysis is notable not separated by sex in this project, but there are importantly no data trends in this direction (**Section 3.3.6, Chapter 3**)

In an ASC valproic acid marmoset model, the authors also found altered total areas of the cell body in their model, with the ASC marmosets showing higher total areas upon reaching adulthood, but notably significantly lower area at 2 months of age (Sanagi et al., 2019). This is interesting as 22q11.2DS MGLs do not exhibit significantly reduced area, but when also considering the human *postmortem* study by Uranova et al. (2018), it suggests the stage of development is relevant. Differences in microglia morphology during brain development has

been described in **Section 1.1.2, Chapter 1**. What did match what was observed in 22q11.2DS MGLs in Sanagi et al. (2019) was that circularity of microglia was significantly increased in their model from 3 months of age all the way to adulthood. However, the authors also observed solidity to be significantly lower in the ASC model at months 3 and 6, whereas solidity did not differ between control and 22q11.2DS MGLs (Sanagi et al., 2019).

Some relevant comparisons to other 22q11.2DS-associated conditions, specifically Parkinson's disease. As well as Alzheimer's disease is also appropriate based on PRS data (**Section 3.3.2, Chapter 3**). Microglia in the substantia nigra of human *postmortem* brain tissue from Parkinson's disease patients appear less ramified compared to control samples as observed in this study on 22q11.2DS MGLs (Doorn et al., 2014). Similarly, in human *postmortem* tissue from Alzheimer's disease patients, a lower amount of ramifications has also been observed, for example in microglia from the inferior parietal lobule (Franco-Bocanegra et al., 2021). This difference in morphological state has not been observed in *postmortem* tissue from individuals with bipolar disorder, at least in the medial frontal gyrus, (Sneeboer et al., 2019).

In addition to aligning findings in 22q11.2DS MGLs with those observed in 22q11.2-associated conditions to validate the model, MGL morphology may have relevance for functional phenotypes (Kettenmann et al., 2011; Vidal-Itriago et al., 2022), with a change to amoeboid morphology potentially being relevant for microglia when performing engulfment of debris as observed in the spinal cord of zebrafish (Morsch et al., 2015). In the developing zebrafish however, the opposite has been found in terms in the context of phagocytotic capacity, with this being increased in ramified microglia (Silva et al., 2021). Functional

studies, such as uptake assays, are necessary to see how these findings overlap in a human model such as the one used in this project.

3.4.5. Altered colocalisation of TMEM119 and IBA1 in both vehicle and LPS-treated 22q11.2DS MGLs compared to control MGLs

Following data published by Snjiders et al. (2021) on schizophrenia *postmortem* temporal cortex tissue showing a significant reduction in TMEM119 positive microglia also positive for IBA1, protein marker expression analysis was extended to assess whether differences could be observed in MGLs. While no differences were observed in intensity analyses with and without LPS for both these markers and including PU.1, colocalisation of TMEM119 and IBA1 was found to be significantly higher in 22q11.2DS MGLs compared to controls. When treated with LPS for 3 hours, control MGLs exhibited a significantly greater change in TMEM119-IBA1 colocalisation, increasing more compared to 22q11.2DS MGLs. As IBA1 is an actin-cross-linking protein associated with M-CSF-induced membrane ruffling (Sasaki et al., 2001), dysregulation of this marker, including lack of localisation-associated change in response to LPS challenge, may suggest an inability of 22q11.2DS MGLs to perform morphological rearrangement, at least at the same speed as control MGLs, which would have been interesting to assess in a live cell experiment but was not performed due to lack of time **(COVID-19 Impact Statement)**.

Snjiders et al (2021) importantly used a different approach when assessing the expression of IBA1 in their microglia. While cell lines used in this project appear heterogenous in terms of 22q11.2 deletions and polygenic risk, when compared to staining in Snjiders et al. (2021), close to 100% of MGLs was qualitatively observed to positively express the proteins IBA1 and TMEM119. As brain microglia are highly heterogeneous, how our cells potentially align

to brain microglia across regions is hence relevant, and this could act as either a strength or limitation to the study, with single-cell approaches being required to determine which sub-populations are present within MGL cultures. Consistent expression of TMEM119 however is relevant when comparing data to microglia studies on Alzheimer's disease, as loss of TMEM119 positive cells have been observed in Alzheimer's disease microglia in human *postmortem* middle temporal gyrus tissue in both white and grey matter (Kenkhuis et al., 2022). This is also the case in temporal cortex *postmortem* tissue from individuals with schizophrenia (Snijders et al., 2021). A notable observation in the previously mentioned ASC valproic acid marmoset model showed additional segmented IBA1 positive thin process-like structures compared to controls (Sanagi et al., 2019). While percentage area covered in the whole cell of MGLs were not significantly different or changed with LPS stimuli, the analysis performed in this project looking at TMEM119 and IBA1 colocalisation supports that expression of TMEM119 and IBA1 is still affected in 22q11.2DS MGLs, which could have implications for functions as TMEM119 is a regulatory homeostatic marker and IBA1 have, for example, been implicated in phagocytosis (Ohsawa et al., 2004; Kenkhuis et al., 2022; Ruan and Elyaman, 2022)

3.4.6. Limitations and considerations for future work

One could argue that the diversity of CNVs within the 22q11.2 region in 22q11.2DS cell lines, and even of CNVs outside the 22q11.2 region in control lines used in this study, results in too much potential variability, questioning the reproducibility and robustness of this model. The information provided and generated for each cell line however allows for consideration of such factors. In an ideal model, one would perhaps consider the implementation of or a switch to an isogenic model, inserting a classic 22q11.2DS CNV in a control line. Alternatively, the CNV in a 22q11.2DS cell line with the classic deletion could

be repaired to control for the potentially added polygenic risk related to the cumulative effect of genes outside the 22q11.2 region. If possible, one could also utilise it alongside other 22q11.2DS lines to support validation of the data (Li et al., 2019). The process of studying larger CNVs rather than single gene variants using CRISPR/Cas9 has now been more well characterised compared to the time of study initiation (Grajcarek et al., 2019; Kotini and Papapetrou, 2020). This highlights a potentially altered study approach for future work focusing on more in-depth characterisation using, for example, cell line 287_SZM_01 which has the classic most common 22q11.2DS deletion. Yet, due to potential diversity of individuals diagnosed with 22q11.2DS, it can also be considered unreasonable to only study one part of this CNV when modelling 22q11.2DS.

Lack of clinical presentation and polygenic risk for conditions potentially associated with microglia could as seen in cell line 191_SZF affect outcome of results, with the protein marker expression of PU.1 in this line compared to other 22q11.2DS cell lines clustering more alongside controls, rendering the result insignificant. The result is still however meaningful, as while elevated PU.1 has been associated with a more a microglia phenotype linked to immune response, reduced PU.1 has contrastingly been suggested to attenuate microglia immune response, including reduction of phagocytic activity (Zhou et al., 2019; Pimenova et al., 2020, 2021). While this work was done in the context of Alzheimer's disease, it is also highly relevant for studying the impact of 22q11.2 CNVs due to the role of microglia in synapse formation and elimination. It could also hence be hypothesised that 191_SZF might continue clustering more alongside control cell lines.

Time-course of experimental design might be the underlying reason why no changes in protein expression was observed in response to LPS challenge. Enforcement of reduced time

in the laboratory, resources and cancellations of ongoing experiments due to national lockdowns made this impossible to characterise as stated in the **COVID-19 Impact Statement**. Future work should consider the potential of more chronic treatment of MGLs as while microglial form does not always insinuate function, LPS treatment has been noted to shift microglia to a more amoeboid state in the past during longer treatments in rodent models and hence other differences could be observed in hiPSC-derived MGLs (Chen et al., 2012; Lively and Schlichter, 2018). Due to the more circular shape of 22q11.2DS MGLs compared to controls when only treated with vehicle, a blunted response in 22q11.2DS MGLs could be predicted. Live-cell motility experiments as performed in Haenseler et al. (2017) and longer treatment studies support future investigations which ideally aims to address whether differences in 22q11.2DS MGL morphological state has implications for functional phenotypes.

3.5 Conclusions

Taking together 22q11.2DS cell line genotype data mining and the polygenic risk data, it is shown that genetic architecture both inside and outside the 22q11.2 region is variable which could have implications for findings. The effect of each variant within the region is unknown, and it is unknown whether this is a cumulative effect due to variability in PRS or whether there is single or sets of fewer variants driving the clinical manifestation. It is necessary to be aware of the potential for protective, non-pathological and diverse phenotypes in 22q11.2DS MGL due to genetic information identified.

The robustness of the Haenseler et al. (2017) protocol was validated. MGLs morphological and spatial proteomic state appears to be affected by 22q11.2DS genotype. Morphological state appears to match human *postmortem* data in 22q11.2DS-associated neurological

disorders with the exception of bipolar type 2 disorder. Spatial proteomic state differences does not exactly replicate observations in human *postmortem* Alzheimer's disease and schizophrenia studies due to staining differences seen in percentage of positive cells, but colocalisation data still indicates that dysregulation TMEM119 and IBA1 protein markers is present. Overall, colocalisation data alongside morphology data indicates that functional assays such as uptake of cargo should be performed. The established genetic information will also support discussions on how this impacts phenotype in future chapters.

This chapter did not address how 22q11.2DS affects non-morphological and protein marker phenotypes potentially affected such as cytokine release and phagocytosis. How 22q11.2DS affects these more complex functions was further investigated following this confirmation of genotype differences and can be found detailed in further chapters.

Chapter 4:

Transcriptomic profiling of 22q11.2DS MGLs and their response to LPS

4.1 Introduction

4.1.1. Utility of bulk RNA sequencing

Bulk RNA sequencing is a sensitive high-throughput tool for studying transcriptomic profiles of multiple samples in parallel (Wang et al., 2009). In the context of microglia, bulk RNA sequencing can be used to identify genes that are differentially expressed under physiological or pathological conditions, such in response to various stimuli, including injury and infections such as those by bacterial toxins like LPS (Bennett et al., 2016; Gosselin et al., 2017; Holtman et al., 2017). This also extend to studying differences in microglia transcriptomic state in a disease context (Carlström et al., 2021). Tissue from idiopathic donors as well as those with genetic predisposition such as deletions in the 22q11.2 region can be analysed for differentially expressed genes (Bhat et al., 2022; Nehme et al., 2022). Comparing bulk RNA sequencing data with other published genomic data further provide better understanding of the molecular mechanisms which differentially expressed genes might affect by using methods such as gene ontology analysis setting a precedence for further functional experiments (Liao et al., 2019). Analysis can also extend to comparisons to published microglia datasets, including identifying overlap in transcriptomic profiles (Jao and Ciernia, 2021). It is critical to note that while bulk RNA sequencing does not separate microglial subpopulations within cultures as with single-cell RNA sequencing as it provides an average gene expression profile of all cells in the sample, but it is a more cost-effective approach to that is suitable for studying the overall transcriptomic profile of a single cell type in

monoculture, keeping in mind that heterogenous cell populations might exist (Wang et al., 2009; Li and Wang, 2021). Analyses approaches by tools such as the MGENrichment application (Jao and Ciernia, 2021) do however allow researchers to partially bridge this gap in monoculture experiments by addressing overlap of microglia monoculture with subpopulation identified by single-cell RNA sequencing.

4.1.2. Relevance for transcriptomic profiling of hiPSC-derived 22q11.2DS MGLs

Immune response in the central nervous system is primarily driven by microglia, which has increasingly been implicated in psychiatric disorders. In a 2017 meta-review assessing blood and cerebrospinal fluid samples, *in vivo* neuroimaging data, and *postmortem* tissue findings, aberrant immune responses such as that of microglia along with altered neuroplasticity was linked to schizophrenia (De Picker et al., 2017). Findings include transcriptomic changes in blood and *postmortem* brain associated with increased innate immune response, increased cytokine levels in blood associated with innate immune response, and increased number of microglia in *postmortem* tissue (De Picker et al., 2017). Aberrant microglia transcriptomic states have also been described in analysis of schizophrenia, ASC, and bipolar disorder *postmortem* brain tissue, and in induced microglia from blood monocytes donated by individuals with schizophrenia (Gupta et al., 2014; Gandal et al., 2018; Ormel et al., 2020). With relevance to non-psychiatric disorders linked with 22q11.2DS such as Parkinson's disease and Alzheimer's disease (relevance discussed in **Chapter 3**), altered microglia transcriptomic state has also been established in both of these disorders looking isolated cells from four different brain regions which included the medial frontal gyrus, superior temporal gyrus, subventricular zone and thalamus (de Paiva Lopes et al., 2022). An effect of 22q11.2DS on the transcriptomic signature has previously been characterised in hiPSC-derived neuronal cells, T cells isolated from peripheral blood and whole peripheral blood,

with profiling of the latter two sample types implicating immune response and cytokine signalling, but it is unknown whether such changes are reflected central nervous system microglia (Jalbrzikowski et al., 2015; Lin et al., 2016; Khan et al., 2020; Lin et al., 2021; Nehme et al., 2022; Raje et al., 2022). RNA sequencing would provide an unbiased perspective on the molecular phenotype of 22q11.2DS microglia as well as provide data that can determine future functional testing.

While there is clearly evidence of aberrant immune response in microglia, large-scale studies have been limited to the use of *postmortem* tissue. In *postmortem* studies, microglia form and function may have throughout lifespan been influenced by environmental cues by local cell types such as neurons (Umpierre and Wu, 2021). *Postmortem* studies also generally reflect end of life, so conclusions on disease processes relevant for development might be limited, but samples are also affected by medication, such as anti-psychotics (Chan et al., 2011), and lifestyle factors such as smoking, which has been shown to affects reduce microglia process and increase cytokine production in animals (Ghosh et al., 2009; Long et al., 2023). In studies of disease, it is hence important to be able to identify what cues are coming from each cell type, so bulk RNA sequencing would be a useful approach in monocultured cells.

Additionally, *postmortem* studies are unable to determine the effect of stimuli that elicits an immune response such as by LPS challenge, which is known to robustly induce an immune response including an increase in cytokine production of proteins such as IL-1 β , IL-6 and TNF- α (Ormel et al., 2020). It is a critical area lacking research, with Ormel et al. (2020) and being the only human studies to characterise an enhanced response to LPS by using induced microglia from blood monocytes donated by individuals with recent-onset schizophrenia, such as by secretion of TNF- α compared to controls. Ormel et al. (2020) did however not assess the transcriptome in schizophrenia samples, so differences in LPS was not compared.

As induced microglia from blood monocytes could potentially retain epigenetic changes, it is an interesting model to study post-pathogenesis, but models that theoretically should not retain any epigenetic modification, such as the hiPSC model, might be more preferred in studying pathogenesis as microglia acquire their homeostatic immune-sensing properties early in development (Kracht et al., 2020). The microglia differentiation protocol used in this project also importantly have a transcriptomic profile similar to fetal microglia (Haenseler et al., 2017). With regard to aforementioned *postmortem* studies which reflect end of life, hiPSCs might be a preferred model due to cells having no previous influence from non-microglial cells while also avoiding potential stress response during isolation.

4.1.3. Importance of exploring the effect of LPS challenge on the hiPSC-derived 22q11.2DS MGL transcriptome

There has been increasing evidence that exposure to infection during brain development and the resulting immune response is an environmental risk factor for psychiatric disorders such as schizophrenia, bipolar disorder and ASC (Canetta et al., 2014; Estes & McAllister, 2016), highlighting the importance of studies microglia in a context-dependent manner. This viral exposure or induction of maternal immune activation can lead to sustained changes in microglia motility and behavioural changes in a Poly:(I:C) mouse model (Ozaki et al., 2020). In humans, it is possible that smaller particles such as maternal cytokines can enter the fetal brain during development due to the blood-brain barrier being established at a later stage (Adinolfi, 1985). As microglia are critical for normal brain development (Paolicelli et al., 2011), inability of microglia to respond to environmental stimuli in a homeostatic manner could as such be a key driver in ASC or schizophrenia pathogenesis. For example, if a chronic elevation of cytokines is induced through this exposure, it would correlate to what is

seen peripheral blood studies suggesting that increased cytokine levels is part of schizophrenia and bipolar disorder aetiology (Lesh et al., 2018).

As human and other animal systems are genetically divergent, use of a human model is critical to truly understand this environmental risk factor. Studies on immune challenges in early developmental models have also primarily been limited to neurons, and while they are also capable of exhibiting an immune response (Bhat et al., 2022), microglia are the primary immune cells of the brain. Couch et al. (2023) was the first study to present transcriptomic profiling of hiPSC-derived MGLs in the context of IL-6 challenge, a cytokine used to model MIA (Graham et al., 2018; Mueller et al., 2021; Ozaki et al., 2020). The publication, using two of the control lines sequenced in this study, described that these hiPSC-derived MGLs are capable of showing a prototypical myeloid response, with differentially up-regulated genes also showing overlap with human brain tissue findings from schizophrenia, ASC and bipolar disorder patients (Gandal et al., 2018; Couch et al., 2023). It is hence interesting to see whether a different broader treatment using LPS is able exhibit a similar response, and whether this response can be replicated in 22q11.2 MGLs. Like IL-6, LPS has been used to model MIA in animal models. Differences in microglia response has been described in these models compared to controls.

It is possible the 22q11.2DS MGLs might, for example, have an enhanced response to LPS compared to controls as seen in Diz-Chaves et al. (2012, 2013), where prenatally stressed mice had an exaggerated response to LPS including induction of more substantial increases in *IL-1 β* and *TNF- α* expression in the hippocamps compared to unstressed mice. Microglia, at least in rodent models, have been shown that they may be capable of launching an exaggerated response following immune challenge in disease conditions, which for example

includes induction of *IL-1 β* transcripts (Palin et al., 2008; Ramaglia et al., 2012; Norden et al., 2015). As previously noted, Ormel et al. (2020) is the only published study to describe an enhanced response using a human *in vitro* model system in the context of schizophrenia, but transcriptomics was not performed on these samples so there is a lack of clarity surrounding the underlying molecular changes that might cause this response. In the context of available data on 22q11.2DS MGLs, this thesis previously in **Chapter 3** identified differences in morphological phenotypes and protein marker colocalisation in both vehicle and LPS-treated conditions when compared to control MGLs. Transcriptomic profiling of these cells will benefit identification of differences underlying molecular mechanisms and potential functional tests.

4.1.4. Aims and hypotheses

With no previous data being available on the transcriptomic profile of 22q11.2DS MGLs, this exploratory hypothesis-free analysis aims to do the following to support choice of further functional testing:

1. Determine the effect of 22q11.2DS on the MGL transcriptomic profile
2. Assess the transcriptomic response of control and 22q11.2DS MGLs to LPS
3. Characterise any differences in LPS transcriptomic response between control and 22q11.2DS MGLs

4.2 Methods

Four control (two male, two female) and three 22q11.2DS (1 male, 2 female) hiPSC lines were differentiated into microglia and treated with either vehicle or LPS for 3 hours. MGLs or macrophages were differentiated as described in **Chapter 2, Section 2.3**, and **Section 2.4**. Treatments with either vehicle or LPS for 3 hours was performed as described in **Chapter 2, Section 2.5**. One biological replicate (defined in **Section 2.8, Chapter 2**) from each of the cell lines in **Table 4.1** were used in this chapter.

4.2.1 RNA library preparation and NovaSeq Sequencing

To obtain RNA sequencing samples, total RNA was extracted as described in **Chapter 2, section 2.6** from MGLs treated with H₂O vehicle or LPS for 3 hours. Samples were submitted for sequencing at the GENEWIZ Ltd, which has now been acquired by Azenta Life Sciences Inc (Burlington, Massachusetts), where libraries were prepared using a polyA selection method with the NEBNext Ultra II RNA Library Prep Kit for Illumina (NEB, Ipswich, MA, USA), quantified with a Qubit 4.0 Fluorometer (Life Technologies, Carlsbad, CA, USA), and quality controlled with RNA Kit on an Agilent 5300 Fragment Analyzer (Agilent Technologies, Palo Alto, CA, USA) to ensure RNA integrity. Libraries were multiplexed and loaded on the Illumina NovaSeq 6000 instrument at a 2x150bp configuration. The associated NovaSeq Control Software (v1.7) was used for image analysis and base calling. Output data provided by GENEWIZ from Azenta Life Sciences and shown in **Table 4.1**. Raw data was provided by GENEWIZ from Azenta Life Sciences in the .fastq format for analysis.

Sample cell line	Treatment	# Reads	Yield (Mbases)	Mean Quality Score	% Bases >= 30
014_CTM_02	Vehicle	22,443,381	6,733	35.05	89.47
014_CTM_02	LPS	20,980,463	6,294	35.43	91.37
CTR_M3_36S	Vehicle	18,885,903	5,666	35.12	89.81
CTR_M3_36S	LPS	22,355,260	6,707	35.11	89.64
007_CTF_10	Vehicle	22,657,058	6,797	35.02	89.12
007_CTF_10	LPS	20,181,578	6,054	34.92	88.71
069_CTF_01	Vehicle	18,601,011	5,580	35.04	89.27
069_CTF_01	LPS	20,717,623	6,215	34.98	88.97
287_SZM_01	Vehicle	21,809,306	6,543	35.23	90.25
287_SZM_01	LPS	22,210,270	6,663	35.32	90.81
191_SZF_13	Vehicle	48,274,164	14,482	35	89.07
191_SZF_13	LPS	22,045,591	6,614	35.17	90
509_CXF_11	Vehicle	22,825,256	6,848	35.15	89.76
509_CXF_11	LPS	21,045,934	6,314	35.29	90.57

Table 4. 1: Overview of sequencing sample details. Initial quality control analysis by GENEWIZ from Azenta

Life Sciences yielded an overall average yield (Mbases) of 6,956, mean quality of 35.00 and % Bases >= 30 of 90 (Individual sample values seen in Table 4.1). Abbreviations: LPS, liposaccharide.

4.2.2. RNAseq sample processing

Initial sample processing was performed within the cloud-based high performance cluster within the Rosalind Research Computing Infrastructure which was accessed through King's College London. Processing was run through the Linux-based software Ubuntu (version 20.04) through secure shell (SSH) login nodes. FASTQC was performed for quality control of RNA sequencing reads (version 0.11.9) (<http://www.bioinformatics.babraham.ac.uk/projects/fastqc/>). FASTQ files were auto-trimmed and mapped to the human reference genome (GRCh38/Hg38) using STAR (Spliced Transcripts Alignment to a Reference) (version 2.7.6a) (Dobin et al., 2013). Binary BAM files generated by STAR was converted to text-based SAM alignments using SAMtools (H. Li et al., 2009). Count matrices were prepared using *featureCounts*, mapping the number of reads onto each gene using Ensembl gene annotations for Hg38 (version 99) (Liao et al., 2014). Output files were then extracted from the cloud server onto a local hard drive. Further processing and downstream analysis were carried out in R version 4.0.2 (R Core Team, 2020). Raw gene counts and filtered by removing unexpressed genes, 20 % of genes with the lowest gene expression, and genes raw gene counts under 10 in all samples. These were identified before the actual filtering occurred and cuts were not carried out in order, meaning that for example that the 20% of genes with lowest raw gene counts included unexpressed genes when being selected for filtering. Gene classifications were then generated using the biomaRt R package (Smedley et al., 2015). Protein coding and non-protein coding genes, which were classified as part of the biomaRt processing, were separated with Microsoft Excel's built-in sorting function using an Excel sheet directly extracted from the biomaRt classification process that included gene biotype in row 1, of which the column consisted of the different such biotypes. All genes that were classified as protein coding genes were kept for analysis.

4.2.3. Differential gene expression

Differential gene expression analysis was then carried out using the DESeq2 R package (version 1.30.1) with the default Wald test in Bioconductor (version 3.12) (Love et al., 2014; Huber et al., 2015). PCA was performed on the DESeq2 processed files using DESeq2's built-in PCA function which uses another R package, *ggplot2* (Wickham, 2016), to help visualise variation between samples. When data was extracted at multiple thresholds, genes not meeting criteria was filtered out using a built-in R function allowing manipulation of large Microsoft Excel documents. Thresholds included the following with their use being stated when appropriate: Benjamini-Hochberg (BH) adjusted P values, or padj , of < 0.05 with LogFoldChange of 1.5, p-value 0.001 with LogFoldChange of 1.5, and p-value 0.001 with LogFoldChange of 0.5. Differential gene expression analysis was performed three ways: Vehicle-treated control vs vehicle-treated 22q11.2DS, vehicle-treated control vs LPS-treated control, and vehicle-treated 22q11.2DS vs LPS-treated 22q11.2DS. When running this analysis, DESeq2 generates normalised gene counts, which was also extracted from the analysis to generate heatmaps of expression levels of chosen genes by extracting normalised gene count values into GraphPad Prism 9.3 for Windows 11 (GraphPad Software, La Jolla California USA, <https://www.graphpad.com/scientific-software/prism/>). To normalise gene counts, DESeq2 uses a median of ratios method where raw counts are divided by sample-specific size factors determined by median ratio of raw gene counts relative to geometric mean expression per gene. Lastly, an interaction effect analysis was also performed using a built-in DESeq2 feature in the DESeq2 R package (version 1.30.1), yielding the difference between the condition effect for 22q11.2DS genotype and the condition effect for the reference control genotype. The threshold for interaction effect analysis was BH adjusted padj of < 0.05 with LogFoldChange of 1.5

4.2.4. Gene enrichment analysis

For each significance threshold generated with DESeq2 analysis, genes were sorted into up- and down-regulated lists based on their positive or negative Log2FoldChange. Microsoft Excel's built-in sorting function was used with an excel sheet consisting of DESeq2 output. Sorting was done using the column with Log2FoldChange in Row 1. Genes not meeting the respective fold change threshold, for example a value of 1.5 or -1.5 Log2FoldChange, were filtered out manually. Subsequently, the same sorting approach was applied to columns with padj or pvalue in row 1 based on threshold utilised. The sheet was then saved as a separate file which was used for analysis. The process was repeated on a backup of the DESeq2 output sheet when starting filtering of genes for the next threshold. This generated a gene list for up-regulated genes and a another for down-regulated genes at each significance threshold. To compare our output with gene lists of other published work on microglia, each list from all thresholds were inputted into the web-based MGENrichment application (Jao and Ciernia, 2021). MGENrichment outputs were filtered for 1 % FDR and only studies using human tissue due to species-related heterogeneity which was discussed in **Section 1.1.5, Chapter 1**. Outputs were also filtered for relevance, with data sets showing overlap with genes of non-relevant conditions to or phenotypes 22q11.2DS being excluded.

4.2.5. Gene ontology analysis

Gene ontology analysis was carried out using WebGestalt (Liao et al., 2019) for each gene list generated and used in gene enrichment analysis. Gene lists were tested for over representation of non-redundant cellular component, biological process and molecular function gene ontology terms. The pathway Reactome database was also searched. A threshold of 5 % FDR was set and values were corrected for multiple testing using the BH method. Top hits across were illustrated regardless of significance output where noted.

4.3 Results

To support clarity in description and discussion of differentially expressed gene (DEG) data, an overview of the signatures generated is provided here:

- Signature A: Vehicle-treated control MGLs vs vehicle-treated 22q11.2DS MGL. (i.e., differences in gene expression between 22q11.2DS MGLs and control MGLs treated with vehicle).
- Signature B: LPS-treated control MGLs vs vehicle-treated control MGLs (i.e., the effect of 3-hour LPS challenge on gene expression in control MGLs).
- Signature C: LPS-treated 22q11.2DS MGLs vs vehicle-treated 22q11.2DS MGLs (i.e., the effect of 3-hour LPS challenge on gene expression in 22q11.2DS MGLs).
- Signature D: Interaction effect of LPS challenge in 22q11.2DS MGLs vs in control MGLs (i.e., how the transcriptional response to 3-hour LPS challenge differs in 22q11.2DS MGLs compared to control MGLs).

4.3.1. Control and 22q11.2DS MGLs express key microglia genes and qualitative confirmation of common deleted genes in 22q11.2DS MGLs cell lines

To support additional validation of the Haenseler et al. (2017) MGL differentiation protocol, a heatmap of key microglia/monocyte genes also assessed by microarray in Haenseler et al. (2017) was generated (**Figure 4.1**). Compared to Haenseler et al. (2017) All genes except for the genes *CLEC6A*, *CNR2*, and *CNRI* were positively expressed in MGLs based on normalised gene counts which had previously been filtered for lowly expressed genes (**Section 4.2.2, Chapter 4** and **Section 4.2.3, Chapter 4**). As these genes have low expression in monocultured hiPSC-derived microglia-like cells in Haenseler et al. (2017), this

still aligns with that dataset, as these could have been excluded during filtering of genes with low or no expression.

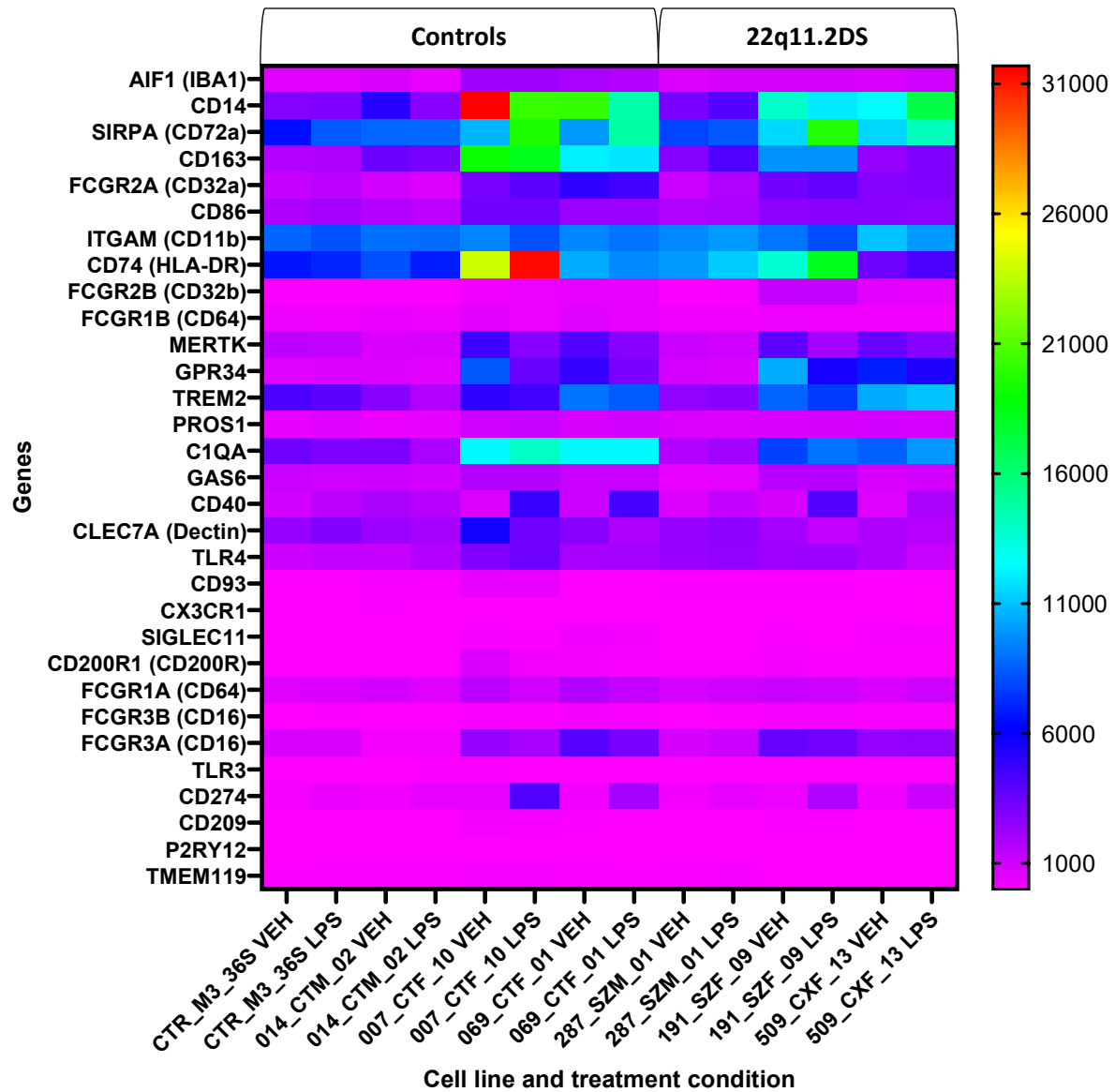


Figure 4. 1: Validation of MGL gene expression based on consensus human microglia/monocyte markers as assessed in Haenseler et al. (2017). Haenseler et al. (2017) used microarray to assess expression of key genes associated with microglia based on the following publications: Melief et al. (2012), Butovsky et al. (2014), and Bennett et al. (2016). Additionally, expression of AIF1 (IBA1) was confirmed based on the increasing use of IBA1 markers in microglia research (Ito et al., 1998; Ohsawa et al., 2004; Kenkhuis et al., 2022). Gene expression values are based on normalised gene counts generated during DEG analyses (Section 4.2.3, Chapter

4). Gene expression values are that of normalised gene counts computed by DESeq2 as part of DEG analysis

Abbreviation: DEG, differentially expressed genes.

To support mining data generated in Section 3.3.1, Chapter 3, and reduction of *COMT* observed in Section 3.3.5, Chapter 3, a handful of commonly deleted genes among 22q11.2DS were selected to qualitatively show expression levels compared to control MGLs (**Figure 4.2**). These includes MRPL40 and DGCR8 which had previously been discussed in **Section 3.4.1, Chapter 3**. This heatmap of expression levels shows that these suspected deleted genes also including *TANGO2* appears reduced in 22q11.2DS MGLs. *TANGO2* deficiency is associated with mitochondrial dysfunction in fibroblasts from patients with TANGO2-related disease (Heiman et al., 2022) and would align with data on 22q11.2DS hiPSC-derived neuronal cells such as that by Li et al. (2019) even though TANGO2 was not specifically assessed in their 22q11.2DS study.

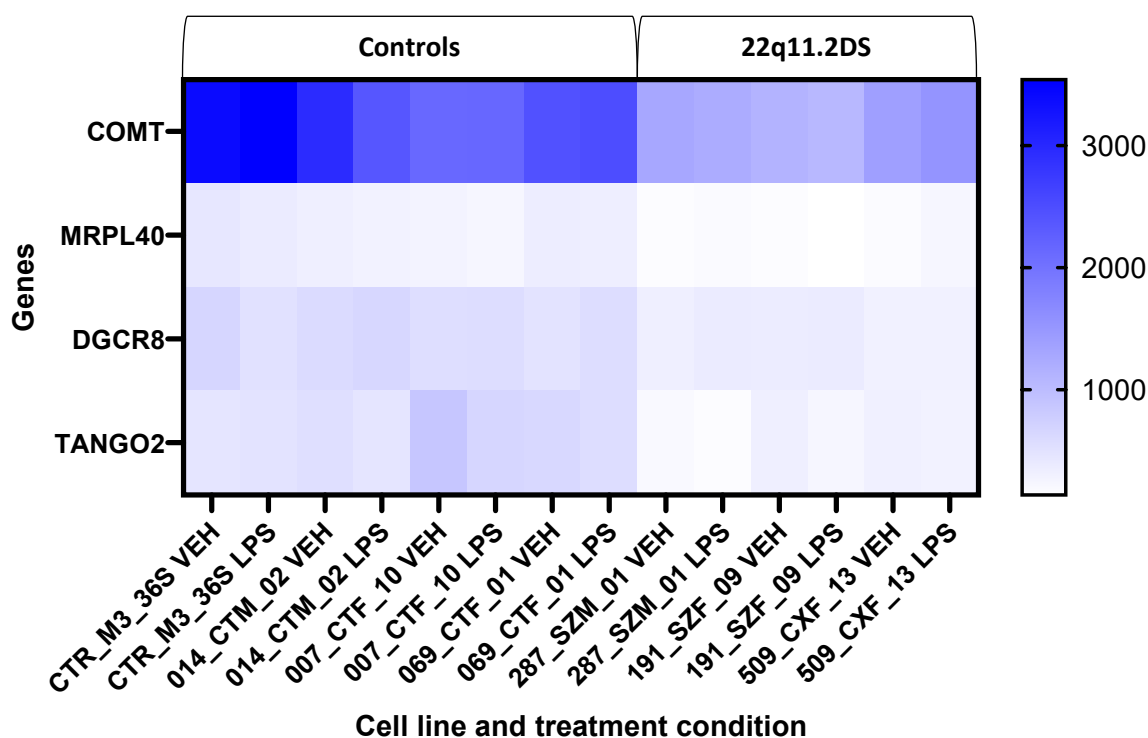


Figure 4. 2: Heatmap showing expression of selected deleted gene common among all 22q11.2DS cell lines. Genes were selected based on mining data from Section 3.3.1, Chapter 3. Gene expression values are that of normalised gene counts computed by DESeq2 as part of DEG analysis. Abbreviation: DEG, differentially expressed genes.

4.3.2. PCA analysis of RNA sequencing data demonstrates presence of variance based on sex and treatment condition, but not control and 22q11.2DS genotypes

To assess whether genetic background and treatment condition represent the primary sources of gene expression variation among samples, a principal component analyses (PCA) was completed on all cell lines used in this experiment, including vehicle- and LPS-treatment samples (**Figure 4.3**). The PCA depicted along principal component 1(PC1) of the x-axis accounts for 43% of the variance across these samples and appears to be representative of the effect of sex. Principal component 2 (PC2), which accounts for 31% of the variance along the y-axis is likely the effect of LPS-treatment. Variance between control and 22q11.2DS MGL same-sex vehicle-treated samples match what has previously been observed in 22q11.2DS

hiPSC-derived neurons with samples not clustering away from each other, however the effect of sex was not as pronounced (Khan et al., 2020; Nehme et al., 2022). The effect of LPS on the whole transcriptome has not been characterised in the context of 22q11.2DS or hiPSC-derived MGLs. However, a response to LPS has been characterised in human monocyte-derived MGLs, with LPS. being a pronounced source of variance in PCA (Smit et al., 2022). In this dataset the response to LPS was not as pronounced in male lines compared to female lines, which did not appear to be the case in Smit et al. (2022) or Ormel et al. (2020). Notable variables in this analysis that that the female 22q11.2DS line 509_CXF_13 separates more extensively from its same-sex control line counterparts compared to the other 22q11.2DS MGLs following LPS challenge. The LPS-treated 22q11.2DS MGL samples of 191_SZF_09 and 287_SZM_01 clusters more alongside their same-sex control line counterparts. It also appears that the control line 014_CTM_02 have had a less broad transcriptomic response to LPS compared to other male lines.

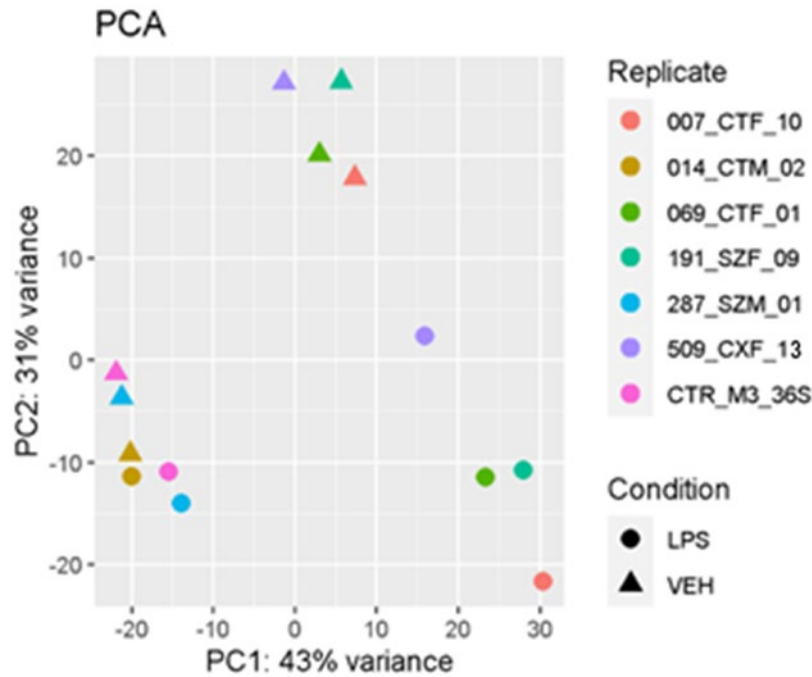


Figure 4. 3: PCA analysis of H₂O vehicle- and LPS-treated control and 22q11.2DS MGLs. 43% of variance is represented by PC1 along the x-axis, while 31% is represented by PC2 along the y-axis. Abbreviations: LPS, liposaccharide; PC1, principal component 1; PC2, principal component 2; PCA, principal component analysis; VEH, vehicle

4.3.3. Differentially expressed genes across different analysis thresholds in Signature A

To characterise differences in transcriptional profile of control and 22q11.2DS MGLs, DEG was assessed at three different thresholds. A stringent Benjamin-Hochberg FDR-corrected pvalue, which in DESeq2 is termed the adjusted pvalue, or padj, of < 0.05 (FDR <5%), along with a Log2FoldChange of 1.5 (StringentT, in analyses: Signature A-StringentT) would be the ideal statistical threshold to identify the most stringent DEG output using DESeq2.

However, due to low sample numbers and heterogeneity of 22q11.2DS hiPSC lines it was elected to additionally explore less strict thresholds for vehicle versus vehicle comparisons, specifically $p < 0.01$ with Log2FoldChange of 1.5 (ModerateT, in analyses: Signature A-ModerateT), and $p < 0.01$ with Log2FoldChange of 0.5 (LenientT, in analyses: Signature A-LenientT).

Reasoning for the inclusion of different thresholds was based on various approaches taken in previously published work. Studies with larger sample size have utilised less stringent threshold than StringentT, for example, a study with a cohort of 111 control subjects and 144 individuals with schizophrenia on cultured neural progenitor cells derived from olfactory neuroepithelium used a significance threshold of FDR <10% (Evgrafov et al., 2020). Evgrafov et al. (2020) detected 80 DEGs at this threshold. As shown in Bhat et al. (2022) which studied hiPSC-derived forebrain cortical neural progenitor cells from 3 control and 3 idiopathic schizophrenia donors at a significance threshold of FDR <5%, a stringent threshold with small sample size such as this study might yield substantially less significant DEGs (1 DEG between control and idiopathic lines). Additionally, the effect of smaller datasets on DEG outputs has also been demonstrated in the context of 22q11.2DS using hiPSC-derived neurons, with Nehme et al. (2022) detecting no significant DEGs at FDR <5% within the 22q11.2 region which should contain a number of deleted genes. However, a substantial number of genes within the region were noted to be reduced with a fold change between -1.5 and -2.0 and they as a result expanded the analyses to a larger number of donors following power analysis. As expanding this dataset to include more donors as done in Nehme et al. (2022) was not plausible due to time restrictions and donors available, an exploratory route was taken using different threshold stringencies when exploring Signature A gene expression, focusing on fold changes and a strict pvalue of <0.01. A fold change cut-off of 1.5 was initially tested, however, key genes suspected to be deleted such as *COMT* (confirmed in **Section 3.3.5, Chapter 3**) did not appear in down-regulated genes at this fold change cut-off, however *COMT* alongside other key genes such as *MPRL40* and *DGCR8* (deletions identified in **Section 3.3.1, Chapter 3**) were detected at a fold change cut-off of 0.5, so this threshold was also assessed.

When using StringentT, 4 down-regulated and 7 up-regulated genes were identified in 22q11.2DS MGLs when compared to controls (**Figure 4.4, Table 4.2, Table 4.3**). Down-regulated genes of note include *CCL13* and *IL1A* (Liu and Quan, 2018; Boche and Gordon, 2022). Deficiency in *IL1A* has in mice microglia been associated with impaired immune response to infection, specifically reduced parasite control and brain immune cell infiltration (Batista et al., 2020). Lower expression of *CCL13* has in hiPSC induced microglia been linked to higher phagocytic activity compared to microglia with high expression of *CCL13* (Dräger et al., 2022). A notable up-regulated gene is also *NLRP2* which has primarily been studied in the context of astrocyte immune response via the NLRP2 inflammasome, which is activated by DAMP ATP, while the microglia immune response has classically been more associated with the NLRP3 inflammasome albeit the focus has notably been on neurodegenerative diseases (Minkiewicz et al., 2013; Scheiblich et al., 2021; Holbrook et al., 2021; Wu et al., 2021; Jung et al., 2022). However, NLRP2 have also been described to be present in other immune cell types, including monocytes and macrophages, which shares similar ontogeny to microglia (Bruey et al., 2004; Fontalba et al., 2007). *NLRP2* has for example been associated with inhibition of the NF- κ B signalling pathway (Bruey et al., 2004; Fontalba et al., 2007), suggesting the this gene is elevated in an attempt to regulate microglia transcriptomic state.

In ModerateT analysis (**Figure 4.5, Table 4.4, Table 4.5**), a total of 28 genes were down-regulated while 26 were up-regulated. The trend of genes associated with aberrant immune states continued, including down-regulation of the genes *IL-6*, *IL-1 β* , and *CXCL10*, which are all implicated in regulation in microglial immune response (Clarner et al., 2015; Ishijima and Nakajima, 2021). Specifically, *CXCL10* for example is up-regulated following viral infection by cytomegalovirus in human primary microglia cultures (Cheeran et al., 2003), while

increases of *IL-6* and *IL-1 β* secretion amount and protein levels have been well established using animal models (Ishijima and Nakajima, 2021). Genes such as *CMPK2* might also be of importance as it belongs to a family of nucleotide kinases that are required for mtDNA synthesis and production of oxidised mtDNA fragments which may act as activating ligands for the NLRP3 inflammasome complex (Zhong et al., 2018). Up-regulated genes are also of note, with *S100B* being associated with regulation of microglial cell functions such as phagocytosis in mouse models and the immortalised BV2 microglial cell line, with the later model also having suggested that up-regulation increase of genes such as the aforementioned *IL-1 β* (Adami et al., 2001; Bianchi et al., 2010). So, while genes such as *IL-6* might be down-regulated, altered transcriptomic states of 22q11.2DS could potentially be explained by use of alternate pathways to perform homeostatic functions. As noted in threshold reasoning, none of the suspected deletions in 22q11.2 regions showed up in ModerateT DEG analysis. This became the primary reason to now further investigate LenientT.

LenientT showed 70 down-regulated genes 85 up-regulated genes (**Figure 4.6, Table 4.6, Table 4.7**). Of these, key deleted genes were confirmed such as *COMT*, *MRPL40* and *DGCR8*. With a number of DEGs now detected, exploratory secondary analyses were undertaken.

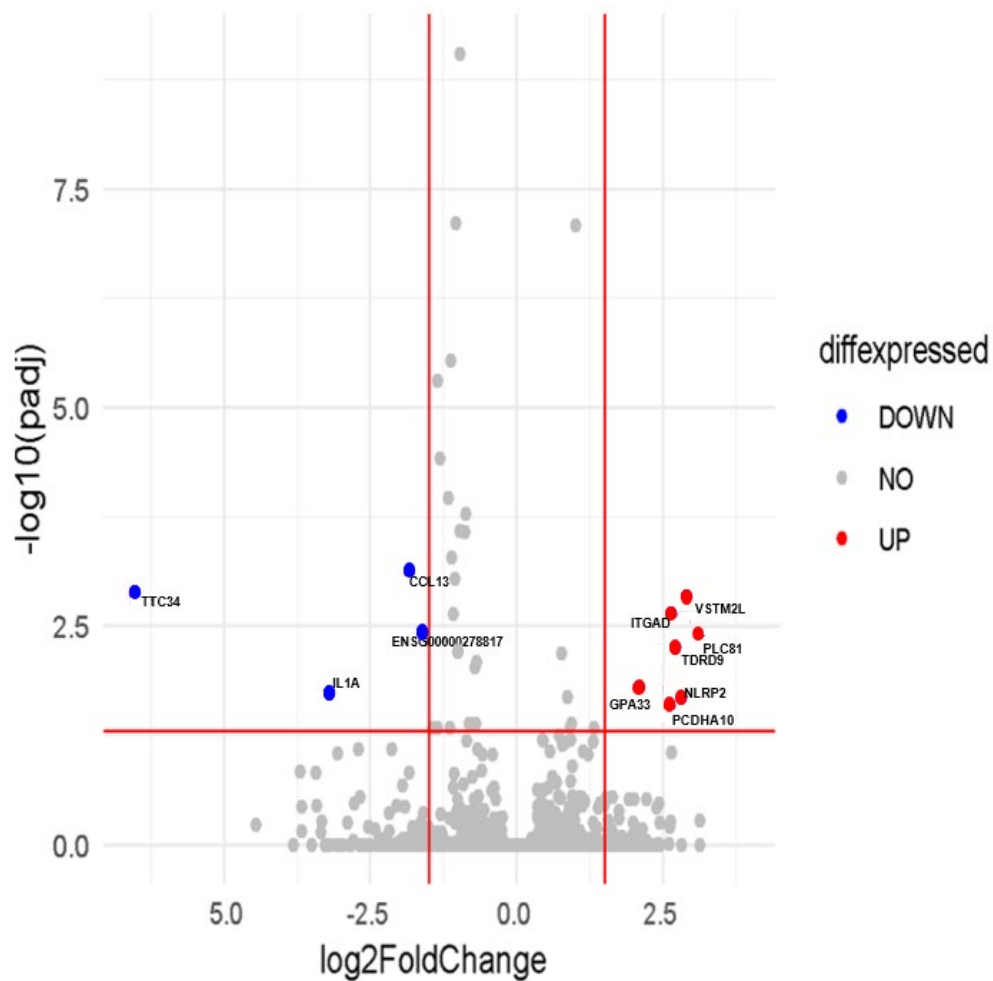


Figure 4. 4: Volcano plot of up and down-regulated genes in *Signature A-StringentT*. UP (red) = up-regulated genes in 22q11.2DS MGLs , DOWN (blue) = down-regulated genes in 22q11.2DS MGLs . NO (grey) = genes not passing the designated threshold. Abbreviations: padj, adjusted pvalue; diffexpressed, differentially expressed.

ENSG00000278817
CCL13
IL1A
TTC34

Table 4. 2: Down-regulated differentially expressed genes in *Signature A-StringentT*. Overview of genes significantly reduced in 22q11.2DS MGLs compared to control MGLs.

PLCB1	ITGAD
VSTM2L	PCDHA10
NLRP2	GPA33
TDRD9	

Table 4. 3: Up-regulated differentially expressed genes in Signature A-StringentT. Overview of genes significantly increased in 22q11.2DS MGLs compared to control MGLs.

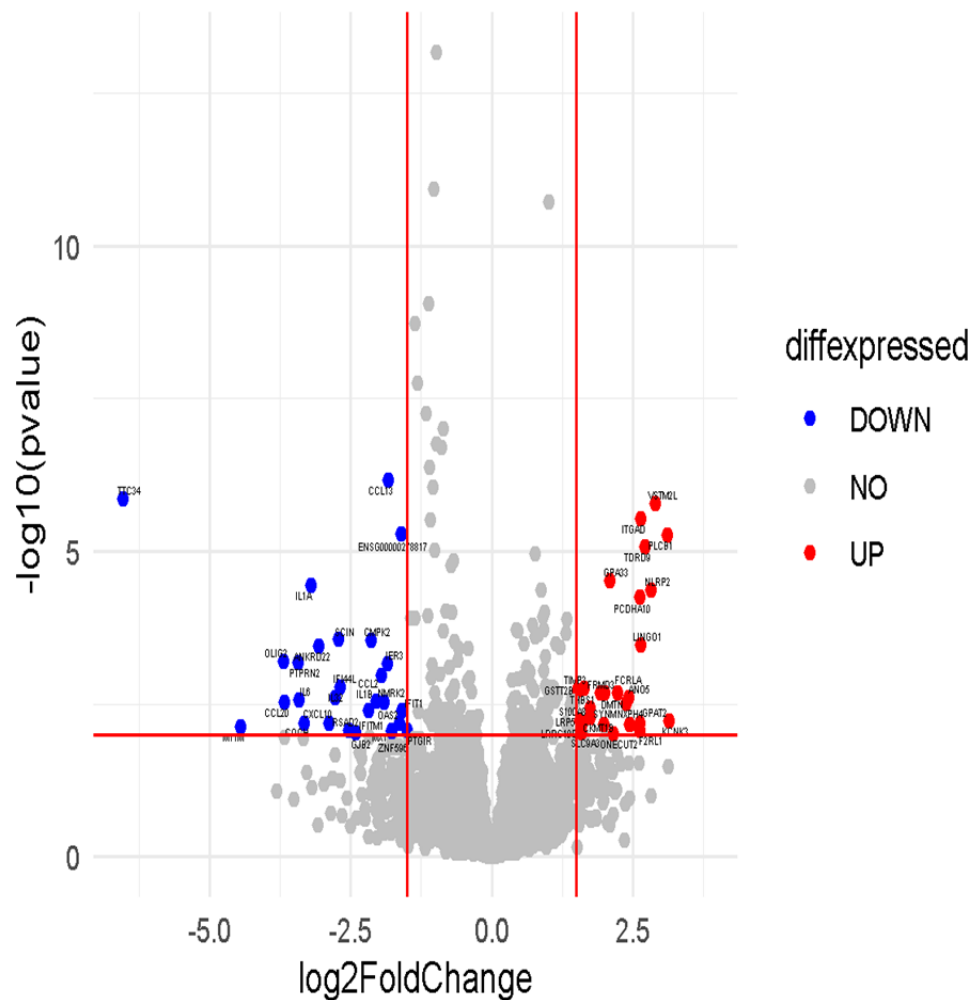


Figure 4. 5: Volcano plot of up and down-regulated in Signature A-ModerateT. UP (red) = up-regulated genes in 22q11.2DS MGLs, DOWN (blue) = down-regulated genes in 22q11.2DS MGLs. NO (grey) = genes not passing the designated threshold. Abbreviations: padj, adjusted pvalue; diffexpressed, differentially expressed.

ANKRD22	IFIT1	
CCL13	IFITM1	OLIG2
CCL2	IL1A	PTGIR
CCL20	IL1B	PTPRN2
CMPK2	IL32	RSAD2
COCH	IL6	SCIN
CXCL10	MT1M	TTC34
GJB2	MX1	ZNF596
IER3	NMRK2	ENSG00000278817
IFI44L	OAS2	

Table 4. 4: Down-regulated differentially expressed genes in Signature A-ModerateT. Overview of genes significantly reduced in 22q11.2DS MGLs compared to control MGLs.

ANO5	KCNK3	
CKMT1B	LINGO1	
DMTN	LRP5	SLC9A3
F2RL1	LRRC10B	SYNM
FCRLA	NLRP2	TDRD9
FRMD3	NXPH4	THBS1
GPA33	ONECUT2	TIMP3
GPAT2	PCDHA10	VSTM2L
GSTT2B	PLCB1	
ITGAD	S100A8	

Table 4. 5: Up-regulated differentially expressed genes in Signature A-ModerateT. Overview of genes significantly increased in 22q11.2DS MGLs compared to control MGLs.

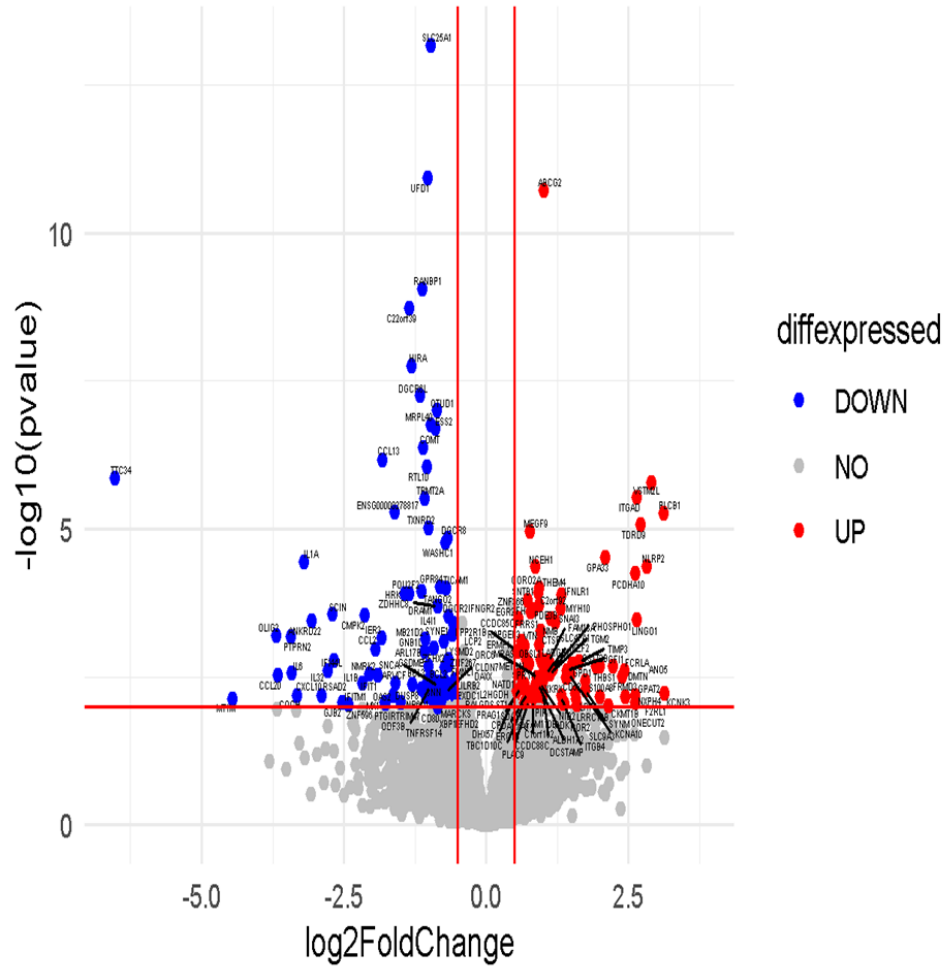


Figure 4. 6: Volcano plot of up and down-regulated genes in Signature A-LenientT. UP (red) = up-regulated genes in 22q11.2DS MGLs , DOWN (blue) = down-regulated genes in 22q11.2DS MGLs . NO (grey) = genes not passing the designated threshold. Abbreviations: padj, adjusted pvalue; diffexpressed, differentially expressed.

ANKRD22	COCH	GJB2	IL1B	NMRK2	RSAD2	
ARL17B	COMT	GNB1L	IL32	NR6A1	RTL10	TTC34
ARVCF	CXCL10	GPR84	IL4I1	OAS2	SCIN	TXNRD2
BCL2	DAXX	GSDME	IL6	ODF3B	SLC25A1	UFD1
BCL3	DGCR2	HIRA	LCP2	OLIG2	SNCA	WASHC1
C22orf39	DGCR6L	HRK	LILRB2	OTUD1	SNN	XBP1
CCL13	DGCR8	IER3	LYSMD2	POU2F2	SYNE1	ZDHHC8
CCL2	DRAM1	IFI44L	MARCKS	PTGIR	TANGO2	ZFHX2
CCL20	DUSP8	IFIT1	MB21D2	PTPRN2	TICAM1	ZNF267
CD80	EFHD2	IFITM1	MRPL40	PXDC1	TNFRSF14	ZNF596
CLDN7	ESS2	IFNGR2	MT1M	RALGDS	TRIM47	ENSG00000278817
CMPK2	FMNL1	IL1A	MX1	RANBP1	TRMT2A	

Table 4. 6: Down-regulated differentially expressed genes in Signature A-LenientT. Overview of genes significantly reduced in 22q11.2DS MGLs compared to control MGLs.

ABCG2	CORO2A	FAM13A	IKZF2	METRNL	ORC6	S100A8	
ADK	CPD	FCRLA	ITGAD	MRAS	PCDHA10	SLC47A1	TGM2
ALDH1A2	CTSF	FH	ITGB4	MYH10	PDE3B	SLC9A3	THBS1
ANO5	DCSTAMP	FRMD3	KCNA10	NATD1	PHOSPHO1	SNAI3	THEM4
ANXA9	DHX57	FRRS1	KCNK3	NCEH1	PIR	SNTB1	TIMP3
C1orf162	DMTN	GFI1	L2HGDH	NID2	PLAC9	SOAT1	VSTM2L
C2orf92	EGR2	GPA33	LARGE1	NLRP2	PLCB1	SPRY4	VTN
CCDC85C	ERMP1	GPAT2	LINGO1	NMB	PPP2R1B	ST14	XKRX
CCDC88C	ERO1B	GPD1	LRP5	NXPH4	PRAG1	SYNM	ZNF366
CD52	F2RL1	GSTT2B	LRRC10B	OBSL1	RAPGEF3	TBC1D10C	
CKMT1B	FAM110B	IFNLRL1	MEGF9	ONECUT2	ROR2	TDRD9	

Table 4. 7: Up-regulated differentially expressed genes in Signature A-LenientT. Overview of genes significantly increased in 22q11.2DS MGLs compared to control MGLs.

4.3.4. Microglia gene set enrichment of differentially expressed in Signature A

To investigate whether DEGs in 22q11.2DS MGLs compared to controls were enriched for genes associated with microglial form, function and disease, up- and down-regulated genes were analysed in the MGENrichment tool, comparing gene sets identified in **Section 4.3.2, Chapter 4** to previously published transcriptome data on human microglia. It was elected to only look at overlap with human datasets based on the potential for species-related heterogeneity which as discussed in **Section 1.1.5, Chapter 1**.

In the DEG outputs of Signature A-StringentT, no significant hits were identified for either up-or down-regulated DEGs (**Table 4.8**).

List name	In list	Description	Tissue	Source
Control vs 22q down-regulated genes		No hits		
Control vs 22q up-regulated genes		No hits		

Table 4. 8: Gene set enrichment analysis of Signature A-StringentT. In list denotes the total number of overlapping genes between 22q11.2DS MGL DEG and the gene data set. The brief description of the data set is extracted from the MGENrichment tool output. Microglia tissue annotation under tissue infers isolated cell. Non-human tissue was excluded from the final data set. Genes assessed were those significantly increased or decreased in 22q11.2DS MGLs compared to control MGLs. Abbreviations: MGL, microglia-like cells

For Signature A-ModerateT, 4 data sets for the down-regulated gene sets and 1 data set from the up-regulated gene set had significant overlap with 5% FDR correction (**Table 4.9**). Up-regulated hits included the microglia interferon response pathway identified in Olah et al. (2020), microglia signature gene data sets (Galatro et al., 2017; Gosselin et al., 2017) and schizophrenia, ASC, and bipolar disorder gene module identified in Gandal et al. (2018). Additionally, along the same lines, the ASC gene module in Gandal et al. (2018) was also significantly associated with the down-regulated gene set at this threshold.

List name	In list	Description	Tissue	Source
Control vs 22q down-regulated genes				
Cluster 4 Microglia interferon response signaling pathway	9	SCRNA-seq Cluster 4 Microglia interferon response signaling pathway	microglia	Olah et al., 2020
core human microglial signature	10	logFC > 3 and p < 0.001 human microglia vs human cortex	microglia	Galatro et al. 2017
geneModules SCZ & ASD & BD	10	WGCNA gene expression modules ASD & SCZ & BD gene enriched	brain	Gandal, et al., 2018
Human microglia signature genes	6	Genes with >10-fold-higher average expression in microglia compared to cortex	microglia	Gosselin, et al. 217
Control vs 22q up-regulated genes				
listname	In list	description	tissue	source
geneModules ASD	9	WGCNA gene expression modules ASD gene enriched	brain	Gandal, et al., 2018

Table 4. 9: Gene set enrichment analysis of Signature A-ModerateT. In list denotes the total number of overlapping genes between 22q11.2DS MGL DEG and the gene data set. The brief description of the data set is extracted from the MGENrichment tool output. Microglia tissue annotation under tissue infers isolated cell. Non-human tissue was excluded from the final data set. Genes assessed were those significantly increased or decreased in 22q11.2DS MGLs compared to control MGLs. Comparison datasets notably refer to ASC as ASD, which kept in the table to ensure that the information stays true to the original publications. ASD is adapted for to ASC in thesis main text. Abbreviations: ASC, autism spectrum condition; ASD, autism spectrum disorder; MGL, microglia-like cells

In Signature A-LenientT, a total of 9 hits were identified passing 5% FDR correction were identified in the down-regulated gene set along with 4 in the up-regulated gene set (**Table 4.10**). For down-regulated DEGs, the additional gene sets with overlap included an microglia anti-inflammatory response cluster in Olah et al. (2020) which was characterised by genes such as *IL-10*, *IL-4*, and *IL-13*, the ASC and schizophrenia module in Gandal et al. (2018), as well as three data sets where Signature A-LenientT down-regulated DEGs overlapped with modules in which genes are expressed higher in ASC, Alzheimer's Disease, and Irritable Bowel Disease compared to controls (Miller et al., 2013; Gandal et al., 2018). For the up-regulated Signature A-LenientT DEGs, additional now significantly overlapping gene sets includes the ASC and schizophrenia module in Gandal et al. (2018) similar to the down-regulated DEGs, as well as another signature microglia gene data set (Gosselin et al., 2017)

List name	In list	Description	Tissue	Source
Down-regulated genes				
geneModules SCZ & ASD & BD	20	WGCNA gene expression modules ASD & SCZ & BD gene enriched	brain	Gandal, et al., 2018
core human microglial signature	20	logFC > 3 and p < 0.001 human microglia vs human cortex	microglia	Galatro et al. 2017
Gandal IBD>Ctrl	33	RNASeq genes higher in Irritable Bowel Disease compared to controls	brain	Gandal, et al., 2018
Human microglia signature genes	14	Genes with >10-fold-higher average expression in microglia compared to cortex	microglia	Gosselin, et al. 217
Cluster 4 Microglia interferon response signaling pathway	11	SCRNA-seq Cluster 4 Microglia interferon response signaling pathway	microglia	Olah et al., 2020
Cluster 5 Microglia anti-inflammatory responses	11	SCRNA-seq Cluster 5 Microglia anti-inflammatory responses	microglia	Olah et al., 2020
Gandal ASD>Ctrl	13	RNASeq genes higher in ASD compared to controls	brain	Gandal, et al., 2018
geneModules ASD & SCZ	19	WGCNA gene expression modules ASD & SCZ gene enriched	brain	Gandal, et al., 2018
Miller AD>Ctrl	4	RNASeq genes higher in Alzheimer's Disease compared to controls	brain	Miller et al., 2013
Up-regulated genes				
Gandal IBD>Ctrl	29	RNASeq genes higher in Irritable Bowel Disease compared to controls	brain	Gandal, et al., 2018
geneModules ASD	19	WGCNA gene expression modules ASD gene enriched	brain	Gandal, et al., 2018
geneModules ASD & SCZ	21	WGCNA gene expression modules ASD & SCZ gene enriched	brain	Gandal, et al., 2018
Human microglia signature genes	8	Genes with >10-fold-higher average expression in microglia compared to cortex	microglia	Gosselin, et al. 2017

Table 4. 10: Gene set enrichment analysis of Signature A-LenientT. In list denotes the total number of

overlapping genes between 22q11.2DS MGL DEG and the gene data set. The brief description of the data set is extracted from the MGENrichment tool output. Microglia tissue annotation under tissue infers isolated cell. Non-human tissue was excluded from the final data set. Genes assessed were those significantly increased or decreased in 22q11.2DS MGLs compared to control MGLs. Comparison datasets notably refer to ASC as ASD, which kept in the table to ensure that the information stays true to the original publications. ASD is adapted for to ASC in thesis main text. Abbreviations: ASC, autism spectrum condition; ASD, autism spectrum disorder; MGL, microglia-like cells

4.3.5. Gene ontology analysis of differentially expressed genes in Signature A

Using the Webgestalt GO analysis tool, gene ontology was assessed in up- and down-regulated gene sets identified in **Chapter 4, Section 4.3.2** against non-redundant biological processes, non-redundant molecular functions, cellular components, as well as the reactome pathway functional datasets.

Similar to microglia gene set enrichment results, Signature A-StringentT DEGs were not significantly associated with any of the assessed processes during gene ontology analysis, but top 10 hits are shown in **Figure 4.7** and **Figure 4.8** for down-regulated DEGs and up-regulated DEGs, respectively.

In Signature A-ModerateT however, a notable number of processes are associated with down-regulated DEGs passing 5% FDR correction while no processes were associated with the up-regulated DEG gene set. Top 10 hits for each category are shown in **Figure 4.9** for down-regulated DEGs, and in **Figure 4.10** for up-regulated DEGs. Associations passing 5% FDR correction for down-regulated DEGs were:

- Non-redundant biological processes: Vascular endothelial growth factor production response to type I interferon, response to chemokine, response to interleukin-1, response to virus, response to interferon-gamma, defense response to other organism, cellular response to biotic stimulus, response to molecule of bacterial origin, cell chemotaxis
- Cellular components: No associations
- Non-redundant molecular functions: Cytokine receptor binding, receptor ligand activity, G protein-coupled receptor binding
- Reactome pathway: interleukin-1 processing, interleukin-10 signaling, interferon alpha/beta signaling, chemokine receptors bind chemokines. interleukin-4 and interleukin-13 signaling, interferon signaling, cytokine signaling in immune system, signaling by interleukins, immune system

Of Signature A-LenientT DEGs, there are less hits passing 5% FDR correction compared to Signature A-ModerateT in the down-regulated control vs 22q11.2DS gene set while there remained no significant hits for up-regulated genes. Top 10 hits for down-regulated DEGs are shown in Figure 4.11, and for up-regulated DEGs in Figure 4.12. Associations passing 5% FDR correction for down-regulated DEGs were:

- Non-redundant biological processes: cytokine metabolic process, response to virus, response to interleukin-1, production of molecular mediator of immune response,

response to molecule of bacterial origin, response to interferon-gamma, cellular response to biotic stimulus, defense response to other organism, viral life cycle

- Cellular components: No associations
- Non-redundant molecular functions: Cytokine receptor binding
- Reactome pathway: interleukin-10 signaling, interferon alpha/beta signaling, cytokine signaling in immune system

The reduction in associated pathways is likely due to an increased number of genes in input causing associated pathways in Signature A-ModerateT causing associations not to pass the 5% FDR correction threshold in Signature A-LenientT. However, a notable difference is also observed in which associations passes significance.

- Common association between Signature A-ModerateT and Signature A-LenientT: Cellular response to biotic stimulus, cytokine receptor binding, cytokine signaling in immune system, defense response to other organism, interferon alpha/beta signaling, interleukin-10 signaling, response to interleukin-1, response to molecule of bacterial origin, response to virus, response to interferon-gamma
- Unique associations in Signature A-LenientT: Cytokine metabolic process, positive regulation of cytokine production, production of molecular mediator of immune response, and viral life cycle
- Unique associations in Signature A-ModerateT: Cell chemotaxis, chemokine receptors bind chemokines, G protein-coupled receptor binding, immune system, interferon signaling, interleukin-1 processing, interleukin-4 and interleukin-13 signaling, receptor ligand activity. response to chemokine. response to type I interferon, signaling by onterleukins. vascular endothelial growth factor production

The differences between thresholds indicates that either of these two thresholds might not be perfect, and more high-powered studies is required to indicate which one is more accurate. However, the common associations which passed 5% FDR correction across both thresholds are likely most indicative of what one would expect in a higher powered study. These common associations indicate that the gene ontology profile of down-regulated genes is akin to what would be expected after LPS treatment, specifically an immune response, or that 22q11.2DS MGLs might respond differently to an immune challenge to potential deficits in cytokine receptor binding and signalling. This suggests that the transcriptomic state of the 22q11.2DS MGL vehicle-treated condition is altered compared to control MGLs. While the functional mechanism by which this happens is unclear, the consistent hits related to cytokines might suggest an abnormality of the 22q11.2DS MGLs in their ability to produce cytokines, and perhaps consequently impact their cytokine secretion during an immune response which is important for microglial state self-regulation (Lau et al., 2021).

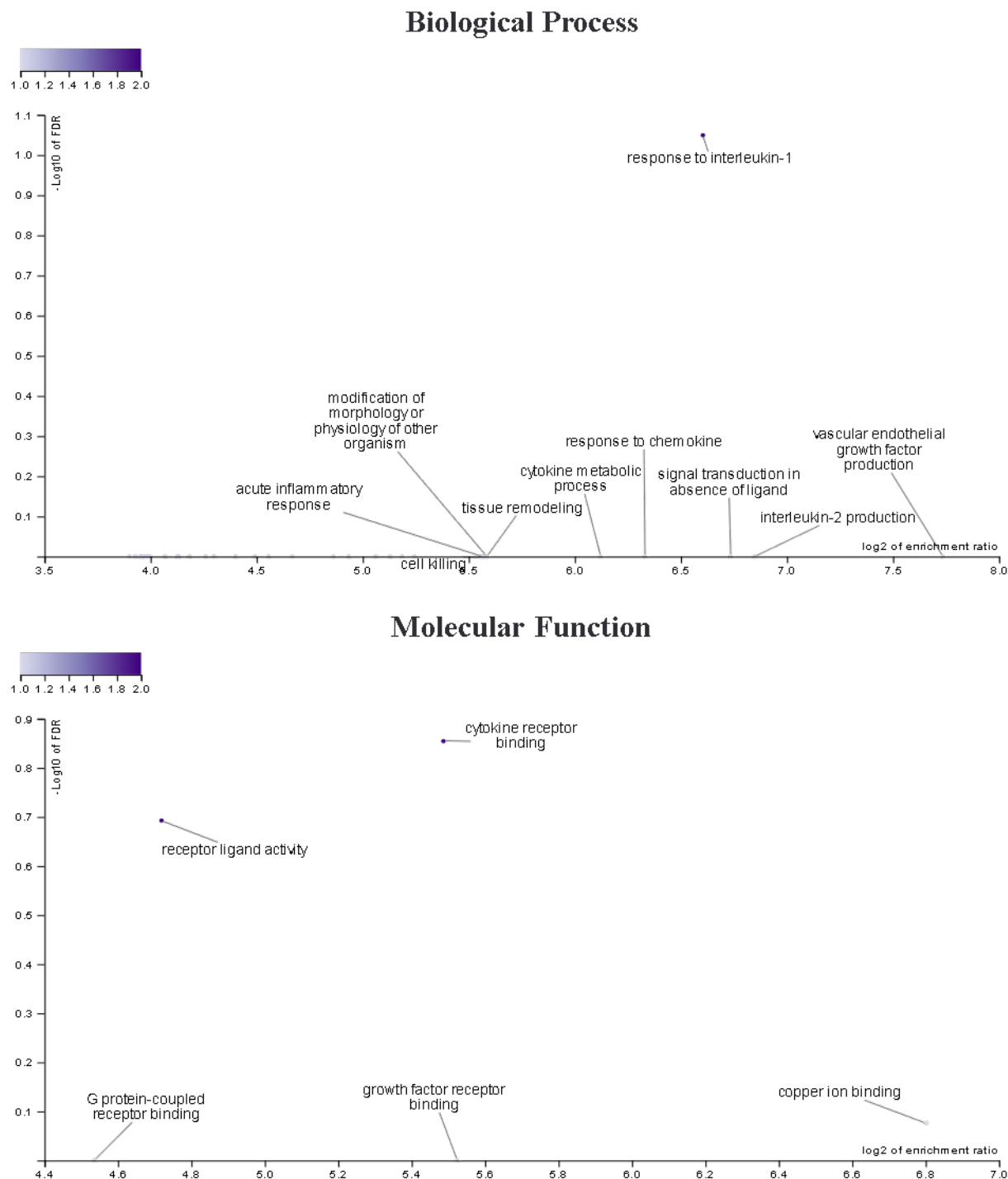


Figure 4. 7: Gene ontology analysis of down-regulated differentially expressed genes in Signature A-StringentT. Processes shown are non-redundant biological process, non-redundant molecular functions and reactome pathways. Figures visualise up to top 10 hits where hits were found regardless of significance. No hits were identified for cellular component association. Differentially expressed genes assessed were those significantly decreased in 22q11.2DS MGLs compared to control MGLs based on StringentT. Abbreviations: MGL, microglia-like cells.

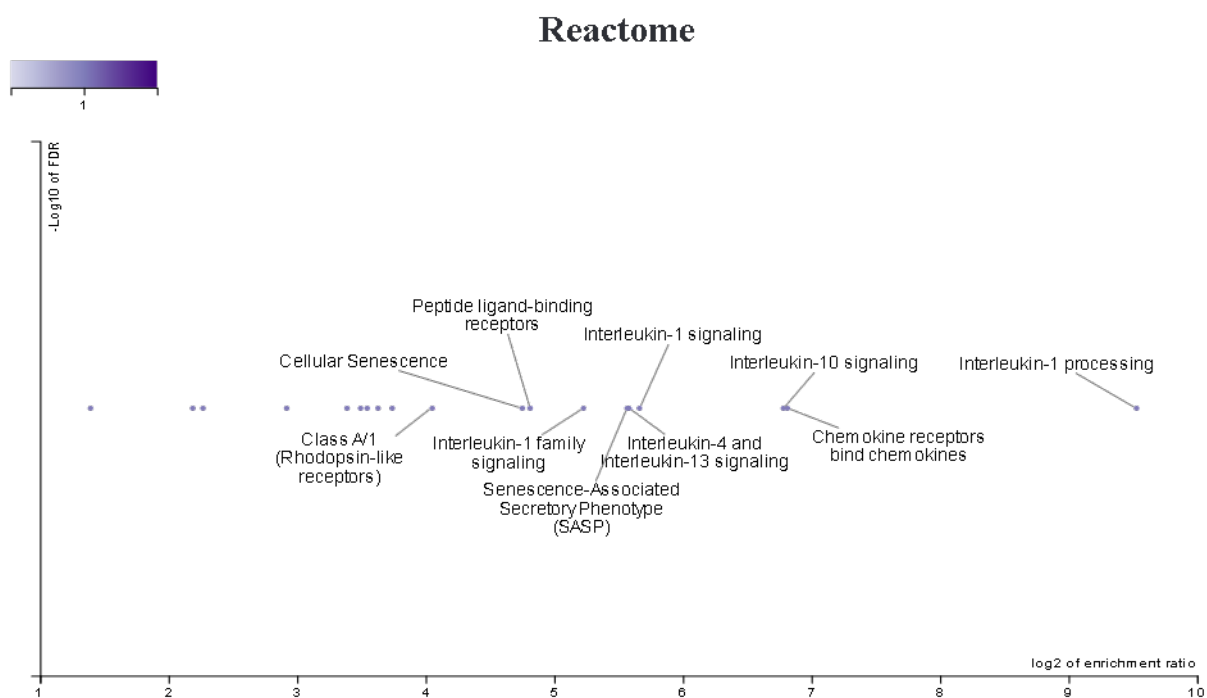


Figure 4. 7 continued: Gene ontology analysis of down-regulated differentially expressed genes in Signature A-StringentT. Processes shown are non-redundant biological process, non-redundant molecular functions and reactome pathways. Figures visualise up to top 10 hits where hits were found regardless of significance. No hits were identified for cellular component association. Differentially expressed genes assessed were those significantly decreased in 22q11.2DS MGLs compared to control MGLs based on StringentT. Abbreviations: MGL, microglia-like cells.

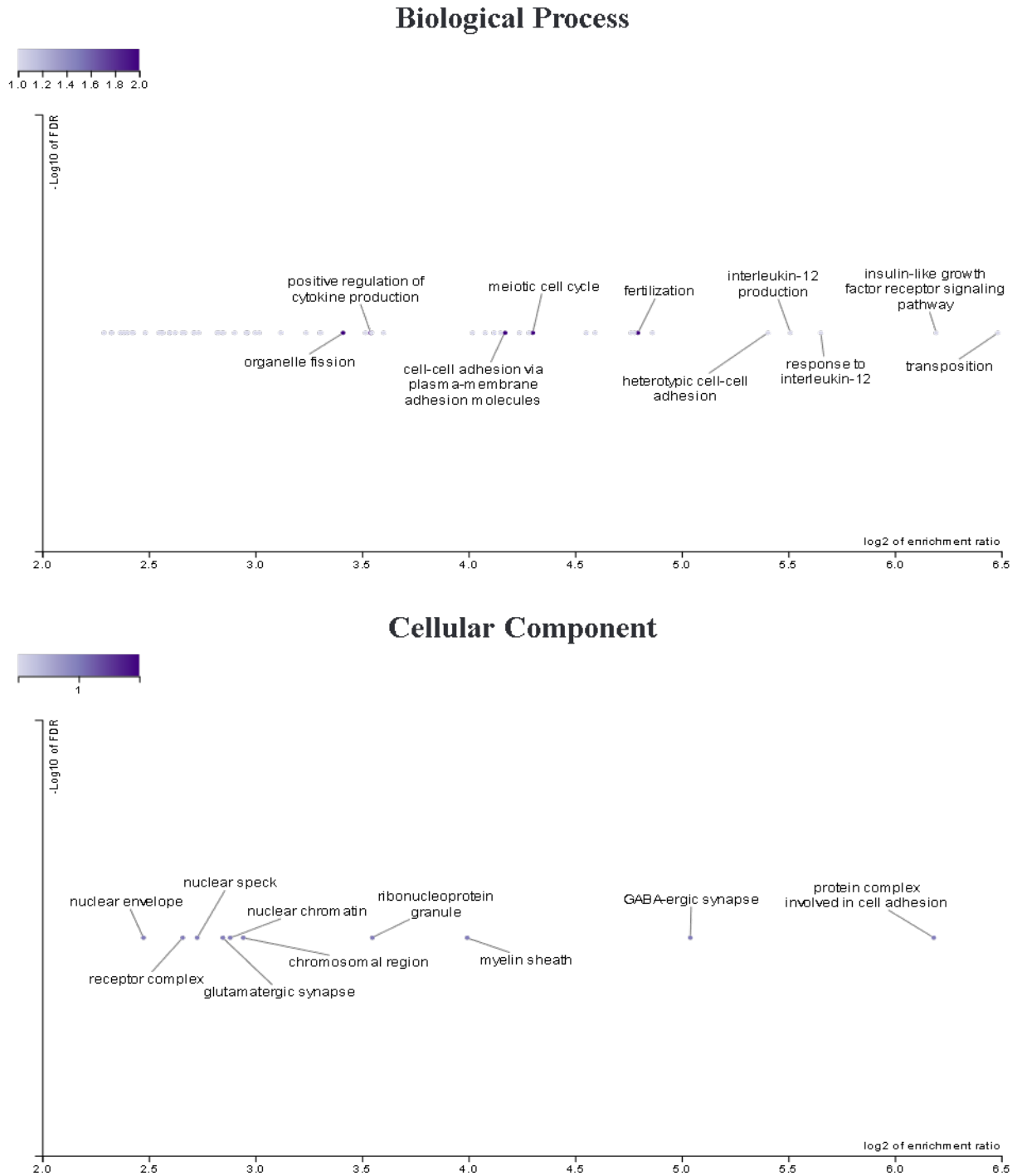


Figure 4. 8: Gene ontology analysis of up-regulated differentially expressed genes in Signature A-StringentT. Processes shown are non-redundant biological process, cellular component, non-redundant molecular functions and reactome pathways. Figures visualise up to top 10 hits where hits were found regardless of significance. Differentially expressed genes assessed were those significantly increased in 22q11.2DS MGLs compared to control MGLs based on StringentT. Abbreviations: MGL, microglia-like cells.

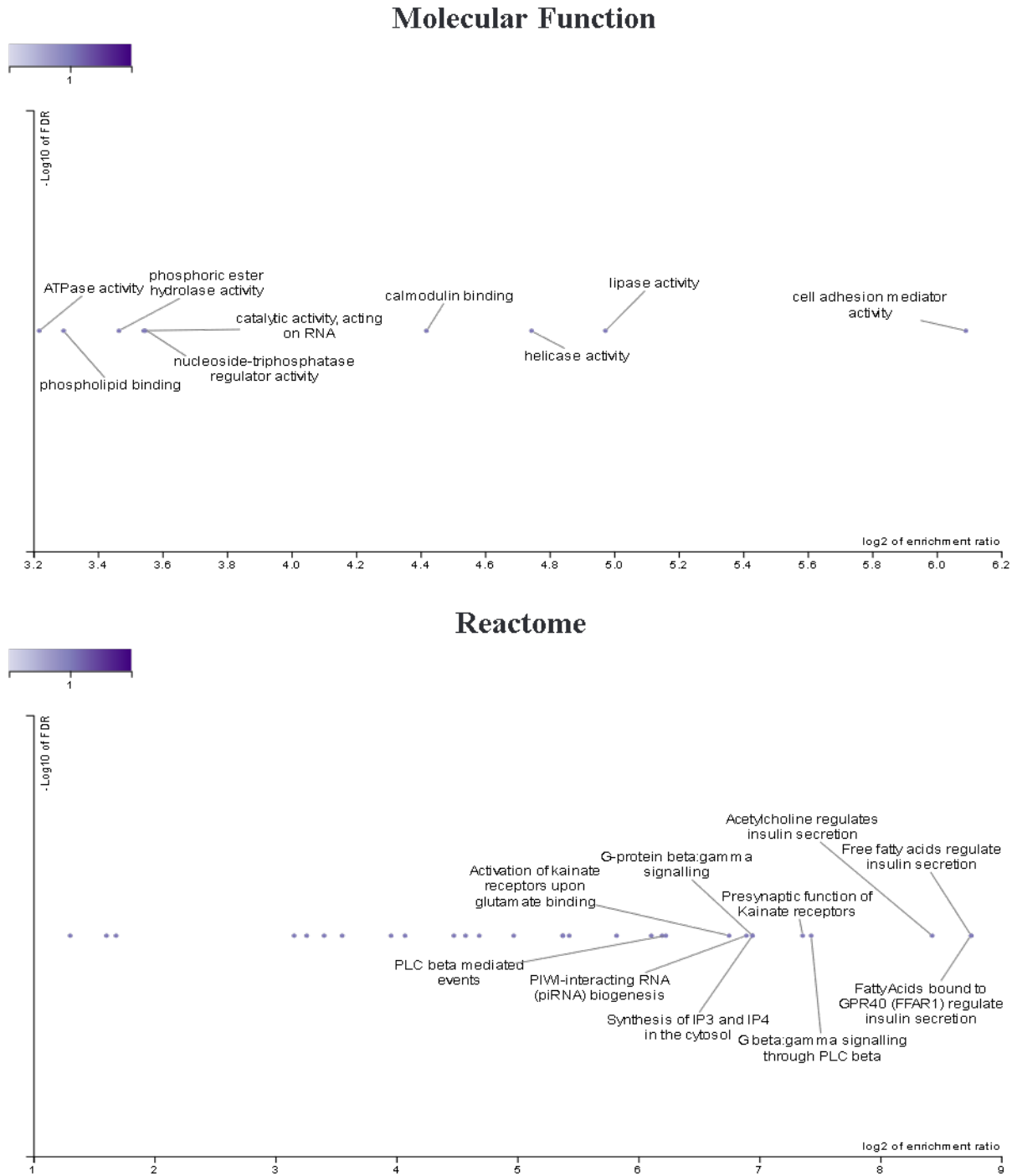


Figure 4. 8 continued: Gene ontology analysis of up-regulated differentially expressed genes in Signature A-StringentT. Processes shown are non-redundant biological process, cellular component, non-redundant molecular functions and reactome pathways. Figures visualise up to top 10 hits where hits were found regardless of significance. Differentially expressed genes assessed were those significantly increased in 22q11.2DS MGLs compared to control MGLs based on StringentT. Abbreviations: MGL, microglia-like cells.

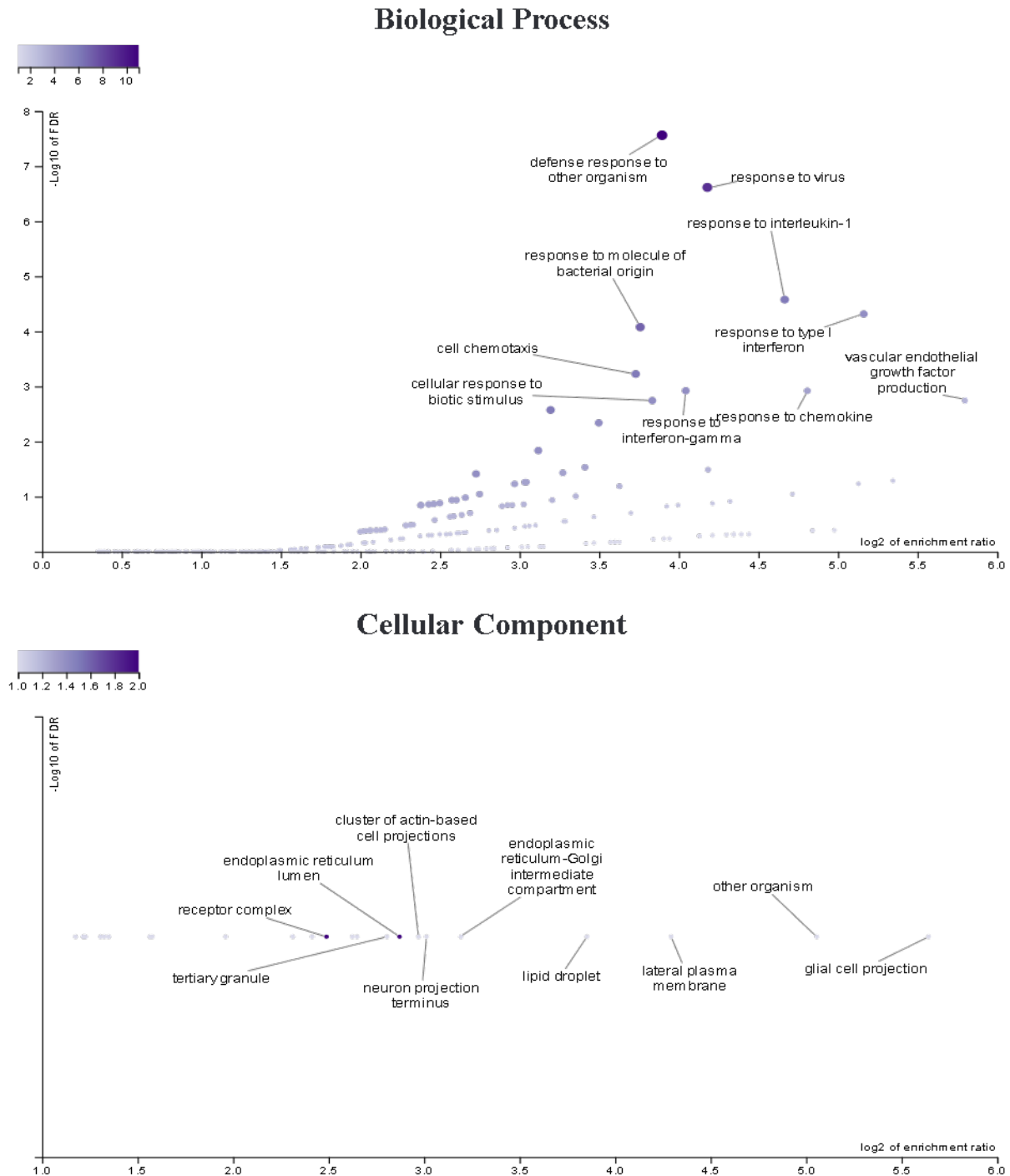


Figure 4. 9: Gene ontology analysis of down-regulated differentially expressed genes in Signature A-ModerateT. Processes shown are non-redundant biological process, cellular component, non-redundant molecular functions and reactome pathways. Figures visualise up to top 10 hits where hits were found regardless of significance. Differentially expressed genes assessed were those significantly decreased in 22q11.2DS MGLs compared to control MGLs based on ModerateT. Abbreviations: MGL, microglia-like cells.

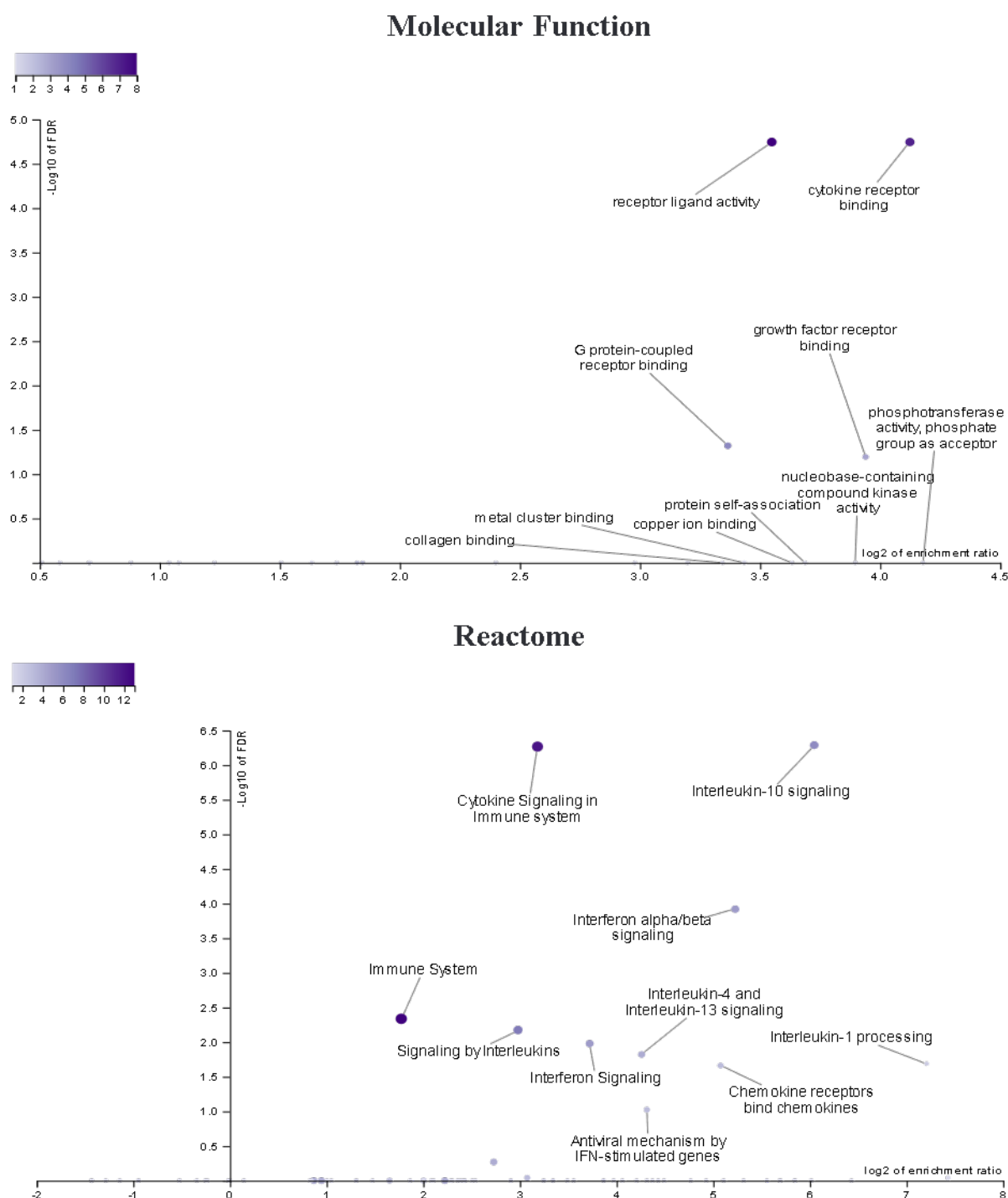


Figure 4. 9 continued: Gene ontology analysis of down-regulated differentially expressed genes in Signature A-ModerateT. Processes shown are non-redundant biological process, cellular component, non-redundant molecular functions and reactome pathways. Figures visualise up to top 10 hits where hits were found regardless of significance. Differentially expressed genes assessed were those significantly decreased in 22q11.2DS MGLs compared to control MGLs based on ModerateT. Abbreviations: MGL, microglia-like cells.

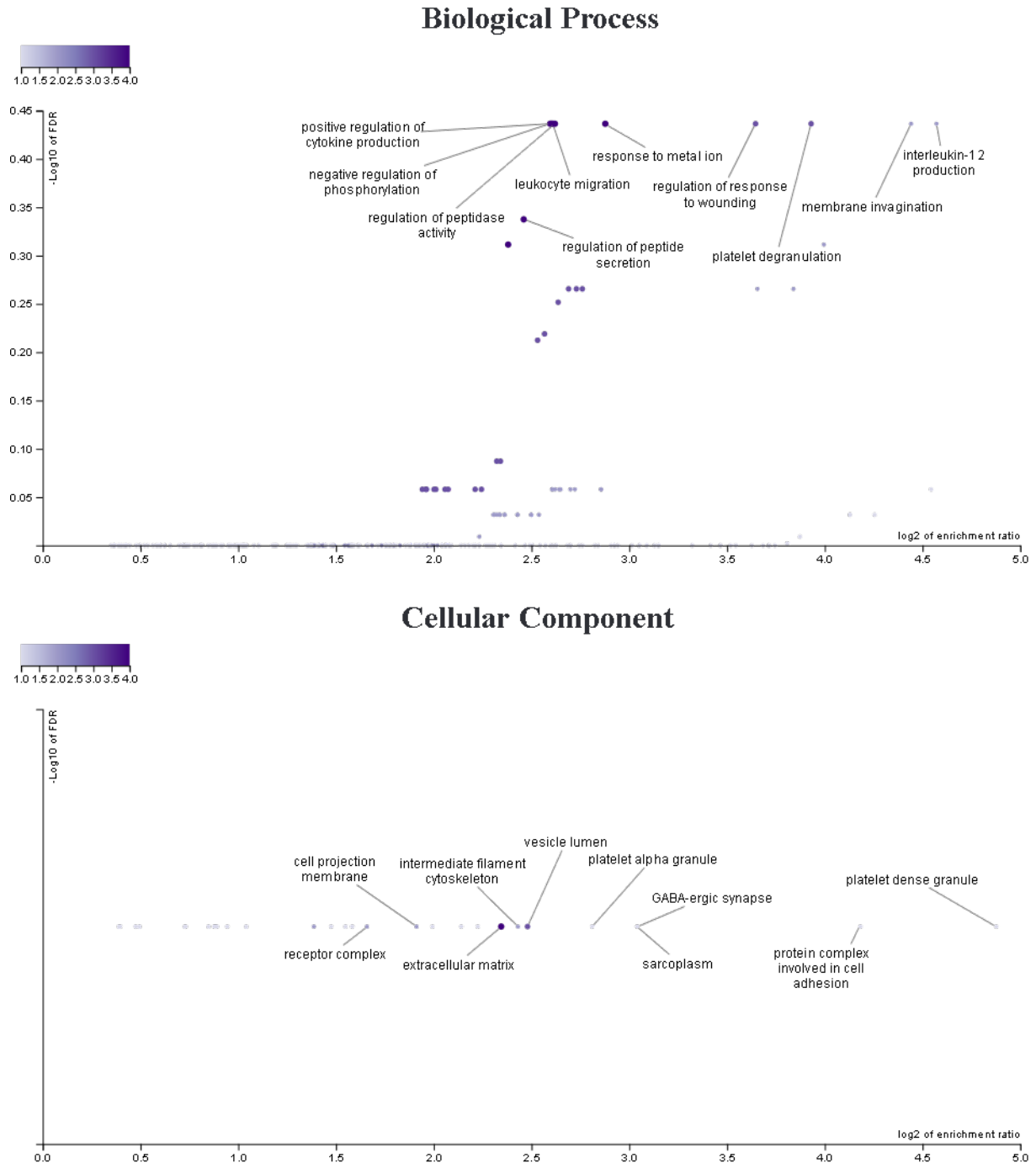


Figure 4. 10: Gene ontology analysis of up-regulated differentially expressed genes in Signature A-ModerateT. Processes shown are non-redundant biological process, cellular component, non-redundant molecular functions and reactome pathways. Figures visualise up to top 10 hits where hits were found regardless of significance. Differentially expressed genes assessed were those significantly increased in 22q11.2DS MGLs compared to control MGLs based on ModerateT. Abbreviations: MGL, microglia-like cells.

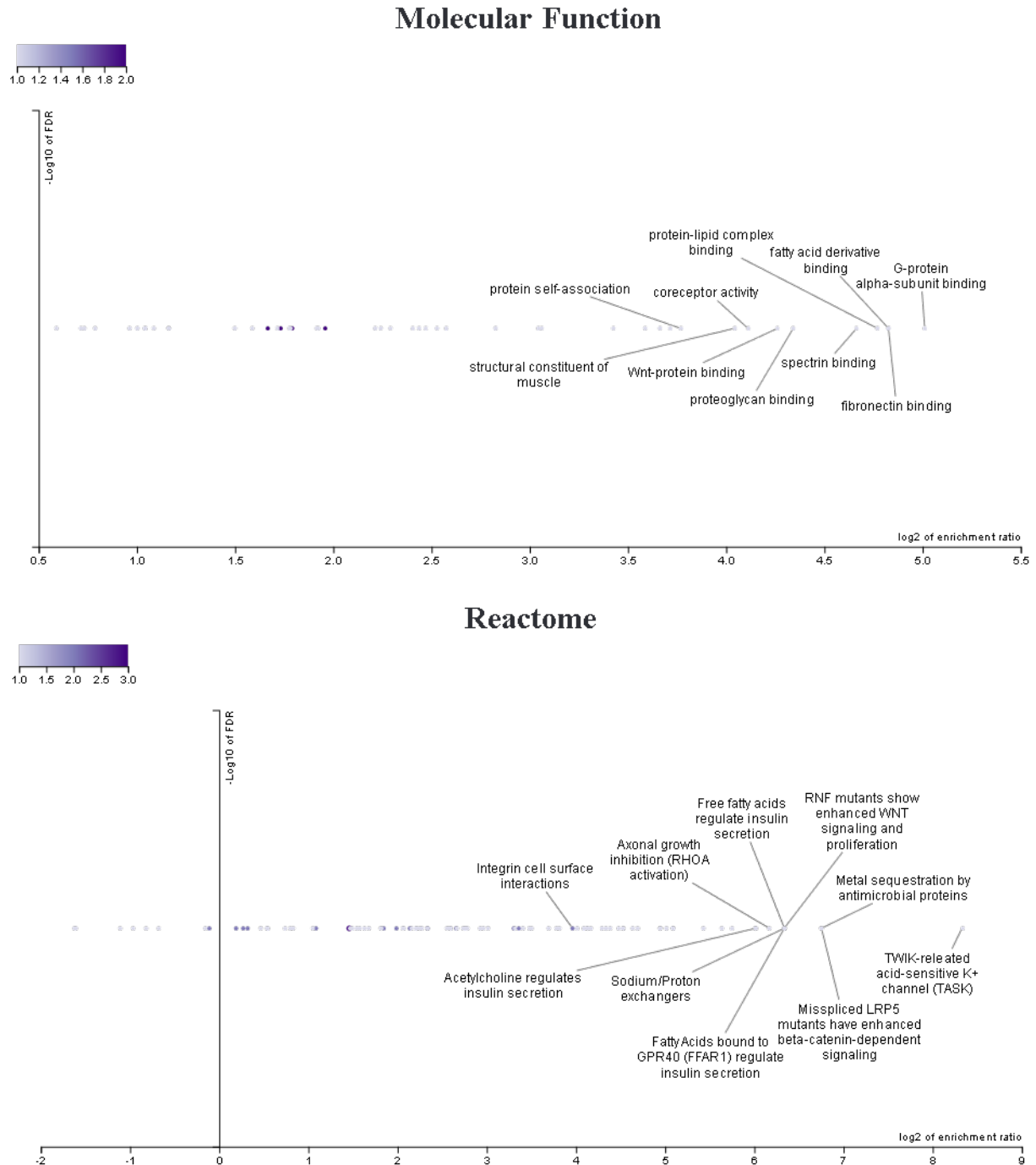


Figure 4. 10 continued: Gene ontology analysis of up-regulated differentially expressed genes in Signature

A-ModerateT. Processes shown are non-redundant biological process, cellular component, non-redundant

molecular functions and reactome pathways. Figures visualise up to top 10 hits where hits were found

regardless of significance. Differentially expressed genes assessed were those significantly increased in

22q11.2DS MGLs compared to control MGLs based on ModerateT. Abbreviations: MGL, microglia-like cells.

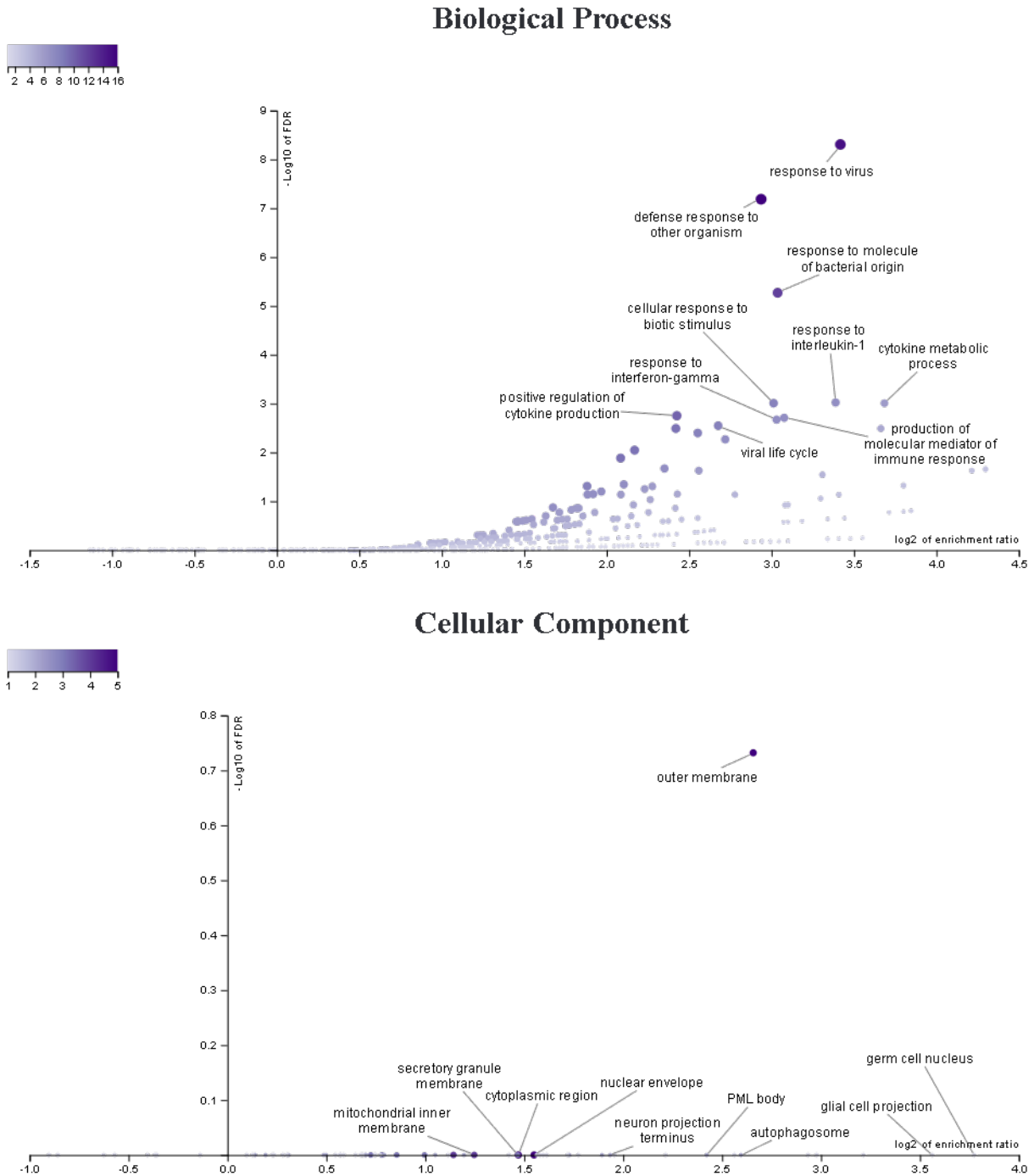


Figure 4. 11: Gene ontology analysis of down-regulated differentially expressed genes in Signature A-LenientT. Processes shown are non-redundant biological process, cellular component, non-redundant molecular functions and reactome pathways. Figures visualise up to top 10 hits where hits were found regardless of significance. Differentially expressed genes assessed were those significantly decreased in 22q11.2DS MGLs compared to control MGLs based on LenientT. Abbreviations: MGL, microglia-like cells.

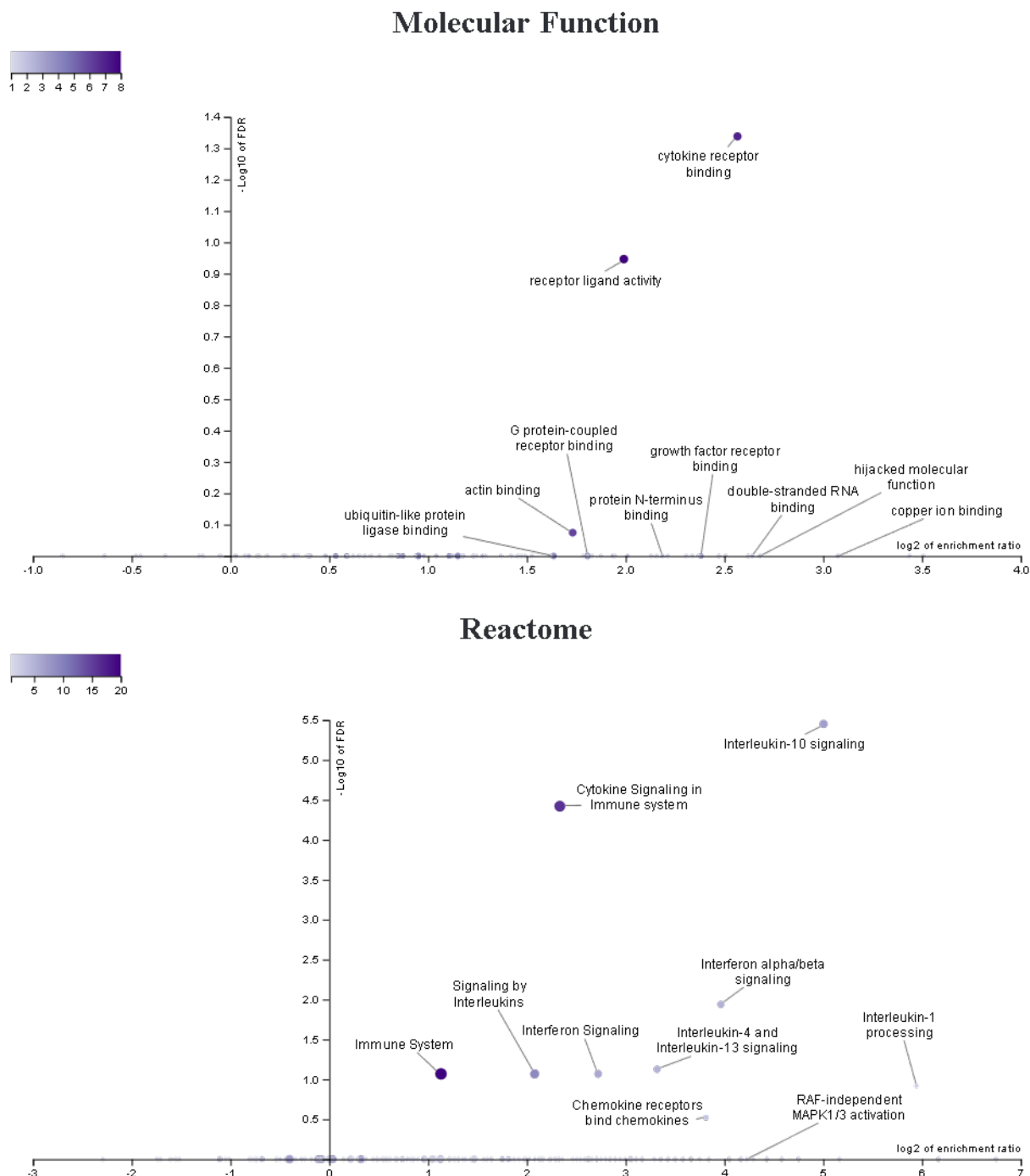


Figure 4. 11 continued: Gene ontology analysis of down-regulated differentially expressed genes in Signature A-LenientT. Processes shown are non-redundant biological process, cellular component, non-redundant molecular functions and reactome pathways. Figures visualise up to top 10 hits where hits were found regardless of significance. Differentially expressed genes assessed were those significantly decreased in 22q11.2DS MGLs compared to control MGLs based on LenientT. Abbreviations: MGL, microglia-like cells.

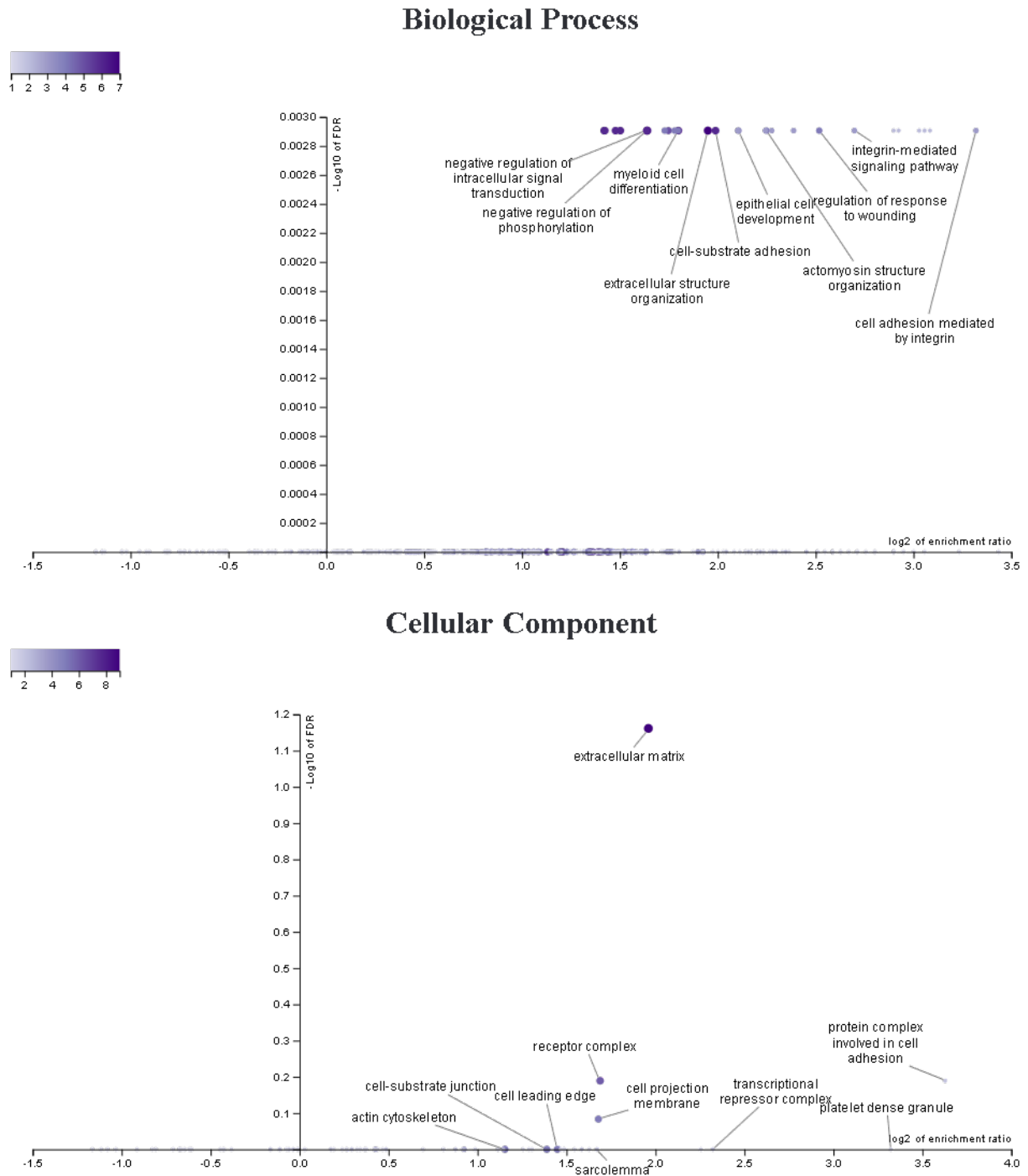


Figure 4. 12: Gene ontology analysis of up-regulated differentially expressed genes in Signature A-LenientT.

Processes shown are non-redundant biological process, cellular component, non-redundant molecular functions and reactome pathways. Figures visualise up to top 10 hits where hits were found regardless of significance.

Differentially expressed genes assessed were those significantly increased in 22q11.2DS MGLs compared to control MGLs based on LenientT. Abbreviations: MGL, microglia-like cells.

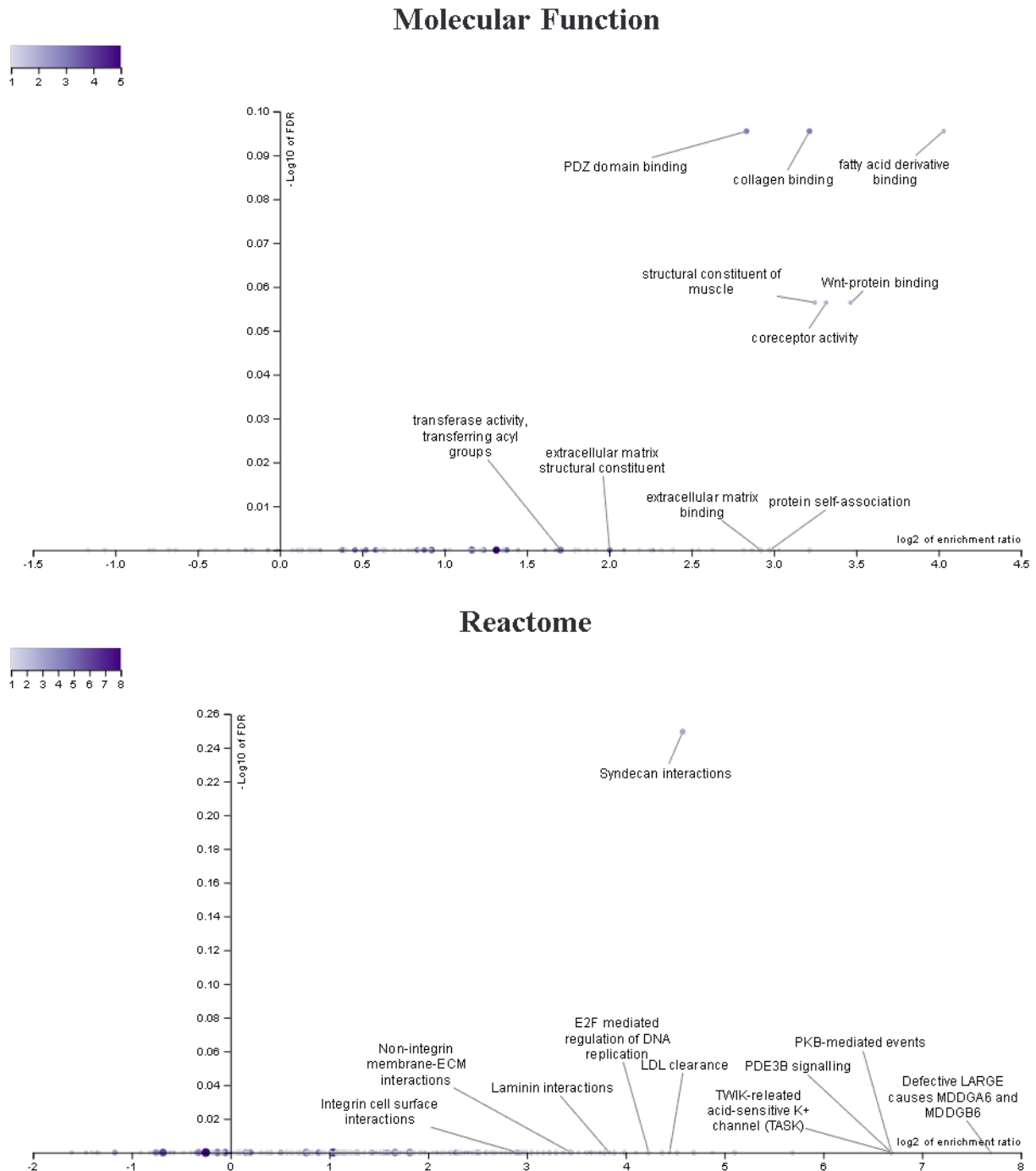


Figure 4. 12 continued: Gene ontology analysis of up-regulated differentially expressed genes in Signature A-LenientT. Processes shown are non-redundant biological process, cellular component, non-redundant molecular functions and reactome pathways. Figures visualise up to top 10 hits where hits were found regardless of significance. Differentially expressed genes assessed were those significantly increased in 22q11.2DS MGLs compared to control MGLs based on LenientT. Abbreviations: MGL, microglia-like cells.

4.3.6. Signature B

Microglia are capable of broad responses to immune challenge. To determine whether MGLs are capable of a wide transcriptomic response, separate control and 22q11.2DS MGLs wells were treated with LPS. Vehicle- and LPS-treated control and 22q11.2DS were analysed separately in order to identify potentially unique transcriptomic responses.

In 3-hour LPS treatment, control MGLs exhibited a large response of 84 up-regulated genes (**Figure 4.13, Table 4.11**). No down-regulated genes passed the threshold which was designated to $p_{adj} < 0.05$ along with a Log2FoldChange of 1.5. No additional thresholds were explored due to the size of the response being deemed sufficient for any secondary analysis. Up-regulated genes largely aligned with what would be expected in response to immune challenge, including *IL-6*, *IL-1 β* and *IL1A* (all noted in **Section 4.3.3, Chapter 4** vehicle comparison), but also genes such as *IRF8* which plays a critical role in transforming microglia state in response to injury, for example being necessary for positive microglial presence in response to peripheral nerve injury as well as viral infection by Japanese encephalitis virus in animal models (Masuda et al., 2012; Tripathi et al. 2021). *IRF8* was also noted to be up-regulated in hiPSC-derived MGLs from neurotypical donors in response to IL-6 as published in Couch et al. (2023). It is notable that *IRF8* has been shown to be reduced in human *postmortem* cortical brain tissue from individuals with schizophrenia (Gandal et al., 2018; Snijders et al., 2021), but this is not the case in 22q11.2DS MGLs when compared to control MGLs in this study (**Section 4.3.3, Chapter 4**).

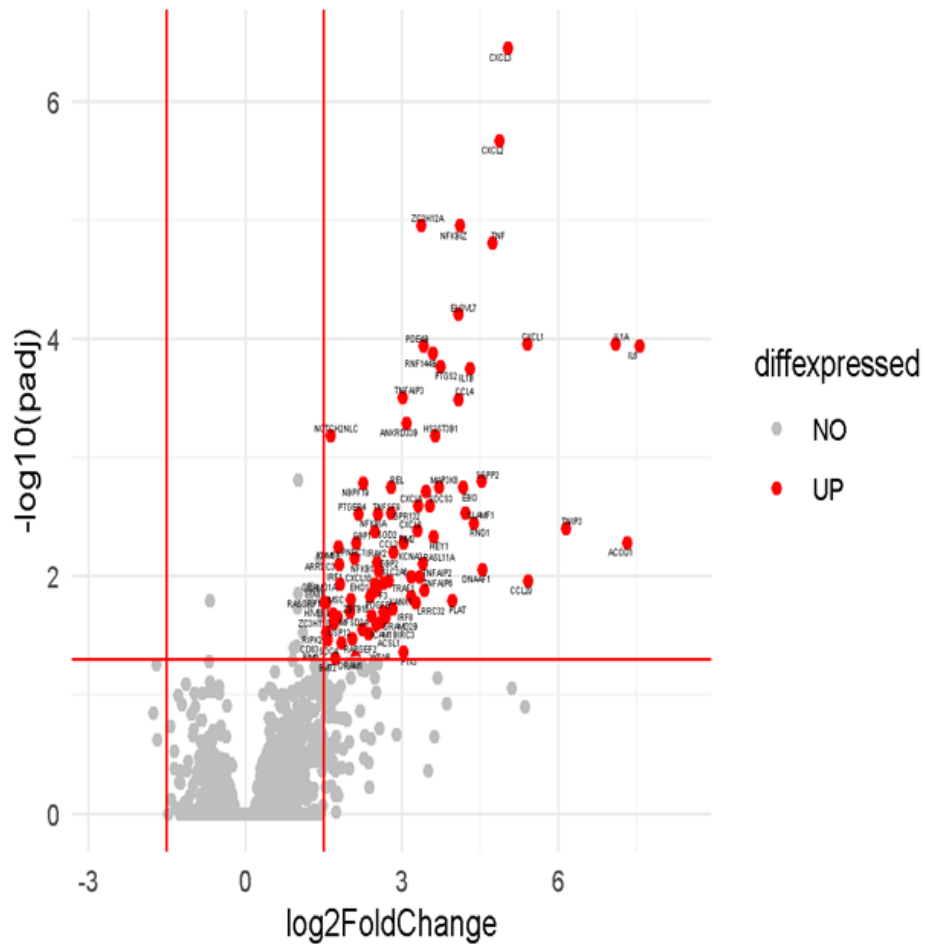


Figure 4. 13: Volcano plot of up and down-regulated genes in Signature B. UP (red) = up-regulated genes in LPS-treated control MGLs compared to vehicle-treated control MGLs, DOWN (blue) = down-regulated genes in LPS-treated MGLs. NO (grey) = genes not passing the designated threshold. Abbreviations: padj, adjusted pvalue; diffexpressed, differentially expressed.

ACOD1	CXCL2	GPR132	IRF8	NOTCH2NLC	RASL11A	TNF
ACSL1	CXCL3	GRAMD1A	KANK1	PDE4B	REL	TNFAIP2
ANKRD33B	CXCL6	GRAMD2B	KCNA3	PDGFB	RIPK2	TNFAIP3
ARRDC3	CXCL8	HEY1	KDM6B	PIM2	RND1	TNFAIP6
BIRC3	DNAAF1	HIVEP1	LRRC32	PIM3	RNF144B	TNFSF9
BMT2	DRAM1	HS3ST3B1	MAP3K8	PLAT	SDC4	TNIP3
CCL20	EBI3	ICAM1	MFSD2A	PNRC1	SGPP2	TRAF1
CCL3	EHD1	IL1A	MSC	PTGER4	SLAMF1	USP12
CCL4	ELOVL7	IL1B	NBPFF19	PTGS2	SLC2A6	WTAP
CD83	F3	IL6	NFKB1	PTX3	SOC3	ZBTB10
CXCL1	GBP1	IRAK2	NFKBIA	RAPGEF2	SOD2	ZC3H12A
CXCL10	GBP2	IRF1	NFKBIZ	RASGRP1	STX11	ZC3H12C

Table 4. 11: Differentially expressed genes in Signature B. Overview of genes significantly increased in 22q11.2DS MGLs compared to control MGLs. No genes were significantly downregulated in Signature B.

In order to assess whether treatment of control MGLs with LPS elicit a transcriptomic response similar to other human microglia data sets, the MGENrichment tool was used. A total of 7 hits were identified following 5% FDR correction (**Table 4.12**). These included data sets associated with microglia cellular stress (Olah et al., 2020), anti-inflammatory responses (Olah et al., 2020) and signature genes (Galatro et al., 2017; Gosselin et al., 2017). This transcriptomic state of control MGLs also link to a psychiatric disorder gene module of schizophrenia, ASC and bipolar disorder (Gandal et al., 2018), as well as a gene data set with genes that are more highly expressed in ASC (Gandal et al., 2018). The latter two hits suggest that the transcriptomic profile of LPS-treated control MGLs might replicate that of microglial states observed in psychiatric disorders.

<i>listname</i>	<i>in list</i>	<i>description</i>	<i>tissue</i>	<i>source</i>
geneModules SCZ & ASD & BD	37	WGCNA gene expression modules ASD & SCZ & BD gene enriched	brain	Gandal, et al., 2018
Cluster 5 Microglia anti-inflammatory responses	23	SCRNA-seq Cluster 5 Microglia anti-inflammatory responses	microglia	Olah et al., 2020
Human microglia signature genes	20	Genes with >10-fold-higher average expression in microglia compared to cortex	microglia	Gosselin, et al. 2017
Gandal ASD>Ctrl	21	RNASeq genes higher in ASD compared to controls	brain	Gandal, et al., 2018
core human microglial signature	22	logFC > 3 and p<0.001 human microglia vs human cortex	microglia	Galatro et al. 2017
Cluster 6 Microglia anti-inflammatory responses	11	SCRNA-seq Cluster 6 Microglia anti-inflammatory responses	microglia	Olah et al., 2020
Cluster 3 Microglia cellular stress	6	SCRNA-seq Cluster 3 Microglia cellular stress	microglia	Olah et al., 2020

Table 4. 12: Gene set enrichment analysis of Signature B. *In list denotes the total number of overlapping DEG in Signature B and the target gene data set. The brief description of the data set is extracted from the MGENrichment tool output. Microglia tissue annotation under tissue infers isolated cells. Non-human tissue was excluded from the final data set. Genes assessed were those significantly increased LPS-treated control MGLs compared to control MGLs based on Signature B DEG data. No genes were significantly decreased. Comparison datasets notably refer to ASC as ASD, which kept in the table to ensure that the information stays true to the original publications. ASD is adapted for to ASC in thesis main text. Abbreviations: ASC, autism spectrum condition; ASD, autism spectrum disorder; BD, bipolar disorder; MGL, microglia-like cells; RNAseq, RNA sequencing; SCRNA-seq, single-cell RNA sequencing; SCZ, schizophrenia; WGCNA, weighted correlation network analysis*

Using the Webgestalt GO analysis tool, gene ontology was assessed in up-regulated gene sets identified against non-redundant biological processes, molecular functions, cellular components, and reactome pathways. Processes associated with up-regulated genes in control MGL LPS-response passing 5% FDR correction were substantial. Top 10 hits for each category are shown in **Figure 4.14**. Associations passing 5% FDR correction were:

- Non-redundant biological processes: Response to interleukin-1, cellular response to biotic stimulus, response to molecule of bacterial origin, response to tumor necrosis factor, positive regulation of response to external stimuli, leukocyte cell-cell adhesion, regulation of inflammatory response, positive regulation of defense response, leukocyte migration, and positive regulation of cytokine production
- Cellular component: No associations

- Non-redundant molecular functions: Cytokine receptor binding, G protein-coupled receptor binding, receptor ligand activity
- Reactome pathways: Interleukin-1 processing, interleukin-10 signaling, chemokine receptors bind chemokines, interleukin-4 and Interleukin-13 signaling, interleukin-1 signaling, interferon gamma signaling, interleukin-1 family signaling, signaling by interleukins, cytokine signaling in immune system, and immune system.

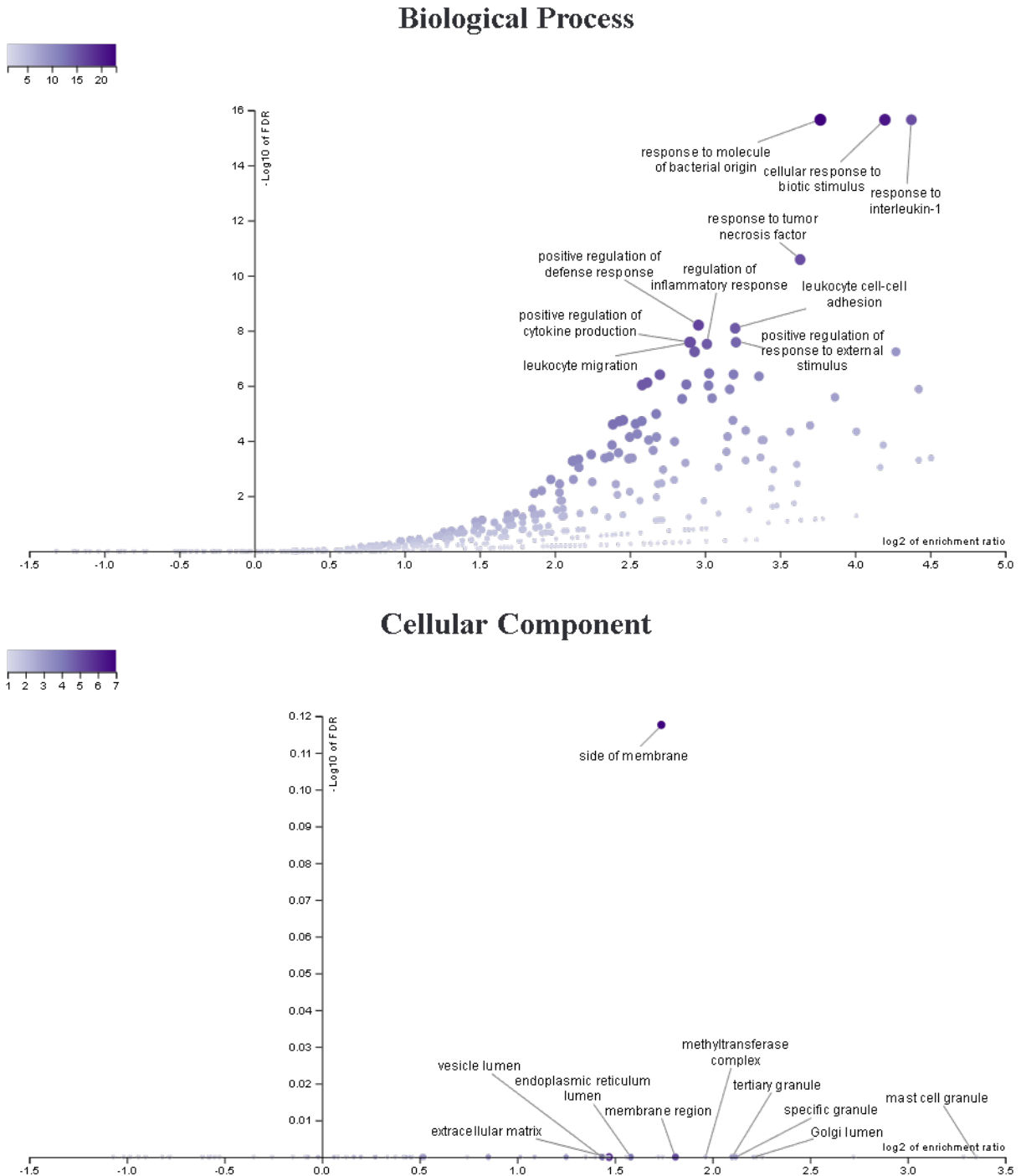


Figure 4. 14: Gene ontology analysis of Signature B. Processes shown are non-redundant biological process, cellular component, non-redundant molecular functions and reactome pathways. Figures visualise up to top 10 hits where hits were found regardless of significance. Genes assessed were those significantly increased LPS-treated 22q11.2DS MGLs compared to 22q11.2DS MGLs based on Signature C DEG data. No genes were

significantly decreased.

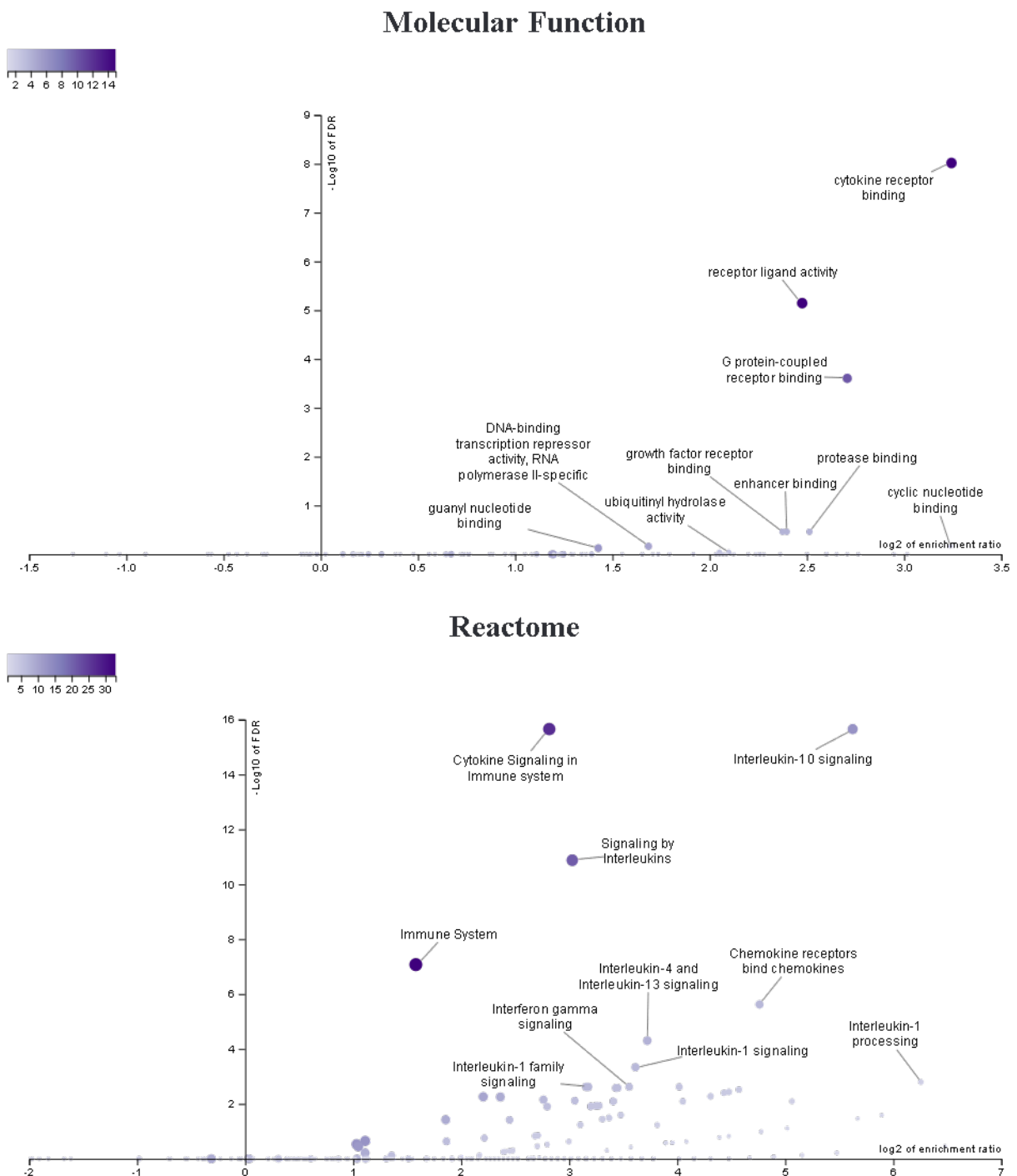


Figure 4. 14 continued: Gene ontology analysis of Signature B. Processes shown are non-redundant biological process, cellular component, non-redundant molecular functions and reactome pathways. Figures visualise up to top 10 hits where hits were found regardless of significance. Genes assessed were those significantly increased LPS-treated 22q11.2DS MGLs compared to 22q11.2DS MGLs based on Signature C DEG data. No genes were significantly decreased.

4.3.7. Signature C

To assess whether 22q11.2DS MGLs, like control MGLs, are capable of a wide response to LPS and whether the CNVs have an impact on this response, RNAseq was analysed separately. The same analysis pipeline was used as with control MGLs.

22q11.2DS MGLs exhibited a similarly sized response to control MGLs with 96 genes being up-regulated (**Figure 4.15, Table 4.13**). However, a surface level difference of 13 genes highlights the need for secondary analysis. In the 22q11.2DS, it is notable that genes that are down-regulated in 22q11.2DS MGLs such as IL-6 and IL1A (**Section 4.3.3, Chapter 4**), are significantly up-regulated in response in LPS-treated compared to vehicle-treated 22q11.2DS MGLs. This shows that 22q11.2DS MGLs are capable of shifting transcriptomic state in response to LPS even with these differences in transcriptomic state between vehicle-treated conditions.

ACOD1	CCL4L2	EBI3	ICAM1	MB21D2	PIM3	SLAMF1	
ACSL1	CD274	EHD1	IER3	MEFV	PLAGL2	SLC2A6	
ACVR2A	CD40	ELOVL7	IFNGR2	MFSD2A	PNRC1	SOC3	
ADORA2A	CD83	FFAR2	IL1A	NFE2L2	PPP1R15A	SOD2	
ANKRD33B	CFAP46	GBP1	IL1B	NFKB1	PTGER4	STX11	TRAF1
ARRDC3	CXCL1	GBP2	IL6	NFKB2	PTGS2	TICAM1	UPB1
BCL3	CXCL10	GCH1	IRAK2	NFKBIA	REL	TLR2	WTAP
BTG2	CXCL2	GPR132	IRF8	NFKBIZ	RELB	TNF	ZBTB10
BTG3	CXCL3	GPR84	KANK1	NKX3-1	RND1	TNFAIP2	ZC3H12A
CCL2	CXCL8	GRAMD1A	KMO	OTUD1	RNF144B	TNFAIP3	
CCL20	DDIT4	GRAMD2B	KYNU	PDE4B	RNF19B	TNFAIP8	
CCL3	DNAAF1	HEY1	MAP3K8	PDGFB	SDC4	TNFSF9	
CCL4	DRAM1	HS3ST3B1	MARCKS	PIM2	SIX5	TNIP1	

Table 4. 13: Differentially expressed genes in Signature C. Overview of genes significantly increased in 22q11.2DS MGLs compared to control MGLs. No genes were significantly downregulated in Signature C.

DEGs were then assessed against other human microglia data sets using the MGENrichment tool. 8 hits were identified following 5% FDR correction (Table 4.14). The associated data sets are the same as that which was observed in the vehicle-treated vs LPS-treated control LPS analysis, with the exception of a data set linked with oxidative phosphorylation, cell cycle, and immediate-early response (Kracht et al., 2020). This is important as it may suggest that the 22q11.2DS MGLs are differentially prepared to respond to environmental stimuli during fetal stages compared to control MGLs.

<i>listname</i>	<i>in list</i>	<i>description</i>	<i>tissue</i>	<i>source</i>
geneModules SCZ & ASD & BD	43	WGCNA gene expression modules ASD & SCZ & BD gene enriched	brain	Gandal, et al., 2018
Cluster 5 Microglia anti-inflammatory responses	31	SCRNA-seqCluster 5 Microglia anti-inflammatory responses	microglia	Olah et al., 2020
core human microglial signature	35	logFC > 3 and p < 0.001 human microglia vs human cortex	microglia	Galatro et al. 2017
Human microglia signature genes	27	Genes with >10-fold-higher average expression in microglia compared to cortex	microglia	Gosselin, et al. 2017
Gandal ASD > Ctrl	30	RNASeq genes higher in ASD compared to controls	brain	Gandal, et al., 2018
Cluster 3 Microglia cellular stress	9	SCRNA-seqCluster 3 Microglia cellular stress	microglia	Olah et al., 2020
Cluster 6 Microglia anti-inflammatory responses	11	SCRNA-seqCluster 6 Microglia anti-inflammatory responses	microglia	Olah et al., 2020
State 6 oxidative phosphorylation, cell cycle, and the immediate-early response	3	SC-RNAseqState 6 oxidative phosphorylation, cell cycle, and the immediate-early response	microglia	Kracht et al. 2020

Table 4. 14: Gene set enrichment analysis of Signature C. *In list* denotes the total number of overlapping DEG in Signature C and the target gene data set. The brief description of the data set is extracted from the MGENrichment tool output. Microglia tissue annotation under tissue infers isolated cells. Non-human tissue was excluded from the final data set. Genes assessed were those significantly increased LPS-treated 22q11.2DS MGLs compared to 22q11.2DS MGLs based on Signature C DEG data. No genes were significantly decreased. Comparison datasets notably refer to ASC as ASD, which kept in the table to ensure that the information stays true to the original publications. ASD is adapted for to ASC in thesis main text. Abbreviations: ASC, autism spectrum condition; ASD, autism spectrum disorder; BD, bipolar disorder; MGL, microglia-like cells; RNAseq, RNA sequencing; SCRNA-seq, single-cell RNA sequencing; SCZ, schizophrenia; WGCNA, weighted correlation network analysis.

Subsequently, the Webgestalt GO analysis tool was used to assess the gene ontology of DEGs against non-redundant biological processes, non-redundant molecular functions, cellular components, and reactome pathways. Similar to LPS response in control MGLs, a large amount of processes passing 5% FDR correction identified. Top 10 hits for each category are shown in **Figure 4.16**. Associations passing 5% FDR correction were:

- Non-redundant biological processes: Response to interleukin-1, cellular response to biotic stimulus, response to molecule of bacterial origin, response to interferon-gamma, response to tumor necrosis factor, negative regulation of cytokine production, positive regulation of response to external stimuli, regulation of inflammatory response, positive regulation of cytokine production, leukocyte migration
- Cellular components: No significant associations

- Non redundant molecular functions: G protein-coupled receptor binding, receptor ligand activity,
- Reactome pathways: Interleukin-1 processing, interleukin-10 signaling, interleukin-4 and Interleukin-13 signaling, interleukin-1 signaling, interferon gamma signaling, interleukin-1 family signaling, signaling by interleukins, RIP-mediated NFkB activation via ZBP1, diseases of immune system, diseases associated with the TLR signaling cascade, chemokine receptors bind chemokines, cytokine signaling in immune system, and immune system.

This ontology analysis highlighted some key differences across Signature B and Signature C.

Signature B had unique associations with:

- Biological processes: Leukocyte cell-cell adhesion, and positive regulation of defense response.
- Non-redundant molecular function: Cytokine receptor binding

Signature C had unique associations with:

- Biological processes: Response to interferon-gamma and negative regulation of cytokine production. In reactome associated hits,
- Reactome pathways: RIP-mediated NFkB activation via ZBP1, diseases of immune system, diseases associated with the TLR signaling cascade.

Differences in associated pathways utilised during LPS response indicate potential use of unique mechanisms during immune response. Hence it would be interesting to further investigate whether uniquely DEGs in Signature B and Signature C are the primary genes driving this difference.

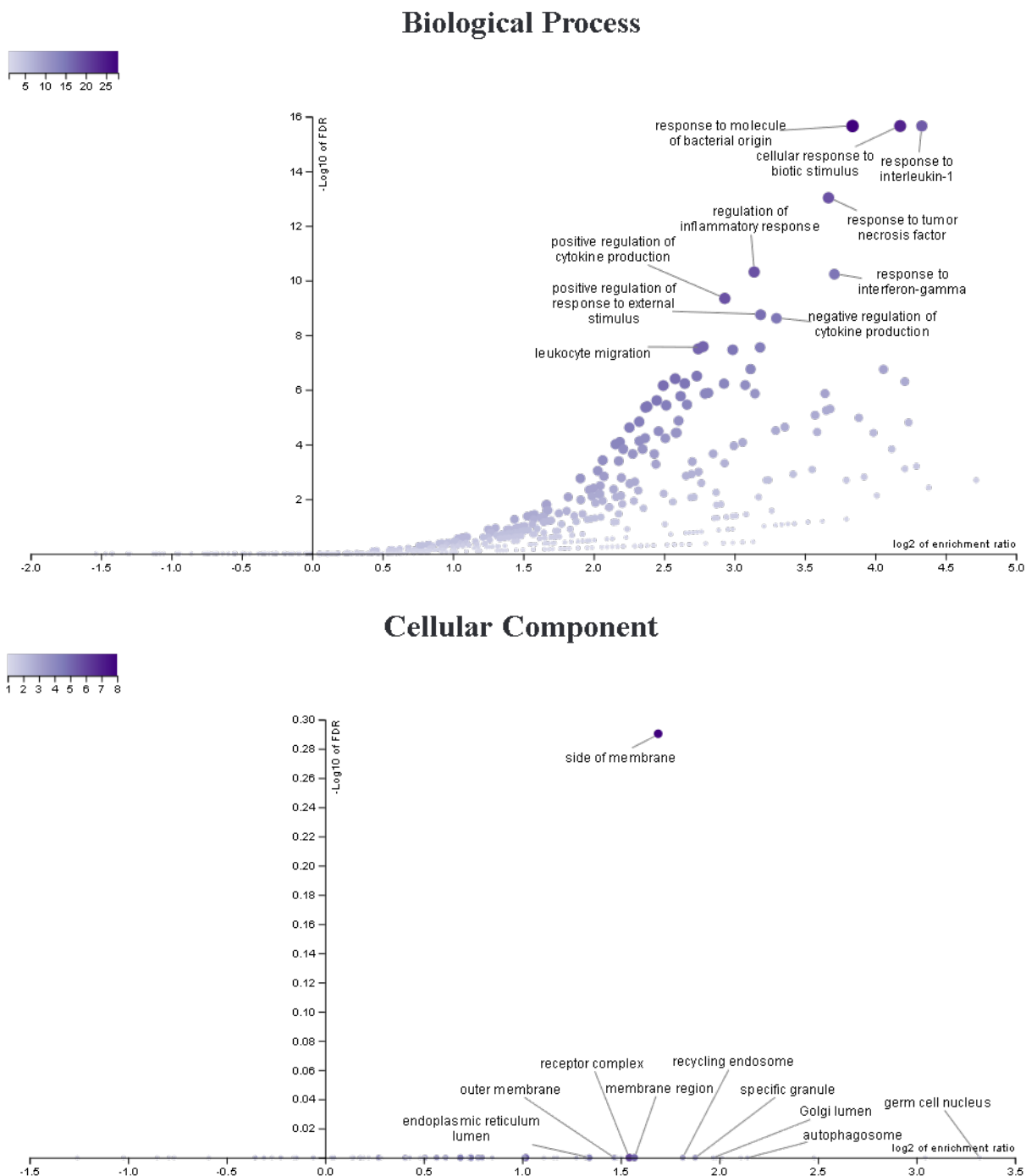


Figure 4. 16: Gene ontology analysis of Signature C. Processes shown are non-redundant biological process, cellular component, non-redundant molecular functions and reactome pathways. Figures visualise up to top 10 hits where hits were found regardless of significance. Genes assessed were those significantly increased LPS-treated 22q11.2DS MGLs compared to 22q11.2DS MGLs based on Signature C DEG data. No genes were significantly decreased.

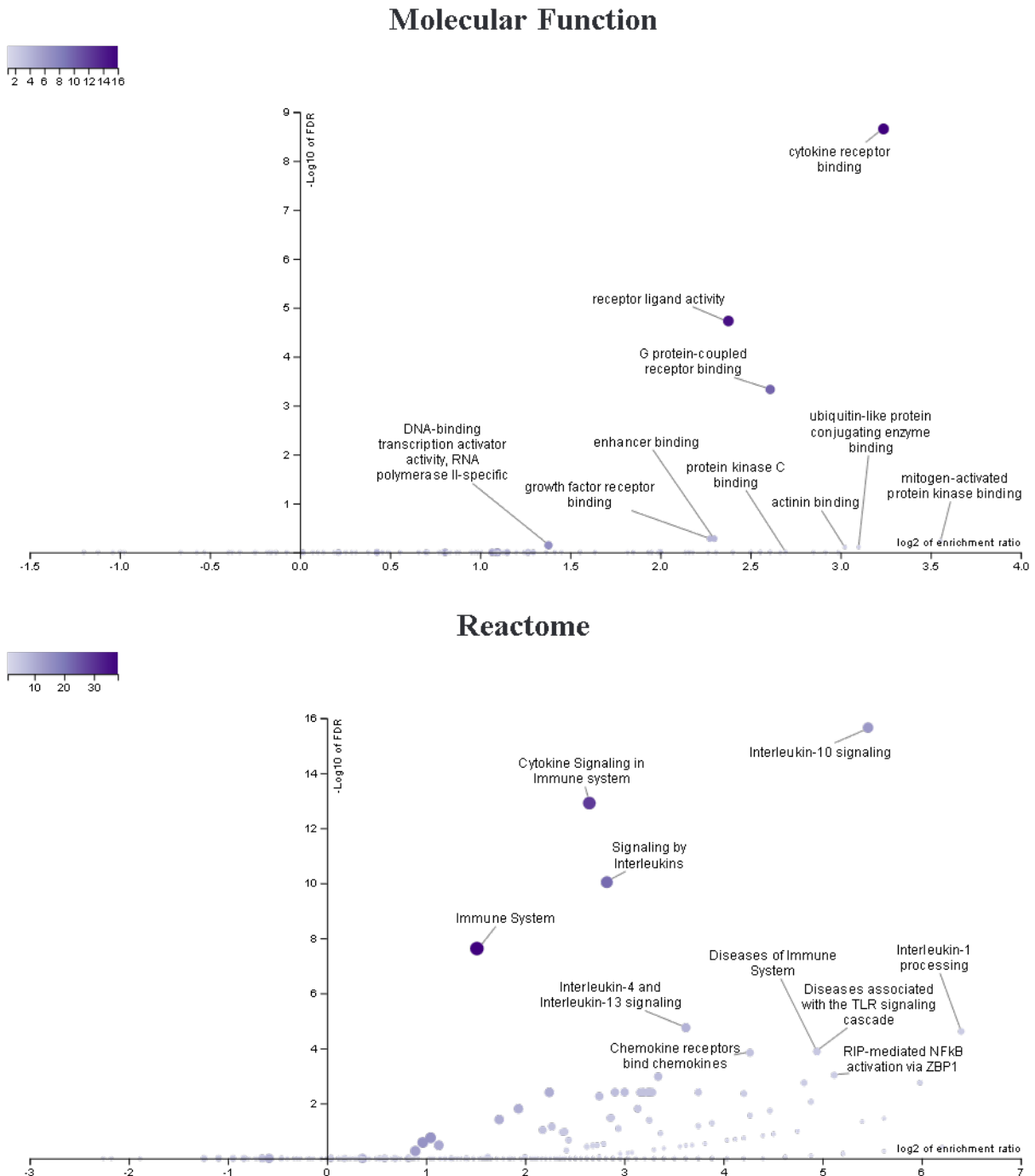


Figure 4. 16 continued: Gene ontology analysis of Signature C. Processes shown are non-redundant biological process, cellular component, non-redundant molecular functions and reactome pathways. Figures visualise up to top 10 hits where hits were found regardless of significance. Genes assessed were those significantly increased LPS-treated 22q11.2DS MGLs compared to 22q11.2DS MGLs based on Signature C DEG data. No genes were significantly decreased.

4.3.8. Common differentially expressed genes between control and 22q11.2DS in response to LPS

To further assess how control and 22q11.2DS MGLs might differentially respond to LPS, differences in DEGs were assessed. As shown in **Figure 4.17**, 61 DEGs were up-regulated in both analyses with 35 being uniquely differentially regulated in vehicle- vs LPS-22q11.2DS MGLs, and 23 in the control MGL analysis. A list of the commonly expressed genes is shown in **Table 4.15**.

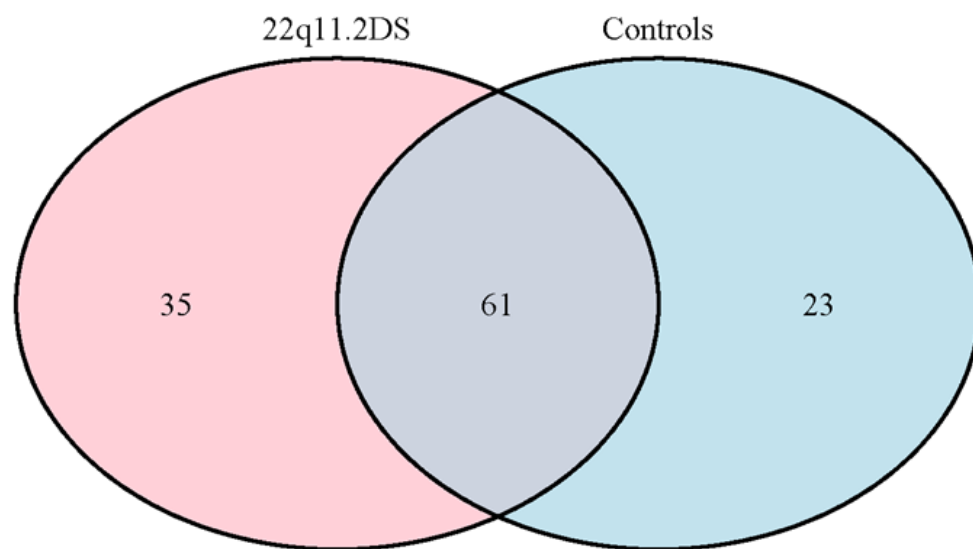


Figure 4. 17: Venn diagram showing the total number of overlapping and uniquely differentially expressed genes in Signature B and Signature C. Number of genes up-regulated in both LPS-treated control and 22q11.2DS MGLs compared to vehicle-treated control and 22q11.2DS, respectively. All of these genes were up-regulated in the LPS condition. No genes were down-regulated in either LPS condition compared to the respective vehicle condition. Red circle represents control MGLs and blue circle represents 22q11.2DS MGLs.

ACOD1	CXCL3	GRAMD2B	MFSD2A	REL	
ACSL1	CXCL8	HEY1	NFKB1	RND1	
ANKRD33B	DNAAF1	HS3ST3B1	NFKBIA	RNF144B	
ARRDC3	DRAM1	ICAM1	NFKBIZ	SDC4	TNFAIP3
CCL20	EBI3	IL1A	PDE4B	SLAMF1	TNFSF9
CCL3	EHD1	IL1B	PDGFB	SLC2A6	TRAF1
CCL4	ELOVL7	IL6	PIM2	SOC3	WTAP
CD83	GBP1	IRAK2	PIM3	SOD2	ZBTB10
CXCL1	GBP2	IRF8	PNRC1	STX11	ZC3H12A
CXCL10	GPR132	KANK1	PTGER4	TNF	
CXCL2	GRAMD1A	MAP3K8	PTGS2	TNFAIP2	

Table 4. 15: Overlap of differentially expressed genes in Signature B and Signature C. Overview of genes up-regulated in both LPS-treated control and 22q11.2DS MGLs compared to vehicle-treated control and 22q11.2DS, respectively. All of these genes were up-regulated in the LPS condition. No genes were down-regulated in either LPS condition compared to the respective vehicle condition.

4.3.9. Microglia gene set enrichment of uniquely differentially expressed genes in LPS treated control and 22q11.2DS MGLs

In an attempt to characterise the unique side of the response to LPS in control and 22q11.2DS, uniquely DEGs was assessed using the MGENrichment tool. An overview of the uniquely DEGs can be found in **Table 4.16** and **Table 4.17**.

BIRC3	LRRC32	
BMT2	MSC	RASL11A
CXCL6	NBPF19	RIPK2
F3	NOTCH2NLC	SGPP2
HIVEP1	PLAT	TNFAIP6
IRF1	PTX3	TNIP3
KCNA3	RAPGEF2	USP12
KDM6B	RASGRP1	ZC3H12C

Table 4. 16: Uniquely differentially expressed genes in Signature B vs Signature C. Overview of genes significantly increased in LPS-treated control MGLs but not significantly increased in LPS-treated 22q11.2DS MGLs. All these genes were up-regulated in LPS-treated control MGLs compared to vehicle-treated control MGLs.

ACVR2A	CD40	KMO	OTUD1	
ADORA2A	CFAP46	KYNU	PLAGL2	
BCL3	DDIT4	MARCKS	PPP1R15A	
BTG2	FFAR2	MB21D2	RELB	TNFAIP8
BTG3	GCH1	MEFV	RNF19B	TNIP1
CCL2	GPR84	NFE2L2	SIX5	UPB1
CCL4L2	IER3	NFKB2	TICAM1	
CD274	IFNGR2	NKX3-1	TLR2	

Table 4. 17: Uniquely differentially expressed genes in Signature C vs Signature B. Overview of genes significantly increased in 22q11.2DS MGLs but not significantly increased in control MGLs in LPS-treated control MGLs but not significantly increased in LPS-treated 22q11.2DS MGLs. All these genes were up-regulated in LPS-treated 22q11.2DS MGLs compared to vehicle-treated 22q11.2DS MGLs.

Following gene set enrichment analysis using MGENrichment of both sets of DEGs, no significant overlap with unique DEGs in Signature B (**Table 4.16**) was identified, however several gene sets were found to overlap with unique DEGs in Signature C (**Table 4.18**, gene list assessed in **Table 4.17**) which passed 5% FDR correction. These overlapping gene sets were associated with human microglial signature (Galatro et al., 2017; Gosselin et al., 2017)), anti-inflammatory responses (Olah et al., 2020), a psychiatric disorder gene module of schizophrenia, ASC and bipolar disorder (Gandal et al., 2018), including one data set with genes that are more highly expressed in ASC (Gandal et al., 2018). Interestingly, there was also overlap with a gene set comprised of immediate early microglia genes during GW 9-18 (Kracht et al., 2020), speculatively suggesting that immune challenge in 22q11.2DS carriers can impact homeostatic transcriptomic state of microglia during brain development differently than immune challenge in non-carriers would.

listname	In list	description	tissue	source
core human microglial signature	14	logFC > 3 and p < 0.001 human microglia vs human cortex	microglia	Galatro et al. 2017
Gandal ASD > Ctrl	13	RNASeq genes higher in ASD compared to controls	brain	Gandal, et al., 2018
Cluster 5 Microglia anti-inflammatory responses	10	SCRNA-seq Cluster 5 Microglia anti-inflammatory responses	microglia	Olah et al., 2020
geneModules SCZ & ASD & BD	12	WGCNA gene expression modules ASD & SCZ & BD gene enriched	brain	Gandal, et al., 2018
Gandal IBD > Ctrl	20	RNASeq genes higher in Irritable Bowel Disease compared to controls	brain	Gandal, et al., 2018
Human microglia signature genes	7	Genes with >10-fold-higher average expression in microglia compared to cortex	microglia	Gosselin, et al. 2017
Cluster 5 marker genes, GW 9-18; immediate early genes	3	SC-RNAseq Cluster 5 marker genes, gestational week 9-18; immediate early genes	microglia	Kracht et al. 2020

Table 4. 18: Gene set enrichment analysis of unique DEGs in Signature C vs Signature B. In list denotes the total number of overlapping DEG in unique Signature C DEGs and the target gene data set. The brief description of the data set is extracted from the MGENrichment tool output. Microglia tissue annotation under tissue infers isolated cells. Non-human tissue was excluded from the final data set. Genes assessed can be seen in Table 4.17. All genes were significantly up-regulated. Comparison datasets notably refer to ASC as ASD, which kept in the table to ensure that the information stays true to the original publications. ASD is adapted for to ASC in thesis main text. Abbreviations: ASC, autism spectrum condition; ASD, autism spectrum disorder; BD, bipolar disorder; GW, gestational week; MGL, microglia-like cells; RNAseq, RNA sequencing; SCRNA-seq, single-cell RNA sequencing; SCZ, schizophrenia; WGCNA, weighted correlation network analysis.

4.3.10. Gene ontology of uniquely differentially expressed genes in Signature B and C

To assess whether differences in Signature B and Signature C was associated with specific gene sets or pathways, downstream analyses was performed on DEGs that were not commonly up-regulated.

No hits were identified using the MGENrichment tool when assessing uniquely DEGs in Signature B (Table 4.16) and Signature C (Table 4.17), gene ontology was subsequently still attempted with Webgestalt GO analysis tool.

No associations passing 5% FDR correction were made with DEGs uniquely differentially regulated in Signature B, but top 10 hits for each category are shown in Figure 4.18. Several

processes were associated with the uniquely DEGs in Signature C. Top 10 hits for each category are shown in **Figure 4.19**. Associations passing 5% FDR correction were:

- Non-redundant biological process: ER-nucleus signaling pathway, chemokine production, response to interferon-gamma, type I interferon production, cellular response to biotic stimulus, response to molecule of bacterial origin, I-kappaB kinase/NF-kappaB signaling, regulation of neurotransmitter levels, positive regulation of cytokine production, regulation of inflammatory response, and diseases of immune system
- Reactome pathway: Diseases associated with the TLR signaling cascade.

This data suggests that cytokine secretion of 22q11.2DS MGLs in response to LPS might be different compared to control MGLs, with underlying differences in signalling pathways potentially the cause of this. Interestingly, this analysis also identified association with regulation of neurotransmitter levels, which is relevant for modulation of microglia immune response (Liu et al., 2016).

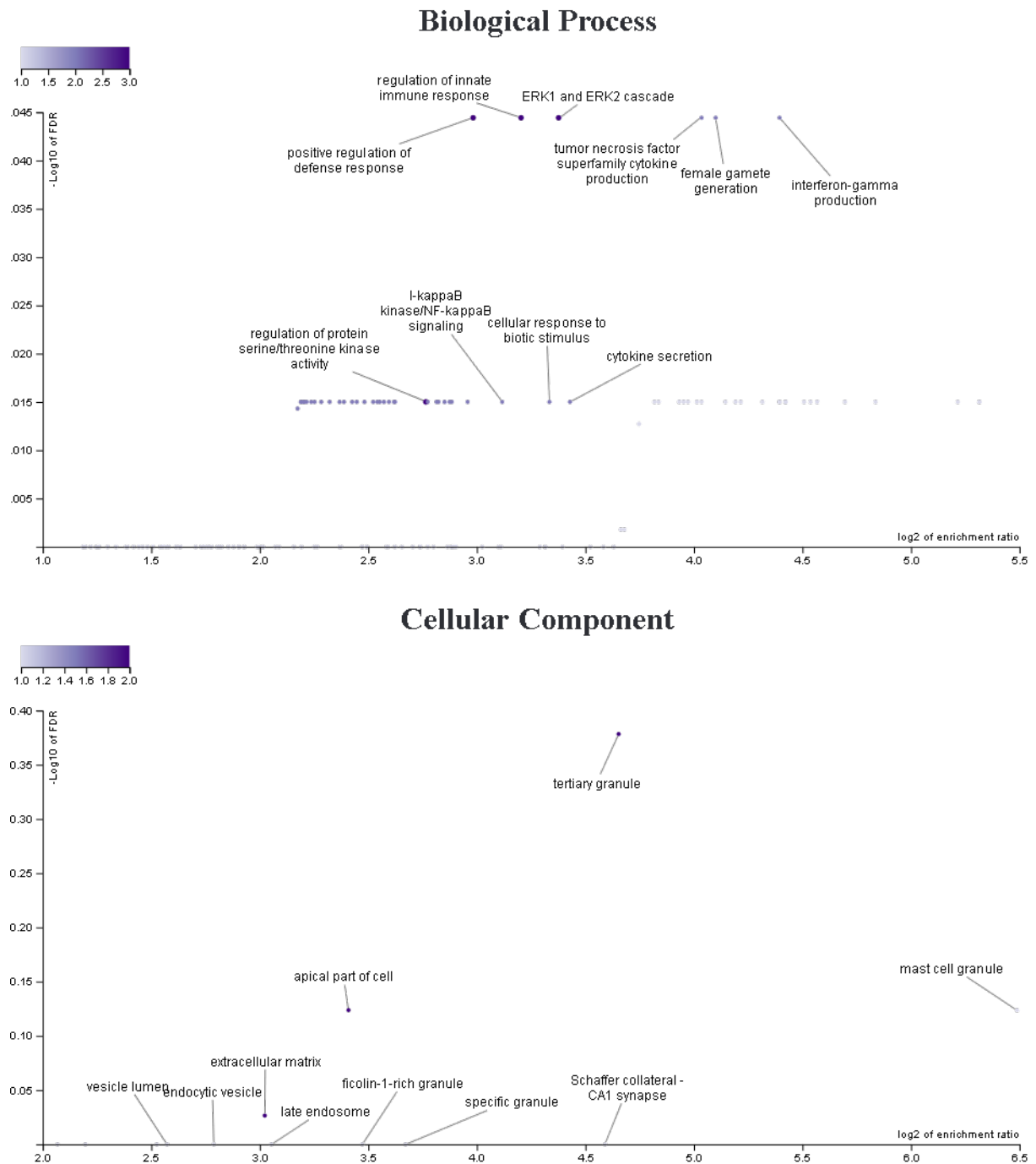


Figure 4. 18: Gene ontology analysis of DEGs up-regulated in Signature B but not Signature C. Processes shown are non-redundant biological process, cellular component, non-redundant molecular functions and reactome pathways. Figures visualise up to top 10 hits where hits were found regardless of significance. Threshold for DEGs was $p_{adj} < 0.05$ along with a $\text{Log}_2\text{FoldChange}$ of 1.5.

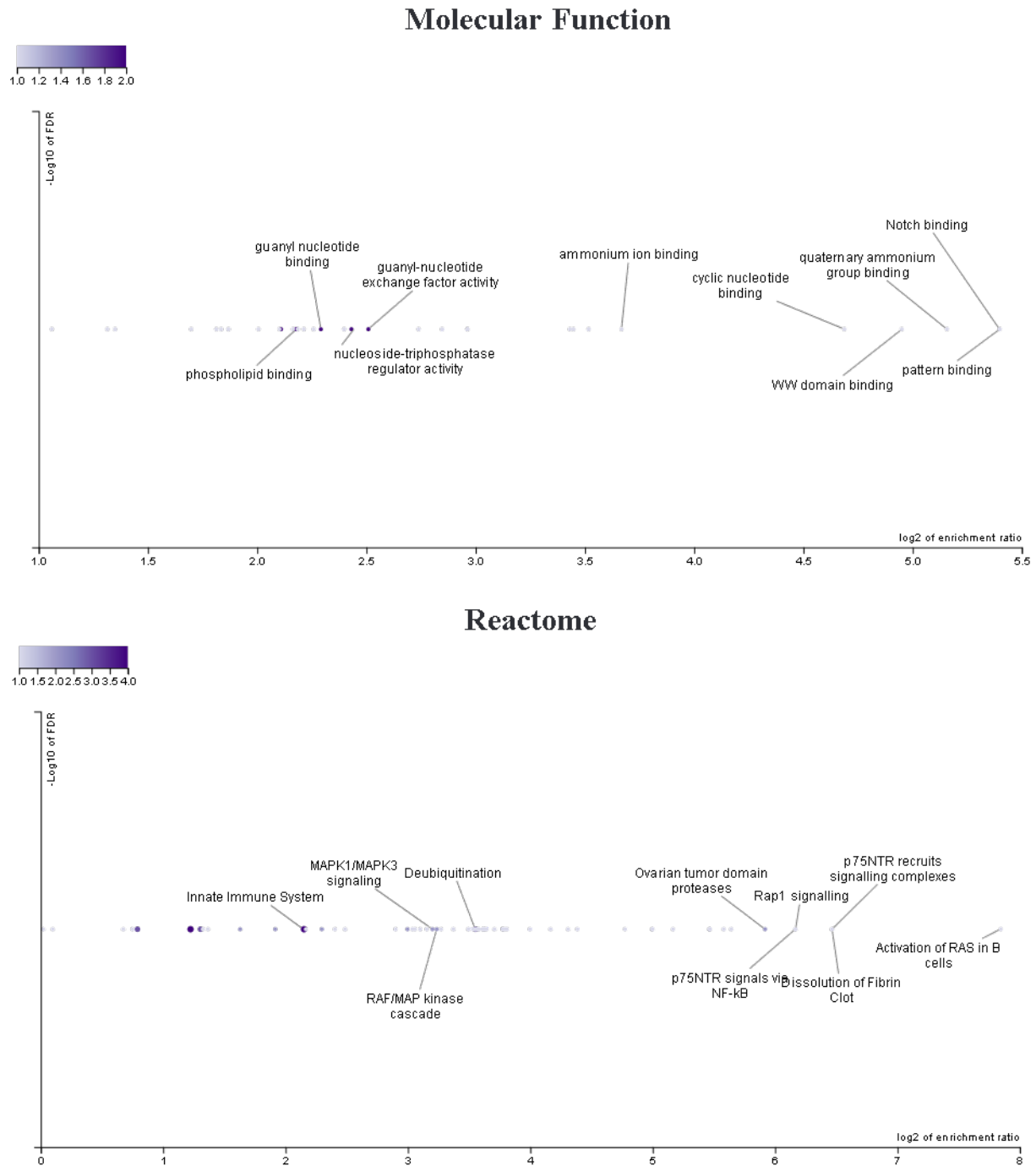


Figure 4. 18 continued: Gene ontology analysis of DEGs up-regulated in Signature B but not Signature C.

Processes shown are non-redundant biological process, cellular component, non-redundant molecular functions and reactome pathways. Figures visualise up to top 10 hits where hits were found regardless of significance.

Threshold for DEGs was $\text{padj} < 0.05$ along with a Log2FoldChange of 1.5.

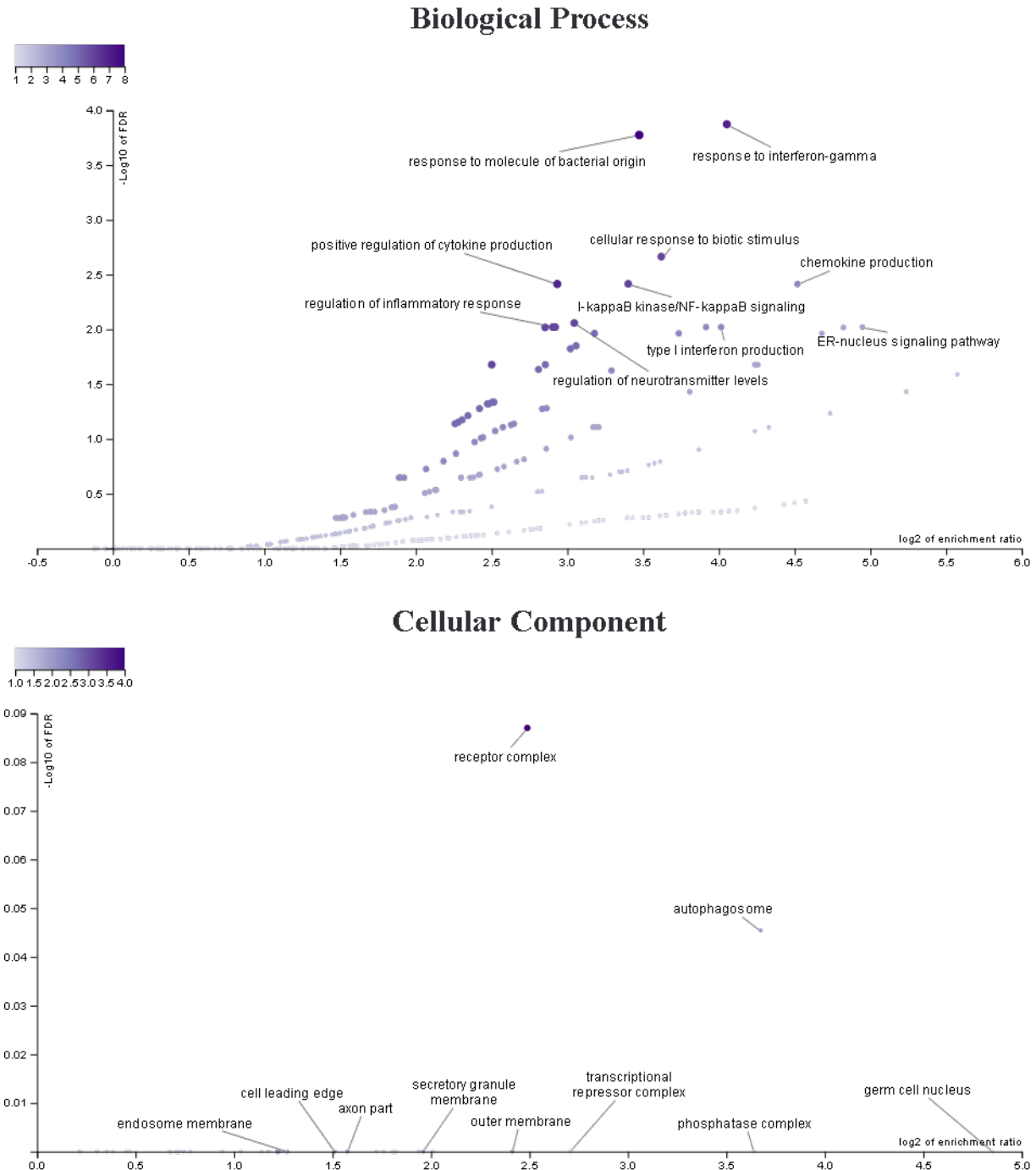


Figure 4. 19: Gene ontology analysis of DEGs up-regulated in Signature C but not Signature B. Processes shown are non-redundant biological process, cellular component, non-redundant molecular functions and reactome pathways. Figures visualise up to top 10 hits where hits were found regardless of significance. Threshold for DEGs was $\text{padj} < 0.05$ along with a Log2FoldChange of 1.5

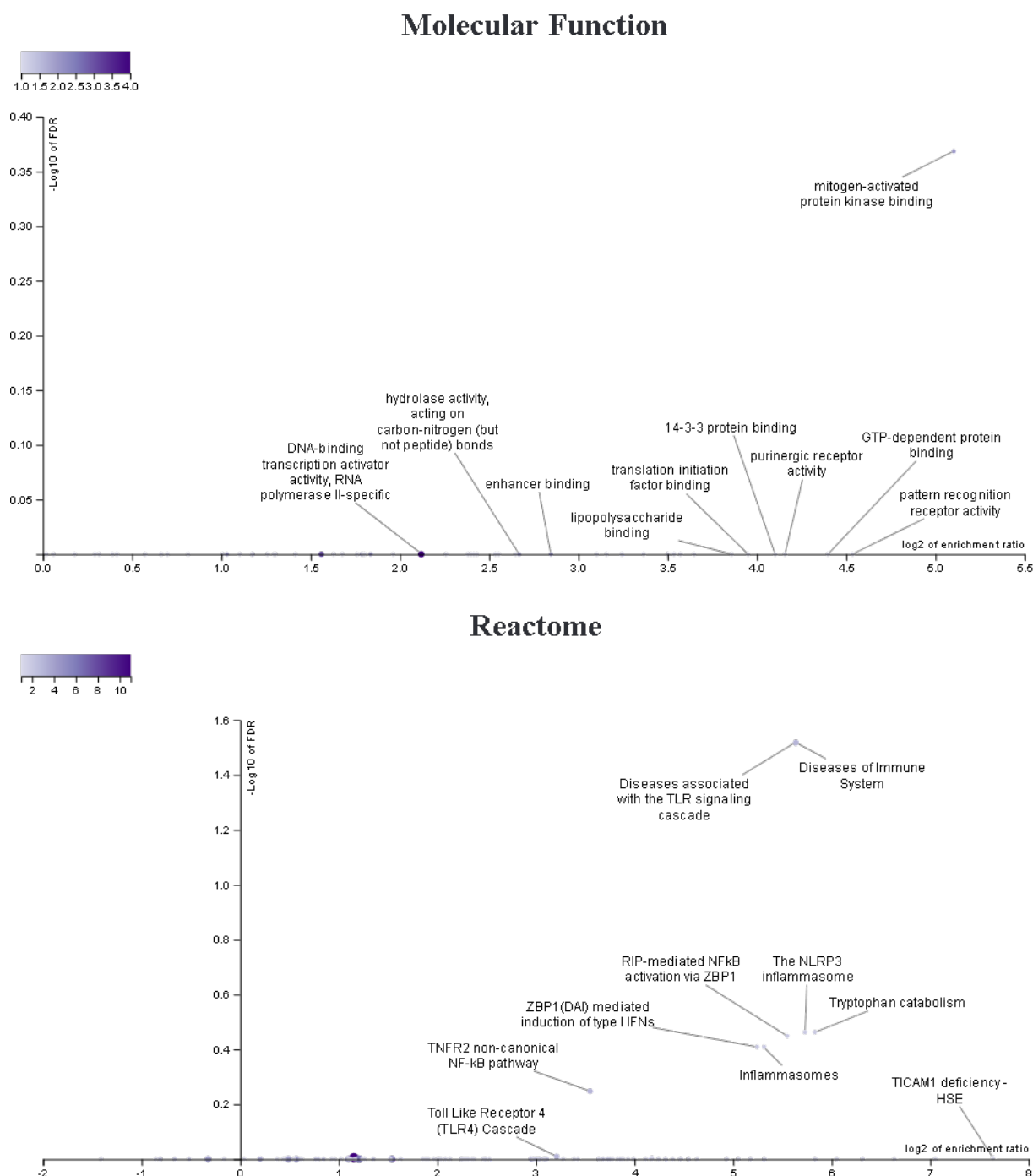


Figure 4. 19 continued: Gene ontology analysis of DEGs up-regulated in Signature C but not Signature B.

Processes shown are non-redundant biological process, cellular component, non-redundant molecular functions and reactome pathways. Figures visualise up to top 10 hits where hits were found regardless of significance.

Threshold for DEGs was $\text{padj} < 0.05$ along with a Log2FoldChange of 1.5

4.3.11. Signature D

Lastly, an interaction analysis was performed to assess how LPS stimulation differentially affects control and 22q11.2DS MGLs. 2 genes passed multiple correction interaction analysis at the $\text{padj} < 0.05$ Log2FoldChange 1.5 threshold, specifically *CXCL10* and *CHN1* (**Figure 4.20**). To see which cell lines drives this difference, normalised gene counts are shown in **Figure 4.21**.

CXCL10 is significantly up-regulated in response to LPS in both control and 22q11.2DS MGLs (**Section 4.3.7, Chapter 4** and **Section 4.3.8, Chapter 4**), but appears to increase more in 22q11.2DS MGLs following treatment. Reduced *CXCL10* expression have been associated with reduced microglial migration in cuprizone-treated knockout mice (Clarner et al., 2015), suggesting that 22q11.2DS MGLs might be in a more responsive state compared to control MGLs. When looking at the normalised count data, the consistently strong response across all 22q11.2DS MGLs is the driver behind this significant difference. *CHN1* was not up-regulated in any of the analyses (**Section 4.3.7, Chapter 4** and **Section 4.3.8, Chapter 4**). The response is more driven by 2 of the 3 22q11.2DS hiPSC lines, with the exclusion being 191_SZF_09 (for genetic background, see **Section 3.3.1, Chapter 3**). The change in control of MGLs is also largely non-existent, with it at times decreasing. This is an interesting finding as *CHN1* is a largely uncharacterised gene in terms of its role in microglia form and function.

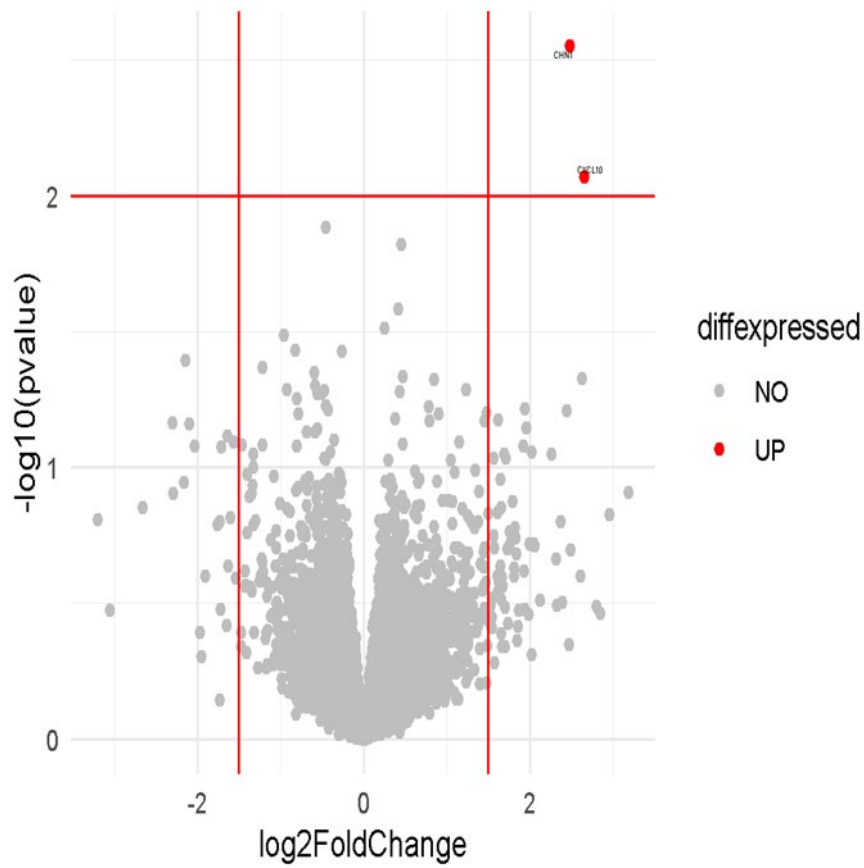


Figure 4. 20: Volcano plot of up- and down-regulated genes in Signature D. UP (red) = genes more up-regulated in LPS-treated 22q11.2DS MGLs compared to LPS-treated control MGLs, DOWN(blue) = genes more down-regulated in LPS-treated 22q11.2DS MGLs compared to LPS-treated control MGLs. NO (grey) = genes not passing the designated threshold. Abbreviations: padj, adjusted pvalue; diffexpressed, differentially expressed.

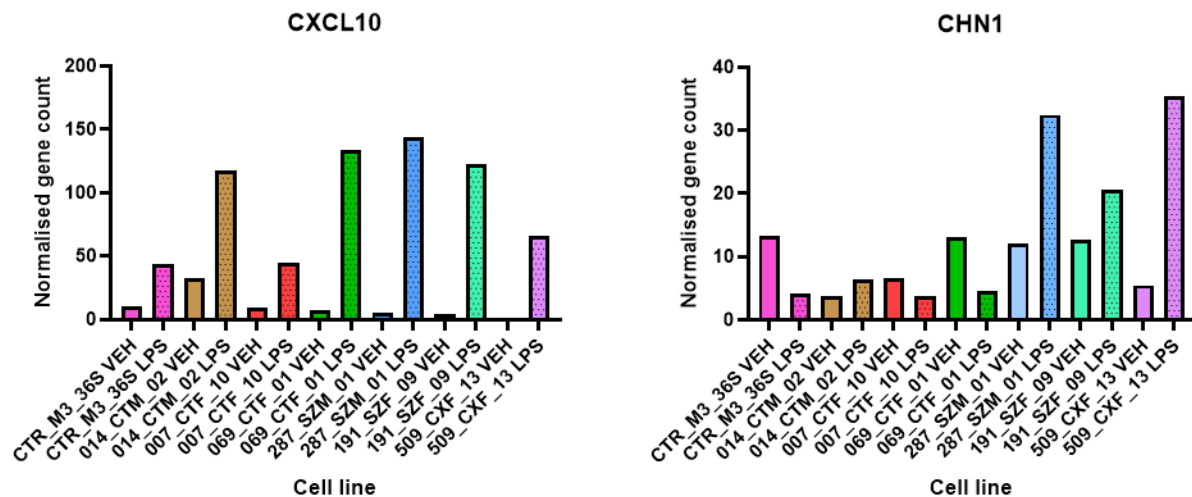


Figure 4. 21: Normalised gene counts of gene hits in Signature D. Figures show vehicle- and LPS-treated control and 22q11.2DS MGLs. Final three letters in cell lines on the x-axis indicates H₂O vehicle treated (VEH) or LPS-treated (LPS). Abbreviations: LPS, lipopolysaccharide; MGL, microglia-like cell; VEH, vehicle.

4.4 Discussion

This chapter provided the first RNA sequencing data on 22q11.2DS MGLs as well hiPSC-derived MGL LPS response in both control and 22q11.2DS cell lines. It critically provided an overview of positive expression of key microglia genes further verifying successful use of the differentiation protocol. While identifying a clear difference between control and 22q11.2DS MGL transcriptomic state in vehicle-treated condition potentially impacting cytokine-associated functions, LPS treatment also confirmed the ability of hiPSC-derived MGLs to exhibit a broadly respond to this challenge. In addition to the latter confirmation, secondary analyses also identified several key differences in how 22q11.2DS utilises different pathways to illicit this response to LPS compared to control lines. The discussion of this exploratory analysis provides are largely speculative perspective on the implications of findings and attempts to identify potential microglia functions that could be investigated in future studies. To help provide an overview of Signature A thresholds and Signature B versus C MGEnrichment analysis a summary is provided in **Figure 4.22**, and **Figure 4.23**, respectively. Similarly, an overview of Signature A thresholds and Signature B versus C gene ontology analysis is provided in **Figure 4.24**, and **Figure 4.25**, respectively.

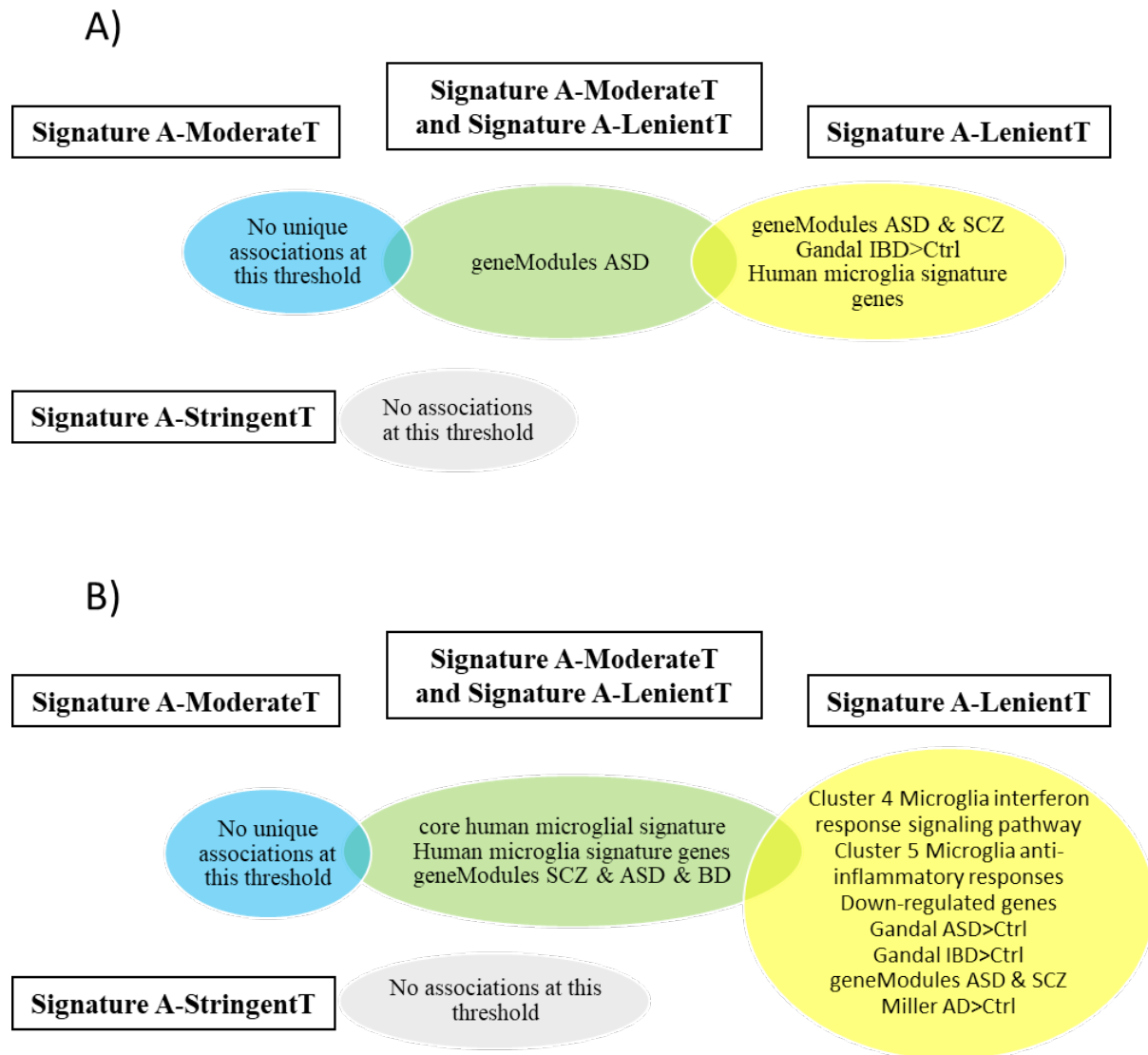


Figure 4. 22: Overview of Signature A MGENrichment gene set enrichment analyses. A) Common and unique significant overlaps between thresholds tested based on up-regulated DEGs. B) Common and unique significant overlaps between thresholds tested based on down-regulated DEGs. These gene sets were initially identified in Table 4.10 and Table 4.11, and specifically not identified in Table 4.9. Comparison datasets notably refer to ASC as ASD, which kept in the tables and figures to ensure that the information stays true to the original publications. ASD is adapted for to ASC in thesis main text. Abbreviations: ASC, autism spectrum condition; ASD, autism spectrum disorder; BD, bipolar disorder; GW, gestational week; MGL, microglia-like cells; RNAseq, RNA sequencing; SCRNA-seq, single-cell RNA sequencing; SCZ, schizophrenia; WGCNA, weighted correlation network analysis.

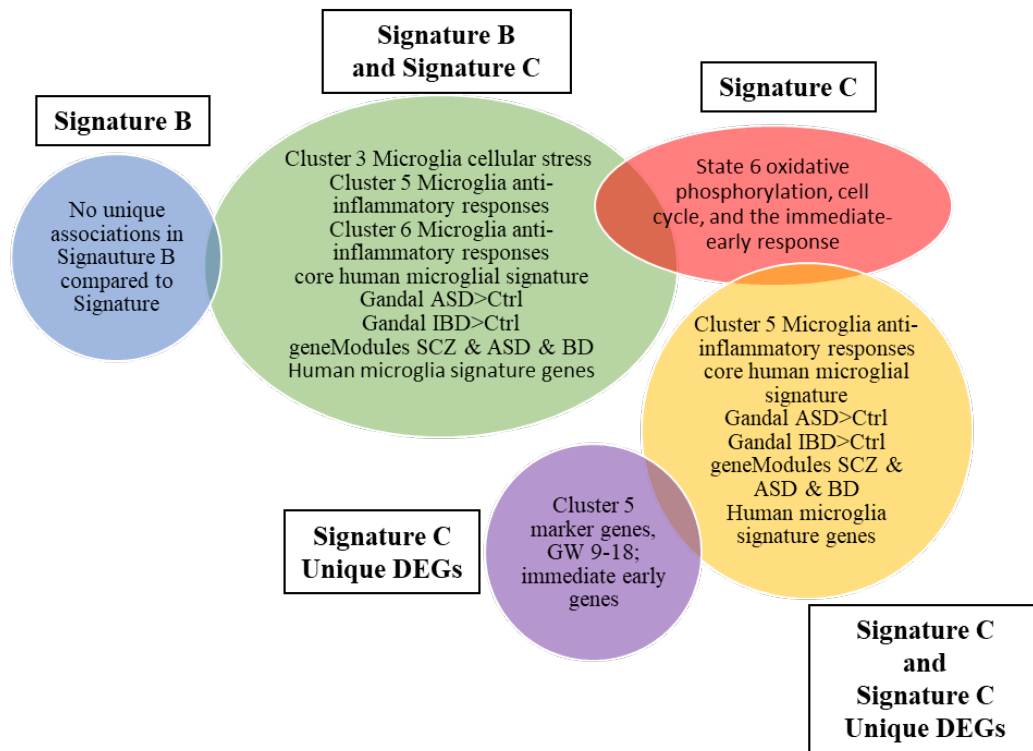


Figure 4. 23: Overview of Signature B and Signature C MGENrichment gene set enrichment analyses. All common and unique significant overlaps with MGENrichment analysis gene sets between Signature A and Signature B. These gene sets were initially identified in Table 4.12, Table 4.14, and Table 4.18. All overlapping genes are up-regulated. Comparison datasets notably refer to ASC as ASD, which kept in the tables and figures to ensure that the information stays true to the original publications. ASD is adapted for to ASC in thesis main text. Abbreviations: ASC, autism spectrum condition; ASD, autism spectrum disorder; BD, bipolar disorder; MGL, microglia-like cells; RNAseq, RNA sequencing; SCRNA-seq, single-cell RNA sequencing; SCZ, schizophrenia; WGCNA, weighted correlation network analysis.

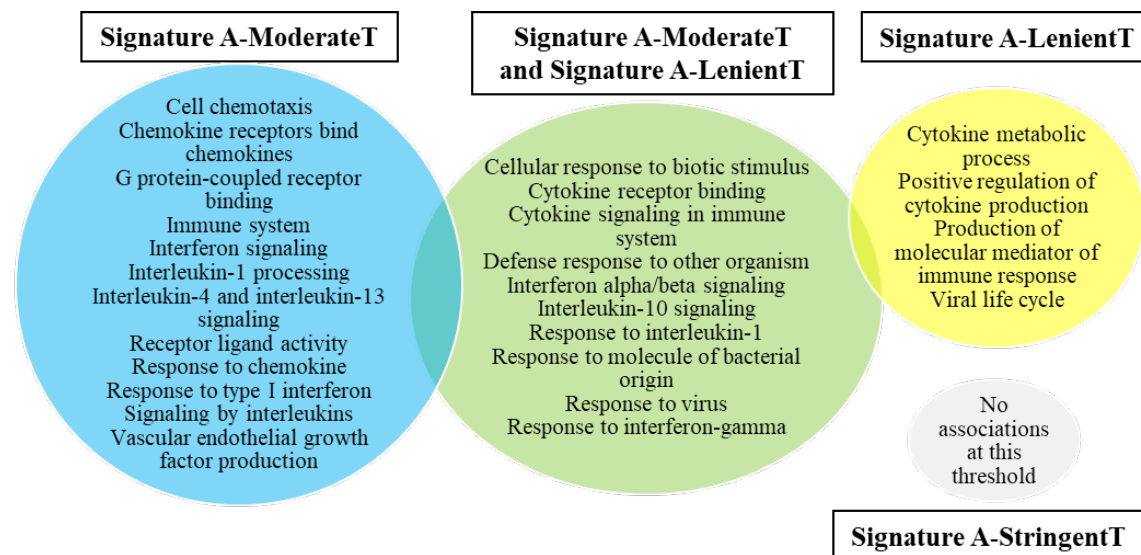


Figure 4. 24: Overview of Signature A gene ontology analyses. Common and unique significant associations between thresholds tested based on down-regulated DEGs. No associations were found with up-regulated DEGs. These associations were initially described in Section 4.3.5, Chapter 4. Processes shown are either non-redundant biological processes, non-redundant molecular functions or reactome pathways. For the relevant category to each association, see associated section.

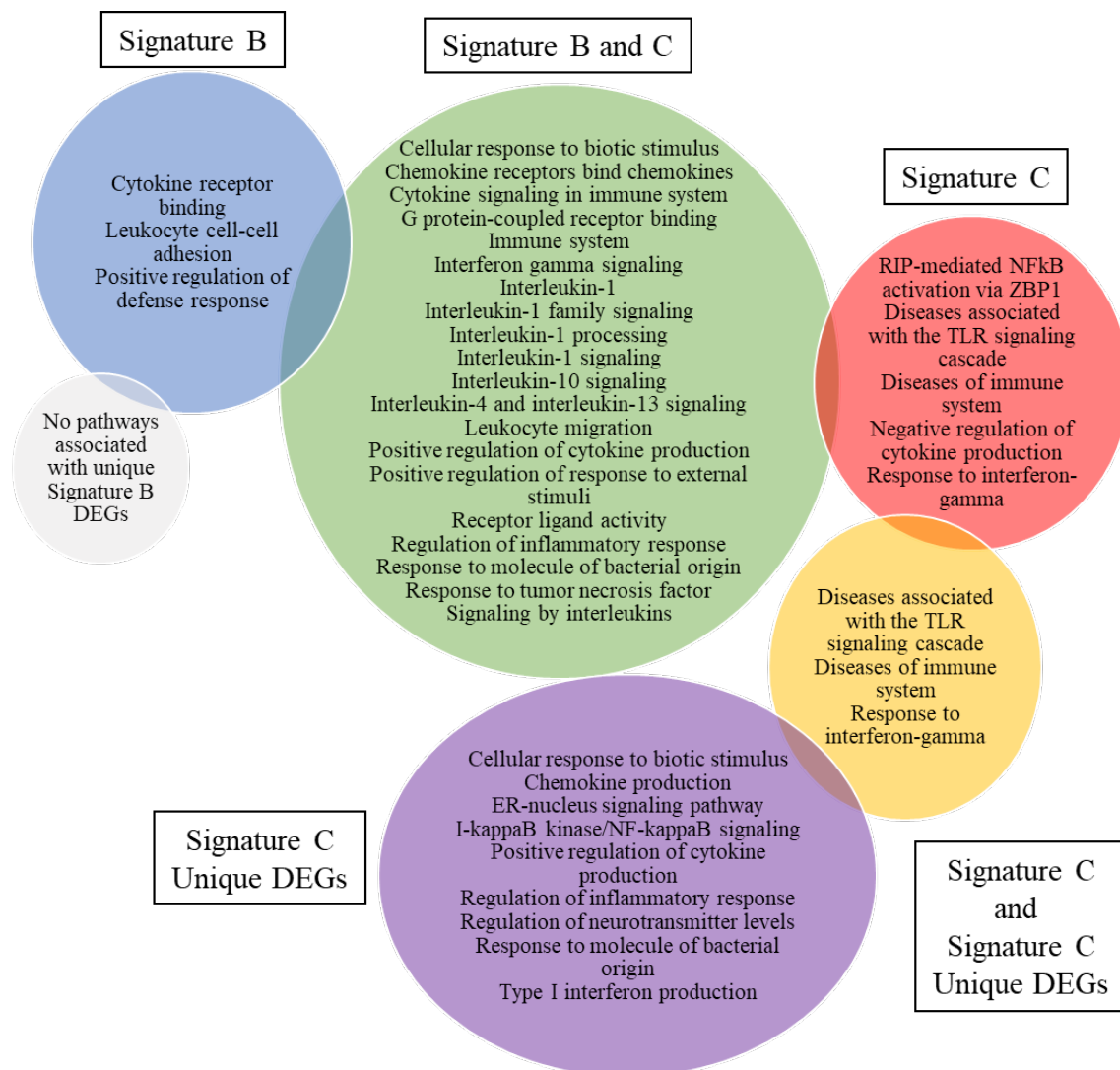


Figure 4. 25: Overview of Signature B and Signature C gene ontology analyses. All common and unique significant overlaps in gene ontology analyses between Signature A and Signature B. All tested DEGs data sets are up-regulated as there was no significantly down-regulated DEGs assess in these Signatures. These associations were initially described in Section 4.3.6, Section 4.3.7, and section 4.3.10, all sections being in Chapter 4. Processes shown are either non-redundant biological processes, non-redundant molecular functions or reactome pathways. For the relevant category to each association, see associated section.

4.4.1. Differentially regulated genes in Signature A are associated with 22q11.2DS-associated conditions and aberrancies in immune response

In initial analysis of Signature A-StringentT, only 11 genes were found to be differentially regulated in 22q11.2DS MGLs compared to controls (**Section 4.3.3, Chapter 4**). As there are no microglia studies to directly compare to, this is a substantially lower number than what have for example been noted in schizophrenia on neural progenitor cells. However, this is not surprising if one considers the much larger sample size of this study, as well as that the threshold of significance was notably less stringent (Evgrafov et al., 2020). In studies with similar sample numbers but on hiPSC-derived neural progenitor and a statistical threshold similar to StringentT by Bhat et al. (2022) on schizophrenia, 1 and 0 DEGs was detected. While this might allude to MGLs potentially being more broadly affected than neuronal cells, it is importantly not clear whether this is a phenotype uniquely caused by presence of 22q11.2 CNVs as Bhat et al (2022) investigated idiopathic cell lines. Even considering the difference in DEGs compared to other hiPSC data sets, no microglia gene sets had significant overlap with up- or down-regulated genes. Similarly, no hits were significant when performing gene ontology analysis on relevant functions and pathways. Because of this, adopting the approach of Evgrafov and colleagues (2020) was deemed an interesting secondary approach. This approach was also supported by a larger study by Nehme et al. (2022) using the hiPSC model comparing 20 different 22q11.2DS lines from donors with various diagnosis with neurotypical controls found 212 DEGs in undifferentiated hiPSCs, 216 DEGs hiPSC-derived neural progenitor cells, 86 in hiPSC-derived neurons. They did however not find any statistically significant DEG in a pilot study looking at only two 22q11.2DS cell lines. As noted in **Section 4.3.3, Chapter 4**, a substantial amount of genes within the 22q11.2 region were noted to be reduced with a fold change between -1.5 and -2.0. While expansion of analyses to more cell lines in this project was not plausible and as there are no universal

consensus for statistical thresholding in low sample size RNA sequencing, the transparency provided with overviews of analysis performed at different thresholds can help support comparisons with future studies with similar or higher statistical power.

Lucratively, testing two less stringent thresholds in Signature A showed a drastically higher amount of significantly up- and down-regulated genes (**Section 4.3.3, Chapter 4**). In what was defined as Signature A-ModerateT, 28 genes were down-regulated and 26 were up-regulated. In Signature A-LenientT, the least stringent threshold, 70 genes were down-regulated and 85 up-regulated. As shown, both of these also yielded notable findings in secondary analyses.

Enrichment analysis of DEGs demonstrated association with psychiatric disorder, Alzheimer's disease and core microglia signature gene sets. Down-regulated DEGs in both Signature A-ModerateT and Signature B-LenientT (**Section 4.3.4, Chapter 4**) also showed association with psychiatric disorders and the microglia signature, confirming that these DEGs in MGLs have relevance to schizophrenia, ASC and bipolar disorder, and that 22q11.2DS impacts homeostatic transcriptomic state in MGLs. Signature B-LenientT down-regulated DEGs were also additionally associated with Alzheimer's disease. These thresholds also point towards evidence for dysregulated interferon response signalling 22q11.2DS MGLs. In Signature A-ModerateT, the association with interferon response signalling is retained, but notable overlaps with Alzheimer's Disease and an anti-inflammatory response gene set is lost. This is, for example, potentially due to being driven by the 22q11.2DS cell line 287_SZM_01, which has high polygenic risk for Alzheimer's Disease compared to other lines in this study (**Section 3.3.2, Chapter 3**). In the up-regulated DEG set analysis, an

overlap with a signature gene set alongside ASC and schizophrenia is seen with Signature A-LenientT DEG, but only the overlap with ASC is retained in Signature A-ModerateT.

Both Signature A-ModerateT and Signature B-LenientT down-regulated DEGs was linked with interferon response signalling in enrichment analysis (**Section 4.3.4, Chapter 4**). Type I and II interferons both contribute to an antiviral state (Warre-Cornish et al., 2020), suggesting that 22q11.2DS might be more susceptible to viral exposure compared to control lines. Type I interferons have also been associated with the function of microglia in influencing neuroimmune milieu, blood-brain-barrier integrity, and regulation of phagocytosis, the latter of which has been suggested to be affected in psychiatric disorders using both induced microglia from blood monocytes and mouse models (McDonough et al., 2017; Sellgren et al., 2019; Meng et al., 2022). This finding also aligns with findings by Gupta et al. (2014), which in a single-cell transcriptomics study found that altered genes in microglia from ASC *postmortem* brain tissue (cerebral cortex, anterior prefrontal cortex, and part of the frontal cortex) is associated with the interferon type 1 pathway, validating this finding in 22q11.2DS MGLs. Additionally, the link with interferon and microglia in Parkinson's Disease has been described by de Paiva Lopes and colleagues (2022), also using isolated cells from four different brain regions including the medial frontal gyrus, superior temporal gyrus, subventricular zone and thalamus. Chronic type II interferon IFN γ treatment on microglia is also associated with a distinct microglia morphological state with retracted processes, increased secretion of IL-1 β , TNF- α , IL-6, and nitric oxide, up-regulation of CD11b and CD68, and population expansion (Papageorgiou et al., 2016). Transient IFN γ treatment has previously been linked to increased neurite outgrowth (McDonough et al., 2017; Warre-Cornish et al., 2020), and 22q11.2DS MGL inability to secrete this cytokine could hence speculatively explain reduced neuronal connectivity in psychiatric disorders. If

one considers data unique to Signature-LenientT, down-regulated DEGs share significant overlap to the gene set associated with anti-inflammatory response. Together, this gene set enrichment analysis may imply that 22q11.2DS MGLs would have an aberrant immune response, which could be either enhanced or blunted compared to control MGLs. However, functional assays would be required to further test this theory such as through assaying secretion of cytokines including IFN γ by the MGLs.

Gene ontology analysis of Signature A-ModerateT and Signature-LenientT (**Section 4.3.5, Chapter 4**) found no association with up-regulated DEG gene set, but further solidifies the association of the down-regulated gene sets with interferon, as well as linking the down-regulated DEGs with interleukin processing and cytokine signalling. Multiple interleukin pathways were identified as potentially involved in this analysis and implications for all hits will be discussed. Reduced processing of IL-1, which is associated with immune response (Liu and Quan, 2018), might imply that 22q11.2DS MGLs might be in an alternate homeostatic state. However, IL-10 signalling, which is a regulator of immune response is also associated with this gene set (Laffer et al., 2019; Shemer et al., 2020). Both IL-4 and IL-13 signalling which are also primarily serve a similar role to IL-10 (Li et al., 2021), are also affected as a consequence of the down-regulated genes. Both can also play a role in inducing the death of microglia in rats when immune response is promoted using LPS (Yang et al., 2002).

IL-4 plays a key role in repressing NF- κ B-dependent transcription of TLR-induced cytokines in primary rhesus macaque (Zuiderwijk-Sick et al., 2021). Both psychiatric disorders and neurodegenerative disease associated with 22q11.2DS have been linked with dysregulation of NF- κ B signalling or associated transcription modulators. This encompasses schizophrenia,

ASC, bipolar disorder, Alzheimer's Disease and Parkinson's Disease with modelling methodology broadly having utilised human *postmortem* tissue, immortalised human and mouse lines, plasma, and primary mouse tissue (Lee et al., 2010; Young et al., 2011; Honarmand Tamizkar et al., 2021; Li et al., 2021; Roman et al., 2021; Murphy et al., 2022; Wang et al., 2022). However, it is not clear what exact role NF- κ B plays in these conditions. In a study on schizophrenia *postmortem* tissue by Murphy and colleagues (2020), they suggest that dysregulation of this pathway might lead to blunting of putative normal immune responses. In line with the ontology analysis of Signature A (**Section 4.3.5, Chapter 4**), this could be related to a difference in the response necessary to attenuate or modulate the initiation of the immune response. *Postmortem* studies on schizophrenia also notably must account to antipsychotic exposure, which they found to positively correlate to NF- κ B mRNAs. Antipsychotics such as clozapine might for example elevate NF- κ B based on a mouse model by Volk et al. (2019), whereas haloperidol and olanzapine has no effect on NF- κ B expression in monkeys in Ibi et al. (2017). HiPSC models using MGLs could provide a better viewpoint of schizophrenia-associated NF- κ B expression including testing effect of antipsychotics.

Compared to IL-4, IL-13, while its role as a cytokine is well characterised, has not historically been associated with psychiatric or neurodegenerative conditions. Regardless, its role in the immune response, mostly characterised in ischemic stroke as well as brain and spinal cord injury models, is related to amelioration of microglia response (Kolosowska et al., 2019; Amo-Aparicio et al., 2021; Li et al., 2021; Chen et al., 2022). One mechanism through which IL-13 acts in amelioration of immune response is inhibition of STAT3 signalling. STAT3 pathway activation has for example in immortalised mouse line N9 and primary mice been associated with phenotypic conversion towards microglial states associated with

immune responses (Qin et al., 2012; Chen et al., 2022; . In an SV40 immortalised human microglia cell line model, exposure to schizophrenia patient serum has been shown to over-activate the STAT3 pathway (van Rees et al., 2018). It is unclear how this would correlate to reduced IL-13 signalling, other than potentially implying that a blunting of cytokine secretion associated with amelioration of the immune response occurs in schizophrenia.

IL-4 and IL-13, while both markers associated with the amelioration of the immune response, may play different roles in pathological conditions. This also extends to the ability of these cytokines to shift microglia metabolic profiles. In a mouse spinal cord injury model used by Amo-Aparicio et al. (2021), IL-13 fails to mediate functional recovery when compared to IL-4. A key difference found in these microglia is that IL-4 can shift microglia metabolism from glycolytic to oxidative phosphorylation, while IL-13 did not (Amo-Aparicio et al., 2021). This is of high relevance when modelling 22q11.2DS, as hiPSC-derived neuronal models investigating this genetic risk factor has found that oxidative phosphorylation is reduced in 22q11.2DS forebrain-like excitatory neurons in donors with schizophrenia, but not those without a schizophrenia diagnosis (Li et al., 2019; Li et al., 2021). In the context of microglia, reduced IL-4 signalling could be causal to a similar state if investigated using hiPSC-derived MGLs.

Having discussed the implications of cytokine dysregulation for microglia inflammation, the role of chemokines should also be noted due to the shown down-regulation of genes associated with chemokine receptor binding. Similarly to cytokines, chemokines play a role in microglia intrinsic form and function regulation as well as being a communication mechanism between other microglia and non-microglial cell types (Salvi et al., 2017). For example, *CCL13*, which in Signature A is down-regulated in 22q11.2DS MGLs compared to

controls at all thresholds, even StringentT, has using an hiPSC-derived microglia model been associated with reduced phagocytosis in microglia with high expression compared to those with low expression (**Section 4.3.3, Chapter 4**; Dräger et al., 2022). *CXCL10*, which is associated with immune response, is also down-regulated (Signature A-ModerateT and Signature A-LenientT in **Section 4.3.3, Chapter 4**). This is in line with down-regulated DEG gene ontology association with IL-10 signalling, which should regulate CXCL10 production (Cheeran et al., 2003, Signature A-ModerateT and Signature A-LenientT in **Section 4.3.5, Chapter 4**). Reduced *CCL20* expression (**Section 4.3.3, Chapter 4**), whose chemokine-associated production is associated with inhibition of immune response not specific to microglia in mice, is also observed in this study (Liao et al., 2020). Together, these data on Signature A suggests that aberrant cytokine and chemokine receptor binding in 22q11.2DS MGL transcriptomic state require functional testing.

4.4.2. Signature B and Signature C showcases broad immune responses, but secondary analysis identifies differences in pathways utilised

With LPS inducing 84 and 96 DEGs in Signature B and Signature C, respectively, this was considered a strong enough response to not loosen the threshold of significance for this analysis (**Section 4.3.6 and Section 4.3.7, Chapter 4**). However, like with the vehicle group comparisons, it is difficult to estimate what a substantial amount of DEGs would be. The closest study in size is on murine microglia treated with LPS or LPS+IFN γ treated their primary cultures for 6 hours rather than 3 hours, with the same concentration before sample collection (Pulido-Salgado et al., 2018). With a total of 4,684 DEGs, identical stringency of thresholding was utilised for analysis (Pulido-Salgado et al., 2018). Similarly, a large response has been shown in induced microglia from blood monocytes also in a 6-hour treatment Ormel et al. (2020), although the exact number of DEGs was not noted, but this

study was on 12 vehicle-treated samples and 13 LPS-treated samples. It is however notable that both studies do not use a minimum fold change when determining DEG thresholds. While this will account for some of the difference, it is unlikely that other minor differences in the analysis pathways also contributes to this difference in DEG number. It is possible that the 6-hour treatment used by these studies is a source of this difference, however. At this treatment time-point, additional genes might be up- or down-regulated in a response to the initial spike in transcriptomic immune response with gene expression levels also potentially being higher or lower. This highlights the importance of studying different time-points, which could decide whether the experiment is focused on, for example, studying the the immediate- or early response of MGLs to LPS.

MGEEnrichment analysis of Signature B and signature C data overlapped with gene sets associated with microglia signature markers, cellular stress and anti-inflammatory response (**Section 4.3.6** and **Section 4.3.7, Chapter 4**). Adding to this, overlaps were also found with schizophrenia, bipolar disorder and ASC data. Because of the converging evidence of microglia involvement in these conditions, it is not necessarily surprising, however, Sneeboer et al. (2019) have previously described that *postmortem* tissues of individuals with bipolar disorder do not exhibit patterns of immune response. The most interesting finding here, however, might be the overlap of Signature C up-regulated DEGs with a gene set associated with oxidative phosphorylation, cell cycle, and immediate-early response. Considering the previously discussed direct vehicle comparison data and published work on 22q11.2DS forebrain-like excitatory neurons showing reduced oxidative phosphorylation in 22q11.2DS lines compared to control lines (**Section 4.4.1, Chapter 4**; Li et al., 2019; Li et al., 2021). Hence 22q11.2DS MGLs might rely more on oxidative phosphorylation rather than

glycolysis during LPS response. However, functional experiments alongside further treatment timepoints would have to be assessed.

A broad immune response was also widely seen in gene ontology analysis for both Signature B and Signature C (**Section 4.3.6** and **Section 4.3.7, Chapter 4**). Even though the pathways were associated with down-regulated DEGs in Signature A, gene ontology of Signature C significantly up-regulated all processes discussed in vehicle-vehicle comparison. This also includes the not previously mentioned link with G-protein receptor binding, in which related genes also play a substantial role in microglia homeostasis and has been linked to a variety of psychiatric disorders including 22q11.2DS-associated conditions ASC, schizophrenia and bipolar disorder (Monfared et al., 2021). Dysregulation of G protein-coupled receptor signalling have also been associated with Parkinson's Disease, with G protein-coupled receptors specifically also the most common drug targets for therapies such as antipsychotics and is typically up-regulated in microglia immune responses (Boczek et al., 2021; Gu et al., 2021; Monfared et al., 2021).

In the analysis of Signature C, a number of additional hits pointed towards NF- κ B-related signalling, suggesting that 22q11.2DS rely more heavily on this pathway compared to control MGLs. Gene ontology analysis suggests that promotion of NF- κ B signalling is unique to or is stronger in Signature C. Of note, potential aberrancies in NF- κ B signalling was also noted through IL-4 signalling in Signature A. Additionally, associations were made to elevations in interferon type 1 production as well as positive regulation of cytokines. This suggests that in response to LPS challenge, 22q11.2DS might produce additional cytokines compared to control MGLs.

Signature C DEGs are also associated with regulation of neurotransmitters, perhaps most notably one of these genes includes *GCH-1* which is an enzyme necessary for BH4 synthesis and thus might impact the increase or decrease of dopamine biosynthesis rate (Vidal and Pacheco, 2020). Increased dopamine has previously been linked with schizophrenia and Parkinson's Disease (Birtwistle and Baldwin, 1998), both of which are conditions associated with 22q11.2DS as noted throughout this thesis. Cell line specific altered dopamine synthesis, metabolism and signaling have also been observed in hiPSC-derived midbrain dopaminergic neurons for 287_SZM_01 and 191_SZF_09, two of the 22q11.2DS lines used in this study (Reid et al., 2022), further solidifying the role that neurotransmitters might play in 22q11.2DS-associated conditions. It should however be noted that BH4 is not only a pivotal cofactor for dopamine, but also serotonin and nitric oxide (Fanet et al., 2021). Both have notably also been implicated in schizophrenia (Nasyrova et al., 2015; Pourhamzeh et al., 2022). In addition to these implications for *GCH-1* dysregulation, it is important to note that work in a zebrafish *GCHI*^{-/-} model has identified a correlation with the gene and brain innate immunity, specifically increased microglial phagocytic activity (Larbalestier et al., 2022). As their model investigated deficiency however, it is unclear how this will connect to the 22q11.2DS in which it is up-regulated. Speculatively it would be interesting to assess whether this increase in *GCHI* causes an attenuated increase in phagocytic activity during LPS response in 22q11.2DS MGL compared to control MGLs.

4.4.3. Signature D analysis reveals potential key drivers in differential response to LPS

Two genes were found to be significantly different in response to LPS in 22q11.2DS MGLs, namely *CXCL10* and *CHN1* (Section 4.3.11, Chapter 4). *CXCL10* was initially found to be significantly down-regulated in vehicle comparisons (Section 4.3.3, Chapter 4). It was previously noted that *CXCL10* is linked with microglia immune response, with a reduction

implying that microglia might be in a more homeostatic state. However, in Signature A, IL-10 signalling, which inhibits its production, is also reduced making the corresponding protein translation output unclear (**Section 4.3.5, Chapter 4**). In Signature B and Signature C, elevated IL-10 signalling is associated with the up-regulated gene set for both signatures but does not appear to be able to sufficiently inhibit microglia response to LPS through by attenuating *CXCL10* based on this analysis. This could mean that up-regulated genes associated with the IL-10 signalling are rather actively de-regulating the production of IL-10 itself, resulting in an enhanced microglia LPS response. This is also the case for IL-4 signalling, which like IL-10 can inhibit *CXCL10* production (Cheeran et al., 2003). This implies that *CXCL10* is a key driver in early 22q11.2DS MGL LPS response. Even so, a critical point identified by Clarner et al., (2015) is that a *CXCL10*-driven immune response might not necessarily enhance affect phagocytic activity of microglia. Functional analysis such as by phagocytosis assays would be necessary to evaluate this.

The role of *CHN1* however is less clear. It has previously been highlighted for further investigation in a population specific expression analysis on *postmortem* tissue from Parkinson Disease prefrontal cortex and substantia nigra regions, and Huntington's Disease motor cortex region (Capurro et al., 2015). The only work on microglia highlighting this gene is a hit in a rat corpus callosum microarray experiment, which suggests that the gene is up-regulated in ramified microglia compared to amoeboid microglia (Parakalan et al., 2012). This suggests that morphology of 22q11.2DS MGLs might become more ramified in response to LPS, although this was not the case after 3 hours of LPS treatment as shown in **Section 3.3.6, Chapter 3**. 3 hours however might be not a long enough treatment period to characterise this potential shift in morphological state even though there though a transcriptomic change is evident.

4.4.4. Limitations and future direction

There are naturally key limitations to this current study with the greatest being the small sample size compared non-hiPSC models. Heterogeneity of the cell lines (**Section 3.3.1, Chapter 3**) could also be a potential source of variance; hence additional replication is warranted. Reducing the stringency threshold in vehicle analysis also impacts how much a single cell line could impact the findings especially in a low power study. Furthermore, it could be argued that confirmation of RNAseq data should be confirmed using experiments such as qPCR which highly correlates with DEGs identified in using RNAseq (Griffith et al., 2010; Shi and He, 2014; Wu et al., 2014; Coenye, 2021). For this thesis, qPCR would have been an implemented experiment to support data validity if time and resources were not available (**COVID-19 Impact Statement**). However, due to the high sensitivity of RNAseq, any discrepancies in such findings is likely due to potential variability of housekeeper genes used in qPCR and probe-based bias based on what region of the cDNA is amplified rather than the RNAseq itself (Dheda et al., 2004; Tuomi et al., 2010). Furthermore, a large number of genes has been identified alongside several pathways affected by more than a single gene, making performing an expression confirmation of each gene unreasonable. While it would be valuable to at least, for example, confirm interaction analysis output of *CXCL10* and *CHN1*, it is argued that instead of qPCR, a focus should rather be put on functional assays linked to the affected pathways, which would not only confirm the findings but potentially illuminate how the transcriptomic differences correlate to differences in microglia phenotype. This is not to undervalue the usefulness of qPCR, rather, it is suggested that for future studies some key genes could be assessed on new cell lines alongside functional assays due to the cost of RNAseq, reducing overall resources required while retaining a link from these donors to new cell lines.

Future work should focus on adding additional cell lines to confirm the data as common phenotypes across 22q11.2DS MGLs. An interesting additional experiment would be to examine the effect of longer treatment. Alternatively, repeated exposures to examine 22q11.2DS MGL self-regulation in between treatments or differences in response to later treatments could be key exploratory assays. First however, functional assays including cytokine production, phagocytosis and metabolic profiling should be prioritised.

4.5 Conclusions

In summary, the use of RNA sequencing on this hiPSC model solidifies that there is an intrinsic effect of 22q11.2DS on transcriptomic state MGL state. Transcriptomic profiling of vehicle- and LPS-treated control and 22q11.2DS MGLs demonstrated overlap of 22q11.2DS MGL transcriptomic profile with 22q11.2DS-related conditions as well as Alzheimer's disease. Differences between control and 22q11.2DS transcriptomic profiles were observed in signalling associated with immune response. Key learnings from Signature A included that 22q11.2DS MGLs transcriptomic state differs to control MGLs even without immune challenge. Signature A analysis also identified that affected functions might include inability to shift metabolic profile, inhibited communication to cells in the local environment via reduced secretion of regulatory cytokines and chemokines, and potential aberrancies in homeostatic functions such as phagocytosis. Signature B and Signature C analyses revealed that both control and 22q11.2DS MGLs can broadly respond to LPS challenge. 22q11.2DS might rely more heavily on alternate pathways such as NF- κ B signalling. Some key genes, being *CXCL10* and *CHN1*, have also been identified as potential drivers of differential response to LPS stimuli based on their function in previous literature and would be relevant to investigate in future research.

Chapter 5:

Functional characterisation of control versus 22q11.2DS hiPSC-derived microglia-like cells

5.1 Introduction

5.1.1. Functional characterisation of 22q11.2DS MGLs based on morphological and transcriptomic profiling

Following morphological and transcriptomic profiling of 22q11.2DS MGLs, several microglia functions were noted as potentially affected. Morphology data (**Chapter 3**) and RNA sequencing data (**Chapter 4**) suggested phagocytic activity might be higher in 22q11.2DS MGLs based on morphological state, DEGs, and potentially IBA1:TMEM119 protein marker colocalisation. Additionally, RNA sequencing data (**Chapter 4**) highlighted genes, pathways and overlap with other human microglia datasets, together providing hints toward differences in cytokine and chemokine signalling, overall suggesting 22q11.2DS MGLs might secrete less cytokines without LPS challenge. Additionally, RNA sequencing data suggests that 22q11.2DS MGLs might struggle to switch metabolic states based on differences in IL-4 signalling, as it can support switching microglia metabolism from glycolytic to oxidative states. This is also supported by 22q11.2DS findings on mitochondria function in hiPSC-derived forebrain-like excitatory neurons which has reduced oxidative phosphorylation compared to control lines (Li et al., 2019). Taken together, while it is unclear how the dysregulation of these functions at morphological and transcriptomic levels affects their functional performance, it provides a number of testable hypotheses related to key microglial functions. The impact of potential validation of these data with functional changes

will support future work with different experiments in more complex model systems to then understand the consequences of these differences, for example whether it impacts neuronal phenotypes in co-cultures or circuit formation in chimeric mice.

Considering the suspected developmental stage of MGLs being in the at a fetal stage (Haenseler et al., 2017), an emphasis is made here to investigate relevant functions during brain development. In addition to providing fundamental homeostatic and innate immune functions, microglia key roles include synapse formation and elimination (Hanger et al., 2020). The key roles of microglia in the central nervous system encompass release of cytokines, which while being a form of cell-cell communication, can also have both protective and damaging effects on nearby neurons and other glia (Smith et al., 2012; Ferro et al., 2021). Understanding whether the development of cytokine release functions is affected can hence provide key insights. Lastly, regarding a potential inability to switch metabolic state, a way to investigate this in microglia is by looking at lysosomes, which help process a mix of energy substrates, regulating microglia metabolism (Kreher et al., 2021).

5.1.2. Microglia-associated phagocytosis in psychiatric disorders

Microglia are not static cells, and as shown in previous chapters, external LPS challenge elicit a response in MGLs. While microglia functions include in synapse formation and elimination, they are also capable of regulating neuronal progenitor pools (Sierra et al., 2010; Schafer et al., 2012; Cunningham et al., 2013; Miyamoto et al., 2016; Weinhard et al., 2018; Wang et al., 2020). Based on previous chapters (**Chapter 3, Chapter 4**), LPS challenge might also might induce increased phagocytosis (Fricker et al., 2012; Scheiblich and Bicker, 2015), to partially assess these microglial functions. 22q11.2DS MGLs might however not need additional stimuli to have higher phagocytic activity compared to control MGLs based

on morphological and transcriptomic as mentioned in **Section 5.5.1, Chapter 5**. In addition to previous data in this project and that it is a fundamental functional property of microglia which should be assessed during all functional characterisation, abnormal synapse elimination observed in psychiatric disorders also suggests that phagocytosis is a relevant mechanism to investigate (Tang et al., 2014; Osimo et al., 2019; Sellgren et al., 2019). Whether their role is over- or under-elimination of synapses however is not entirely clear, as well as whether it applies to all 22q11.2DS-associated psychiatric disorders. Excessive synaptic pruning is well supported in schizophrenia literature and has been proposed to occur excessively in a complement-dependent manner based on rodent models and a key study on human induced microglia from blood monocytes by Sellgren and colleagues (Stevens et al., 2007; Schafer et al., 2012; Sekar et al., 2016; Sellgren et al., 2019). Disruption of C3 also appears to be involved in ASC based on a knockdown mice model (Fagan et al., 2017). However, in contrast to schizophrenia models, potential deficits in synaptic pruning has been implied. This is based on observations of increased dendritic spine density in ASC *postmortem* tissue in layer V pyramidal neurons within the temporal lobe, which were replicated in ASC mouse models with autophagy deficiency, highlighting relevance of also studying lysosomal markers as 22q11.2DS is a risk factor for both ASC and schizophrenia (Tang et al., 2014; Yim and Mizushima, 2020; Iyer et al., 2022).

5.1.3. The role of lysosomes in microglial functions

Pathways and transcription programmes associated with lysosome-mediated signalling can control the switch between anabolism and catabolism in cells, regulating cellular metabolism through lysosomal biogenesis and autophagy (Ballabio and Bonifacino, 2020). Lysosomes are also specifically connected to the role of microglia in central nervous system development through release of BDNF and CatS, supporting remodelling of the extracellular matrix and

through this synaptic architecture (Kreher et al., 2021). Lysosomal activity is related to key functions including phagocytosis and degradation of digested material (Gray et al., 2016; Wong et al., 2017; Hipolito et al., 2018; Ballabio and Bonifacino, 2020; Lancaster et al., 2021; Zhang et al., 2021). Deficiencies in autophagy has been linked to ASD-like behaviours in mouse models and assessing inferred lysosome content of cells is hence relevant for study in 22q11.2DS MGLs alongside phagocytosis assays (Tang et al., 2014; Kim et al., 2017). Lysosome content within cells can be inferred using markers of acidic compartments within cells, which primarily includes lysosomes, such as lysotracker (Peri and Nüsslein-Volhard, 2008; Solomon et al., 2022). Outside of disease conditions, lysosomal activity in microglia is also increased following immune challenge provided such as through LPS (200 ng/mL) treatment as shown in primary mouse microglia and in immortalised J774 macrophages (Majumdar et al., 2007), and in newborn rat primary microglia also systemically challenged with LPS (10 ng/mL) (Liu et al., 2008). This is relevant when assessing 22q11.2DS MGLs, as a genotype effect during LPS challenge has been alluded to in **Chapter 3** and **Chapter 4**.

5.1.4. Relevance of studying cytokine secretion by control and 22q11.2DS microglia

Several articles have published evidence of peripheral cytokine elevations in psychiatric disorders (Naudin et al., 1996; Miller et al., 2011; Kordulewska et al., 2019; Zhao et al., 2021). In the CNS however, while presence of alternate microglial states has been proposed (**Section 1.2.4, Chapter 1**), it requires further characterisation using human model systems, their cytokine secretion phenotype for example has not been clearly established in in this setting. While data on patient CNS cytokine levels are largely unavailable, expected 22q11.2DS MGL cytokine secretion profiles might include elevations of IL-1 β , IL-2, IL-6, IL-8 and TNF α , which would match serum data from individuals with ASC and schizophrenia (Naudin et al., 1996; Miller et al., 2011; Smith et al., 2012; Kordulewska et al.,

2019; Zhao et al., 2021). While elevations of IL-6 and IL-8 have also been associated with severity of clinical symptoms in schizophrenia (Dahan et al., 2018), it is important to highlight that hiPSC models would not characterise this stage of disease. Rather, microglia during developmental stages might have an entirely different secretion profile.

Transcriptomic data shown in **Chapter 4** vehicle comparisons suggest that cytokine levels are actually decreased in 22q11.2DS MGLs based on down-regulated DEG association with cytokine signalling and production pathways, yet one could critically also hypothesise that the overall impact of DEGs on pathways results in increased secretion, and hence functional validation is critical.

Differences compared to control MGLs observed at the transcriptomic level in 22q11.2DS MGL during LPS challenge is also important to consider. In fact, there is two lines of evidence suggesting that microglia in schizophrenia and ASC might have an enhanced response to LPS challenge. First, as described by Parrott et al. (2021), ASC-associated *FMRI* knockout mice exhibit an enhanced response to LPS at different doses (1 ng/mL, 10 ng/mL, and 100 ng/mL) and treatment lengths. TNF α secretion was enhanced in the LPS condition with 1 ng/mL and 10 ng/mL LPS after 6 hours, and 100 ng/mL after 24 and 48 hours. IL-6 secretion was enhanced in the LPS condition with 10 ng/mL LPS after 6 hours, and with 1 ng/mL and 100 ng/mL LPS after 24 hours, with no differences at 48 hours. In the context of schizophrenia, Ormel et al. (2020) has also described an enhanced response to LPS (100 ng/mL) in TNF α secretion in human induced microglia from blood monocytes donated by individuals with schizophrenia following 6 hours of treatment. Hence it is critical to evaluate the effect of LPS treatment on 22q11.2DS MGLs, and whether a similar effect extends to other cytokines.

5.1.5. Aims and hypotheses

Based on this short review of literature, the overarching aim of this chapter is to perform functional validation of previously obtained data.

In line with the review and obtained data, it is hypothesised that 22q11.2DS have a higher phagocytic activity compared to control MGLs without LPS challenge. 22q11.2DS MGL lysosome levels (inferred by staining of acidic compartments) will not increase to the same degree as control MGLs in response to LPS based on rodent ASC data. This would be in line with a further hypothesis that 22q11.2DS MGL uptake will not substantially increase following LPS stimuli. Considering the evidence provided by RNA sequencing of 22q11.2DS MGLs, it is hypothesised that 22q11.2DS MGLs will contrast observations in patient serum. When compared to control MGLs, 22q11.2DS MGLs will exhibit reduced cytokine production in vehicle comparisons, but an enhanced response will occur during treatment with LPS based on available ASC and schizophrenia data.

In terms of null hypotheses, it is anticipated that there will be no statistically significant disparities in phagocytic activity between 22q11.2DS and control MGLs in the absence of LPS challenge. There will be no statistically significant divergence of lysosome level change or uptake levels between 22q11.2DS MGLs and control MGLs following LPS challenge. 22q11.2DS MGLs will not have statistically significant lower levels of cytokines when compared to control MGLs in vehicle comparisons, and their cytokine production levels following LPS challenge will be statistically similar to those of control MGLs. asserting an absence of statistically significant differences in both scenarios.

To investigate these hypotheses, this chapter aims to:

1. Establish if there are differences in the uptake of a range of cargoes by 22q11.2DS MGLs vs. neurotypical control MGLs with and without LPS challenge
2. Determine differences in 22q11.2DS MGL lysotracker levels with and without LPS challenge compared to neurotypical control MGLs
3. Characterise differences between 22q11.2DS MGL and control MGLs cytokine secretion profiles with and without LPS challenge

5.2 Methods

All cell lines used in across this project (**Section 2.1, Chapter 2**) including five control (three male, two female) and three 22q11.2DS (1 male, 2 female) hiPSC lines were differentiated into microglia and treated with either vehicle or LPS for 3 hours as described in **Section 2.2.3** and **Section 2.2.4, Chapter 2** for uptake and lysosome level assays. For the cytokine assay, two less control lines (male lines 014_CTM_02, and 127_CTM_03) were used, with MGLs also being treated with LPS for 24 hours instead of 3 hours as per **Section 2.2.4**. Experiment design and statistical analysis was performed as per **Section 2.7** and **Section 2.8, Chapter 2**, respectively.

5.2.1 Cargo uptake and lysotracker red™ assay

In vitro cell culture studies can easily assess different endocytic pathways of microglia including phagocytosis and pinocytosis (Maguire et al., 2022), with hiPSC-derived MGLs providing a starting point in studying human models to account for species-related heterogeneity (**Section 1.1.5, Chapter 1**). Fluorescently tagged constructs can be used to assess the level of activity within a set time-period. Microglia phagocytosis have been described to plateau after 3 hours, with LPS-treated microglia phagocytosis being enhanced compared to non-treated microglia (He et al., 2021), hence this is perhaps a reasonable time-period to study phagocytosis. Bioparticles which are pHrodo labelled provide additional simplicity (Haenseler et al., 2017; Maguire et al., 2022). Adding cargos of various predetermined sizes to cultures to be taken up by the microglia allows for a prediction of what pathway will be used by the cells (Hall-Roberts et al., 2021; Maguire et al., 2022; Solomon et al., 2022). Cargos over 0.5 µm in diameter would be expected to promote the use of phagosomes to take up the material, utilising the phagocytosis pathway (Freeman and

Grinstein, 2014). Smaller cargo down to >200 nm in diameter would predict use of micropinocytosis (Rennick et al., 2021). The last commonly investigated pathway is clathrin-mediated endocytosis which is primarily responsible for uptake of material <120 nm (Kaksonen and Roux, 2018). In both macropinocytosis and clathrin-mediated endocytosis, aggregates of particles such as large fibrillar β -amyloid may rather enable phagosomes even though β -amyloid usually enables clathrin-mediated endocytosis and macropinocytosis (Koenigsnecht-Talboo and Landreth, 2005; Ries and Sastre, 2016; Abud et al., 2017; Hall-Roberts et al., 2021). Inhibitors of these pathways are often used as negative control to ascertain expected endocytic uptake mechanism, especially in aggregate-prone proteins.

To assess uptake of different cargoes and microglial lysosomal content, pMacpres were seeded at a 1.5×10^5 per well with wells containing a single sterile glass coverslips within Nunclon Delta Surface 12-well plates (Thermo Scientific, 163320). On day 14 of differentiation to microglia, with a 100% medium change, cells were treated with either vehicle (H_2O) or LPS (100 ng/ml) for 3 hours. At hour 2 of this treatment, the respective experiment cargo or 75 nM LysoTracker DND-99 (L7528, ThermoFisher) was added to the wells, incubating along with the final 60 minutes of LPS treatment. Uptake of three different cargoes was assessed, which included fluorescein isothiocyanate (FITC)-Dextran 4kD (46946, Sigma), Alexa Fluor™ 594-zymosan (Z23374, ThermoFisher) and previously published in-house mouse brain purified ^{td}Tomato-tagged synaptosomes (Solomon et al., 2022). Three different cargo was investigated to control for the effect of cargo size, which microglial choice of primary uptake mechanism is dependent on (Maguire et al., 2022). To confirm the primary uptake mechanism being phagocytosis, a separate well for each cargo with one coverslip was pre-treated with 10 μ M Cytochalasin D (Cayman), an actin polymerisation inhibitor, for 2 hours prior to addition of cargos to inhibit actin polymerisation. Cytochalasin D has been shown to inhibit both

phagocytosis and micropinocytosis (Brenner and Korn, 1979; Kanlaya et al., 2013; Hall-Roberts et al., 2021; Obst et al., 2021; Maguire et al., 2022) Wells were washed carefully using sterile 0.1M PBS and fixed with 4% paraformaldehyde diluted in 0.1M PBS for 20 minutes at room temperature. Samples were then stored in 0.1M PBS (+0.05% sodium azide w/v) at 4°C until staining and confocal microscopy. To visualise the microglia cell membrane, coverslips were incubated with Sambucus Nigra Lectin far red (SNL, excitation peak 650 nm and emission peak 670 nm, CL-1305-1, Vector) for one hour at a concentration of 1:400. Coverslips were then mounted on slides with VECTASHIELD® HardSet™ Antifade Mounting Medium with DAPI (H-1500-10). For the zymosan and FITC-dextran uptake assays, images were acquired using a 63x oil immersion lens (numerical aperture 1.40) on a Leica SP5 (TCS-SP5, Leica) confocal microscope. For the mouse brain purified ^{td}Tomato-tagged synaptosome uptake and lysotracker red™ experiments, images were acquired using a Nikon A1R inverted confocal microscope (Nikon A1 Piezo Z Drive Nikon A1plus, Nikon) at the WCIC (<https://www.kclwcic.co.uk/>) using a 60 x oil immersion lens (numerical aperture 1.49). Image acquisition for both microscopes were set up to acquire multiple channels as necessary of singular planes and 18 Z stacks, which was sufficient to cover SNL cell membrane fluorescence signal, with step size 0.9 µm at a resolution of 1024 × 1024 yx. In Leica SP5 image acquisition, lasers used were 405 nm (DAPI; blue), 488nm (green), 561 nm (red) and 633 nm (far red). In the Nikon A1R, lasers used were 405.7 nm (DAPI; blue), 561.9 nm (red) and 638.9 nm (far-red). Optical section was set by pinhole size which was 28.0970625798212 (a.u.) and 1.0 (a.u.) when using the Nikon A1R and Leica SP5, respectively. All threshold settings were optimised to work for all fields of view then applied universally across all images. This was in Leica image acquisition optimised using the Smart gain function, while the laser power setting was adapted in Nikon A1R optimisation of image acquisition.

Three images were acquired per coverslip for each different differentiation (experimental design: **Section 2.8, Chapter 2**), totalling n=9 images per condition for each cell line. Acquired images were analysed in 3D maximum projection using IMARIS Version 9.0.2. No additional pre-processing was performed before setting intensity thresholds. A constant threshold for SNL and one for each cargo was used across conditions, extracting 3D volume of uptake (cargo within cells) and 3D total cell volume within fields to then calculate uptake 3D volume per total cell volume. Any positive cargo outside of the cells were masked from the data extraction using the integrated function of the software. For control MGL vehicle vs 22q11.2DS vehicle comparison, the percentage of cargo or lysotracker volume within SNL cellular volume was calculated. Effect of LPS treatment was analysed and visualised as a fold change of the percentage of cargo or lysotracker volume within SNL cellular volume, comparing the percentage in the 3-hour LPS condition to the H₂O vehicle condition for each biological replicate. This 3D reconstruction analysis approach has previously been used by Solomon et al. (2022)

5.2.2 Cytokine secretion assay

Cytokine secretion of MGL into culture media were measured using the V-PLEX Proinflammatory Panel 1 Human Kit (MSD, K15049D-1) according to manufacturer's instructions. This captured N=10 cytokines, being IFN- γ , IL-1 β , IL-2, IL-4, IL-6, IL-8, IL-10, IL-12p70, IL-13, and TNF- α . Culture media was collected from matured 14-day differentiated MGLs from each donor cell line treated with 24 hours with either LPS (100 ng/ml) or vehicle (H₂O). Aliquots were made and frozen at collection. For preparation, media aliquots were defrosted for the first time and immediately was plated onto the V-PLEX kit 96-well plates, which is pre-coated with capture antibodies, provided as part of the kit. Samples were plated at 50uL in duplicates with n=3 technical replicates, being wells, for each biological replicate,

and incubated for 2 hours at room temperature. Media was not diluted using the diluent provided in the kit. Individual wells were then washed three times with the washing buffer provided in the kit. The antibody solution was then incubated for 2 hours at room temperature. Wells were washed aa further three times using the kit's washing buffer before performing reading the plate with the wells containing the read buffer provided in the kit. The cytokines concentration was determined with the electrochemiluminescent labels with the plate being inserted into the MSD instrument (MESO QUICKPLEX SQ 120). The DISCOVERY WORKBENCH® 4.0 software was to calibrate at samples against a reference calibrator which is generated by MSD and to extract raw data which included calculated cytokine concertation. Detection ranges for were (Protein: range): IFN- γ : 0.37–938 pg/mL, IL-1 β : 0.05–375 pg/mL, IL-2: 0.09–938 pg/mL, IL-4: 0.02–158 pg/mL, IL-6: 0.06–488 pg/mL, IL-8: 0.07–375 pg/mL, IL-10: 0.04–233 pg/mL, IL-12p70: 0.11–315 pg/mL, IL-13: 0.24–353 pg/mL, and TNF- α : 0.04–248 pg/mL. No samples were below the limit for detection. The mean calculated cytokine concentrations for each biological replicate were calculated in Microsoft Excel. For control MGL vehicle vs 22q11.2DS vehicle comparison, values were log transformed to support data visualisation. Effect of LPS treatment was analysed and visualised as a fold change of the 24-hour LPS condition compared to the H2O vehicle condition using the raw untransformed mean calculated cytokine concentration for each biological replicate.

5.3 Results

5.3.1 Effect of 22q11.2DS on particle uptake is dependent on cargo size

To assess whether 22q11.2 CNVs influences cargo uptake by microglia, three different cargos representing different sizes were used to consider potential effects on different uptake mechanisms. Two larger particles, zymosan (approx size 3 μm) and ^{125}I Tomato tagged mouse brain synaptosomes, were used to assess phagocytosis (**Figure 5.1** and **Figure 5.2**). To investigate whether effect is similar in smaller particles, permeability of dextran at a molecular weight of 4kDa was also assessed (**Figure 5.3**). This dextran product ranges from 3-5kDa in size, and hence the maximum diameter is estimated to be around 2.2 nm diameter in size.

In the absence of LPS-stimulation, when comparing MGL from 22q11.2DS donor lines (N=3) to neurotypical controls (N=5) the inferred phagocytosis of both pHrodo zymosan particles and ^{125}I Tomato mouse brain synaptosomes were significantly increased in the 22q11.2ds lines ($p < 0.01$, **Figure 5.1B** and **Figure 5.2B**). By contrast, there were no statically significant differences between 22q11.2DS and neurotypical donor lines in dextran uptake (**Figure 5.3B**). When comparing the effect of LPS stimulation on uptake of these cargoes using a fold-change measure for each donor line. Interestingly, the neurotypical control lines on average demonstrated a statistically significant larger fold-change in the inferred phagocytosis of pHrodo zymosan ($p < 0.01$, **Figure 5.1B**) and ^{125}I Tomato mouse brain synaptosomes ($p < 0.05$, **Figure 5.B**). By contrast, LPS stimulation increased uptake of dextran 4kDa in MGLs irrespective of genotype ($p < 0.05$, **Figure 5.3B**), but to a similar extent.

Some notable variability by cell line included in vehicle comparisons was that 191_SZF_09 MGLs phagocytosis of synaptosomes was not similar to that of other 22q11.2DS cell lines, and more closely clustered with control MGLs. However, this was not the case in the context of LPS treatment. This could be related to cell line heterogeneity characterised in **Section 3.3.1, Chapter 3**.

Importantly, across all conditions tested the inclusion of cytochalasin D (n=1 biological replicate per cargo for each condition). Cytochalasin D qualitatively inhibited uptake of cargo across conditions. However, it was not completely blocked, with around 1% of the total volume of cells containing cargo in experiments on zymosan or mouse brain purified ^{td}Tomato-tagged synaptosomes (**Figure 5.1C** and **Figure 5.2C**). Uptake was also substantially inhibited in the dextran experiment, however not to the same extent (**Figure 5.3C**). This is likely due to the difference in endocytic pathways used, and it is hence not necessarily surprising as cytochalasin D is broadly characterised to inhibit phagocytosis and macropinocytosis, with its effect on clathrin-mediated endocytosis, which dextran of this size is most likely to fall under, being reduced or even contrasting (Gottlieb et al., 1993; Kuhn et al., 2014). Together, this suggests that phagocytosis is affected in 22q11.2DS MGLs, but clathrin-mediated endocytosis is not.

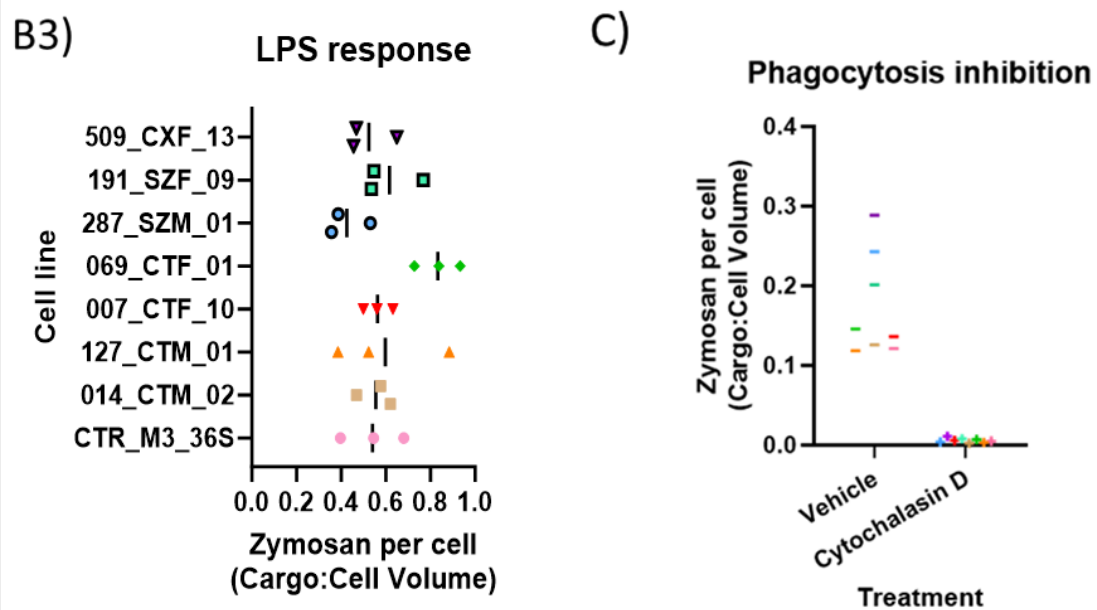
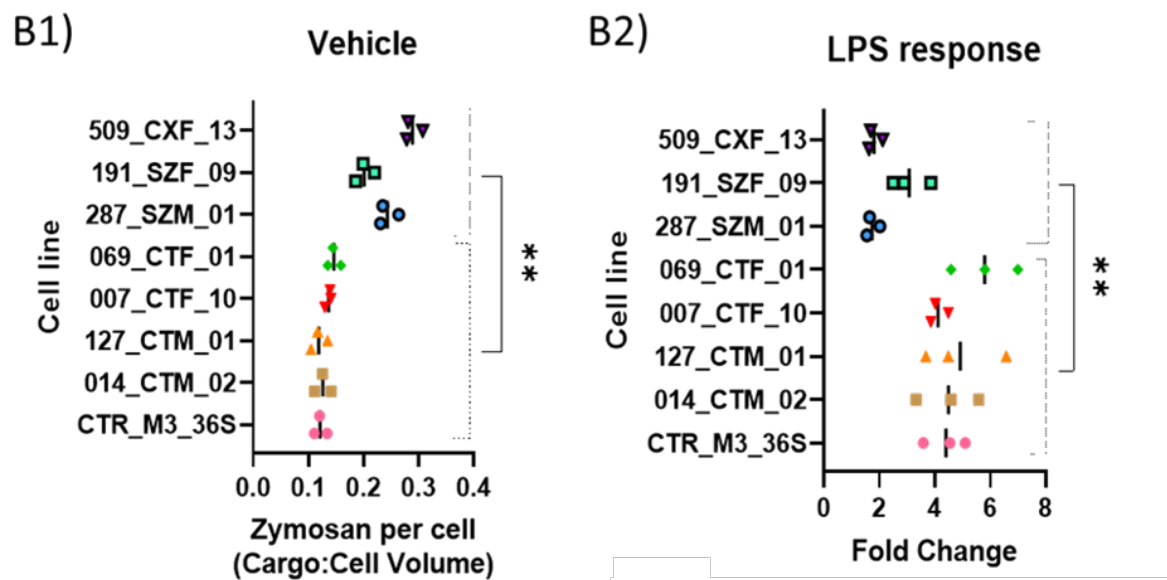
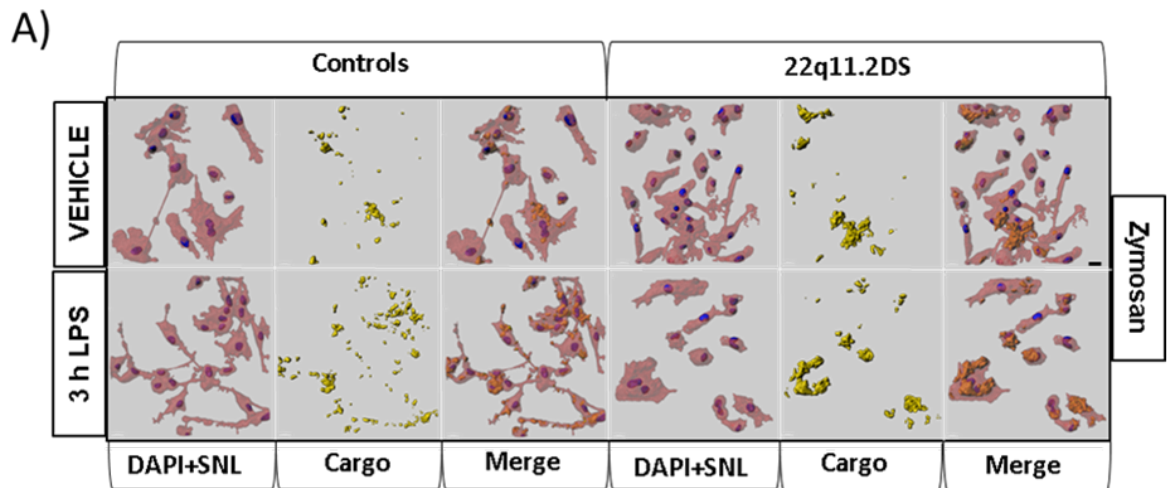
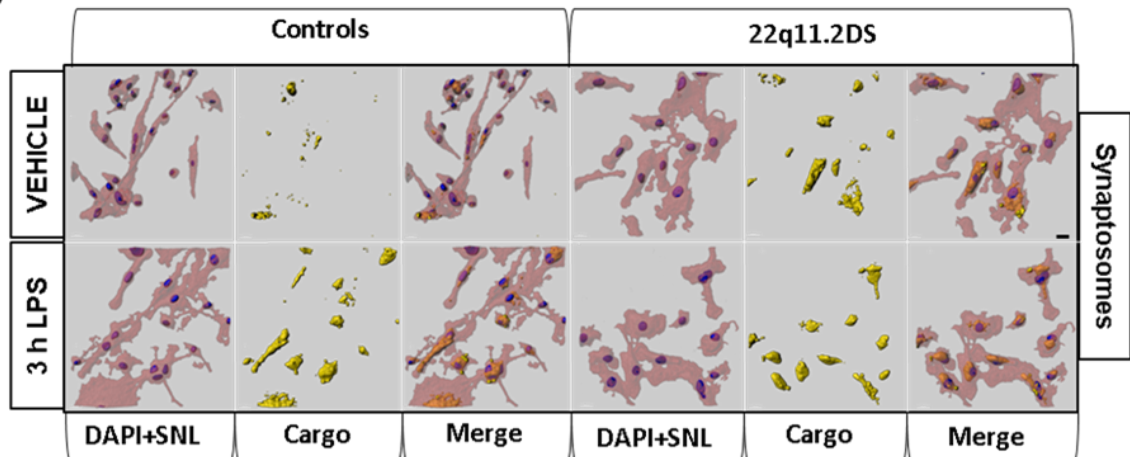


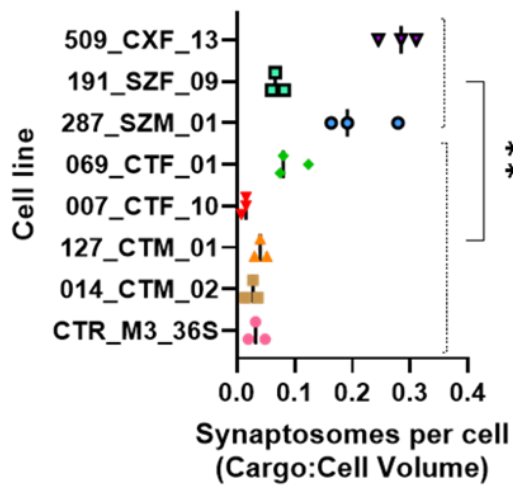
Figure 5. 1: Effect of 22q11.2DS on uptake of Alexa Fluor™ 594-zymosan in vehicle- and LPS-treated conditions. A) Fluorescent confocal illustration of control and 22q11.2DS MGL zymosan uptake following treatment with vehicle or LPS for 3 hours. Scale bar = 20 μm . B) Comparison of vehicle- and LPS-treated control vs 22q11.2DS MGLs. 1) Statistical comparison: Control vehicle versus 22q11.2DS vehicle. 2) Statistical comparison: Effect of LPS treatment as a fold change of the 3-hour LPS condition compared to the vehicle condition. 3) Overview of control LPS and 22q11.2DS LPS uptake values. C) Qualitative effect of inhibition of phagocytosis on zymosan uptake using cytochalasin D (n=1 biological replicate per condition). Colour coding shows the corresponding effect on each cell line. Internalised zymosan particles was determined as a proportion of total cell area covered. Total cell area was detected using SNL staining (far red). Statistical comparison groups consisted of N=3 day 14 differentiated 22q11.2DS MGLs vs N=5 day 14 differentiated control MGLs, with n=3 biological replicates being performed for each cell line. For statistical comparisons, means of control MGLs were compared to means of 22q11.2DS MGLs in one statistical test, not separately for each cell line. For each cell line, the mean of all biological replicates was calculated and used during statistical analysis. Data was checked for normal distribution. Unpaired two-tailed parametric t-test was used for statistical comparisons. Significant p values are indicated at follows ** = $p < 0.01$. Bars represent the mean of n=3 biological replicates for each cell line.

A)



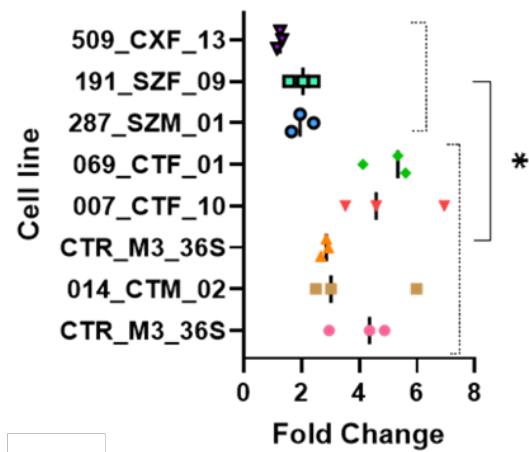
B1)

Vehicle



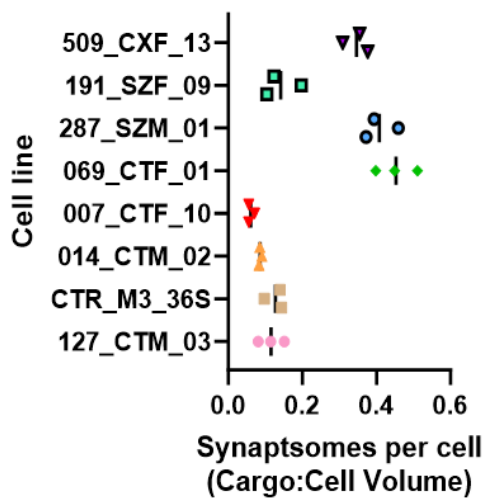
B2)

LPS response



B3)

LPS response



C)

Phagocytosis inhibition

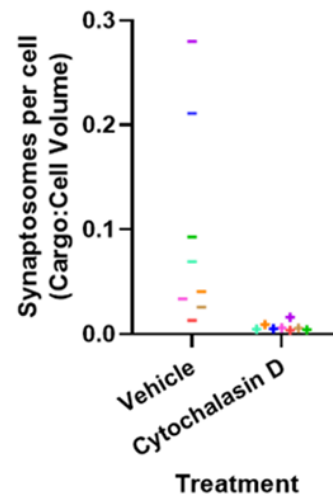
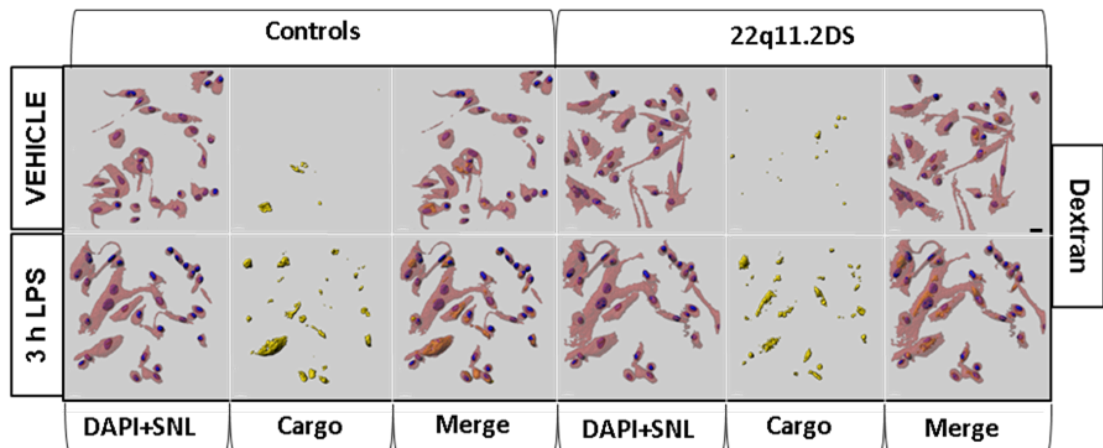
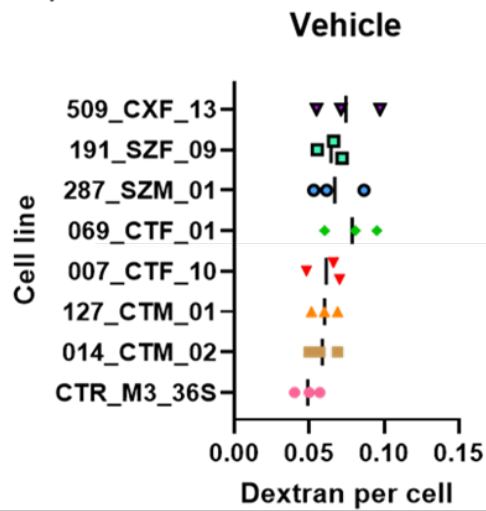


Figure 5. 2: Effect of 22q11.2DS on uptake of mouse brain purified ^{td}Tomato-tagged synaptosomes in vehicle- and LPS-treated conditions. A) Fluorescent confocal illustration of control and 22q11.2DS MGL synaptosome uptake following treatment with vehicle or LPS for 3 hours. Scale bar = 20 μ m. B) Comparison of vehicle- and LPS-treated control vs 22q11.2DS MGLs. 1) Statistical comparison: Control vehicle versus 22q11.2DS vehicle. 2) Statistical comparison: Effect of LPS treatment as a fold change of the 3-hour LPS condition compared to the vehicle condition. 3) Overview of control LPS and 22q11.2DS LPS uptake values. C) Qualitative effect of inhibition of phagocytosis on zymosan uptake using cytochalasin D (n=1 biological replicate per condition). Colour coding shows the corresponding effect on each cell line. Internalised synaptosome particles was determined as a proportion of total cell area covered. Total cell area was detected using SNL staining (far red). Statistical comparison groups consisted of N=3 day 14 differentiated 22q11.2DS MGLs vs N=5 day 14 differentiated control MGLs, with n=3 biological replicates being performed for each cell line. For statistical comparisons, means of control MGLs were compared to means of 22q11.2DS MGLs in one statistical test, not separately for each cell line. For each cell line, the mean of all biological replicates was calculated and used during statistical analysis. Data was checked for normal distribution. Unpaired two-tailed parametric t-test was used for statistical comparisons. Significant p values are indicated at follows: * = $p < 0.05$, ** = $p < 0.01$. Bars represent the mean of n=3 biological replicates for each cell line.

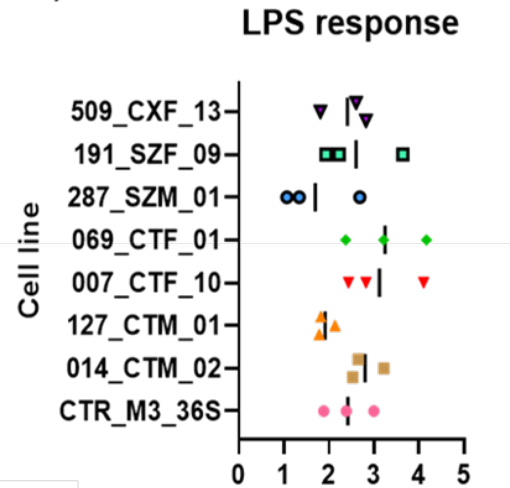
A)



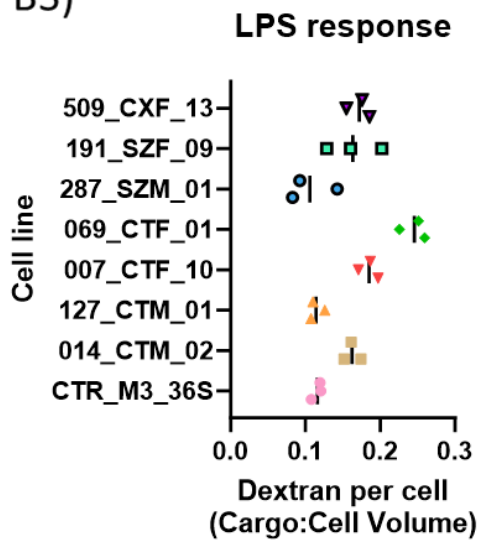
B1)



B2)



B3)



C)

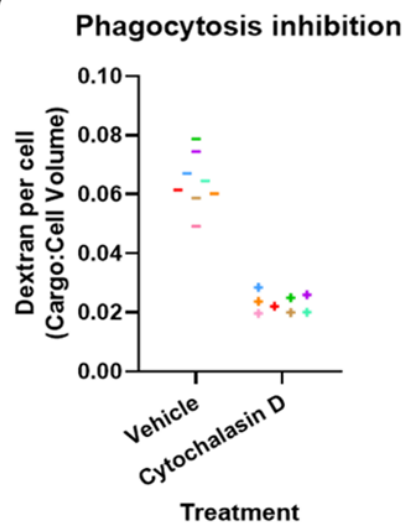


Figure 5. 3: Effect of 22q11.2DS on uptake of 4 kDa FITC-dextran (green) in vehicle- and LPS-treated conditions. A) Fluorescent confocal illustration of control and 22q11.2DS MGL dextran uptake following treatment with vehicle or LPS for 3 hours. Scale bar = 20 μm . B) Comparison of vehicle- and LPS-treated control vs 22q11.2DS MGLs. 1) Statistical comparison: Control vehicle versus 22q11.2DS vehicle. 2) Statistical comparison: Effect of LPS treatment as a fold change of the 3-hour LPS condition compared to the vehicle condition. 3) Overview of control LPS and 22q11.2DS LPS uptake values. While response to LPS challenge was not significantly different between 22q11.2DS and control MGLs ($p < 0.05$), uptake of FITC-dextran during LPS challenge was significantly increased in both groups. C) Qualitative effect of inhibition of phagocytosis on dextran uptake using cytochalasin D ($n=1$ biological replicate per condition). Colour coding shows the corresponding effect on each cell line. Internalised dextran particles were determined as a proportion of total cell area covered. Total cell area was detected using SNL staining (far red). Statistical comparison groups consisted of $N=3$ day 14 differentiated 22q11.2DS MGLs vs $N=5$ day 14 differentiated control MGLs, with $n=3$ biological replicates being performed for each cell line. For statistical comparisons, means of control MGLs were compared to means of 22q11.2DS MGLs in one statistical test, not separately for each cell line. For each cell line, the mean of all biological replicates was calculated and used during statistical analysis. Data was checked for normal distribution. Unpaired two-tailed parametric t-test was used for statistical comparisons. Bars represent the mean of $n=3$ biological replicates for each cell line.

5.3.2 Abnormal lysosome:cell body ratio in 22q11.2DS MGLs compared to controls

To assess the volume of lysosomes within MGLs from 22q11.2DS donors (N=3) compared to neurotypical control donors (N=5), the same method used in uptake analysis was adopted, with total volume of lysosomes being compared to the volume of cells (**Section 5.2.1**). Lysotracker red™ which stains acidic compartments of cells, being primarily lysosomes, was used for assessment. In the basal state, there were no statistically significant differences in inferred lysosome to cell volume ratio between control and 22q11.2DS donor lines (**Figure 5.4A**). By contrast, following 3 hour exposure to LPS (100 ng/ml) MGLs differentiated from control donors demonstrated a statistically significant increase in inferred lysosome to cell volume ratio when compared to the 22q11.2DS donor lines ($p < 0.05$, **Figure 5.4B2 and 5.C**). It is notable that the control line CTR_M3_36S vehicle data points (**Figure 5.4A**) was more similar to that of 22q11.2DS cell lines and the cause of this is not clear. These data suggest a decreased ability of 22q11.2DS MGLs to generate acidic endolysosomal vesicles in response to LPS challenge.

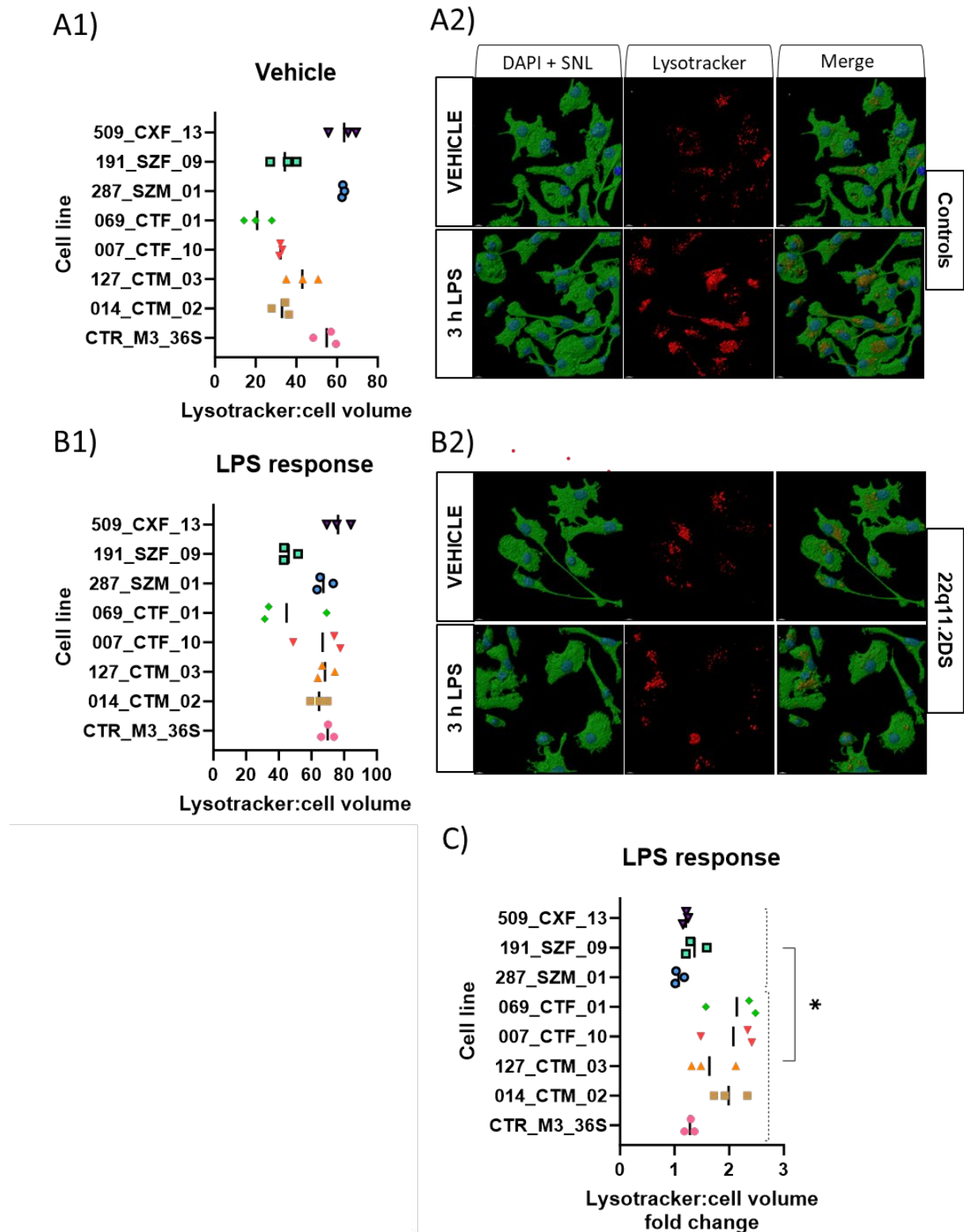


Figure 5. 4: Effect of 22q11.2DS on MGL acidic endolysosomal vesicle levels. A) Control vehicle and 22q11.2DS vehicle comparison. 1) Statistical analysis of lysotracker protein expression in control and 22q11.2DS MGLs treated with vehicle for 3 hours. 2) Illustration of lysotracker content in control and

22q11.2DS MGLs treated with H₂O vehicle for 3 hours (scale bar = 10 μ m). B) Control LPS and 22q11.2DS LPS comparison. 1) Overview of control LPS and 22q11.2DS LPS uptake values. 2) Illustration of lysotracker content in control and 22q11.2DS MGLs treated with LPS for 3 hours (scale bar = 10 μ m). C) Statistical analysis assessing the effect of LPS on lysotracker protein expression in control and 22q11.2DS MGLs treated with either vehicle or LPS for 3 hours. Effect of LPS treatment is shown as a fold change of the 3-hour LPS condition compared to the H₂O vehicle condition. Comparison groups consisted of N=3 day 14 differentiated 22q11.2DS MGLs vs N=5 day 14 differentiated control MGLs, with n=3 biological replicates being performed for each cell line. For statistical comparisons, means of control MGLs were compared to means of 22q11.2DS MGLs in one statistical test, not separately for each cell line. For each cell line, the mean of all biological replicates was calculated and used during statistical analysis. Data was checked for normal distribution. Unpaired two-tailed parametric t-test was used for statistical comparisons. Significant p values are indicated at follows: * = $p < 0.05$. Bars represent the mean of n=3 biological replicates for each cell line.

5.3.3 Altered cytokine release in 22q11.2DS MGL culture media compared to controls

To assess cytokine secretion into the culture media from MGLs differentiated from control and 22q11.2DS MGLs, the cells were exposed for 24 hours to LPS or vehicle, a different treatment length compared to the uptake experiments. This was based on experiments performed in other work published in Couch et al. (2023) using the same differentiation protocol as this study, which demonstrated detection of cytokines and chemokines at 3 and 24 hours, but higher cytokine concentrations at 24 hours. The longer treatment length also was chosen to ensure MGLs had time to respond, ensuring cytokine secretion into the media at levels above the limit of detection using the commercial assay kit (**Section 5.2.2, Chapter 5**)

Using the vehicle-treated samples to assess baseline conditions, a statistically significant reduction in the levels of both of IL-6 (adjusted $p < 0.05$) and IFN γ (adjusted $p < 0.01$) were observed when comparing media from 22q11.2ds donor lines (N=3) to control donor lines (N=3) (**Figure 5.5**). It is of note that in analysis of vehicle vs vehicle analysis that MGLs

from the control line CTR_M3_36S had similar secretion levels to all 22q11.2DS MGLs of IL-1 β , perhaps resulting in a not significant difference (adjusted $p < 0.070$), but it is unclear whether this is due to a sex difference or a CTR_M3_36S specific genotype as only one male control line was used for this experiment..

To assess the impact of genotype on cytokine secretion into the media following LPS stimulation, fold-change in cytokine secretion was compared (**Section 5.2.2, Chapter 5**) for each cytokine measured by the assay kit between control and 22q11.2DS donor lines. Of note, the fold change in the levels of IL-10 and TNF α were significantly lower (adjusted $p < 0.05$ for both cytokines) in the media samples from the 22q11.2DS lines as compared to controls (**Figure 5.6**) By contrast, the fold change for IL-6 was significantly higher (adjusted $p < 0.0001$) in the media samples from 22q11.2DS lines as compared to control lines (**Figure 5.6**). Statistical difference in IL-10 was likely driven by 007_CTF_10 control line, as the other control lines had more similar fold change to that of 22q11.2DS. 007_CTF_10 also notable had higher fold change in IL-1 β secretion compared to all other cell lines. The reason for this is unclear, with no previous data indicating why this is the case. Other notable variance is apparent increased in IL-2 secretion in the 287_SZM_01 and 509_CXF_13 22q11.2DS lines, but 191_SZF_09 secretion fold change was more aligned to that of control lines. Together, this data confirms altered cytokine secretion in 22q11.2DS under basal conditions and highlights some interesting differences in the response to LPS as a function of genotype, with some notable variance being highlighted across both comparisons.

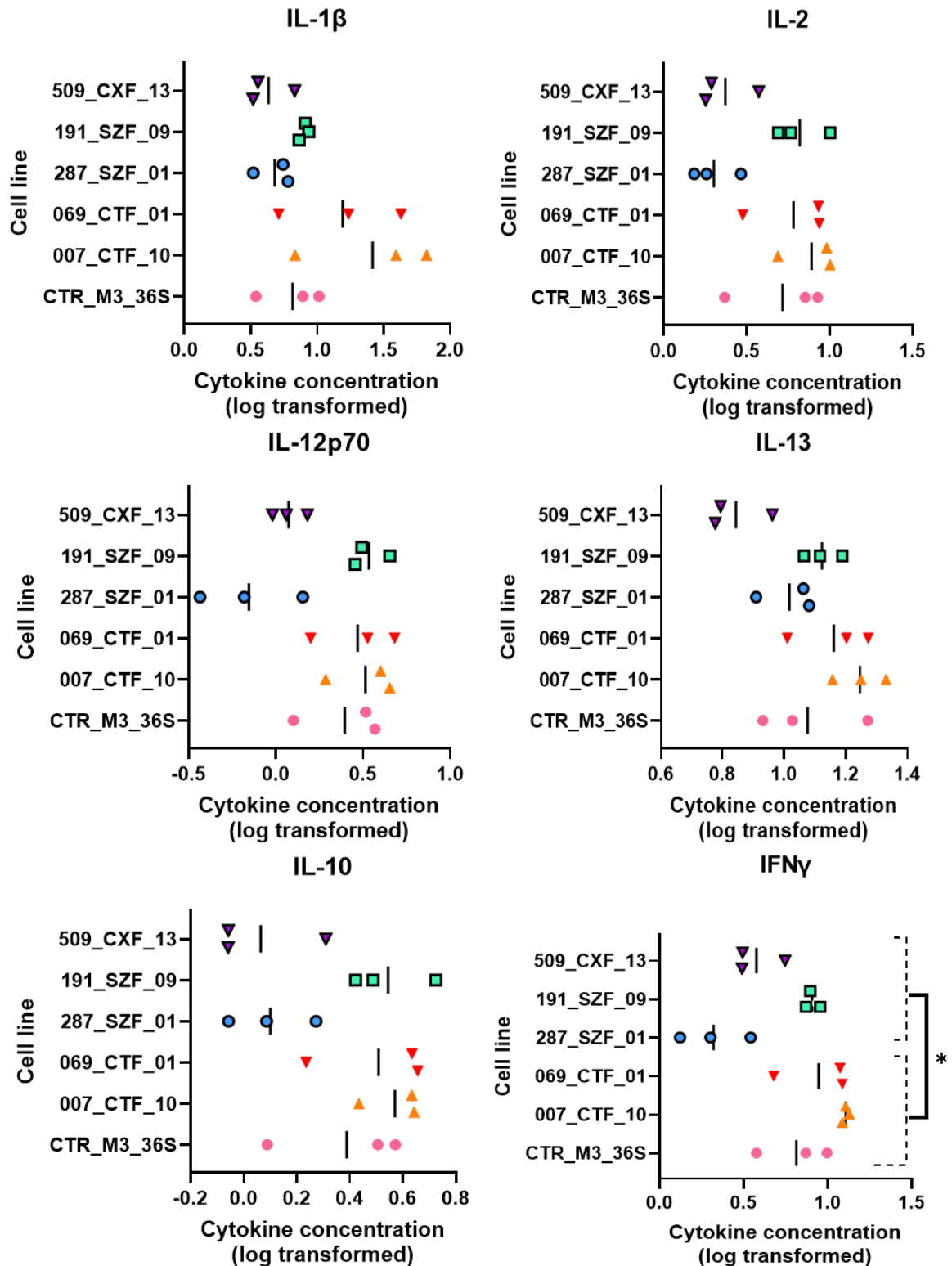


Figure 5. 5: Effect of 22q11.2DS on cytokine release. Statistical comparison between control and 22q11.2DS lines treated H2O vehicles for 24 hours. Before analysis and illustration, data was transformed using Log2 transformation to help better visualise differences across replicates. Comparison groups consisted of N=3 day 14 differentiated 22q11.2DS MGLs vs N=3 day 14 differentiated control MGLs, with n=3 biological replicates

being performed for each cell line. For statistical comparisons, means of control MGLs were compared to means of 22q11.2DS MGLs in one statistical test, not separately for each cell line. For each cell line, the mean of all biological replicates was calculated and used during statistical analysis. Data was checked for normal distribution. Unpaired two-tailed parametric t-test was used for statistical comparisons. Statistics were corrected for multiple comparisons using the Bonferroni-Dunn method. Significant *p* values are indicated as follows: * = *p* < 0.05, ** = *p* < 0.01. Bars represent the mean of *n*=3 biological replicates for each cell line.

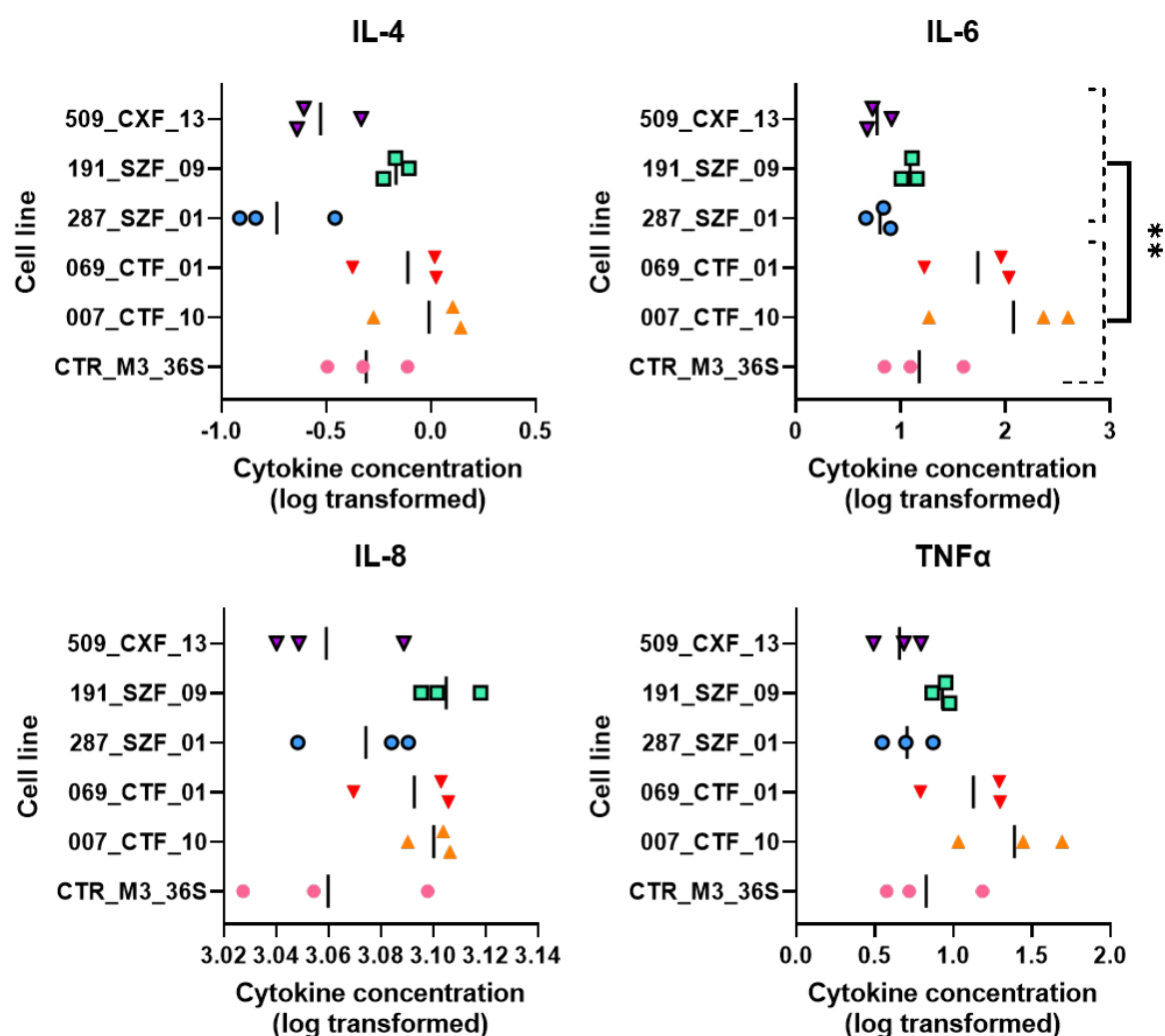
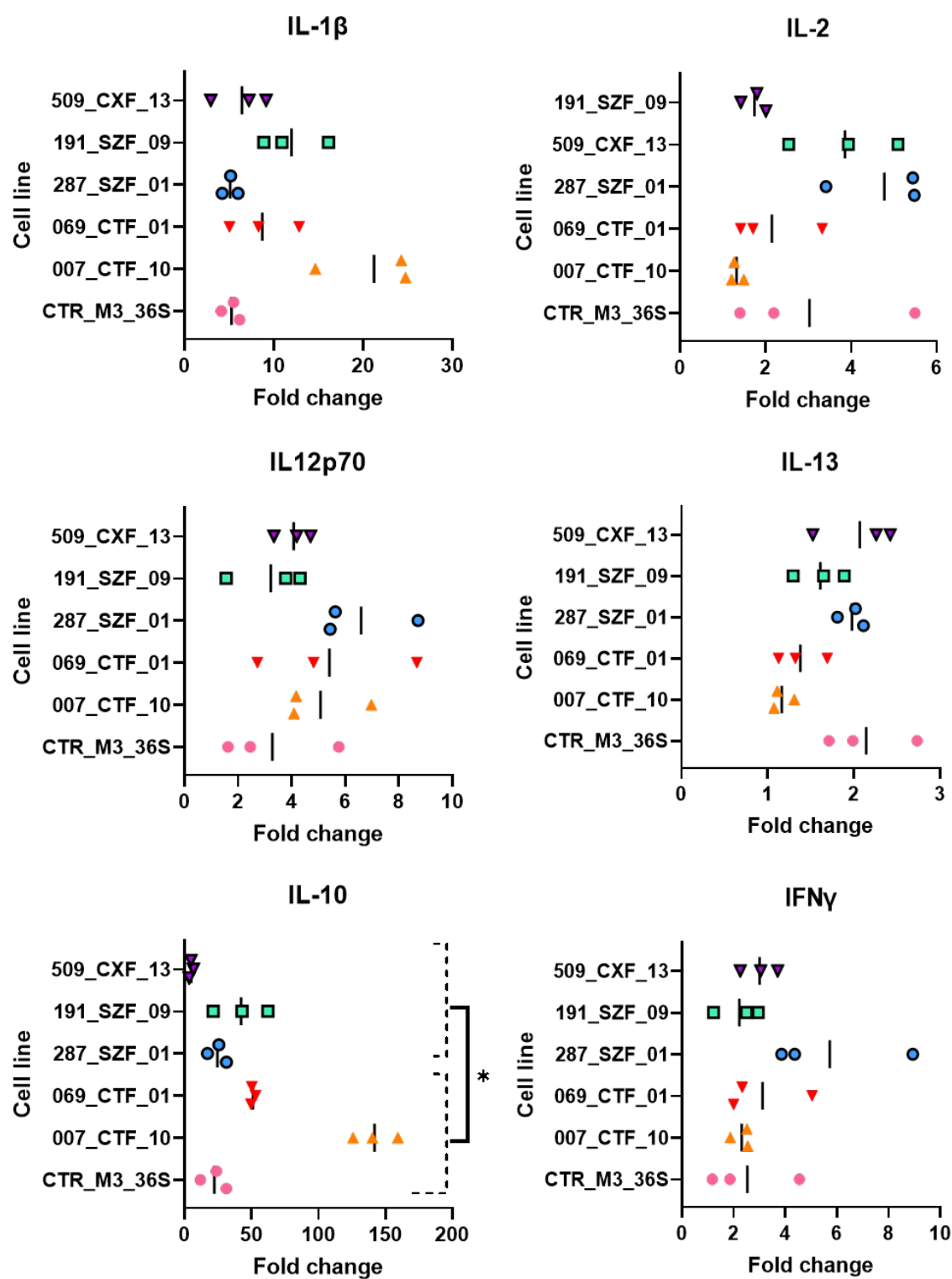


Figure 5. 5 Continued: Effect of 22q11.2DS on cytokine release. Statistical comparison between control and 22q11.2DS lines treated H2O vehicles for 24 hours. Before analysis and illustration, data was transformed using Log2 transformation to help better visualise differences across replicates. Comparison groups consisted of *N*=3 day 14 differentiated 22q11.2DS MGLs vs *N*=3 day 14 differentiated control MGLs, with *n*=3 biological replicates being performed for each cell line. For statistical comparisons, means of control MGLs were

*compared to means of 22q11.2DS MGLs in one statistical test, not separately for each cell line. For each cell line, the mean of all biological replicates was calculated and used during statistical analysis. Data was checked for normal distribution. Unpaired two-tailed parametric t-test was used for statistical comparisons. Statistics were corrected for multiple comparisons using the Bonferroni-Dunn method. Significant p values are indicated at follows: * = $p < 0.05$, ** = $p < 0.01$. Bars represent the mean of $n=3$ biological replicates for each cell line.*



being performed for each cell line. For statistical comparisons, means of control MGLs were compared to means of 22q11.2DS MGLs in one statistical test, not separately for each cell line. For each cell line, the mean of all biological replicates was calculated and used during statistical analysis. Data was checked for normal distribution. Unpaired two-tailed parametric t-test was used for statistical comparisons. Statistics were corrected for multiple comparisons using the Bonferroni-Dunn method. Significant *p* values are indicated as follows: * = *p* < 0.05, **** = *p* < 0.0001. Bars represent the mean of *n*=3 biological replicates for each cell line.

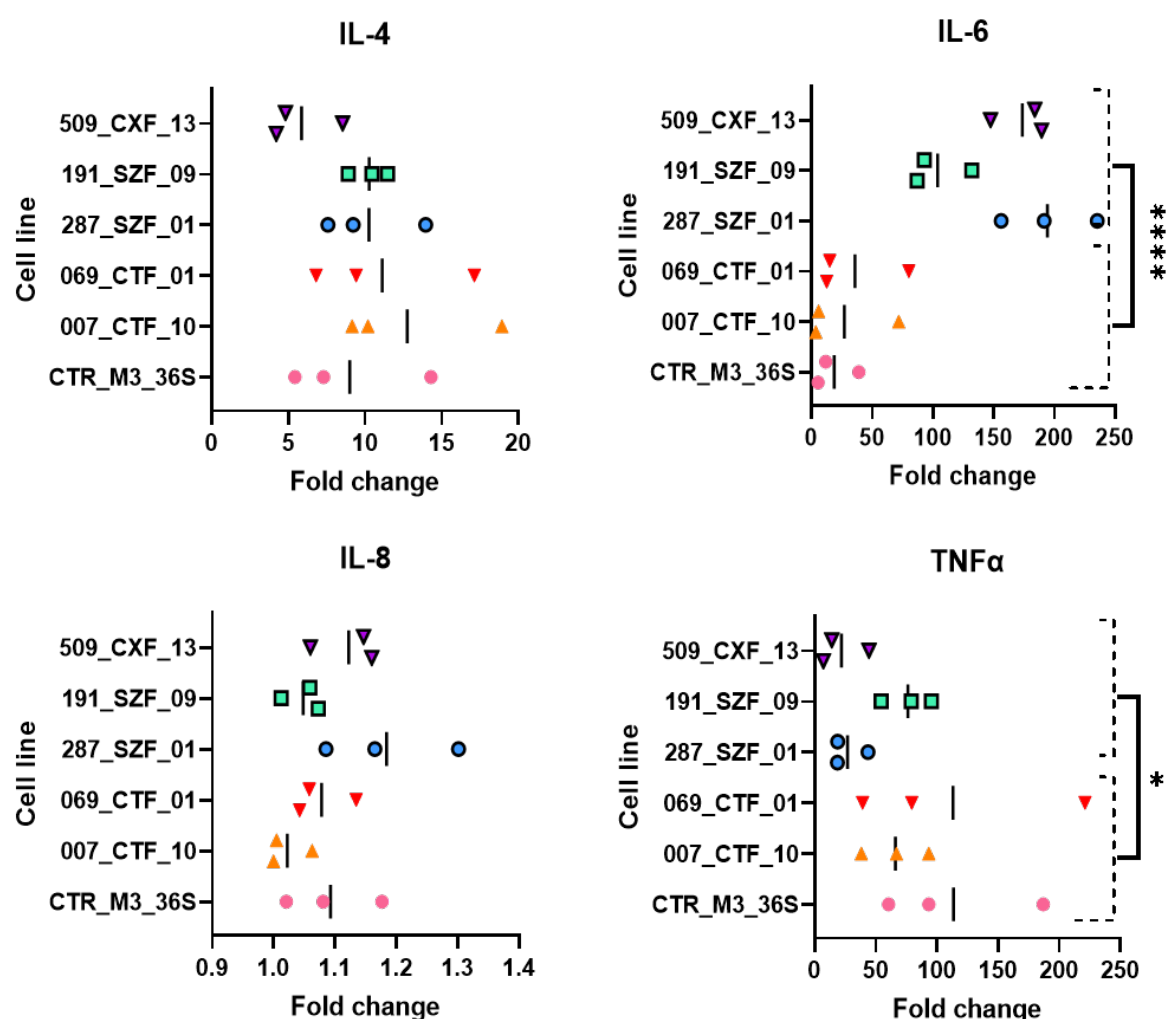


Figure 5. 6 Continued. Effect of 22q11.2DS on cytokine release when treated with LPS. Statistical comparison of control and 22q11.2DS lines treated with LPS for 24 hours. Effect of LPS treatment is shown as a fold change of the 3-hour LPS condition compared to the H2O vehicle condition. Comparison groups consisted of *N*=3 day 14 differentiated 22q11.2DS MGLs vs *N*=3 day 14 differentiated control MGLs, with *n*=3 biological replicates being performed for each cell line. For statistical comparisons, means of control MGLs were compared to means of

22q11.2DS MGLs in one statistical test, not separately for each cell line. For each cell line, the mean of all biological replicates was calculated and used during statistical analysis. Data was checked for normal distribution. Unpaired two-tailed parametric t-test was used for statistical comparisons. Statistics were corrected for multiple comparisons using the Bonferroni-Dunn method. Significant p values are indicated at follows: * = $p < 0.05$, **** = $p < 0.0001$. Bars represent the mean of $n=3$ biological replicates for each cell line.

5.4 Discussion

This chapter provided the first evidence of 22q11.2DS affecting two key functions of MGLs, namely phagocytosis of different cargos and secretion of cytokines, with a complex pattern of effects due to genotype and treatment (LPS vs. vehicle). Significant genotype differences in phagocytosis were increased inferred phagocytosis of Alexa Fluor™ 594-zymosan and ^{td}Tomato-tagged synaptosomes by 22q11.2DS MGLs compared to control MGLs, with no differences being observed in FITC-dextran uptake. With 3-hour LPS challenge, phagocytosis of Alexa Fluor™ 594-zymosan and ^{td}Tomato-tagged synaptosomes changed significantly more in control MGLs compared to 22q11.2DS MGLs, with again no changes being observed in FITC-dextran uptake. With regard to cytokine secretion, 22q11.2DS MGL secrete significantly less IFN γ and IL-6 compared to control MGLs, but when challenged with LPS for 24 hours, IL-6 secretion significantly increased more in 22q11.2DS compared to control MGLs. In contrast, IL-10 and TNF α secretion increased significantly more in control MGLs compared to 22q11.2DS MGLs. Additionally, this chapter provided the first evidence of a 22q11.2DS-associated effect on generating acidic vesicles such as lysosomes when treated with LPS, as after 3 hours of LPS challenge, change in lysotracker levels was significantly higher in control MGLs compared to 22q11.2DS MGLs.

5.4.1 Genotype effects of 22q11.2DS on MGL phagocytosis is cargo and context-dependent

Differential effects of psychiatric disorder risk genes on microglia phagocytosis have previously been described in schizophrenia and ASC *in vitro* genetic risk models outside the context of LPS challenge. In ASC, TMEM59-deficient mouse microglia have been shown to have impaired capacity for synaptic engulfment with complementing *in vivo* data in the same

model (Meng et al., 2022). Specifically, this study suggested that reduced phagocytosis of excitatory synapses distorts the excitatory-inhibitory neuronal activity balance (Meng et al., 2022). This contrasts what was observed in this study and what has previously been observed in schizophrenia models. Patient-derived induced microglia not of hiPSC or yolk sac origin have been used to associate the schizophrenia Complement *C4* risk variant to increased engulfment of synaptic material (Sellgren et al., 2017, 2019). While this project has not shown whether the effect of 22q11.2DS is a complement dependent process, findings by Sellgren and colleagues (2017, 2019) aligns with results of this project, specifically increased phagocytosis of zymosan beads and mouse brain purified ^{td}Tomato-tagged synaptosomes. Combining phagocytosis data with morphology data described in **Chapter 3** suggesting that 22q11.2DS MGLs have a more amoeboid-like morphology, it supports studies such as Morsch et al. (2015) that show enhanced engulfment of debris in as in zebrafish microglia with amoeboid-like morphology compared to more ramified morphological states. Importantly, there is also opposing data which was also shown in zebrafish have demonstrated higher phagocytosis by in less spherical subset of microglia (Silva et al., 2021). It is also unclear how changes in proteomic colocalization of TMEM119 and IBA1 both with and without LPS fits into this (**Chapter 3**) due to their role in homeostasis and potential role in phagocytosis, respectively, as changes in mean protein marker expression levels were not observed (**Chapter 3**, Ohsawa et al., 2004; Kenkhuis et al., 2022; Ruan and Elyaman, 2022). Transcriptomic data on 22q11.2DS MGLs (**Chapter 4**), support increased phagocytosis by 22q11.2DS MGLs due to elevated *S100B*, which as described in the chapter has been associated with regulation of phagocytosis in mice, including the immortalised BV2 mouse microglial cell line (Adami et al., 2001; Bianchi et al., 2010).

Findings on vehicle-treated 22q11.2DS MGLs compared to vehicle-treated control MGLs in this study has a preference towards aligning with the data from the schizophrenia data (Sellgren et al., 2017, 2019), suggesting that 22q11.2DS might preferentially be more of a model of schizophrenia than ASC (Meng et al., 2022). However, due the limited data available to compare to, one cannot say for certain. It must also be considered that schizophrenia and ASC might arise from the same individual, like the donor of 287_SZM_01, and potentially an imbalance of the circuitry one way or the other is responsible. This is importantly still an interesting finding, as it speculatively supports a reason for why treatments such as antipsychotics may vary in efficacy (Howes et al., 2022). Reducing microglia phagocytosis activity by way of minocycline (Sellgren et al., 2019), may hence potentially have no or maybe even an adverse effect in circuitry where genetic risk factors mediating microglia function causes reduced pruning.

LPS challenge has previously been demonstrated to increase phagocytosis FluoSphere® Carboxylate-Modified Microspheres (2 µm, yellow-green fluorescent (505/515) in a 1 hour window following 24 hours of LPS treatment using induced microglia not of hiPSC or yolk sac origin (Ormel et al., 2020). While Ormel et al (2020) also utilised schizophrenia patient lines in their study, phagocytosis was only assessed in neurotypical samples. In this project a 3 hour treatment was selected as microglia phagocytosis have been described to plateau after 3 hours, with LPS-treated microglia phagocytosis being enhanced compared to non-treated microglia (He et al., 2021). Following LPS challenge in this project, control MGL phagocytosis of zymosan beads and mouse brain purified ^{td}Tomato-tagged synaptosomes increased significantly more than in 22q11.2DS MGLs. Hence based on aforementioned zebrafish microglia data observed by Silva et al (2021) suggesting higher phagocytosis in less spherical microglia and, one could speculatively one could consider the idea that 22q11.2DS

MGLs have reduced phagocytic capacity due to their more circular morphological state (**Chapter 3**), so while uptake is increased compared to control MGLs in vehicle conditions, their morphological state prevents them from responding to LPS challenge of 3 hours in a similar way to control MGLs.

It is clear that 22q11.2DS effects on MGLs are cargo-dependent, with no changes being observed in FITC-dextran across both vehicle and LPS condition comparisons. Hence the effect of 22q11.2DS MGLs is likely on specific uptake mechanisms. It is apparent that cytochalasin D does not inhibit uptake of FITC-dextran to the same extent as other cargos, which is possibly due to uptake of being primarily via clathrin-mediated endocytosis pathways. As seen in this study however, an effect of cytochalasin D on dextran uptake has previously been characterised, although it appears to be cell line dependent, with cytochalasin D increasing uptake of dextran in A431 (epidermal) cancer lines but reducing it in HeLa (cervical) cancer lines (Al Soraj et al., 2012).. Hence as there is no previously published work on use of cytochalasin D to inhibit uptake of particles the size of 4kDa in microglia, it is hence critical to further characterise this uptake mechanism in MGLs, including through the use of other inhibitors such as dynasore (Macia et al., 2006; Maguire et al., 2022).

Importantly, cytochalasin D treatment on microglia has previously been demonstrated to inhibit uptake of dead human neuroblastoma cells (SH-SY5Y cell line) and rat cortical synaptosomes (Hall-Roberts et al., 2020; Obst et al., 2021). Hence while additional characterisation is necessary to understand the role of cytochalasin D on microglia uptake of FITC-dextran, findings on phagocytosis and potential pinocytosis of zymosan beads and mouse brain purified ^{td}Tomato-tagged synaptosomes is supported by these previous studies.

5.4.2 22q11.2DS MGL acidity is not increased the level of control MGLs in response to LPS

Findings in LPS-challenged control MGLs replicates complement data from mouse microglia (Majumdar et al., 2007; Tanaka et al., 2013), having elevated lysosome markers in response to immune challenge such as LPS or injury, while 22q11.2DS lysosome levels remain unchanged. This could potentially infer an inability of 22q11.2DS MGLs to regulate their metabolic state to the same degree as control MGLs and an inability to additional phagocytic activity, which would be relevant to test in future work (**Section 5.4.4, Chapter 5**)

Alternatively, this aberrant lysosome level response can mean that cells are unable to degrade ingested material. In LPS-treated 22q11.2DS MGLs, there is no significant increase their phagocytosis of zymosan or mouse brain purified ^{td}Tomato-tagged synaptosomes compared to LPS-treated control MGLs, yet 22q11.2DS MGLs take up a significantly greater amount of these cargo in vehicle conditions. This further supports an idea explored in **Section 5.4.1, Chapter 5** that 22q11.2DS MGLs are at capacity, potentially also due to their more circular morphological state (**Chapter 3**). As 22q11.2DS MGLs potentially do not increase inferred lysotracker levels in response to LPS, there are likely not a sufficient number of lysosomes to accommodate additional need for degradation. This speculatively would explain 22q11.2DS MGL response to not recruit phagosomes in order to take up additional cargo, or even to not utilise potential motility processes to migrate towards cargo, as they are clearly capable of phagocytosis. However, it should be noted that that the number of cells within each culture taking up cargo was not quantified due to COVID-19-related time restrictions (**COVID-19 Impact Statement**). This would have further supported this theory in assessing whether there are less cells in 22q11.2DS MGLs that are actively performing phagocytosis functions, or whether all are actively phagocytising cargo. Additionally, assessing colocalisation of

cargo and acidic compartment could potentially support that debris accumulates in lysosomes, but due to the specificity of lysotracker, at least one other stain, such as CD68, would be necessary to confirm this (Wu et al., 2021)

A deficiency in intrinsic microglia autophagy, the cells' ability to degrade material within the cytoplasm, has previously been suggested to cause social behavioural phenotypes linked with ASC (Kim et al., 2016). The study by Kim et al. (2016) showed that in *atg7*-deficient mice, ASC model driven by impaired autophagy, altered connectivity was between brain regions. Additionally, by using primary microglia that were given synaptosomes, they showed that synaptosome degradation was inefficient and delayed in *atg7*-deficient microglia. Lastly, mice with *Atg7*-deficient microglia had increased spine density, suggesting that synaptic pruning was inhibited. This was also replicated in a co-culture with primary neurons. This well characterised phenotype shown in Kim et al. (2016), while in mice, highlights a very plausible hypothesis for 22q11.2DS MGLs which combines previous schizophrenia and ASC data on phagocytosis. Clearly, 22q11.2DS MGLs exhibit exaggerated phagocytosis while not stimulated but are not able to increase it to the same extent as otherwise healthy control MGLs when prompted, which is in line with previous schizophrenia data (Sellgren et al., 2019). However, if one then considers what is shown with the lysotracker assay, 22q11.2DS MGLs are unlikely to be able to keep up this uptake in the long-term, as well as being unable to phagocytose additional cargo when needed. This is in line with previous ASC data suggesting impaired synaptic pruning (Tang et al., 2014). Hence it could be hypothesised that the elevated synaptic pruning seen in schizophrenia is a temporary phenotype, at least in individuals where these two conditions are co-occurring.

5.4.3 22q11.2DS MGLs have context-dependent abnormalities in cytokine secretion

Based on vehicle vs vehicle comparisons, cytokine levels do not all match differences observed in schizophrenia or ASC serum and cerebrospinal fluid levels (Naudin et al., 1996; Miller et al., 2011; Schwieler et al., 2015; Dahan et al., 2018; Kordulewska et al., 2019; Zhao et al., 2021), which could be due to this model assessing a stage pre-pathogenesis.

Differences in vehicle comparisons included IFN γ and IL-6, but it is also notable that IL-1 β trended towards statistical significance and was possibly caused by no cell line variability in CTR_M3_36S. There were key differences following LPS stimuli, with IL-6 secretion increasing significantly more in 22q11.2DS MGLs after 24 hours compared to control MGLs.

However, secretion change of IL-10 and TNF α was significantly higher in control MGLs.

This supports findings that MGLs responds with enhanced cytokine secretion following challenge using other agents, such as IL-6 or a combination of LPS (100 ng/mL) / IFN γ (100 ng/mL) (Haenseler et al., 2017; Couch et al., 2023), and that transcriptomic response to LPS is different in control MGLs and 22q11.2DS MGLs (**Chapter 4**). However, findings in this study contradicts findings by Ormel et al. (2020) also using 100 ng/mL LPS, which found enhanced TNF α secretion without increased IL-6 secretion in human microglia induced from blood monocytes donated by individuals with schizophrenia compared to control lines.

Critically, Ormel et al. (2020) treated cells for 6 hours rather than 24, so it could be a time-dependent difference which would have to be investigated in the future. Additionally, Ormel et al. (2020) likely is investigating a post-pathogenesis stage of schizophrenia as these cells are not reprogrammed, and these induced microglia do not share a similar ontogeny to MGLs (Haenseler et al., 2017). The enhanced LPS response observed is partially in line with findings in an ASC-associated *Fmr1* knockout mouse model, which also found enhanced IL-6 secretion compared to controls after 24 hours, but critically this model also, like Ormel et al. (2020) for enhanced TNF α secretion (Parrott et al., 2021), so further work is necessary to

determine whether this is an *Fmr1* knockout-related effect, or the difference is due to species heterogeneity (**Section 1.1.5, Chapter 1**).

The potential implications of changes in the type II interferon IFN γ were previously discussed extensively in **Section 4.4.1, Chapter 4**, with data generated in this chapter supporting evidence of reduced IFN and other cytokine signalling in vehicle comparisons as observed in **Chapter 4**, including differential down-regulation *IL-6*. It is however important to note that decreased IFN γ have previously been observed to be reduced in whole blood cultures and not changed in serum from individuals with schizophrenia, but observed to be increased in serum from individuals with ASC (Wilke et al., 1996; Potvin et al., 2008; Saghazadeh et al., 2019). This section hence will focus more on the relevance of differences in *IL-6*, *IL-10* and *TNF α* .

On the topic of *IL-6*, findings in vehicle versus vehicle comparisons contradicts the literature on schizophrenia and ASC meta-analyses (Potvin et al., 2008; Saghazadeh et al., 2019). This also extends non-serum experiments assessing protein levels in *postmortem* tissue in ASC (Wei et al., 2011), while another similar experiment has shown no change in schizophrenia except for on the mRNA level (Izumi et al., 2021). Of note, the latter did show reduced protein *IL-10* levels in the tissue. In schizophrenia, another meta-analysis has pointed out that *IL-6* is acutely increased in individuals with first-episode psychosis and inpatients experiencing relapse (Miller et al., 2011). This study by Miller et al. (2011) suggests that *IL-6* can be a state marker of clinical status, which is relevant to findings in this study showing that the fold change of *IL-6* in 22q11.2DS MGLs is significantly higher than that of control MGLs when exposed to LPS. It is possible that an abnormal spike in *IL-6* following LPS challenge affirms these findings.

Chronic elevation of IL-6 has been observed following MIA in mice as well in adults with childhood trauma, which is risk factor associated with psychosis symptoms (Schäfer and Fisher, 2011; Baumeister et al., 2016; Toutountzidis et al., 2022). As there are no studies on individuals pre- and post-diagnosis of schizophrenia assessing their serum, it is unclear what their IL-6 levels were beforehand. It naturally makes sense that landscape is sparse on findings related to this type of experiment due to the difficulty of obtaining such data. In the context of hiPSC studies, it is, speculatively, possible that LPS treatment is an inducer of what would be a chronically activated microglia state.

Fitting with this theory is the lower fold change of IL-10 in 22q11.2DS MGLs compared to controls. As an anti-inflammatory cytokine, it is no surprise that reduction of IL-10 has been shown to drive microglia to states associated with classic microglia activation and when treated with LPS it is up-regulated, serving to help modulate the immune response (Lobo-Silva et al., 2016; Laffer et al., 2019). Reduced IL-10 has also been previously found in serum of individuals with schizophrenia, bipolar disorder, and ASC (Kunz et al., 2011; Saghazadeh et al., 2019), as well as having been associated with symptom severity in schizophrenia (Chenniappan et al., 2020). Mouse models outside of the psychiatric disorder field has also shown that IL-10 serves an important role in not only preventing hyperactivation of microglia, but also exacerbation of immune response (Shemer et al., 2020; Weston et al., 2021). Therefore, reduced IL-10 response compared to controls in 22q11.2DS MGLs is likely either partially or if not the underlying reason behind the elevated IL-6 response in 22q11.2DS MGLs.

Elevated TNF α in control LPS response may suggest differences in the way MGLs respond to LPS stimuli. This could speculatively be associated with abnormalities in signalling pathway, with for example 22q11.2DS MGLs relying more on NF- κ B-related signalling based on transcriptomic state data at 3 hours of LPS treatment (**Chapter 4**). In LPS response, IL-6 and TNF α are induced by a specific combination of MAPKs (Ishijima and Nakajima, 2021). By using a rat model, Ishijima and Nakajima (2021) observed that nitric oxide is more preferentially involved in the signalling cascade resulting in IL-6 and IL-1 β secretion following stimuli with LPS, while JNK/p38, ERK/JNK, ERK/JNK/p38, and PKC α inhibition results in reduced secretion of TNF α while retaining IL-6 and IL-1 β elevation. 22q11.2DS MGLs might be more reliant on or prefer nitric oxide signalling in their LPS response, which notably is linked to NF- κ B signalling, matching 22q11.2DS MGL transcriptomic response profile in **Chapter 4** (Baig et al., 2015; Brás et al., 2020). Alternatively, aberrancies in JNK/p38, ERK/JNK, ERK/JNK/p38, or PKC α -associated signalling, while not specifically identified in transcriptome analysis at this scale, might be the root cause. This would support notions of altered signalling in at least one of these which have been characterised across psychiatric disorders including schizophrenia, bipolar disorder, and ASC (Kyosseva, 2004; Funk et al., 2012; Lang et al., 2014; Robson et al., 2018; Musi et al., 2020). A straightforward future experiment to start assessing signalling abnormalities in 22q11.2DS MGLs and support findings in this project would perhaps be to look at NF- κ B activation. This could for example be tested by assessing nuclear NF- κ B protein, such as RelA fluorescence intensity fold changes by immunocytochemistry (Lee et al., 2014; Ernst et al., 2018)

The difference in response is also important for how the microglia communicates with neurons through these cytokines (Chamera et al., 2020), which is an interesting avenue for

future work. While there is a clear understanding that neuronal activity can shape the function of microglia, research on bidirectional communication between microglia and neurons is lacking (Ferro et al., 2021). For example, it is well known how fractalkine (CX3CR1-CX3CL1) signalling between the two cell types works, with chemokine CX3CL1 secreted by neurons acting as an off-signal for microglia, keeping them in a resting surveillance state in rodents (Cardona et al., 2006; Arnoux and Audinat, 2015; Szepesi et al., 2018), highlighting the importance of later studies on chemokines. The effects of specific microglia-secreted chemokines and cytokines are however not as well understood, however treatments on neural stem cells with microglia-conditioned media have previously demonstrated protective effects, highlighting the importance of their role during development (Nagata et al., 1993; Polazzi et al., 2009; Vay et al., 2018). Absence of circulating TNF α could have detrimental effects neuronal progenitor proliferation through unbalanced TNFR1 and TNFR2 neuronal receptor signalling (Chen and Palmer, 2013; Papazian et al., 2021), although how this would translate to environments pushed towards a pro-inflammatory state is unclear. Perhaps the most important finding here, however, is the little discussed in this chapter reduced secretion of IFN γ , which could negatively impact neurite outgrowth (Warre-Cornish et al., 2020).

5.4.4 Limitations and future directions

The experimental design in this study provides N=3 biological replicates per cell line for each experiment. Inclusion of mouse brain purified ^{td}Tomato-tagged synaptosomes critically provided biological material relevant to schizophrenia and ASC phenotypes (Kim et al., 2017; Sellgren et al., 2019). However, a number of factors could have been improved to strengthen the findings of this study.

In uptake experiments the dextran condition effectively acts as an additional control for phagocytosis experiments, acting more to show that cytochalasin D successfully inhibits phagocytosis rather than clathrin-mediated endocytosis. For a future experiment, addition of a compound such as dynasore, which inhibits this uptake mechanism would be of benefit (Macia et al., 2006; Maguire et al., 2022). The addition of another differently sized physiologically relevant cargo, like β -amyloid based on cell line 287_SZM_01 having higher PRS for Alzheimer's disease and 069_CTF_01 potentially having an Alzheimer's disease associated SNP (**Section 3.3.2, Chapter 3** and **Section 2.1, Chapter 2**, respectively), would also be relevant as it would assess a combination of clathrin-mediated endocytosis and macropinocytosis pending on aggregation (Mandrekar et al., 2009; Joshi et al., 2021; Maguire et al., 2022). Another cargo options could also include α -Syn protein, which would have relevance for 22q11.2DS-associated risk of Parkinson's disease, however, as found by Choi et al. 2020, uptake inhibition cargos such as cytochalasin D or Dynasore actually increased α -Syn protein uptake, so alternatives would have to also be tested (Boot et al., 2018; Choi et al., 2020). Of perhaps highest relevance to the uptake assays, cell survival assays were not performed, making it possible that final cell number were variable across cell lines at the end up differentiation during the experiment. This could impact uptake as the number of cells taking up cargo could theoretically be different across cell lines, perhaps leading to higher uptake per cell in lower density wells. Phagocytosis findings should also in the future be confirmed in co-culture, by for example assessing uptake of fluorescent cargos as in this study. It would alternatively be worth investigating changes in synaptic elements such as PSD95 in co-culture as the cargos used in this project are critically not biologically human (Solomon et al., 2022).

Metabolic regulation of microglia extends beyond the responsibility of lysosomes, particularly to the mitochondria, and a complete view of MGL metabolism is lacking in this study. Mitochondrial function can affect and be affected by microglial state (Ghosh et al., 2018). In order to further detangle the puzzle of dysregulated metabolic shift in 22q11.2DS MGLs a natural next step would be to assess mitochondrial function. This could be performed by using standard approaches such as staining for associated proteins and quantifying gene expression, or using more state-based approaches measuring oxygen consumption rate (Li et al., 2019; Li, Tran, et al., 2021; Mallach et al., 2021; Piers et al., 2020; Reich et al., 2021; Solomon et al., 2022). Mitochondrial fragmentation induced by LPS in immortalised murine BV2 microglia, can also for example alter Ca^{2+} homeostasis (Pereira et al., 2021). Reliable calcium homeostasis is critical for microglia, as it has for example been argued that it is necessary for normal sensing of tissue dyshomeostasis, with it occurring mostly during pathological conditions, and is mediated by Ca^{2+} release from the intracellular Ca^{2+} stores (Eichhoff et al., 2011; Pan and Garaschuk, 2022). Hence investigation of the effect of 22q11.2DS on MGLs could also potentially be extended to characterisation of Ca^{2+} levels using for example live cell calcium imaging (Solomon et al., 2022; Pan and Garaschuk, 2022).

There is also a need to further assess the role of the differentially secreted cytokines, as well as extending this analysis to chemokines as RNA sequencing data also points towards dysregulated chemokine signalling (**Chapter 4**). This is due to the importance of cell to cell communication, which is clearly established between neurons and microglia (Chamera et al., 2020; Ferro et al., 2021). The most straightforward method would be assessing the effect of 22q11.2DS MGL-conditioned media on hiPSC-derived neuronal cell types such as cortical interneurons or midbrain dopaminergic neurons that might be implicated in schizophrenia

(Park et al., 2020; Rogdaki et al., 2021; Reid et al., 2022), but also perhaps astrocytes due to their established crosstalk although it is difficult to predict which astrocyte mechanism could be impacted based on current findings (Matejuk and Ransohoff, 2020). Naturally, control MGL-conditioned media would be used as a comparison. As it has been shown that media from BV2 cells treated with 1ug/ml LPS and 1ug/ml polyI-C can affect metabolism in hiPSC-derived cortical interneurons, with lines donated by individuals with schizophrenia showing prolonged metabolic defect (Park et al., 2020), it would be interesting to assess what metabolic effect conditioned 22q11.2 MGL media would have on neuronal cell types. It would also be interesting to consider the effect on neuronal cell types differentiated from 22q11.2DS hiPSCs to assess whether 22q11.2DS neuronal cells responds differently to 22q11.2DS or control MGL conditioned media. Alternatively, the effect of each differentially secreted cytokine could be assessed individually or together, through ELISAs or through a panel kit as used in this study. While chemokines such as CXCL10 and CCL13 might be of particular interest due to RNA sequencing data (**Chapter 4**), and complement cascade components such as C1q is of interest due to increased phagocytosis observed by 22q11.2DS MGLs in this chapter (Stevens et al., 2007), a full profiling of everything secreted by the MGLs might have to be considered to rule out missing out on the beneficial or detrimental effect of other secreted molecules.

In addition to the potential future functional experiments highlighted, a single longer or repeated exposures are key potential experimental alterations that could be implemented into future experiments. This would be relevant to assess theories such as that of an initial environmental challenge is a driver behind future pathology in these potentially susceptible 22q11.2DS MGLs, which might make baseline cytokine phenotype more akin those observed *in vivo*. Another relevant function that has not been looked at is also motility of 22q11.2DS

MGLs, which could be assessed using live cell imaging (Haenseler et al., 2017; Couch et al., 2023). As previously noted, pathways involved should also be further validated. Co-cultures are also a critical step, which can support assessment of differences in synapse formation and engulfment of synaptic material such as PSD95 (Solomon et al. 2022).

5.5 Conclusions

In summary, functional characterisation based on previous morphological and transcriptomic profiling and psychiatric disorder literature revealed a context dependent effect of 22q11.2DS on MGL phagocytosis, acidic endolysosomal vesicles, and cytokine secretion. Perhaps the most notable finding being reduced secretion of cytokines in the vehicle-treated condition compared to control MGLs. This does however give rise to theories such as that environmental stimulus, modelled with LPS in study, could potentially initiate long-standing effect on the cellular environment and serum levels seen in patients. LPS-treatment of hiPSC-derived MGLs could provide a potential alternative model of MIA through if effects of LPS are later validated to be long-standing, with 22q11.2DS MGLs also speculatively increasing susceptibility to psychiatric disorders rather than driving the pathogenesis. Longer term experiments also assessing repeated exposure is however also necessary. Future studies to extend these findings has also been proposed, including extending metabolic characterisation to mitochondrial function as well as assessing the effect of 22q11.2DS MGL-conditioned media on hiPSC-derived neuronal cells.

Chapter 6: General Discussion

6.1 Overview and discussion of key findings

Converging lines of evidence support a role for microglia in the pathophysiology of psychiatric disorders with a neurodevelopmental origin. This project investigated the effect of a highly penetrant risk factor associated with schizophrenia and ASC, 22q11.2DS, as no previous evidence exists on 22q11.2DS in the context of microglia. Additionally, previous human *in vitro* studies on microglia in the context of ASC and schizophrenia have not been completed using human high-risk donor cell lines where microglia are derived from a yolk sac-like origin. Hence, this thesis aimed to contribute novelty to the field by characterising the impact of 22q11.2DS on intrinsic microglia form and function using hiPSC-derived MGLs with an emphasis on phenotypes that be associated with ASC and schizophrenia. To do so, the following characterisation of 22q11.2DS cell lines and differentiated 22q11.2DS MGLs was performed which also successfully validated the MGL differentiation protocol (results are summarised in **Table 6.1**):

- Chapter 3:
 - Confirmation of 22q11.2DS genotype and calculation of PRS to account for factors also outside the 22q11.2 region
 - Morphological state and protein marker analyses with and without 3-hour LPS challenge
- Chapter 4:
 - Transcriptomic state profiling with and without 3-hour LPS challenge, encompassing DEGs, gene set enrichment, and gene ontology analyses,
- Chapter 5:

- Uptake characterisation using a range of cargoes with and without 3-hour LPS challenge
- Analysis of inferred lysosome levels using lysotracker with and without 3-hour LPS challenge
- Cytokine secretion profiling of 10 different cytokines with and without 24-hour LPS challenge

<i>Phenotype investigated</i>	<i>Key findings</i>	<i>Notes</i>
HiPSC genetic variance	<ul style="list-style-type: none"> All cell lines used in this study carry at least one CNV detected by Infinium Psycharray except for CTR_M3_36S CNVs in the 22q11.2 region across 22q11.2DS hiPSCs are heterogenous, with duplications also being present in 191_SZF_09 and 509_CXF_13. Number of CNVs per 22q11.2DS cell lines: <ul style="list-style-type: none"> 287_SZM_01: 1 deletion 191_SZF_09: 4 deletions, 3 duplications, 1 double deletion 509_CXF_13: 1 deletion, 2 duplications 	014_CTM_02 and 069_CTF_01 were not part of the Infinium Psycharray dataset
HiPSC polygenic risk	<ul style="list-style-type: none"> Highest risk for schizophrenia: 509_CXF, 287_SZM, 007_CTF Highest risk for ASC: 191_SZF, 287_SZM, CTR_M3 Highest risk for bipolar disorder type 2: 287_SZM, 127_ZTM, 007_CTF Highest risk for Parkinson's disease: 287_SZM, CTR_M3, 007_CTF Highest risk for Alzheimer's disease: 287_SZM, 191_SZF, 007_CTF 	Cell lines with the highest associated polygenic risk shown from left to right
Morphological state	<ul style="list-style-type: none"> Vehicle-treated 22q11.2DS MGLs have higher circularity, with cultures overall being more amoeboid and less bipolar compared to vehicle-treated control MGLs After 3 hours of LPS treatment, the control MGL population become more amoeboid, but the 22q11.2DS MGL population does not 	
Proteomic state	<ul style="list-style-type: none"> No differences in PU.1, IBA1, and TMEM119 expression Colocalisation of TMEM119:IBA1 is higher in vehicle-treated 22q11.2DS MGLs compared to vehicle-treated control MGLs Colocalisation of TMEM119:IBA1 is increased in control MGLs when treated with LPS for 3 hours, but not to the same extent in 22q11.2DS MGLs Colocalisation of TMEM119:IBA1 in 22q11.2DS MGLs did not appear to change in response to LPS 	Potential variance across 22q11.2DS cell lines were observed in PU.1 and IBA1 fluorescence intensity in across conditions
Transcriptomic state	<ul style="list-style-type: none"> 7 genes were up-regulated and 4 were down-regulated in vehicle-treated 22q11.2DS MGLs compared to vehicle-treated control MGLs. <ul style="list-style-type: none"> Notable genes: <i>CCL13</i>, <i>NLRP2</i>, and <i>IL1A</i> Following 3 hours of LPS treatment, control MGLs uniquely up-regulated 23 genes, while 22q11.2DS MGLs uniquely up-regulated 35 genes In the LPS-treated condition, differentially expressed genes in both control and 22q11.2DS MGLs were associate with psychiatric disorder datasets, but genes differentially expressed in the 22q11.2DS MGL LPS response had more overlaps Genes differentially expressed in the 22q11.2DS MGL LPS response also had unique overlaps with datasets associated with oxidative phosphorylation, microglia signature genes, anti-inflammatory genes, and GW9-18 of microglia development While both control and 22q11.2DS MGL genes differentially expressed following LPS treatment were associated with pathways linked to immune response. 	<p>For vehicle comparisons, results of only the most stringent statistical significance threshold are shown here</p> <p>Summaries of all associated gene sets and pathways can be found at the beginning of the Chapter 4.4 (Figures 4.22-25)</p>

	<ul style="list-style-type: none"> Differences in their immune response during gene ontology analysis, including in cytokine, chemokine, interferon, and neurotransmitter associated pathways, with 22q11.2DS MGL LPS response also being likely to more heavily rely on ER-nucleus-, TLR-, and NF-κB-signalling following the initial exposure to LPS 	Tables with all differentially expressed genes are provided in the relevant sections in Chapter 4
Phagocytic state	<ul style="list-style-type: none"> Vehicle-treated 22q11.2DS MGLs phagocytose more Alexa Fluor™ 594-zymosan and mouse brain purified ^{td}Tomato-tagged synaptosomes compared to vehicle-treated control MGLs Uptake of Alexa Fluor™ 594-zymosan and mouse brain purified ^{td}Tomato-tagged synaptosomes increased more in control MGLs compared to 22q11.2DS MGLs when treated with LPS for 3 hours relative to uptake in the vehicle condition No differences were observed in uptake of 4 kDa FITC-dextran across statistical comparison of conditions 	Uptake of the control line 069_CTF_01 following LPS was more like that of 22q11.2DS MGL cell lines except 191_SZF_09, which aligned more with other control lines
Metabolic state	<ul style="list-style-type: none"> When assessing inferred lysosomes levels with lysotracker, no differences were found between vehicle-treated control MGLs and 22q11.2DS MGLs. Inferred lysosome levels appeared to more greatly increased in control MGLs compared to 22q11.2DS MGLs when treated with LPS for 3 hours 	
Secretory state	<ul style="list-style-type: none"> Vehicle-treated 22q11.2DS MGL had lower secretion of IFNγ and IL-6 compared to vehicle treated control MGLs Following 24-hour treatment with LPS, IL-6 secretion more increased to a greater extent in 22q11.2DS MGLs compared to control MGLs, while TNFα and IL-10 increased to a greater extent in control MGLs compared to 22q11.2DS MGLs 	Greater TNFα and IL-10 increase in control MGLs following LPS treatment are likely driven by variance across control cell lines

Table 6. 1: Overview of key thesis findings. These experimental results are detailed in the following chapters alongside additional experiments and analysis: Chapter 3: Exact location of and genes within CNVs in 22q11.2DS cell lines, HiPSC genetic variance, hiPSC polygenic risk, morphological state, and proteomic state. Chapter 4: Transcriptomic state. Chapter 5: Phagocytic state, metabolic state, and secretory state. Abbreviations: ASC, autism spectrum condition; CNV, copy number variant; HiPSC, human induced pluripotent stem cell; LPS, lipopolysaccharide; MGL, microglia-like cell.

6.1.1 Genetic heterogeneity of cell lines

Firstly, genotyping data of 22q11.2DS donor cell lines were extensively characterised (Section 3.3.1, Chapter 3). Heterogeneity amongst 22q11.2DS lines was observed, with a combination of deletions and duplications being detected across the three lines. The only commonly affected region across the 22q11.2 region for all three 22q11.2DS lines were LCR-A to LCR-B, but the whole LCR-A to LCR-B region was only deleted in 287_SZM_01 and 509_CXF_13, with 191_SZF_09 having a four segments affected within this region, including two deleted segments, one double deleted segment, as well as one duplication as per Section 3.3.1, Chapter 3, where other differences are also highlighted. This is notable, as both of the cell lines with deletions fully spanning LCR-A to LCR-B, 287_SZM_01 and 509_CXF_13, has a diagnosis of ASC. A deletion spanning LCR-A to LCR-B deletion in the context of 22q11.2DS has been associated with 39-44% increased rate of ASC diagnosis compared to a 0% rate in individuals whose deletion does not include LCR-A to LCR-B (Clements et al., 2017) The available information on the clinical status of the 22q11.2DS donor lines also confirmed that one individual, 287_SZM_01, had a diagnosis of schizophrenia, which was also notably the only donor with the most common deletion spanning LCR-A to LCR-D (Section 3.3.1, Chapter 3). Nonetheless it was observed from the genetic data that all donors carried deletions in key genes *COMT*, *MRPL40* and *DGCR8* which has been proposed to be drivers of 22q11.2DS phenotypes (Section 3.3.1, Chapter 3) (Kimoto et al., 2012; Devaraju et al., 2016; Nogami et al., 2021), with *COMT* deletion also being qualitatively confirmed using qPCR (Section 3.3.5, Chapter 3) and all these three genes being detected as down-regulated DEG using RNA sequencing with LenientT thresholding (Section 4.3.3, Chapter 3). Due to potential protective effects of 1.5-3Mb duplications within or spanning LCR-A to LCR-D towards schizophrenia, key genes within these large duplications could also speculatively play similar roles as the deleted driver genes

(Rees et al., 2014), which is relevant for 191_SZF_09, whose clinical status is asymptomatic, and carries three segmented duplications spread across LCR-A to LCR-D (**Section 3.3.1, Chapter 3**). PRS calculation also revealed substantially heterogeneous risk for 22q11.2DS-associated ASC, schizophrenia, bipolar disorder type II and Parkinson's Disease, as well as Alzheimer's Disease across cell lines as described in **Section 3.3.2, Chapter 3**. Control lines, excluding 069_CTF_01 and 127_CTM_03 which were not test, did not have elevated polygenic towards these disorders relative to other cell lines. Notable findings included 287_SZM_01 having high polygenic risk towards Alzheimer's disease and Parkinson's disease, 509_CXF_13 having high polygenic risk towards schizophrenia and low polygenic risk towards Parkinson's disease, and 191_SZF_09 having no difference in polygenic risk, relative to other cell lines. Overall, variability in PRS across these conditions established a potentially source of variability noted in assays where cell line to cell line variance was noted, for example in **Section 5.3.1, Chapter 5**, where 191_SZF_09 uptake of synaptosomes were noted to align more with control lines in vehicle comparisons.

6.1.2 Genotype-driven differences between control and 22q11.2DS MGLs

Following confirmation that hiPSC-derived MGLs take on microglia-like phenotypes, and that 22q11.2DS influences morphology and TMEM119-IBA1 colocalisation (**Section 3.3.6 and Section 3.3.7, Chapter 3**), RNA sequencing of differentiated MGLs was performed to explore overall changes in transcriptomic profile of cell lines with 22q11.2DS (**Chapter 4**). DEG analysis confirmed several down-regulated genes expected in 22q11.2DS cell lines based on genotyped deletions in **Section 3.3.1, Chapter 3**, and highlighted down-regulated genes such as *CCL13* and up-regulated genes such as *SI00B* that are associated with that regulate microglia phagocytic activity (**Section 4.3.3, Chapter 4**). Reductions in cytokine signalling and regulation pathways was also observed in 22q11.2DS MGLs (**Section 4.3.5,**

Chapter 4), yet the associated specific signalling pathways was primarily related to anti-inflammatory cytokines, suggesting that 22q11.2DS MGLs could exhibit reduced cytokine secretion, with some affected pathways such as IL-4 being associated with metabolic state change. **Chapter 5**, assessing functional properties based on data in **Chapter 3** and **Chapter 4**, showed that 22q11.2DS MGLs have higher phagocytic activity compared to control MGLs in vehicle comparisons without elevated inferred lysosome levels using lysotracker. When assessing cytokine secretion without immune challenge, IFN γ and IL-6 secretion were reduced in 22q11.2DS MGLs compared to control MGLs (**Section, 5.3.3, Chapter 5**). Reduced IFN γ secretion would potentially have implications on neuronal connectivity (McDonough et al., 2017; Warre-Cornish et al., 2020). With IL-6 also reduced, speculatively, an abnormal spike in secretion might be necessary to address potential infections. As there is no increase of inferred lysosome levels by lysotracker in 22q11.2DS MGLs and uptake of cargo by phagocytosis or macropinocytosis is increased compared to control MGLs (**Section 5.3.1, Chapter 5**), speculatively 22q11.2DS MGLs might not be able to accommodate additional workloads, suggesting that 22q11.2DS could impact microglial adaptive immunity.

6.1.3 Distinct phenotype in 22q11.2DS MGLs following LPS challenge

Differences in 22q11.2DS MGLs compared to control MGLs were also observed in response to LPS (**Chapter 3, Chapter 4, Chapter 5**). Initially, it was found that 22q11.2DS do not shift morphological state compared to control MGLs following LPS challenge, at least by the 3-hour mark, with control MGLs reducing their polarity (**Section 3.3.6, Chapter 3**). A reduced change was also observed in TMEM119:IBA1 colocalisation, also supporting that reduced ability to shift state at the proteomic within 3 hours (**Section 3.3.7, Chapter 3**). At the transcriptomic level, as control MGLs, 22q11.2DS MGLs exhibit a broad response to LPS. There is however uniqueness to the 22q11.2DS MGL response, including a higher

number of DEGs and the unique DEGs in 22q11.2DS MGLs being associated with immune response pathways not detected in uniquely DEGs in control MGLs, such as I-kappaB kinase/NF-kappaB signaling (**Section 4.3.10, Chapter 4**). Unique control DEGs had no pathway association (**Section 4.3.10, Chapter 4**), suggesting reliance on different pathways during response to LPS. Differences in associated pathways extended to cytokine production, which was supported by observations using a functional cytokine secretion assay (**Section 4.3.10, Chapter 4; Section 5.3.3, Chapter 5**). An enhanced response was observed in the fold change of IL-6, which was originally lower in vehicle comparisons, in 22q11.2DS MGLs compared to control MGLs, while enhanced secretion response by control MGLs compared to 22q11.2DS MGLs was observed in TNF α and IL-10 (**Section 5.3.3, Chapter 5**). The overall 22q11.2DS MGL transcriptomic LPS response was also uniquely linked to a oxidative phosphorylation gene set (**Section 5.3.6, Chapter 4**), suggesting that 22q11.2DS MGLs, do not shift metabolic state towards a heavier reliance on glycolysis, which is thought to occur during microglia immune challenge, while unstimulated microglia are thought to rely more on oxidative phosphorylation although this data is primarily based on murine immortalised BV2 data (Voloboueva et al., 2013; Gimeno-Bayón et al., 2014; Ghosh et al., 2018; Lauro and Limatola, 2020). Metabolic state of microglia is hence an avenue for future work as it was not directly assessed in this project. Although not directly related to assessing metabolic state, an important finding in this project is significantly lower fold change in lysotracker staining in 22q11.2DS MGLs compared to control MGLs was observed following LPS challenge (**Section 5.3.2, Chapter 5**). This is relevant, as while lysosome levels are inferred by lysotracker in study, the lysosome has been implicated in the maintenance of glycolysis, with lysosome inhibition for example causing reduced glycolytic gene expression (Syu et al., 2017; Ramachandran et al., 2019; Wang et al., 2019; Gu et al., 2021). This data is primarily based on animal models and not tested in microglia, so should not be assumed to

translate without further testing, however, inhibited glycogen metabolism has been observed in a *Atg7* knockout mouse model that has also been used to model ASC and demonstrated deficiencies in autophagy (Tang et al., 2014; Kern et al., 2016; Kim et al., 2017).

Additionally, this lack of lysotracker level change also indicates an explanation for why 22q11.2DS MGLs are unable to take up more cargo during LPS treatment compared to control MGLs potentially due to a ceiling effect of time-dependent effect (**Section 5.3.1** and **Section 5.3.2, Chapter 5**), as they might be unable to degrade cargo already taken up.

This is also in line with the interaction effect on *CHN1* and *CXCL10* found in transcriptomic profiling of the LPS response, suggesting that gene expression of these genes in response to LPS increased more in 22q11.2DS MGLs compared to control MGLs (**Section 3.3.11, Chapter 4**). *CXCL10* which can drive immune response phenotype without associated elevated phagocytic uptake based on mouse data (Cheeran et al., 2003), suggesting that it could be a key driver in the unique 22q11.2DS MGL LPS response which might also rely more heavily on NF- κ B signalling compared to control MGLs (**Section 5.3.10, Chapter 5**). A *CXCL10*-driven immune response could in a homeostatic environment be inhibited by IL-10 based on microglia data from a human primary fetal tissue model (Clarner et al., 2015), but fold change of IL-10 secretion is significantly higher in control MGLs compared to 22q11.2DS MGLs, which suggests that this pathway is not appropriately regulated in 22q11.2DS MGLs, although it should be noted that high variability was seen in the IL-10 data between lines (**Section 5.3.3, Chapter 5**). The interaction effect observed in *CHN1* on the other hand supports the idea that 22q11.2DS MGLs could be able to switch morphological state to become more ramified based on transcriptomic microarray data from a rat model, which showed that this gene is more highly expressed in ramified microglia (Parakalan et al., 2012). However, as morphological state change was not observed in

22q11.2DS MGLs in response to LPS at 3 hours (**Section 3.3.6, Chapter 3**), it could imply 22q11.2DS MGLs take longer to respond or is trying to respond to but is unable to due to other factors which are not clear. Together, these data highlight mechanisms in microglia that could contribute to increased risk of schizophrenia and ASC. With further characterisation and potentially more mature MGLs, these mechanisms could also be useful to assess microglia contribution in neurodegenerative disorders based on 22q11.2DS-associated risk and PRS (**Section 3.3.2, Chapter 3**) for Parkinson's disease, and based on PRS **Section 3.3.2, Chapter 3**) in 287_SZM_01 and suspected SNP in 069_CTF_01 (**Section 2.1, Chapter 2**), for Alzheimer's disease. Studies investigating the repeated response to immune challenge and different treatment lengths are warranted to assess whether 22q11.2DS MGLs can return to their unique homeostatic state re-regulate after stimuli in a similar manner to control MGLs. Additionally, it would assess whether environmental challenges impacting microglia is a driver behind future pathology later in the life of individuals with 22q11.2DS.

6.2 Implications

Experiments performed in this study demonstrated the potential of using hiPSC-derived MGLs for studies requiring investigation of an immune response. The results also highlight the importance of utilising functional assays to complement RNA sequencing data sets. Whether 22q11.2DS MGLs can reliably be used to study microglia contribution to psychiatric disorders such as schizophrenia and ASC with a putative neurodevelopmental, but also neurodegenerative disorders like Parkinson's disease, is unclear. Experiments driven by converging lines of evidence for the implication of microglia across these conditions in this project did however yield significant findings, highlighting mechanisms which could contribute to elevated risk. 22q11.2DS MGL phenotypes observed in this study could

importantly alongside previous 22q11.2DS-associated findings in hiPSC-derived neuronal cells be further investigated on a larger scale with idiopathic donors, or by controlling for 22q11.2DS donor clinical status, as it does appear clear that mechanisms associated with 22q11.2DS is not limited to single cell type.

6.2.1 Studying microglia and their immune response *in vitro* using hiPSCs

The ability of hiPSC-derived MGLs to shift from homeostatic states towards defense response states is evident when utilising the TLR4 agonist LPS. 22q11.2DS did also not impact the ability of MGLs to perform broad transcriptomic LPS response but showed that differences in the MGL transcriptome impacts and promotes changes in functional immune response, also showcasing that these MGLs can be used to model pathologies where there are suspected differences. This supports findings in other studies which have investigated the effect of gene variants on hiPSC-derived MGLs (Garcia-Reitboeck et al., 2018; Solomon et al., 2022). In this model it also is shown that dependent on genetic background, MGLs can respond differently to immune challenge such as by LPS. This allows for unique opportunities in modelling of severe systemic CNS infection or other developmental insults at the fetal stage, which in the context of psychiatric disorders being related to MIA. While this thesis has primarily focused on conditions associated with neurodevelopment, there are also opportunities to use this model in age-related neurodegenerative diseases. Potential hypersensitivity could for example be hypothesised based on a study on peripheral monocytes treated with LPS in Parkinson's Disease (Grozdanov et al., 2014), which as noted 22q11.2DS is a genetic risk factor for. As demonstrated by Haenseler et al. (2017), this differentiation protocol has also been shown to work with genetically modified lines, specifically the integration of a lentivector containing the RFP allowing easy tracking of MGLs in multi-cell cultures, although it is necessary to investigate whether this will work in a disease context. In

more complex model system starting with co-cultures, choice of neuronal subtypes will also be critical, with for example dopaminergic neuronal subtypes being relevant for schizophrenia and Parkinson's disease (Okarmus et al., 2021; Reid et al., 2022). Lastly, the value of utilising a microglia model system with a well characterised authentic ontogeny should be reemphasised (van Wilgenburg et al., 2013; Buchrieser et al., 2017; Haenseler et al., 2017), as alternative human *in vitro* model systems which have attempted to utilise induced microglia from blood monocytes to model schizophrenia lack this (Sellgren et al., 2017, 2019; Ormel et al., 2020). Microglia originate from *MYB*-independent yolk sac derived fetal macrophages, while adult blood monocytes, which in these protocols are induced from, are derived from *MYB*-dependent hematopoietic stem cells in the bone marrow (**Section 1.1.2, Chapter 1**; van Wilgenburg et al., 2013; Hoeffel and Ginhoux, 2015; Buchrieser et al., 2017; Haenseler et al., 2017). As such, hiPSC-derived MGLs are a suitable model system to study pathogenesis, and while induced microglia from blood monocytes could be argued to be suitable post-diagnosis, it still lacks authentic microglial ontogeny.

6.2.2 Understating the contribution of microglia to 22q11.2DS-associated conditions

This is the first characterisation of microglia using an hiPSC model investigating the potential mechanisms associated with ASC and schizophrenia. The effect of highly penetrant risk factor 22q11.2DS on MGLs has both aligns and contrasts with key mechanisms observed in other human *in vitro* model systems, including *postmortem* tissue and induced microglia from blood monocytes. In the context of induced microglia from blood monocytes donated by individuals with idiopathic schizophrenia, this thesis shows that 22q11.2DS MGLs replicates findings by Sellgren and colleagues (2017, 2019), showing that alike the induced microglia, 22q11.2DS MGLs demonstrate increased phagocytosis of synaptic material (**Section 5.3.1, Chapter 5**), although notably this thesis used ^{td}Tomato tagged mouse brain synaptosomes,

Sellgren and colleagues used synaptosomes prepared from hiPSC-neural progenitor cell cultures and adult human *postmortem* brain tissue. This thesis did not, like Sellgren et al. (2019), investigate whether this occurred in complement-dependent manner. These studies did not however look at other microglial functions (Sellgren et al., 2017, 2019). Ormel and colleagues (2020), using the same model, did not assess phagocytosis in idiopathic schizophrenia lines, but as in this thesis saw increased phagocytosis in LPS-treated controls. Also like with 22q11.2DS MGLs this thesis, induced microglia from schizophrenia lines did not appear to cluster away from control lines in PCA. A transcriptomic response to LPS was also shown in control lines like in this thesis by DEGs and gene ontology analysis, but this was not assessed in idiopathic schizophrenia samples. Induced microglia from idiopathic schizophrenia donors were however tested for IL-6 and TNF α cytokine secretion and compared to controls with and without LPS, although it is notable that treatment times were different so findings could be dependent on this (6 hours versus 24 hours in this thesis). No differences were noted at basal state in Ormel et al. (2020), yet completely contrasting findings in this thesis, an enhanced response was observed in TNF α secretion, whereas in this thesis control MGLs had a higher fold change in TNF α compared to 22q11.2DS MGLs, and IL-6 secretion was enhanced in 22q11.2DS MGLs compared to control MGLs. The induced microglia system has importantly currently not been applied in the context of ASC. While there are no hiPSC-derived microglia studies looking at ASC and schizophrenia, there are some notable findings in the context of Parkinson's disease that could be of relevance. Matching findings in this thesis, hiPSC lines donated by individuals with idiopathic Parkinson's disease differentiated into microglia exhibit increased phagocytic activity (Badanjak et al., 2021). Additionally, hiPSC-derived microglia with a Parkinson's disease-associated *LRRK2* mutation found aberrant lysosome-related response, or specifically lack of response, to LPS based on colocalisation of transferrin and LAMP2, which would be a

potential next step in assessing the relevance of lack of inferred lysosome level change by lysotracker which was observed in 22q11.2DS MGLs during this project.

When considering relevant human *postmortem* tissue findings, there are notable findings in the context of morphological state, protein marker expression, and transcriptomic state, but functional data is not available in this model. In the context of morphological state and protein marker expression, less ramification and higher circularity observed in 22q11.2DS MGLs compared to control MGLs aligned with the majority of *postmortem* in the context of ASC, schizophrenia, but also notably neurodegenerative diseases Parkinson's disease and Alzheimer's disease (Morgan et al., 2010; Doorn et al., 2014; Lee et al., 2017; Uranova et al., 2018; Fetit et al., 2021; Franco-Bocanegra et al., 2021; Gober et al., 2021). Contrasting findings have been identified by De Picker et al. (2021), which found that microglia in the prefrontal cortex of individuals with schizophrenia were more spherical, although this could be attributed to differences in analysis methods or condition onset as per Uranova et al. (2018). Although a different analysis approach was used due to noted differences in percentage positive cells in MGL cultures, a difference in 22q11.2DS MGL TMEM119:IBA1 colocalisation compared to control MGLs was also observed following analysis inspired by Sneeboer et al. (2019) which found a reduction in TMEM119 positive microglia also positive for IBA1. From a transcriptomic state standpoint, MGENrichment analysis found notable overlap with large *postmortem* study by Gandal and colleagues (2018), which profiled whole brain samples, but it does infer that DEGs in 22q11.2DS MGL might be enriched in ASC, schizophrenia, and bipolar disorder tissue based on overlap with this identified module. In vehicle comparisons (Signature A), this specifically was for down-regulated DEGs, but up-regulated DEGs also had overlap with an ASC gene expression module, and a schizophrenia and ASC gene expression module. However, it is notable that down-regulated DEGs also had

overlap with a dataset of up-regulated DEGs in ASC as well another dataset of up-regulate DEGs in Alzheimer's disease from Millet et al. (2013), but the relevance of this is unclear. Other relevant findings were associated to the Gandal et al. (2018) study, finding that overlap in Signature C (LPS-treated 22q11.2DS MGLs) up-regulated DEGs was observed with the aforementioned schizophrenia, ASC and bipolar disorder module and with the DEGs increased in ASC compared to control samples dataset from the same study. This was also the case in Signature B (LPS-treated control MGLs), with the relevance is again being unclear.

As seen above, most findings in this study are novel findings in human models even when reviewing literature across 22q11.2DS-associated conditions. Based on the findings in this thesis and problems with microglia nomenclature, the observed unique microglia phenotype is difficult to define. Considering this, and data from LPS treatments, it is clear several mechanisms identified, which were summarised and discussed **Section 6.1, Chapter 6**, could be further investigated to continue trying to understand to what extent microglia contribute to 22q11.2DS-associated conditions. While associated phenotypes are exhibited based on comparisons in this section, there is no clear indication whether these observations are linked to these disorders at the current experiment scale. Differences in clinical status, including one donor with schizophrenia and ASC, one donor with ASC, and one asymptomatic donor, while also considering variability in polygenic risk, also contribute to lack of clarity in understanding in what the drivers, or end result, of observed phenotypes are. Hence, based on findings in this project, it remains unclear whether 22q11.2DS MGLs are a model which can be reliably used to understand the contribution of microglia to 22q11.2DS-associated conditions.

6.3 Limitations and future work

Limitations within these sections considers methods used by more than one results chapter and future work recommendations are based on all work completed. Limitations of experimental designs that were uniquely relevant to specific chapters were discussed within associated chapters.

6.3.1 The hiPSC model and hiPSC-derived MGLs

Spontaneous differentiation is hallmark of hiPSC cell cultures which could potential affect differentiated phenotypes, however, in this thesis akin to the original protocol a highly pure population of MGLs are generated (Haenseler et al., 2017; Yamamoto et al., 2022). One must also consider the difficulty of replication across laboratories as there are many protocols that are used to generate hiPSC-derived microglia (**Section 1.3.2, Chapter 1**), making it unclear whether the phenotype showed in this thesis can be replicated by other protocols. Supporting this, a study on hiPSC-derived neurons, Volpato et al. (2018) demonstrated that even when five different laboratories use the same cell lines with the same protocol, and underwent the same training to generate a neuronal phenotype, scatters appear in RNA sequencing and proteomics analyses while astrocyte:neuron ratios also differed. While it is possible microglia are less heterogeneous than neurons, they remain a highly diverse cell type (**Section 1.1.5, Chapter 1**). Considering all of this, it is no surprise biological replication and statistical power is an issue in hiPSC research when most laboratories are only able to perform smaller scale studies. Variability was even seen during this study, with minimum and maximum values of defined biological replicates being variable in multiple experiments. While a 22q11.2DS donor number of three was investigated, this not necessarily enough statistical power to demonstrate anything beyond a trend. To this point, in order to obtain 80% genome

wide power, approximately 28,500 individuals are required as estimated by a schizophrenia GWAS study (Fromer et al., 2016), but this importantly did not account for individuals with high penetrance CNVs such as those seen in 22q11.2DS. In situations like this study whereby obtaining additional donors are unfeasible, clones of cell lines could be used to strengthen the definition of biological replicate and perhaps reduce variation. To additionally support mitigation of variance in this project, hiPSC were differentiated into factories at similar passage numbers (Volpato et al., 2018; Volpato and Webber, 2020), while additionally matching factory harvest number for experiments across cell lines although the impact of not matching it was not quantified.

While key microglia-related functions were assessed in this study confirming their phenotype, some limitations should be acknowledged regarding the use of hiPSC-derived microglia. While combating the problem of species-associated heterogeneity in this thesis, microglia remain highly heterogenous in terms of sex and regional specificity (Hanamsagar et al., 2017; Nelson et al., 2017; Thion et al., 2018; Masuda et al., 2019; Ewald et al., 2020). In the context of sex differences, these published data indicate potential differences in microglial development rate, phagocytic capacity, inflammatory control genes, soma size, MHCI, MHCII and P2RY12 expression (Loram et al., 2012; Nelson et al., 2017; Thion et al., 2018; Ewald et al., 2020; Patel et al., 2022). Increased MHCI, which is seen in males, might for example affected synaptic pruning functions (Schafer et al., 2012), while a higher amount immune response control genes, which is seen in females, might for example speculatively contribute to the sex-specific susceptibility to ASC and schizophrenia (Aleman et al., 2003; Werling and Geschwind, 2013; Giordano et al., 2021). While this has not been previously studied in hiPSC-derived microglia models, this study lacks enough female control cell lines to quantify such difference in terms of control lines, even without considering the lack of

sufficient 22q11.2DS cell lines, with both a higher number of male and female 22q11.2DS donor lines being necessary to assess the impact in the genetic risk context. There is also currently no way to control for regional heterogeneity in monoculture, although use of other growth factors and cytokines during differentiation could potentially drive the MGLs towards a different phenotype. Expanding cultures with regionally specific neurons is perhaps the most viable solution to support studies on neuron-microglia interaction. The impact of this is significant as the heterogeneity even extends to white and grey matter in schizophrenia (Gober et al., 2021), potentially reducing the viability of morphology assays. Gober and colleagues (2022) found that soma size of microglia being found to be higher in SCZ grey matter, but not white matter, compared to controls, even though arborisation was lower in schizophrenia compared to controls in both sections which match findings in this study.

6.3.2 Studying CNVs and 22q11.2DS

While observations can be linked to 22q11.2DS-associated deletions as all 22q11.2DS contain a linked CNV, it is unclear if any specific parts of these CNVs are drivers of the observed phenotypes in this study. There are also qualitative trends suggesting that clinical profile, for example when donor has neither schizophrenia nor ASC, could be a predictor of how closely cell lines align with symptomatic vs control lines such as in synaptosome data on the 22q11.2DS line 191_SZF_09, which aligned more with control lines (**Section 5.3.1, Chapter 5**). As the number asymptomatic 22q11.2DS lines were not equal to the number of symptomatic lines, this is not controlled for in this thesis. The potential implications are clear based on findings by Li et al. (2019), which found a different phenotype in asymptomatic donors with 22q11.2DS versus donors with 22q11.2DS and with schizophrenia using hiPSC-derived neurons, finding that mitochondrial deficits observed in cell lines from donors with 22q11.2DS and schizophrenia was not present in donors with 22q11.2DS but without

schizophrenia. Furthermore, it is unknown whether findings can clinically translate to schizophrenia, as only one 22q11.2DS donor has this diagnosis. Atypical microglial states is not a phenotype that is limited to psychiatric disorders, and it has multiple times been noted that 22q11.2DS is associated with increased risk for Parkinson's Disease, with 509_CXF_13 having high relative polygenic compared to other lines towards Parkinson's disease, and that there might be elevated risk for Alzheimer's disease in two cell lines (Control line 069_CTF_01 and 22q11.2DS line 287_SZM_01), even if this model is assumed to look at the fetal stage of development. It should however be considered that early microglia phenotypes may exist in Parkinson's Disease. A theory in the Parkinson's disease space revolves around pathogenesis being a result of aberrant re-activation of developmental pathways (Schwamborn, 2018). Abnormalities present during development might infer susceptibility to this re-activation later in life. This stage of development in Parkinson's disease is not well understood, but as such the potential contribution of microglia to this susceptibility should be considered even though the emphasis of this project is on schizophrenia and ASC.

Study of a highly penetrant CNV in this study proved problematic due to the presence of additional CNVs including unexpected duplications two out of the three 22q11.2DS cell lines. Data is hence limited in terms of linking genetic factors to diagnosis as well as understanding to what degree each CNV contributes to MGL phenotypes. Together with PRS data, this thesis hence underlines key problems in studying CNVs using hiPSCs regardless of its potential promise (Kirov et al., 2014; Drakulic et al., 2020), highlighting the importance of acquiring as much genetic and clinical information as possible, and that use of highly penetrant genetic variants is not straightforward (Hoekstra et al., 2017). There are several ways study designs could be changed to mitigate these limitations. Following initiation of this project, the study of altering gene variants using CRISPR/Cas9 has evolved and alteration of

larger CNVs are now possible (Grajcarek et al., 2019; Kotini and Papapetrou, 2020).

Possibilities expand to correction of specific CNVs within 22q11.2DS cell lines, which would help reveal the true effect of these CNVs by examining single homogenous lesions, be that of either deletions or duplications. Ideally, cell lines chosen would be confirmed to only have one larger CNV at this location following genotyping, but in this project only 287_SZM_01 fits this description. Furthermore, 287_SZM_01 has a diagnosis of both schizophrenia and ASC, making it more difficult to unravel what genes are key drivers in the pathogenesis of each disorder. 509_CXF_13 is a potential candidate for the study of ASC using this approach, but it is also unclear whether deletions or duplications are driving the pathology in this cell line, and extensive editing and testing would be required. Alternatively, rather than using the isogenic cell line approach, scale of experiments could be increased. To design an ideal study on 22q11.2DS using hiPSCs without isogenic cell lines, several points would have to be controlled. First, donors should only present with a single diagnosis. Second, asymptomatic donors should be used as additional controls. Third, sex of donors should be equally matched to controls and diagnosed donors. Fourth, both sexes should be investigated simultaneously. Lastly, a minimum of three cell lines per condition should be used, hence requiring a total of 18 donor cell lines ignoring the ideal scenario where several clones are also used per donor in according with a Stem Cell Reports consensus statement (<https://www.cell.com/stem-cell-reports/authors>). This is also without consideration of the feasibility of acquiring such cell lines and need to have at least closely resembling CNVs. This design is completely unfeasible for even high-performing academic laboratories considering the cost of hiPSC maintenance and required experiments, and hence the using of gene editing approaches to create isogenic cell lines following full donor characterisation is recommended for the majority of laboratories.

6.3.3 General future considerations for examining whether microglia play a role in schizophrenia and ASC by using 22q11.2DS MGLs

In monoculture experiments, future studies on the LPS response or with or agents such be considered due to differences observed in 22q11.2DS MGL response compared to that of control MGLs. Studies could investigate this using multiple methods, including examining 22q11.2DS MGL self-regulation back to their unique homeostatic state, by using single exposure, repeated exposure, as well as long-term chronic exposure. Together, these experiments, repeating a similar style as performed in this project with additional timepoints, secreted chemokines, but adding experiments such as mitochondrial activity assays, could potentially elucidate further differences in the 22q11.2DS MGL LPS response compared to control MGLs. Exploratory proteomic studies would be beneficial and could for example serve to assess whether there are differences in expression of select mitochondrial and lysosomal proteins. This would serve future studies that might look at metabolic state and autophagy based on findings in this study and evidence of mitochondrial deficits in hiPSC-derived neurons (Li et al., 2019, 2021). Differences in epigenetic modification following LPS challenge would be an interesting experiment using for example ATAC and ChIP sequencing to assess whether “infection by LPS” induces a lasting epigenetic profile. Background justifying these analyses exists, as epigenetics regulate the innate immune memory of microglia, but remains not investigated in this cell type even though it has been implicated in both schizophrenia and ASC (Mendizabal et al., 2019; Ciernia et al., 2020; Zhang et al., 2022). The hiPSC model is a very useful model of such change early in development due to wiping of the epigenome during reprogramming, with potential residuals also being attenuated during passaging (Gao et al., 2017; de Boni et al., 2018; Poetsch et al., 2022; Polit et al., 2023). Ideally, effect of molecules such as IL-6, implicated in MIA (S. E. P. Smith et al., 2007; Couch et al., 2023), would also be assessed, with single-cell approaches

being an opportunity to estimate heterogeneity of microglia populations and to thoroughly characterise multi-cell cultures.

Regardless of the potential problems with multi-cell culture systems making it difficult to study microglia-specific effects, they are a critical step forward for future work. This is because, for example, co-culture with hiPSC-derived cortical neurons does affect microglia phenotype by regulating them into a more ramified state with attenuated secretion (Haenseler et al., 2017), and it would be important to understand whether this is also true for 22q11.2DS MGLs. Even the type of neuron is relevant, as media levels of SerpinE1 could be up-or down-regulated depending on co-culture with cortical neuron progenitors or spinal motor neurons, respectively (Haenseler et al., 2017; Vahsen et al., 2022). This is relevant for modelling psychiatric disorders, as it has been implicated in maturation of hiPSC-derived interneurons (Genestine et al., 2021), as well as associated to susceptibility to major depression and schizophrenia (Campbell et al., 2008; Tsai et al., 2008; Levitt and Campbell, 2009; Jeffries et al., 2018). Using a well characterised regionally appropriate neuronal phenotype would also help control for microglial regional heterogeneity. Organoid models would add an additional layer to this complexity, increasing possibilities of microglial interactions while remaining in a easily manipulated tissue culture environment (Lancaster et al., 2013; Lancaster and Knoblich, 2014; Ormel et al., 2018; Sabate-Soler et al., 2022; Zhang et al., 2023). More translational modelling could also potentially be extended to humanised animal systems. A chimeric model, where transplantation of developing hematopoietic stem cells results in microglia can acquire an expression profile closely resembling human *ex vivo* microglia, provide an excellent opportunity to study the effect of microglia with behavioural implication (Hasselmann et al., 2019; Mancuso et al., 2019; Svoboda et al., 2019; Hasselmann and Blurton-Jones, 2020). While these models may be limited as they have not

formally demonstrated authentic ontogeny, it remains possible that their ontogeny is authentic. This is also true for any mono- or co-culture system where *MYB*-independence has not been characterised. In the case of the chimeric system, any doubt could potentially be mitigated if a system where transplantation with *MYB*-independent yolk sac derived fetal macrophages are characterised to successfully integrate. Additionally, as shown by Hasselman et al. (2019), xenotransplanted microglia can respond to peripheral LPS challenge in the chimeric mouse. This not only allows for the study of early microglia stress during development but also in ageing. The chimeric animal model provides an opportunity to, for example, study the contribution of 22q11.2DS MGLs to Parkinsonism, which could be possible using transplanted 22q11.2DS cells and comparing different stages of the chimeric animal lifespan.

6.4 Concluding remarks

Data from this thesis demonstrated an impact of 22q11.2DS on microglia form and function. Due to heterogeneity of donor clinical status, CNV sizes and locations, and PRS, no clear link can be made to any 22q11.2DS-associated conditions. However, characterisation of 22q11.2DS MGLs compared to neurotypical controls contributed towards identifying phenotypes that could in the future be further examined while addressing limitations of this project. At this scale of research, alternative approaches include investing in generating an isogenic cell from a 22q11.2DS donor with a single CNV alongside a singular diagnosis. While the use of CNVs has potential, the possibility to generate data at a reasonable scale is not an option for the majority of academic labs. Donor selectivity is critical, with individuals needing to present with either schizophrenia or ASC should investigation into one be preferred. Likely this would be the case, as while they have overlapping genetic risk factors, calculated PRS serves to underline differences even when some overlapping factors are present. Characterisation of PRS on a larger scale would also serve to identify cell lines with high or at least similar scores that could be preferably chosen for future work. Regardless, the findings of this thesis ultimately provide the first data on an hiPSC model of microglia which highlights the impact of 22q11.2DS on key microglial functions that could contribute the pathophysiology of 22q11.2DS-associated conditions.

Bibliography

- Abels, E. R., Nieland, L., Hickman, S., Broekman, M. L. D., El Khoury, J., & Maas, S. L. N. (2021). Comparative Analysis Identifies Similarities between the Human and Murine Microglial Sensomes. *International Journal of Molecular Sciences*, 22(3), 1495. <https://doi.org/10.3390/ijms22031495>
- Absinta, M., Maric, D., Gharagozloo, M., Garton, T., Smith, M. D., Jin, J., Fitzgerald, K. C., Song, A., Liu, P., Lin, J.-P., Wu, T., Johnson, K. R., McGavern, D. B., Schafer, D. P., & Reich, D. S. (2021). A lymphocyte-microglia-astrocyte axis in chronic active multiple sclerosis. *Nature*, 597(7878), 709–714.
- Abud, E. M., Ramirez, R. N., Martinez, E. S., Healy, L. M., Nguyen, C. H. H., Newman, S. A., Yeromin, A. V., Scarfone, V. M., Marsh, S. E., Fimbres, C., Caraway, C. A., Fote, G. M., Madany, A. M., Agrawal, A., Kayed, R., Gyls, K. H., Cahalan, M. D., Cummings, B. J., Antel, J. P., ... Blurton-Jones, M. (2017). iPSC-Derived Human Microglia-like Cells to Study Neurological Diseases. *Neuron*, 94(2), 278-293.e9.
- Adami, C., Sorci, G., Blasi, E., Agnietti, A. L., Bistoni, F., & Donato, R. (2001). S100B expression in and effects on microglia. *Glia*, 33(2), 131–142.
- Adhya, D., Swarup, V., Nagy, R., Dutan, L., Shum, C., Valencia-Alarcón, E. P., Jozwik, K. M., Mendez, M. A., Horder, J., Loth, E., Nowosiad, P., Lee, I., Skuse, D., Flinter, F. A., Murphy, D., McAlonan, G., Geschwind, D. H., Price, J., Carroll, J., ... Baron-Cohen, S. (2021). Atypical Neurogenesis in Induced Pluripotent Stem Cells From Autistic Individuals. *Biological Psychiatry*, 89(5), 486–496.
- Adinolfi, M. (1985). The development of the human blood-CSF-brain barrier. *Developmental Medicine and Child Neurology*, 27(4), 532–537.
- Akiyama, H., & McGeer, P. L. (1990). Brain microglia constitutively express beta-2 integrins. *Journal of Neuroimmunology*, 30(1), 81–93.
- Al Soraj, M., He, L., Peynshaert, K., Cousaert, J., Vercauteren, D., Braeckmans, K., De Smedt, S. C., & Jones, A. T. (2012). SiRNA and pharmacological inhibition of endocytic pathways to characterize the differential role of macropinocytosis and the actin cytoskeleton on cellular uptake of dextran and cationic cell penetrating peptides octaarginine (R8) and HIV-Tat. *Journal of Controlled Release*, 161(1), 132–141.
- Aleman, A., Kahn, R. S., & Selten, J.-P. (2003). Sex Differences in the Risk of Schizophrenia: Evidence From Meta-analysis. *Archives of General Psychiatry*, 60(6), 565–571.
- Almeida, S., Zhang, Z., Coppola, G., Mao, W., Futai, K., Karydas, A., Geschwind, M. D., Tartaglia, M. C., Gao, F., Gianni, D., Sena-Esteves, M., Geschwind, D. H., Miller, B. L., Farese, R. V., & Gao, F.-B. (2012). Induced pluripotent stem cell models of progranulin-deficient frontotemporal dementia uncover specific reversible neuronal defects. *Cell Reports*, 2(4), 789–798.
- Alver, M., Mancini, V., Läll, K., Schneider, M., Romano, L., Mägi, R., Dermitzakis, E. T., Eliez, S., & Reymond, A. (2022). Contribution of schizophrenia polygenic burden to longitudinal phenotypic variance in 22q11.2 deletion syndrome. *Molecular Psychiatry*, 27(10), Article 10.
- American Psychiatric Association (APA). (2013). *Diagnostic and Statistical Manual of Mental Disorders* (5th edition (DSM-5)). American Psychiatric Publishing.
- Amo-Aparicio, J., Garcia-Garcia, J., Francos-Quijorna, I., Urpi, A., Esteve-Codina, A., Gut, M., Quintana, A., & Lopez-Vales, R. (2021). Interleukin-4 and interleukin-13 induce different metabolic profiles in microglia and macrophages that relate with divergent outcomes after spinal cord injury. *Theranostics*, 11(20), 9805–9820.

- Andersen, M. S., Bandres-Ciga, S., Reynolds, R. H., Hardy, J., Ryten, M., Krohn, L., Gan-Or, Z., Holtman, I. R., Pihlstrøm, L., & the International Parkinson's Disease Genomics Consortium. (2021). Heritability Enrichment Implicates Microglia in Parkinson's Disease Pathogenesis. *Annals of Neurology*, 89(5), 942–951.
- Andoh, M., & Koyama, R. (2021). Microglia regulate synaptic development and plasticity. *Developmental Neurobiology*, 81(5), 568–590.
- Angkustsiri, K., Goodlin-Jones, B., Deprey, L., Brahmabhatt, K., Harris, S., & Simon, T. J. (2014). Social Impairments in Chromosome 22q11.2 Deletion Syndrome (22q11.2DS): Autism Spectrum Disorder or a Different Endophenotype? *Journal of Autism and Developmental Disorders*, 44(4), 739–746.
- Antaki, D., Guevara, J., Maihofer, A. X., Klein, M., Gujral, M., Grove, J., Carey, C. E., Hong, O., Arranz, M. J., Hervas, A., Corsello, C., Vaux, K. K., Muotri, A. R., Iakoucheva, L. M., Courchesne, E., Pierce, K., Gleeson, J. G., Robinson, E. B., Nievergelt, C. M., & Sebat, J. (2022). A phenotypic spectrum of autism is attributable to the combined effects of rare variants, polygenic risk and sex. *Nature Genetics*, 54(9), Article 9.
- Aresvik, D. M., Lima, K., Øverland, T., Mollnes, T. E., & Abrahamsen, T. G. (2016). Increased Levels of Interferon-Inducible Protein 10 (IP-10) in 22q11.2 Deletion Syndrome. *Scandinavian Journal of Immunology*, 83(3), 188–194.
- Arioka, Y., Shishido, E., Kushima, I., Suzuki, T., Saito, R., Aiba, A., Mori, D., & Ozaki, N. (2021). Chromosome 22q11.2 deletion causes PERK-dependent vulnerability in dopaminergic neurons. *EBioMedicine*, 63.
- Arnoux, I., & Audinat, E. (2015). Fractalkine Signaling and Microglia Functions in the Developing Brain. *Neural Plasticity*, 2015, 689404.
- Askew, K., Li, K., Olmos-Alonso, A., Garcia-Moreno, F., Liang, Y., Richardson, P., Tipton, T., Chapman, M. A., Riecken, K., Beccari, S., Sierra, A., Molnár, Z., Cragg, M. S., Garaschuk, O., Perry, V. H., & Gomez-Nicola, D. (2017). Coupled Proliferation and Apoptosis Maintain the Rapid Turnover of Microglia in the Adult Brain. *Cell Reports*, 18(2), 391–405.
- Atladóttir, H. O., Thorsen, P., Østergaard, L., Schendel, D. E., Lemcke, S., Abdallah, M., & Parner, E. T. (2010). Maternal infection requiring hospitalization during pregnancy and autism spectrum disorders. *Journal of Autism and Developmental Disorders*, 40(12), 1423–1430.
- Bachstetter, A. D., Van Eldik, L. J., Schmitt, F. A., Neltner, J. H., Ighodaro, E. T., Webster, S. J., Patel, E., Abner, E. L., Kryscio, R. J., & Nelson, P. T. (2015). Disease-related microglia heterogeneity in the hippocampus of Alzheimer's disease, dementia with Lewy bodies, and hippocampal sclerosis of aging. *Acta Neuropathologica Communications*, 3, 32.
- Badanjak, K., Mulica, P., Smajic, S., Delcambre, S., Tranchevent, L.-C., Diederich, N., Rauen, T., Schwamborn, J. C., Glaab, E., Cowley, S. A., Antony, P. M. A., Pereira, S. L., Venegas, C., & Grünewald, A. (2021). iPSC-Derived Microglia as a Model to Study Inflammation in Idiopathic Parkinson's Disease. *Frontiers in Cell and Developmental Biology*, 9.
- Baig, M. S., Zaichick, S. V., Mao, M., de Abreu, A. L., Bakhshi, F. R., Hart, P. C., Saqib, U., Deng, J., Chatterjee, S., Block, M. L., Vogel, S. M., Malik, A. B., Consolaro, M. E. L., Christman, J. W., Minshall, R. D., Gantner, B. N., & Bonini, M. G. (2015). NOS1-derived nitric oxide promotes NF-κB transcriptional activity through inhibition of suppressor of cytokine signaling-1. *The Journal of Experimental Medicine*, 212(10), 1725–1738.
- Ballabio, A., & Bonifacino, J. S. (2020). Lysosomes as dynamic regulators of cell and organismal homeostasis. *Nature Reviews. Molecular Cell Biology*, 21(2), 101–118.

- Banerjee, P., Paza, E., Perkins, E. M., James, O. G., Kenkhuis, B., Lloyd, A. F., Burr, K., Story, D., Yusuf, D., He, X., Backofen, R., Dando, O., Chandran, S., & Priller, J. (2020). Generation of pure monocultures of human microglia-like cells from induced pluripotent stem cells. *Stem Cell Research*, 49, 102046.
- Basilico, B., Ferrucci, L., Ratano, P., Golia, M. T., Grimaldi, A., Rosito, M., Ferretti, V., Reverte, I., Sanchini, C., Marrone, M. C., Giubettini, M., De Turre, V., Salerno, D., Garofalo, S., St-Pierre, M.-K., Carrier, M., Renzi, M., Pagani, F., Modi, B., ... Ragozzino, D. (2022). Microglia control glutamatergic synapses in the adult mouse hippocampus. *Glia*, 70(1), 173–195.
- Bassett, A. S., & Chow, E. W. C. (2008). Schizophrenia and 22q11.2 deletion syndrome. *Current Psychiatry Reports*, 10(2), 148–157.
- Bassett, A. S., Costain, G., Fung, W. L. A., Russell, K. J., Pierce, L., Kapadia, R., Carter, R. F., Chow, E. W. C., & Forsythe, P. J. (2010). Clinically detectable copy number variations in a Canadian catchment population of schizophrenia. *Journal of Psychiatric Research*, 44(15), 1005–1009.
- Bassett, A. S., Lowther, C., Merico, D., Costain, G., Chow, E. W. C., van Amelsvoort, T., McDonald-McGinn, D., Gur, R. E., Swillen, A., Van den Bree, M., Murphy, K., Gothelf, D., Bearden, C. E., Eliez, S., Kates, W., Philip, N., Sashi, V., Campbell, L., Vorstman, J., ... International 22q11.2DS Brain and Behavior Consortium. (2017). Rare Genome-Wide Copy Number Variation and Expression of Schizophrenia in 22q11.2 Deletion Syndrome. *The American Journal of Psychiatry*, 174(11), 1054–1063.
- Batista, S. J., Still, K. M., Johanson, D., Thompson, J. A., O'Brien, C. A., Lukens, J. R., & Harris, T. H. (2020). Gasdermin-D-dependent IL-1 α release from microglia promotes protective immunity during chronic *Toxoplasma gondii* infection. *Nature Communications*, 11(1), Article 1.
- Bauman, M. D., Iosif, A.-M., Smith, S. E. P., Bregere, C., Amaral, D. G., & Patterson, P. H. (2014). Activation of the maternal immune system during pregnancy alters behavioral development of rhesus monkey offspring. *Biological Psychiatry*, 75(4), 332–341.
- Baumeister, D., Akhtar, R., Ciufolini, S., Pariante, C. M., & Mondelli, V. (2016). Childhood trauma and adulthood inflammation: A meta-analysis of peripheral C-reactive protein, interleukin-6 and tumour necrosis factor- α . *Molecular Psychiatry*, 21(5), Article 5.
- Beaino, W., Janssen, B., Vugts, D. J., de Vries, H. E., & Windhorst, A. D. (2021). Towards PET imaging of the dynamic phenotypes of microglia. *Clinical and Experimental Immunology*, 206(3), 282–300.
- Beers, D. R., Henkel, J. S., Xiao, Q., Zhao, W., Wang, J., Yen, A. A., Siklos, L., McKercher, S. R., & Appel, S. H. (2006). Wild-type microglia extend survival in PU.1 knockout mice with familial amyotrophic lateral sclerosis. *Proceedings of the National Academy of Sciences of the United States of America*, 103(43), 16021–16026.
- Bennett, M. L., Bennett, F. C., Liddel, S. A., Ajami, B., Zamanian, J. L., Fernhoff, N. B., Mulinyawe, S. B., Bohlen, C. J., Adil, A., Tucker, A., Weissman, I. L., Chang, E. F., Li, G., Grant, G. A., Hayden Gephart, M. G., & Barres, B. A. (2016). New tools for studying microglia in the mouse and human CNS. *Proceedings of the National Academy of Sciences of the United States of America*, 113(12), E1738–E1746.
- Ben-Reuven, L., & Reiner, O. (2016). Modeling the autistic cell: iPSCs recapitulate developmental principles of syndromic and nonsyndromic ASD. *Development, Growth & Differentiation*, 58(5), 481–491.
- Bergen, S. E., Ploner, A., Howrigan, D., CNV Analysis Group and the Schizophrenia Working Group of the Psychiatric Genomics Consortium, O'Donovan, M. C., Smoller, J. W., Sullivan, P. F., Sebat, J., Neale, B., & Kendler, K. S. (2019). Joint Contributions of Rare Copy Number Variants and Common SNPs to Risk for Schizophrenia. *The American Journal of Psychiatry*, 176(1), 29–35.

- Bergon, A., Belzeaux, R., Comte, M., Pelletier, F., Hervé, M., Gardiner, E. J., Beveridge, N. J., Liu, B., Carr, V., Scott, R. J., Kelly, B., Cairns, M. J., Kumarasinghe, N., Schall, U., Blin, O., Boucraut, J., Tooney, P. A., Fakra, E., & Ibrahim, E. C. (2015). CX3CR1 is dysregulated in blood and brain from schizophrenia patients. *Schizophrenia Research*, 168(1–2), 434–443.
- Bessis, A., Béchade, C., Bernard, D., & Roumier, A. (2007). Microglial control of neuronal death and synaptic properties. *Glia*, 55(3), 233–238.
- Bhat, A., Irizar, H., Couch, A. C. M., Raval, P., Duarte, R. R. R., Dutan Polit, L., Hanger, B., Powell, T., Deans, P. J. M., Shum, C., Nagy, R., McAlonan, G., Iyegbe, C. O., Price, J., Bramon, E., Bhattacharyya, S., Vernon, A. C., & Srivastava, D. P. (2022). Attenuated transcriptional response to pro-inflammatory cytokines in schizophrenia hiPSC-derived neural progenitor cells. *Brain, Behavior, and Immunity*, 105, 82–97.
- Bianchi, R., Giambanco, I., & Donato, R. (2010). S100B/RAGE-dependent activation of microglia via NF-kappaB and AP-1 Co-regulation of COX-2 expression by S100B, IL-1beta and TNF-alpha. *Neurobiology of Aging*, 31(4), 665–677.
- Biber, K., Neumann, H., Inoue, K., & Boddeke, H. W. G. M. (2007). Neuronal ‘On’ and ‘Off’ signals control microglia. *Trends in Neurosciences*, 30(11), 596–602.
- Birtwistle, J., & Baldwin, D. (1998). Role of dopamine in schizophrenia and Parkinson’s disease. *British Journal of Nursing (Mark Allen Publishing)*, 7(14), 832–834, 836, 838–841.
- Bloomfield, P. S., Bonsall, D., Wells, L., Dormann, D., Howes, O., & De Paola, V. (2018). The effects of haloperidol on microglial morphology and translocator protein levels: An in vivo study in rats using an automated cell evaluation pipeline. *Journal of Psychopharmacology (Oxford, England)*, 32(11), 1264–1272.
- Boche, D., & Gordon, M. N. (2022). Diversity of transcriptomic microglial phenotypes in aging and Alzheimer’s disease. *Alzheimer’s & Dementia*, 18(2), 360–376.
- Boczek, T., Mackiewicz, J., Sobolczyk, M., Wawrzyniak, J., Lisek, M., Ferenc, B., Guo, F., & Zylinska, L. (2021). The Role of G Protein-Coupled Receptors (GPCRs) and Calcium Signaling in Schizophrenia. Focus on GPCRs Activated by Neurotransmitters and Chemokines. *Cells*, 10(5), 1228.
- Bölte, S., Girdler, S., & Marschik, P. B. (2019). The contribution of environmental exposure to the etiology of autism spectrum disorder. *Cellular and Molecular Life Sciences: CMLS*, 76(7), 1275–1297.
- Boot, E., Bassett, A. S., & Marras, C. (2018). 22q11.2 Deletion Syndrome–Associated Parkinson’s Disease. *Movement Disorders Clinical Practice*, 6(1), 11–16.
- Böttcher, C., Schlickeiser, S., Sneeboer, M. A. M., Kunkel, D., Knop, A., Paza, E., Fidzinski, P., Kraus, L., Snijders, G. J. L., Kahn, R. S., Schulz, A. R., Mei, H. E., Hol, E. M., Siegmund, B., Glaubien, R., Spruth, E. J., de Witte, L. D., & Priller, J. (2019). Human microglia regional heterogeneity and phenotypes determined by multiplexed single-cell mass cytometry. *Nature Neuroscience*, 22(1), Article 1.
- Bowie, C. R., & Harvey, P. D. (2006). Cognitive deficits and functional outcome in schizophrenia. *Neuropsychiatric Disease and Treatment*, 2(4), 531–536.
- Brás, J. P., Bravo, J., Freitas, J., Barbosa, M. A., Santos, S. G., Summavielle, T., & Almeida, M. I. (2020). TNF-alpha-induced microglia activation requires miR-342: Impact on NF-kB signaling and neurotoxicity. *Cell Death & Disease*, 11(6), 415.

- Brenner, S. L., & Korn, E. D. (1979). Substoichiometric concentrations of cytochalasin D inhibit actin polymerization. Additional evidence for an F-actin treadmill. *The Journal of Biological Chemistry*, 254(20), 9982–9985.
- Brown, A. S., & Derkits, E. J. (2010). Prenatal infection and schizophrenia: A review of epidemiologic and translational studies. *The American Journal of Psychiatry*, 167(3), 261–280.
- Brown, A. S., & Meyer, U. (2018). Maternal Immune Activation and Neuropsychiatric Illness: A Translational Research Perspective. *American Journal of Psychiatry*, 175(11), 1073–1083.
- Brown, A. S., Sourander, A., Hinkka-Yli-Salomäki, S., McKeague, I. W., Sundvall, J., & Surcel, H.-M. (2014). Elevated maternal C-reactive protein and autism in a national birth cohort. *Molecular Psychiatry*, 19(2), 259–264.
- Bruey, J. M., Bruey-Sedano, N., Newman, R., Chandler, S., Stehlik, C., & Reed, J. C. (2004). PAN1/NALP2/PYPAF2, an inducible inflammatory mediator that regulates NF-kappaB and caspase-1 activation in macrophages. *The Journal of Biological Chemistry*, 279(50), 51897–51907.
- Buchrieser, J., James, W., & Moore, M. D. (2017). Human Induced Pluripotent Stem Cell-Derived Macrophages Share Ontogeny with MYB-Independent Tissue-Resident Macrophages. *Stem Cell Reports*, 8(2), 334–345.
- Buckley, P. F., Miller, B. J., Lehrer, D. S., & Castle, D. J. (2009). Psychiatric comorbidities and schizophrenia. *Schizophrenia Bulletin*, 35(2), 383–402.
- Butovsky, O., Jedrychowski, M. P., Moore, C. S., Cialic, R., Lanser, A. J., Gabriely, G., Koeglsperger, T., Dake, B., Wu, P. M., Doykan, C. E., Fanek, Z., Liu, L., Chen, Z., Rothstein, J. D., Ransohoff, R. M., Gygi, S. P., Antel, J. P., & Weiner, H. L. (2014). Identification of a unique TGF- β -dependent molecular and functional signature in microglia. *Nature Neuroscience*, 17(1), 131–143.
- Butovsky, O., & Weiner, H. L. (2018). Microglial signatures and their role in health and disease. *Nature Reviews. Neuroscience*, 19(10), 622–635.
- Bystron, I., Blakemore, C., & Rakic, P. (2008). Development of the human cerebral cortex: Boulder Committee revisited. *Nature Reviews. Neuroscience*, 9(2), 110–122.
- Caballano-Infantes, E., Díaz, I., Hitos, A. B., Cahuana G. M., Martínez-Ruiz, A., Soria-Juan, B., Rodríguez-Griñolo, R., Hmadcha, A., Martín, F., Soria, B., Tejedo, J. R., & Bedoya, F. J. (2021). Stemness of Human Pluripotent Cells: Hypoxia-Like Response Induced by Low Nitric Oxide. *Antioxidants (Basel)*, 10(9): 1408
- Cabirol, M.-J., Cardoit, L., Courtand, G., Mayeur, M.-E., Simmers, J., Pascual, O., & Thoby-Brisson, M. (2022). Microglia shape the embryonic development of mammalian respiratory networks. *ELife*, 11, e80352.
- Cakir, B., Tanaka, Y., Kiral, F. R., Xiang, Y., Dagliyan, O., Wang, J., Lee, M., Greaney, A. M., Yang, W. S., duBoulay, C., Kural, M. H., Patterson, B., Zhong, M., Kim, J., Bai, Y., Min, W., Niklason, L. E., Patra, P., & Park, I.-H. (2022). Expression of the transcription factor PU.1 induces the generation of microglia-like cells in human cortical organoids. *Nature Communications*, 13(1), Article 1.
- Campbell, D. B., Li, C., Sutcliffe, J. S., Persico, A. M., & Levitt, P. (2008). Genetic evidence implicating multiple genes in the MET receptor tyrosine kinase pathway in autism spectrum disorder. *Autism Research: Official Journal of the International Society for Autism Research*, 1(3), 159–168.
- Canetta, S., Sourander, A., Surcel, H.-M., Hinkka-Yli-Salomäki, S., Leiviskä, J., Kellendonk, C., McKeague, I. W., & Brown, A. S. (2014). Elevated maternal C-reactive protein and increased risk of schizophrenia in a national birth cohort. *The American Journal of Psychiatry*, 171(9), 960–968.

- Capurro, A., Bodea, L.-G., Schaefer, P., Luthi-Carter, R., & Perreau, V. M. (2015). Computational deconvolution of genome wide expression data from Parkinson's and Huntington's disease brain tissues using population-specific expression analysis. *Frontiers in Neuroscience*, 8, 441.
- Cardona, A. E., Pioro, E. P., Sasse, M. E., Kostenko, V., Cardona, S. M., Dijkstra, I. M., Huang, D., Kidd, G., Dombrowski, S., Dutta, R., Lee, J.-C., Cook, D. N., Jung, S., Lira, S. A., Littman, D. R., & Ransohoff, R. M. (2006). Control of microglial neurotoxicity by the fractalkine receptor. *Nature Neuroscience*, 9(7), 917–924.
- Carlström, E. L., Niazi, A., Etemadikhah, M., Halvardson, J., Enroth, S., Stockmeier, C. A., Rajkowska, G., Nilsson, B., & Feuk, L. (2021). Transcriptome Analysis of Post-Mortem Brain Tissue Reveals Up-Regulation of the Complement Cascade in a Subgroup of Schizophrenia Patients. *Genes*, 12(8), 1242.
- Chamera, K., Trojan, E., Szuster-Głuszcak, M., & Basta-Kaim, A. (2020). The Potential Role of Dysfunctions in Neuron-Microglia Communication in the Pathogenesis of Brain Disorders. *Current Neuropharmacology*, 18(5), 408–430.
- Chan, M. K., Tsang, T. M., Harris, L. W., Guest, P. C., Holmes, E., & Bahn, S. (2011). Evidence for disease and antipsychotic medication effects in post-mortem brain from schizophrenia patients. *Molecular Psychiatry*, 16(12), 1189–1202.
- Charlson, F. J., Ferrari, A. J., Santomauro, D. F., Diminic, S., Stockings, E., Scott, J. G., McGrath, J. J., & Whiteford, H. A. (2018). Global Epidemiology and Burden of Schizophrenia: Findings From the Global Burden of Disease Study 2016. *Schizophrenia Bulletin*, 44(6), 1195–1203.
- Cheeran, M. C.-J., Hu, S., Sheng, W. S., Peterson, P. K., & Lokensgard, J. R. (2003). CXCL10 Production from Cytomegalovirus-Stimulated Microglia Is Regulated by both Human and Viral Interleukin-10. *Journal of Virology*, 77(8), 4502–4515.
- Chen, C.-H., Cheng, M.-C., Huang, A., Hu, T.-M., Ping, L.-Y., & Chang, Y.-S. (2020). Detection of Rare Methyl-CpG Binding Protein 2 Gene Missense Mutations in Patients With Schizophrenia. *Frontiers in Genetics*, 11, 476.
- Chen, D., Li, J., Huang, Y., Wei, P., Miao, W., Yang, Y., & Gao, Y. (2022). Interleukin 13 promotes long-term recovery after ischemic stroke by inhibiting the activation of STAT3. *Journal of Neuroinflammation*, 19(1), 112.
- Chen, J., Lu, Y., Cue, J. M., Patel, N., Zheng, J. J., Cummings, M. J., & Do, J. (2022). Genetic Relationship between Alzheimer's Disease and Schizophrenia. *Alzheimer's & Dementia*, 18(S3), e065861.
- Chen, S.-W., Hung, Y.-S., Fuh, J.-L., Chen, N.-J., Chu, Y.-S., Chen, S.-C., Fann, M.-J., & Wong, Y.-H. (2021). Efficient conversion of human induced pluripotent stem cells into microglia by defined transcription factors. *Stem Cell Reports*, 16(5), 1363–1380.
- Chen, Z., Jalabi, W., Shpargel, K. B., Farabaugh, K. T., Dutta, R., Yin, X., Kidd, G. J., Bergmann, C. C., Stohlman, S. A., & Trapp, B. D. (2012). Lipopolysaccharide-induced microglial activation and neuroprotection against experimental brain injury is independent of hematogenous TLR4. *The Journal of Neuroscience: The Official Journal of the Society for Neuroscience*, 32(34), 11706–11715.
- Chen, Z., & Palmer, T. D. (2013). Differential roles of TNFR1 and TNFR2 signaling in adult hippocampal neurogenesis. *Brain, Behavior, and Immunity*, 30, 45–53.
- Chenniappan, R., Nandeesha, H., Kattimani, S., & Nanjaiah, N. D. (2020). Interleukin-17 and Interleukin-10 Association with Disease Progression in Schizophrenia. *Annals of Neurosciences*, 27(1), 24–28.
- Chiu, I. M., Morimoto, E. T. A., Goodarzi, H., Liao, J. T., O'Keeffe, S., Phatnani, H. P., Muratet, M., Carroll, M. C., Levy, S., Tavazoie, S., Myers, R. M., & Maniatis, T. (2013). A neurodegeneration-specific

- gene-expression signature of acutely isolated microglia from an amyotrophic lateral sclerosis mouse model. *Cell Reports*, 4(2), 385–401.
- Cho, K. H., Cheong, J. S., Kim, J. H., Abe, H., Murakami, G., & Cho, B. H. (2013). Site-specific distribution of CD68-positive microglial cells in the brains of human midterm fetuses: A topographical relationship with growing axons. *BioMed Research International*, 2013, 762303.
- Choi, B. H., & Lapham, L. W. (1978). Radial glia in the human fetal cerebrum: A combined Golgi, immunofluorescent and electron microscopic study. *Brain Research*, 148(2), 295–311.
- Choi, I., Zhang, Y., Seegobin, S. P., Pruvost, M., Wang, Q., Purtell, K., Zhang, B., & Yue, Z. (2020). Microglia clear neuron-released α -synuclein via selective autophagy and prevent neurodegeneration. *Nature Communications*, 11(1), Article 1.
- Choi, S. W., Mak, T. S. H., & O'Reilly, P. F. (2020). A guide to performing Polygenic Risk Score analyses. *Nature Protocols*, 15(9), 2759–2772.
- Ciernia, A. V., Link, V. M., Careaga, M., LaSalle, J. M., & Ashwood, P. (2020). Genetic variants drive altered epigenetic regulation of endotoxin response in BTBR macrophages. *Brain, Behavior, and Immunity*, 89, 20–31.
- Clarner, T., Janssen, K., Nellessen, L., Stangel, M., Skripuletz, T., Krauspe, B., Hess, F.-M., Denecke, B., Beutner, C., Linnartz-Gerlach, B., Neumann, H., Vallières, L., Amor, S., Ohl, K., Tenbrock, K., Beyer, C., & Kipp, M. (2015). CXCL10 triggers early microglial activation in the cuprizone model. *Journal of Immunology (Baltimore, Md.: 1950)*, 194(7), 3400–3413.
- Clements, C. C., Wenger, T. L., Zoltowski, A. R., Bertollo, J. R., Miller, J. S., de Marchena, A. B., Mitteer, L. M., Carey, J. C., Yerys, B. E., Zackai, E. H., Emanuel, B. S., McDonald-McGinn, D. M., & Schultz, R. T. (2017). Critical region within 22q11.2 linked to higher rate of autism spectrum disorder. *Molecular Autism*, 8, 58.
- Cleynen, I., Engchuan, W., Hestand, M. S., Heung, T., Holleman, A. M., Johnston, H. R., Monfeuga, T., McDonald-McGinn, D. M., Gur, R. E., Morrow, B. E., Swillen, A., Vorstman, J. A. S., Bearden, C. E., Chow, E. W. C., van den Bree, M., Emanuel, B. S., Vermeesch, J. R., Warren, S. T., Owen, M. J., ... Bassett, A. S. (2021). Genetic contributors to risk of schizophrenia in the presence of a 22q11.2 deletion. *Molecular Psychiatry*, 26(8), 4496–4510.
- Coales, I., Tsartsalis, S., Fancy, N., Weinert, M., Clode, D., Owen, D., & Matthews, P. M. (2022). Alzheimer's disease-related transcriptional sex differences in myeloid cells. *Journal of Neuroinflammation*, 19(1), 247.
- Cocks, G., Curran, S., Gami, P., Uwanogho, D., Jeffries, A. R., Kathuria, A., Lucchesi, W., Wood, V., Dixon, R., Ogilvie, C., Steckler, T., & Price, J. (2014). The utility of patient specific induced pluripotent stem cells for the modelling of Autistic Spectrum Disorders. *Psychopharmacology*, 231(6), 1079–1088.
- Coenye, T. (2021). Do results obtained with RNA-sequencing require independent verification? *Biofilm*, 3, 100043.
- Coleman, J. R. I. (2022). Feasibility and application of polygenic score analysis to the morphology of human-induced pluripotent stem cells. *Molecular Genetics and Genomics*, 297(4), 1111–1122.
- Corley, E., Holleran, L., Fahey, L., Corvin, A., Morris, D. W., & Donohoe, G. (2021). Microglial-expressed genetic risk variants, cognitive function and brain volume in patients with schizophrenia and healthy controls. *Translational Psychiatry*, 11(1), 490.
- Correll, C. U., Solmi, M., Croatto, G., Schneider, L. K., Rohani-Montez, S. C., Fairley, L., Smith, N., Bitter, I., Gorwood, P., Taipale, H., & Tiihonen, J. (2022). Mortality in people with schizophrenia: A systematic

- review and meta-analysis of relative risk and aggravating or attenuating factors. *World Psychiatry: Official Journal of the World Psychiatric Association (WPA)*, 21(2), 248–271.
- Corvin, A., & Morris, D. W. (2014). Genome-wide Association Studies: Findings at the Major Histocompatibility Complex Locus in Psychosis. *Biological Psychiatry*, 75(4), 276–283.
- Cotel, M.-C., Lenartowicz, E. M., Natesan, S., Modo, M. M., Cooper, J. D., Williams, S. C. R., Kapur, S., & Vernon, A. C. (2015). Microglial activation in the rat brain following chronic antipsychotic treatment at clinically relevant doses. *European Neuropsychopharmacology: The Journal of the European College of Neuropsychopharmacology*, 25(11), 2098–2107.
- Couch, A. C. M., Solomon, S., Duarte, R. R. R., Marrocu, A., Sun, Y., Sichlinger, L., Matuleviciute, R., Polit, L. D., Hanger, B., Brown, A., Kordasti, S., Srivastava, D. P., & Vernon, A. C. (2023). Acute IL-6 exposure triggers canonical IL6Ra signaling in hiPSC microglia, but not neural progenitor cells. *Brain, Behavior, and Immunity*, 110, 43–59.
- Coutinho, E., Menassa, D. A., Jacobson, L., West, S. J., Domingos, J., Moloney, T. C., Lang, B., Harrison, P. J., Bennett, D. L. H., Bannerman, D., & Vincent, A. (2017). Persistent microglial activation and synaptic loss with behavioral abnormalities in mouse offspring exposed to CASPR2-antibodies in utero. *Acta Neuropathologica*, 134(4), 567–583.
- Crockett, A. M., Ryan, S. K., Vásquez, A. H., Canning, C., Kanyuch, N., Kebir, H., Ceja, G., Gesualdi, J., Zackai, E., McDonald-McGinn, D., Viaene, A., Kapoor, R., Benallegue, N., Gur, R., Anderson, S. A., & Alvarez, J. I. (2021). Disruption of the blood–brain barrier in 22q11.2 deletion syndrome. *Brain*, 144(5), 1351–1360.
- Császár, E., Lénárt, N., Cserép, C., Környei, Z., Fekete, R., Pósfai, B., Balázsfi, D., Hangya, B., Schwarcz, A. D., Szabadits, E., Szöllösi, D., Szigeti, K., Máthé, D., West, B. L., Sviatkó, K., Brás, A. R., Mariani, J.-C., Kliwer, A., Lenkei, Z., ... Dénes, Á. (2022). Microglia modulate blood flow, neurovascular coupling, and hypoperfusion via purinergic actions. *Journal of Experimental Medicine*, 219(3).
- Cserép, C., Schwarcz, A. D., Pósfai, B., László, Z. I., Kellermayer, A., Környei, Z., Kisfali, M., Nyerges, M., Lele, Z., Katona, I., & Ádám Dénes, null. (2022). Microglial control of neuronal development via somatic purinergic junctions. *Cell Reports*, 40(12), 111369.
- Cuadros, M. A., Sepulveda, M. R., Martin-Oliva, D., Marín-Teva, J. L., & Neubrand, V. E. (2022). Microglia and Microglia-Like Cells: Similar but Different. *Frontiers in Cellular Neuroscience*, 16.
- Cunningham, C. L., Martínez-Cerdeño, V., & Noctor, S. C. (2013). Microglia regulate the number of neural precursor cells in the developing cerebral cortex. *The Journal of Neuroscience: The Official Journal of the Society for Neuroscience*, 33(10), 4216–4233.
- Cuomo, A. S. E., Seaton, D. D., McCarthy, D. J., Martinez, I., Bonder, M. J., Garcia-Bernardo, J., Amatya, S., Madrigal, P., Isaacson, A., Buettner, F., Knights, A., Natarajan, K. N., Vallier, L., Marioni, J. C., Chhatriwala, M., & Stegle, O. (2020). Single-cell RNA-sequencing of differentiating iPS cells reveals dynamic genetic effects on gene expression. *Nature Communications*, 11(1), Article 1.
- da Fonseca, A. C. C., Matias, D., Garcia, C., Amaral, R., Geraldo, L. H., Freitas, C., & Lima, F. R. S. (2014). The impact of microglial activation on blood-brain barrier in brain diseases. *Frontiers in Cellular Neuroscience*, 8, 362.
- Da Pozzo, E., Tremolanti, C., Costa, B., Giacomelli, C., Milenkovic, V. M., Bader, S., Wetzels, C. H., Rupprecht, R., Taliani, S., Da Settimo, F., & Martini, C. (2019). Microglial Pro-Inflammatory and Anti-Inflammatory Phenotypes Are Modulated by Translocator Protein Activation. *International Journal of Molecular Sciences*, 20(18), 4467.

- Dahan, S., Bragazzi, N. L., Yogev, A., Bar-Gad, M., Barak, V., Amital, H., & Amital, D. (2018). The relationship between serum cytokine levels and degree of psychosis in patients with schizophrenia. *Psychiatry Research*, 268, 467–472.
- D'Alò, G. L., De Crescenzo, F., Amato, L., Cruciani, F., Davoli, M., Fulceri, F., Minozzi, S., Mitrova, Z., Morgano, G. P., Nardocci, F., Saulle, R., Schünemann, H. J., Scattoni, M. L., & ISACAGuideline Working Group. (2021). Impact of antipsychotics in children and adolescents with autism spectrum disorder: A systematic review and meta-analysis. *Health and Quality of Life Outcomes*, 19(1), 33.
- Davalos, D., Grutzendler, J., Yang, G., Kim, J. V., Zuo, Y., Jung, S., Littman, D. R., Dustin, M. L., & Gan, W.-B. (2005). ATP mediates rapid microglial response to local brain injury in vivo. *Nature Neuroscience*, 8(6), 752–758.
- Davies, D. S., Ma, J., Jegathees, T., & Goldsbury, C. (2017). Microglia show altered morphology and reduced arborization in human brain during aging and Alzheimer's disease. *Brain Pathology (Zurich, Switzerland)*, 27(6), 795–808.
- Davies, R. W., Fiksinski, A. M., Breetvelt, E. J., Williams, N. M., Hooper, S. R., Monfeuga, T., Bassett, A. S., Owen, M. J., Gur, R. E., Morrow, B. E., McDonald-McGinn, D. M., Swillen, A., Chow, E. W. C., van den Bree, M., Emanuel, B. S., Vermeesch, J. R., van Amelsvoort, T., Arango, C., Armando, M., ... Vorstman, J. A. S. (2020). Using common genetic variation to examine phenotypic expression and risk prediction in 22q11.2 deletion syndrome. *Nature Medicine*, 26(12), 1912–1918.
- De Biase, L. M., Schuebel, K. E., Fufeld, Z. H., Jair, K., Hawes, I. A., Cimbri, R., Zhang, H.-Y., Liu, Q.-R., Shen, H., Xi, Z.-X., Goldman, D., & Bonci, A. (2017). Local Cues Establish and Maintain Region-Specific Phenotypes of Basal Ganglia Microglia. *Neuron*, 95(2), 341–356.e6.
- de Boni, L., Gasparoni, G., Haubenreich, C., Tierling, S., Schmitt, I., Peitz, M., Koch, P., Walter, J., Wüllner, U., & Brüstle, O. (2018). DNA methylation alterations in iPSC- and hESC-derived neurons: Potential implications for neurological disease modeling. *Clinical Epigenetics*, 10(1), 13.
- de Groot, C. J., Hupples, W., Sminia, T., Kraal, G., & Dijkstra, C. D. (1992). Determination of the origin and nature of brain macrophages and microglial cells in mouse central nervous system, using non-radioactive in situ hybridization and immunoperoxidase techniques. *Glia*, 6(4), 301–309.
- de Haas, A. H., Boddeke, H. W. G. M., & Biber, K. (2008). Region-specific expression of immunoregulatory proteins on microglia in the healthy CNS. *Glia*, 56(8), 888–894.
- de Paiva Lopes, K., Snijders, G. J. L., Humphrey, J., Allan, A., Sneeboer, M., Navarro, E., Schilder, B. M., Vialle, R. A., Parks, M., Missall, R., van Zuiden, W., Gigase, F., Kübler, R., van Berlekom, A. B., Hicks, E. M., Böttcher, C., Priller, J., Kahn, R. S., de Witte, L. D., & Raj, T. (2022). Genetic analysis of the human microglia transcriptome across brain regions, aging and disease pathologies. *Nature Genetics*, 54(1), 4–17.
- De Picker, L. J., Morrens, M., Chance, S. A., & Boche, D. (2017). Microglia and Brain Plasticity in Acute Psychosis and Schizophrenia Illness Course: A Meta-Review. *Frontiers in Psychiatry*, 8, 238.
- De Picker, L. J., Victoriano, G. M., Richards, R., Gorvett, A. J., Lyons, S., Buckland, G. R., Tofani, T., Norman, J. L., Chatelet, D. S., Nicoll, J. A. R., & Boche, D. (2021). Immune environment of the brain in schizophrenia and during the psychotic episode: A human post-mortem study. *Brain, Behavior, and Immunity*, 97, 319–327.
- De Picker, L., & Morrens, M. (2020). Perspective: Solving the Heterogeneity Conundrum of TSPO PET Imaging in Psychosis. *Frontiers in Psychiatry*, 11, 362.
- Deczkowska, A., Keren-Shaul, H., Weiner, A., Colonna, M., Schwartz, M., & Amit, I. (2018). Disease-Associated Microglia: A Universal Immune Sensor of Neurodegeneration. *Cell*, 173(5), 1073–1081.

- del Río-Hortega, P. (1919). *El “tercer elemento” de los centros nerviosos [The “third element” of the nerve centers]. I to IV(9)*, 68–166.
- del Río-Hortega, P. (1932). *Microglia, in Cytology and Cellular Pathology of the Nervous System* (Penfield W, Vol. 2). P. B. Hoeber, Inc.
- del Río-Hortega, P. (1939). THE MICROGLIA. *The Lancet*, 233(6036), 1023–1026.
- Deng, X.-L., Feng, L., Wang, Z.-X., Zhao, Y.-E., Zhan, Q., Wu, X.-M., Xiao, B., & Shu, Y. (2020). The Runx1/Notch1 Signaling Pathway Participates in M1/M2 Microglia Polarization in a Mouse Model of Temporal Lobe Epilepsy and in BV-2 Cells. *Neurochemical Research*, 45(9), 2204–2216.
- Dermitzakis, I., Manthou, M. E., Meditskou, S., Tremblay, M.-È., Petratos, S., Zoupi, L., Boziki, M., Kesidou, E., Simeonidou, C., & Theotokis, P. (2023). Origin and Emergence of Microglia in the CNS—An Interesting (Hi)story of an Eccentric Cell. *Current Issues in Molecular Biology*, 45(3), Article 3.
- Devaraju, P., Yu, J., Eddins, D., Mellado-Lagarde, M. M., Earls, L. R., Westmoreland, J. J., Quarato, G., Green, D. R., & Zakharenko, S. S. (2017). Haploinsufficiency of the 22q11.2 microdeletion gene Mrpl40 disrupts short-term synaptic plasticity and working memory through dysregulation of mitochondrial calcium. *Molecular Psychiatry*, 22(9), Article 9.
- Dheda, K., Huggett, J. F., Bustin, S. A., Johnson, M. A., Rook, G., & Zumla, A. (2004). Validation of housekeeping genes for normalizing RNA expression in real-time PCR. *BioTechniques*, 37(1), 112–119.
- Diz-Chaves, Y., Astiz, M., Bellini, M. J., & Garcia-Segura, L. M. (2013). Prenatal stress increases the expression of proinflammatory cytokines and exacerbates the inflammatory response to LPS in the hippocampal formation of adult male mice. *Brain, Behavior, and Immunity*, 28, 196–206.
- Diz-Chaves, Y., Pernía, O., Carrero, P., & Garcia-Segura, L. M. (2012). Prenatal stress causes alterations in the morphology of microglia and the inflammatory response of the hippocampus of adult female mice. *Journal of Neuroinflammation*, 9, 71.
- Dobin, A., Davis, C. A., Schlesinger, F., Drenkow, J., Zaleski, C., Jha, S., Batut, P., Chaisson, M., & Gingeras, T. R. (2013). STAR: Ultrafast universal RNA-seq aligner. *Bioinformatics (Oxford, England)*, 29(1), 15–21.
- Doorn, K. J., Moors, T., Drukarch, B., van de Berg, W. D., Lucassen, P. J., & van Dam, A.-M. (2014). Microglial phenotypes and toll-like receptor 2 in the substantia nigra and hippocampus of incidental Lewy body disease cases and Parkinson’s disease patients. *Acta Neuropathologica Communications*, 2(1), 90.
- Douvaras, P., Sun, B., Wang, M., Kruglikov, I., Lallo, G., Zimmer, M., Terrenoire, C., Zhang, B., Gandy, S., Schadt, E., Freytes, D. O., Noggle, S., & Fossati, V. (2017). Directed Differentiation of Human Pluripotent Stem Cells to Microglia. *Stem Cell Reports*, 8(6), 1516–1524.
- Dräger, N. M., Sattler, S. M., Huang, C. T.-L., Teter, O. M., Leng, K., Hashemi, S. H., Hong, J., Aviles, G., Clelland, C. D., Zhan, L., Udeochu, J. C., Kodama, L., Singleton, A. B., Nalls, M. A., Ichida, J., Ward, M. E., Faghri, F., Gan, L., & Kampmann, M. (2022). A CRISPRi/a platform in human iPSC-derived microglia uncovers regulators of disease states. *Nature Neuroscience*, 25(9), Article 9.
- Drakulic, D., Djurovic, S., Syed, Y. A., Trattaro, S., Caporale, N., Falk, A., Ofir, R., Heine, V. M., Chawner, S. J. R. A., Rodriguez-Moreno, A., van den Bree, M. B. M., Testa, G., Petrakis, S., & Harwood, A. J. (2020). Copy number variants (CNVs): A powerful tool for iPSC-based modelling of ASD. *Molecular Autism*, 11(1), 42.

- Dubbelaar, M. L., Kracht, L., Eggen, B. J. L., & Boddeke, E. W. G. M. (2018). The Kaleidoscope of Microglial Phenotypes. *Frontiers in Immunology*, 9, 1753.
- Dunaevsky, A., & Bergdolt, L. (2019). Brain changes in a maternal Immune activation model of neurodevelopmental brain disorders. *Progress in Neurobiology*, 175, 1–19.
- Durbin, R. (2014). Efficient haplotype matching and storage using the positional Burrows-Wheeler transform (PBWT). *Bioinformatics (Oxford, England)*, 30(9), 1266–1272.
- Edmonson, C. A., Ziats, M. N., & Rennert, O. M. (2016). A Non-inflammatory Role for Microglia in Autism Spectrum Disorders. *Frontiers in Neurology*, 7, 9.
- Edmonson, C., Ziats, M. N., & Rennert, O. M. (2014). Altered glial marker expression in autistic post-mortem prefrontal cortex and cerebellum. *Molecular Autism*, 5(1), 3.
- Eichhoff, G., Brawek, B., & Garaschuk, O. (2011). Microglial calcium signal acts as a rapid sensor of single neuron damage in vivo. *Biochimica et Biophysica Acta (BBA) - Molecular Cell Research*, 1813(5), 1014–1024.
- Eme-Scolan, E., & Dando, S. J. (2020). Tools and Approaches for Studying Microglia In vivo. *Frontiers in Immunology*, 11.
- Ernst, O., Vayttaden, S. J., & Fraser, I. D. C. (2018). Measurement of NF-κB activation in TLR-activated macrophages. *Methods in Molecular Biology (Clifton, N.J.)*, 1714, 67–78.
- Esiri, M. M., al Izzi, M. S., & Reading, M. C. (1991). Macrophages, microglial cells, and HLA-DR antigens in fetal and infant brain. *Journal of Clinical Pathology*, 44(2), 102–106.
- Estes, M. L., & McAllister, A. K. (2016). Maternal immune activation: Implications for neuropsychiatric disorders. *Science (New York, N.Y.)*, 353(6301), 772–777. <https://doi.org/10.1126/science.aag3194>
- Evgrafov, O. V., Armoskus, C., Wrobel, B. B., Spitsyna, V. N., Souaiaia, T., Herstein, J. S., Walker, C. P., Nguyen, J. D., Camarena, A., Weitz, J. R., Kim, J. M. “Hugo”, Lopez Duarte, E., Wang, K., Simpson, G. M., Sobell, J. L., Medeiros, H., Pato, M. T., Pato, C. N., & Knowles, J. A. (2020). Gene Expression in Patient-Derived Neural Progenitors Implicates WNT5A Signaling in the Etiology of Schizophrenia. *Biological Psychiatry*, 88(3), 236–247.
- Ewald, A. C., Kiernan, E. A., Roopra, A. S., Radcliff, A. B., Timko, R. R., Baker, T. L., & Watters, J. J. (2020). Sex- and Region-Specific Differences in the Transcriptomes of Rat Microglia from the Brainstem and Cervical Spinal Cord. *Journal of Pharmacology and Experimental Therapeutics*, 375(1), 210–222.
- Fabrick, B., Haastert, E., Galea, I., Polfliet, M., Döpp, E., Heuvel, M., van den Berg, T., Groot, C., Valk, P., & Dijkstra, C. (2005). CD163-positive perivascular macrophages in the human CNS express molecules for antigen recognition and presentation. *Glia*, 51, 297–305.
- Fagan, K., Crider, A., Ahmed, A. O., & Pillai, A. (2017). Complement C3 Expression Is Decreased in Autism Spectrum Disorder Subjects and Contributes to Behavioral Deficits in Rodents. *Molecular Neuropsychiatry*, 3(1), 19–27.
- Fagerlund, I., Dougalis, A., Shakirzyanova, A., Gómez-Budia, M., Pelkonen, A., Kontinen, H., Ohtonen, S., Fazaludeen, M. F., Koskivi, M., Kuusisto, J., Hernández, D., Pebay, A., Koistinaho, J., Rauramaa, T., Lehtonen, Š., Korhonen, P., & Malm, T. (2022). Microglia-like Cells Promote Neuronal Functions in Cerebral Organoids. *Cells*, 11(1), Article 1.
- Fanet, H., Capuron, L., Castanon, N., Calon, F., & Vancassel, S. (2021). Tetrahydrobiopterin (BH4) Pathway: From Metabolism to Neuropsychiatry. *Current Neuropsychiatry*, 19(5), 591–609.

- Fedoroff, S., Zhai, R., & Novak, J. P. (1997). Microglia and astroglia have a common progenitor cell. *Journal of Neuroscience Research*, 50(3), 477–486.
- Fernández de Cossío, L., Guzmán, A., van der Veldt, S., & Luheshi, G. N. (2017). Prenatal infection leads to ASD-like behavior and altered synaptic pruning in the mouse offspring. *Brain, Behavior, and Immunity*, 63, 88–98.
- Ferro, A., Auguste, Y. S. S., & Cheadle, L. (2021). Microglia, Cytokines, and Neural Activity: Unexpected Interactions in Brain Development and Function. *Frontiers in Immunology*, 12.
- Fetit, R., Hillary, R. F., Price, D. J., & Lawrie, S. M. (2021). The neuropathology of autism: A systematic review of post-mortem studies of autism and related disorders. *Neuroscience & Biobehavioral Reviews*, 129, 35–62.
- Fiksinski, A. M., Breetvelt, E. J., Duijff, S. N., Bassett, A. S., Kahn, R. S., & Vorstman, J. a. S. (2017). Autism Spectrum and psychosis risk in the 22q11.2 deletion syndrome. Findings from a prospective longitudinal study. *Schizophrenia Research*, 188, 59–62.
- Flaherty, E., Zhu, S., Barretto, N., Cheng, E., Deans, P. J. M., Fernando, M. B., Schrode, N., Francoeur, N., Antoine, A., Alganem, K., Halpern, M., Deikus, G., Shah, H., Fitzgerald, M., Ladran, I., Gochman, P., Rapoport, J., Tsankova, N. M., McCullumsmith, R., ... Brennand, K. J. (2019). Neuronal impact of patient-specific aberrant NRXN1 α splicing. *Nature Genetics*, 51(12), 1679–1690.
- Fontalba, A., Gutierrez, O., & Fernandez-Luna, J. L. (2007). NLRP2, an Inhibitor of the NF- κ B Pathway, Is Transcriptionally Activated by NF- κ B and Exhibits a Nonfunctional Allelic Variant1. *The Journal of Immunology*, 179(12), 8519–8524.
- Forsyth, J. K., Nachun, D., Gandal, M. J., Geschwind, D. H., Anderson, A. E., Coppola, G., & Bearden, C. E. (2020). Synaptic and Gene Regulatory Mechanisms in Schizophrenia, Autism, and 22q11.2 Copy Number Variant-Mediated Risk for Neuropsychiatric Disorders. *Biological Psychiatry*, 87(2), 150–163.
- Franco-Bocanegra, D. K., Gourari, Y., McAuley, C., Chatelet, D. S., Johnston, D. A., Nicoll, J. A. R., & Boche, D. (2021). Microglial morphology in Alzheimer's disease and after A β immunotherapy. *Scientific Reports*, 11, 15955.
- Freeman, S. A., & Grinstein, S. (2014). Phagocytosis: Receptors, signal integration, and the cytoskeleton. *Immunological Reviews*, 262(1), 193–215.
- Fricker, M., Oliva-Martín, M. J., & Brown, G. C. (2012). Primary phagocytosis of viable neurons by microglia activated with LPS or A β is dependent on calreticulin/LRP phagocytic signalling. *Journal of Neuroinflammation*, 9(1), 196.
- Fromer, M., Roussos, P., Sieberts, S. K., Johnson, J. S., Kavanagh, D. H., Perumal, T. M., Ruderfer, D. M., Oh, E. C., Topol, A., Shah, H. R., Klei, L. L., Kramer, R., Pinto, D., Gümüş, Z. H., Cicek, A. E., Dang, K. K., Browne, A., Lu, C., Xie, L., ... Sklar, P. (2016). Gene expression elucidates functional impact of polygenic risk for schizophrenia. *Nature Neuroscience*, 19(11), 1442–1453.
- Fujita, S., & Kitamura, T. (1975). Origin of brain macrophages and the nature of the so-called microglia. *Acta Neuropathologica. Supplementum*, Suppl 6, 291–296.
- Funk, A. J., McCullumsmith, R. E., Haroutunian, V., & Meador-Woodruff, J. H. (2012). Abnormal activity of the MAPK- and cAMP-associated signaling pathways in frontal cortical areas in postmortem brain in schizophrenia. *Neuropsychopharmacology: Official Publication of the American College of Neuropsychopharmacology*, 37(4), 896–905.
- Gabriel, E., Albanna, W., Pasquini, G., Ramani, A., Josipovic, N., Mariappan, A., Schinzel, F., Karch, C. M., Bao, G., Gottardo, M., Suren, A. A., Hescheler, J., Nagel-Wolfrum, K., Persico, V., Rizzoli, S. O.,

- Altmüller, J., Riparbelli, M. G., Callaini, G., Goureau, O., ... Gopalakrishnan, J. (2021). Human brain organoids assemble functionally integrated bilateral optic vesicles. *Cell Stem Cell*, 28(10), 1740-1757.e8.
- Galatro, T. F., Holtman, I. R., Lerario, A. M., Vainchtein, I. D., Brouwer, N., Sola, P. R., Veras, M. M., Pereira, T. F., Leite, R. E. P., Möller, T., Wes, P. D., Sogayar, M. C., Laman, J. D., den Dunnen, W., Pasqualucci, C. A., Oba-Shinjo, S. M., Boddeke, E. W. G. M., Marie, S. K. N., & Eggen, B. J. L. (2017). Transcriptomic analysis of purified human cortical microglia reveals age-associated changes. *Nature Neuroscience*, 20(8), Article 8.
- Gallo, N. B., Berisha, A., & Van Aelst, L. (2022). Microglia regulate chandelier cell axo-axonic synaptogenesis. *Proceedings of the National Academy of Sciences*, 119(11), e2114476119.
- Gandal, M. J., Zhang, P., Hadjimichael, E., & Walker, R. (2018). Transcriptome-wide isoform-level dysregulation in ASD, schizophrenia, and bipolar disorder. *Science*, 362(6420), eaat8127.
- Gao, S., Hou, X., Jiang, Y., Xu, Z., Cai, T., Chen, J., & Chang, G. (2017). Integrated analysis of hematopoietic differentiation outcomes and molecular characterization reveals unbiased differentiation capacity and minor transcriptional memory in HPC/HSC-iPSCs. *Stem Cell Research & Therapy*, 8(1), 13.
- García-Gutiérrez, M. S., Navarrete, F., Sala, F., Gasparyan, A., Austrich-Olivares, A., & Manzanares, J. (2020). Biomarkers in Psychiatry: Concept, Definition, Types and Relevance to the Clinical Reality. *Frontiers in Psychiatry*, 11.
- Garcia-Reitboeck, P., Phillips, A., Piers, T. M., Villegas-Llerena, C., Butler, M., Mallach, A., Rodrigues, C., Arber, C. E., Heslegrave, A., Zetterberg, H., Neumann, H., Neame, S., Houlden, H., Hardy, J., & Pocock, J. M. (2018). Human Induced Pluripotent Stem Cell-Derived Microglia-Like Cells Harboring TREM2 Missense Mutations Show Specific Deficits in Phagocytosis. *Cell Reports*, 24(9), 2300–2311.
- Genestine, M., Ambriz, D., Crabtree, G. W., Dummer, P., Molotkova, A., Quintero, M., Mela, A., Biswas, S., Feng, H., Zhang, C., Canoll, P., Hargus, G., Agalliu, D., Gogos, J. A., & Au, E. (2021). Vascular-derived SPARC and SerpinE1 regulate interneuron tangential migration and accelerate functional maturation of human stem cell-derived interneurons. *ELife*, 10, e56063.
- Ghimire, S., Mantziou, V., Moris, N., & Martinez Arias, A. (2021). Human gastrulation: The embryo and its models. *Developmental Biology*, 474, 100–108. <https://doi.org/10.1016/j.ydbio.2021.01.006>
- Ghosh, D., Mishra, M. K., Das, S., Kaushik, D. K., & Basu, A. (2009). Tobacco carcinogen induces microglial activation and subsequent neuronal damage. *Journal of Neurochemistry*, 110(3), 1070–1081.
- Ghosh, S., Castillo, E., Frias, E. S., & Swanson, R. A. (2018). Bioenergetic regulation of microglia. *Glia*, 66(6), 1200–1212.
- Gilmore, J. H., Fredrik Jarskog, L., Vadlamudi, S., & Lauder, J. M. (2004). Prenatal Infection and Risk for Schizophrenia: IL-1 β , IL-6, and TNF α Inhibit Cortical Neuron Dendrite Development. *Neuropsychopharmacology*, 29(7), Article 7.
- Gimeno-Bayón, J., López-López, A., Rodríguez, M. J., & Mahy, N. (2014). Glucose pathways adaptation supports acquisition of activated microglia phenotype. *Journal of Neuroscience Research*, 92(6), 723–731.
- Ginhoux, F., Greter, M., Leboeuf, M., Nandi, S., See, P., Gokhan, S., Mehler, M. F., Conway, S. J., Ng, L. G., Stanley, E. R., Samokhvalov, I. M., & Merad, M. (2010). Fate Mapping Analysis Reveals That Adult Microglia Derive from Primitive Macrophages. *Science*, 330(6005), 841–845.
- Ginhoux, F., Lim, S., Hoeffel, G., Low, D., & Huber, T. (2013). Origin and differentiation of microglia. *Frontiers in Cellular Neuroscience*, 7, 45.

- Giordano, G. M., Bucci, P., Mucci, A., Pezzella, P., & Galderisi, S. (2021). Gender Differences in Clinical and Psychosocial Features Among Persons With Schizophrenia: A Mini Review. *Frontiers in Psychiatry*, 12.
- Gober, R., Ardalán, M., Shiadeh, S. M. J., Duque, L., Garamszegi, S. P., Ascona, M., Barreda, A., Sun, X., Mallard, C., & Vontell, R. T. (2021). Microglia activation in postmortem brains with schizophrenia demonstrates distinct morphological changes between brain regions. *Brain Pathology*, 32(1), e13003.
- Gogos, A., Ney, L. J., Seymour, N., Van Rheenen, T. E., & Felmingham, K. L. (2019). Sex differences in schizophrenia, bipolar disorder, and post-traumatic stress disorder: Are gonadal hormones the link? *British Journal of Pharmacology*, 176(21), 4119–4135.
- Gokhale, A., Hartwig, C., Freeman, A. A. H., Bassell, J. L., Zlatić, S. A., Savas, C. S., Vadlamudi, T., Abudulai, F., Pham, T. T., Crocker, A., Werner, E., Wen, Z., Repetto, G. M., Gogos, J. A., Claypool, S. M., Forsyth, J. K., Bearden, C. E., Glausier, J., Lewis, D. A., ... Faundez, V. (2019). Systems Analysis of the 22q11.2 Microdeletion Syndrome Converges on a Mitochondrial Interactome Necessary for Synapse Function and Behavior. *Journal of Neuroscience*, 39(18), 3561–3581.
- Gómez Morillas, A., Besson, V. C., & Lerouet, D. (2021). Microglia and Neuroinflammation: What Place for P2RY12? *International Journal of Molecular Sciences*, 22(4), 1636.
- Gonzalez, D. M., Gregory, J., & Brennand, K. J. (2017). The Importance of Non-neuronal Cell Types in hiPSC-Based Disease Modeling and Drug Screening. *Frontiers in Cell and Developmental Biology*, 5.
- Gosling, C. J., Cartigny, A., Mellier, B. C., Solanes, A., Radua, J., & Delorme, R. (2022). Correction: Efficacy of psychosocial interventions for Autism spectrum disorder: an umbrella review. *Molecular Psychiatry*, 27(9), Article 9.
- Gosselin, D., Skola, D., Coufal, N. G., Holtman, I. R., Schlachetzki, J. C. M., Sajti, E., Jaeger, B. N., O'Connor, C., Fitzpatrick, C., Pasillas, M. P., Pena, M., Adair, A., Gonda, D. G., Levy, M. L., Ransohoff, R. M., Gage, F. H., & Glass, C. K. (2017). An environment-dependent transcriptional network specifies human microglia identity. *Science (New York, N.Y.)*, 356(6344), eaal3222.
- Gothelf, D., Frisch, A., Munitz, H., Rockah, R., Laufer, N., Mozes, T., Hermesh, H., Weizman, A., & Frydman, M. (1999). Clinical characteristics of schizophrenia associated with velo-cardio-facial syndrome. *Schizophrenia Research*, 35(2), 105–112.
- Gottlieb, T. A., Ivanov, I. E., Adesnik, M., & Sabatini, D. D. (1993). Actin microfilaments play a critical role in endocytosis at the apical but not the basolateral surface of polarized epithelial cells. *The Journal of Cell Biology*, 120(3), 695–710.
- Grabert, K., Michoel, T., Karavolos, M. H., Clohisey, S., Baillie, J. K., Stevens, M. P., Freeman, T. C., Summers, K. M., & McColl, B. W. (2016). Microglial brain region-dependent diversity and selective regional sensitivities to aging. *Nature Neuroscience*, 19(3), 504–516.
- Graham, A. M., Rasmussen, J. M., Rudolph, M. D., Heim, C. M., Gilmore, J. H., Styner, M., Potkin, S. G., Entringer, S., Wadhwa, P. D., Fair, D. A., & Buss, C. (2018). Maternal Systemic Interleukin-6 During Pregnancy Is Associated With Newborn Amygdala Phenotypes and Subsequent Behavior at 2 Years of Age. *Biological Psychiatry*, 83(2), 109–119.
- Grajcarek, J., Monlong, J., Nishinaka-Arai, Y., Nakamura, M., Nagai, M., Matsuo, S., Loughheed, D., Sakurai, H., Saito, M. K., Bourque, G., & Woltjen, K. (2019). Genome-wide microhomologies enable precise template-free editing of biologically relevant deletion mutations. *Nature Communications*, 10(1), Article 1.

- Gray, M. A., Choy, C. H., Dayam, R. M., Escobar, E. O., Somerville, A., Xiao, X., Ferguson, S. M., & Botelho, R. J. (2016). Phagocytosis enhances lysosomal and bactericidal properties by activating the transcription factor TFEB. *Current Biology : CB*, 26(15), 1955–1964.
- Griffith, M., Griffith, O. L., Mwenifumbo, J., Goya, R., Morrissy, A. S., Morin, R. D., Corbett, R., Tang, M. J., Hou, Y.-C., Pugh, T. J., Robertson, G., Chittaranjan, S., Ally, A., Asano, J. K., Chan, S. Y., Li, H. I., McDonald, H., Teague, K., Zhao, Y., ... Marra, M. A. (2010). Alternative expression analysis by RNA sequencing. *Nature Methods*, 7(10), 843–847.
- Grinde, D., Øverland, T., Lima, K., Schjalm, C., Mollnes, T. E., & Abrahamsen, T. G. (2020). Complement Activation in 22q11.2 Deletion Syndrome. *Journal of Clinical Immunology*, 40(3), 515–523.
- Grove, J., Ripke, S., Als, T. D., Mattheisen, M., Walters, R. K., Won, H., Pallesen, J., Agerbo, E., Andreassen, O. A., Anney, R., Awashti, S., Belliveau, R., Bettella, F., Buxbaum, J. D., Bybjerg-Grauholm, J., Bækvad-Hansen, M., Cerrato, F., Chambert, K., Christensen, J. H., ... Børglum, A. D. (2019). Identification of common genetic risk variants for autism spectrum disorder. *Nature Genetics*, 51(3), 431–444.
- Grozdanov, V., Bliederaeuser, C., Ruf, W. P., Roth, V., Fundel-Clemens, K., Zondler, L., Brenner, D., Martin-Villalba, A., Hengerer, B., Kassubek, J., Ludolph, A. C., Weishaupt, J. H., & Danzer, K. M. (2014). Inflammatory dysregulation of blood monocytes in Parkinson's disease patients. *Acta Neuropathologica*, 128(5), 651–663.
- Gu, C., Chen, Y., Chen, Y., Liu, C.-F., Zhu, Z., & Wang, M. (2021). Role of G Protein-Coupled Receptors in Microglial Activation: Implication in Parkinson's Disease. *Frontiers in Aging Neuroscience*, 13, 768156.
- Gu, J., Geng, M., Qi, M., Wang, L., Zhang, Y., & Gao, J. (2021). The role of lysosomal membrane proteins in glucose and lipid metabolism. *FASEB Journal: Official Publication of the Federation of American Societies for Experimental Biology*, 35(10), e21848.
- Guo, X., Delio, M., Haque, N., Castellanos, R., Hestand, M. S., Vermeesch, J. R., Morrow, B. E., & Zheng, D. (2016). Variant discovery and breakpoint region prediction for studying the human 22q11.2 deletion using BAC clone and whole genome sequencing analysis. *Human Molecular Genetics*, 25(17), 3754–3767.
- Gupta, S., Ellis, S. E., Ashar, F. N., Moes, A., Bader, J. S., Zhan, J., West, A. B., & Arking, D. E. (2014). Transcriptome analysis reveals dysregulation of innate immune response genes and neuronal activity-dependent genes in autism. *Nature Communications*, 5(1), Article 1.
- Haddad, P. M., & Correll, C. U. (2018). The acute efficacy of antipsychotics in schizophrenia: A review of recent meta-analyses. *Therapeutic Advances in Psychopharmacology*, 8(11), 303–318.
- Haenseler, W., Sansom, S. N., Buchrieser, J., Newey, S. E., Moore, C. S., Nicholls, F. J., Chintawar, S., Schnell, C., Antel, J. P., Allen, N. D., Cader, M. Z., Wade-Martins, R., James, W. S., & Cowley, S. A. (2017). A Highly Efficient Human Pluripotent Stem Cell Microglia Model Displays a Neuronal-Co-culture-Specific Expression Profile and Inflammatory Response. *Stem Cell Reports*, 8(6), 1727–1742.
- Hall-Roberts, H., Agarwal, D., Obst, J., Smith, T. B., Monzón-Sandoval, J., Di Daniel, E., Webber, C., James, W. S., Mead, E., Davis, J. B., & Cowley, S. A. (2020a). TREM2 Alzheimer's variant R47H causes similar transcriptional dysregulation to knockout, yet only subtle functional phenotypes in human iPSC-derived macrophages. *Alzheimer's Research & Therapy*, 12(1), 151.
- Hall-Roberts, H., Agarwal, D., Obst, J., Smith, T. B., Monzón-Sandoval, J., Di Daniel, E., Webber, C., James, W. S., Mead, E., Davis, J. B., & Cowley, S. A. (2020b). TREM2 Alzheimer's variant R47H causes similar transcriptional dysregulation to knockout, yet only subtle functional phenotypes in human iPSC-derived macrophages. *Alzheimer's Research & Therapy*, 12(1), 151.

- Hall-Roberts, H., Daniel, E. D., James, W. S., Davis, J. B., & Cowley, S. A. (2021). In vitro Quantitative Imaging Assay for Phagocytosis of Dead Neuroblastoma Cells by iPSC-Macrophages. *JoVE (Journal of Visualized Experiments)*, 168, e62217.
- Hammond, T. R., Dufort, C., Dissing-Olesen, L., Giera, S., Young, A., Wysoker, A., Walker, A. J., Gergits, F., Segel, M., Nemesh, J., Marsh, S. E., Saunders, A., Macosko, E., Ginhoux, F., Chen, J., Franklin, R. J. M., Piao, X., McCarroll, S. A., & Stevens, B. (2019). Single-Cell RNA Sequencing of Microglia throughout the Mouse Lifespan and in the Injured Brain Reveals Complex Cell-State Changes. *Immunity*, 50(1), 253–271.e6.
- Hanamsagar, R., Alter, M. D., Block, C. S., Sullivan, H., Bolton, J. L., & Bilbo, S. D. (2017). Generation of a microglial developmental index in mice and in humans reveals a sex difference in maturation and immune reactivity. *Glia*, 65(9), 1504–1520.
- Handunnetthi, L., Saatci, D., Hamley, J. C., & Knight, J. C. (2021). Maternal immune activation downregulates schizophrenia genes in the foetal mouse brain. *Brain Communications*, 3(4), fcab275.
- Hanger, B., Couch, A., Rajendran, L., Srivastava, D. P., & Vernon, A. C. (2020). Emerging Developments in Human Induced Pluripotent Stem Cell-Derived Microglia: Implications for Modelling Psychiatric Disorders With a Neurodevelopmental Origin. *Frontiers in Psychiatry*, 11, 789.
- Hao, C., Richardson, A., & Fedoroff, S. (1991). Macrophage-like cells originate from neuroepithelium in culture: Characterization and properties of the macrophage-like cells. *International Journal of Developmental Neuroscience: The Official Journal of the International Society for Developmental Neuroscience*, 9(1), 1–14.
- Hasselmann, J., & Blurton-Jones, M. (2020). Human iPSC-derived microglia: A growing toolset to study the brain's innate immune cells. *Glia*, 68(4), 721–739.
- Hasselmann, J., Coburn, M. A., England, W., Figueroa Velez, D. X., Kiani Shabestari, S., Tu, C. H., McQuade, A., Kolahdouzan, M., Echeverria, K., Claes, C., Nakayama, T., Azevedo, R., Coufal, N. G., Han, C. Z., Cummings, B. J., Davtyan, H., Glass, C. K., Healy, L. M., Gandhi, S. P., ... Blurton-Jones, M. (2019). Development of a Chimeric Model to Study and Manipulate Human Microglia In Vivo. *Neuron*, 103(6), 1016–1033.e10.
- Hattori, Y. (2023). The microglia-blood vessel interactions in the developing brain. *Neuroscience Research*, 187, 58–66.
- Hayes, L. N., An, K., Carloni, E., Li, F., Vincent, E., Trippaers, C., Paranjpe, M., Dölen, G., Goff, L. A., Ramos, A., Kano, S.-I., & Sawa, A. (2022). Prenatal immune stress blunts microglia reactivity, impairing neurocircuitry. *Nature*, 610(7931), 327–334.
- He, Y., Taylor, N., Yao, X., & Bhattacharya, A. (2021). Mouse primary microglia respond differently to LPS and poly(I:C) in vitro. *Scientific Reports*, 11, 10447.
- Hefendehl, J. K., Neher, J. J., Sühs, R. B., Kohsaka, S., Skodras, A., & Jucker, M. (2014). Homeostatic and injury-induced microglia behavior in the aging brain. *Aging Cell*, 13(1), 60–69.
- Heiman, P., Mohsen, A.-W., Karunanidhi, A., St Croix, C., Watkins, S., Koppes, E., Haas, R., Vockley, J., & Ghaloul-Gonzalez, L. (2022). Mitochondrial dysfunction associated with TANGO2 deficiency. *Scientific Reports*, 12(1), 3045.
- Hickman, S. E., Kingery, N. D., Ohsumi, T. K., Borowsky, M. L., Wang, L., Means, T. K., & El Khoury, J. (2013). The microglial sensome revealed by direct RNA sequencing. *Nature Neuroscience*, 16(12), Article 12.

- Hipolito, V. E. B., Ospina-Escobar, E., & Botelho, R. J. (2018). Lysosome remodelling and adaptation during phagocyte activation. *Cellular Microbiology*, 20(4).
- Hoeffel, G., & Ginhoux, F. (2015). Ontogeny of Tissue-Resident Macrophages. *Frontiers in Immunology*, 6, 486.
- Hoekstra, S. D., Stringer, S., Heine, V. M., & Posthuma, D. (2017). Genetically-Informed Patient Selection for iPSC Studies of Complex Diseases May Aid in Reducing Cellular Heterogeneity. *Frontiers in Cellular Neuroscience*, 11.
- Holbrook, J. A., Jarosz-Griffiths, H. H., Caseley, E., Lara-Reyna, S., Poulter, J. A., Williams-Gray, C. H., Peckham, D., & McDermott, M. F. (2021). Neurodegenerative Disease and the NLRP3 Inflammasome. *Frontiers in Pharmacology*, 12, 643254.
- Holtman, I. R., Raj, D. D., Miller, J. A., Schaafsma, W., Yin, Z., Brouwer, N., Wes, P. D., Möller, T., Orre, M., Kamphuis, W., Hol, E. M., Boddeke, E. W. G. M., & Eggen, B. J. L. (2015). Induction of a common microglia gene expression signature by aging and neurodegenerative conditions: A co-expression meta-analysis. *Acta Neuropathologica Communications*, 3(1), 31.
- Holtman, I. R., Skola, D., & Glass, C. K. (2017). Transcriptional control of microglia phenotypes in health and disease. *The Journal of Clinical Investigation*, 127(9), 3220–3229.
- Honarmand Tamizkar, K., Badrlou, E., Aslani, T., Brand, S., Arsang-Jang, S., Ghafouri-Fard, S., & Taheri, M. (2021). Dysregulation of NF- κ B-Associated LncRNAs in Autism Spectrum Disorder. *Frontiers in Molecular Neuroscience*, 14.
- Hoogland, I. C. M., Houbolt, C., van Westerloo, D. J., van Gool, W. A., & van de Beek, D. (2015). Systemic inflammation and microglial activation: Systematic review of animal experiments. *Journal of Neuroinflammation*, 12(1), 114.
- Howes, O. D., Thase, M. E., & Pillinger, T. (2022). Treatment resistance in psychiatry: State of the art and new directions. *Molecular Psychiatry*, 27(1), 58–72.
- Hu, K. (2014). Vectorology and factor delivery in induced pluripotent stem cell reprogramming. *Stem Cells and Development*, 23(12), 1301–1315.
- Huang, Y., Xu, Z., Xiong, S., Sun, F., Qin, G., Hu, G., Wang, J., Zhao, L., Liang, Y.-X., Wu, T., Lu, Z., Humayun, M. S., So, K.-F., Pan, Y., Li, N., Yuan, T.-F., Rao, Y., & Peng, B. (2018). Repopulated microglia are solely derived from the proliferation of residual microglia after acute depletion. *Nature Neuroscience*, 21(4), 530–540.
- Huber, W., Carey, V. J., Gentleman, R., Anders, S., Carlson, M., Carvalho, B. S., Bravo, H. C., Davis, S., Gatto, L., Girke, T., Gottardo, R., Hahne, F., Hansen, K. D., Irizarry, R. A., Lawrence, M., Love, M. I., MacDonald, J., Obenchain, V., Oleś, A. K., ... Morgan, M. (2015). Orchestrating high-throughput genomic analysis with Bioconductor. *Nature Methods*, 12(2), Article 2.
- Hume, D. A., Perry, V. H., & Gordon, S. (1983). Immunohistochemical localization of a macrophage-specific antigen in developing mouse retina: Phagocytosis of dying neurons and differentiation of microglial cells to form a regular array in the plexiform layers. *The Journal of Cell Biology*, 97(1), 253–257.
- Hutchins, K. D., Dickson, D. W., Rashbaum, W. K., & Lyman, W. D. (1990). Localization of morphologically distinct microglial populations in the developing human fetal brain: Implications for ontogeny. *Brain Research. Developmental Brain Research*, 55(1), 95–102.
- Huttenlocher, P. R. (1979). Synaptic density in human frontal cortex—Developmental changes and effects of aging. *Brain Research*, 163(2), 195–205.

- Ibi, D., de la Fuente Revenga, M., Kezunovic, N., Muguruza, C., Saunders, J. M., Gaitonde, S. A., Moreno, J. L., Ijaz, M. K., Santosh, V., Kozlenkov, A., Holloway, T., Seto, J., García-Bea, A., Kurita, M., Mosley, G. E., Jiang, Y., Christoffel, D. J., Callado, L. F., Russo, S. J., ... González-Maeso, J. (2017). Antipsychotic-induced Hdac2 transcription via NF- κ B leads to synaptic and cognitive side effects. *Nature Neuroscience*, 20(9), Article 9.
- Ihnatovych, I., Birkaya, B., Notari, E., & Szigeti, K. (2020). iPSC-Derived Microglia for Modeling Human-Specific DAMP and PAMP Responses in the Context of Alzheimer's Disease. *International Journal of Molecular Sciences*, 21(24), 9668.
- Illes, P., Verkhratsky, A., & Tang, Y. (2021). Surveilling microglia dampens neuronal activity: Operation of a purinergically mediated negative feedback mechanism. *Signal Transduction and Targeted Therapy*, 6(1), Article 1.
- Ishijima, T., & Nakajima, K. (2021). Inflammatory cytokines TNF α , IL-1 β , and IL-6 are induced in endotoxin-stimulated microglia through different signaling cascades. *Science Progress*, 104(4), 00368504211054985.
- Ito, D., Imai, Y., Ohsawa, K., Nakajima, K., Fukuuchi, Y., & Kohsaka, S. (1998). Microglia-specific localisation of a novel calcium binding protein, Iba1. *Brain Research. Molecular Brain Research*, 57(1), 1–9.
- Iyer, H., Shen, K., Meireles, A. M., & Talbot, W. S. (2022). A lysosomal regulatory circuit essential for the development and function of microglia. *Science Advances*, 8(35), eabp8321.
- Izumi, R., Hino, M., Wada, A., Nagaoka, A., Kawamura, T., Mori, T., Sainouchi, M., Kakita, A., Kasai, K., Kunii, Y., & Yabe, H. (2021). Detailed Postmortem Profiling of Inflammatory Mediators Expression Revealed Post-inflammatory Alternation in the Superior Temporal Gyrus of Schizophrenia. *Frontiers in Psychiatry*, 12.
- Jacob, R., & Chowdhury, A. N. (2008). Metabolic comorbidity in schizophrenia. *Indian Journal of Medical Sciences*, 62(1), 23–31.
- Jain, R. W., & Yong, V. W. (2022). B cells in central nervous system disease: Diversity, locations and pathophysiology. *Nature Reviews Immunology*, 22(8), Article 8.
- Jakovcevski, I., Filipovic, R., Mo, Z., Rakic, S., & Zecevic, N. (2009). Oligodendrocyte development and the onset of myelination in the human fetal brain. *Frontiers in Neuroanatomy*, 3, 5.
- Jalbrzikowski, M., Lazaro, M. T., Gao, F., Huang, A., Chow, C., Geschwind, D. H., Coppola, G., & Bearden, C. E. (2015). Transcriptome Profiling of Peripheral Blood in 22q11.2 Deletion Syndrome Reveals Functional Pathways Related to Psychosis and Autism Spectrum Disorder. *PLoS ONE*, 10(7), e0132542.
- Janossy, G., Bofill, M., Poulter, L. W., Rawlings, E., Burford, G. D., Navarrete, C., Ziegler, A., & Kelemen, E. (1986). Separate ontogeny of two macrophage-like accessory cell populations in the human fetus. *Journal of Immunology (Baltimore, Md.: 1950)*, 136(12), 4354–4361.
- Jansen, I. E., Savage, J. E., Watanabe, K., Bryois, J., Williams, D. M., Steinberg, S., Sealock, J., Karlsson, I. K., Hägg, S., Athanasiu, L., Voyle, N., Proitsi, P., Witoelar, A., Stringer, S., Aarsland, D., Almdahl, I. S., Andersen, F., Bergh, S., Bettella, F., ... Posthuma, D. (2019). Genome-wide meta-analysis identifies new loci and functional pathways influencing Alzheimer's disease risk. *Nature Genetics*, 51(3), 404–413.
- Jao, J., & Ciernia, A. V. (2021). MGENrichment: A web application for microglia gene list enrichment analysis. *PLoS Computational Biology*, 17(11), e1009160.

- Jeffries, C. D., Perkins, D. O., Fournier, M., Do, K. Q., Cuenod, M., Khadimallah, I., Domenici, E., Addington, J., Bearden, C. E., Cadenhead, K. S., Cannon, T. D., Cornblatt, B. A., Mathalon, D. H., McGlashan, T. H., Seidman, L. J., Tsuang, M., Walker, E. F., & Woods, S. W. (2018). Networks of blood proteins in the neuroimmunology of schizophrenia. *Translational Psychiatry*, 8, 112.
- Jensen, A. R., Lane, A. L., Werner, B. A., McLees, S. E., Fletcher, T. S., & Frye, R. E. (2022). Modern Biomarkers for Autism Spectrum Disorder: Future Directions. *Molecular Diagnosis & Therapy*, 26(5), 483–495.
- Johnson, T., Saatci, D., & Handunnetthi, L. (2022). Maternal immune activation induces methylation changes in schizophrenia genes. *PloS One*, 17(11), e0278155.
- Joshi, P., Riffel, F., Satoh, K., Enomoto, M., Qamar, S., Scheiblich, H., Villacampa, N., Kumar, S., Theil, S., Parhizkar, S., Haass, C., Heneka, M. T., Fraser, P. E., St George-Hyslop, P., & Walter, J. (2021). Differential interaction with TREM2 modulates microglial uptake of modified A β species. *Glia*, 69(12), 2917–2932.
- Jung, E. S., Suh, K., Han, J., Kim, H., Kang, H.-S., Choi, W.-S., & Mook-Jung, I. (2022). Amyloid- β activates NLRP3 inflammasomes by affecting microglial immunometabolism through the Syk-AMPK pathway. *Aging Cell*, 21(5), e13623.
- Kahn, R. S., Sommer, I. E., Murray, R. M., Meyer-Lindenberg, A., Weinberger, D. R., Cannon, T. D., O'Donovan, M., Correll, C. U., Kane, J. M., van Os, J., & Insel, T. R. (2015). Schizophrenia. *Nature Reviews Disease Primers*, 1(1), Article 1.
- Kaidanovich-Beilin, O., Lipina, T., Vukobradovic, I., Roder, J., & Woodgett, J. R. (2011). Assessment of Social Interaction Behaviors. *Journal of Visualized Experiments: JoVE*, 48, 2473.
- Kaksonen, M., & Roux, A. (2018). Mechanisms of clathrin-mediated endocytosis. *Nature Reviews. Molecular Cell Biology*, 19(5), 313–326.
- Kana, V., Desland, F. A., Casanova-Acebes, M., Ayata, P., Badimon, A., Nabel, E., Yamamuro, K., Sneeboer, M., Tan, I.-L., Flanigan, M. E., Rose, S. A., Chang, C., Leader, A., Le Bourhis, H., Sweet, E. S., Tung, N., Wroblewska, A., Lavin, Y., See, P., ... Merad, M. (2019). CSF-1 controls cerebellar microglia and is required for motor function and social interaction. *The Journal of Experimental Medicine*, 216(10), 2265–2281.
- Kanlaya, R., Sintiprungrat, K., Chaiyarit, S., & Thongboonkerd, V. (2013). Macropinocytosis is the Major Mechanism for Endocytosis of Calcium Oxalate Crystals into Renal Tubular Cells. *Cell Biochemistry and Biophysics*, 67(3), 1171–1179.
- Karayorgou, M., Simon, T. J., & Gogos, J. A. (2010). 22q11.2 microdeletions: Linking DNA structural variation to brain dysfunction and schizophrenia. *Nature Reviews. Neuroscience*, 11(6), 402–416.
- Karbarz, M. (2020). Consequences of 22q11.2 Microdeletion on the Genome, Individual and Population Levels. *Genes*, 11(9), 977.
- Karlsson, K. R., Cowley, S., Martinez, F. O., Shaw, M., Minger, S. L., & James, W. (2008). Homogeneous monocytes and macrophages from human embryonic stem cells following coculture-free differentiation in M-CSF and IL-3. *Experimental Hematology*, 36(9), 1167–1175.
- Kathuria, A., Lopez-Lengowski, K., Jagtap, S. S., McPhie, D., Perlis, R. H., Cohen, B. M., & Karmacharya, R. (2020). Transcriptomic Landscape and Functional Characterization of Induced Pluripotent Stem Cell-Derived Cerebral Organoids in Schizophrenia. *JAMA Psychiatry*, 77(7), 745–754.

- Kathuria, A., Lopez-Lengowski, K., Watmuff, B., McPhie, D., Cohen, B. M., & Karmacharya, R. (2019). Synaptic deficits in iPSC-derived cortical interneurons in schizophrenia are mediated by NLGN2 and rescued by N-acetylcysteine. *Translational Psychiatry*, 9(1), Article 1.
- Kenkhuis, B., Somarakis, A., Kleindouwel, L. R. T., van Roon-Mom, W. M. C., Höllt, T., & van der Weerd, L. (2022). Co-expression patterns of microglia markers Iba1, TMEM119 and P2RY12 in Alzheimer's disease. *Neurobiology of Disease*, 167, 105684.
- Kern, L., Spreckels, J., Nist, A., Stiewe, T., Skevaki, C., Greene, B., Mernberger, M., & Elsässer, H.-P. (2016). Altered glycogen metabolism causes hepatomegaly following an Atg7 deletion. *Cell and Tissue Research*, 366(3), 651–665.
- Kettenmann, H., Hanisch, U.-K., Noda, M., & Verkhratsky, A. (2011). Physiology of Microglia. *Physiological Reviews*, 91(2), 461–553.
- Kettenmann, H., Kirchhoff, F., & Verkhratsky, A. (2013). Microglia: New roles for the synaptic stripper. *Neuron*, 77(1), 10–18.
- Khan, T. A., Revah, O., Gordon, A., Yoon, S.-J., Krawisz, A. K., Goold, C., Sun, Y., Kim, C. H., Tian, Y., Li, M.-Y., Schaepe, J. M., Ikeda, K., Amin, N. D., Sakai, N., Yazawa, M., Kushan, L., Nishino, S., Porteus, M. H., Rapoport, J. L., ... Pasca, S. P. (2020). Neuronal defects in a human cellular model of 22q11.2 deletion syndrome. *Nature Medicine*, 26(12), Article 12.
- Kiehl, T. R., Chow, E. W. C., Mikulis, D. J., George, S. R., & Bassett, A. S. (2009). Neuropathologic features in adults with 22q11.2 deletion syndrome. *Cerebral Cortex (New York, N.Y.: 1991)*, 19(1), 153–164.
- Kierdorf, K., Erny, D., Goldmann, T., Sander, V., Schulz, C., Perdiguero, E. G., Wieghofer, P., Heinrich, A., Riemke, P., Hölscher, C., Müller, D. N., Luckow, B., Brocker, T., Debowski, K., Fritz, G., Opdenakker, G., Diefenbach, A., Biber, K., Heikenwalder, M., ... Prinz, M. (2013). Microglia emerge from erythromyeloid precursors via Pu.1- and Irf8-dependent pathways. *Nature Neuroscience*, 16(3), Article 3.
- Kierdorf, K., & Prinz, M. (2013). Factors regulating microglia activation. *Frontiers in Cellular Neuroscience*, 7.
- Kim, H.-J., Cho, M.-H., Shim, W. H., Kim, J. K., Jeon, E.-Y., Kim, D.-H., & Yoon, S.-Y. (2017). Deficient autophagy in microglia impairs synaptic pruning and causes social behavioral defects. *Molecular Psychiatry*, 22(11), Article 11.
- Kimoto, S., Muraki, K., Toritsuka, M., Mugikura, S., Kajiwar, K., Kishimoto, T., Illingworth, E., & Tanigaki, K. (2012). Selective overexpression of Comt in prefrontal cortex rescues schizophrenia-like phenotypes in a mouse model of 22q11 deletion syndrome. *Translational Psychiatry*, 2(8), e146.
- Kirov, G., Rees, E., Walters, J. T. R., Escott-Price, V., Georgieva, L., Richards, A. L., Chambert, K. D., Davies, G., Legge, S. E., Moran, J. L., McCarroll, S. A., O'Donovan, M. C., & Owen, M. J. (2014). The penetrance of copy number variations for schizophrenia and developmental delay. *Biological Psychiatry*, 75(5), 378–385.
- Kirov, G., Rujescu, D., Ingason, A., Collier, D. A., O'Donovan, M. C., & Owen, M. J. (2009). Neurexin 1 (NRXN1) Deletions in Schizophrenia. *Schizophrenia Bulletin*, 35(5), 851–854.
- Kisler, K., Nikolakopoulou, A. M., & Zlokovic, B. V. (2021). Microglia have a grip on brain microvasculature. *Nature Communications*, 12(1), Article 1.
- Koenigsknecht-Talboo, J., & Landreth, G. E. (2005). Microglial phagocytosis induced by fibrillar beta-amyloid and IgGs are differentially regulated by proinflammatory cytokines. *The Journal of Neuroscience: The Official Journal of the Society for Neuroscience*, 25(36), 8240–8249.

- Kolosowska, N., Keuters, M. H., Wojciechowski, S., Keksa-Goldsteine, V., Laine, M., Malm, T., Goldsteins, G., Koistinaho, J., & Dhungana, H. (2019). Peripheral Administration of IL-13 Induces Anti-inflammatory Microglial/Macrophage Responses and Provides Neuroprotection in Ischemic Stroke. *Neurotherapeutics: The Journal of the American Society for Experimental NeuroTherapeutics*, 16(4), 1304–1319.
- Konishi, H., Kiyama, H., & Ueno, M. (2019). Dual functions of microglia in the formation and refinement of neural circuits during development. *International Journal of Developmental Neuroscience: The Official Journal of the International Society for Developmental Neuroscience*, 77, 18–25.
- Kordulewska, N. K., Kostyra, E., Piskorz-Ogórek, K., Moszyńska, M., Cieślińska, A., Fiedorowicz, E., & Jarmołowska, B. (2019). Serum cytokine levels in children with spectrum autism disorder: Differences in pro- and anti-inflammatory balance. *Journal of Neuroimmunology*, 337, 577066.
- Kotini, A. G., & Papapetrou, E. P. (2020). Engineering of targeted megabase-scale deletions in human induced pluripotent stem cells. *Experimental Hematology*, 87, 25–32.
- Kracht, L., Borggrewe, M., Eskandar, S., Brouwer, N., Chuva de Sousa Lopes, S. M., Laman, J. D., Scherjon, S. A., Prins, J. R., Kooistra, S. M., & Eggen, B. J. L. (2020). Human fetal microglia acquire homeostatic immune-sensing properties early in development. *Science (New York, N.Y.)*, 369(6503), 530–537.
- Kraguljac, N. V., McDonald, W. M., Widge, A. S., Rodriguez, C. I., Tohen, M., & Nemeroff, C. B. (2021). Neuroimaging Biomarkers in Schizophrenia. *The American Journal of Psychiatry*, 178(6), 509–521.
- Kreher, C., Favret, J., Maulik, M., & Shin, D. (2021). Lysosomal Functions in Glia Associated with Neurodegeneration. *Biomolecules*, 11(3), 400.
- Kuhn, D. A., Vanhecke, D., Michen, B., Blank, F., Gehr, P., Petri-Fink, A., & Rothen-Rutishauser, B. (2014). Different endocytotic uptake mechanisms for nanoparticles in epithelial cells and macrophages. *Beilstein Journal of Nanotechnology*, 5, 1625–1636.
- Kunz, M., Ceresér, K. M., Goi, P. D., Fries, G. R., Teixeira, A. L., Fernandes, B. S., Belmonte-de-Abreu, P. S., Kauer-Sant'Anna, M., Kapczinski, F., & Gama, C. S. (2011). Serum levels of IL-6, IL-10 and TNF- α in patients with bipolar disorder and schizophrenia: Differences in pro- and anti-inflammatory balance. *Revista Brasileira De Psiquiatria (Sao Paulo, Brazil: 1999)*, 33(3), 268–274.
- Kyosseva, S. V. (2004). Differential expression of mitogen-activated protein kinases and immediate early genes fos and jun in thalamus in schizophrenia. *Progress in Neuro-Psychopharmacology and Biological Psychiatry*, 28(6), 997–1006.
- Laffer, B., Bauer, D., Wasmuth, S., Busch, M., Jalilvand, T. V., Thanos, S., Meyer zu Hörste, G., Loser, K., Langmann, T., Heiligenhaus, A., & Kasper, M. (2019). Loss of IL-10 Promotes Differentiation of Microglia to a M1 Phenotype. *Frontiers in Cellular Neuroscience*, 13, 430.
- Lancaster, C. E., Fountain, A., Dayam, R. M., Somerville, E., Sheth, J., Jacobelli, V., Somerville, A., Terebiznik, M. R., & Botelho, R. J. (2021). Phagosome resolution regenerates lysosomes and maintains the degradative capacity in phagocytes. *The Journal of Cell Biology*, 220(9), e202005072.
- Lancaster, M. A., & Knoblich, J. A. (2014). Generation of cerebral organoids from human pluripotent stem cells. *Nature Protocols*, 9(10), 2329–2340.
- Lancaster, M. A., Renner, M., Martin, C.-A., Wenzel, D., Bicknell, L. S., Hurles, M. E., Homfray, T., Penninger, J. M., Jackson, A. P., & Knoblich, J. A. (2013). Cerebral organoids model human brain development and microcephaly. *Nature*, 501(7467), Article 7467.
- Lang, B., Pu, J., Hunter, I., Liu, M., Martin-Granados, C., Reilly, T. J., Gao, G.-D., Guan, Z.-L., Li, W.-D., Shi, Y.-Y., He, G., He, L., Stefánsson, H., St Clair, D., Blackwood, D. H., McCaig, C. D., & Shen, S.

- (2014). Recurrent deletions of ULK4 in schizophrenia: A gene crucial for neuritogenesis and neuronal motility. *Journal of Cell Science*, 127(Pt 3), 630–640.
- Larbalestier, H., Keatinge, M., Watson, L., White, E., Gowda, S., Wei, W., Koler, K., Semenova, S. A., Elkin, A. M., Rimmer, N., Sweeney, S. T., Mazzolini, J., Sieger, D., Hide, W., McDearmid, J., Panula, P., MacDonald, R. B., & Bandmann, O. (2022). GCH1 Deficiency Activates Brain Innate Immune Response and Impairs Tyrosine Hydroxylase Homeostasis. *The Journal of Neuroscience*, 42(4), 702–716.
- Lau, S.-F., Fu, A. K. Y., & Ip, N. Y. (2021). Cytokine signaling convergence regulates the microglial state transition in Alzheimer's disease. *Cellular and Molecular Life Sciences: CMLS*, 78(10), 4703–4712.
- Lauro, C., & Limatola, C. (2020). Metabolic Reprograming of Microglia in the Regulation of the Innate Inflammatory Response. *Frontiers in Immunology*, 11, 493.
- Lavis, S., Guillermier, M., Hérard, A.-S., Petit, F., Delahaye, M., Van Camp, N., Ben Haim, L., Lebon, V., Remy, P., Dollé, F., Delzescaux, T., Bonvento, G., Hantraye, P., & Escartin, C. (2012). Reactive Astrocytes Overexpress TSPO and Are Detected by TSPO Positron Emission Tomography Imaging. *The Journal of Neuroscience*, 32(32), 10809–10818.
- Lawson, L. J., Perry, V. H., Dri, P., & Gordon, S. (1990). Heterogeneity in the distribution and morphology of microglia in the normal adult mouse brain. *Neuroscience*, 39(1), 151–170.
- Lawson, L. J., Perry, V. H., & Gordon, S. (1992). Turnover of resident microglia in the normal adult mouse brain. *Neuroscience*, 48(2), 405–415.
- Lee, A. S., Azmitia, E. C., & Whitaker-Azmitia, P. M. (2017). Developmental microglial priming in postmortem autism spectrum disorder temporal cortex. *Brain, Behavior, and Immunity*, 62, 193–202.
- Lee, B. K., Magnusson, C., Gardner, R. M., Blomström, Å., Newschaffer, C. J., Burstyn, I., Karlsson, H., & Dalman, C. (2015). Maternal hospitalization with infection during pregnancy and risk of autism spectrum disorders. *Brain, Behavior, and Immunity*, 44, 100–105.
- Lee, M., Cho, T., Jantaratnotai, N., Wang, Y. T., McGeer, E., & McGeer, P. L. (2010). Depletion of GSH in glial cells induces neurotoxicity: Relevance to aging and degenerative neurological diseases. *FASEB Journal*, 24(7), 2533–2545.
- Lee, R. E. C., Walker, S. R., Savery, K., Frank, D. A., & Gaudet, S. (2014). Fold-change of nuclear NF-κB determines TNF-induced transcription in single cells. *Molecular Cell*, 53(6), 867–879.
- Lee, S. H., Goddard, M. E., Wray, N. R., & Visscher, P. M. (2012). A better coefficient of determination for genetic profile analysis. *Genetic Epidemiology*, 36(3), 214–224.
- Lehrman, E. K., Wilton, D. K., Litvina, E. Y., Welsh, C. A., Chang, S. T., Frouin, A., Walker, A. J., Heller, M. D., Umemori, H., Chen, C., & Stevens, B. (2018). CD47 protects synapses from excess microglia-mediated pruning during development. *Neuron*, 100(1), 120-134.e6.
- Lenz, K. M., Nugent, B. M., Haliyur, R., & McCarthy, M. M. (2013). Microglia Are Essential to Masculinization of Brain and Behavior. *The Journal of Neuroscience*, 33(7), 2761–2772.
- Lesh, T. A., Careaga, M., Rose, D. R., McAllister, A. K., Van de Water, J., Carter, C. S., & Ashwood, P. (2018). Cytokine alterations in first-episode schizophrenia and bipolar disorder: Relationships to brain structure and symptoms. *Journal of Neuroinflammation*, 15(1), 165.
- Levinson, D. F., Duan, J., Oh, S., Wang, K., Sanders, A. R., Shi, J., Zhang, N., Mowry, B. J., Olincy, A., Amin, F., Cloninger, C. R., Silverman, J. M., Buccola, N. G., Byerley, W. F., Black, D. W., Kendler, K. S., Freedman, R., Dudbridge, F., Pe'er, I., ... Gejman, P. V. (2011). Copy number variants in

- schizophrenia: Confirmation of five previous findings and new evidence for 3q29 microdeletions and VIPR2 duplications. *The American Journal of Psychiatry*, 168(3), 302–316.
- Levitt, P., & Campbell, D. B. (2009). The genetic and neurobiologic compass points toward common signaling dysfunctions in autism spectrum disorders. *The Journal of Clinical Investigation*, 119(4), 747–754.
- Li, H., Handsaker, B., Wysoker, A., Fennell, T., Ruan, J., Homer, N., Marth, G., Abecasis, G., Durbin, R., & 1000 Genome Project Data Processing Subgroup. (2009). The Sequence Alignment/Map format and SAMtools. *Bioinformatics (Oxford, England)*, 25(16), 2078–2079.
- Li, J., Ryan, S. K., Deboer, E., Cook, K., Fitzgerald, S., Lachman, H. M., Wallace, D. C., Goldberg, E. M., & Anderson, S. A. (2019). Mitochondrial deficits in human iPSC-derived neurons from patients with 22q11.2 deletion syndrome and schizophrenia. *Translational Psychiatry*, 9(1), Article 1.
- Li, J., Shui, X., Sun, R., Wan, L., Zhang, B., Xiao, B., & Luo, Z. (2021). Microglial Phenotypic Transition: Signaling Pathways and Influencing Modulators Involved in Regulation in Central Nervous System Diseases. *Frontiers in Cellular Neuroscience*, 15.
- Li, J., Tran, O. T., Crowley, T. B., Moore, T. M., Zackai, E. H., Emanuel, B. S., McDonald-McGinn, D. M., Gur, R. E., Wallace, D. C., & Anderson, S. A. (2021). Association of Mitochondrial Biogenesis With Variable Penetrance of Schizophrenia. *JAMA Psychiatry*, 78(8), 911–921.
- Li, J.-W., Zong, Y., Cao, X.-P., Tan, L., & Tan, L. (2018). Microglial priming in Alzheimer's disease. *Annals of Translational Medicine*, 6(10), 176.
- Li, Q., & Barres, B. A. (2018). Microglia and macrophages in brain homeostasis and disease. *Nature Reviews Immunology*, 18(4), Article 4.
- Li, Q., Li, Y., Liu, B., Chen, Q., Xing, X., Xu, G., & Yang, W. (2022). Prevalence of Autism Spectrum Disorder Among Children and Adolescents in the United States From 2019 to 2020. *JAMA Pediatrics*, 176(9), 943–945.
- Li, X., & Wang, C.-Y. (2021). From bulk, single-cell to spatial RNA sequencing. *International Journal of Oral Science*, 13(1), Article 1.
- Li, Y., Sun, Z., Zhu, H., Sun, Y., Shteyman, D. B., Markx, S., Leong, K. W., Xu, B., & Fu, B. M. (2023). Inhibition of Abl Kinase by Imatinib Can Rescue the Compromised Barrier Function of 22q11.2DS Patient-iPSC-Derived Blood–Brain Barriers. *Cells*, 12(3), Article 3.
- Li, Y., Xia, Y., Yin, S., Wan, F., Hu, J., Kou, L., Sun, Y., Wu, J., Zhou, Q., Huang, J., Xiong, N., & Wang, T. (2021). Targeting Microglial α -Synuclein/TLRs/NF-kappaB/NLRP3 Inflammasome Axis in Parkinson's Disease. *Frontiers in Immunology*, 12, 719807.
- Li, Y., Xia, Y., Zhu, H., Luu, E., Huang, G., Sun, Y., Sun, K., Markx, S., Leong, K. W., Xu, B., & Fu, B. M. (2021). Investigation of Neurodevelopmental Deficits of 22 q11.2 Deletion Syndrome with a Patient-iPSC-Derived Blood-Brain Barrier Model. *Cells*, 10(10), 2576.
- Liao, L.-S., Zhang, M.-W., Gu, Y.-J., & Sun, X.-C. (2020). Targeting CCL20 inhibits subarachnoid hemorrhage-related neuroinflammation in mice. *Aging (Albany NY)*, 12(14), 14849–14862.
- Liao, Y., Smyth, G. K., & Shi, W. (2014). featureCounts: An efficient general purpose program for assigning sequence reads to genomic features. *Bioinformatics*, 30(7), 923–930.
- Liao, Y., Wang, J., Jaehnig, E. J., Shi, Z., & Zhang, B. (2019). WebGestalt 2019: Gene set analysis toolkit with revamped UIs and APIs. *Nucleic Acids Research*, 47(W1), W199–W205.

- Lim, S.-H., Park, E., You, B., Jung, Y., Park, A.-R., Park, S. G., & Lee, J.-R. (2013). Neuronal Synapse Formation Induced by Microglia and Interleukin 10. *PLOS ONE*, 8(11), e81218.
- Lin, A., Forsyth, J. K., Hoftman, G. D., Kushan-Wells, L., Jalbrzikowski, M., Dokuru, D., Coppola, G., Fikinski, A., Zinkstok, J., Vorstman, J., Nachun, D., & Bearden, C. E. (2021). Transcriptomic profiling of whole blood in 22q11.2 reciprocal copy number variants reveals that cell proportion highly impacts gene expression. *Brain, Behavior, & Immunity - Health*, 18, 100386.
- Lin, H., Lee, E., Hestir, K., Leo, C., Huang, M., Bosch, E., Halenbeck, R., Wu, G., Zhou, A., Behrens, D., Hollenbaugh, D., Linnemann, T., Qin, M., Wong, J., Chu, K., Doberstein, S. K., & Williams, L. T. (2008). Discovery of a cytokine and its receptor by functional screening of the extracellular proteome. *Science (New York, N.Y.)*, 320(5877), 807–811.
- Lin, J.-R., Zhao, Y., Jabalameli, M. R., Nguyen, N., Mitra, J., Swillen, A., Vorstman, J. A. S., Chow, E. W. C., van den Bree, M., Emanuel, B. S., Vermeesch, J. R., Owen, M. J., Williams, N. M., Bassett, A. S., McDonald-McGinn, D. M., Gur, R. E., Bearden, C. E., Morrow, B. E., Lachman, H. M., & Zhang, Z. D. (2023). Rare coding variants as risk modifiers of the 22q11.2 deletion implicate postnatal cortical development in syndromic schizophrenia. *Molecular Psychiatry*, 1–10.
- Lin, M., Pedrosa, E., Hrabovsky, A., Chen, J., Puliafito, B. R., Gilbert, S. R., Zheng, D., & Lachman, H. M. (2016). Integrative transcriptome network analysis of iPSC-derived neurons from schizophrenia and schizoaffective disorder patients with 22q11.2 deletion. *BMC Systems Biology*, 10(1), 105.
- Lituma, P. J., Woo, E., O'Hara, B. F., Castillo, P. E., Sibinga, N. E. S., & Nandi, S. (2021). Altered synaptic connectivity and brain function in mice lacking microglial adapter protein Iba1. *Proceedings of the National Academy of Sciences of the United States of America*, 118(46), e2115539118.
- Liu, H., Leak, R. K., & Hu, X. (2016). Neurotransmitter receptors on microglia. *Stroke and Vascular Neurology*, 1(2), 52–58.
- Liu, J., Hong, Z., Ding, J., Liu, J., Zhang, J., & Chen, S. (2008). Predominant release of lysosomal enzymes by newborn rat microglia after LPS treatment revealed by proteomic studies. *Journal of Proteome Research*, 7(5), 2033–2049.
- Liu, L.-R., Liu, J.-C., Bao, J.-S., Bai, Q.-Q., & Wang, G.-Q. (2020). Interaction of Microglia and Astrocytes in the Neurovascular Unit. *Frontiers in Immunology*, 11, 1024.
- Liu, X., & Quan, N. (2018). Microglia and CNS Interleukin-1: Beyond Immunological Concepts. *Frontiers in Neurology*, 9.
- Lively, S., & Schlichter, L. C. (2018). Microglia Responses to Pro-inflammatory Stimuli (LPS, IFN γ +TNF α) and Reprogramming by Resolving Cytokines (IL-4, IL-10). *Frontiers in Cellular Neuroscience*, 12, 215.
- Llobet, L., Montoya, J., López-Gallardo, E., & Ruiz-Pesini, E. (2015). Side Effects of Culture Media Antibiotics on Cell Differentiation. *Tissue Engineering. Part C, Methods*, 21(11), 1143–1147.
- Lobo-Silva, D., Carriche, G. M., Castro, A. G., Roque, S., & Saraiva, M. (2016). Balancing the immune response in the brain: IL-10 and its regulation. *Journal of Neuroinflammation*, 13(1), 297.
- Loh, P.-R., Danecek, P., Palamara, P. F., Fuchsberger, C., A Reshef, Y., K Finucane, H., Schoenherr, S., Forer, L., McCarthy, S., Abecasis, G. R., Durbin, R., & L Price, A. (2016). Reference-based phasing using the Haplotype Reference Consortium panel. *Nature Genetics*, 48(11), Article 11.
- Lombardo, M. V., Moon, H. M., Su, J., Palmer, T. D., Courchesne, E., & Pramparo, T. (2018). Maternal immune activation dysregulation of the fetal brain transcriptome and relevance to the pathophysiology of autism spectrum disorder. *Molecular Psychiatry*, 23(4), 1001–1013.

- Long, D., Zhang, Y., Liu, A., Shen, L., Wei, H., Lou, Q., Hu, S., Chen, D., Chai, X., & Wang, D. (2023). Microglia sustain anterior cingulate cortex neuronal hyperactivity in nicotine-induced pain. *Journal of Neuroinflammation*, 20(1), 81.
- Lopez-Lengowski, K., Kathuria, A., & Karmacharya, R. (2021). Co-culturing microglia and cortical neurons differentiated from human induced pluripotent stem cells. *Journal of Visualized Experiments : JoVE*, 175, 10.3791/62480.
- Loram, L. C., Sholar, P. W., Taylor, F. R., Wiesler, J. L., Babb, J. A., Strand, K. A., Berkelhammer, D., Day, H. E. W., Maier, S. F., & Watkins, L. R. (2012). Sex and estradiol influence glial pro-inflammatory responses to lipopolysaccharide in rats. *Psychoneuroendocrinology*, 37(10), 1688–1699.
- Lord, C., Brugha, T. S., Charman, T., Cusack, J., Dumas, G., Frazier, T., Jones, E. J. H., Jones, R. M., Pickles, A., State, M. W., Taylor, J. L., & Veenstra-VanderWeele, J. (2020). Autism spectrum disorder. *Nature Reviews Disease Primers*, 6(1), Article 1.
- Love, M. I., Huber, W., & Anders, S. (2014). Moderated estimation of fold change and dispersion for RNA-seq data with DESeq2. *Genome Biology*, 15(12), 550.
- Lund, R. J., Nikula, T., Rahkonen, N., Närvä, E., Baker, D., Harrison, N., Andrews, P., Otonkoski, T., & Lahesmaa, T. (2012). High-throughput karyotyping of human pluripotent stem cells. *Stem Cell Res*, 9(3): 192–195.
- Lyu, J., Xie, D., Bhatia, T. N., Leak, R. K., Hu, X., & Jiang, X. (2021). Microglial/Macrophage polarization and function in brain injury and repair after stroke. *CNS Neuroscience & Therapeutics*, 27(5), 515–527.
- Macia, E., Ehrlich, M., Massol, R., Boucrot, E., Brunner, C., & Kirchhausen, T. (2006). Dynasore, a cell-permeable inhibitor of dynamin. *Developmental Cell*, 10(6), 839–850.
- Maezawa, I., & Jin, L.-W. (2010). Rett syndrome microglia damage dendrites and synapses by the elevated release of glutamate. *The Journal of Neuroscience: The Official Journal of the Society for Neuroscience*, 30(15), 5346–5356.
- Maguire, E., Connor-Robson, N., Shaw, B., O'Donoghue, R., Stöberl, N., & Hall-Roberts, H. (2022). Assaying Microglia Functions In Vitro. *Cells*, 11(21), Article 21. <https://doi.org/10.3390/cells11213414>
- Majumdar, A., Cruz, D., Asamoah, N., Buxbaum, A., Sohar, I., Lobel, P., & Maxfield, F. R. (2007). Activation of Microglia Acidifies Lysosomes and Leads to Degradation of Alzheimer Amyloid Fibrils. *Molecular Biology of the Cell*, 18(4), 1490–1496.
- Malkova, N. V., Yu, C. Z., Hsiao, E. Y., Moore, M. J., & Patterson, P. H. (2012). Maternal immune activation yields offspring displaying mouse versions of the three core symptoms of autism. *Brain, Behavior, and Immunity*, 26(4), 607–616.
- Mallach, A., Gobom, J., Arber, C., Piers, T. M., Hardy, J., Wray, S., Zetterberg, H., & Pocock, J. (2021). Differential Stimulation of Pluripotent Stem Cell-Derived Human Microglia Leads to Exosomal Proteomic Changes Affecting Neurons. *Cells*, 10(11), 2866.
- Mancuso, R., Van Den Daele, J., Fattorelli, N., Wolfs, L., Balusu, S., Burton, O., Liston, A., Sierksma, A., Fourné, Y., Poovathingal, S., Arranz-Mendigüen, A., Sala Frigerio, C., Claes, C., Serneels, L., Theys, T., Perry, V. H., Verfaillie, C., Fiers, M., & De Strooper, B. (2019). Stem-cell-derived human microglia transplanted in mouse brain to study human disease. *Nature Neuroscience*, 22(12), Article 12.
- Mandrekar, S., Jiang, Q., Lee, C. Y. D., Koenigsknecht-Talboo, J., Holtzman, D. M., & Landreth, G. E. (2009). Microglia mediate the clearance of soluble Aβ through fluid phase macropinocytosis. *The Journal of Neuroscience: The Official Journal of the Society for Neuroscience*, 29(13), 4252–4262.

- Manolio, T. A., Collins, F. S., Cox, N. J., Goldstein, D. B., Hindorff, L. A., Hunter, D. J., McCarthy, M. I., Ramos, E. M., Cardon, L. R., Chakravarti, A., Cho, J. H., Guttmacher, A. E., Kong, A., Kruglyak, L., Mardis, E., Rotimi, C. N., Slatkin, M., Valle, D., Whittemore, A. S., ... Visscher, P. M. (2009). Finding the missing heritability of complex diseases. *Nature*, 461(7265), 747–753.
- Mansur, F., Teles E Silva, A. L., Gomes, A. K. S., Magdalon, J., de Souza, J. S., Griesi-Oliveira, K., Passos-Bueno, M. R., & Sertié, A. L. (2021). Complement C4 Is Reduced in iPSC-Derived Astrocytes of Autism Spectrum Disorder Subjects. *International Journal of Molecular Sciences*, 22(14), 7579.
- Marín-Teva, J., Dusart, I., Colin, C., Gervais, A., van Rooijen, N., & Mallat, M. (2004). Microglia promote the death of developing Purkinje cells. *Neuron*, 41(4).
- Marques, T. R., Ashok, A. H., Pillinger, T., Veronese, M., Turkheimer, F. E., Dazzan, P., Sommer, I. E. C., & Howes, O. D. (2019). Neuroinflammation in schizophrenia: Meta-analysis of in vivo microglial imaging studies. *Psychological Medicine*, 49(13), 2186–2196.
- Marshall, C. R., Howrigan, D. P., Merico, D., Thiruvahindrapuram, B., Wu, W., Greer, D. S., Antaki, D., Shetty, A., Holmans, P. A., Pinto, D., Gujral, M., Brandler, W. M., Malhotra, D., Wang, Z., Fajardo, K. V. F., Maile, M. S., Ripke, S., Agartz, I., Albus, M., ... Sebat, J. (2017). Contribution of copy number variants to schizophrenia from a genome-wide study of 41,321 subjects. *Nature Genetics*, 49(1), 27–35.
- Martinez, D., Slifstein, M., Broft, A., Mawlawi, O., Hwang, D.-R., Huang, Y., Cooper, T., Kegeles, L., Zarahn, E., Abi-Dargham, A., Haber, S. N., & Laruelle, M. (2003). Imaging human mesolimbic dopamine transmission with positron emission tomography. Part II: Amphetamine-induced dopamine release in the functional subdivisions of the striatum. *Journal of Cerebral Blood Flow and Metabolism: Official Journal of the International Society of Cerebral Blood Flow and Metabolism*, 23(3), 285–300.
- Masuda, T., Sankowski, R., Staszewski, O., Böttcher, C., Amann, L., Sagar, null, Scheiwe, C., Nessler, S., Kunz, P., van Loo, G., Coenen, V. A., Reinacher, P. C., Michel, A., Sure, U., Gold, R., Grün, D., Priller, J., Stadelmann, C., Prinz, M. (2019). Spatial and temporal heterogeneity of mouse and human microglia at single-cell resolution. *Nature*, 566(7744), 388–392.
- Masuda, T., Tsuda, M., Yoshinaga, R., Tozaki-Saitoh, H., Ozato, K., Tamura, T., & Inoue, K. (2012). IRF8 is a critical transcription factor for transforming microglia into a reactive phenotype. *Cell Reports*, 1(4), 334–340.
- Matcovitch-Natan, O., Winter, D. R., Giladi, A., Vargas Aguilar, S., Spinrad, A., Sarrazin, S., Ben-Yehuda, H., David, E., Zelada González, F., Perrin, P., Keren-Shaul, H., Gury, M., Lara-Astaiso, D., Thaiss, C. A., Cohen, M., Bahar Halpern, K., Baruch, K., Deczkowska, A., Lorenzo-Vivas, E., ... Amit, I. (2016). Microglia development follows a stepwise program to regulate brain homeostasis. *Science (New York, N.Y.)*, 353(6301), aad8670.
- Matejuk, A., & Ransohoff, R. M. (2020). Crosstalk Between Astrocytes and Microglia: An Overview. *Frontiers in Immunology*, 11.
- Mattei, D., Ivanov, A., Ferrai, C., Jordan, P., Guneykaya, D., Buonfiglioli, A., Schaafsma, W., Przanowski, P., Deuther-Conrad, W., Brust, P., Hesse, S., Patt, M., Sabri, O., Ross, T. L., Eggen, B. J. L., Boddeke, E. W. G. M., Kaminska, B., Beule, D., Pombo, A., ... Wolf, S. A. (2017). Maternal immune activation results in complex microglial transcriptome signature in the adult offspring that is reversed by minocycline treatment. *Translational Psychiatry*, 7(5), e1120.
- Matthiesen, S., Jahnke, R., & Knittler, M. R. (2021). A Straightforward Hypoxic Cell Culture Method Suitable for Standard Incubators. *Methods Protoc*, 4(2): 25.
- McCutcheon, R., Beck, K., Jauhar, S., & Howes, O. D. (2018). Defining the Locus of Dopaminergic Dysfunction in Schizophrenia: A Meta-analysis and Test of the Mesolimbic Hypothesis. *Schizophrenia Bulletin*, 44(6), 1301–1311.

- McDonald-McGinn, D. M., Hain, H. S., Emanuel, B. S., & Zackai, E. H. (2020). 22q11.2 Deletion Syndrome. In M. P. Adam, G. M. Mirzaa, R. A. Pagon, S. E. Wallace, L. J. Bean, K. W. Gripp, & A. Amemiya (Eds.), *GeneReviews*®. University of Washington, Seattle.
- McDonald-McGinn, D. M., Sullivan, K. E., Marino, B., Philip, N., Swillen, A., Vorstman, J. A. S., Zackai, E. H., Emanuel, B. S., Vermeesch, J. R., Morrow, B. E., Scambler, P. J., & Bassett, A. S. (2015). 22q11.2 deletion syndrome. *Nature Reviews Disease Primers*, 1(1), Article 1.
- McDonough, A., Lee, R. V., & Weinstein, J. R. (2017). Microglial Interferon Signaling and White Matter. *Neurochemical Research*, 42(9), 2625–2638.
- McKercher, S. R., Torbett, B. E., Anderson, K. L., Henkel, G. W., Vestal, D. J., Baribault, H., Klemsz, M., Feeney, A. J., Wu, G. E., Paige, C. J., & Maki, R. A. (1996). Targeted disruption of the PU.1 gene results in multiple hematopoietic abnormalities. *The EMBO Journal*, 15(20), 5647–5658.
- McNamara, N. B., Munro, D. A. D., Bestard-Cuche, N., Uyeda, A., Bogie, J. F. J., Hoffmann, A., Holloway, R. K., Molina-Gonzalez, I., Askew, K. E., Mitchell, S., Mungall, W., Dodds, M., Dittmayer, C., Moss, J., Rose, J., Szymkowiak, S., Amann, L., McColl, B. W., Prinz, M., ... Miron, V. E. (2023). Microglia regulate central nervous system myelin growth and integrity. *Nature*, 613(7942), Article 7942.
- McQuade, A., Coburn, M., Tu, C. H., Hasselmann, J., Davtyan, H., & Blurton-Jones, M. (2018). Development and validation of a simplified method to generate human microglia from pluripotent stem cells. *Molecular Neurodegeneration*, 13(1), 67.
- Mekori-Domachevsky, E., Taler, M., Shoenfeld, Y., Gurevich, M., Sonis, P., Weisman, O., Weizman, A., & Gothelf, D. (2017). Elevated Proinflammatory Markers in 22q11.2 Deletion Syndrome Are Associated With Psychosis and Cognitive Deficits. *The Journal of Clinical Psychiatry*, 78(9), 9052.
- Melief, J., Koning, N., Schuurman, K. G., Van De Garde, M. D. B., Smolders, J., Hoek, R. M., Van Eijk, M., Hamann, J., & Huitinga, I. (2012). Phenotyping primary human microglia: Tight regulation of LPS responsiveness. *Glia*, 60(10), 1506–1517.
- Menassa, D. A., & Gomez-Nicola, D. (2018). Microglial Dynamics During Human Brain Development. *Frontiers in Immunology*, 9, 1014.
- Menassa, D. A., Muntslag, T. A. O., Martin-Estebané, M., Barry-Carroll, L., Chapman, M. A., Adorjan, I., Tyler, T., Turnbull, B., Rose-Zerilli, M. J. J., Nicoll, J. A. R., Krsnik, Z., Kostovic, I., & Gomez-Nicola, D. (2022). The spatiotemporal dynamics of microglia across the human lifespan. *Developmental Cell*, 57(17), 2127–2139.e6.
- Mendizabal, I., Berto, S., Usui, N., Toriumi, K., Chatterjee, P., Douglas, C., Huh, I., Jeong, H., Layman, T., Tamminga, C. A., Preuss, T. M., Konopka, G., & Yi, S. V. (2019). Cell type-specific epigenetic links to schizophrenia risk in the brain. *Genome Biology*, 20(1), 135.
- Meng, J., Han, L., Zheng, N., Wang, T., Xu, H., Jiang, Y., Wang, Z., Liu, Z., Zheng, Q., Zhang, X., Luo, H., Can, D., Lu, J., Xu, H., & Zhang, Y. (2022). Microglial Tmem59 Deficiency Impairs Phagocytosis of Synapse and Leads to Autism-Like Behaviors in Mice. *The Journal of Neuroscience*, 42(25), 4958–4979.
- Migliaccio, G., Migliaccio, A. R., Petti, S., Mavilio, F., Russo, G., Lazzaro, D., Testa, U., Marinucci, M., & Peschle, C. (1986). Human embryonic hemopoiesis. Kinetics of progenitors and precursors underlying the yolk sac—Liver transition. *The Journal of Clinical Investigation*, 78(1), 51–60.
- Miller, B. J., Buckley, P., Seabolt, W., Mellor, A., & Kirkpatrick, B. (2011). Meta-Analysis of Cytokine Alterations in Schizophrenia: Clinical Status and Antipsychotic Effects. *Biological Psychiatry*, 70(7), 663–671.

- Miller, J. A., Woltjer, R. L., Goodenbour, J. M., Horvath, S., & Geschwind, D. H. (2013). Genes and pathways underlying regional and cell type changes in Alzheimer's disease. *Genome Medicine*, 5(5), 48.
- Minkiewicz, J., de Rivero Vaccari, J. P., & Keane, R. W. (2013). Human astrocytes express a novel NLRP2 inflammasome. *Glia*, 61(7), 1113–1121.
- Miyamoto, A., Wake, H., Ishikawa, A. W., Eto, K., Shibata, K., Murakoshi, H., Koizumi, S., Moorhouse, A. J., Yoshimura, Y., & Nabekura, J. (2016). Microglia contact induces synapse formation in developing somatosensory cortex. *Nature Communications*, 7(1), Article 1.
- Modabbernia, A., Velthorst, E., & Reichenberg, A. (2017). Environmental risk factors for autism: An evidence-based review of systematic reviews and meta-analyses. *Molecular Autism*, 8, 13.
- Mohammadi, A., Rashidi, E., & Amooeian, V. G. (2018). Brain, blood, cerebrospinal fluid, and serum biomarkers in schizophrenia. *Psychiatry Research*, 265, 25–38.
- Mondelli, V., Vernon, A. C., Turkheimer, F., Dazzan, P., & Pariante, C. M. (2017). Brain microglia in psychiatric disorders. *The Lancet. Psychiatry*, 4(7), 563–572.
- Monfared, R. V., Alhassen, W., Truong, T. M., Gonzales, M. A. M., Vachirakorntong, V., Chen, S., Baldi, P., Civelli, O., & Alachkar, A. (2021). Transcriptome Profiling of Dysregulated GPCRs Reveals Overlapping Patterns across Psychiatric Disorders and Age-Disease Interactions. *Cells*, 10(11), 2967.
- Monier, A., Adle-Biasette, H., Delezoide, A.-L., Evrard, P., Gressens, P., & Verney, C. (2007). Entry and distribution of microglial cells in human embryonic and fetal cerebral cortex. *Journal of Neuropathology and Experimental Neurology*, 66(5), 372–382.
- Monier, A., Evrard, P., Gressens, P., & Verney, C. (2006). Distribution and differentiation of microglia in the human encephalon during the first two trimesters of gestation. *The Journal of Comparative Neurology*, 499(4), 565–582.
- Montilla, A., Ruiz, A., Marquez, M., Sierra, A., Matute, C., & Domercq, M. (2021). Role of Mitochondrial Dynamics in Microglial Activation and Metabolic Switch. *ImmunoHorizons*, 5(8), 615–626.
- Morgan, J. T., Chana, G., Pardo, C. A., Achim, C., Semendeferi, K., Buckwalter, J., Courchesne, E., & Everall, I. P. (2010). Microglial Activation and Increased Microglial Density Observed in the Dorsolateral Prefrontal Cortex in Autism. *Biological Psychiatry*, 68(4), 368–376.
- Morsch, M., Radford, R., Lee, A., Don, E. K., Badrock, A. P., Hall, T. E., Cole, N. J., & Chung, R. (2015). In vivo characterization of microglial engulfment of dying neurons in the zebrafish spinal cord. *Frontiers in Cellular Neuroscience*, 9, 321.
- Mueller, F. S., Scarborough, J., Schalbetter, S. M., Richetto, J., Kim, E., Couch, A., Yee, Y., Lerch, J. P., Vernon, A. C., Weber-Stadlbauer, U., & Meyer, U. (2021). Behavioral, neuroanatomical, and molecular correlates of resilience and susceptibility to maternal immune activation. *Molecular Psychiatry*, 26(2), Article 2.
- Muffat, J., Li, Y., Yuan, B., Mitalipova, M., Omer, A., Corcoran, S., Bakiasi, G., Tsai, L.-H., Aubourg, P., Ransohoff, R. M., & Jaenisch, R. (2016). Efficient derivation of microglia-like cells from human pluripotent stem cells. *Nature Medicine*, 22(11), 1358–1367.
- Mukai, J., Cannavò, E., Crabtree, G. W., Sun, Z., Diamantopoulou, A., Thakur, P., Chang, C.-Y., Cai, Y., Lomvardas, S., Takata, A., Xu, B., & Gogos, J. A. (2019). Recapitulation and Reversal of Schizophrenia-Related Phenotypes in Setd1a-Deficient Mice. *Neuron*, 104(3), 471–487.e12.
- Mullins, N., Forstner, A. J., O'Connell, K. S., Coombes, B., Coleman, J. R. I., Qiao, Z., Als, T. D., Bigdeli, T. B., Børte, S., Bryois, J., Charney, A. W., Drange, O. K., Gandal, M. J., Hagensaars, S. P., Ikeda, M.,

- Kamitaki, N., Kim, M., Krebs, K., Panagiotaropoulou, G., ... Andreassen, O. A. (2021). Genome-wide association study of more than 40,000 bipolar disorder cases provides new insights into the underlying biology. *Nature Genetics*, 53(6), 817–829.
- Murabe, Y., & Sano, Y. (1982). Morphological studies on neuroglia. VI. Postnatal development of microglial cells. *Cell and Tissue Research*, 225(3), 469–485.
- Murabe, Y., & Sano, Y. (1983). Morphological studies on neuroglia. VII. Distribution of ‘brain macrophages’ in brains of neonatal and adult rats, as determined by means of immunohistochemistry. *Cell and Tissue Research*, 229(1), 85–95.
- Murai, N., Mitalipova, M., & Jaenisch, R. (2020). Functional analysis of CX3CR1 in human induced pluripotent stem (iPS) cell-derived microglia-like cells. *The European Journal of Neuroscience*, 52(7), 3667–3678.
- Murphy, C. E., Lawther, A. J., Webster, M. J., Asai, M., Kondo, Y., Matsumoto, M., Walker, A. K., & Weickert, C. S. (2020). Nuclear factor kappa B activation appears weaker in schizophrenia patients with high brain cytokines than in non-schizophrenic controls with high brain cytokines. *Journal of Neuroinflammation*, 17(1), 215.
- Murphy, C. E., Walker, A. K., O'Donnell, M., Galletly, C., Lloyd, A. R., Liu, D., Weickert, C. S., & Weickert, T. W. (2022). Peripheral NF-κB dysregulation in people with schizophrenia drives inflammation: Putative anti-inflammatory functions of NF-κB kinases. *Translational Psychiatry*, 12(1), Article 1.
- Murphy, K. C., Jones, L. A., & Owen, M. J. (1999). High Rates of Schizophrenia in Adults With Velo-Cardio-Facial Syndrome. *Archives of General Psychiatry*, 56(10), 940–945.
- Musi, C. A., Agrò, G., Santarella, F., Iervasi, E., & Borsello, T. (2020). JNK3 as Therapeutic Target and Biomarker in Neurodegenerative and Neurodevelopmental Brain Diseases. *Cells*, 9(10), E2190.
- Nagata, K., Nakajima, K., Takemoto, N., Saito, H., & Kohsaka, S. (1993). Microglia-derived plasminogen enhances neurite outgrowth from explant cultures of rat brain. *International Journal of Developmental Neuroscience: The Official Journal of the International Society for Developmental Neuroscience*, 11(2), 227–237.
- Nakamura, Y., Si, Q. S., & Kataoka, K. (1999). Lipopolysaccharide-induced microglial activation in culture: Temporal profiles of morphological change and release of cytokines and nitric oxide. *Neuroscience Research*, 35(2), 95–100.
- Nalls, M. A., Blauwendraat, C., Vallerger, C. L., Heilbron, K., Bandres-Ciga, S., Chang, D., Tan, M., Kia, D. A., Noyce, A. J., Xue, A., Bras, J., Young, E., von Coelln, R., Simón-Sánchez, J., Schulte, C., Sharma, M., Krohn, L., Pihlström, L., Siitonen, A., ... Zhang, F. (2019). Identification of novel risk loci, causal insights, and heritable risk for Parkinson's disease: A meta-analysis of genome-wide association studies. *The Lancet Neurology*, 18(12), 1091–1102.
- Napoli, E., Tassone, F., Wong, S., Angkustsiri, K., Simon, T. J., Song, G., & Giulivi, C. (2015). Mitochondrial Citrate Transporter-dependent Metabolic Signature in the 22q11.2 Deletion Syndrome *. *Journal of Biological Chemistry*, 290(38), 23240–23253.
- Nasyrova, R. F., Ivashchenko, D. V., Ivanov, M. V., & Neznanov, N. G. (2015). Role of nitric oxide and related molecules in schizophrenia pathogenesis: Biochemical, genetic and clinical aspects. *Frontiers in Physiology*, 6, 139.
- Naudin, J., Mège, J. L., Azorin, J. M., & Dassa, D. (1996). Elevated circulating levels of IL-6 in schizophrenia. *Schizophrenia Research*, 20(3), 269–273.
- Nehme, R., Pietiläinen, O., Artomov, M., Tegtmeier, M., Valakh, V., Lehtonen, L., Bell, C., Singh, T., Trehan, A., Sherwood, J., Manning, D., Peirent, E., Malik, R., Guss, E. J., Hawes, D., Beccard, A., Bara, A. M.,

- Hazelbaker, D. Z., Zuccaro, E., ... Eggen, K. (2022). The 22q11.2 region regulates presynaptic gene-products linked to schizophrenia. *Nature Communications*, 13, 3690.
- Nelson, L. H., & Lenz, K. M. (2017). Microglia depletion in early life programs persistent changes in social, mood-related, and locomotor behavior in male and female rats. *Behavioural Brain Research*, 316, 279–293.
- Nelson, L. H., Warden, S., & Lenz, K. M. (2017). Sex differences in microglial phagocytosis in the neonatal hippocampus. *Brain, Behavior, and Immunity*, 64, 11–22.
- Niarchou, M., Calkins, M. E., Moore, T. M., Tang, S. X., McDonald-McGinn, D. M., Zackai, E. H., Emanuel, B. S., Gur, R. C., & Gur, R. E. (2018). Attention Deficit Hyperactivity Disorder Symptoms and Psychosis in 22q11.2 Deletion Syndrome. *Schizophrenia Bulletin*, 44(4), 824–833.
- Nimmerjahn, A., Kirchhoff, F., & Helmchen, F. (2005). Resting microglial cells are highly dynamic surveillants of brain parenchyma in vivo. *Science (New York, N.Y.)*, 308(5726), 1314–1318.
- Niraula, A., Sheridan, J. F., & Godbout, J. P. (2017). Microglia Priming with Aging and Stress. *Neuropsychopharmacology: Official Publication of the American College of Neuropsychopharmacology*, 42(1), 318–333.
- Norden, D. M., Muccigrosso, M. M., & Godbout, J. P. (2015). Microglial Priming and Enhanced Reactivity to Secondary Insult in Aging, and Traumatic CNS injury, and Neurodegenerative Disease. *Neuropharmacology*, 96(0 0), 29–41.
- Notter, T., Coughlin, J. M., Gschwind, T., Weber-Stadlbauer, U., Wang, Y., Kassiou, M., Vernon, A. C., Benke, D., Pomper, M. G., Sawa, A., & Meyer, U. (2018). Translational evaluation of translocator protein as a marker of neuroinflammation in schizophrenia. *Molecular Psychiatry*, 23(2), 323–334.
- Nygaard, A. B., Jørgensen, C. B., Cirera, S., & Fredholm, M. (2007). Selection of reference genes for gene expression studies in pig tissues using SYBR green qPCR. *BMC Mol Biol*, 8: 67.
- Obst, J., Hall-Roberts, H. L., Smith, T. B., Kreuzer, M., Magno, L., Di Daniel, E., Davis, J. B., & Mead, E. (2021). PLCγ2 regulates TREM2 signalling and integrin-mediated adhesion and migration of human iPSC-derived macrophages. *Scientific Reports*, 11(1), Article 1.
- Oehmichen, M., Wiethölter, H., & Greaves, M. F. (1979). Immunological Analysis of Human Microglia: Lack of Monocytic and Lymphoid Membrane Differentiation Antigens. *Journal of Neuropathology & Experimental Neurology*, 38(2), 99–103.
- Oehmichen, M., Wiethölter, H., Grüniger, H., & Gencic, M. (1979). Features and distribution of intracerebrally injected peritoneal macrophages. *Experimentelle Pathologie*, 17(2), 71–76.
- Ohsawa, K., Imai, Y., Sasaki, Y., & Kohsaka, S. (2004). Microglia/macrophage-specific protein Iba1 binds to fimbria and enhances its actin-bundling activity. *Journal of Neurochemistry*, 88(4), 844–856.
- Okarmus, J., Havelund, J. F., Ryding, M., Schmidt, S. I., Bogetofte, H., Heon-Roberts, R., Wade-Martins, R., Cowley, S. A., Ryan, B. J., Færgeman, N. J., Hyttel, P., & Meyer, M. (2021). Identification of bioactive metabolites in human iPSC-derived dopaminergic neurons with PARK2 mutation: Altered mitochondrial and energy metabolism. *Stem Cell Reports*, 16(6), 1510–1526.
- Olah, M., Menon, V., Habib, N., Taga, M. F., Ma, Y., Yung, C. J., Cimpean, M., Khairallah, A., Coronas-Samano, G., Sankowski, R., Grün, D., Kroshilina, A. A., Dionne, D., Sarkis, R. A., Cosgrove, G. R., Helgager, J., Golden, J. A., Pennell, P. B., Prinz, M., ... De Jager, P. L. (2020). Single cell RNA sequencing of human microglia uncovers a subset associated with Alzheimer's disease. *Nature Communications*, 11(1), Article 1.

- Onay, H., Kacamak, D., Kavasoglu, A. N., Akgun, B., Yalcinli, M., Kose, S., & Ozbaran, B. (2016). Mutation analysis of the NRXN1 gene in autism spectrum disorders. *Balkan Journal of Medical Genetics: BJMG*, 19(2), 17–22.
- Ormel, P. R., Böttcher, C., Gigase, F. A. J., Missall, R. D., van Zuiden, W., Fernández Zapata, M. C., Ilhan, D., de Goeij, M., Udine, E., Sommer, I. E. C., Priller, J., Raj, T., Kahn, R. S., Hol, E. M., & de Witte, L. D. (2020). A characterization of the molecular phenotype and inflammatory response of schizophrenia patient-derived microglia-like cells. *Brain, Behavior, and Immunity*, 90, 196–207.
- Ormel, P. R., Vieira de Sá, R., van Bodegraven, E. J., Karst, H., Harschnitz, O., Sneeboer, M. A. M., Johansen, L. E., van Dijk, R. E., Scheefhals, N., Berdenis van Berlekom, A., Ribes Martínez, E., Kling, S., MacGillavry, H. D., van den Berg, L. H., Kahn, R. S., Hol, E. M., de Witte, L. D., & Pasterkamp, R. J. (2018). Microglia innately develop within cerebral organoids. *Nature Communications*, 9(1), 4167.
- Osimo, E. F., Beck, K., Reis Marques, T., & Howes, O. D. (2019). Synaptic loss in schizophrenia: A meta-analysis and systematic review of synaptic protein and mRNA measures. *Molecular Psychiatry*, 24(4), Article 4.
- Ouchi, Y., Banno, Y., Shimizu, Y., Ando, S., Hasegawa, H., Adachi, K., & Iwamoto, T. (2013). Reduced Adult Hippocampal Neurogenesis and Working Memory Deficits in the Dgcr8-Deficient Mouse Model of 22q11.2 Deletion-Associated Schizophrenia Can Be Rescued by IGF2. *Journal of Neuroscience*, 33(22), 9408–9419.
- Ousley, O., Evans, A. N., Fernandez-Carriba, S., Smearman, E. L., Rockers, K., Morrier, M. J., Evans, D. W., Coleman, K., & Cubells, J. (2017a). Examining the Overlap between Autism Spectrum Disorder and 22q11.2 Deletion Syndrome. *International Journal of Molecular Sciences*, 18(5), 1071.
- Ousley, O., Evans, A. N., Fernandez-Carriba, S., Smearman, E. L., Rockers, K., Morrier, M. J., Evans, D. W., Coleman, K., & Cubells, J. (2017b). Examining the Overlap between Autism Spectrum Disorder and 22q11.2 Deletion Syndrome. *International Journal of Molecular Sciences*, 18(5), 1071.
- Owen, D. R., Narayan, N., Wells, L., Healy, L., Smyth, E., Rabiner, E. A., Galloway, D., Williams, J. B., Lehr, J., Mandhair, H., Peferoen, L. A., Taylor, P. C., Amor, S., Antel, J. P., Matthews, P. M., & Moore, C. S. (2017). Pro-inflammatory activation of primary microglia and macrophages increases 18 kDa translocator protein expression in rodents but not humans. *Journal of Cerebral Blood Flow and Metabolism: Official Journal of the International Society of Cerebral Blood Flow and Metabolism*, 37(8), 2679–2690.
- Ozaki, K., Kato, D., Ikegami, A., Hashimoto, A., Sugio, S., Guo, Z., Shibushita, M., Tatematsu, T., Haruwaka, K., Moorhouse, A. J., Yamada, H., & Wake, H. (2020). Maternal immune activation induces sustained changes in fetal microglia motility. *Scientific Reports*, 10(1), 21378.
- Page, S. C., Sripathy, S. R., Farinelli, F., Ye, Z., Wang, Y., Hiler, D. J., Pattie, E. A., Nguyen, C. V., Tippani, M., Moses, R. L., Chen, H.-Y., Tran, M. N., Eagles, N. J., Stolz, J. M., Catallini, J. L., Soudry, O. R., Dickinson, D., Berman, K. F., Apud, J. A., ... Maher, B. J. (2022). Electrophysiological measures from human iPSC-derived neurons are associated with schizophrenia clinical status and predict individual cognitive performance. *Proceedings of the National Academy of Sciences of the United States of America*, 119(3), e2109395119.
- Palin, K., Cunningham, C., Forse, P., Perry, V. H., & Platt, N. (2008). Systemic inflammation switches the inflammatory cytokine profile in CNS Wallerian degeneration. *Neurobiology of Disease*, 30(1), 19–29.
- Pan, K., & Garaschuk, O. (2022). The role of intracellular calcium-store-mediated calcium signals in in vivo sensor and effector functions of microglia. *The Journal of Physiology*.
- Pandya, H., Shen, M. J., Ichikawa, D. M., Sedlock, A. B., Choi, Y., Johnson, K. R., Kim, G., Brown, M. A., Elkhouloun, A. G., Maric, D., Sweeney, C. L., Gossa, S., Malech, H. L., McGavern, D. B., & Park, J. K.

- (2017). Differentiation of human and murine induced pluripotent stem cells to microglia-like cells. *Nature Neuroscience*, 20(5), 753–759.
- Paolicelli, R. C., Bolasco, G., Pagani, F., Maggi, L., Scianni, M., Panzanelli, P., Giustetto, M., Ferreira, T. A., Guiducci, E., Dumas, L., Ragozzino, D., & Gross, C. T. (2011). Synaptic Pruning by Microglia Is Necessary for Normal Brain Development. *Science*, 333(6048), 1456–1458.
- Paolicelli, R. C., & Ferretti, M. T. (2017). Function and Dysfunction of Microglia during Brain Development: Consequences for Synapses and Neural Circuits. *Frontiers in Synaptic Neuroscience*, 9, 9.
- Paolicelli, R. C., Sierra, A., Stevens, B., Tremblay, M.-E., Aguzzi, A., Ajami, B., Amit, I., Audinat, E., Bechmann, I., Bennett, M., Bennett, F., Bessis, A., Biber, K., Bilbo, S., Blurton-Jones, M., Boddeke, E., Brites, D., Brône, B., Brown, G. C., ... Wyss-Coray, T. (2022). Microglia states and nomenclature: A field at its crossroads. *Neuron*, 110(21), 3458–3483.
- Papageorgiou, I. E., Lewen, A., Galow, L. V., Cesetti, T., Scheffel, J., Regen, T., Hanisch, U.-K., & Kann, O. (2016). TLR4-activated microglia require IFN- γ to induce severe neuronal dysfunction and death in situ. *Proceedings of the National Academy of Sciences of the United States of America*, 113(1), 212–217.
- Papatheodorou, I., Moreno, P., Manning, J., Fuentes, A. M.-P., George, N., Fexova, S., Fonseca, N. A., Füllgrabe, A., Green, M., Huang, N., Huerta, L., Iqbal, H., Jianu, M., Mohammed, S., Zhao, L., Jarnuczak, A. F., Jupp, S., Marioni, J., Meyer, K., ... Brazma, A. (2020). Expression Atlas update: From tissues to single cells. *Nucleic Acids Research*, 48(D1), D77–D83.
- Papazian, I., Tsoukala, E., Boutou, A., Karamita, M., Kambas, K., Iliopoulou, L., Fischer, R., Kontermann, R. E., Denis, M. C., Kollias, G., Lassmann, H., & Probert, L. (2021). Fundamentally different roles of neuronal TNF receptors in CNS pathology: TNFR1 and IKK β promote microglial responses and tissue injury in demyelination while TNFR2 protects against excitotoxicity in mice. *Journal of Neuroinflammation*, 18(1), 222.
- Pape, K., Tamouza, R., Leboyer, M., & Zipp, F. (2019). Immunoneuropsychiatry—Novel perspectives on brain disorders. *Nature Reviews Neurology*, 15(6), Article 6.
- Parakalan, R., Jiang, B., Nimmi, B., Janani, M., Jayapal, M., Lu, J., Tay, S. S. W., Ling, E.-A., & Dheen, S. T. (2012). Transcriptome analysis of amoeboid and ramified microglia isolated from the corpus callosum of rat brain. *BMC Neuroscience*, 13, 64.
- Paraschivescu, C., Barbosa, S., Lorivel, T., Glaichenhaus, N., & Davidovic, L. (2020). Cytokine changes associated with the maternal immune activation (MIA) model of autism: A penalized regression approach. *PLoS ONE*, 15(8), e0231609.
- Pardo, C. A., Vargas, D. L., & Zimmerman, A. W. (2005). Immunity, neuroglia and neuroinflammation in autism. *International Review of Psychiatry (Abingdon, England)*, 17(6), 485–495.
- Park, G.-H., Noh, H., Shao, Z., Ni, P., Qin, Y., Liu, D., Beaudreault, C. P., Park, J. S., Abani, C. P., Park, J. M., Le, D. T., Gonzalez, S. Z., Guan, Y., Cohen, B. M., McPhie, D. L., Coyle, J. T., Lanz, T. A., Xi, H. S., Yin, C., ... Chung, S. (2020). Activated microglia cause metabolic disruptions in developmental cortical interneuron that persist in schizophrenia-patient-derived interneurons. *Nature Neuroscience*, 23(11), 1352–1364.
- Parrott, J. M., Oster, T., & Lee, H. Y. (2021). Altered inflammatory response in FMRP-deficient microglia. *iScience*, 24(11), 103293.
- Patel, K. R., Cherian, J., Gohil, K., & Atkinson, D. (2014). Schizophrenia: Overview and Treatment Options. *Pharmacy and Therapeutics*, 39(9), 638–645.

- Patel, T., Carnwath, T. P., Wang, X., Allen, M., Lincoln, S. J., Lewis-Tuffin, L. J., Quicksall, Z. S., Lin, S., Tutor-New, F. Q., Ho, C. C. G., Min, Y., Malphrus, K. G., Nguyen, T. T., Martin, E., Garcia, C. A., Alkharboosh, R. M., Grewal, S., Chaichana, K., Wharen, R., ... Ertekin-Taner, N. (2022). Transcriptional landscape of human microglia implicates age, sex, and APOE-related immunometabolic pathway perturbations. *Aging Cell*, 21(5), e13606.
- Patlak, C. S., Blasberg, R. G., & Fenstermacher, J. D. (1983). Graphical evaluation of blood-to-brain transfer constants from multiple-time uptake data. *Journal of Cerebral Blood Flow and Metabolism: Official Journal of the International Society of Cerebral Blood Flow and Metabolism*, 3(1), 1–7.
- Pereira, O. R., Ramos, V. M., Cabral-Costa, J. V., & Kowaltowski, A. J. (2021). Changes in mitochondrial morphology modulate LPS-induced loss of calcium homeostasis in BV-2 microglial cells. *Journal of Bioenergetics and Biomembranes*, 53(2), 109–118.
- Peri, F., & Nüsslein-Volhard, C. (2008). Live imaging of neuronal degradation by microglia reveals a role for v0-ATPase a1 in phagosomal fusion in vivo. *Cell*, 133(5), 916–927.
- Perry, V. H., Hume, D. A., & Gordon, S. (1985). Immunohistochemical localization of macrophages and microglia in the adult and developing mouse brain. *Neuroscience*, 15(2), 313–326.
- Petanjek, Z., Berger, B., & Esclapez, M. (2009). Origins of cortical GABAergic neurons in the cynomolgus monkey. *Cerebral Cortex (New York, N.Y.: 1991)*, 19(2), 249–262.
- Pey, P., Pearce, R. K., Kalaitzakis, M. E., Griffin, W. S., & Gentleman, S. M. (2014). Phenotypic profile of alternative activation marker CD163 is different in Alzheimer's and Parkinson's disease. *21*.
- Piers, T. M., Cosker, K., Mallach, A., Johnson, G. T., Guerreiro, R., Hardy, J., & Pocock, J. M. (2020). A locked immunometabolic switch underlies TREM2 R47H loss of function in human iPSC-derived microglia. *The FASEB Journal*, 34(2), 2436–2450. <https://doi.org/10.1096/fj.201902447R>
- Pike, A. F., Longhena, F., Faustini, G., van Eik, J.-M., Gombert, I., Herrebout, M. A. C., Fayed, M. M. H. E., Sandre, M., Varanita, T., Teunissen, C. E., Hoozemans, J. J. M., Bellucci, A., Veerhuis, R., & Bubacco, L. (2022). Dopamine signaling modulates microglial NLRP3 inflammasome activation: Implications for Parkinson's disease. *Journal of Neuroinflammation*, 19(1), 50.
- Pimenova, A. A., Herbinet, M., Gupta, I., Machlovi, S. I., Bowles, K. R., Marcora, E., & Goate, A. M. (2021). Alzheimer's-associated PU.1 expression levels regulate microglial inflammatory response. *Neurobiology of Disease*, 148, 105217. <https://doi.org/10.1016/j.nbd.2020.105217>
- Pimenova, A. A., Herbinet, M., Gupta, I., Machlovi, S., Marcora, E., & Goate, A. M. (2020). Protective low expression of PU.1 reduces microglial inflammatory and phagocytic response. *Alzheimer's & Dementia*, 16(S2), e041201.
- Plavén-Sigray, P., Matheson, G. J., Collste, K., Ashok, A. H., Coughlin, J. M., Howes, O. D., Mizrahi, R., Pomper, M. G., Rusjan, P., Veronese, M., Wang, Y., & Cervenka, S. (2018). Positron Emission Tomography Studies of the Glial Cell Marker Translocator Protein in Patients With Psychosis: A Meta-analysis Using Individual Participant Data. *Biological Psychiatry*, 84(6), 433–442.
- Poetsch, M. S., Strano, A., & Guan, K. (2022). Human Induced Pluripotent Stem Cells: From Cell Origin, Genomic Stability, and Epigenetic Memory to Translational Medicine. *Stem Cells*, 40(6), 546–555.
- Polazzi, E., Altamira, L. E. P., Eleuteri, S., Barbaro, R., Casadio, C., Contestabile, A., & Monti, B. (2009). Neuroprotection of microglial conditioned medium on 6-hydroxydopamine-induced neuronal death: Role of transforming growth factor beta-2. *Journal of Neurochemistry*, 110(2), 545–556.
- Polit, L. D., Eidhof, I., McNeill, R. V., Warre-Cornish, K. M., Ohki, C. M. Y., Walter, N. M., Sala, C., Verpelli, C., Radtke, F., Galderisi, S., Mucci, A., Collo, G., Edenhofer, F., Castrén, M. L., Réthelyi, J. M.,

- Ejlersen, M., Hohmann, S. S., Ilieva, M. S., Lukjanska, R., ... Srivastava, D. P. (2023). Recommendations, guidelines, and best practice for the use of human induced pluripotent stem cells for neuropharmacological studies of neuropsychiatric disorders. *Neuroscience Applied*, 101125.
- Potkin, S. G., Kane, J. M., Correll, C. U., Lindenmayer, J.-P., Agid, O., Marder, S. R., Olfson, M., & Howes, O. D. (2020). The neurobiology of treatment-resistant schizophrenia: Paths to antipsychotic resistance and a roadmap for future research. *NPJ Schizophrenia*, 6(1), 1.
- Potvin, S., Stip, E., Sepehry, A. A., Gendron, A., Bah, R., & Kouassi, E. (2008). Inflammatory Cytokine Alterations in Schizophrenia: A Systematic Quantitative Review. *Biological Psychiatry*, 63(8), 801–808.
- Pourhamzeh, M., Moravej, F. G., Arabi, M., Shahriari, E., Mehrabi, S., Ward, R., Ahadi, R., & Joghataei, M. T. (2022). The Roles of Serotonin in Neuropsychiatric Disorders. *Cellular and Molecular Neurobiology*, 42(6), 1671–1692.
- Pulido-Salgado, M., Vidal-Taboada, J. M., Barriga, G. G.-D., Solà, C., & Saura, J. (2018). RNA-Seq transcriptomic profiling of primary murine microglia treated with LPS or LPS + IFN γ . *Scientific Reports*, 8, 16096.
- Qin, H., Holdbrooks, A. T., Liu, Y., Reynolds, S. L., Yanagisawa, L. L., & Benveniste, E. N. (2012). SOCS3 Deficiency Promotes M1 Macrophage Polarization and Inflammation. *Journal of Immunology (Baltimore, Md. : 1950)*, 189(7), 3439–3448.
- Raje, N. R., Noel-MacDonnell, J. R., Shortt, K. A., Gigliotti, N. M., Chan, M. A., & Heruth, D. P. (2022). T Cell Transcriptome in Chromosome 22q11.2 Deletion Syndrome. *Journal of Immunology (Baltimore, Md.: 1950)*, 209(5), 874–885.
- Rakic, P. (1988). Specification of cerebral cortical areas. *Science (New York, N.Y.)*, 241(4862), 170–176.
- Ramachandran, P. V., Savini, M., Folick, A. K., Hu, K., Masand, R., Graham, B. H., & Wang, M. C. (2019). Lysosomal Signaling Promotes Longevity through Adjusting Mitochondrial Activity. *Developmental Cell*, 48(5), 685–696.e5.
- Ramaglia, V., Hughes, T. R., Donev, R. M., Ruseva, M. M., Wu, X., Huitinga, I., Baas, F., Neal, J. W., & Morgan, B. P. (2012). C3-dependent mechanism of microglial priming relevant to multiple sclerosis. *Proceedings of the National Academy of Sciences of the United States of America*, 109(3), 965–970.
- Ransohoff, R. M. (2016). A polarizing question: Do M1 and M2 microglia exist? *Nature Neuroscience*, 19(8), Article 8.
- Rees, E., Kirov, G., Sanders, A., Walters, J. T. R., Chambert, K. D., Shi, J., Szatkiewicz, J., O'Dushlaine, C., Richards, A. L., Green, E. K., Jones, I., Davies, G., Legge, S. E., Moran, J. L., Pato, C., Pato, M., Genovese, G., Levinson, D., Duan, J., ... Owen, M. J. (2014). Evidence that duplications of 22q11.2 protect against schizophrenia. *Molecular Psychiatry*, 19(1), 37–40.
- Reich, M., Paris, I., Ebeling, M., Dahm, N., Schweitzer, C., Reinhardt, D., Schmucki, R., Prasad, M., Köchl, F., Leist, M., Cowley, S. A., Zhang, J. D., Patsch, C., Gutbier, S., & Britschgi, M. (2021). Alzheimer's Risk Gene TREM2 Determines Functional Properties of New Type of Human iPSC-Derived Microglia. *Frontiers in Immunology*, 11, 617860.
- Reid, M. J., Rogdaki, M., Dutan, L., Hanger, B., Sabad, K., Nagy, R., Adhya, D., Baron-Cohen, S., McAlonan, G., Price, J., Vernon, A. C., Howes, O. D., & Srivastava, D. P. (2022). Cell line specific alterations in genes associated with dopamine metabolism and signaling in midbrain dopaminergic neurons derived from 22q11.2 deletion carriers with elevated dopamine synthesis capacity. *Schizophrenia Research*, S0920-9964(22)00184-0.

- Rennick, J. J., Johnston, A. P. R., & Parton, R. G. (2021). Key principles and methods for studying the endocytosis of biological and nanoparticle therapeutics. *Nature Nanotechnology*, 16(3), Article 3.
- Réu, P., Khosravi, A., Bernard, S., Mold, J. E., Salehpour, M., Alkass, K., Perl, S., Tisdale, J., Possnert, G., Druid, H., & Frisén, J. (2017). The Lifespan and Turnover of Microglia in the Human Brain. *Cell Reports*, 20(4), 779–784.
- Rezaie, P., Bohl, J., & Ulfing, N. (2004). Anomalous alterations affecting microglia in the central nervous system of a fetus at 12 weeks of gestation: Case report. *Acta Neuropathologica*, 107(2), 176–180.
- Rezaie, P., & Male, D. (1999). Colonisation of the developing human brain and spinal cord by microglia: A review. *Microscopy Research and Technique*, 45(6), 359–382.
- Ribolsi, M., Fiori Nastro, F., Pelle, M., Medici, C., Sacchetto, S., Lisi, G., Riccioni, A., Siracusano, M., Mazzone, L., & Di Lorenzo, G. (2022). Recognizing Psychosis in Autism Spectrum Disorder. *Frontiers in Psychiatry*, 13, 768586.
- Ries, M., & Sastre, M. (2016). Mechanisms of A β Clearance and Degradation by Glial Cells. *Frontiers in Aging Neuroscience*, 8, 160.
- Robinson, J. T., Thorvaldsdóttir, H., Winckler, W., Guttman, M., Lander, E. S., Getz, G., & Mesirov, J. P. (2011). Integrative genomics viewer. *Nature Biotechnology*, 29(1), Article 1.
- Robson, M. J., Quinlan, M. A., Margolis, K. G., Gajewski-Kurdiel, P. A., Veenstra-VanderWeele, J., Gershon, M. D., Watterson, D. M., & Blakely, R. D. (2018). P38 α MAPK signaling drives pharmacologically reversible brain and gastrointestinal phenotypes in the SERT Ala56 mouse. *Proceedings of the National Academy of Sciences of the United States of America*, 115(43), E10245–E10254.
- Rodriguez, J. I., & Kern, J. K. (2011). Evidence of microglial activation in autism and its possible role in brain underconnectivity. *Neuron Glia Biology*, 7(2–4), 205–213.
- Rogdaki, M., Devroye, C., Ciampoli, M., Veronese, M., Ashok, A. H., McCutcheon, R. A., Jauhar, S., Bonoldi, I., Gudbrandsen, M., Daly, E., van Amelsvoort, T., Van Den Bree, M., Owen, M. J., Turkheimer, F., Papaleo, F., & Howes, O. D. (2021). Striatal dopaminergic alterations in individuals with copy number variants at the 22q11.2 genetic locus and their implications for psychosis risk: A [18F]-DOPA PET study. *Molecular Psychiatry*.
- Roman, K. M., Jenkins, A. K., Lewis, D. A., & Volk, D. W. (2021). Involvement of the nuclear factor- κ B transcriptional complex in prefrontal cortex immune activation in bipolar disorder. *Translational Psychiatry*, 11, 40.
- Ross, P. J., Zhang, W.-B., Mok, R. S. F., Zaslavsky, K., Deneault, E., D’Abate, L., Rodrigues, D. C., Yuen, R. K. C., Faheem, M., Mufteev, M., Piekna, A., Wei, W., Pasceri, P., Landa, R. J., Nagy, A., Varga, B., Salter, M. W., Scherer, S. W., & Ellis, J. (2020). Synaptic Dysfunction in Human Neurons With Autism-Associated Deletions in PTCHD1-AS. *Biological Psychiatry*, 87(2), 139–149.
- Ruan, C., & Elyaman, W. (2022). A New Understanding of TMEM119 as a Marker of Microglia. *Frontiers in Cellular Neuroscience*, 16, 902372.
- Ryu, A. H., Eckalbar, W. L., Kreimer, A., Yosef, N., & Ahituv, N. (2017). Use antibiotics in cell culture with caution: Genome-wide identification of antibiotic-induced changes in gene expression and regulation. *Scientific Reports*, 7(1), 7533.
- Sabate-Soler, S., Nickels, S. L., Saraiva, C., Berger, E., Dubonyte, U., Barmppa, K., Lan, Y. J., Kouno, T., Jarazo, J., Robertson, G., Sharif, J., Koseki, H., Thome, C., Shin, J. W., Cowley, S. A., & Schwamborn, J. C. (2022). Microglia integration into human midbrain organoids leads to increased neuronal maturation and functionality. *Glia*, 70(7), 1267–1288.

- Saghazadeh, A., Ataeinia, B., Keynejad, K., Abdolalizadeh, A., Hirbod-Mobarakeh, A., & Rezaei, N. (2019). A meta-analysis of pro-inflammatory cytokines in autism spectrum disorders: Effects of age, gender, and latitude. *Journal of Psychiatric Research*, 115, 90–102.
- Salari, N., Rasoulpoor, S., Rasoulpoor, S., Shohaimi, S., Jafarpour, S., Abdoli, N., Khaledi-Paveh, B., & Mohammadi, M. (2022). The global prevalence of autism spectrum disorder: A comprehensive systematic review and meta-analysis. *Italian Journal of Pediatrics*, 48(1), 112.
- Salter, M. W., & Stevens, B. (2017). Microglia emerge as central players in brain disease. *Nature Medicine*, 23(9), Article 9.
- Salvi, V., Sozio, F., Sozzani, S., & Del Prete, A. (2017). Role of Atypical Chemokine Receptors in Microglial Activation and Polarization. *Frontiers in Aging Neuroscience*, 9, 148.
- Sanagi, T., Sasaki, T., Nakagaki, K., Minamimoto, T., Kohsaka, S., & Ichinohe, N. (2019). Segmented Iba1-Positive Processes of Microglia in Autism Model Marmosets. *Frontiers in Cellular Neuroscience*, 13, 344.
- Sandiego, C. M., Gallezot, J.-D., Pittman, B., Nabulsi, N., Lim, K., Lin, S.-F., Matuskey, D., Lee, J.-Y., O'Connor, K. C., Huang, Y., Carson, R. E., Hannestad, J., & Cosgrove, K. P. (2015). Imaging robust microglial activation after lipopolysaccharide administration in humans with PET. *Proceedings of the National Academy of Sciences of the United States of America*, 112(40), 12468–12473.
- Sankowski, R., Böttcher, C., Masuda, T., Geirsdottir, L., Sagar, Sindram, E., Seredenina, T., Muhs, A., Scheiwe, C., Shah, M. J., Heiland, D. H., Schnell, O., Grün, D., Priller, J., & Prinz, M. (2019). Mapping microglia states in the human brain through the integration of high-dimensional techniques. *Nature Neuroscience*, 22(12), Article 12.
- Sasaki, Y., Ohsawa, K., Kanazawa, H., Kohsaka, S., & Imai, Y. (2001). Iba1 is an actin-cross-linking protein in macrophages/microglia. *Biochemical and Biophysical Research Communications*, 286(2), 292–297.
- Schaefer, M. R., Williams, M., Kulpa, D. A., Blakely, P. K., Yaffee, A. Q., & Collins, K. L. (2008). A Novel Trafficking Signal within the HLA-C Cytoplasmic Tail Allows Regulated Expression Upon Differentiation of Macrophages. *Journal of Immunology (Baltimore, Md. : 1950)*, 180(12), 7804–7817.
- Schafer, D. P., Lehrman, E. K., Kautzman, A. G., Koyama, R., Mardinly, A. R., Yamasaki, R., Ransohoff, R. M., Greenberg, M. E., Barres, B. A., & Stevens, B. (2012). Microglia Sculpt Postnatal Neural Circuits in an Activity and Complement-Dependent Manner. *Neuron*, 74(4), 691–705.
- Schäfer, I., & Fisher, H. L. (2011). Childhood trauma and psychosis—What is the evidence? *Dialogues in Clinical Neuroscience*, 13(3), 360–365.
- Scheiblich, H., & Bicker, G. (2015). Regulation of microglial migration, phagocytosis, and neurite outgrowth by HO-1/CO signaling. *Developmental Neurobiology*, 75(8), 854–876.
- Scheiblich, H., Bousset, L., Schwartz, S., Griep, A., Latz, E., Melki, R., & Heneka, M. T. (2021). Microglial NLRP3 Inflammasome Activation upon TLR2 and TLR5 Ligation by Distinct α -Synuclein Assemblies. *The Journal of Immunology*, 207(8), 2143–2154.
- Schendel, D., Munk Laursen, T., Albiñana, C., Vilhjalmsón, B., Ladd-Acosta, C., Fallin, M. D., Benke, K., Lee, B., Grove, J., Kalkbrenner, A., Ejlskov, L., Hougaard, D., Bybjerg-Grauholm, J., Baekvad-Hansen, M., Børglum, A. D., Werge, T., Nordentoft, M., Mortensen, P. B., & Agerbo, E. (2022). Evaluating the interrelations between the autism polygenic score and psychiatric family history in risk for autism. *Autism Research: Official Journal of the International Society for Autism Research*, 15(1), 171–182.

- Schindelin, J., Arganda-Carreras, I., Frise, E., Kaynig, V., Longair, M., Pietzsch, T., Preibisch, S., Rueden, C., Saalfeld, S., Schmid, B., Tinevez, J.-Y., White, D. J., Hartenstein, V., Eliceiri, K., Tomancak, P., & Cardona, A. (2012). Fiji—An Open Source platform for biological image analysis. *Nature Methods*, 9(7), 10.1038/nmeth.2019.
- Schneider, M., Debbané, M., Bassett, A. S., Chow, E. W. C., Fung, W. L. A., van den Bree, M. B. M., Owen, M., Murphy, K. C., Niarchou, M., Kates, W. R., Antshel, K. M., Fremont, W., McDonald-McGinn, D. M., Gur, R. E., Zackai, E. H., Vorstman, J., Duijff, S. N., Klaassen, P. W. J., Swillen, A., ... Eliez, S. (2014). Psychiatric Disorders From Childhood to Adulthood in 22q11.2 Deletion Syndrome: Results From the International Consortium on Brain and Behavior in 22q11.2 Deletion Syndrome. *American Journal of Psychiatry*, 171(6), 627–639.
- Schulz, C., Gomez Perdiguero, E., Chorro, L., Szabo-Rogers, H., Cagnard, N., Kierdorf, K., Prinz, M., Wu, B., Jacobsen, S. E. W., Pollard, J. W., Frampton, J., Liu, K. J., & Geissmann, F. (2012). A lineage of myeloid cells independent of Myb and hematopoietic stem cells. *Science (New York, N.Y.)*, 336(6077), 86–90.
- Schwamborn, J. C. (2018). Is Parkinson's Disease a Neurodevelopmental Disorder and Will Brain Organoids Help Us to Understand It? *Stem Cells and Development*, 27(14), 968–975.
- Schwarz, J. M., Sholar, P. W., & Bilbo, S. D. (2012). Sex differences in microglial colonization of the developing rat brain. *Journal of Neurochemistry*, 120(6), 948–963.
- Schwieler, L., Larsson, M. K., Skogh, E., Kegel, M. E., Orhan, F., Abdelmoaty, S., Finn, A., Bhat, M., Samuelsson, M., Lundberg, K., Dahl, M.-L., Sellgren, C., Schuppe-Koistinen, I., Svensson, C. I., Erhardt, S., & Engberg, G. (2015). Increased levels of IL-6 in the cerebrospinal fluid of patients with chronic schizophrenia—Significance for activation of the kynurenine pathway. *Journal of Psychiatry & Neuroscience : JPN*, 40(2), 126–133.
- Sekar, A., Bialas, A. R., de Rivera, H., Davis, A., Hammond, T. R., Kamitaki, N., Tooley, K., Presumey, J., Baum, M., Van Doren, V., Genovese, G., Rose, S. A., Handsaker, R. E., Daly, M. J., Carroll, M. C., Stevens, B., & McCarroll, S. A. (2016). Schizophrenia risk from complex variation of complement component 4. *Nature*, 530(7589), Article 7589.
- Sellgren, C. M., Gracias, J., Watmuff, B., Biag, J. D., Thanos, J. M., Whittredge, P. B., Fu, T., Worringer, K., Brown, H. E., Wang, J., Kaykas, A., Karmacharya, R., Goold, C. P., Sheridan, S. D., & Perlis, R. H. (2019). Increased synapse elimination by microglia in schizophrenia patient-derived models of synaptic pruning. *Nature Neuroscience*, 22(3), Article 3.
- Sellgren, C. M., Sheridan, S. D., Gracias, J., Xuan, D., Fu, T., & Perlis, R. H. (2017). Patient-specific models of microglia-mediated engulfment of synapses and neural progenitors. *Molecular Psychiatry*, 22(2), Article 2.
- Sharma, S. R., Gonda, X., & Tarazi, F. I. (2018). Autism Spectrum Disorder: Classification, diagnosis and therapy. *Pharmacology & Therapeutics*, 190, 91–104.
- Shemer, A., Scheyltjens, I., Frumer, G. R., Kim, J.-S., Grozovski, J., Ayanaw, S., Dassa, B., Van Hove, H., Chappell-Maor, L., Boura-Halfon, S., Leshkowitz, D., Mueller, W., Maggio, N., Movahedi, K., & Jung, S. (2020). Interleukin-10 Prevents Pathological Microglia Hyperactivation following Peripheral Endotoxin Challenge. *Immunity*, 53(5), 1033-1049.e7.
- Shi, Y., & He, M. (2014). Differential gene expression identified by RNA-Seq and qPCR in two sizes of pearl oyster (*Pinctada fucata*). *Gene*, 538(2), 313–322.
- Shprintzen, R. J., Goldberg, R., Golding-Kushner, K. J., & Marion, R. W. (1992). Late-onset psychosis in the velo-cardio-facial syndrome. *American Journal of Medical Genetics*, 42(1), 141–142.

- Shum, C., Dutan, L., Annuario, E., Warre-Cornish, K., Taylor, S. E., Taylor, R. D., Andreae, L. C., Buckley, N. J., Price, J., Bhattacharyya, S., & Srivastava, D. P. (2020). Δ^9 -tetrahydrocannabinol and 2-AG decreases neurite outgrowth and differentially affects ERK1/2 and Akt signaling in hiPSC-derived cortical neurons. *Molecular and Cellular Neurosciences*, 103, 103463.
- Sierra, A., Encinas, J. M., Deudero, J. J. P., Chancey, J. H., Enikolopov, G., Overstreet-Wadiche, L. S., Tsirka, S. E., & Maletic-Savatic, M. (2010). Microglia shape adult hippocampal neurogenesis through apoptosis-coupled phagocytosis. *Cell Stem Cell*, 7(4), 483–495.
- Silva, N. J., Dorman, L. C., Vainchtein, I. D., Horneck, N. C., & Molofsky, A. V. (2021). In situ and transcriptomic identification of microglia in synapse-rich regions of the developing zebrafish brain. *Nature Communications*, 12(1), Article 1.
- Simpson, D., Gharehagzlou, A., Da Silva, T., Labrie-Cleary, C., Wilson, A. A., Meyer, J. H., Mizrahi, R., & Rusjan, P. M. (2022). In vivo imaging translocator protein (TSPO) in autism spectrum disorder. *Neuropsychopharmacology: Official Publication of the American College of Neuropsychopharmacology*, 47(7), 1421–1427.
- Singh, T., Kurki, M. I., Curtis, D., Purcell, S. M., Crooks, L., McRae, J., Suvisaari, J., Chheda, H., Blackwood, D., Breen, G., Pietiläinen, O., Gerety, S. S., Ayub, M., Blyth, M., Cole, T., Collier, D., Coomber, E. L., Craddock, N., Daly, M. J., ... Barrett, J. C. (2016). Rare loss-of-function variants in SETD1A are associated with schizophrenia and developmental disorders. *Nature Neuroscience*, 19(4), 571–577.
- Sinkus, M. L., Graw, S., Freedman, R., Ross, R. G., Lester, H. A., & Leonard, S. (2015). The human CHRNA7 and CHRFAM7A genes: A review of the genetics, regulation, and function. *Neuropharmacology*, 96(Pt B), 274–288.
- Skene, N. G., Bryois, J., Bakken, T. E., Breen, G., Crowley, J. J., Gaspar, H. A., Giusti-Rodriguez, P., Hodge, R. D., Miller, J. A., Muñoz-Manchado, A. B., O'Donovan, M. C., Owen, M. J., Pardiñas, A. F., Ryge, J., Walters, J. T. R., Linnarsson, S., Lein, E. S., Sullivan, P. F., & Hjerling-Leffler, J. (2018). Genetic identification of brain cell types underlying schizophrenia. *Nature Genetics*, 50(6), 825–833.
- Smedley, D., Haider, S., Durinck, S., Pandini, L., Provero, P., Allen, J., Arnaiz, O., Awedh, M. H., Baldock, R., Barbiera, G., Bardou, P., Beck, T., Blake, A., Bonierbale, M., Brookes, A. J., Bucci, G., Buetti, I., Burge, S., Cabau, C., ... Kasprzyk, A. (2015). The BioMart community portal: An innovative alternative to large, centralized data repositories. *Nucleic Acids Research*, 43(W1), W589–W598.
- Smeland, O. B., Bahrami, S., Frei, O., Shadrin, A., O'Connell, K., Savage, J., Watanabe, K., Krull, F., Bettella, F., Steen, N. E., Ueland, T., Posthuma, D., Djurovic, S., Dale, A. M., & Andreassen, O. A. (2020). Genome-wide analysis reveals extensive genetic overlap between schizophrenia, bipolar disorder, and intelligence. *Molecular Psychiatry*, 25(4), 844–853.
- Smeland, O. B., Frei, O., Fan, C.-C., Shadrin, A., Dale, A. M., & Andreassen, O. A. (2019). The emerging pattern of shared polygenic architecture of psychiatric disorders, conceptual and methodological challenges. *Psychiatric Genetics*, 29(5), 152.
- Smigielski, L., Jagannath, V., Rössler, W., Walitza, S., & Grünblatt, E. (2020). Epigenetic mechanisms in schizophrenia and other psychotic disorders: A systematic review of empirical human findings. *Molecular Psychiatry*, 25(8), 1718–1748.
- Smit, T., Ormel, P. R., Sluijs, J. A., Hulshof, L. A., Middeldorp, J., de Witte, L. D., Hol, E. M., & Donega, V. (2022). Transcriptomic and functional analysis of A β 1-42 oligomer-stimulated human monocyte-derived microglia-like cells. *Brain, Behavior, and Immunity*, 100, 219–230.
- Smith, A. M., Gibbons, H. M., Oldfield, R. L., Bergin, P. M., Mee, E. W., Faull, R. L. M., & Dragunow, M. (2013). The transcription factor PU.1 is critical for viability and function of human brain microglia. *Glia*, 61(6), 929–942.

- Smith, J. A., Das, A., Ray, S. K., & Banik, N. L. (2012). Role of pro-inflammatory cytokines released from microglia in neurodegenerative diseases. *Brain Research Bulletin*, 87(1), 10–20.
- Smith, S. E. P., Li, J., Garbett, K., Mirnics, K., & Patterson, P. H. (2007). Maternal immune activation alters fetal brain development through interleukin-6. *The Journal of Neuroscience: The Official Journal of the Society for Neuroscience*, 27(40), 10695–10702.
- Smolders, S., Notter, T., Smolders, S. M. T., Rigo, J.-M., & Brône, B. (2018). Controversies and prospects about microglia in maternal immune activation models for neurodevelopmental disorders. *Brain, Behavior, and Immunity*, 73, 51–65.
- Sneeboer, M., Snijders, G., Berdowski, W., Fernández-Andreu, A., van Mierlo, H., Berdenis van Berlekom, A., Litjens, M., Kahn, R., Hol, E., & Witte, L. (2019). Microglia in post-mortem brain tissue of patients with bipolar disorder are not immune activated. *Translational Psychiatry*, 9.
- Snijders, G. J. L. J., van Zuiden, W., Sneeboer, M. A. M., Berdenis van Berlekom, A., van der Geest, A. T., Schnieder, T., MacIntyre, D. J., Hol, E. M., Kahn, R. S., & de Witte, L. D. (2021). A loss of mature microglial markers without immune activation in schizophrenia. *Glia*, 69(5), 1251–1267.
- Solomon, S., Sampathkumar, N. K., Carre, I., Mondal, M., Chennell, G., Vernon, A. C., Ruepp, M.-D., & Mitchell, J. C. (2022). Heterozygous expression of the Alzheimer's disease-protective PLC γ 2 P522R variant enhances A β clearance while preserving synapses. *Cellular and Molecular Life Sciences*, 79(8), 453.
- Speicher, A. M., Korn, L., Csáti, J., Gonzalez-Cano, L., Heming, M., Thomas, C., Schroeter, C. B., Schafflick, D., Li, X., Gola, L., Engler, A., Kaehne, T., Vallier, L., Meuth, S. G., Meyer zu Hörste, G., Kovac, S., Wiendl, H., Schöler, H. R., & Pawlowski, M. (2022). Deterministic programming of human pluripotent stem cells into microglia facilitates studying their role in health and disease. *Proceedings of the National Academy of Sciences*, 119(43), e2123476119.
- Squarzoni, P., Oller, G., Hoeffel, G., Pont-Lezica, L., Rostaing, P., Low, D., Bessis, A., Ginhoux, F., & Garel, S. (2014). Microglia Modulate Wiring of the Embryonic Forebrain. *Cell Reports*, 8(5), 1271–1279.
- Srinivasan, K., Friedman, B. A., Etxeberria, A., Huntley, M. A., van der Brug, M. P., Foreman, O., Paw, J. S., Modrusan, Z., Beach, T. G., Serrano, G. E., & Hansen, D. V. (2020). Alzheimer's Patient Microglia Exhibit Enhanced Aging and Unique Transcriptional Activation. *Cell Reports*, 31(13), 107843.
- Stanley, E. R., & Chitu, V. (2014). CSF-1 receptor signaling in myeloid cells. *Cold Spring Harbor Perspectives in Biology*, 6(6), a021857.
- Stępnicki, P., Kondej, M., & Kaczor, A. A. (2018). Current Concepts and Treatments of Schizophrenia. *Molecules (Basel, Switzerland)*, 23(8), 2087.
- Stevens, B., Allen, N. J., Vazquez, L. E., Howell, G. R., Christopherson, K. S., Nouri, N., Micheva, K. D., Mehalow, A. K., Huberman, A. D., Stafford, B., Sher, A., Litke, A. M., Lambris, J. D., Smith, S. J., John, S. W. M., & Barres, B. A. (2007). The Classical Complement Cascade Mediates CNS Synapse Elimination. *Cell*, 131(6), 1164–1178.
- Stilo, S. A., & Murray, R. M. (2019). Non-Genetic Factors in Schizophrenia. *Current Psychiatry Reports*, 21(10), 100.
- Streit, W. J., Graeber, M. B., & Kreutzberg, G. W. (1988). Functional plasticity of microglia: A review. *Glia*, 1(5), 301–307.
- Sullivan, S., Stacey, G. N., Akazawa, C., Aoyama, N., Baptista, R., Bedford, P., Bennaceur Griscelli, A., Chandra, A., Elwood, N., Girard, M., Kawamata, S., Hanatani, T., Latsis, T., Lin, S., Ludwig, T. E.,

- Malygina, T., Mack, A., Mountford, J. C., Noggle, S., ... Song, J. (2018). Quality control guidelines for clinical-grade human induced pluripotent stem cell lines. *Regenerative Medicine*, 13(7), 859–866.
- Suzuki, K., Sugihara, G., Ouchi, Y., Nakamura, K., Futatsubashi, M., Takebayashi, K., Yoshihara, Y., Omata, K., Matsumoto, K., Tsuchiya, K. J., Iwata, Y., Tsujii, M., Sugiyama, T., & Mori, N. (2013). Microglial activation in young adults with autism spectrum disorder. *JAMA Psychiatry*, 70(1), 49–58.
- Suzuki, T., Higgins, P. J., & Crawford, D. R. (2000). Control selection for RNA quantitation. *Biotechniques*, 29(2):332-7.
- Svoboda, D. S., Barrasa, M. I., Shu, J., Rietjens, R., Zhang, S., Mitalipova, M., Berube, P., Fu, D., Shultz, L. D., Bell, G. W., & Jaenisch, R. (2019). Human iPSC-derived microglia assume a primary microglia-like state after transplantation into the neonatal mouse brain. *Proceedings of the National Academy of Sciences of the United States of America*, 116(50), 25293–25303.
- Swinnen, N., Smolders, S., Avila, A., Notelaers, K., Paesen, R., Ameloot, M., Brône, B., Legendre, P., & Rigo, J.-M. (2013). Complex invasion pattern of the cerebral cortex by microglial cells during development of the mouse embryo. *Glia*, 61(2), 150–163.
- Syu, J.-S., Baba, T., Huang, J.-Y., Ogawa, H., Hsieh, C.-H., Hu, J.-X., Chen, T.-Y., Lin, T.-C., Tsuchiya, M., Morohashi, K.-I., Huang, B.-M., Lu, F., & Wang, C.-Y. (2017). Lysosomal activity maintains glycolysis and cyclin E1 expression by mediating Ad4BP/SF-1 stability for proper steroidogenic cell growth. *Scientific Reports*, 7, 240.
- Szepesi, Z., Manouchehrian, O., Bachiller, S., & Deierborg, T. (2018). Bidirectional Microglia-Neuron Communication in Health and Disease. *Frontiers in Cellular Neuroscience*, 12, 323.
- Takahashi, K., Tanabe, K., Ohnuki, M., Narita, M., Ichisaka, T., Tomoda, K., & Yamanaka, S. (2007). Induction of pluripotent stem cells from adult human fibroblasts by defined factors. *Cell*, 131(5), 861–872.
- Takahashi, K., & Yamanaka, S. (2006). Induction of pluripotent stem cells from mouse embryonic and adult fibroblast cultures by defined factors. *Cell*, 126(4), 663–676.
- Takata, K., Kozaki, T., Lee, C. Z. W., Thion, M. S., Otsuka, M., Lim, S., Utami, K. H., Fidan, K., Park, D. S., Malleret, B., Chakarov, S., See, P., Low, D., Low, G., Garcia-Miralles, M., Zeng, R., Zhang, J., Goh, C. C., Gul, A., ... Ginhoux, F. (2017). Induced-Pluripotent-Stem-Cell-Derived Primitive Macrophages Provide a Platform for Modeling Tissue-Resident Macrophage Differentiation and Function. *Immunity*, 47(1), 183-198.e6.
- Tanabe, S., & Yamashita, T. (2018). B-1a lymphocytes promote oligodendrogenesis during brain development. *Nature Neuroscience*, 21(4), 506–516.
- Tanaka, A., To, J., O'Brien, B., Donnelly, S., & Lund, M. (2017). Selection of reliable reference genes for the normalisation of gene expression levels following time course LPS stimulation of murine bone marrow derived macrophages. *BMC Immunol*, 18: 43.
- Tanaka, Y., Matsuwaki, T., Yamanouchi, K., & Nishihara, M. (2013). Increased lysosomal biogenesis in activated microglia and exacerbated neuronal damage after traumatic brain injury in progranulin-deficient mice. *Neuroscience*, 250, 8–19.
- Tang, G., Gudsnek, K., Kuo, S.-H., Cotrina, M. L., Rosoklija, G., Sosunov, A., Sonders, M. S., Kanter, E., Castagna, C., Yamamoto, A., Yue, Z., Arancio, O., Peterson, B. S., Champagne, F., Dwork, A. J., Goldman, J., & Sulzer, D. (2014). Loss of mTOR-Dependent Macroautophagy Causes Autistic-like Synaptic Pruning Deficits. *Neuron*, 83(5), 1131–1143.
- Tavian, M., & Peault, B. (2005). Embryonic development of the human hematopoietic system. *The International Journal of Developmental Biology*, 49(2–3), Article 2–3.

- Tewari, M., Khan, M., Verma, M., Coppens, J., Kemp, J. M., Bucholz, R., Mercier, P., & Egan, T. M. (2021). Physiology of cultured human microglia maintained in a defined culture medium. *ImmunoHorizons*, 5(4), 257–272.
- The 1000 Genomes Project Consortium, Abecasis, G. R., Altshuler, D. M., Durbin, R. M., Abecasis, G. R., Bentley, D. R., Chakravarti, A., Clark, A. G., Donnelly, P., Eichler, E. E., Flicek, P., Gabriel, S. B., Gibbs, R. A., Green, E. D., Hurles, M. E., Knoppers, B. M., Korbel, J. O., Lander, E. S., Lee, C., ... National Eye Institute, N. (2015). A global reference for human genetic variation. *Nature*, 526(7571), Article 7571.
- The Haplotype Reference Consortium, Das, S., Kretzschmar, W., Delaneau, O., Wood, A. R., Teumer, A., Kang, H. M., Fuchsberger, C., Danecek, P., Sharp, K., Luo, Y., Sidore, C., Kwong, A., Timpson, N., Koskinen, S., Vrieze, S., Scott, L. J., Zhang, H., Mahajan, A., ... the Haplotype Reference Consortium. (2016). A reference panel of 64,976 haplotypes for genotype imputation. *Nature Genetics*, 48(10), Article 10.
- Thion, M. S., Low, D., Silvín, A., Chen, J., Grisel, P., Schulte-Schrepping, J., Blecher, R., Ulas, T., Squarizoni, P., Hoeffel, G., Couplier, F., Siopi, E., David, F. S., Scholz, C., Shihui, F., Lum, J., Amoyo, A. A., Larbi, A., Poidinger, M., ... Garel, S. (2018). Microbiome Influences Prenatal and Adult Microglia in a Sex-Specific Manner. *Cell*, 172(3), 500-516.e16.
- Thorvaldsdóttir, H., Robinson, J. T., & Mesirov, J. P. (2013). Integrative Genomics Viewer (IGV): High-performance genomics data visualization and exploration. *Briefings in Bioinformatics*, 14(2), 178–192.
- Timmerman, R., Burm, S. M., & Bajramovic, J. J. (2018). An Overview of in vitro Methods to Study Microglia. *Frontiers in Cellular Neuroscience*, 12, 242.
- Toutountzidis, D., Gale, T. M., Irvine, K., Sharma, S., & Laws, K. R. (2022). Childhood trauma and schizotypy in non-clinical samples: A systematic review and meta-analysis. *PloS One*, 17(6), e0270494.
- Toyoshima, M., Akamatsu, W., Okada, Y., Ohnishi, T., Balan, S., Hisano, Y., Iwayama, Y., Toyota, T., Matsumoto, T., Itasaka, N., Sugiyama, S., Tanaka, M., Yano, M., Dean, B., Okano, H., & Yoshikawa, T. (2016). Analysis of induced pluripotent stem cells carrying 22q11.2 deletion. *Translational Psychiatry*, 6(11), e934.
- Tremblay, M.-È., Zettel, M. L., Ison, J. R., Allen, P. D., & Majewska, A. K. (2012). Effects of aging and sensory loss on glial cells in mouse visual and auditory cortices. *Glia*, 60(4), 541–558.
- Tripathi, A., Singh Rawat, B., Addya, S., Surjit, M., Tailor, P., Vrati, S., & Banerjee, A. (2021). Lack of Interferon (IFN) Regulatory Factor 8 Associated with Restricted IFN- γ Response Augmented Japanese Encephalitis Virus Replication in the Mouse Brain. *Journal of Virology*, 95(21), e00406-21.
- Trubetskoy, V., Pardiñas, A. F., Qi, T., Panagiotaropoulou, G., Awasthi, S., Bigdeli, T. B., Bryois, J., Chen, C.-Y., Dennison, C. A., Hall, L. S., Lam, M., Watanabe, K., Frei, O., Ge, T., Harwood, J. C., Koopmans, F., Magnusson, S., Richards, A. L., Sidorenko, J., ... Schizophrenia Working Group of the Psychiatric Genomics Consortium. (2022). Mapping genomic loci implicates genes and synaptic biology in schizophrenia. *Nature*, 604(7906), 502–508.
- Trudler, D., Nazor, K. L., Eisele, Y. S., Grabauskas, T., Dolatabadi, N., Parker, J., Sultan, A., Zhong, Z., Goodwin, M. S., Levites, Y., Golde, T. E., Kelly, J. W., Sierks, M. R., Schork, N. J., Karin, M., Ambasadhan, R., & Lipton, S. A. (2021). Soluble α -synuclein-antibody complexes activate the NLRP3 inflammasome in hiPSC-derived microglia. *Proceedings of the National Academy of Sciences of the United States of America*, 118(15), e2025847118.
- Tsai, S.-J., Hong, C.-J., Liou, Y.-J., Yu, Y. W.-Y., & Chen, T.-J. (2008). Plasminogen activator inhibitor-1 gene is associated with major depression and antidepressant treatment response. *Pharmacogenetics and Genomics*, 18(10), 869–875.

- Tuomi, J. M., Voorbraak, F., Jones, D. L., & Ruijter, J. M. (2010). Bias in the Cq value observed with hydrolysis probe based quantitative PCR can be corrected with the estimated PCR efficiency value. *Methods*, 50(4), 313–322.
- Uchino, S., & Waga, C. (2013). SHANK3 as an autism spectrum disorder-associated gene. *Brain & Development*, 35(2), 106–110.
- Umpierre, A. D., & Wu, L.-J. (2021). How microglia sense and regulate neuronal activity. *Glia*, 69(7), 1637–1653.
- Uranova, N. A., Vikhreva, O. V., Rakhmanova, V. I., & Orlovskaya, D. D. (2018). Ultrastructural pathology of oligodendrocytes adjacent to microglia in prefrontal white matter in schizophrenia. *NPJ Schizophrenia*, 4(1), 26.
- Vahsen, B. F., Gray, E., Candalija, A., Cramb, K. M. L., Scaber, J., Dafinca, R., Katsikoudi, A., Xu, Y., Farrimond, L., Wade-Martins, R., James, W. S., Turner, M. R., Cowley, S. A., & Talbot, K. (2022). Human iPSC co-culture model to investigate the interaction between microglia and motor neurons. *Scientific Reports*, 12(1), Article 1.
- van der Poel, M., Ulas, T., Mizze, M. R., Hsiao, C.-C., Miedema, S. S. M., Adelia, Schuurman, K. G., Helder, B., Tas, S. W., Schultze, J. L., Hamann, J., & Huitinga, I. (2019). Transcriptional profiling of human microglia reveals grey–white matter heterogeneity and multiple sclerosis-associated changes. *Nature Communications*, 10(1), Article 1.
- van Rees, G. F., Lago, S. G., Cox, D. A., Tomasik, J., Rustogi, N., Weigelt, K., Ozcan, S., Cooper, J., Drexhage, H., Leweke, F. M., & Bahn, S. (2018). Evidence of microglial activation following exposure to serum from first-onset drug-naïve schizophrenia patients. *Brain, Behavior, and Immunity*, 67, 364–373.
- van Wilgenburg, B., Browne, C., Vowles, J., & Cowley, S. A. (2013). Efficient, long term production of monocyte-derived macrophages from human pluripotent stem cells under partly-defined and fully-defined conditions. *PloS One*, 8(8), e71098.
- Vanhee, S., De Mulder, K., Van Caeneghem, Y., Verstichel, G., Van Roy, N., Menten, B., Velghe, I., Philippé, J., De Bleser, D., Lambrecht, B. N., Taghon, T., Leclercq, G., Kerre, T., & Vandekerckhove, B. (2015). In vitro human embryonic stem cell hematopoiesis mimics MYB-independent yolk sac hematopoiesis. *Haematologica*, 100(2), 157–166.
- Vargas, D. L., Nascimbene, C., Krishnan, C., Zimmerman, A. W., & Pardo, C. A. (2005). Neuroglial activation and neuroinflammation in the brain of patients with autism. *Annals of Neurology*, 57(1), 67–81.
- Vay, S. U., Flitsch, L. J., Rabenstein, M., Rogall, R., Blaschke, S., Kleinhaus, J., Reinert, N., Bach, A., Fink, G. R., Schroeter, M., & Rueger, M. A. (2018). The plasticity of primary microglia and their multifaceted effects on endogenous neural stem cells in vitro and in vivo. *Journal of Neuroinflammation*, 15(1), 226.
- Verney, C., Monier, A., Fallet-Bianco, C., & Gressens, P. (2010). Early microglial colonization of the human forebrain and possible involvement in periventricular white-matter injury of preterm infants. *Journal of Anatomy*, 217(4), 436–448.
- Vidal, P. M., & Pacheco, R. (2020). The Cross-Talk Between the Dopaminergic and the Immune System Involved in Schizophrenia. *Frontiers in Pharmacology*, 11.
- Vidal-Itriago, A., Radford, R. A. W., Aramideh, J. A., Maurel, C., Scherer, N. M., Don, E. K., Lee, A., Chung, R. S., Graeber, M. B., & Morsch, M. (2022). Microglia morphophysiological diversity and its implications for the CNS. *Frontiers in Immunology*, 13, 997786.

- Villa, A., Gelosa, P., Castiglioni, L., Cimino, M., Rizzi, N., Pepe, G., Lolli, F., Marcello, E., Sironi, L., Vegeto, E., & Maggi, A. (2018). Sex-Specific Features of Microglia from Adult Mice. *Cell Reports*, 23(12), 3501–3511.
- Volk, D. W., Moroco, A. E., Roman, K. M., Edelson, J. R., & Lewis, D. A. (2019). The Role of the Nuclear Factor- κ B Transcriptional Complex in Cortical Immune Activation in Schizophrenia. *Biological Psychiatry*, 85(1), 25–34.
- Voloboueva, L. A., Emery, J. F., Sun, X., & Giffard, R. G. (2013). Inflammatory response of microglial BV-2 cells includes a glycolytic shift and is modulated by mitochondrial glucose-regulated protein 75/mortalin. *FEBS Letters*, 587(6), 756–762.
- Volpato, V., Smith, J., Sandor, C., Ried, J. S., Baud, A., Handel, A., Newey, S. E., Wessely, F., Attar, M., Whiteley, E., Chintawar, S., Verheyen, A., Barta, T., Lako, M., Armstrong, L., Muschet, C., Artati, A., Cusulin, C., Christensen, K., ... Lakics, V. (2018). Reproducibility of Molecular Phenotypes after Long-Term Differentiation to Human iPSC-Derived Neurons: A Multi-Site Omics Study. *Stem Cell Reports*, 11(4), 897–911.
- Volpato, V., & Webber, C. (2020). Addressing variability in iPSC-derived models of human disease: Guidelines to promote reproducibility. *Disease Models & Mechanisms*, 13(1), dmm042317.
- Vorstman, J. A. S., Breetvelt, E. J., Thode, K. I., Chow, E. W. C., & Bassett, A. S. (2013). Expression of autism spectrum and schizophrenia in patients with a 22q11.2 deletion. *Schizophrenia Research*, 143(1), 55–59.
- Vorstman, J. A. S., Morcus, M. E. J., Duijff, S. N., Klaassen, P. W. J., Heineman-de Boer, J. A., Beemer, F. A., Swaab, H., Kahn, R. S., & van Engeland, H. (2006). The 22q11.2 deletion in children: High rate of autistic disorders and early onset of psychotic symptoms. *Journal of the American Academy of Child and Adolescent Psychiatry*, 45(9), 1104–1113.
- Wakselman, S., Béchade, C., Roumier, A., Bernard, D., Triller, A., & Bessis, A. (2008). Developmental neuronal death in hippocampus requires the microglial CD11b integrin and DAP12 immunoreceptor. *The Journal of Neuroscience : The Official Journal of the Society for Neuroscience*, 28(32).
- Wang, C., Fan, L., Khawaja, R. R., Liu, B., Zhan, L., Kodama, L., Chin, M., Li, Y., Le, D., Zhou, Y., Condello, C., Grinberg, L. T., Seeley, W. W., Miller, B. L., Mok, S.-A., Gestwicki, J. E., Cuervo, A. M., Luo, W., & Gan, L. (2022). Microglial NF- κ B drives tau spreading and toxicity in a mouse model of tauopathy. *Nature Communications*, 13(1), Article 1.
- Wang, C., Yue, H., Hu, Z., Shen, Y., Ma, J., Li, J., Wang, X.-D., Wang, L., Sun, B., Shi, P., Wang, L., & Gu, Y. (2020). Microglia mediate forgetting via complement-dependent synaptic elimination. *Science*, 367(6478), 688–694.
- Wang, L., Pavlou, S., Du, X., Bhuckory, M., Xu, H., & Chen, M. (2019). Glucose transporter 1 critically controls microglial activation through facilitating glycolysis. *Molecular Neurodegeneration*, 14, 2.
- Wang, X., Bryan, C., LaMantia, A.-S., & Mendelowitz, D. (2017). Altered neurobiological function of brainstem hypoglossal neurons in DiGeorge/22q11.2 Deletion Syndrome. *Neuroscience*, 359, 1–7.
- Wang, Z., Gerstein, M., & Snyder, M. (2009). RNA-Seq: A revolutionary tool for transcriptomics. *Nature Reviews. Genetics*, 10(1), 57–63.
- Warre-Cornish, K., Perfect, L., Nagy, R., Duarte, R. R. R., Reid, M. J., Raval, P., Mueller, A., Evans, A. L., Couch, A., Ghevaert, C., McAlonan, G., Loth, E., Murphy, D., Powell, T. R., Vernon, A. C., Srivastava, D. P., & Price, J. (2020). Interferon- γ signaling in human iPSC-derived neurons recapitulates neurodevelopmental disorder phenotypes. *Science Advances*, 6(34), eaay9506.

- Washer, S. J., Perez-Alcantara, M., Chen, Y., Steer, J., James, W. S., Trynka, G., Bassett, A. R., & Cowley, S. A. (2022). Single-cell transcriptomics defines an improved, validated monoculture protocol for differentiation of human iPSC to microglia. *Scientific Reports*, 12, 19454.
- Wei, C., El Hindi, S., Li, J., Fornoni, A., Goes, N., Sageshima, J., Maignel, D., Karumanchi, S. A., Yap, H.-K., Saleem, M., Zhang, Q., Nikolic, B., Chaudhuri, A., Daftarian, P., Salido, E., Torres, A., Salifu, M., Sarwal, M. M., Schaefer, F., ... Reiser, J. (2011). Circulating urokinase receptor as a cause of focal segmental glomerulosclerosis. *Nature Medicine*, 17(8), 952–960. <https://doi.org/10.1038/nm.2411>
- Weinberger, D. R. (2019). Polygenic Risk Scores in Clinical Schizophrenia Research. *The American Journal of Psychiatry*, 176(1), 3–4.
- Weinhard, L., di Bartolomei, G., Bolasco, G., Machado, P., Schieber, N. L., Neniskyte, U., Exiga, M., Vadiasute, A., Raggioli, A., Schertel, A., Schwab, Y., & Gross, C. T. (2018). Microglia remodel synapses by presynaptic trogocytosis and spine head filopodia induction. *Nature Communications*, 9(1), Article 1.
- Wendimu, M. Y., & Hooks, S. B. (2022). Microglia Phenotypes in Aging and Neurodegenerative Diseases. *Cells*, 11(13), 2091. <https://doi.org/10.3390/cells11132091>
- Wenger, T. L., Miller, J. S., DePolo, L. M., de Marchena, A. B., Clements, C. C., Emanuel, B. S., Zackai, E. H., McDonald-McGinn, D. M., & Schultz, R. T. (2016). 22q11.2 duplication syndrome: Elevated rate of autism spectrum disorder and need for medical screening. *Molecular Autism*, 7, 27.
- Werling, D. M., & Geschwind, D. H. (2013). Sex differences in autism spectrum disorders. *Current Opinion in Neurology*, 26(2), 146–153.
- Weston, L. L., Jiang, S., Chisholm, D., Jantzie, L. L., & Bhaskar, K. (2021). Interleukin-10 deficiency exacerbates inflammation-induced tau pathology. *Journal of Neuroinflammation*, 18(1), 161.
- Wickham, H. (2016). *ggplot2: Elegant Graphics for Data Analysis*. Springer-Verlag New York. <https://ggplot2.tidyverse.org/authors.html>
- Wilke, I., Arolt, V., Rothermundt, M., Weitzsch, Ch., Hornberg, M., & Kirchner, H. (1996). Investigations of cytokine production in whole blood cultures of paranoid and residual schizophrenic patients. *European Archives of Psychiatry and Clinical Neuroscience*, 246(5), 279–284.
- Williams, J. A., Burgess, S., Suckling, J., Lalouis, P. A., Batool, F., Griffiths, S. L., Palmer, E., Karwath, A., Barsky, A., Gkoutos, G. V., Wood, S., Barnes, N. M., David, A. S., Donohoe, G., Neill, J. C., Deakin, B., Khandaker, G. M., Upthegrove, R., & PIMS Collaboration. (2022). Inflammation and Brain Structure in Schizophrenia and Other Neuropsychiatric Disorders: A Mendelian Randomization Study. *JAMA Psychiatry*, 79(5), 498–507.
- Wong, C.-O., Gregory, S., Hu, H., Chao, Y., Sepúlveda, V. E., He, Y., Li-Kroeger, D., Goldman, W. E., Bellen, H. J., & Venkatachalam, K. (2017). Lysosomal Degradation is Required for Sustained Phagocytosis of Bacteria by Macrophages. *Cell Host & Microbe*, 21(6), 719-730.e6.
- Wood, G. W., Gollahon, K. A., Tilzer, S. A., Vats, T., & Morantz, R. A. (1979). The failure of microglia in normal brain to exhibit mononuclear phagocyte markers. *Journal of Neuropathology and Experimental Neurology*, 38(4), 369–376.
- Wu, A. R., Neff, N. F., Kalisky, T., Dalerba, P., Treutlein, B., Rothenberg, M. E., Mburu, F. M., Mantalas, G. L., Sim, S., Clarke, M. F., & Quake, S. R. (2014). Quantitative assessment of single-cell RNA-sequencing methods. *Nature Methods*, 11(1), 41–46.

- Wu, A.-G., Zhou, X.-G., Qiao, G., Yu, L., Tang, Y., Yan, L., Qiu, W.-Q., Pan, R., Yu, C.-L., Law, B. Y.-K., Qin, D.-L., & Wu, J.-M. (2021). Targeting microglial autophagic degradation in NLRP3 inflammasome-mediated neurodegenerative diseases. *Ageing Research Reviews*, 65, 101202.
- Wu, Y., Dissing-Olesen, L., MacVicar, B. A., & Stevens, B. (2015). Microglia: Dynamic Mediators of Synapse Development and Plasticity. *Trends in Immunology*, 36(10), 605–613.
- Wu, Y., Shao, W., Todd, T. W., Tong, J., Yue, M., Koga, S., Castanedes-Casey, M., Librero, A. L., Lee, C. W., Mackenzie, I. R., Dickson, D. W., Zhang, Y.-J., Petrucelli, L., & Prudencio, M. (2021). Microglial lysosome dysfunction contributes to white matter pathology and TDP-43 proteinopathy in GRN-associated FTD. *Cell Reports*, 36(8), 109581.
- Xu, L., Ye, X., Wang, Q., Xu, B., Zhong, J., Chen, Y., & Wang, L. (2021). T-cell infiltration, contribution and regulation in the central nervous system post-traumatic injury. *Cell Proliferation*, 54(8), e13092.
- Xu, Z.-X., Kim, G. H., Tan, J.-W., Riso, A. E., Sun, Y., Xu, E. Y., Liao, G.-Y., Xu, H., Lee, S.-H., Do, N.-Y., Lee, C. H., Clipperton-Allen, A. E., Kwon, S., Page, D. T., Lee, K. J., & Xu, B. (2020). Elevated protein synthesis in microglia causes autism-like synaptic and behavioral aberrations. *Nature Communications*, 11(1), Article 1.
- Yamamoto, T., Arita, M., Kuroda, H., Suzuki, T., & Kawamata, S. (2022). Improving the differentiation potential of pluripotent stem cells by optimizing culture conditions. *Scientific Reports*, 12(1), Article 1.
- Yang, M.-S., Park, E. J., Sohn, S., Kwon, H. J., Shin, W.-H., Pyo, H. K., Jin, B., Choi, K. S., Jou, I., & Joe, E.-H. (2002). Interleukin-13 and -4 induce death of activated microglia. *Glia*, 38(4), 273–280.
- Yang, X., He, G., Hao, Y., Chen, C., Li, M., Wang, Y., Zhang, G., & Yu, Z. (2010). The role of the JAK2-STAT3 pathway in pro-inflammatory responses of EMF-stimulated N9 microglial cells. *Journal of Neuroinflammation*, 7(1), 54.
- Yilmaz, M., Yalcin, E., Presumey, J., Aw, E., Ma, M., Whelan, C. W., Stevens, B., McCarroll, S. A., & Carroll, M. C. (2021). Overexpression of schizophrenia susceptibility factor human complement C4A promotes excessive synaptic loss and behavioral changes in mice. *Nature Neuroscience*, 24(2), 214–224.
- Yim, W. W.-Y., & Mizushima, N. (2020). Lysosome biology in autophagy. *Cell Discovery*, 6(1), Article 1.
- Young, A. M. H., Campbell, E., Lynch, S., Suckling, J., & Powis, S. J. (2011). Aberrant NF-KappaB Expression in Autism Spectrum Condition: A Mechanism for Neuroinflammation. *Frontiers in Psychiatry*, 2, 27.
- Yu, J., Vodyanik, M. A., Smuga-Otto, K., Antosiewicz-Bourget, J., Frane, J. L., Tian, S., Nie, J., Jonsdottir, G. A., Ruotti, V., Stewart, R., Slukvin, I. I., & Thomson, J. A. (2007). Induced pluripotent stem cell lines derived from human somatic cells. *Science*, 318(5858):1917-20.
- Zablotsky, B., Black, L. I., & Blumberg, S. J. (2017). Estimated Prevalence of Children With Diagnosed Developmental Disabilities in the United States, 2014-2016. *NCHS Data Brief*, 291, 1–8.
- Zhan, Y., Paolicelli, R. C., Sforzini, F., Weinhard, L., Bolasco, G., Pagani, F., Vyssotski, A. L., Bifone, A., Gozzi, A., Ragozzino, D., & Gross, C. T. (2014). Deficient neuron-microglia signaling results in impaired functional brain connectivity and social behavior. *Nature Neuroscience*, 17(3), Article 3.
- Zhang, S., Meng, Y., Zhou, L., Qiu, L., Wang, H., Su, D., Zhang, B., Chan, K.-M., & Han, J. (2022). Targeting epigenetic regulators for inflammation: Mechanisms and intervention therapy.
- Zhang, W., Jiang, J., Xu, Z., Yan, H., Tang, B., Liu, C., Chen, C., & Meng, Q. (2023). Microglia-containing human brain organoids for the study of brain development and pathology. *Molecular Psychiatry*, 28(1), Article 1.

- Zhang, X., Dong, H., Zhang, S., Lu, S., Sun, J., & Qian, Y. (2015). Enhancement of LPS-induced microglial inflammation response via TLR4 under high glucose conditions. *Cellular Physiology and Biochemistry: International Journal of Experimental Cellular Physiology, Biochemistry, and Pharmacology*, 35(4), 1571–1581.
- Zhang, Y., Chen, K., Sloan, S. A., Bennett, M. L., Scholze, A. R., O’Keeffe, S., Phatnani, H. P., Guarnieri, P., Caneda, C., Ruderisch, N., Deng, S., Liddelow, S. A..., & Wu, J. Q. (2014). An RNA-sequencing transcriptome and splicing database of glia, neurons, and vascular cells of the cerebral cortex. *The Journal of Neuroscience: The Official Journal of the Society for Neuroscience*, 34(36), 11929–11947.
- Zhang, Z., Yue, P., Lu, T., Wang, Y., Wei, Y., & Wei, X. (2021). Role of lysosomes in physiological activities, diseases, and therapy. *Journal of Hematology & Oncology*, 14(1), 79.
- Zhao, D., Lin, M., Chen, J., Pedrosa, E., Hrabovsky, A., Fourcade, H. M., Zheng, D., & Lachman, H. M. (2015). MicroRNA Profiling of Neurons Generated Using Induced Pluripotent Stem Cells Derived from Patients with Schizophrenia and Schizoaffective Disorder, and 22q11.2 Del. *PLOS ONE*, 10(7), e0132387.
- Zhao, H., Zhang, H., Liu, S., Luo, W., Jiang, Y., & Gao, J. (2021). Association of Peripheral Blood Levels of Cytokines With Autism Spectrum Disorder: A Meta-Analysis. *Frontiers in Psychiatry*, 12, 670200.
- Zhao, W., Hu, B., Zhang, X., & Wang, P. (2020). *Pen-strep influence macrophage mechanical property and mechano-response to microenvironment* (p. 2020.04.09.034884). bioRxiv.
- Zhong, S., Zhang, S., Fan, X., Wu, Q., Yan, L., Dong, J., Zhang, H., Li, L., Sun, L., Pan, N., Xu, X., Tang, F., Zhang, J., Qiao, J., & Wang, X. (2018). A single-cell RNA-seq survey of the developmental landscape of the human prefrontal cortex. *Nature*, 555(7697), Article 7697. <https://doi.org/10.1038/nature25980>
- Zhong, Z., Liang, S., Sanchez-Lopez, E., He, F., Shalapour, S., Lin, X.-J., Wong, J., Ding, S., Seki, E., Schnabl, B., Hevener, A. L., Greenberg, H. B., Kisseleva, T., & Karin, M. (2018). New mitochondrial DNA synthesis enables NLRP3 inflammasome activation. *Nature*, 560(7717), 198–203.
- Zhou, N., Liu, K., Sun, Y., Cao, Y., & Yang, J. (2019). Transcriptional mechanism of IRF8 and PU.1 governs microglial activation in neurodegenerative condition. *Protein & Cell*, 10(2), 87–103.
- Zhu, F., Zhang, L., Liu, F., Wu, R., Guo, W., Ou, J., Zhang, X., & Zhao, J. (2018). Altered Serum Tumor Necrosis Factor and Interleukin-1 β in First-Episode Drug-Naïve and Chronic Schizophrenia. *Frontiers in Neuroscience*, 12, 296.
- Zrzavy, T., Machado-Santos, J., Christine, S., Baumgartner, C., Weiner, H. L., Butovsky, O., & Lassmann, H. (2018). Dominant role of microglial and macrophage innate immune responses in human ischemic infarcts. *Brain Pathology*, 28(6), 791–805.
- Zuiderwijk-Sick, E. A., van der Putten, C., Timmerman, R., Veth, J., Pasini, E. M., van Straalen, L., van der Valk, P., Amor, S., & Bajramovic, J. J. (2021). Exposure of Microglia to Interleukin-4 Represses NF- κ B-Dependent Transcription of Toll-Like Receptor-Induced Cytokines. *Frontiers in Immunology*, 12.
- Zürcher, N. R., Loggia, M. L., Mullett, J. E., Tseng, C., Bhanot, A., Richey, L., Hightower, B. G., Wu, C., Parmar, A. J., Butterfield, R. I., Dubois, J. M., Chonde, D. B., Izquierdo-Garcia, D..., & Hooker, J. M. (2021). [11C]PBR28 MR-PET imaging reveals lower regional brain expression of translocator protein (TSPO) in young adult males with autism spectrum disorder. *Molecular Psychiatry*, 26(5), 1659–1669.
- Zusso, M., Methot, L., Lo, R., Greenhalgh, A. D., David, S., & Stifani, S. (2012). Regulation of Postnatal Forebrain Amoeboid Microglial Cell Proliferation and Development by the Transcription Factor Runx1. *The Journal of Neuroscience*, 32(33), 11285–11298.